Pacific Northwest
NATIONAL LABORATORY

Proudly Operated by **Battelle** *Since 1965*

Deep Vadose Zone Treatability Test of Soil Desiccation for the Hanford Central Plateau: Final Report

February 2018

MJ Truex   VL Freedman
GB Chronister   ML Rockhold
CE Strickland   WJ Greenwood
CD Johnson   JE Peterson
GD Tartakovsky   SS Hubbard
M Oostrom   AL Ward
RE Clayton
TC Johnson

U.S. DEPARTMENT OF
ENERGY

DISCLAIMER

This report was prepared as an account of work sponsored by an agency of the United States Government. Neither the United States Government nor any agency thereof, nor Battelle Memorial Institute, nor any of their employees, makes **any warranty, express or implied, or assumes any legal liability or responsibility for the accuracy, completeness, or usefulness of any information, apparatus, product, or process disclosed, or represents that its use would not infringe privately owned rights**. Reference herein to any specific commercial product, process, or service by trade name, trademark, manufacturer, or otherwise does not necessarily constitute or imply its endorsement, recommendation, or favoring by the United States Government or any agency thereof, or Battelle Memorial Institute. The views and opinions of authors expressed herein do not necessarily state or reflect those of the United States Government or any agency thereof.

PACIFIC NORTHWEST NATIONAL LABORATORY
operated by
BATTELLE
for the
UNITED STATES DEPARTMENT OF ENERGY
under Contract DE-AC05-76RL01830

Printed in the United States of America

Available to DOE and DOE contractors from the
Office of Scientific and Technical Information,
P.O. Box 62, Oak Ridge, TN 37831-0062;
ph: (865) 576-8401
fax: (865) 576-5728
email: reports@adonis.osti.gov

Available to the public from the National Technical Information Service
5301 Shawnee Rd., Alexandria, VA 22312
ph: (800) 553-NTIS (6847)
email: orders@ntis.gov <http://www.ntis.gov/about/form.aspx>
Online ordering: http://www.ntis.gov

This document was printed on recycled paper.
(8/2010)

Deep Vadose Zone Treatability Test of Soil Desiccation for the Hanford Central Plateau: Final Report

MJ Truex   VL Freedman
GB Chronister[1] ML Rockhold
CE Strickland   WJ Greenwood
CD Johnson   JE Peterson[2]
GD Tartakovsky   SS Hubbard[2]
M Oostrom   AL Ward
RE Clayton
TC Johnson

February 2018

Pacific Northwest National Laboratory
Richland, Washington 99352

[1]CH2M Hill Plateau Remediation Company
[2]Lawrence Berkley National Laboratory

Summary

Over decades of operation, the U.S. Department of Energy (DOE) and its predecessors have released nearly 2 trillion L (450 billion gal) of liquid into the vadose zone at the Hanford Site. Much of this liquid waste discharge into the vadose zone occurred in the Central Plateau, a 200 km^2 (75 mi^2) area that includes approximately 800 waste sites. Some of the inorganic and radionuclide contaminants in the deep vadose zone at the Hanford Site are at depths where direct exposure pathways (human health or ecological) are not of concern, but may need to be remediated to protect groundwater (DOE 2008a; Dresel et al. 2011). The Tri-Party Agencies (DOE, U.S. Environmental Protection Agency, and Washington State Department of Ecology) established Milestone M-015-50, which directed DOE to submit a treatability test plan for remediation of Tc-99 and uranium in the deep vadose zone. These contaminants are mobile in the subsurface environment and have been detected at high concentrations deep in the vadose zone, and at some locations have reached groundwater. Testing technologies for remediating Tc-99 and uranium will also provide information relevant for remediating other contaminants in the vadose zone. The desiccation test described herein was conducted as an element of the test plan published in March 2008 to meet Milestone M-015-50 (DOE 2008a). Desiccation was tested as a potential vadose zone remediation technology to be used in conjunction with a surface infiltration barrier to protect groundwater.

The desiccation field test was conducted at the Hanford Site 200-BC-1 Operable Unit. This operable unit contains 26 cribs and trenches that received about 110 million L (29 million gal) of liquid waste primarily in the mid-1950s. The waste contained about 410 curies of Tc-99 (Corbin et al. 2005). There is no evidence the contamination has reached groundwater, located about 100 m (330 ft) below ground surface (bgs) in this area. Initial characterization efforts indicated the Tc-99 inventory is located mostly at a depth in the vadose zone of between about 30 and 70 m (98 and 230 ft) bgs. However, transport model predictions have indicated the potential for this contamination to adversely impact groundwater in the future (Ward et al. 2004).

The test was conducted to provide information about desiccation that is intended for use in subsequent feasibility studies for waste sites with inorganic and radionuclide contaminants in the deep vadose zone. Field-scale test site characterization was conducted to support this treatability test, as described in a characterization work plan (DOE 2008b). Results of the characterization effort have been previously reported in DOE (2010a) and Um et al. (2009). A field test plan (DOE 2010b) was prepared and used to guide the desiccation field testing effort. Laboratory and numerical modeling efforts (Truex et al. 2011; Ward et al. 2008; Oostrom et al. 2009, 2011, 2012a,b) preceded and accompanied the field test and are incorporated herein as their results pertain to assessment of desiccation for future feasibility studies.

The desiccation technology relies on removal of water from a portion of the subsurface such that the resultant low moisture conditions inhibit downward movement of water and dissolved contaminants. Implementation requires establishing sufficiently dry conditions within the targeted zone to inhibit downward water transport effectively. Nominally, the targeted desiccation zone would need to extend laterally across the portion of the vadose zone where contaminants have the potential to move downward at a flux that would cause groundwater contaminant concentrations above the groundwater remediation objective. Overall objectives for the field test were to provide technical data as a design basis for desiccation, demonstrate desiccation at the field scale, and provide scale-up information for use in subsequent feasibility studies. Key performance factors identified for the field test included providing

field-scale information to evaluate 1) the location and extent of the desiccated zone within the subsurface, 2) the desiccation rate, 3) the achievable end-state moisture conditions within the desiccated zone, and 4) the rate and extent of moisture content increase after desiccation is completed.

The objectives outlined in the field test plan (DOE 2010b) were successfully addressed through the field testing and associated laboratory and modeling efforts conducted as part of this treatability test. A design basis to apply desiccation for vadose zone remediation was developed and is available for use in subsequent feasibility and remedial design efforts. Analysis of data and use of numerical simulations indicate that full-scale designs can be made more cost effective than the design of the field test (which was designed to collect specific data, not as a full-scale remediation) through use of ambient air as the injected dry gas and use of an injection-only design (i.e., no extraction well). Using desiccation performance calculations developed from the treatability test information, a nominal Hanford Site design with a 10-year operating period and an injection rate of 170 m^3/h (100 cfm) per meter of well screen leads to an injection well spacing on the order of 25+ m (80+ ft) (4–6 wells per hectare) (2–3 wells per acre).

The field test successfully provided information addressing key performance factors for desiccation. In the relatively short 6-month duration of the field test, a zone of the subsurface about 3-m (10-ft) thick out to a radius of about 3 m (10 ft) was desiccated, creating conditions that reduce the rate of moisture and contaminant movement toward the groundwater. Moisture content of the subsurface was also reduced to a lesser extent over a larger portion of the test area. The distribution of desiccation was controlled by permeability contrasts that affect the injected gas flow patterns. The lateral and vertical distribution of drying from the injection well was influenced by the subsurface heterogeneity with initial drying in higher permeability zones. Desiccation removed over 18,000 kg of water from the test zone within the 164-day desiccation period (with 151 days of air injection during that time) and reduced volumetric moisture content in over 1300 m^3 of soil with values lower than 0.04 m^3/m^3 in 225 m^3 of the test site and lower than 0.01 m^3/m^3 in 68 m^3.

The rate and extent of desiccation observed in the field test was consistent with laboratory data and associated modeling calculations also conducted as part of the overall treatability test effort. These efforts demonstrated that the desiccation rate is related to the water-holding capacity of the injected gas, which is a function of temperature and is influenced by evaporative cooling processes during desiccation. Thus, the overall desiccation rate and extent are controlled by the water-holding capacity of the injected gas, temperature, and number of pore volumes of dry gas that contact the targeted treatment zone. With sufficient time, moisture content can be reduced to near zero through evaporative processes during desiccation as shown in both laboratory tests and the field test. In the field test, a range of desiccation responses were induced over the finite duration of the test as observed by the range in moisture-content values at the end of desiccation. The distribution of desiccation depended on the radial distance from the injection well and the pattern of injected gas flow. While a full-scale remediation using desiccation would be operated long enough to achieve a more uniform low moisture content throughout the targeted treatment zone, the field test was conducted to provide a range of desiccation intensity so that post-desiccation rewetting could be evaluated for different desiccation conditions.

Over time, the rate of moisture rewetting of the desiccated zones is a function of the hydraulic gradient, water relative permeability, and porous media unsaturated flow properties. Rewetting data over a period of 6 years after the end of active desiccation are consistent with expectations based on related laboratory data and numerical simulation analyses. Because the rewetting process is predictable, feasibility study

efforts can use the information herein and site-specific analyses to determine appropriate configurations for applying a desiccation zone in conjunction with a surface barrier.

Acronyms and Abbreviations

ARAR	applicable or relevant and appropriate requirement
bgs	below ground surface
CERCLA	*Comprehensive Environmental Response, Compensation, and Liability Act of 1980*
cfm	cubic feet per minute
C_R	count ratio
DOE	U.S. Department of Energy
DPHP	dual-probe heat pulse
DQO	data quality objective
EC	electrical conductivity
ERT	electrical resistivity tomography
GPR	ground-penetrating radar
HDU	heat dissipation unit
Ksat	saturated hydraulic conductivity
PNNL	Pacific Northwest National Laboratory
PSQ	principal study question
PVC	polyvinyl chloride
TCP	thermocouple psychrometer
VMC	volumetric moisture content
VMC_0	ratio of volumetric moisture content at the starting time
VMCt	ratio of volumetric moisture content at time 't'

Contents

Figures

Tables

1.0   Introduction

Although the depth of some inorganic and radionuclide contamination in the vadose zone at the Hanford Site is beyond the point where direct exposure pathways are relevant, remediation may still be required to protect groundwater (DOE 2008a). However, remediation options for contamination deep in the vadose zone are limited by the physical and hydrogeologic properties of the vadose zone (Dresel et al. 2011). In response to the Tri-Party Agreement Milestone M-015-50, the *Deep Vadose Treatability Test Plan for the Hanford Central Plateau* was issued in March 2008 (DOE 2008a). This overall plan is for a treatability test program to evaluate potential deep vadose zone remedies for groundwater protection at the Hanford Site. As part of this program, evaluation of vadose zone desiccation was planned (DOE 2010a,b) and a field test of desiccation was conducted (Truex et al. 2012a,b, 2013a), including post-desiccation monitoring that has been documented over time in interim data summary reports (Truex et al. 2013b, 2014, 2015). Prior to implementation, field test site characterization was conducted as described in a characterization work plan (DOE 2008b). Results of the characterization effort have been previously reported (DOE 2010a; Um et al. 2009). A comprehensive documentation of the desiccation field test, including the final post-desiccation monitoring data, is included herein as a final desiccation treatability test report.

The Hanford Site 200-BC-1 Operable Unit (the BC Cribs and Trenches Area) has subsurface conditions that serve as an example of vadose zone contamination issues and was selected as the location of the desiccation field test site. This operable unit contains 26 cribs and trenches (engineered features used to infiltrate liquid waste into the ground) that received about 110 million liters of liquid waste, primarily in the mid-1950s. The waste contained about 410 curies of technetium-99 (Tc-99) (Corbin et al. 2005). There is no evidence that the contamination has reached groundwater, located about 100 m (330 ft) below ground surface (bgs) in this area. Initial characterization efforts indicated that the Tc-99 inventory is located mostly at a depth in the vadose zone of between about 30 and 70 m (98 and 230 ft) bgs. However, transport model predictions have indicated that the potential exists for this contamination to adversely affect groundwater in the future (Ward et al. 2004). The groundwater contaminant concentrations that can result from vadose zone contamination are a function of the rate of contaminant movement through the vadose zone. For remediation, contaminant discharge from the vadose zone to the groundwater must be maintained at a magnitude low enough to achieve groundwater protection goals.

Desiccation of a portion of the vadose zone, in conjunction with a surface infiltration barrier, has the potential to minimize migration of deep vadose zone contaminants towards the water table (Truex et al. 2011). To apply desiccation, a dry gas is injected into the subsurface (Figure 1.1). The dry gas evaporates water from the porous medium until the gas reaches 100% relative humidity, after which the gas can no longer evaporate water. Once the gas reaches 100% relative humidity and moves outside the desiccation zone, it mingles with other soil gas which is also has a natural state of 100% relative humidity. Thus, the pore water removed by desiccation is transformed to humidity in the soil gas, which does not have secondary effects. Evaporation can remove pore water and may result in very low moisture contents and decreased water relative permeability in the desiccated zone (Ward et al. 2008; Oostrom et al. 2009, 2012a and b; Truex et al. 2011, 2012a and b, 2013a and b, 2014). Because of these desiccation-induced changes, the future rate of movement of moisture and contaminants through this zone is decreased. Importantly, desiccation is complementary to application of a surface infiltration barrier. When a surface infiltration barrier is applied, the subsurface moisture conditions re-equilibrate to the lower recharge rate beneath the barrier. However, the moisture (and associated contaminants) present

deep in the vadose zone take time to equilibrate to the new conditions and, over this time period (which depends on the initial moisture conditions and the thickness of the vadose zone), the rate of moisture (and contaminant) movement toward the groundwater declines from pre-barrier rates to the recharge rate associated with the barrier. Desiccation can be applied to rapidly decrease the moisture content in the deep vadose zone to levels at and below the long-term moisture conditions that are associated with a surface barrier. Thus, the combination of desiccation and a surface barrier rapidly reaches and then maintains low contaminant flux conditions in the vadose zone.
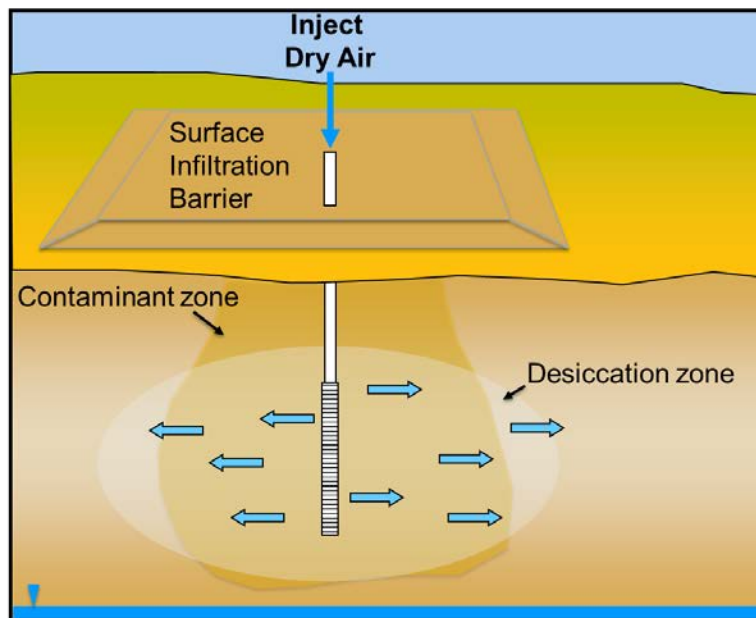
Figure 1.1. Conceptual Depiction of Desiccation and a Surface Barrier

Laboratory and modeling studies have been conducted to study desiccation and provide a technical basis for its use as a potential remedy in conjunction with a surface infiltration barrier (Truex et al. 2011; Ward et al. 2008; Oostrom et al. 2009, 2011, 2012a,b). In these studies, the overall performance of desiccation in limiting water and contaminant flux through the vadose zone to the groundwater was shown to be a function of the final moisture content in the desiccated zone, contaminant concentration, sediment properties, size of the desiccated zone, the hydraulic properties and conditions in surrounding subsurface zones, and the net surface recharge rate. In the laboratory, desiccation was shown to be capable of reducing the moisture content to below the residual moisture content of the porous medium. Key factors that impact the effectiveness of desiccation are the initial moisture content in the zone being desiccated, permeability contrasts between adjacent sediment layers, and temperature and relative humidity of the injected gas.

The rate of desiccation in the laboratory was directly related to the water-holding capacity of the injected dry gas, the initial moisture content, and the number of pore volumes of dry gas transported through the porous medium. Because the transport of dry gas is directly related to the permeability of the porous medium, higher permeability zones in soil columns and flow cells packed with heterogeneous media dried more quickly than lower permeability zones. Laboratory studies have also demonstrated the concentration of solutes in the pore water does not significantly affect the desiccation rate for solute concentrations ranging up to 5.8M of sodium nitrate.

Truex et al. (2011) examined rewetting of desiccated zones in the laboratory and found that vapor-phase rewetting from adjacent humid soil gas, in the absence of advective soil gas movement, occurs slowly by diffusion of water vapor and increases the moisture content of desiccated porous medium to a limited extent, nominally to near the residual moisture content for the porous medium. The aqueous-phase rewetting rate was found to be a function of the relative aqueous-phase permeability of the porous medium and hydraulic capillary pressure gradients.

Modeling studies (Truex et al. 2011; Ward et al. 2008) demonstrated the desiccation rate is increased with higher temperature and lower relative humidity of the injected dry gas, consistent with laboratory studies where the thermodynamic factors controlling the water-holding capacity of the injected dry gas were correlated with the desiccation rate. Truex et al. (2011) demonstrated through numerical modeling that combinations of a surface infiltration barrier and subsurface desiccation enhanced protection of groundwater compared to no-treatment or surface-barrier-only scenarios. The effectiveness of desiccation was related to the thickness and vertical location of the imposed desiccated zone in relation to the location of the elevated moisture and contaminant conditions. While the concentration of solutes increased in the desiccated zone in these simulations, this effect did not lead to a significant high-concentration pulse to the groundwater.

This report is the final treatability test report for desiccation, meeting the requirements for this test in the *Deep Vadose Treatability Test Plan for the Hanford Central Plateau* (DOE 2008a). The field test described herein builds on the above technical basis developed for desiccation and provides information about desiccation that is intended for use in subsequent feasibility studies for waste sites with inorganic and radionuclide contaminants in the deep vadose zone. This report is organized following the guidelines for reporting of *Comprehensive Environmental Response, Compensation, and Liability Act of 1980* (CERCLA) treatability tests (EPA 1992). Section 2.0 provides the conclusions and recommendations for the study. The test approach is described in Section 3.0, followed by a presentation of the detailed results in Section 4.0. Quality assurance and the cost and schedule for the project are presented in Sections 5.0 and 6.0, respectively.

2.0   Conclusions and Recommendations

2.1   Overall Conclusions

The objectives for the field test were to provide technical data as a design basis for desiccation, demonstrate desiccation at the field scale, and provide scale-up information for use in subsequent feasibility tests. The objectives outlined in the field test plan (DOE 2010b) were successfully addressed through the field testing and associated laboratory and modeling efforts conducted as part of this treatability test. In the field test, a portion of the subsurface was desiccated, creating conditions that reduce the rate of moisture and contaminant movement toward the groundwater. A design basis to apply desiccation for vadose zone remediation was developed and is available for use in subsequent feasibility study and remedial design efforts. Post-desiccation monitoring quantified the rewetting process in support of developing an overall performance assessment for application of desiccation. Overall, the desiccation test at the 200-BC-1 Operable Unit field test site provides sufficient information for desiccation to be applied in conjunction with a surface infiltration barrier and to be considered as a potential vadose zone remedy in future feasibility studies as summarized below and described in this report and the referenced material.

Although desiccation could be applied alone, it would require continued periodic application to remove water that enters the vadose zone by surface infiltration. As appropriate, this type of application could be evaluated for specific sites as part of a feasibility study. However, desiccation is complementary to application of a surface infiltration barrier. When a surface infiltration barrier is applied, the subsurface moisture conditions re-equilibrate to the lower recharge rate beneath the barrier. The moisture (and associated contaminants) present deep in the vadose zone takes time to equilibrate to the new conditions and, over this time period (which depends on the initial moisture conditions and the thickness of the vadose zone), the rate of moisture (and contaminant) movement toward the groundwater declines from pre-barrier rates to the recharge rate associated with the barrier. During this time of equilibration, contaminant flux to the groundwater may occur at an unacceptable rate. Desiccation can be applied to rapidly decrease the moisture content in the deep vadose zone to levels at and below the long-term moisture conditions that are associated with a surface barrier. Thus, the combination of desiccation and a surface barrier rapidly reaches and then maintains low contaminant flux conditions in the vadose zone. In this way, desiccation enhances the performance of a surface barrier, addressing deep contamination by rapidly decreasing moisture and reaching low recharge conditions that limit the contaminant flux to groundwater. For desiccation only or remediation alternatives that are a combination of a surface barrier and desiccation, it may be relevant to consider the cost of using these approaches to keep contaminant flux to the groundwater low enough to prevent a groundwater plume of concern compared to the cost of active groundwater remediation.

The treatability test was conducted to provide information about desiccation that is intended for use at waste sites with inorganic and radionuclide contaminants in the deep vadose zone. While desiccation was demonstrated at a site contaminated primarily with Tc-99, its mode of action associated with changing moisture conditions is also relevant to other inorganic and radionuclide contaminants. Volatile contaminants (e.g., organics) would be impacted by the air injection process used to induce desiccation and are not part of this desiccation treatability test. The active desiccation portion of the field test occurred over a duration of 164 days (with 151 days of air injection during that time), ending on June 30, 2011 (Truex et al. 2012a). The desiccation phase was then followed by 6 years of monitoring at the site.

For the test, which used an injection and extraction well design to help meet tests objectives, the injection and extraction wells were 12 m (39 ft) apart with multiple monitored locations surrounding the injection well. A clustered monitoring approach was used in the test whereby a "sensor borehole" containing sensors, gas-sampling ports, and electrical resistance tomography electrodes was placed nominally adjacent to a cased, unscreened "logging well" that was used to conduct neutron moisture logging and cross-hole ground-penetrating radar (GPR). Monitoring with the in situ sensors and geophysical techniques was continued during the post-desiccation (rewetting) phase of the test through July 2017.

The field test demonstrated that desiccation can be applied at the field scale and reduce subsurface moisture content to levels expected to decrease future water and contaminant movement, if applied in conjunction with a surface barrier. The distribution, rate, and extent of desiccation observed in the field were impacted by subsurface heterogeneity; however, over time, the moisture content in initially wetter, lower permeability zones of limited extent was also reduced. Field test results were consistent with expectations based on previous laboratory and modeling efforts that investigated aspects of the desiccation process. The field test targeted a desiccation zone that had significant contrasts in permeability to investigate the performance of desiccation across multiple types of subsurface conditions. As discussed in this report, full-scale application of desiccation would seek target depth intervals for dry gas injection that enable creation of thick desiccated zones and avoid zones where injected gas flow would be minimal.

While the desiccation field test was applied at a relatively shallow location (9.1 to 15.2 m [30 to 50 ft] bgs), there is no inherent limitation for extending the information from the treatability test to use deeper in the vadose zone or over thicker desiccation intervals. Scaling information is provided in this report that enables consideration of the volume of the target desiccation zone and the starting moisture content. Application to deeper or thicker zones would be accomplished with deeper wells or longer well screens, which can be readily included in a design based on the information herein (Sections 2.1 and 2.2). The rate of desiccation is a function of the rate of air injection. Thus, design for a specific site would need to consider the air permeability and its effect on the air injection rate and associated desiccation time. Permeable areas such as the sand and gravel zones of the Hanford formation would support higher air injection rates than less permeable areas such as zones with higher silt content (e.g., parts of the Hanford and Ringold formations, the Cold Creek Unit). Lower air injection rates do not preclude use of desiccation, but would increase the timeframe needed to desiccate a target zone relative to the timeframe for the same target zone size in a more permeable formation.

The test results and related laboratory and modeling efforts provide information to guide design and implementation of desiccation. Desiccation observed in the field test was consistent with design calculations and simulations based on the water-holding capacity of the injected gas. In addition, the distribution of desiccated zones met expectations; higher permeability zones dried first, followed by expansion of desiccation into lower-permeability zones over time. Analysis of data and use of numerical simulations indicate that full-scale designs can be made more cost effective than the design of the field test (which was designed to collect specific data, not as a full-scale remediation) by using ambient air as the injected dry gas and by using an injection-only design (i.e., no extraction well). Detailed descriptions of pre-desiccation data and the active desiccation test results are available in the following reports and articles.

Reports

- Truex, MJ, CE Strickland, M Oostrom, CD Johnson, GD Tartakovsky TC Johnson, RE Clayton, and GB Chronister. 2015. *Deep Vadose Zone Treatability Test for the Hanford Central Plateau: Interim Post-Desiccation Monitoring Results, Fiscal Year 2015*. PNNL-24706, Pacific Northwest National Laboratory, Richland, WA.

- Truex MJ, M Oostrom, CE Strickland, TC Johnson, CD Johnson, RE Clayton, and GB Chronister. 2014. *Deep Vadose Zone Treatability Test for the Hanford Central Plateau: Interim Post-Desiccation Monitoring Results, Fiscal Year 2014*. PNNL-23731 Pacific Northwest National Laboratory, Richland, Washington.

- Truex MJ, M Oostrom, CE Strickland, TC Johnson, CD Johnson, RE Clayton, and GB Chronister. 2013. *Deep Vadose Zone Treatability Test for the Hanford Central Plateau: Interim Post-Desiccation Monitoring Results*. PNNL-22826, Pacific Northwest National Laboratory, Richland, Washington.

- Truex MJ, M Oostrom, CE Strickland, TC Johnson, VL Freedman, CD Johnson, WJ Greenwood, AL Ward, RE Clayton, MJ Lindberg, JE Peterson, SS Hubbard, GB Chronister, and MW Benecke. 2012. *Deep Vadose Zone Treatability Test for the Hanford Central Plateau: Soil Desiccation Pilot Test Results*. PNNL-21369, Pacific Northwest National Laboratory, Richland, Washington.

- Truex MJ, M Oostrom, VL Freedman, C Strickland, and AL Ward. 2011. *Laboratory and Modeling Evaluations in Support of Field Testing for Desiccation at the Hanford Site*. PNNL-20146, Pacific Northwest National Laboratory, Richland, Washington.

- DOE/RL (U.S. Department of Energy, Richland Operations Office). 2010. *Characterization of the Soil Desiccation Pilot Test Site*. DOE/RL-2009-119, Rev. 0, Richland, Washington.

- Um W, RJ Serne, MJ Truex, AL Ward, MM Valenta, CF Brown, C Iovin, KN Geiszler, IV Kutnyakov, ET Clayton, H-S Chang, SR Baum, and DM Smith. 2009. *Characterization of Sediments from the Soil Desiccation Pilot Test (SDPT) Site in the BC Cribs and Trenches Area*. PNNL-18800, Pacific Northwest National Laboratory, Richland, Washington.

- Ward AL, M Oostrom, and DH Bacon. 2008. *Experimental and Numerical Investigations of Soil Desiccation for Vadose Zone Remediation: Report for Fiscal Year 2007*. PNNL-17274, Pacific Northwest National Laboratory, Richland, Washington.

Articles

- Truex MJ, TC Johnson, CE Strickland, JE Peterson, and SS Hubbard. 2013. "Monitoring Vadose Zone Desiccation with Geophysical Methods." *Vadose Zone Journal* doi:10.2136/vzj2012.0147

- Oostrom M, VL Freedman, TW Wietsma, and MJ Truex. 2012. "Effects of porous medium heterogeneity on vadose zone desiccation: Intermediate-scale laboratory experiments and simulations." *Vadose Zone Journal* doi:10.2136/vzj2011.0168.

- Truex MJ, M Oostrom, CE Strickland, GB Chronister, MW Benecke, and CD Johnson. 2012. "Field-Scale Assessment of Desiccation Implementation for Deep Vadose Zone Contaminants." *Vadose Zone Journal* doi:10.2136/vzj2011.0144

- Chronister GB, MJ Truex, and MW Benecke. 2012. "Soil Desiccation Techniques - Strategies for Immobilization of Deep Vadose Contaminants at the Hanford Central Plateau." In *Proceedings of Waste Management Symposia 2012*.

- Truex MJ, M Oostrom, JE Szecsody, CE Strickland, GB Chronister, and MW Benecke. 2012. "Technical Basis for Gas-Phase Vadose Zone Remediation Technologies at Hanford: A Review." In *Proceedings of Waste Management Symposia 2012*.

- Oostrom M, TW Wietsma, CE Strickland, VL Freedman, and MJ Truex. 2012. "Instrument Testing during Desiccation and Rewetting at the Intermediate Laboratory Scale." *Vadose Zone Journal* doi:10.2136/vzj2011.0089.

- Oostrom M, GD Tartakovsky, TW Wietsma, MJ Truex, and JH Dane. 2011. "Determination of Water Saturation in Relatively Dry and Desiccated Porous Media Using Gas-Phase Partitioning Tracer Tests." *Vadose Zone Journal* 10:1–8; doi:10.2136/vzj2010.0101.

- Oostrom M, TW Wietsma, JH Dane, MJ Truex, and AL Ward. 2009. "Desiccation of Unsaturated Porous Media: Intermediate-Scale Experiments and Numerical Simulation." *Vadose Zone Journal* 8:643–650.

Desiccation is intended to help meet remediation goals in conjunction with a surface barrier by slowing the movement of contaminated moisture through the vadose zone and reducing the flux of contaminants into the groundwater. The rate at which moisture returns to the desiccated zone, here termed the rewetting rate, is important in the overall long-term performance of desiccation as part of a remedy.

Rewetting phenomena and rates have previously been studied through laboratory and modeling efforts. Laboratory data quantifying the rewetting process were collected and reported by Truex et al. (2011). Key conclusions were that vapor-phase rewetting can occur but this vapor-phase process only rewets the desiccated zone to a small extent, essentially to a level below the residual moisture content. Rewetting by aqueous transport occurs, consistent with standard hydraulic phenomena, such that desiccating to very low moisture content and creating very low aqueous phase hydraulic conductivity conditions leads to low rates of aqueous transport rewetting.

Previous modeling efforts (Truex et al. 2012a, 2013b) concluded that the initial rate of rewetting is a function of the porous media properties of both the desiccated zone and the subsurface surrounding this zone, as well as the moisture content distribution at the end of active desiccation. After active desiccation, the moisture content distribution in the target zone will trend back toward the equilibrium moisture conditions for the porous media properties. Vapor-phase rewetting will occur, but has a negligible impact on the overall rewetting process. Advective rewetting in the aqueous phase strongly depends on the recharge rate, porous media permeability within and surrounding the desiccated zone, the moisture content surrounding the desiccated zone, and the total thickness of the desiccated zone. For example, at the C7527 and C7529 monitoring locations closest to injection well, the thicker desiccated zones have shown the least rewetting. These thicker desiccated zones were associated with areas of high injected air flow due to the presence of coarser, lower-moisture content sediments. Rewetting of these zones has primarily occurred from moisture in the vadose zone above the desiccated zone. Analysis of rewetting in this zone after two years of rewetting was presented in Truex et al. (2013b). Additional rewetting analysis (Truex et al. 2015 and herein) demonstrated the importance of 3-D moisture migration,

and a dominant effect of vertical moisture migration due to drainage of water from the vadose zone above the desiccated zone and recharge.

Data from 6 years of monitoring after active desiccation was ended show moisture redistribution in the subsurface at the test site associated with rewetting of desiccated areas. Areas that were moderately desiccated have largely returned to near pre-test conditions. Rewetting is continuing for highly desiccated areas. Analysis (Truex et al. 2015 and herein) demonstrates that the rewetting is partly from a local redistribution of water from wetter to dryer zones, but is primarily related to the vertical moisture migration rate from above the desiccation zone associated with moisture in the subsurface and the recharge rate. Qualitatively, trends of moisture redistribution over a broad zone in the vicinity of the test site are observed in the GPR and electrical resistivity tomography (ERT) data.

Over time, the rate of moisture rewetting of the desiccated zones is a function of the recharge rate, hydraulic gradient, water relative permeability, and porous media unsaturated flow properties. Rewetting data for the test site since the end of active desiccation are consistent with expectations based on related laboratory data and numerical simulation analyses for the test site configuration. Analysis of the current data and associated numerical modeling have shown that the rewetting process and rate can be reasonably estimated (Truex et al. 2015 and herein). Based on this analysis, desiccation can be applied to augment the performance of a surface barrier in reducing the flux of vadose-zone contaminants to the groundwater. Desiccation would need to be applied as a relatively thick zone (or combination of zones) to accelerate the transition of vadose zone moisture conditions to the low moisture, low recharge conditions that are induced beneath a surface barrier. While the same long-term moisture and recharge conditions are obtained for both a surface-barrier-only remedy and a remedy using desiccation in combination with a surface barrier, the latter configuration more rapidly obtains these conditions and decreases the flux of contaminants located deep in the vadose zone where there is a delay before the moisture and recharge effects of a surface barrier can occur. During that delay, deep vadose zone contamination flux can proceed at rates associated with pre-surface-barrier conditions that may not be protective of groundwater. Recommendations associated with configurations for a remedy using desiccation in combination with a surface barrier are provided in Section 2.2.

2.2 Recommendations

The field test results provide a basis to recommend design features for consideration in future feasibility studies for the vadose zone. A description of key design elements and an example conceptual full-scale desiccation design are presented below to highlight the recommended approach and integrate the primary conclusions from the laboratory, modeling, and field testing efforts conducted as a part of the desiccation treatability test. There are two aspects to the design recommendation. The first aspect is the configuration of a targeted desiccation zone with respect to 1) subsurface hydrology, moisture, and contaminant distribution and 2) integration with a surface infiltration barrier. The second aspect is the equipment, layout, and operational approach to desiccate a targeted zone.

Site-specific information will be important to consider in evaluating desiccation in future feasibility studies and for remedial design. Categories of information to support these efforts are listed below. This test report and the associated field planning documents (DOE 2008b, 2010a,b) can be used as resources for details of relevant site data and data collection methods for desiccation, including:

- Subsurface hydrology, moisture, and contaminant distribution

- Surface recharge rate and distribution – because a focused zone of surface infiltration (e.g., caused by surface water drainage and accumulation in a localized area) may cause unwanted accelerated transport and rewetting in a localized zone, this type of recharge condition needs to be evaluated for the site

- Air permeability of the targeted desiccation zone(s)

- Subsurface infrastructure that may affect injected air flow patterns

- Contaminant transport parameters needed to estimate contaminant flux to groundwater

- Surface barrier design inputs

2.2.1 Desiccation Remediation Configuration

One driver for selection of the target zone for desiccation is the ability to cost-effectively distribute dry air in the subsurface. While moisture in finer-textured sediment is important, the desiccation approach should focus on providing injected dry-air flow with moisture removal in coarser, higher-permeability zones. After desiccation conditions are reached in the higher-permeability zones, cyclic operation of the desiccation system can be applied as needed. In this approach, the injection system is cycled off to allow local moisture re-equilibration to occur where moisture in the lower-permeability zones moves into adjacent desiccated higher-permeability zones. The system can then be cycled back on to remove this water. Using this type of cycled operational approach, desiccation could be applied as a stand-alone remedy, but would require continued periodic application to remove water that enters the vadose zone by surface infiltration. As appropriate, this type of stand-alone application could be evaluated for specific sites as part of a feasibility study. However, desiccation is complementary to application of a surface infiltration barrier. In many cases, desiccation would need to be considered as a near-term action to enhance the effectiveness of a surface barrier in meeting short- and long-term objectives for groundwater protection. The surface barrier is an important component because it provides passive long-term reduction of the recharge rate, which is the long-term driver for contaminant flux to the groundwater.

The subsurface contaminant and moisture distribution is another driver for selection of the target zone for desiccation. Desiccation within and toward the lower depths of the contaminated zone is important because this target directly slows current contaminant movement toward the groundwater in addition to more rapidly reaching the moisture conditions associated with low recharge under a surface barrier. Desiccating larger potions of the contaminated zone improves performance, but the increased cost of desiccation needs to be considered. Thus, simulations should be applied to determine the best combination of desiccation target and surface barrier design that will meet needs for protection of groundwater (in conjunction with a surface barrier) at the lowest cost. For a given subsurface contaminant and moisture distribution, a surface barrier may provide effective conditions to protect groundwater in the long-term by limiting the flux of moisture and contaminants to the groundwater. The desiccation design should target the portion of the contamination that will move into the groundwater

during the transition time while the long-term barrier conditions are being established (i.e., the drainage of moisture down to the steady long-term conditions under a barrier). Thus, there are two aspects for assessing the feasibility of a combined desiccation/surface-barrier remedy:

1. Can long-term groundwater protection objectives be met with a surface barrier?

2. Is there a portion of the contaminated zone that causes near-term exceedance of groundwater protection objectives and can be addressed by desiccation?

Analysis of a combined desiccation/surface-barrier remedy for a feasibility study as described above will need to consider the site-specific conditions. For this treatability test report, an example of the type of simulations that could support a feasibility study analysis was prepared with a focus on the vadose zone transport aspects of the analysis. For a feasibility study, contaminant transport in the vadose zone would need to be linked with the groundwater conditions below the site to predict groundwater concentration profiles for comparison to groundwater protection objectives. In this example, demonstration of how desiccation configuration variations affect the contaminant flux to groundwater is discussed using the contaminant flux to groundwater as a relative metric to compare the effect of different configurations.

For the example, a 3-D numerical model of the 200-BC-1 cribs area was configured using the eSTOMP software (http://stomp.pnnl.gov/estomp_guide/eSTOMP_guide.stm) to model contaminant transport from the surface to the water table. The model configuration was an extension of the model used by Truex et al (2015) to evaluate rewetting phenomena. In the Truex et al. (2015) model, characterization information from the desiccation site was used to develop a layered approximation of the subsurface within the desiccation zone. Data for vertical variation in hydraulic properties and neutron moisture logging data were used by Truex et al. (2015) to define the vertical distribution of hydraulic properties. These layers of hydraulic properties were then assumed to extend horizontally to the lateral edges of the domain. A courser discretization with uniform hydraulic properties was used by Truex et al. (2015) to model the subsurface between the bottom of the desiccation zone and the water table. For the model configuration herein, the same layering of hydraulic properties in the desiccation zone was applied and extended to the new lateral boundaries of the modeling domain. This sequence of layers was then repeated multiple times to develop a scenario of layering for the zone between the bottom of the desiccation zone and the water table. Figure 2.1 shows this layering and the vertical discretization in Truex et al. (2015) compared to the vertical discretization in the cribs-size model used herein. As part of this configuration change, the model grid cell thickness was the same as used in the desiccation zone by Truex et al. (2015) except that the maximum allowed thickness was set to 0.5 m. The scenario of continuing altering layers of silt and sands throughout the full vadose zone thickness is consistent with the characterization information in Serne et al. (2009), though the configuration in the model is not intended to exactly replicate the observed layers. The intent of the model is to provide an example of desiccation performance, not a site-specific model of the 200-BC-1 Operable Unit cribs.

The model lateral domain in relation to the cribs is shown in Figure 2.2. The lateral dimensions were selected so that the vadose zone contamination introduced by the cribs remained inside the model domain. Crib dimensions were modeled based on the information in WIDS Summary Reports, Last et al. (2006), and Maxfield (1979). Crib discharges were modeled using the inventory information in Kincaid et al. (2006) where the Tc-99 concentration was calculated as the ratio of the inventory mass and the discharged liquid volume. The surface recharge as input to the ground surface of the model was varied over time to represent the four time periods and associated conditions shown in Table 2.1. These periods correspond

to pre-Hanford conditions (before 11/1955), the operational period (11/1955 – 6/1981), the post-operational period (6/1981 – 12/2014), and the remediation scenario (after 12/2014). Four vertical desiccation intervals were considered as part of the remediation scenario 3: 40t-45d; 20t-55d; 40t-65d; and 20t-75d (nomenclature example: the interval '40t-45d' is a 40-m [131-ft] thick desiccation zone that is centered on a depth of 45 m [148 ft] bgs). For the desiccation scenarios, desiccation was implemented by imposing a -5 bar water pressure in the selected zone at the beginning of the remediation period. The -5 bar pressure is consistent with pressures measured during the desiccation test. While it would require some time to achieve full desiccation to this level, that desiccation time is small in comparison with the overall simulation time and was therefore neglected.

While the simulations are for example purposes and not intended to specifically model the 200-BC-1 cribs area, the simulated depth of Tc-99 contamination at the year 2010 was compared to the observed depth of Tc-99 contamination observed by Serne et al. (2009) in borehole C5923, located within the cribs area. The observed Tc-99 depth in the borehole was about 20-m above the water table at that location. As shown in Figure 2.3, the simulated Tc-99 depth is approximately the same. Note that the simulated Tc-99 is deeper directly below the cribs at that same time. Because the simulated and observed Tc-99 depths (borehole C5923) were similar, the model configuration was deemed appropriate for use to provide results of contaminant flux to groundwater that can be used for relative comparison of performance for the selected example desiccation configurations.

Figure 2.4 shows a series of 2-D sections of simulated historical Tc-99 contaminant zone progress over time from 1960 to 2015. At the year 2015, in all of the desiccation scenarios, desiccation was imposed over the lateral extent shown in Figure 2.4i and Figure 2.4j to intersect the contaminated zone. These lateral dimensions are consistent with the dimensions of the active desiccation conceptual design presented in Section 2.2.2.2. Several desiccation scenarios with different vertical intervals of desiccation were conducted to examine how the relative thickness and position of the desiccation zone with respect to the contamination and the groundwater affect the performance in limiting contaminant flux to the groundwater. Figure 2.5 shows the four desiccation vertical interval scenarios with the scenario labeled to indicate the thickness of the desiccated zone and its depth (at the centerline). The scenarios examined are summarized below.

- Interval '40t-45d' is a 40-m (131-ft) thick desiccation zone that is centered on a depth of 45 m (148 ft) bgs

- Interval '20t-55d' is a 20-m (66-ft) thick desiccation zone that is centered on a depth of 45 m (180 ft) bgs

- Interval '40t-65d' is a 40-m (131-ft) thick desiccation zone that is centered on a depth of 45 m (213 ft) bgs

- Interval '20t-75d' is a 20-m (66-ft) thick desiccation zone that is centered on a depth of 45 m (246 ft) bgs

Simulation results are summarized in Figure 2.6. This figure compares the cumulative Tc-99 mass over time, Tc-99 flux across the water table, and the water flux that migrates into the groundwater for 1) a no-action scenario, 2) a surface-barrier-only scenario, and 3) the selected set of combined desiccation/surface-barrier scenarios. The cumulative Tc-99 plot shows how much Tc-99 crosses the water table in the simulation period compared to the total of ~140 Ci of Tc-99 that are in the simulated domain and cross into the water for the no-action scenario. Tc-99 flux across the water table is the target

for remediation to decrease relative to the no-action scenario because Tc-99 flux is proportional to Tc-99 concentration in the groundwater. The water flux is related to the Tc-99 flux and provides a means to distinguish between the action of a surface barrier only and a combination of a surface barrier and desiccation.

While a barrier-only scenario reduces the Tc-99 flux to groundwater, near-term fluxes (earlier than the year 2200) are not significantly decreased. Comparison of the water flux plots for the no-action and the barrier only scenarios (Figure 2.6C and Figure 2.6F) shows that the barrier-only scenario does not decrease the water flux prior to 2200. This water flux occurs due to drainage as the subsurface transitions toward the barrier-controlled flux and is the target for desiccation. Desiccation, consistent with results presented by Truex et al. (2011), decreases the near-term Tc-99 flux to groundwater compared to the no-action and barrier-only scenarios, though the amount of decrease depends on where the desiccation is applied and the thickness of the desiccation zone.

Thick desiccation zones (10 m [33ft]or greater) would likely be needed for desiccation to provide a significant benefit in groundwater protection over a barrier-only scenario for the contaminant and environmental conditions at sites like the 200-BC-1 Operable Unit cribs area. For example, comparing the results of the 40t-45d (Figure 2.6G, H, I) to the results of 20t-55d (Figure 2.6J, K, L) where the bottom of each desiccation zone is the same shows how the thinner zone misses removal of some moisture that causes an increased flux during the simulation period. Simulation results also show that desiccation toward the bottom of the contaminated zone is important to minimize the near-term Tc-99 flux. This result can be observed comparing the very near-term (first 500 years) Tc-99 flux for 40t-45d (Figure 2.6H) to the near-term flux for 40t-65d (Figure 2.6N). However, this comparison also reveals that the 40t-65d scenario (Figure 2.6N) misses removal of some moisture higher in the vadose zone that causes an increased flux during the simulation period.

For a site-specific application, simulations such as shown in this example, but also coupled to the groundwater to estimate resultant contaminant concentrations, can be used to identify an appropriate desiccation design and to evaluate whether desiccation in conjunction with a surface barrier will meet the site remedial action objectives. Based on the example results, the combined desiccation/surface barrier scenario is most protective of groundwater and desiccation is necessary to limit the flux to groundwater of contaminants located deep in the vadose zone.
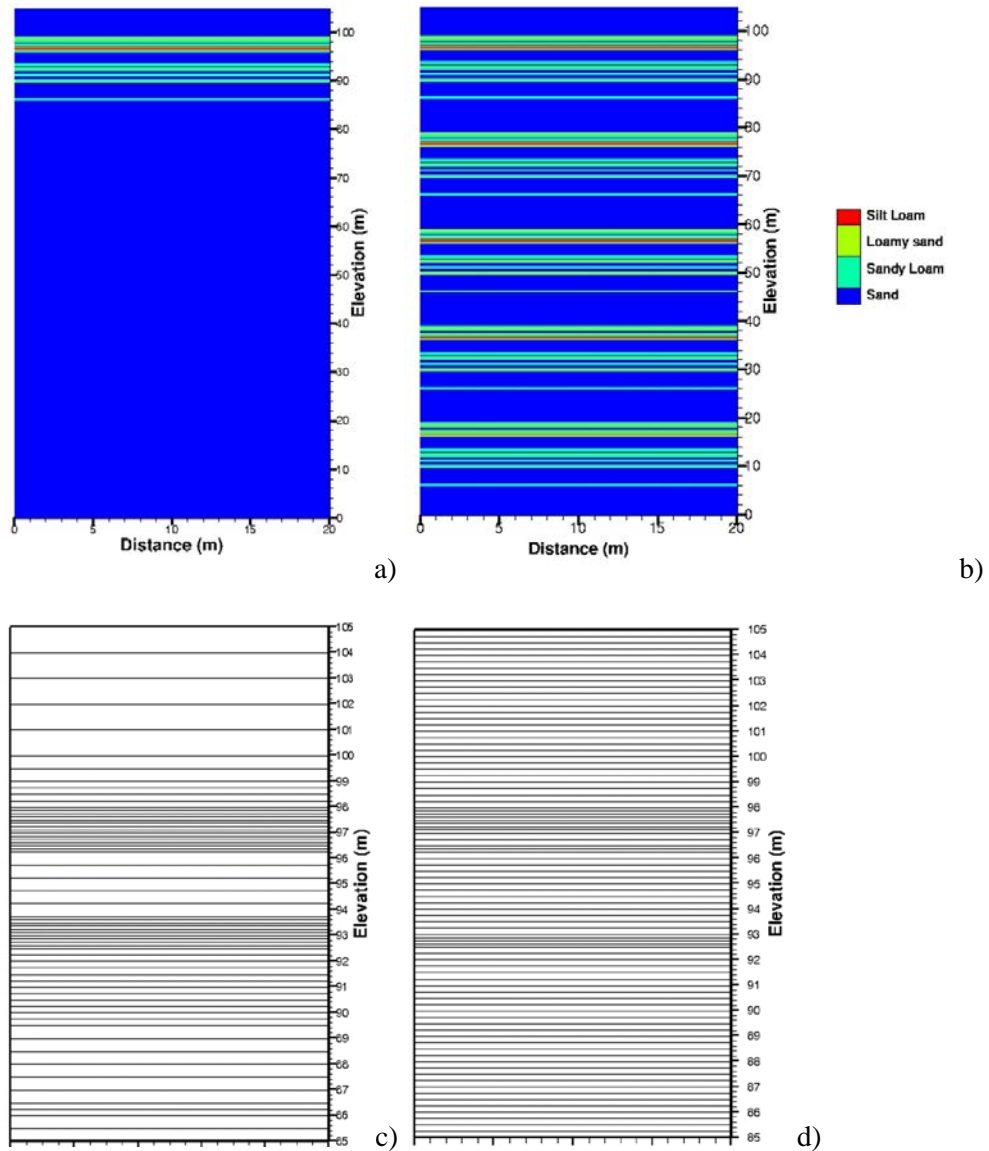
Figure 2.1. Lithology Layering Used in a) Truex et.al (2015) Model and b) the Cribs-Area Model. Porous media properties for each category are described by Truex et al. (2015). Vertical discretization in the c) Truex et.al (2015) model and d) the cribs-area model.
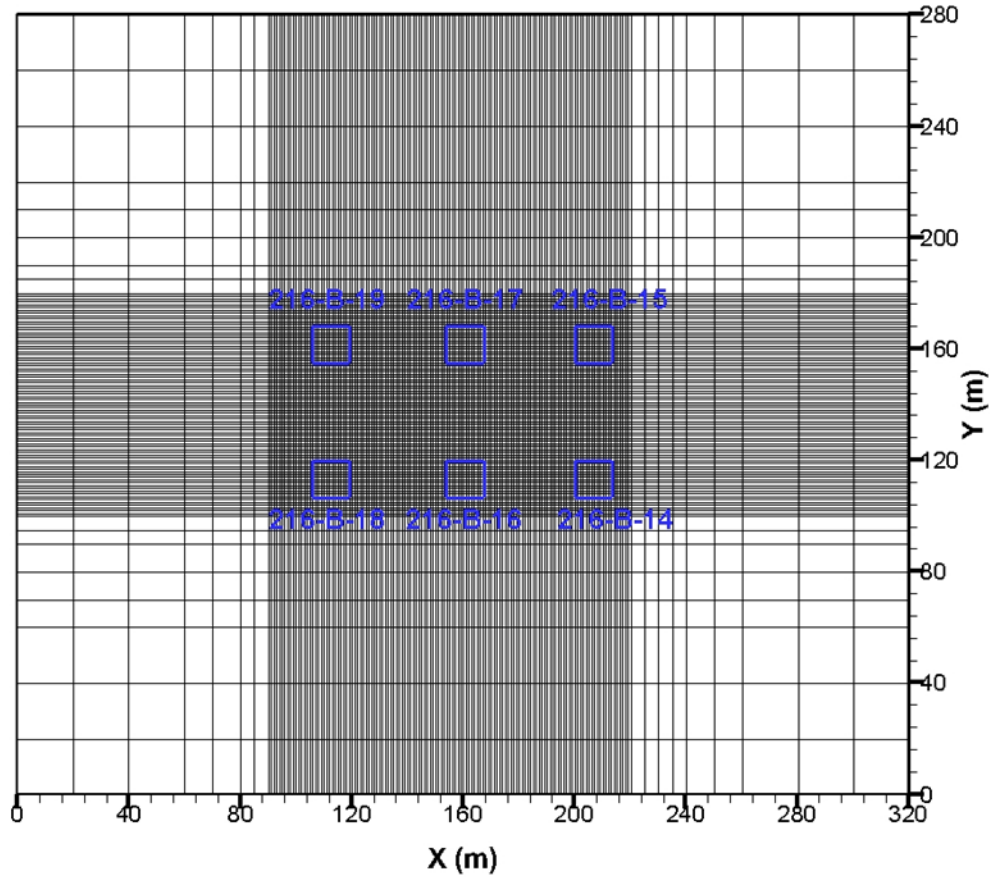
Figure 2.2. Model Lateral Domain and Domain Discretization for the Cribs-Area Model
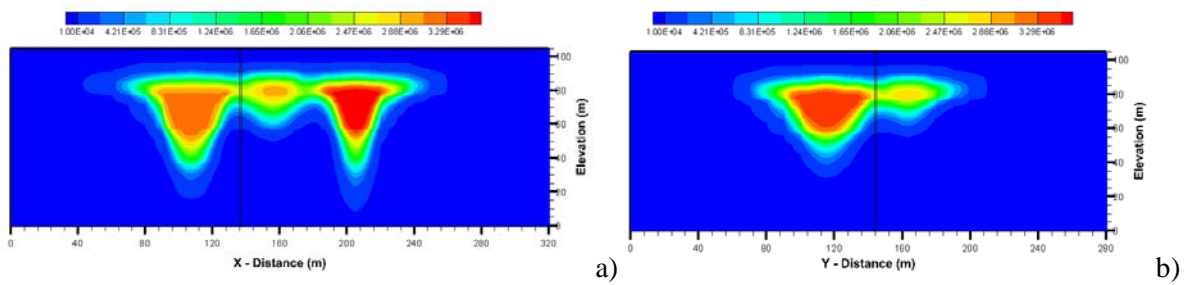
Figure 2.3. Simulated Pore-Water Tc-99 Concentration (pCi/L) at Year 2010. Cross-sections are through the model at the location of borehole C5923 for the model a) X-plane; b) Y-plane.

2.11
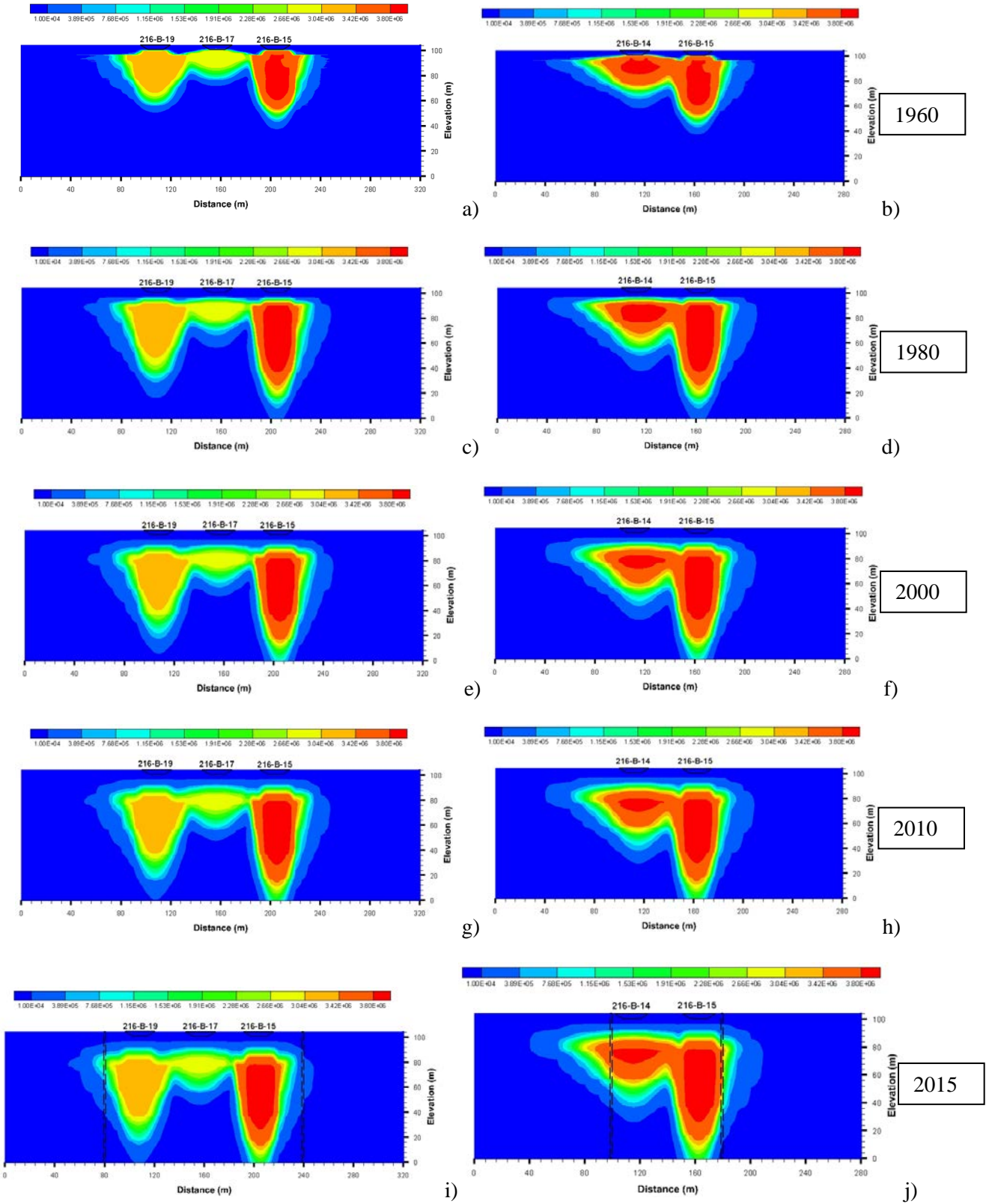
Figure 2.4. Simulated Historical Progression of Pore-Water Tc-99 Concentrations over Time beneath the Cribs for the a, c, e, g, i) X-plane (through cribs -15, -17, and -19); b, d, f, h, j) Y-plane

(through cribs (-14 and -15) at 1960, 1980, 2000, 2010, and 2015, Respectively. The lateral extent of the simulated desiccation zone is shown in figures i and j.
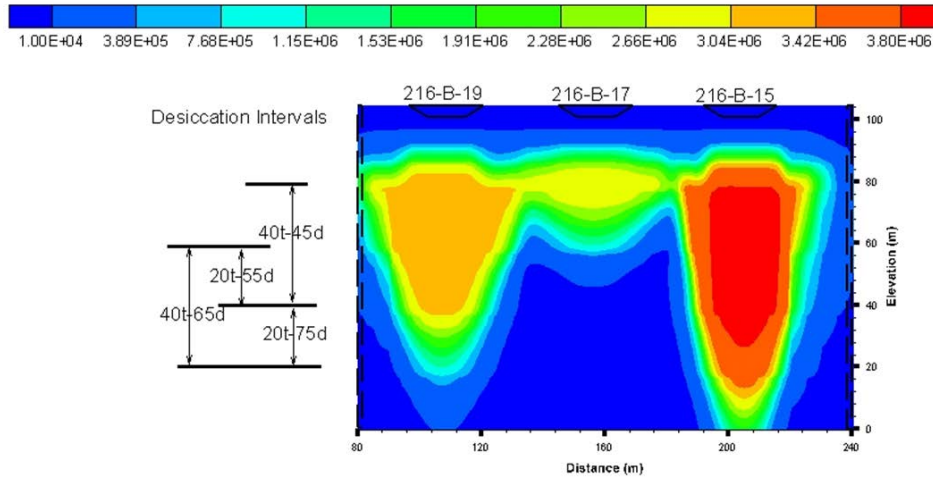
Figure 2.5. Selected Vertical Intervals for Desiccation Scenarios. The nomenclature for the desiccation vertical interval defines the thickness of the desiccated interval in meters and the depth of the center of the desiccation zone in meters below ground surface. For example, the interval '40t-45d' is a 40-m (131-ft) thick desiccation zone that is centered on a depth of 45 m (148 ft) bgs. The color mapping is the simulated pore-water Tc-99 concentration (pCi/L) at year 2015. Each scenario used the lateral dimensions shown in Figure 2.4i and Figure 2.4j.

2.14
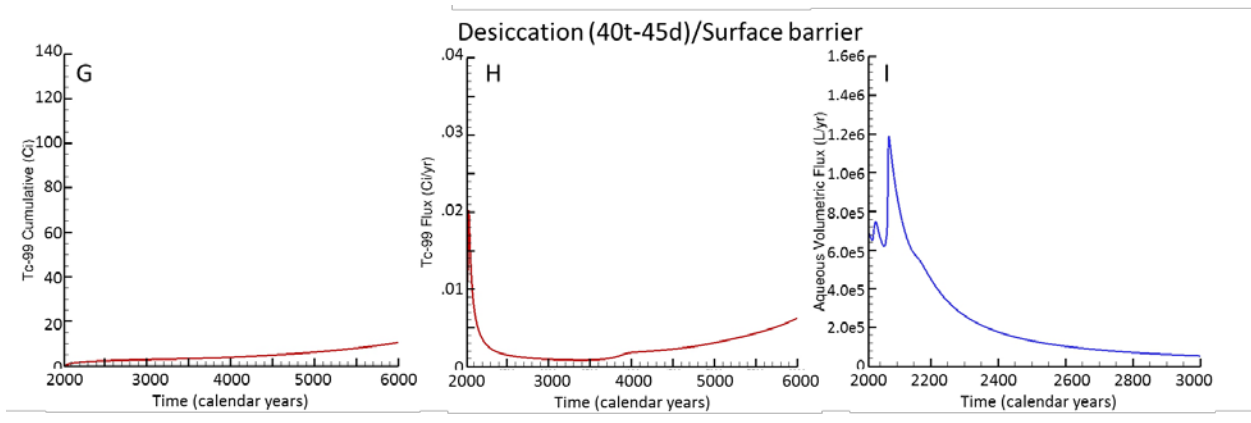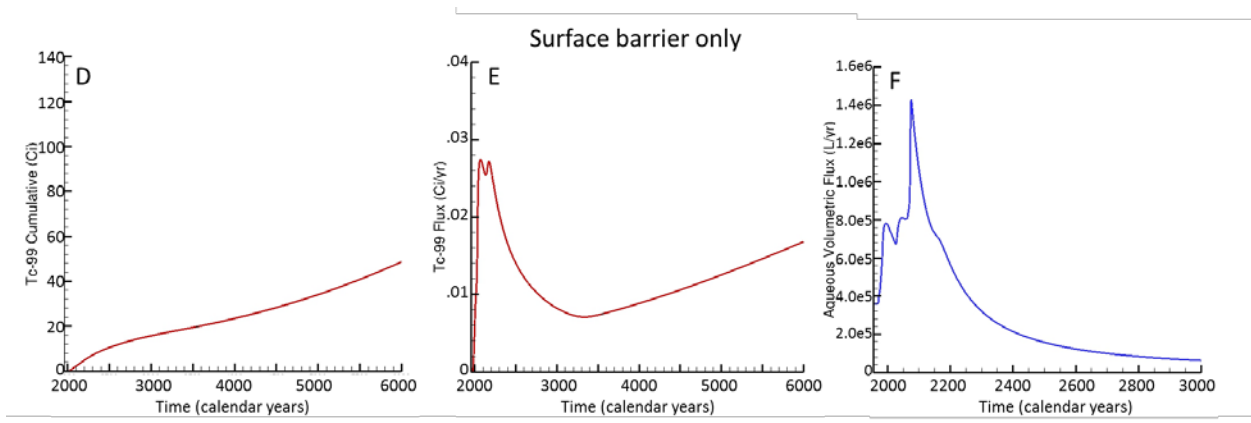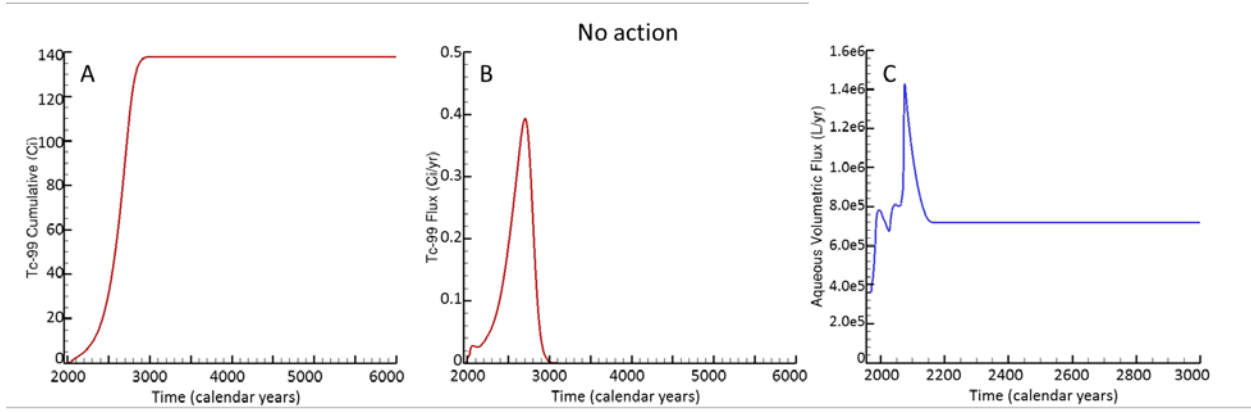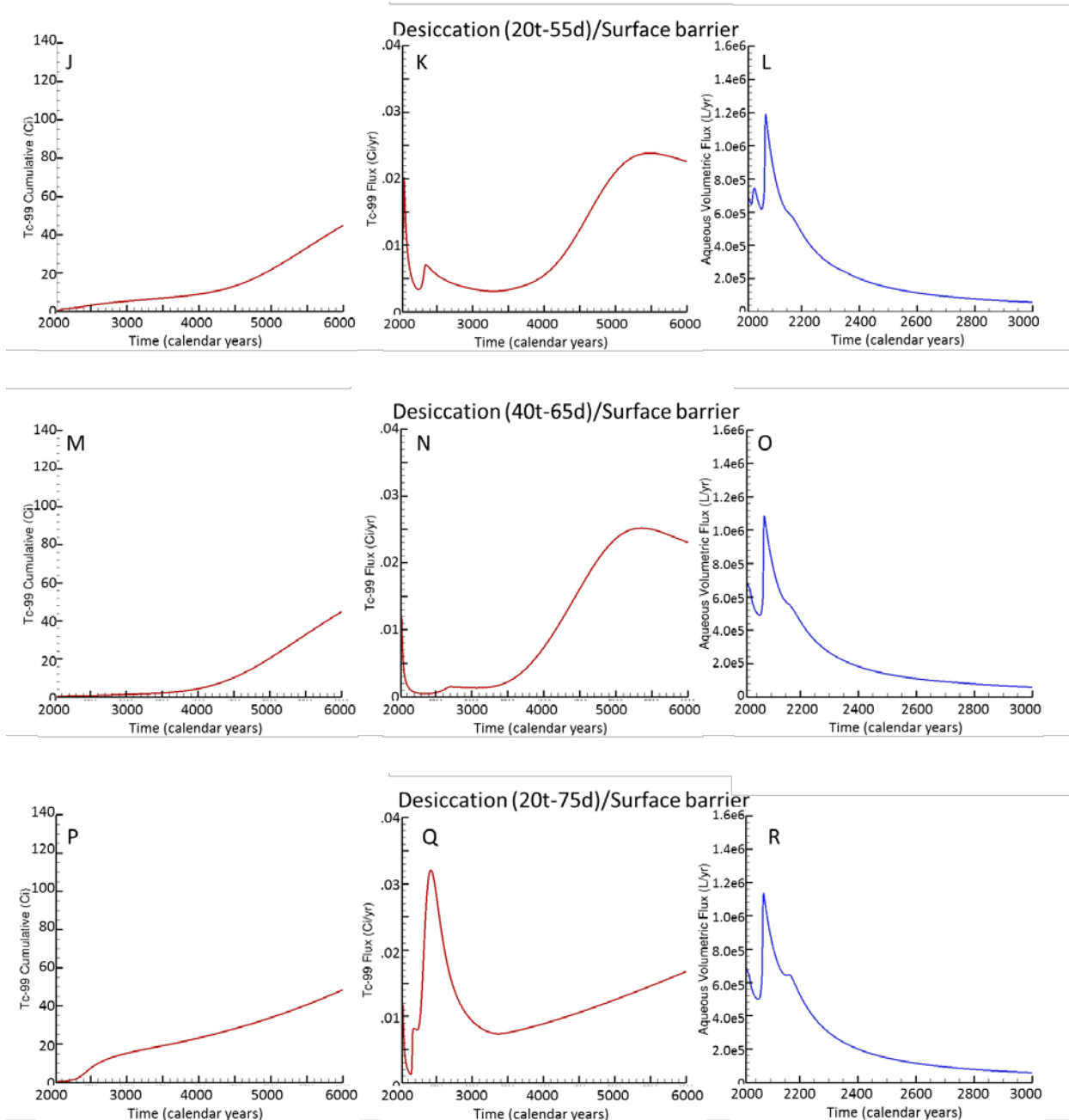
Figure 2.6. Simulated Temporal Profiles of Tc-99 Cumulative Mass, Tc-99 Mass Discharge, and Water Flux across the Water Table for Each Row Left to Right, Respectively. See **Figure 2.5** desiccation scenario legend nomenclature. Plots in each row are A, B, C) No-action scenario; D, E, F) Surface-barrier only scenario; G, H, I) Desiccation (40t-45d)/Surface barrier; J, K, L) Desiccation (20t-55d)/Surface barrier; M, N, O) Desiccation (40t-65d)/Surface barrier; P, Q, R) Desiccation (20t-75d)/Surface barrier.

Table 2.1. Model Input Ground-Surface Recharge Distribution for Simulation Scenarios

Scenario	Pre-operational	11/1955 to	6/1981 to	After 12/2014

2.15

	(pre-11/1955) Input (mm/y)	6/1981 Input (mm/y)	12/2014 Input (mm/y)	Input (mm/y)
1. Baseline: no action	4	30	8	8
2. Surface barrier only	4	30	8	0.5
3. Surface barrier and desiccation (multiple)	4	30	8	0.5

2.2.2   Desiccation Implementation Design

Design considerations for active desiccation are described below.

2.2.2.1   Key Design Elements

For full-scale desiccation, the following key design elements should be considered and were incorporated into the example design that follows.

- Ambient air can be injected to induce desiccation at the Hanford Site except during ambient conditions when the temperature is above 30°C and concurrently, the relative humidity is above 70% (Section 4.2.4).

- No extraction well is needed as long as the injection well is 1) deep enough that injected air exhaust at the surface is very diffuse; or 2) for shallow applications, a gas barrier is used to move injected gas laterally and ensure that injected air exhaust at the surface is very diffuse (movement of air at the surface is only an issue when low temperatures can cause water condensation) (Section 4.2.4). Note that injected gas reached 100% humidity and is then no different than the soil gas surrounding the desiccation zone. However, because soil gas movement is induced, if soil gas moves into a zone with lower temperature, there can be condensation. For this reason, the gas flux at the ground surface needs to be considered if low temperatures are expected. An extraction well limits flux of injected gas out the ground surface, but it is also possible to have suitable conditions with only an injection well as described above.

- Designs can consider heating to 20°C to help enhance the desiccation rate. Potentially, however, systems could operate without heating of air, although some additional operational constraints may be needed.

- While operational time is variable, longer operational time will lead to a larger radius of influence for each injection well. Because the desiccation occurs in both lateral and vertical directions from a well, the design should consider the combination of well screen length, air distribution, well spacing, and operating time to optimize the balance between capital and operational costs. Scoping calculations (Section 4.2.4) and injection simulations (Section 4.2.4) from the treatability test results can be used to help guide these decisions for well spacing. As shown in the example conceptual design, a nominal Hanford Site design with a 10-year operating period leads to a well spacing on the order of 25+ m (80+ ft) (4–6 wells per hectare) (2–3 wells per acre) for application in the Hanford formation. (Less permeable formations or those with more initial moisture would require a longer operating period.)

- Temperature changes can be used as a useful indicator of subsurface gas flow and desiccation patterns, with limitations based on the spacing/density of monitoring locations and interpolation uncertainty. Providing a constant temperature influent gas temperature would help facilitate interpretation of temperature data. Of the other monitoring processes, ERT is likely useful for larger scale applications and can be set to collect data autonomously to provide volumetric images of desiccation progress that would be useful in supporting operational decisions (Section 4.2.3).

- Neutron moisture logging provides valuable information about the extent of desiccation at selected locations that can be directly correlated to desiccation performance goals, with limitations based on the spacing/density of monitoring locations. When used jointly with temperature and ERT data, periodic neutron moisture data can guide decisions for when desiccation can be shut down (Section 4.2.3).

- Post-desiccation monitoring with neutron logging and ERT can be applied to determine the rate of rewetting (moisture re-equilibration within the desiccated zone) and whether additional desiccation cycles are needed (Section 4.2.3).

- Additional desiccation cycles can be conducted as needed to remove more moisture from a target area that contains low-permeability zones. Each successive cycle would require less time than the previous cycle to reach a similar ending condition.

2.2.2.2   Example Conceptual Design

Using the above design elements, an example conceptual design for full-scale desiccation was developed. No specific performance modeling or analyses were conducted as part of this example to determine the depth or thickness necessary to meet overall performance requirements for protection of groundwater. Rather, scoping calculations and the key design elements were translated into an example design to address a relevant areal extent for desiccation application and conceptually depict the type of design that future feasibility study evaluations can use based on the information obtained in the treatability test of desiccation.

The example conceptual design nominally covers the areal dimensions (80 by 160 m [262 by 525 ft]) of the cribs portion of the 200-BC-1 Operable Unit. Figure 2.7 shows a conceptual layout of 11 injection wells to cover this area (about 5 wells per hectare [2.5 wells/acre] desiccated). Each well uses a 10-m (33-ft) well screen with an injection rate of 1700 m^3/h (1000 cfm) (170 m^3/h [100 cfm] per meter of well screen). At this injection rate, the expected injection pressure is less than 1.4 atm (20 psi) based on the pneumatic properties at the field test site.
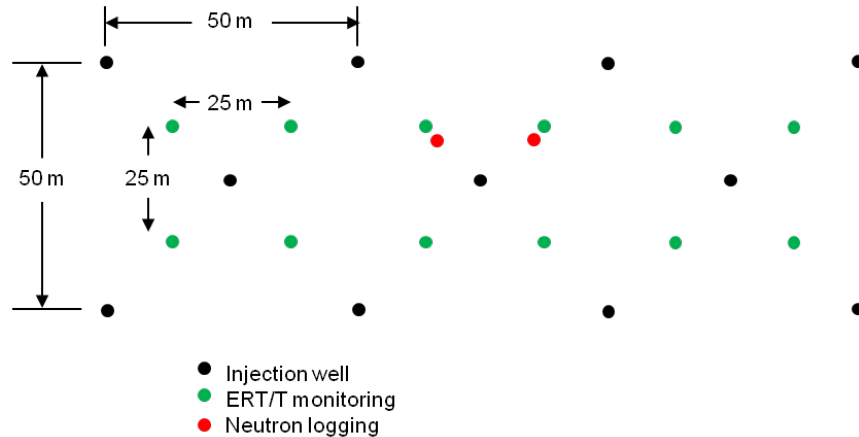
Figure 2.7. Example Well Layout Concept for Cribs Portion of BC Cribs and Trenches

To estimate desiccation volume, it was assumed the volumetric soil moisture content in the desiccated zone needs to be reduced by on average 0.065 (m^3/m^3). Assuming that injection of ambient air is 75% as efficient as use of anhydrous gas, 0.00017 m^3-soil are desiccated for every cubic meter of ambient air injected (see also Section 4.2.4.4). Over a 10-year operating period, the nominal lateral radius of influence from each injection well is about 24 m. For the cribs portion of the 200-BC-1 Operable Unit, it was assumed the desiccation would occur deep enough that a surface gas barrier is not needed during active desiccation (see Section 4.2.4). However, for long-term effectiveness, emplacement of infiltration control at the surface is needed to limit the recharge rate (Truex et al. 2011). For full-scale monitoring, the conceptual design uses two access boreholes installed to conduct neutron moisture logging. Temperature and ERT monitoring are conducted by installing electrodes and thermistors in 12 locations. However, the feasibility design may elect to use fewer monitoring locations. A total of 25 boreholes (11 as 4-in. diameter wells screened for injection, 2 as 2-in. diameter cased wells for neutron probe access, and 12 as boreholes instrumented with thermistors and ERT electrodes) are used in the design.

Several types of above ground equipment would be needed for implementation. The system would require 11 air blowers capable of 1700 m^3/h (1000 cfm) and 1.4 atm (20 psi) pressure. Moderate heating of the injected gas to maintain a minimum of 20°C is anticipated to be needed to assist in maintaining desiccation at near 75% of the rate with anhydrous gas injection. However, a study of average meteorological conditions could be used to refine the design in terms of the need for heating and the portion of the year during which heating would be needed. Thermistor and ERT monitoring could be implemented with data loggers and a data computer for autonomous operation, similar to the system used in the field test.

An operating period of 10 years was used to obtain desiccation coverage of the targeted area for the conceptual design example. In future feasibility studies, an assumption of additional desiccation cycles after moisture re-equilibration (estimated as 5 years of no-operation) may be warranted. For these additional cycles, the operating period required would diminish each time because much less moisture would need to be removed. As an estimate, if the first additional cycle needed to remove 25% of the water removed in the first application, 2.5 years of operation would be required. If the next application needed to remove 50% of the water removed in the previous application, 1.5 years of operation would be required. The need for these additional desiccation cycles depends on the number and characteristics of low-permeability zones present in the targeted desiccation zone. As a baseline, future feasibility studies

could consider at least one additional desiccation cycle after moisture re-equilibration from the first desiccation application.

As discussed in Section 2.2.1, the thickness of the desiccation zone needs to be evaluated to determine an effective thickness for use in combination with a surface barrier to meet groundwater protection objectives. The above implementation example is based on a screened interval of 10 m (33 ft). Scaling of injection flow rate would be needed if a thicker desiccation zone is need for a specific application.

3.0 Approach

3.1 Objectives

Test objectives were developed and presented in the field test plan (DOE 2010b). These objectives are summarized in the bulleted items below and have the overall goal of providing information about desiccation such that the technology can be effectively evaluated in subsequent feasibility studies for waste sites with inorganic and radionuclide contaminants in the deep vadose zone.

- Design Parameters: Determine the design parameters for applying soil desiccation, including operational parameters such as injected nitrogen flow rate and injected temperature, and identifying soil moisture reduction targets to achieve acceptable reduction of contaminant transport in the vadose zone.

- Desiccation Field Test Performance: Demonstrate field-scale desiccation for targeted areas within the vadose zone.

  – Quantify the nitrogen flow, water extraction rate, and other operational parameters to evaluate implementability of the process on a large scale.

  – Determine the extent of soil moisture reduction in the targeted treatment zone to evaluate the short-term effectiveness of the process.

  – After desiccation is completed, determine the rate of change in soil moisture for the desiccated zone.

  – Determine the best types of instrumentation for monitoring key subsurface and operational parameters to provide feedback to operations and evaluate long-term effectiveness.

- Scale-up Assessment: Determine the number of injection and extraction wells, screened intervals, type of equipment and instrumentation, and operational strategy such that costs for full-scale application can be effectively estimated.

3.2 Experimental Design and Procedures

The experimental design and procedures are summarized below with subsections on Test Site Background (3.2.1), Test Layout and Operations (3.2.2), Equipment and Materials (3.2.3), Sampling and Analysis (3.2.44), Data Management (3.2.5), and Deviations from the Test Plan (3.2.6).

3.2.1 Test Site Background

The field treatability test for desiccation was conducted in the Hanford Site 200-BC-1 Operable Unit, commonly referred to as the BC Cribs and Trenches Area (Figure 3.1). The 6 cribs and 20 trenches at this operable unit received about 110 million L of aqueous waste containing high nitrate and radionuclide concentrations, primarily from Hanford Site operations in the mid-1950s. The site was selected for the field test because relatively high concentrations of mobile Tc-99 contamination and high moisture contents are present at relatively shallow depths, facilitating test operations, yet representing conditions found deeper in the vadose zone where desiccation could be considered as part of a remedy. The test area is located between adjacent waste disposal cribs where the subsurface was impacted by lateral movement

of crib discharges in the subsurface but drilling and other test operations could take place outside the hazardous footprint of the former disposal cribs. Figure 3.2 shows the vertical stratigraphy, technetium, and moisture distribution at the injection well location in relation to the well screen interval. Porous media grain-size variations in the test interval generally range from sands to loamy sands with some zones of silty sand and silt, similar to the porous media observed throughout the full depth interval.
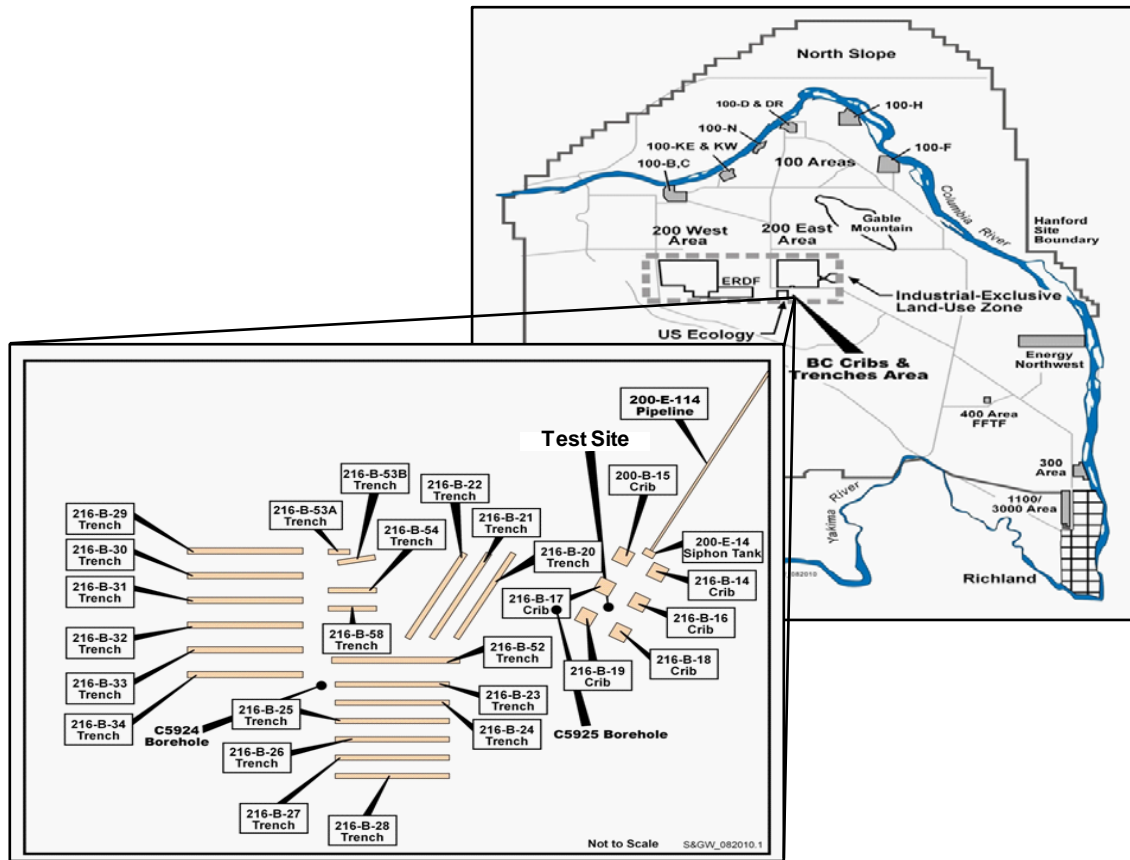
Figure 3.1. Test Site Location in the BC Cribs and Trenches Area (inset, 200-BC-1 Operable Unit) of the Hanford Site (map) (after DOE 2010b). Note the test site is centered around borehole C7523, one of three characterization boreholes (C7523, C7524, C7525) from site investigation activities associated with electrical resistivity studies at the site (Serne et al. 2009).

Previous characterization of the cribs region indicated a plume of mobile contamination beneath the cribs (Serne et al. 2009). Nature and extent of the plume is defined by waste stream composition, the quantity of waste discharged, and the heterogeneity of the vadose zone sediments. At the test site, centered around the 299-E13-62 borehole and located between the 216-B-17 and 216-B-19 Cribs, significant concentrations of Tc-99 and nitrate contamination were observed from approximately 12.2 m (40 ft) bgs to approximately 76.2 m (250 ft) bgs. Local contaminant maxima were observed at 15.2 m (50 ft), 27.4–29.0 m (90–95 ft), 38.1–39.6 m (125–130 ft), and 67.1–70.1 m (220–230 ft) bgs.

Near-surface contamination within the footprint of the 216-B-14 Crib has been characterized by geophysical logging of shallow boreholes (DOE 2009). High concentrations of Cs-137 were observed, with peak concentrations located near the bottom of the as-built crib excavation and extending several

feet deeper. Sr-90 is expected to coexist with the Cs-137, based on characterization of the 216-B-26 Trench that included sampling for that radionuclide (Ward et al. 2004). Note that in contrast to the excavation-based treatability test (DOE 2009), the desiccation field treatability test avoided high-activity contamination associated with the footprint of the cribs, and instead focused on mobile contamination that has migrated laterally and vertically from the cribs.
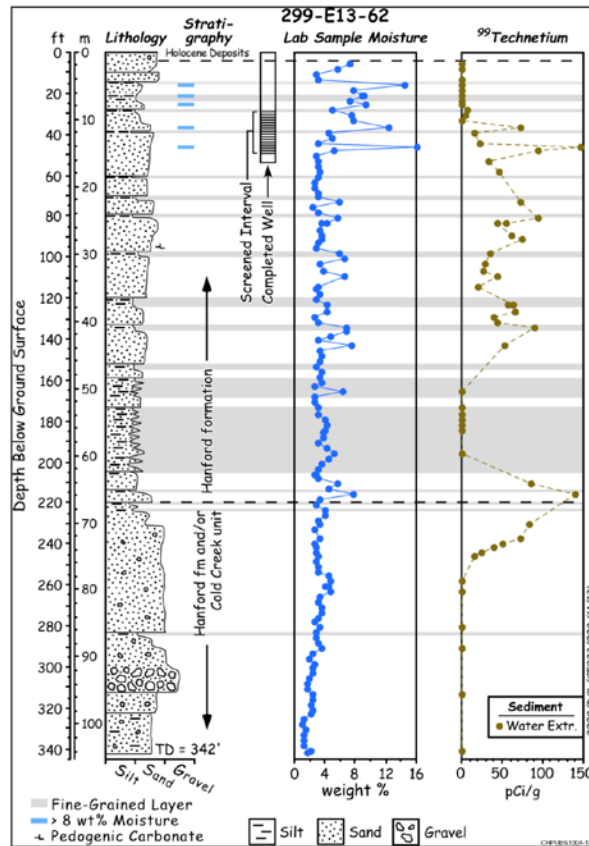
Figure 3.2. Injection Well Borehole Data and Screened Interval (after DOE 2010b)

Although the overall objective of the Deep Vadose Zone Treatability Test Plan is to address groundwater threat from mobile contaminants deep in the vadose zone, the desiccation field test focused on the shallowest component of significant Tc-99 and nitrate contamination centered near 13.7–15.2 m (45–50 ft) bgs. Installation of injection/extraction wells and monitoring instrumentation was less costly at this depth while allowing critical elements of soil desiccation to be evaluated. The deep vadose zone was mimicked by covering the ground surface with an impermeable barrier to limit surface interaction with the test injection and extraction operations.

3.2.2   Test Layout and Operations

The desiccation technology relies on removal of water from a portion of the subsurface such that the resultant low moisture conditions inhibit downward movement of water and dissolved contaminants. Implementation requires establishing sufficiently dry conditions within the targeted zone to effectively inhibit downward water transport. Nominally, the targeted zone would need to extend laterally across the

portion of the vadose zone where contaminants have the potential to move downward at a flux that will impact groundwater above the remediation objective groundwater concentration. Thus, the experimental design was developed to evaluate the process of establishing a desiccated zone that extends laterally away from a dry gas injection well within a specific depth interval of the vadose zone. To obtain this type of desiccation zone, the field test design used a dipole configuration with injection of nitrogen and extraction of soil gas through wells screened in a target depth interval to favor soil gas flow within this interval and within a defined monitoring zone (Figure 3.3).
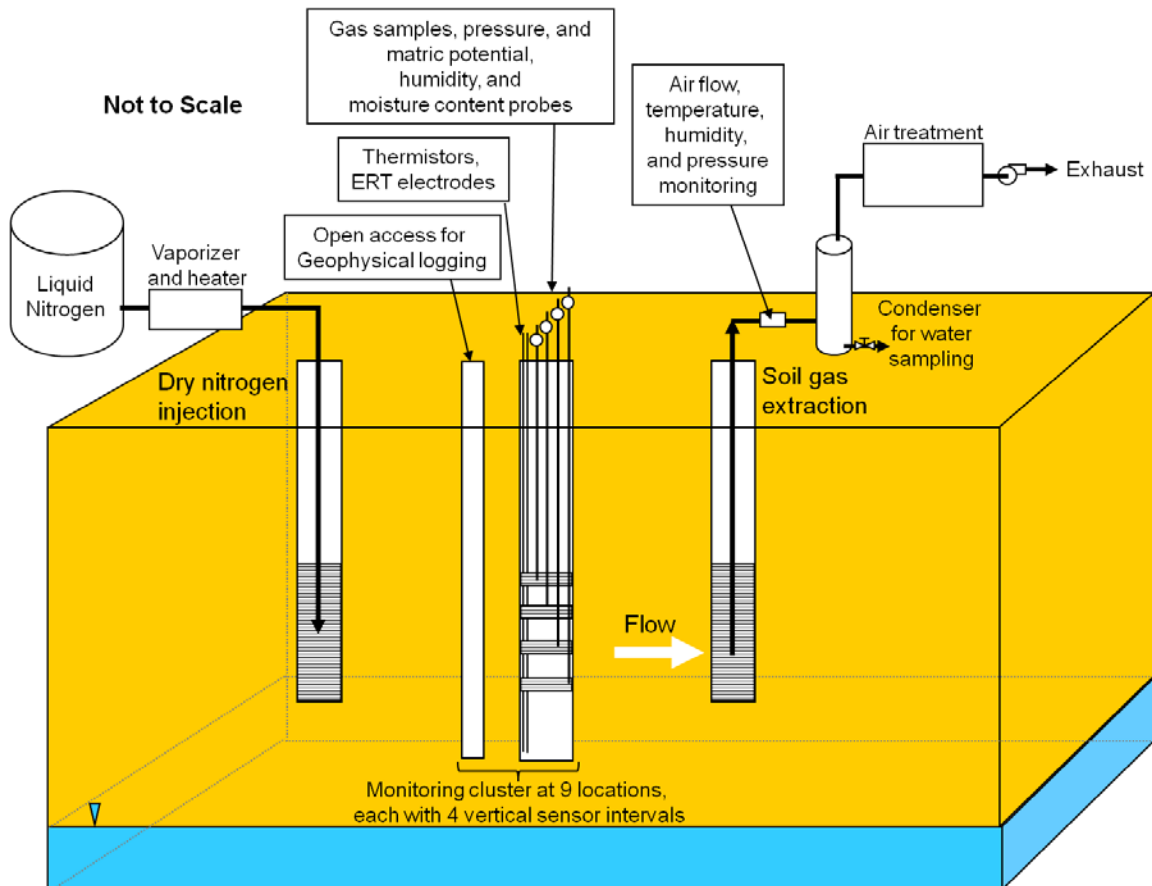
Figure 3.3. Basic Components of the Desiccation Field Test System

The general operational and in situ monitoring strategy is depicted in Figure 3.3. Dry nitrogen gas produced from liquid nitrogen tankers was injected at a controlled temperature of 20°C into a screened interval from 9.1 to 15.2 m (30 to 50 ft) bgs. Equipment testing, including trial nitrogen gas injections and the initial tracer test, occurred between November 22 and December 6, 2010. The active desiccation portion of the field test occurred with nitrogen injection at a stable flow rate of 510 m³/h (300 cubic feet per minute [cfm]) from January 17, 2011, through June 30, 2011, (164 days) except during a 13-day interval from April 21 through May 4, 2011, when there was no injection due to an equipment issue. Extraction of soil gas from a well screened from 9.1 to 15.2 m (30 to 50 ft) bgs was maintained for the full test duration at a stable flow rate of 170 m³/h (100 cfm). Extracted soil gas was routed through a heat exchanger to condense water that was collected and periodically sampled. The injection and extraction wells were 12 m (39 ft) apart. Figure 3.4 depicts the lateral layout of injection and extraction wells and the monitoring locations. Distances from the injection well to the monitoring locations are listed in Table

3.1. A 30-m by 45-m (100-ft by 148-ft) gas-impermeable membrane barrier was installed at the surface centered over the well network.
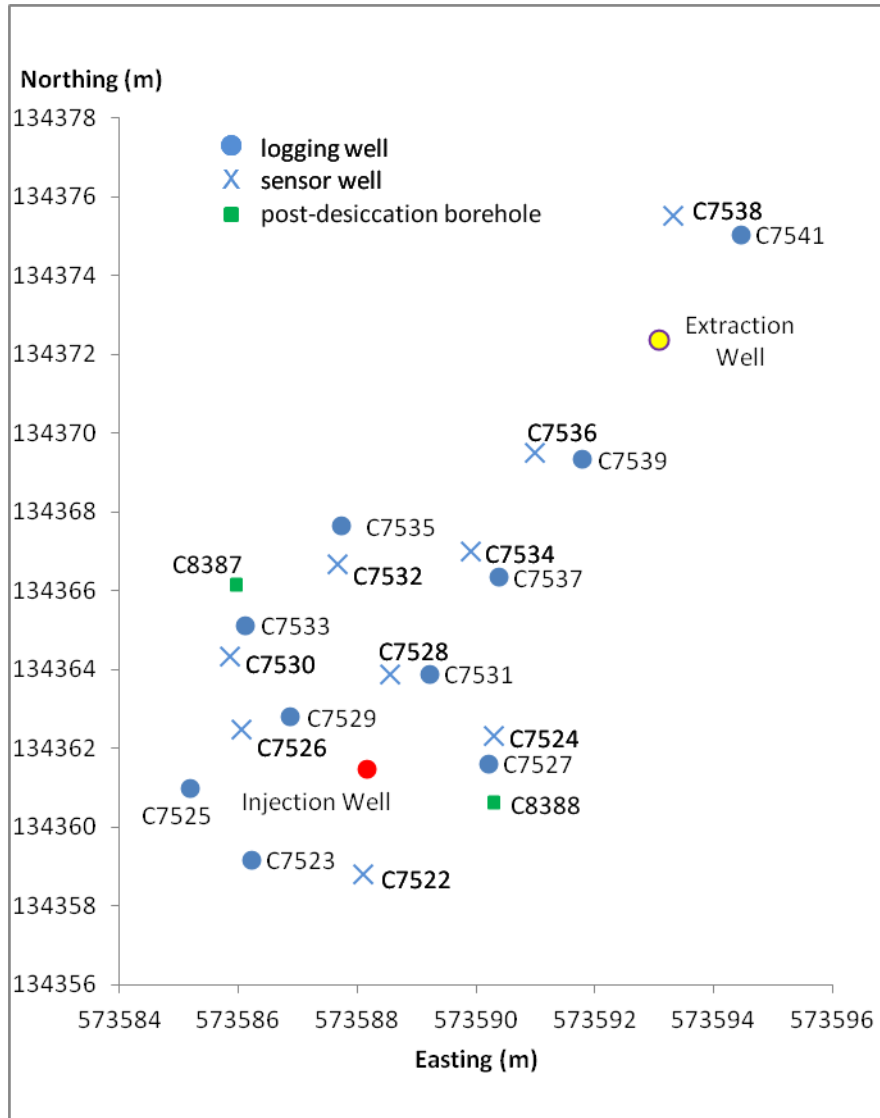
Figure 3.4. Location of Test Site Logging Wells, Sensor Boreholes, and Post-desiccation Boreholes for Collection of Sediment Samples. A background sensor borehole (C7540, not shown) was 15 m (50 ft) southeast from the injection well.

Table 3.1. Field Site Monitoring Locations

Monitoring Location	Distance from Injection Well (m)
C7526-S	2.33
C7529-L	1.85
C7524-S	2.28
C7527-L	2.04
C7528-S	2.43
C7531-L	2.62
C7522-S	2.68
C7523-L	3.02
C7525-L	3.02
C7530-S	3.67
C7533-L	4.18
C7534-S	5.79
C7537-L	5.34
C7532-S	5.22
C7535-L	6.18
C7536-S	8.49
C7539-L	8.64
C7538-S	14.96
C7541-L	14.94

An "S" designation is a borehole that contained in situ sensors. An "L" designation is for cased wells that were used for logging access.

A clustered monitoring approach was used in the test whereby a borehole (sensor borehole) containing sensors, gas-sampling ports, and electrical resistance tomography electrodes was placed nominally adjacent to a cased, unscreened well (logging well) that was used to conduct neutron moisture logging and for application of cross-hole GPR. Sensor boreholes contained four intervals of 100-mesh (> 0.125 and < 0.149 mm) Colorado sand (Colorado Silica, Colorado Springs, Colorado) containing matric potential sensors, moisture content sensors, humidity sensors (sensors described in Section 3.2.2.1), and porous polyethylene gas sampling ports (model X-6081, Porex Technologies Corporation) separated by granular bentonite. The sand intervals were placed nominally at 9.5–10.1, 11–11.6, 12.5–13.1, and 14–14.6 m (31–33, 36–38, 41–43, and 46–48 ft) bgs to provide vertically discrete monitoring across the injection/extraction well screen interval. The boreholes contained thermistor temperature sensors every 0.6 m (2 ft) from 3 to 21.3 m (10 to 70 ft) bgs and electrical resistivity electrodes every 1.5 m (5 ft) within the bentonite intervals of the borehole fill material from 3 to 21.3 m (10 to 70 ft) bgs. ERT electrodes were placed within the bentonite zones with tubing installed to enable addition of water around each electrode to locally hydrate the bentonite and maintain effective coupling between the electrode and the subsurface. Electrical connectivity was checked periodically during the test and water added when necessary to maintain adequate coupling. Logging wells to provide access for neutron moisture logging and cross-hole GPR extended to 21.3 m (70 ft) bgs with a 2-in. polyvinyl chloride (PVC) casing (plugged at the bottom) in a 4-in. diameter borehole and 100-mesh Colorado sand in the annular space.

3.2.2.1 Borehole Sensor Descriptions

Thermistors (USP8242 encapsulated negative temperature coefficient thermistors, U.S. Sensor, Orange, California) were used to monitor temperature. To achieve accurate temperature measurements over the range of interest, a fifth-order polynomial was used to relate resistance to temperature for each of the thermistors used in the field test. The manufacturer's calibration relationship was verified for a subset of the thermistors in a precision water bath spanning the 0°C–40°C temperature range with measured accuracies better than 0.07°C.

Temperatures were logged continuously (10-minute intervals) at each thermistor. The three-dimensional temperature field was estimated at selected times using the same interpolation technique that was used for the neutron moisture data. In addition to providing important information concerning desiccation progress, the temperature field data are also used to correct the ERT-derived electrical conductivity to a standard temperature prior to using the ERT data for estimating volumetric water content.

Matric potential data were collected using heat dissipation unit (HDU) sensors (229-L HDU, Campbell Scientific, Inc., Logan, UT) to indirectly determine the air-water capillary pressure. A 50-mA current excitation module was used to supply current to the HDU sensors. The HDU temperature was measured prior to heating and again at 1 s and 30 s after the onset of heating; these values were used to compute the associated matric potential (Oostrom et al. 2012a). The measurement range of the units is typically from -0.01 to -2.5 MPa (-0.1 to -25 bar) with an accuracy of 1 kPa (Flint et al. 2002). The procedure described by Bilskie et al. (2007) was used for HDU calibration, which simplifies the extended procedure forwarded by Flint et al. (2002) by only requiring calibration data in the range up to -70 kPa. Once installed, the sand zones containing the HDU sensors were allowed to equilibrate with the conditions in the native formation before the injection operations were initiated.

Thermocouple psychrometer (TCP) units (PST-55, Wescor Inc., Logan, UT) were also installed to collect matric potential data. A TCP determines the capillary pressure by essentially making very precise measurements of equilibrium vapor pressure (Brown and Bartos 1982). The capillary pressure is computed using Kelvin's law for vapor pressure lowering. The sensor consists of two adjacent thermocouples. The primary thermocouple is surrounded by a porous membrane or stainless-steel screen that allows contact with the sediment sample. The other thermocouple is sealed in the sensor housing preventing any vapor contact. The temperature depression of the wet sensing junction relative to the dry depends upon the relative humidity of the surrounding air. The units were calibrated in solutions of known water potential. The TCP have a capillary pressure range of -0.2 to -8 MPa (-2 to -80 bar) with an accuracy of 30 kPa. Practical difficulties in applying this sensor are due to the extreme sensitivity to any thermal differences between the sensor and sample, as well as pressure and temperature effects on the measurement. Sensors were calibrated using NaCl solutions spanning the capillary pressure range from -0.2 to -8 MPa (-2 to -80 bar) at temperatures of 10°C, 20°C, and 30°C. Twenty-milliliter glass vials were each filled with separate NaCl solutions and an individual TCP was immersed in the salt solution using caps that centered the TCP within each vial. Using this procedure, a linear relationship between the sensor output and the matric potential was obtained for each sensor over the range from -0.2 MPa to -5 MPa (-2 to -50 bar). At larger capillary pressures, the functional dependence became nonlinear for all of the TCPs.

Dual-probe heat pulse (DPHP) sensors (Specific Heat Sensors, East 30 Sensors, Pullman, WA) were used to measure water content. The sensor type (described in detail in Campbell et al. 1991) consists of two

parallel hypodermic tubes separated by a fixed distance. A heating element is placed in one tube and a thermistor or thermocouple is located in the other tube. A controlled heat pulse is generated by the heating element and the temperature rise is measured. The maximum temperature rise T_m (°C) for each measurement is related to the soil volumetric heat capacity C (J °C^{-1} m^{-3}), probe spacing r (m), and the amount of heat delivered q (J m^{-1}) as follows (Basinger et al. 2003).

$$T_m = \frac{q}{e\pi r^2 C} \qquad (3.1)$$

The heat capacity is a composite of the effects from both the liquid and solid components and can be described using the relationship:

$$C = C_w \theta + \rho_b c_s \qquad (3.2)$$

where C_w is the volumetric heat capacity of water, ρ_b is the soil bulk density, and c_s is the specific heat of the soil component. The soil volumetric water content can then be estimated by combining Equations (3.1) and (3.2), as follows:

$$\theta = \frac{\left(\dfrac{q}{e\pi r^2 T_m} - \rho_b c_s\right)}{C_w} \qquad (3.3)$$

A direct calibration relation was obtained for each of the DPHP sensors. Six different mixtures of water and sediment were made for each porous medium and the maximum temperature rise was subsequently measured for each sensor. For the 100-mesh sand and the Hanford Site sediment, the mixtures consisted of 0, 15, 30, 45, 60, and 75 g water per 1000 g porous medium. For the 200-mesh sand, the mixtures were 0, 30, 60, 90, 120, and 150 g water per 1000 g porous medium. Calibration of this sensor type was highly dependent on tube separation.

Soil gas relative humidity was monitored using a CS215 capacitive relative humidity and temperature sensor (Campbell Scientific, Inc., Logan, UT) with the electronics integral to the unit. The signal excitation and measurement are all completed within the device, followed by a conversion to a digital signal that can be monitored remotely. The sensing element is housed within a sintered high-density polyethylene filter to protect it from impact and environmental conditions. Each humidity probe is factory calibrated and the accuracy of the device is 2% within the 10% to 90% relative humidity range and 4% from 0% to 100% relative humidity. Temperature dependence is better than 2%; from 20°C to 60°C.

Some of the borehole sensors, including TCP units (PST-55, Wescor Inc., Logan, Utah) and DPHP sensors (Specific Heat Sensors, East 30 Sensors, Pullman, Washington), were not tracked during the rewetting period due to poor responses and failures of these sensors observed during the active desiccation phase (Truex et al. 2012a).

3.2.2.2   Neutron Moisture Logging Measurements

Soil moisture content determination using neutron scattering probes has become a standard method over the past several decades (Hignett and Evett 2002). A neutron probe consists of a high energy neutron source, a low energy or thermal neutron detector, and the electronics required for counting and storing the measured response. A fast neutron source placed within moist soil develops a dense cloud of thermal neutrons around it and a thermal neutron detector placed near the source samples the density of the generated cloud. The concentration of thermalized neutrons is affected by both soil density and elemental composition. Elements that absorb neutrons are often in low concentration in the soil solid phase and when clay content is also low, the neutron probe response is mainly affected by changes in moisture content (Greacen et al. 1981; Hignett and Evett 2002). For the desiccation field test, neutron probes were deployed periodically in wells at the site to collect neutron moisture logs with data at discrete depth intervals in the subsurface. Neutron probe data were converted to volumetric moisture content using a site-specific relationship that was developed from core measurements of gravimetric moisture content and bulk density.

Neutron moisture logging was conducted using a CPN 503DR Hydroprobe (InstroTek Inc., Raleigh, NC). Neutron probe measurements were acquired at depth increments of approximately 7.5 cm using a count time of 30 s and then converted to count ratio (C_R) by dividing each measurement by the standard count. Neutron moisture logging was conducted by S.M. Stoller Corporation at the logging well locations and by Pacific Northwest National Laboratory (PNNL) at the injection well.

Neutron probe data were converted to volumetric moisture content using a site specific relationship that was developed from core measurements of gravimetric moisture content and bulk density. Core samples were collected adjacent to logging location C7527 after the active desiccation phase of the test. For this type of neutron probe, and over the normal range of soil moisture content, the calibration relationship between instrument response and volumetric moisture content for a specific soil is approximately linear (Hignett and Evett 2002). However, numerical instrument response simulations have shown a nearly linear relationship between probe counts and volumetric moisture content over the range from 0.05 to 0.3 m^3/m^3, and non-linear behavior at very low moisture contents <0.05 m^3/m^3 (Ward and Wittman 2009; Li et al. 2003).

Soil textures were identified from the post-desiccation core samples (6 to 18 m [20 to 59 ft]bgs) and ranged from medium sand to loamy sand with the exception of one sample of sandy silt. Clay content can also affect moisture content calibration (Greacen et al. 1981); however, clay content was low at the desiccation field site, ranging between 2.4% and 8%. Using the relationship developed by Greacen et al. (1981), the contribution of the clay hydrogen-equivalent water content was small, ranging from 0.018-0.025 m^3/m^3 with a maximum difference of 0.007 m^3/m^3 between the soils present at the desiccation field site.

For sites with multiple soil layers, separate linear calibrations for individual soil layers may be appropriate (Yao et al. 2004). Samples were grouped into sand and loamy sand texture materials. Neutron moisture probe C_R data were plotted with corresponding post-desiccation laboratory-measured volumetric moisture content (computed using measured gravimetric moisture content and bulk density) from samples at the same depth, laterally within 0.9 m (3 ft) of the neutron logging well (Figure 3.5). With the assumption that soil moisture content values are not substantially different at that lateral distance from the logging well, the laboratory data can be used to establish a calibration for the neutron moisture

probe data. While air flow preferentially occurred through sand layers, adjacent loamy sand layers were also seen to desiccate. For desiccation, very dry conditions (<0.01 m^3/m^3) not typically used in neutron probe calibrations were measured within some depth intervals in post-desiccation core samples. While the neutron count ratio data and corresponding laboratory measured moisture content for all samples followed a relatively linear relationship above approximately 0.05 m^3/m^3, the calibration relationship shows non-linear behavior at lower moisture content values (Figure 3.5).

Prior to desiccation, the range of moisture contents was 0.05-0.35 m^3/m^3 as determined from samples collected during installation of the injection well about 2 m (6.5 ft) away from the post-desiccation borehole. Using only samples above 0.05 m^3/m^3, a linear calibration relationship is observed for both sand and loamy sand. Post-desiccation volumetric moisture contents for some of the very dry core samples within the highly desiccated zones (loamy sand and sand textures) were 0.004 +/- 0.002 m^3/m^3 from laboratory gravimetric analyses, with corresponding count ratios of 0.21 +/- 0.007 (Figure 3.5). For the loamy sand, using the linear relationship based on only samples above 0.05 m^3/m^3 would predict a count ratio of 0.34 for a moisture content of 0.004 m^3/m^3, substantially different from the actual observations. Linear relationships over the full range of data could be applied but provide a poor fit to the data. For this study, a non-linear neutron probe calibration relationship captures the response for both soil types and provides a better fit to the data over the full range (Figure 3.5). Regression of volumetric moisture content (θ) (see Truex et al. 2012a) and C_R data for all core samples resulted in the relationship $\theta = 0.714C_R^2 - 0.1363C_R$, with a root mean square error of 0.015 for θ and a coefficient of determination of 0.93.

Volumetric moisture content values from neutron logging events were interpolated to a finely spaced grid encompassing the logging wells using a weighted inverse-distance interpolation scheme. Due to the high vertical resolution of the data along the logging wells, the corresponding low lateral resolution, and the expected high lateral correlation in moisture content, a 5 to 1 horizontal to vertical weighting was selected in the interpolation. This interpolation provides a smoothed three-dimensional estimate of volumetric moisture content distribution. Subtracting the pre-desiccation interpolation from subsequent interpolations provides an estimated change in volumetric moisture content with time.
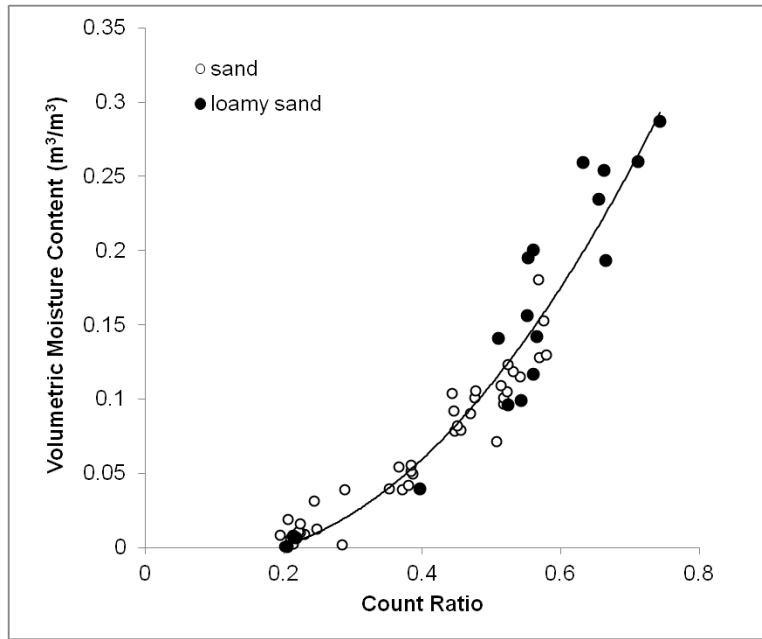
Figure 3.5. Calibration Relation for Neutron Moisture Probe Count Ratio Data and Corresponding
Laboratory-Measured Volumetric Moisture Content

3.2.2.3   Cross-Hole Electrical Resistivity Measurements

ERT is a method of remotely imaging the electrical conductivity (EC) of the subsurface (Figure 3.6).
Electrodes installed along the ground surface and/or within boreholes are used to strategically inject
currents and measure the resulting potentials to produce a data set that is used to reconstruct the
subsurface EC structure (Daily and Owen 1991; Johnson et al. 2010). With respect to soil desiccation,
EC is a useful metric for characterizing the subsurface because it is governed by properties that influence
gas flow, including soil texture and moisture content. EC is also a useful metric for monitoring
desiccation because it is sensitive to moisture content and temperature (Slater and Lesmes 2002), the two
primary properties altered during desiccation.

Figure 3.6. Control System for Electrical Resistivity Tomography

The ERT electrode array deployed in this study was first used to characterize pre-desiccation subsurface structure, providing important three-dimensional information regarding permeability and likely gas flow pathways. During desiccation, the same array was used to image three-dimensional changes in EC from background caused primarily by decreasing moisture content but also by evaporative cooling.

3.11

ERT surveys were collected twice per day during the desiccation phase, and weekly during the post-desiccation phase. The resulting changes in EC were temperature-corrected and converted to changes in moisture content using a site-specific, laboratory-validated relationship (Archie 1942). Results of pre-desiccation and desiccation ERT monitoring are provided by Truex et al. (2012a, 2013a).

ERT data were collected prior to and during desiccation using 99 electrodes—11 electrodes in each of the 9 sensor wells. Full forward and reciprocal measurements were collected twice per day to estimate data noise and quality, and each data set contained 6114 measurements after filtering. Measurements were collected using an 8-channel MPT DAS-1 impedance tomography system.[1] These data were inverted with isotropic regularization smoothing constraints on an unstructured tetrahedral mesh with 354,544 elements using the imaging software described by Johnson et al. (2010). The EC data collected from the ERT system provide a means to image changes in the volumetric moisture content over time in three dimensions.

The bulk EC of the subsurface has been widely observed to follow the empirical Archie's Law (Archie 1942) in clean (i.e., clay free), non-conductive sands. Archie's Law is given by Equation (3.4):

$$EC = \frac{1}{a}\sigma_f \phi^m S_w^n \qquad (3.4)$$

where
a = tortuosity factor
σ_f = fluid conductivity
ϕ = porosity
S_w = water saturation
m = cementation exponent
n = saturation exponent.

The relationship between temporal changes in water saturation and the corresponding changes in electrical conductivity that occur during subsurface desiccation are simplified under the following assumptions:

1. Parameters a, ϕ, and m are constant in time. This assumption is justified if each of these parameters, dependent on the textural properties of the soil, do not change significantly during desiccation.

2. The parameter σ_f is constant in time. This assumption is not strictly valid because ionic concentrations increase as pore water is evaporated during desiccation. However, σ_f becomes independent of water content at a critical saturation limit, or the lower saturation limit where mineral precipitation begins. In addition, core-scale testing on site sediments shows the electrical conductivity response to be primarily governed by decreases in saturation as opposed to increases in fluid conductivity during desiccation. Therefore, it was assumed that fluid conductivity did not change during desiccation.

3. The parameter n is independent of saturation. This assumption is generally valid except at low saturation (<~5%) where n has been observed to decrease with decreasing saturation (Han et al. 2009; Hamammoto et al. 2010). Laboratory testing on site sediments has shown n to be ~2.0 within the saturation range indicated by neutron moisture data during the desiccation test.

---

[1] http://www.mpt3d.com/.

3.12

Because desiccation is a nonisothermal process, the effects of temperature on bulk conductivity must also be considered. The temperature dependence of bulk conductivity in the vadose zone depends on water content, but is always monotonic. A decrease in temperature will cause a corresponding decrease in bulk conductivity and vice versa. Laboratory testing on site sediments showed a temperature dependence of 0.00013 S/m C° at 5% volumetric moisture content and 0.00023 S/m C° at 12% volumetric moisture content, consistent with published values (Friedman 2005; Ruijin et al. 2011). A constant value of 0.00020 S/m C° was assumed for the temperature dependence and used to correct all electrical conductivity results to a temperature of 20°C based on the interpolated temperature field.

With the assumptions stated in 1–3 above, a desiccation induced change in saturation can be expressed in terms of the corresponding change in bulk conductivity as shown in Equation (3.5):

$$\frac{S_t}{S_0} = 10^{\frac{1}{n}log_{10}\left(\frac{EC_t}{EC_0}\right)} \tag{3.5}$$

where S_t is the saturation at time t, S_0 is the pre-desiccation baseline saturation, and EC_t and EC_0 are the corresponding bulk conductivity at time t and pre-desiccation. Note that the ratios of volumetric moisture content and saturation are equivalent. Thus, the EC data from ERT provide a means to image changes in the volumetric moisture content over time in three dimensions with high temporal resolution due to the ability to autonomously collect ERT data.

3.2.2.4 Cross-Hole Ground-Penetrating Radar Measurements

GPR methods are also commonly used to characterize or monitor subsurface moisture content. GPR systems consist of an impulse generator which repeatedly sends a particular voltage and frequency source to a transmitting antenna (Figure 3.7). Cross-hole GPR methods involve lowering a transmitter into a wellbore and measuring the energy with a receiving antenna that is lowered down another wellbore, and moving the transmitting and receiving antennas manually to different positions in the wellbores to facilitate transmission of the energy through a large fraction of the targeted area.

Soil electrical permittivity is strongly dependent on moisture content because of the large difference between water and bulk soil permittivity. The relative permittivity of water is approximately 80, compared to values between 3 and 7 for typical soil mineral components. The permittivity can be determined from the observed velocity of an electromagnetic pulse propagating through the soil matrix. Studies have demonstrated that GPR methods can effectively estimate subsurface moisture content using measured electromagnetic velocities (Hubbard et al. 1997;

Figure 3.7. Ground-Penetrating Radar Data Collection Equipment

van Overmeeren et al. 1997; Huisman et al. 2001). In general, the electromagnetic velocity depends on both the permittivity and conductivity; however, when the conductivity is sufficiently low (i.e., low-loss conditions), GPR-derived velocities can be used to accurately determine permittivity and therefore moisture content.

At the desiccation site, cross-borehole GPR surveys were conducted with the transmitting and receiving antennae placed in separate boreholes to measure the electromagnetic velocity between boreholes. Using measurements acquired from antennae located at many different vertical positions within each borehole, a 2-D image of properties between boreholes can be produced (Jackson and Tweeton 1994). These images can provide information that can be interpreted with respect to the geologic structure and moisture content between boreholes (Binley et. al 2002; Day-Lewis et al. 2002). For the desiccation field test, 2-D images of electromagnetic velocity were generated with GPR and converted to volumetric moisture content changes using an established petrophysical relationship assuming low-loss conditions (Topp and Ferré 2002; Evett 2005). At the desiccation site, the electrical conductivity varies between 0 and 0.250 S/m and the low-loss assumption is not valid at all locations. Thus, GPR data are analyzed and interpreted in conjunction with the subsurface EC data provided by the ERT system.

GPR data was collected with a PulseEKKO 100 using 100 MHz borehole antennae (Sensors and Software, Inc., Mississauga, Ontario, Canada). Multiple offset gather surveys were periodically collected in a set of four logging well pairs (using locations C7523, C7531, C7537, C7539, and the injection well). From these data, two-dimensional electromagnetic velocity images were constructed using MIGRATOM, a curved ray inversion software (Jackson and Tweeton 1994).

Electromagnetic velocity is a function of the various electromagnetic properties of the media through which the electromagnetic wave propagates. The material properties are seldom known so to simplify the relationship, assumptions are often adopted. The first assumption is the media does not contain significant quantities of ferromagnetic materials such that the magnetic permeability of the media is equal to that of free space. Another assumption is that low-loss conditions are present—that is, the electrical conductivity is much less than the product of the frequency of the electromagnetic wave and the electrical permittivity, and the electromagnetic velocity only depends on the electrical permittivity. When these assumptions are valid, it has been shown that the volumetric moisture content, θ, is a linear function of the square root of the soil apparent electrical permittivity, ε_a (Ledieu et al. 1986; White and Zegelin 1995; Topp and Ferré 2002):

$$\theta = A\sqrt{\varepsilon_a} + B \qquad (3.6)$$

The term apparent is used here to mean the permittivity value that is inferred from measurement of the velocity of an electromagnetic wave at a given frequency.

For the desiccation site, a linear regression of GPR-determined electromagnetic velocity values in the vicinity of each logging well and the corresponding neutron moisture data were used to determine the coefficients A and B in Equation (3.6). At the desiccation site, the electrical conductivity varies between 0–0.250 S/m and the low-loss assumption is not valid at all locations. Only data from locations with electrical conductivity less than 0.025 S/m were used in determining the coefficients A and B and were found to be very close to those obtained from the modified form of Topp's equation (Topp and Ferré 2002). Given the good fit to data from the field site, Topp's equation was used to convert GPR-derived permittivity to volumetric moisture content. Note this approach is a standard method to estimate moisture

3.14

content from GPR data with the above assumptions. Interpretation of GPR data for conditions with higher electrical conductivity may be impacted by violation of the low-loss assumption.

3.2.2.5   Gas-Phase Tracer Test System

To examine subsurface gas flow patterns of the injected gas, a tracer test was conducted at the beginning of desiccation operations. Because pure nitrogen gas was used as the injected gas and the subsurface soil gas prior to injection contained nominally atmospheric concentrations of oxygen, the breakthrough of injected nitrogen gas was determined by monitoring the displacement of oxygen. Oxygen concentrations were monitored at the gas-sampling ports during initial nitrogen injection operations with an injection flow rate of 510 m^3/h (300 cfm) and extraction of soil gas at 170 m^3/h (100 cfm) at the extraction well, the same flow conditions that were used for the full desiccation operational period. Zirconium oxide sensors (model 65 oxygen probe analyzer, Advanced Micro Instruments, Huntington Beach, California) were used to measure oxygen

Tracer Test Oxygen Sensor System

concentration in extracted soil gas. Soil gas was extracted from sampling ports and routed through the oxygen sensors with a gas pump (model UNMP830 KNDC, KNF Neuberger Inc., Trenton, New Jersey). A gas flow rate of 0.5 L/min was metered and measured with an adjustable flow meter (model FMA-4491, Advanced Equipment Inc.) and maintained throughout the duration of the tracer test. An array of six independent oxygen sensor, pump, and flow meter assemblies were used to simultaneously measure oxygen levels at different sampling ports. A data acquisition and control system (model CR1000, Campbell Scientific Inc., Logan, UT) was used to record the sensor output.

3.2.2.6   Above Ground Equipment and Overall Data Collection System

Figure 3.8 shows the general test layout including the primary above-ground equipment for gas injection and extraction.
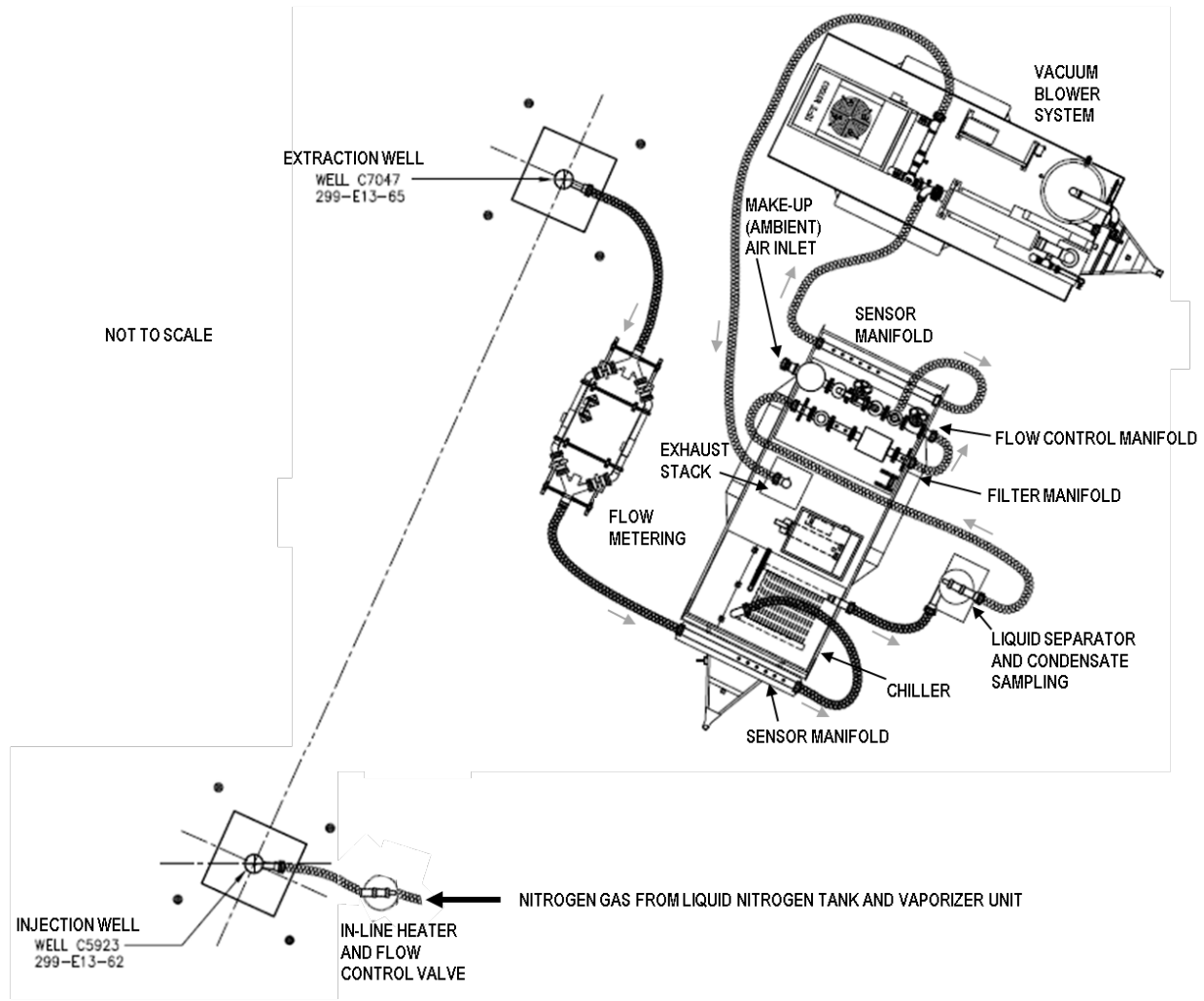
Figure 3.8. Test Site Injection and Extraction Equipment

Injection System. Liquid nitrogen tankers (two, 5000 gallon) were connected to a vaporizer unit to provide the gaseous nitrogen source for injection. An in-line heater with a temperature controller was used to maintain the injection temperature at 20°C (except during portions of June when an ambient temperature of greater than 20°C caused the injection gas temperature to be higher than 20°C). Nitrogen gas was plumbed to the injection well which was configured to enable gas injection and provide access for geophysical measurements through a stilling well (Figure 3.9). Data collected for the injection system included a manual log of nitrogen use and electronic sensors and logging for nitrogen gas flow rate and temperature.
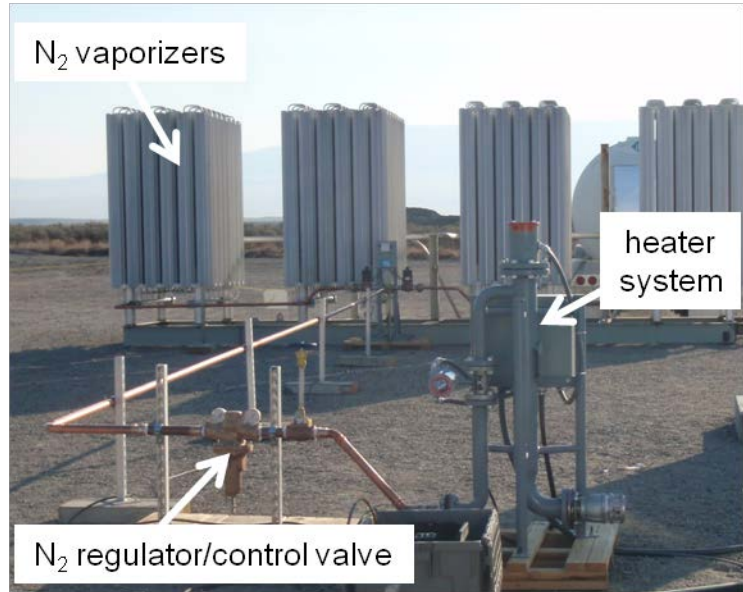
Nitrogen Gas Injection System

Liquid Nitrogen Supply to Produce Nitrogen Gas for Injection
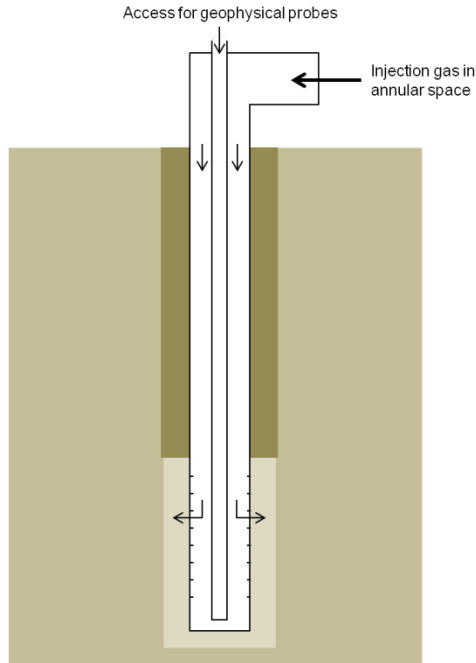
Figure 3.9. Stilling Well Design for Desiccation Field Test
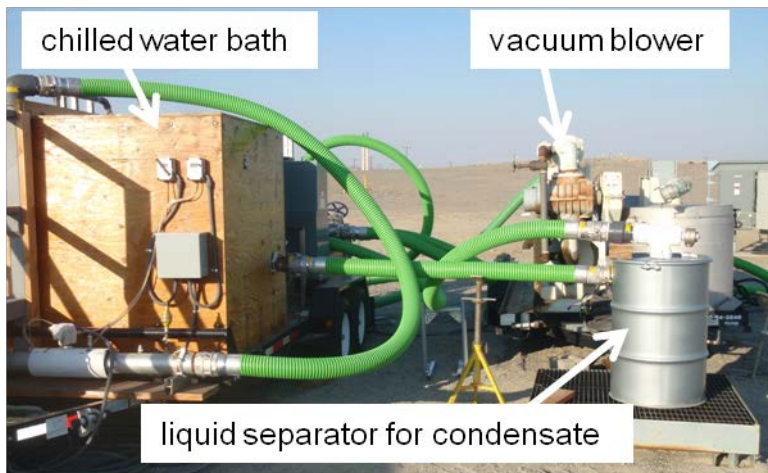
Major Extraction System Components

Extraction System. A vacuum blower system that had been previously used at the 200-PW-1 Operable Unit was used to extract soil gas from the extraction well. The extraction well was plumbed to a manifold with sensors for gas flow rate, temperature, pressure, and relative humidity. The gas was then routed through a custom-built chilled water bath and a commercial liquid separator drum to remove water from the extracted gas. Gas was then routed through a HEPA-grade filter and then to the vacuum blower which exhausted to atmosphere. Gas flow rate was controlled by a valve that enabled throttling of the extraction well gas flow and a valve that controlled the amount of makeup air added to the system just upstream of the blower. Gas flow rate, temperature, and pressure were monitored using sensors just up and down stream of the blower.

Data Collection System. Sensor data for the field test were collected using CR3000 (Campbell Scientific Inc., Logan, Utah) data loggers (DPHP, HDU, Thermistor, Pressure transducer, and Flow meters) or CR7X data loggers (TCP sensors). The separate data logger was used for the TCPs because these sensors generate extremely low voltage signals and required the use of electronics capable of measuring nanovolt

level signals. Data were continuously and automatically retrieved from the data loggers and stored on a Dell T3400 computer located at the field site. A Raven X cellular phone modem (Sierra Wireless, Richmond, British Columbia, Canada) was installed which allowed for remote monitoring of the data acquisition system and data transfer.

3.2.3 Equipment and Materials

Primary equipment and materials for the test are summarized in Section 3.2.2.

3.2.4 Sampling and Analysis

Condensate collected in the liquid separator (Figure 3.8) was periodically drained and transferred to waste storage drums for subsequent waste disposal. During draining operations on December 2, 2010, February 3, 2011, and June 13, 2011, samples were collected and sent to the laboratory for analysis of Tc-99, nitrate, and gross beta concentrations.

3.2.5 Data Management

Data from sensors was maintained on both data loggers and an on-site computer and backed up periodically to an office computer. Sensor data were imported to spreadsheets at least twice per month during active desiccation and every 3 months during the rewetting phase. The spreadsheets were used to convert raw sensor data to the required outputs, to plot results, and to serve as an additional data storage file for the plotted data. Manual test logs were maintained to document primary test events and for operations where no electronic sensor was available (e.g., condensate collection). The electronic and manual data are stored as part of CH2M Hill Plateau Remediation Company and PNNL project records and are documented in project reports in the reports, journal articles, and conference proceedings listed in Section 2.1 and in this report.

3.2.6 Deviations from Work Plan

The field test plan was followed for the test with the following exception. While initial results with gas-phase tracers for monitoring desiccation were favorable in artificial porous media, Oostrom et al. (2011) showed that significant sorption of all gas-phase tracers, even those injected as conservative tracers, occurred once sediments were desiccated. Because the injection point for the tracers would have been the injection well where significant desiccation occurs rapidly, gas-phase tracers were not viable for the test. Instead, the oxygen displacement tracer technique described in Section 3.2.2.4 was applied to evaluate soil gas flow patterns.

4.0 Detailed Results

Results of the field test are presented in the next two sections. First, the results from sensors and geophysical monitoring are presented in Section 4.1. The data are then assessed with respect to the field test objectives in Section 4.2.

4.1 Field Data Summary

The field test of desiccation was conducted to collect data on technology implementation (Section 4.1.1), to quantify the performance of the desiccation process (Section 4.1.2), and to quantify the stability of the desiccated zone (i.e., the rate of rewetting) (Section 4.1.3). The sections below compile the data with respect to each of these basic field test elements.

4.1.1 Desiccation Implementation

Implementation of an in situ technology needs to consider the subsurface properties of the target application site. For the field test, these types of data were collected to set a baseline for the desiccation operations (Section 4.1.1.1). Operational data were then collected during the test to describe test conditions (Section 4.1.1.2) as a foundation for interpreting the sensor and geophysical data that are indicators of subsurface desiccation performance (Section 4.1.2).

4.1.1.1 Pre-Desiccation Data

Bulk air permeability. Step and constant rate discharge tests were conducted as described in *Characterization of the Soil Desiccation Pilot Test Site* (DOE 2010a). These data can be used to evaluate the injection and extraction pressure requirements.

Vertical distribution of permeability. At the injection and extraction well locations, particle size distribution and neutron logging information are available (DOE 2010a; Serne et al. 2009; Um et al. 2009). The vertical distribution of permeability is related to the distribution of injected gas flow. As shown by laboratory and field data, finer, wetter zones will dry more slowly than coarser, dryer zones.

Initial moisture and contaminant distribution. Borehole neutron logs and laboratory analysis of samples were conducted to evaluate the vertical distribution of moisture and contaminant concentrations at the injection and extraction well locations (Figure 4.1) (Serne et al. 2009; Um et al. 2009). In addition, interpolated pre-desiccation neutron logging data (Figure 4.2) and 2-D cross-hole GPR images (Figure 4.3) provide an interpretation of the initial distribution of moisture. The baseline ERT conductivity image (Figure 4.4) can also be interpreted in terms of lithology and contaminant distributions.
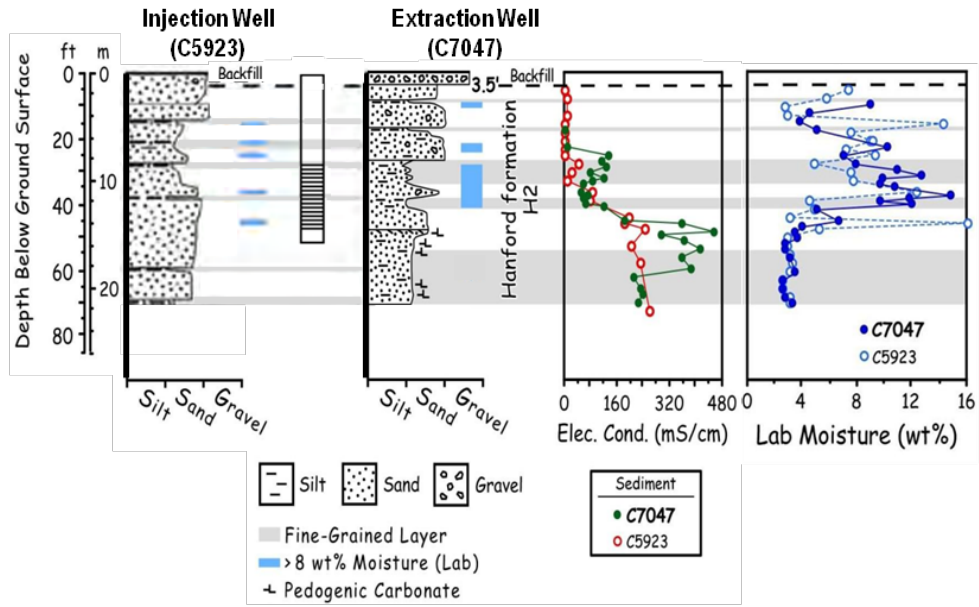
Figure 4.1. Injection and Extraction Well Borehole Initial Laboratory Moisture Content, Extracted Pore Water Electrical Conductivity, and Well Screened Interval (after DOE 2010a; Serne et al. 2008; Um et al. 2009).
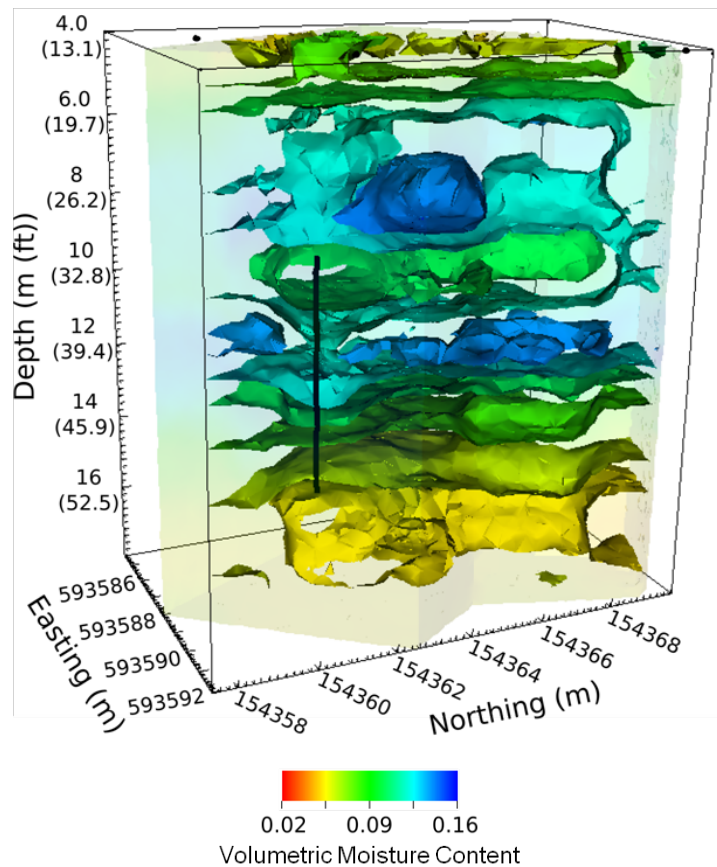
Figure 4.2. 3-D Interpolation of Initial Volumetric Moisture Content from Neutron Moisture Logging Data prior to Desiccation. Neutron moisture data from are from logging at locations C7523–C7537 (Figure 3.4).
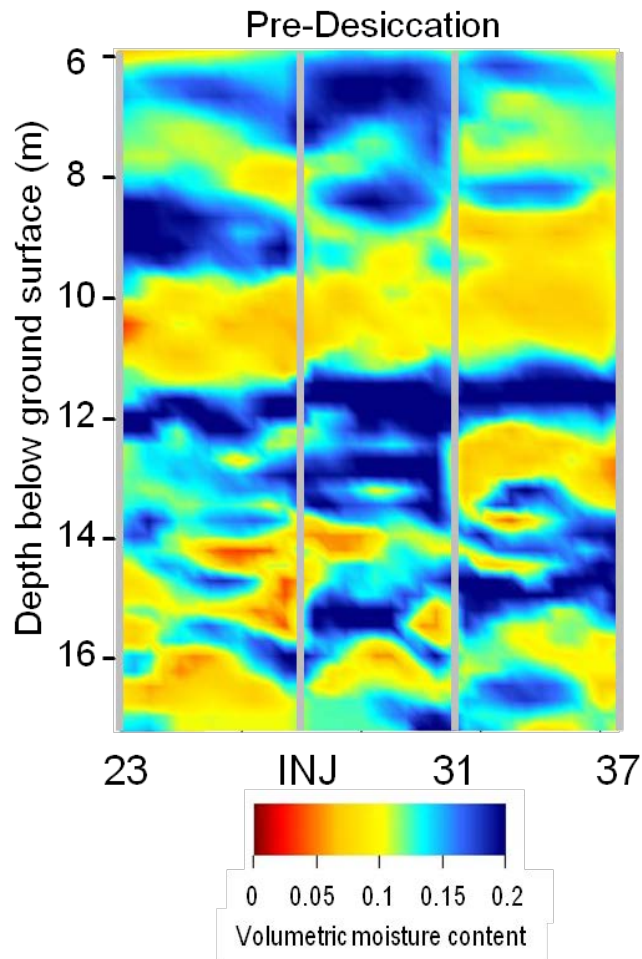
Figure 4.3. 2-D Interpretation of Initial Volumetric Moisture Content from Cross-Hole Ground-Penetrating Radar Data prior to Desiccation. Locations are shown as INJ (injection well) and logging well locations indicated by the last two numbers in the location identifier (e.g., 23 = C7523).
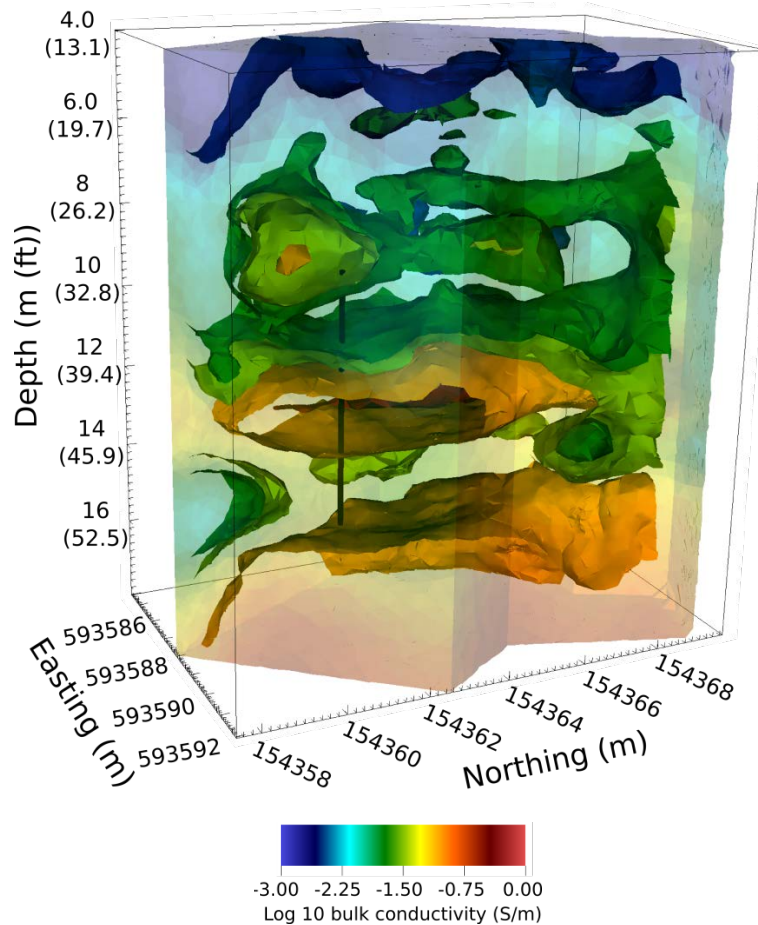
Figure 4.4. 3-D Pre-desiccation Bulk Conductivity At Desiccation Treatability Test Site as Determined via ERT. Elevated conductivities (warmer colors) are associated with finer grained material and/or elevated ionic strength (i.e., nitrate). Lower bulk conductivity is associated with coarser grained, less contaminated zones.

Injected gas flow and distribution. The rate of desiccation is proportional to the rate of dry gas flow through the targeted zone. Injected gas flow distribution is impacted by the heterogeneity in air permeability. Based on the pre-test stratigraphic information, it was expected that soil gas flow would not be uniform in the treatment zone. Tracers were used as a means to examine the degree of variability in the soil gas flow distribution. Tracer response was monitored at four vertical points at each monitoring location. Thus, the resolution of the gas flow permeability is limited to the distribution of these monitoring locations. Because pure nitrogen gas was injected, the movement of injected nitrogen could be tracked by measuring the displacement of soil gas oxygen. Figure 4.5 shows that breakthrough of injected nitrogen occurs first in the 14.3 m (47 ft) and 12.8 m (42 ft) bgs intervals. Injected nitrogen flow is much slower in the upper intervals (9.8 m [32 ft] and 11.3 m [37 ft] bgs). These data suggested that most of the injected dry gas would travel through the lower portion of the test site.
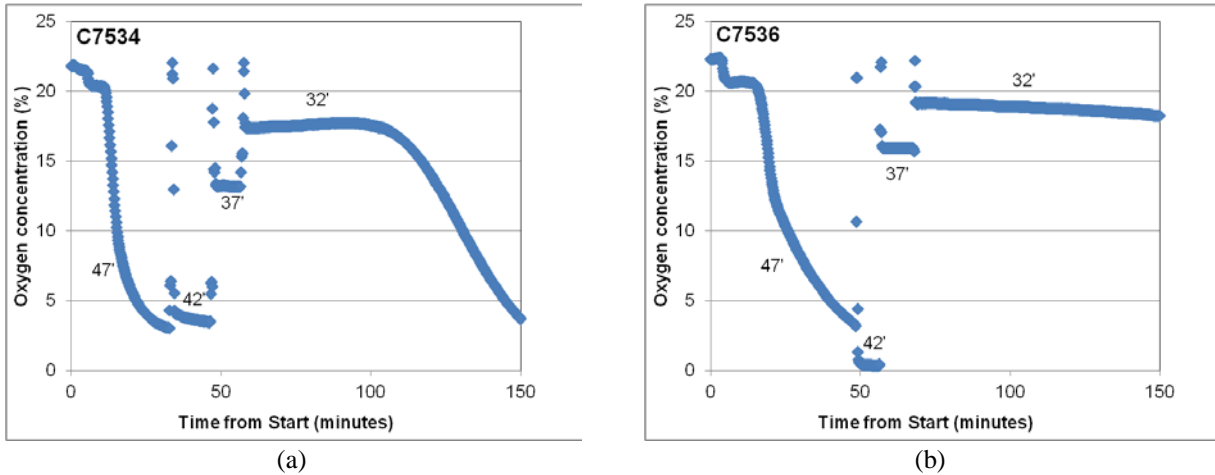
Figure 4.5. Oxygen Response (inverse of injected nitrogen gas tracer breakthrough) at the C7534 and C7536 Locations along the Axis between the Injection and Extraction Wells. Data are for a test with an injection rate of 510 m³/h (300 cfm) and an extraction rate of 170 m³/h (100 cfm). Separate curves are for readings at the different gas sample port vertical positions as denoted in feet below ground surface (e.g., 47').

Baseline in situ sensor data. Monitoring for desiccation involved monitoring for changes from baseline conditions induced by the desiccation process. One type of monitoring was conducted using in situ sensors for temperature, humidity, moisture content, and matric potential. In situ sensors were emplaced in a borehole configured in four depth interval monitoring zones, nominally at 9.9, 11.4, 13, and 14.5 m (32.5, 37.5, 42.5, and 47.5 ft) bgs. The 100-mesh sand used in each of the sensor intervals was added dry and had to equilibrate to the surrounding native formation moisture conditions as shown in with example sensor responses in Figure 4.6 through Figure 4.8. Specific probes are not identified in these figures; the end of the equilibration represents the starting point for active desiccation monitoring which is shown in more detail in Section 4.1.2. These moisture conditions are specific to the emplaced sand properties (the saturation-pressure relationship) in equilibrium with the mixture of native material present adjacent to the sand pack.
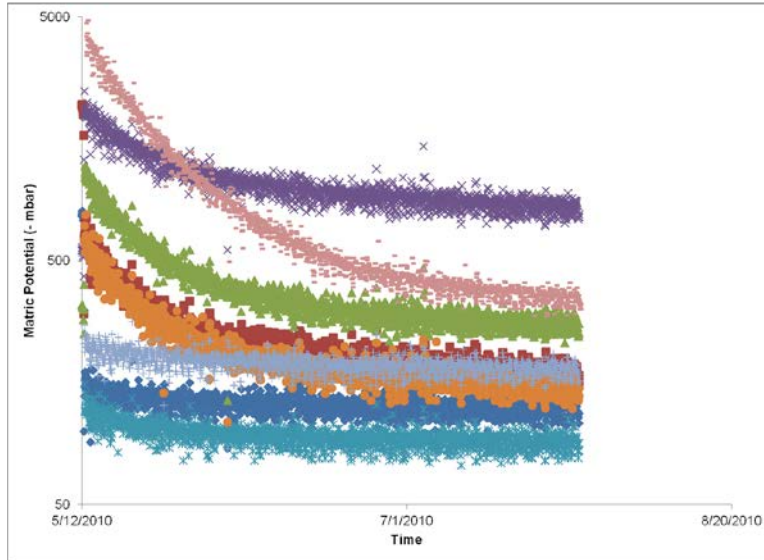
Figure 4.6. Equilibration Response for Heat Dissipation Units
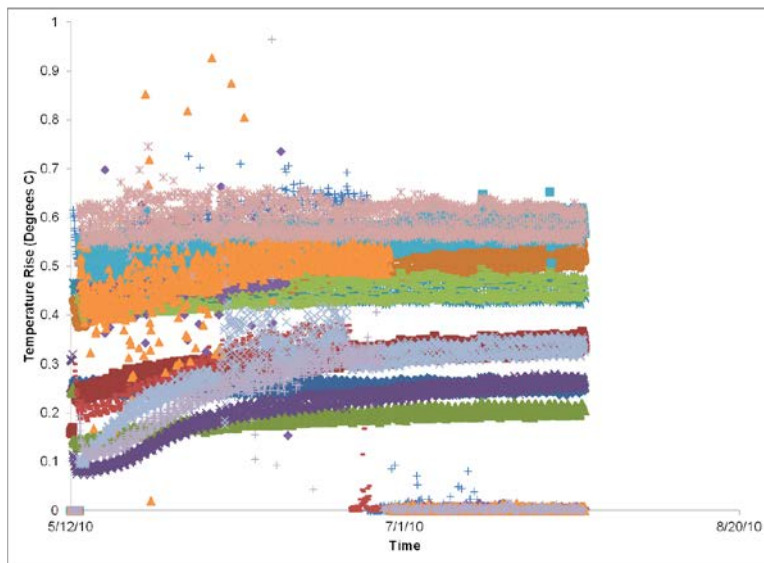
Figure 4.7. Equilibration Response for Dual-Probe Heat-Pulse Sensors. Note that several probes failed at the end of June 2010.
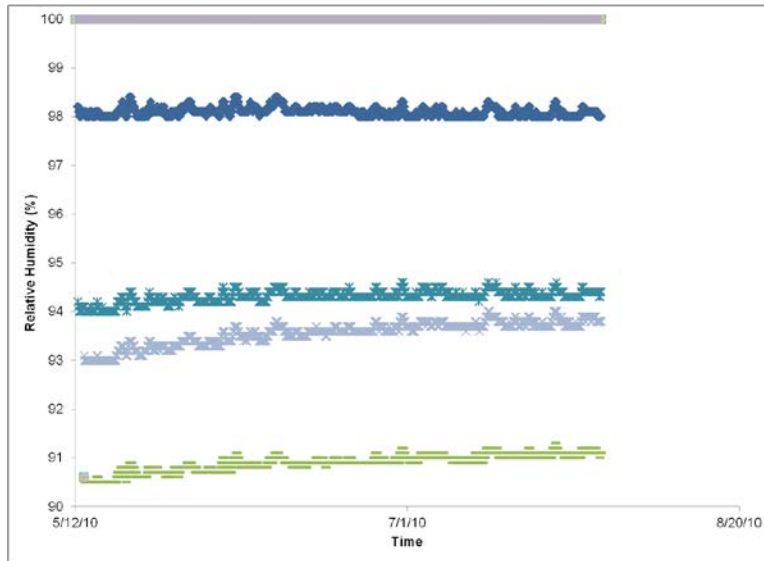
Figure 4.8. Equilibration Response for Humidity Probes

4.1.1.2   Desiccation Operational Data

Operational data were collected during injection and extraction operations at the test site. Of these parameters, the injected gas flow rate and temperature are key drivers for desiccation. Dry nitrogen (relative humidity of zero) was used for the injection gas during the test (Table 4.1). If ambient air were used, then the relative humidity of the injection gas would also be an important parameter as discussed in Section 4.2.4. Extraction parameters were also measured to define test conditions, but are not specifically related to the desiccation rate other than the impact on soil gas flow rates and patterns. Figure 4.9 shows the operational parameter data of injection gas flow and extraction flow rate for the duration of active desiccation. Injection gas temperature was held essentially constant at about 20°C. The extracted gas relative humidity was also measured. However, this parameter is significantly impacted by the temperature at the monitoring location. Because the monitoring location was above ground and not immediately at the extraction well, changes in temperature impacted the measured value. Based on the measured progression of the desiccated zone (other data), there is no expectation that the extracted soil gas would have less than a relative humidity of 100%.

Table 4.1. Summary of Injected Gas Volumes

Time On		Time Off		Cumulative Volume Injection (m^3)
11/22/2010	09:00	11/23/2010	10:24	12,812
11/29/2010	11:13	11/30/2010	08:20	16,354
12/2/2010	09:40	12/6/2010	11:40	32,969
1/17/2011	15:35	4/21/2011	13:00	1,108,884
5/2/2011	12:30	5/2/2011	12:45	1,109,014
5/4/2011	10:15	6/30/2011	13:55	1,799,790
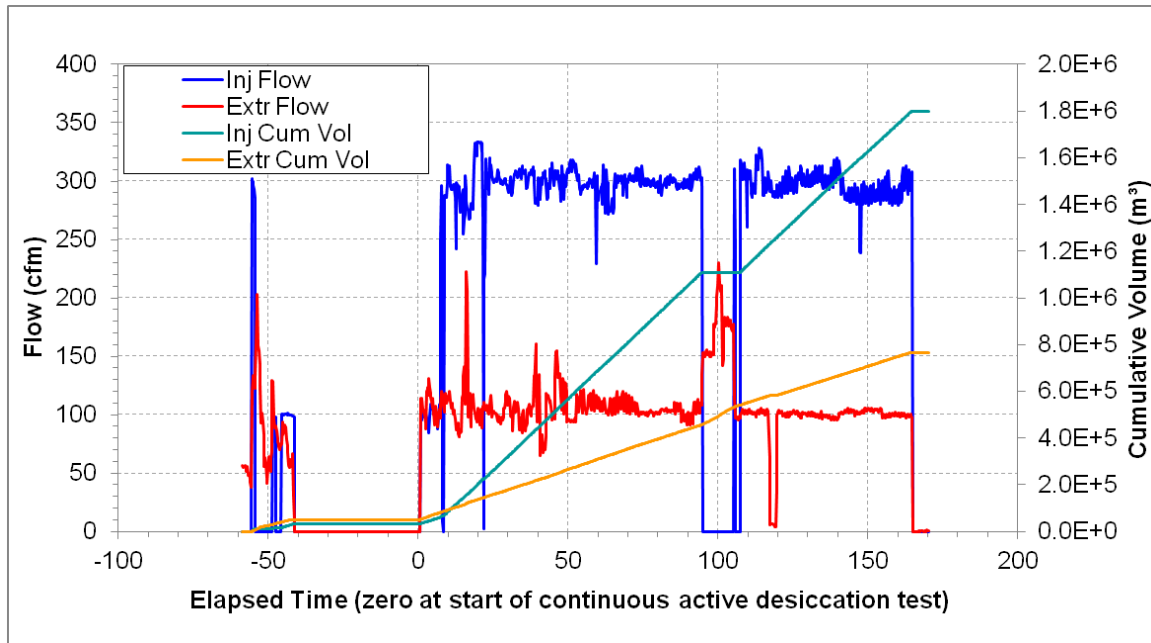
Figure 4.9. Flow Conditions and Cumulative Volumes for Field Test Operations

As desiccation progressed, reduced moisture was expected to increase the air permeability of the subsurface. Tracer data was collected again at day 107 (Figure 4.10) to examine the difference in injected gas flow rate distribution compared to the pre-desiccation tracer test results (Figure 4.5). This assessment along with other data to evaluate the distribution of dry gas from the injection well can be used to assess the uniformity of the desiccation process. Figure 4.10 shows the day 107 tracer data compared to the initial tracer response. Both the initial and day 107 tracer data show a very short term drop in oxygen that is interpreted as a small fast-path for injected gas flow. The fast-path response is accentuated in the day 107 tracer response, as would be expected with desiccation making this path more permeable and potentially larger in size. The bulk gas response occurs later in time as the more gradual drop in oxygen concentration for both the day 107 and initial tracer data. The time of this bulk drop is very similar for both day 107 and initial tracer, indicating that the impact of desiccation on the bulk gas flow was small at day 107. Note that these responses are for wells where only a minor desiccation response was observed; the dominant desiccation response occurred closer to the injection well.

4.8
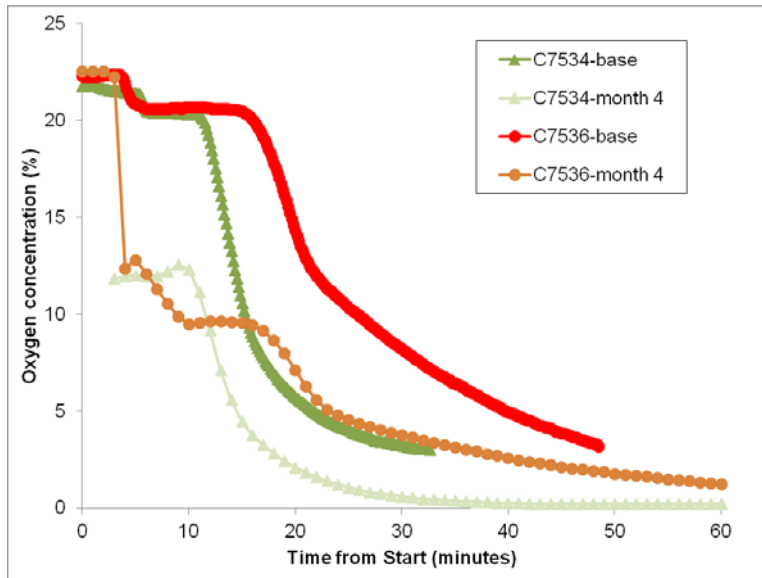
Figure 4.10. Comparison of Baseline and Day 107 (month 4) Tracer Responses at the 47 ft (14.3 m) bgs Depth Interval for Monitoring Locations C7534 and C7536

4.1.2   Active Desiccation

Performance of the desiccation process in terms of reducing the moisture content was quantified using several types of data and analyses. Both discrete and spatial analyses were used in assessing the active desiccation process. Data from individual sensors and single logging locations are presented first, followed by data analyzed to provide spatial information about the desiccation process. The final section presents results of analyses on condensate collected during active desiccation.

4.1.2.1   Sensor and Discrete Location Data

The lateral locations of sensor boreholes containing in situ sensors and ERT electrodes and the location of wells for neutron moisture logging and GPR access are shown in Figure 3.4 (Section 3.2.2). In situ sensors were emplaced to provide a detailed temporal response to desiccation at the monitoring locations. Temperature data over time at the nominal sensor interval depths are presented in Figure 4.11 through Figure 4.14. Matric potential (HDUs), moisture content (DPHP sensors), and humidity data are presented at the sensor depth intervals in Figure 4.15 through Figure 4.26. None of the TCPs provided meaningful data. Periodically, neutron moisture logging was conducted to examine how the vertical profile of moisture content changed at the monitoring locations (Figure 4.27 through Figure 4.33). A summary of changes in neutron moisture probe during active desiccation are presented in Figure 4.34 through Figure 4.36. Neutron moisture information at the injection well (Figure 4.37) shows locations of dominant injected gas flow at those intervals that start drying first (e.g., flow occurs mainly in the upper and lower portion of the screen).

At the completion of active desiccation, two boreholes were drilled to collect samples for laboratory analysis of moisture content and for Tc-99 and nitrate concentration. Data for the core analyses are contained in Appendix A and summarized on Table 4.2.
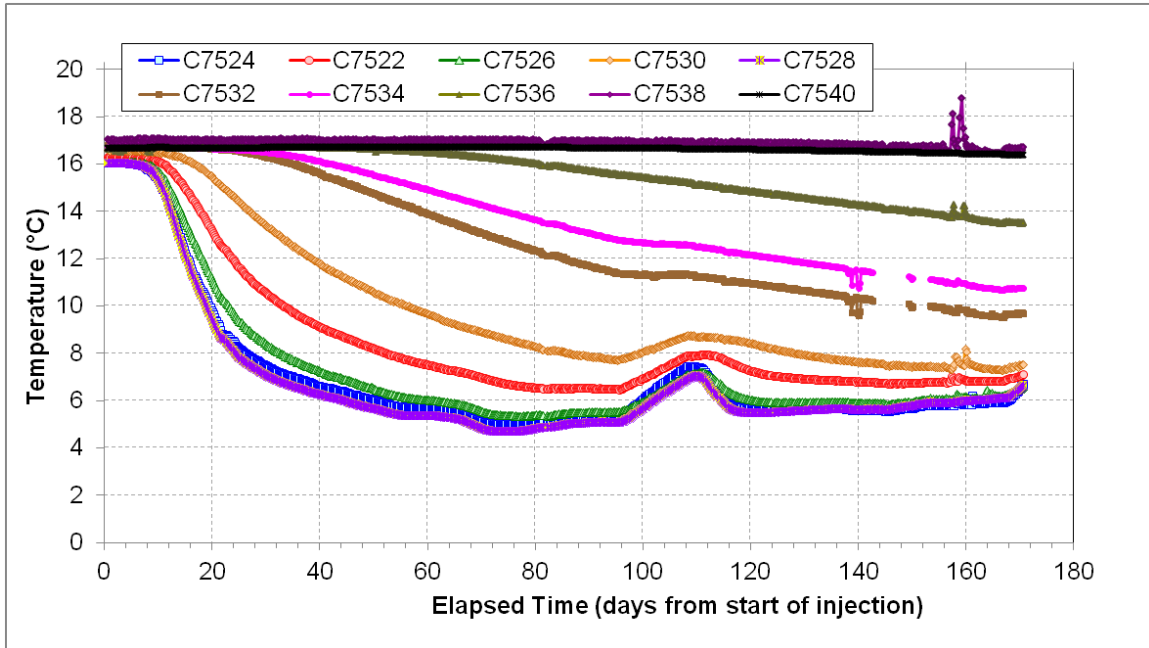
Figure 4.11. Temperature Response over Time for the Sensors at a Depth of 32.5 ft (9.9 m) Below Ground Surface
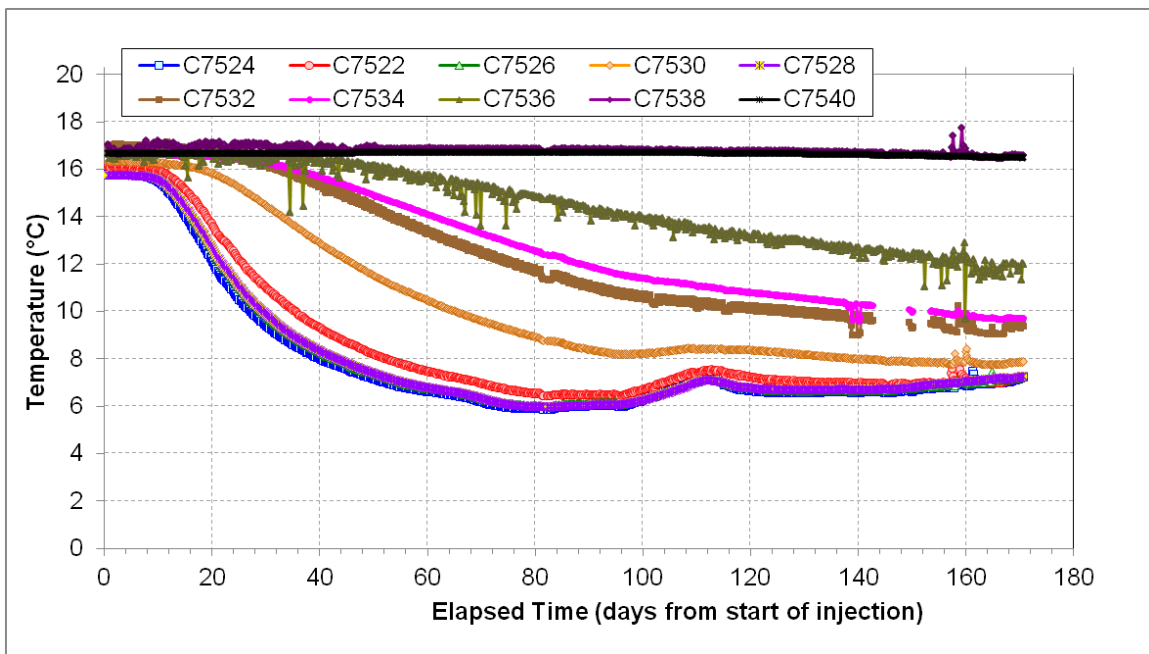
Figure 4.12. Temperature Response over Time for the Sensors at a Depth of 36.5 ft (11.1 m) Below Ground Surface
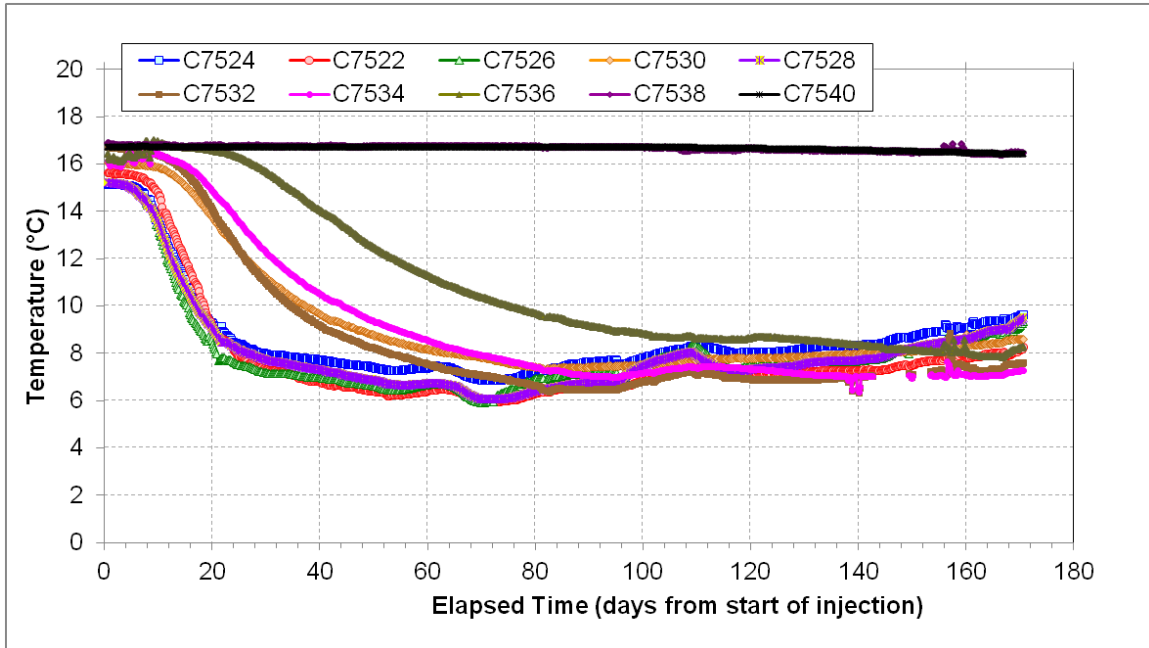
Figure 4.13. Temperature Response over Time for the Sensors at a Depth of 42.5 ft (13 m) Below Ground Surface
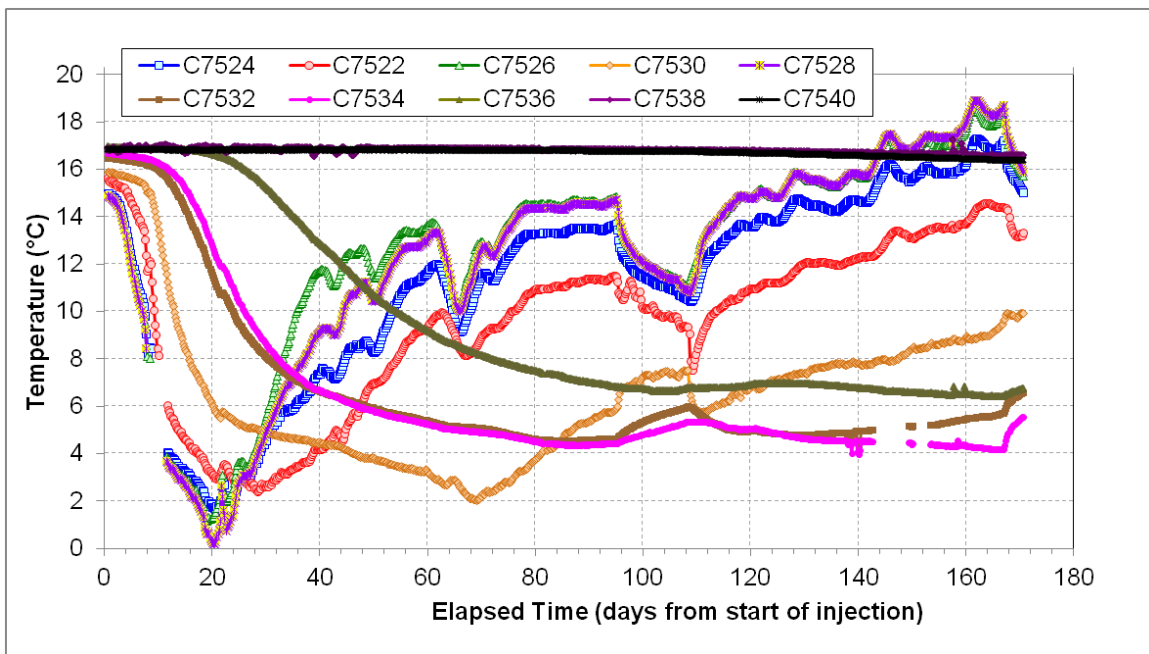
Figure 4.14. Temperature Response over Time for the Sensors at a Depth of 46.5 ft (14.2 m) Below Ground Surface
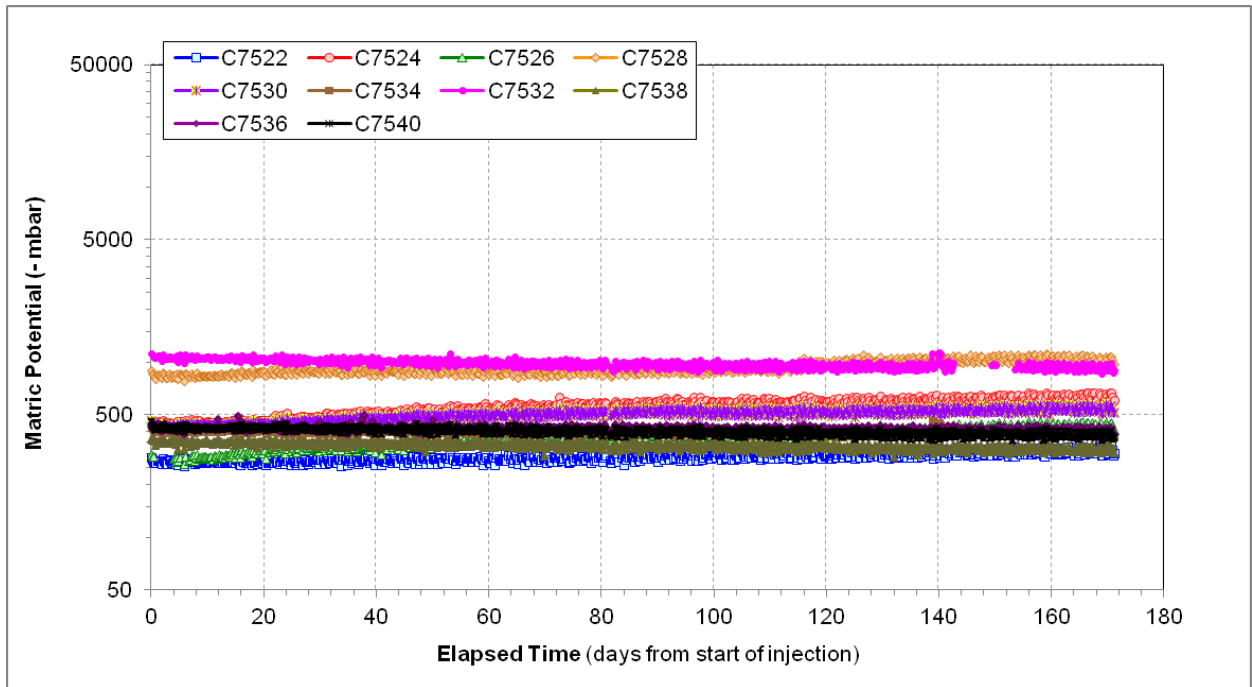
Figure 4.15. Heat Dissipation Unit (matric potential) Response over Time for the Sensors at a Depth of 32.5 ft (9.9 m) Below Ground Surface
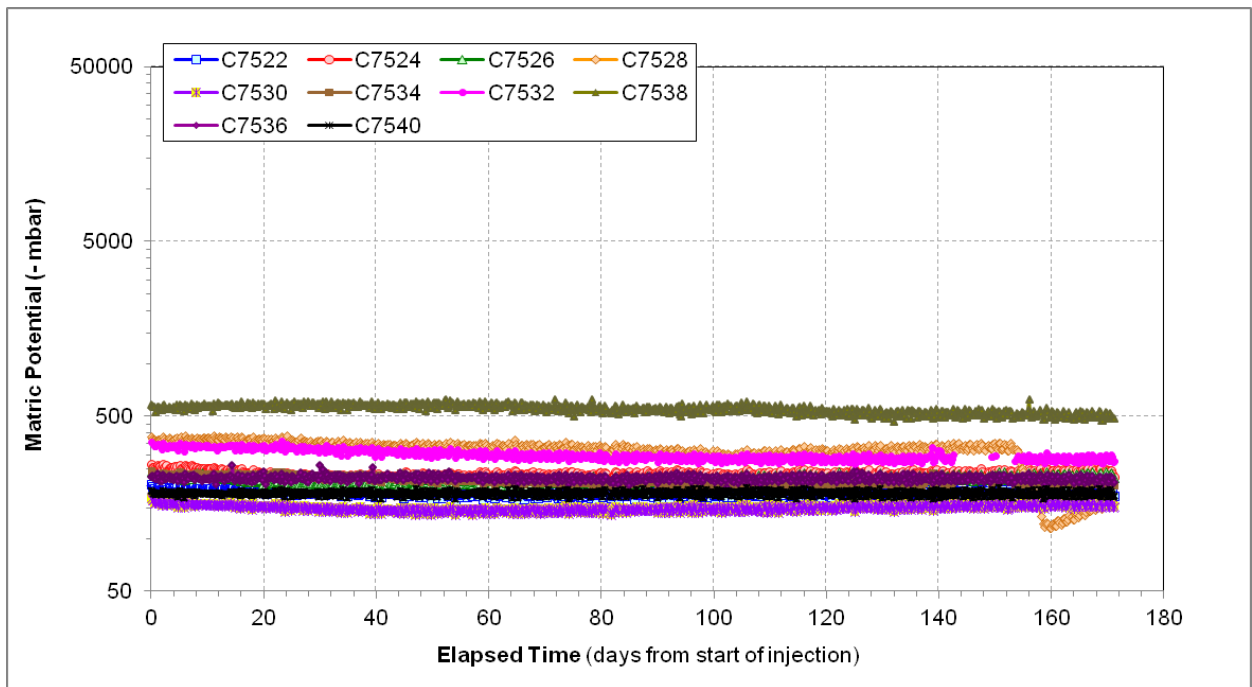
Figure 4.16. Heat Dissipation Unit (matric potential) Response over Time for the Sensors at a Depth of 37.5 ft (11.4 m) Below Ground Surface
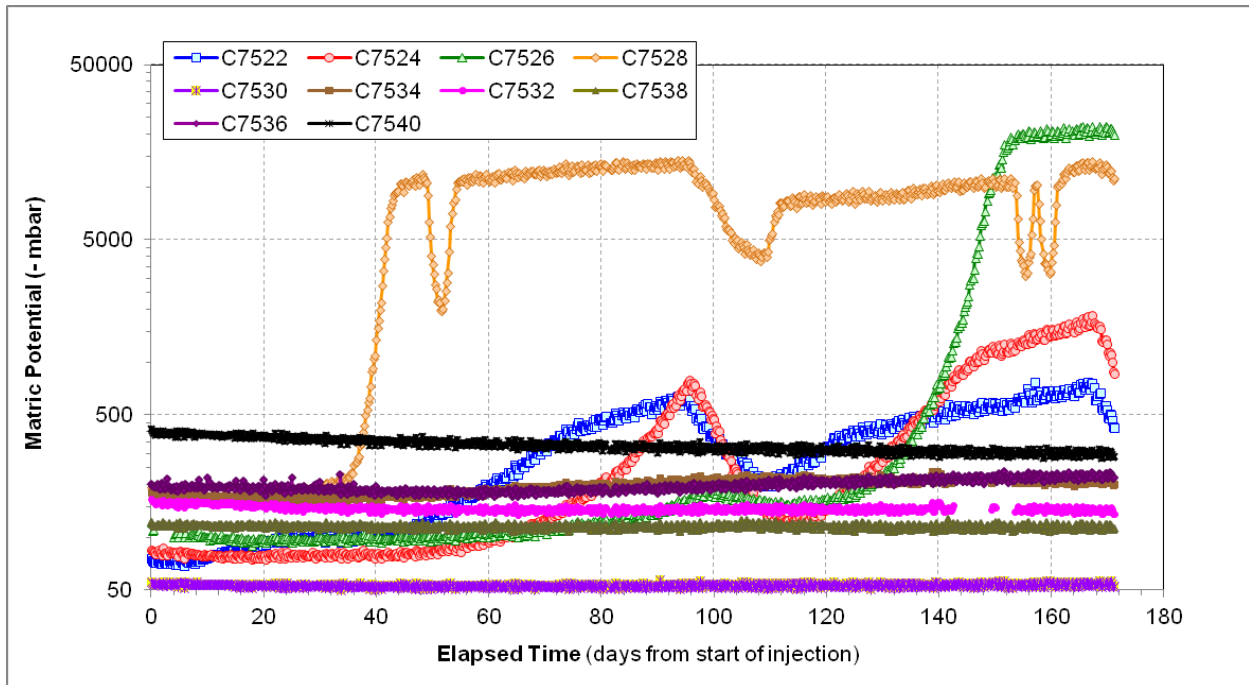
Figure 4.17. Heat Dissipation Unit (matric potential) Response over Time for the Sensors at a Depth of 42.5 ft (13 m) Below Ground Surface
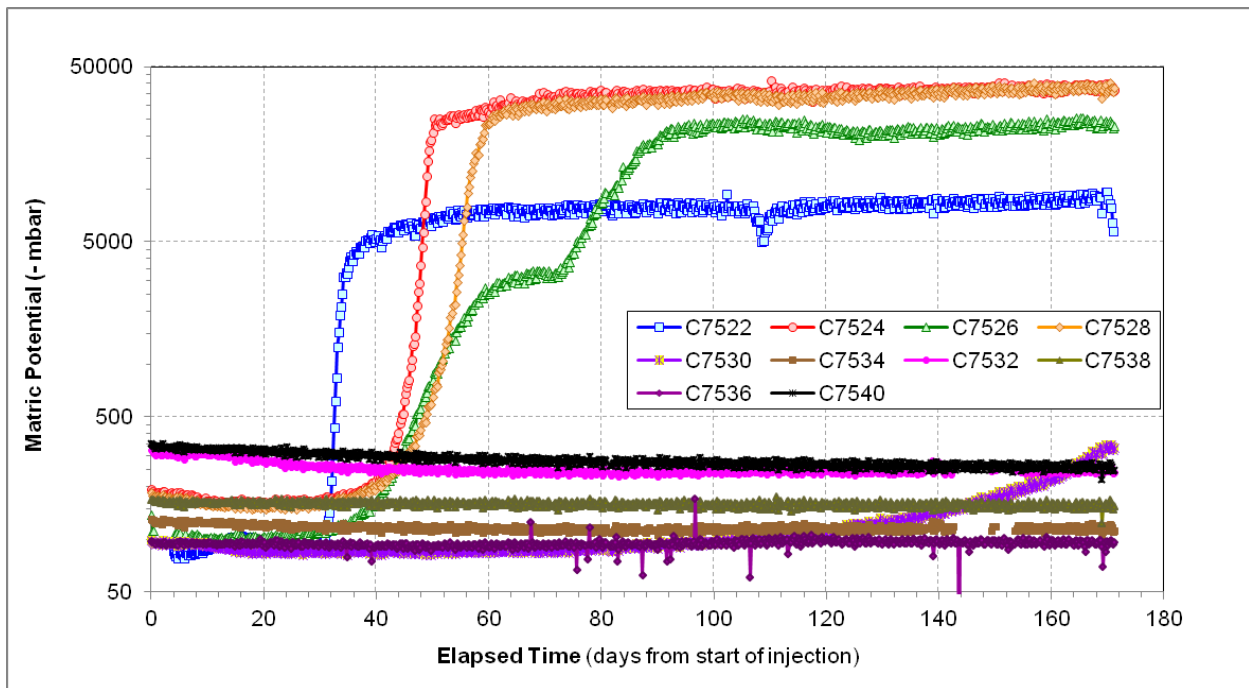
Figure 4.18. Heat Dissipation Unit (matric potential) Response over Time for the Sensors at a Depth of 47.5 ft (14.5 m) Below Ground Surface
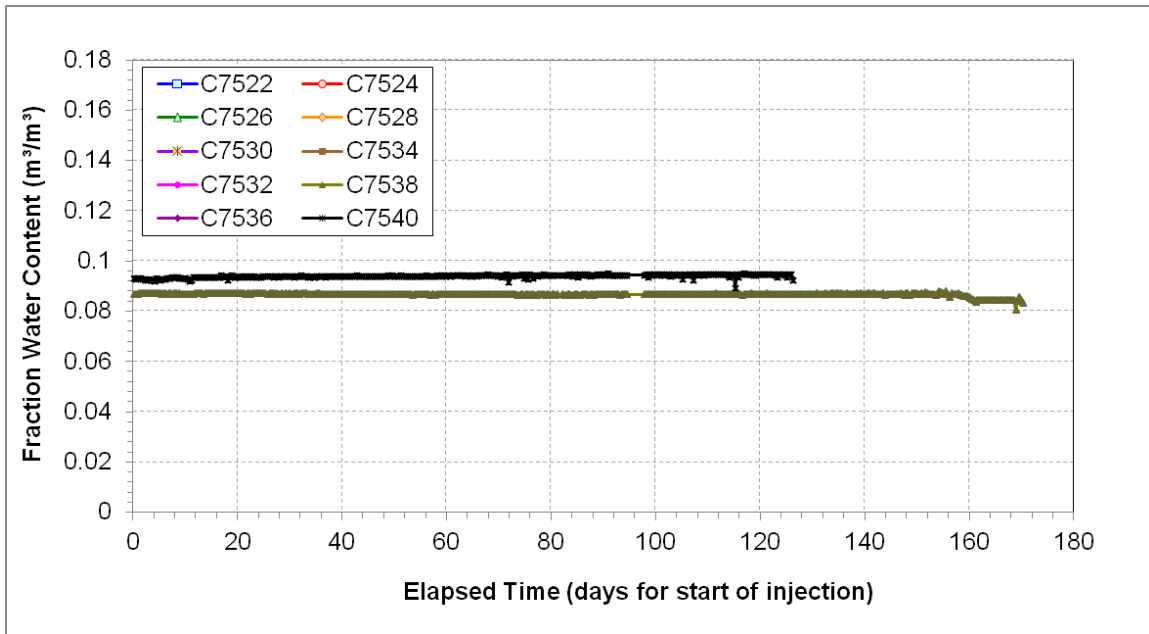
Figure 4.19. Dual-Probe Heat-Pulse Sensor (moisture content) Response over Time for the Sensors at a Depth of 32.5 ft (9.9 m) Below Ground Surface
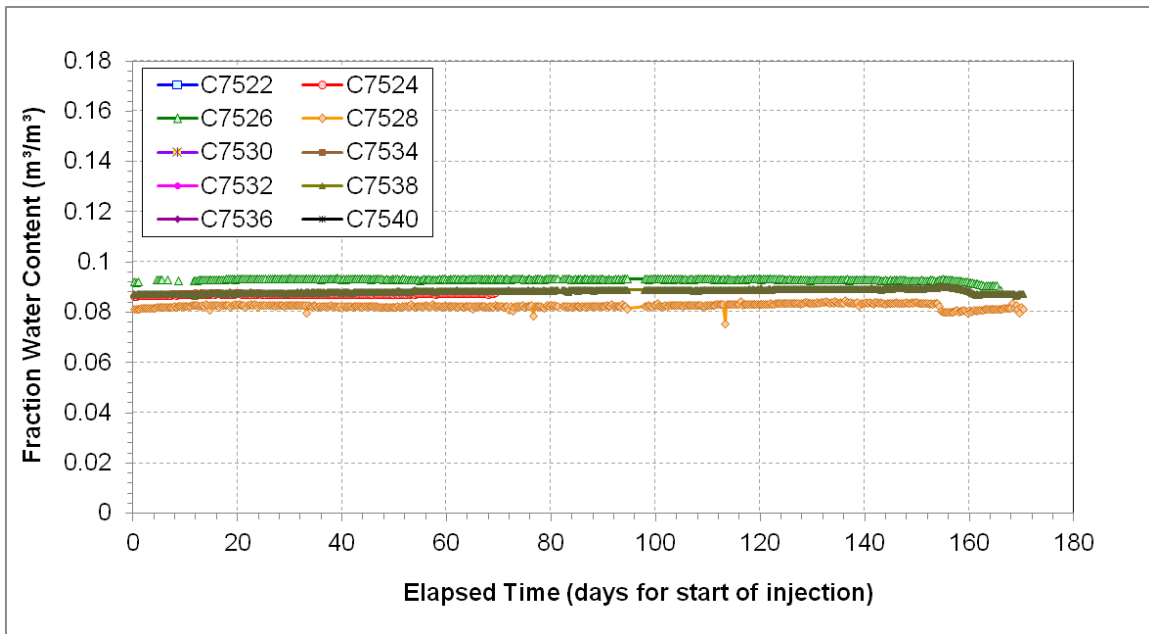
Figure 4.20. Dual-Probe Heat-Pulse Sensor (moisture content) Response over Time for the Sensors at a Depth of 37.5 ft (11.4 m) Below Ground Surface

4.14
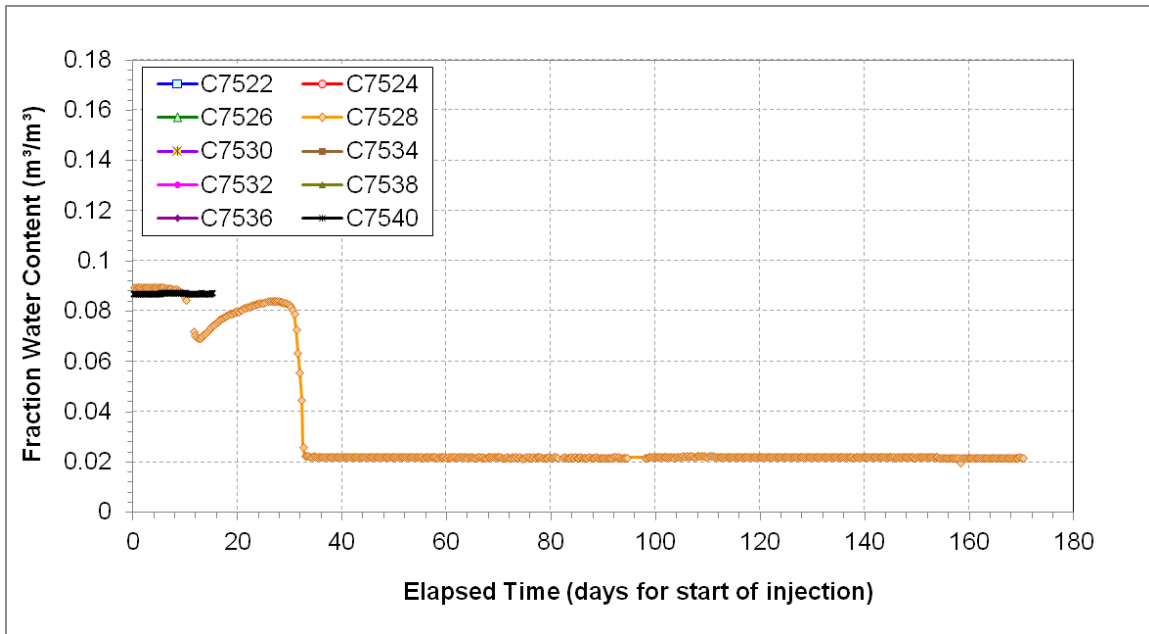
Figure 4.21. Dual-Probe Heat-Pulse Sensor (moisture content) Response over Time for the Sensors at a Depth of 42.5 ft (13 m) Below Ground Surface
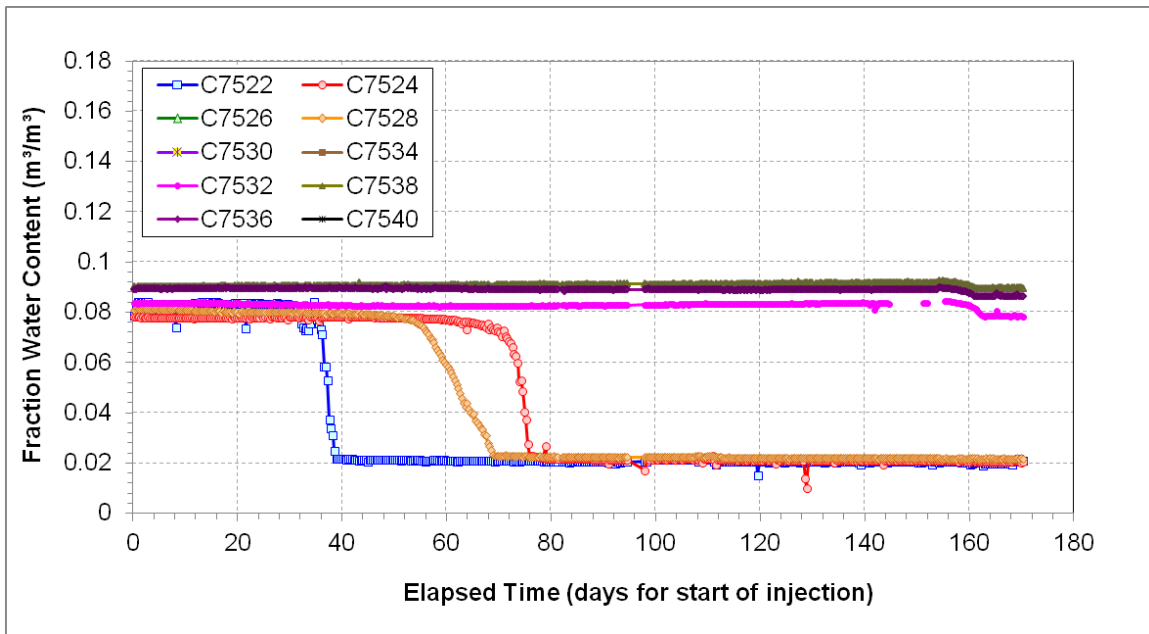
Figure 4.22. Dual-Probe Heat-Pulse Sensor (moisture content) Response over Time for the Sensors at a Depth of 47.5 ft (14.5 m) Below Ground Surface
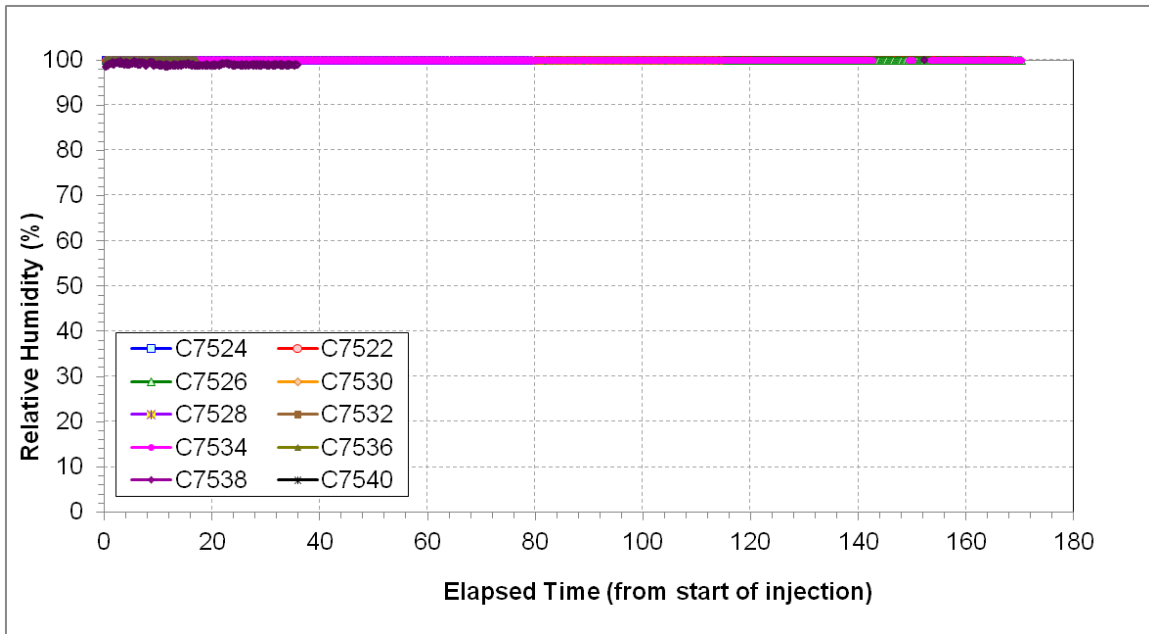
Figure 4.23. Relative Humidity Probe Response over Time for the Sensors at a Depth of 32.5 ft (9.9 m) Below Ground Surface
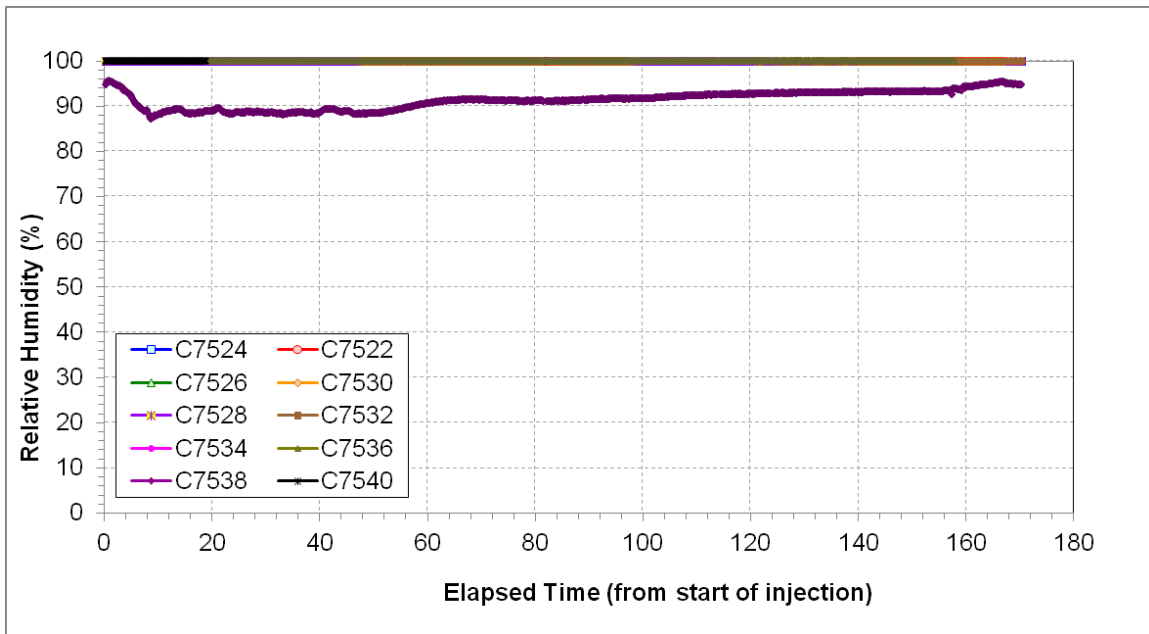
Figure 4.24. Relative Humidity Probe Response over Time for the Sensors at a Depth of 37.5 ft (11.4 m) Below Ground Surface
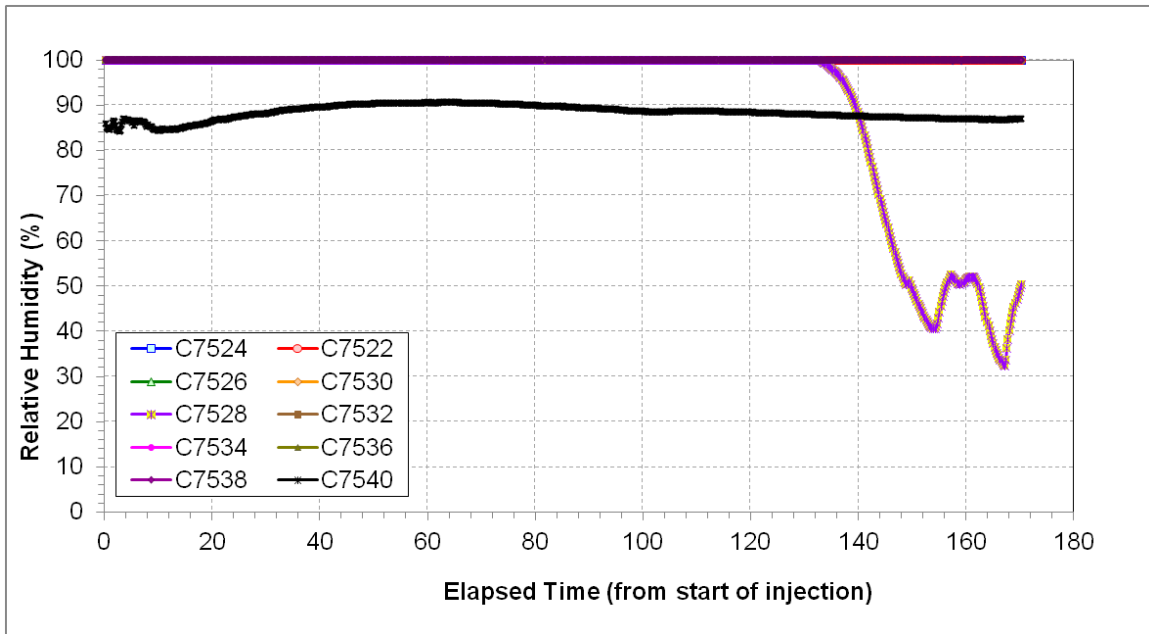
Figure 4.25. Relative Humidity Probe Response over Time for the Sensors at a Depth of 42.5 ft (13 m) Below Ground Surface
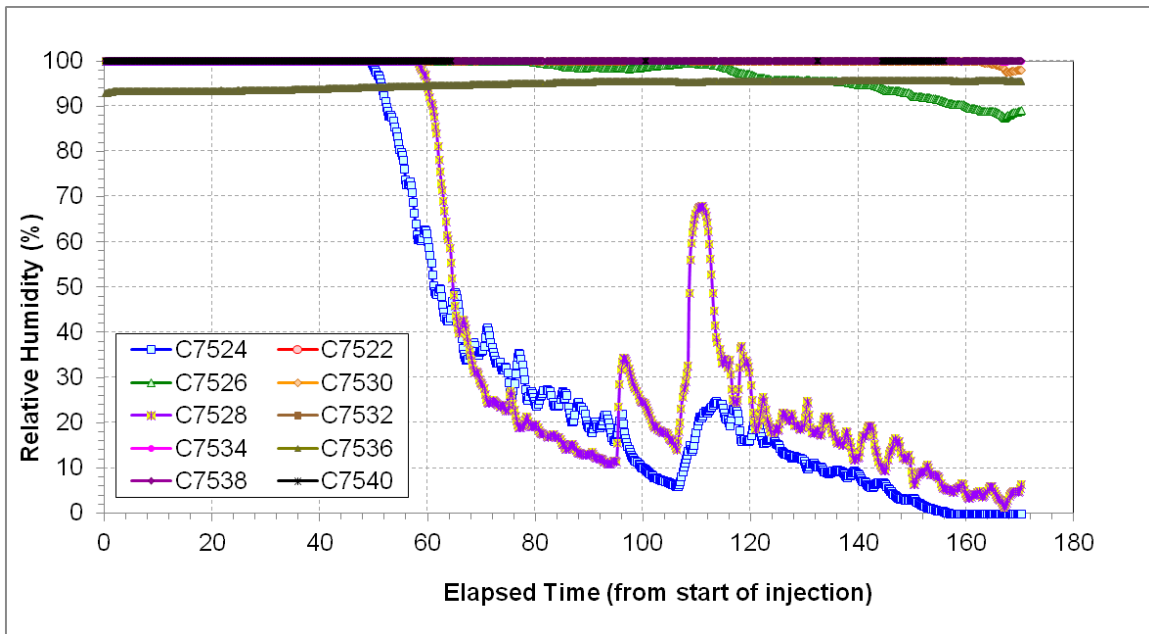
Figure 4.26. Relative Humidity Probe Response over Time for the Sensors at a Depth of 47.5 ft (14.5 m) Below Ground Surface
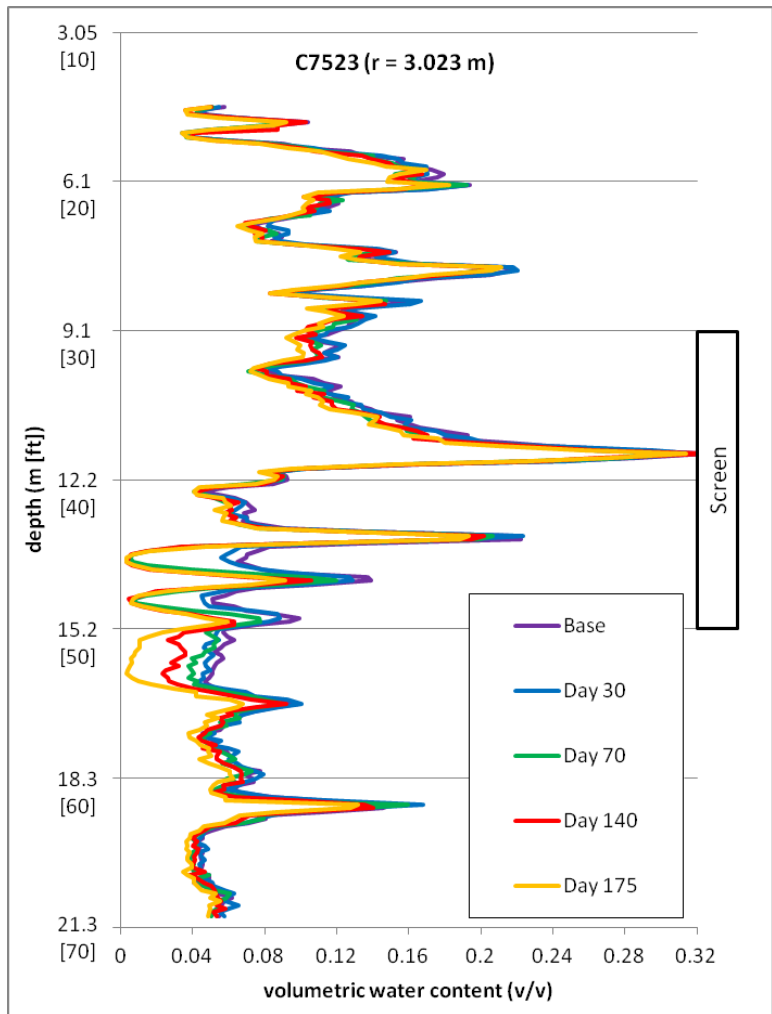
Figure 4.27. Neutron Moisture Probe Response over Time for Location C7523 (3.023 m [9.8 ft] from injection well). The base time is a logging event in December 2010, prior to the continuous active desiccation period. Other data are for logging events in nominal days from the start of active desiccation.
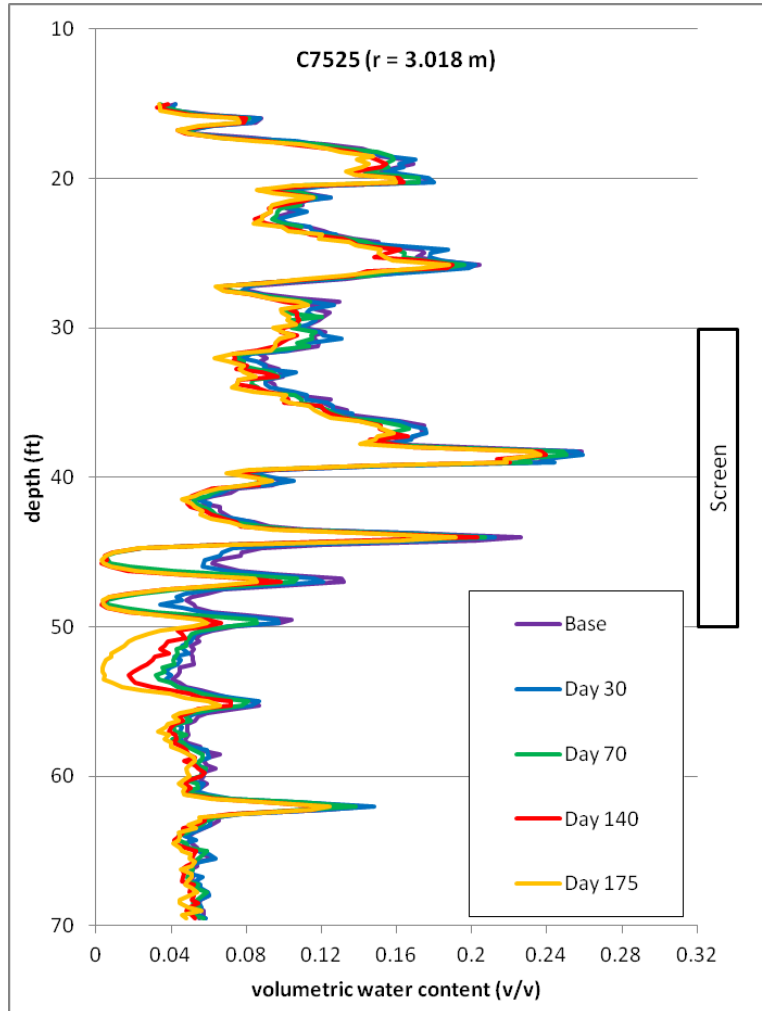
Figure 4.28. Neutron Moisture Probe Response over Time for Location C7525 (3.018 m [9.8 ft] from injection well). The base time is a logging event in December 2010, prior to the continuous active desiccation period. Other data are for logging events in nominal days from the start of active desiccation.
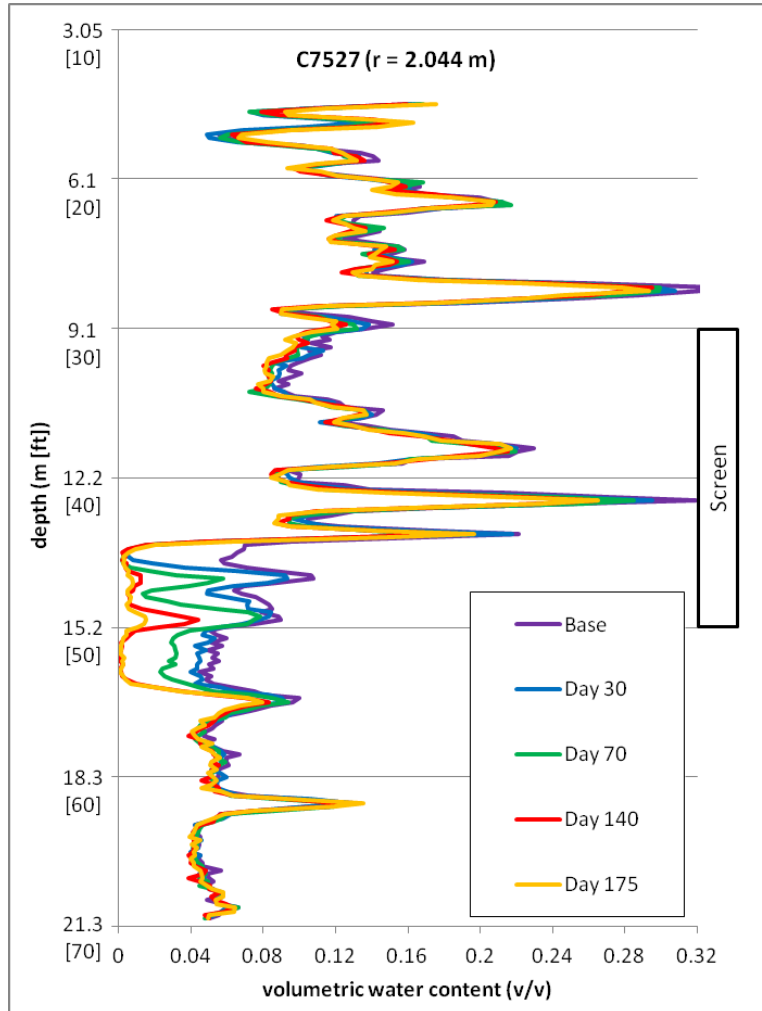
Figure 4.29. Neutron Moisture Probe Response over Time for Location C7527 (2.044 m [6.6 ft] from injection well). The base time is a logging event in December 2010, prior to the continuous active desiccation period. Other data are for logging events in nominal days from the start of active desiccation.
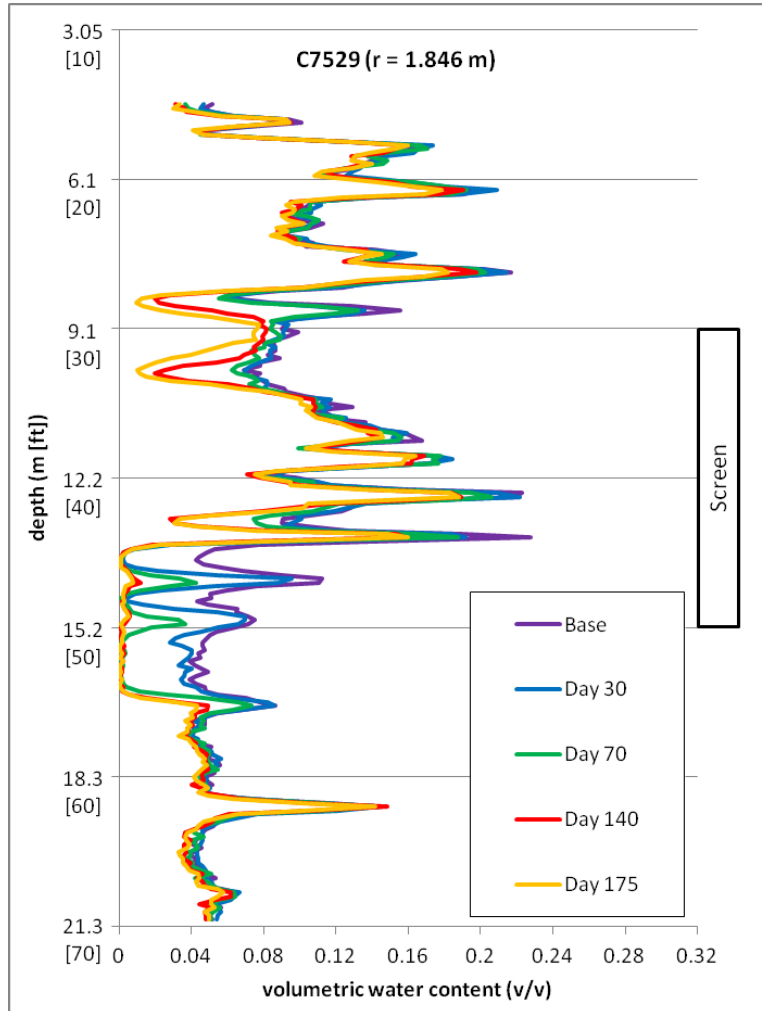
Figure 4.30. Neutron Moisture Probe Response over Time for Location C7529 (1.846 m [6 ft] from injection well). The base time is a logging event in December 2010, prior to the continuous active desiccation period. Other data are for logging events in nominal days from the start of active desiccation.
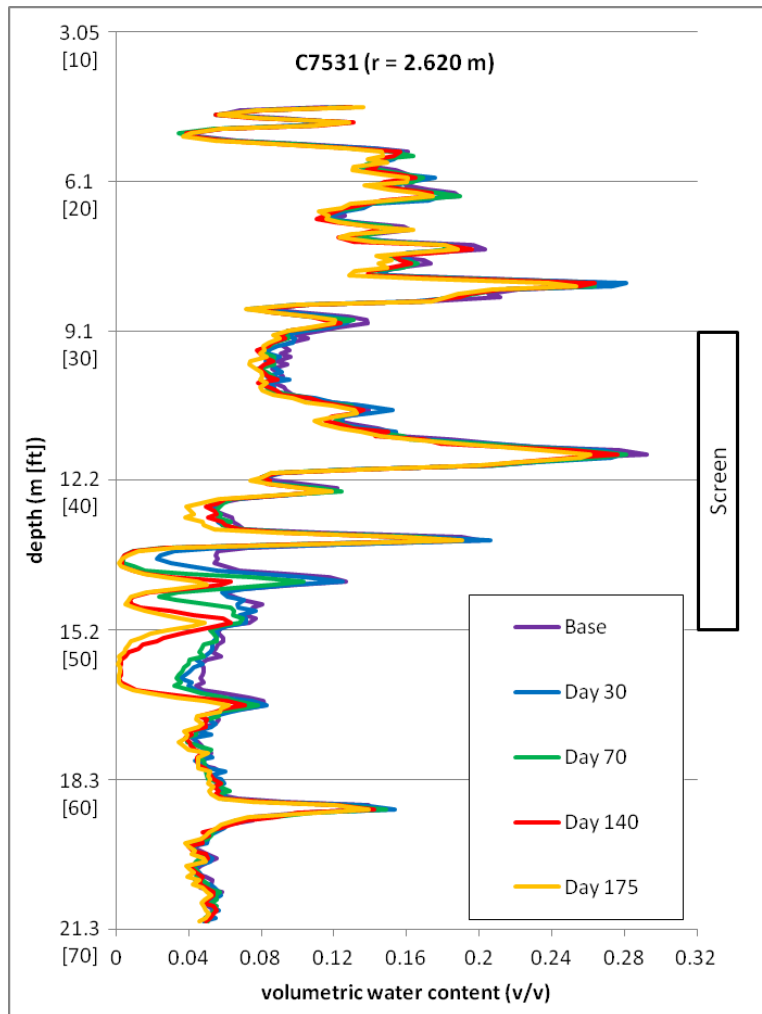
Figure 4.31. Neutron Moisture Probe Response over Time for Location C7531 (2.620 m [8.5 ft] from injection well). This location is along the axis between the injection and extraction wells. The base time is a logging event in December 2010, prior to the continuous active desiccation period. Other data are for logging events in nominal days from the start of active desiccation.
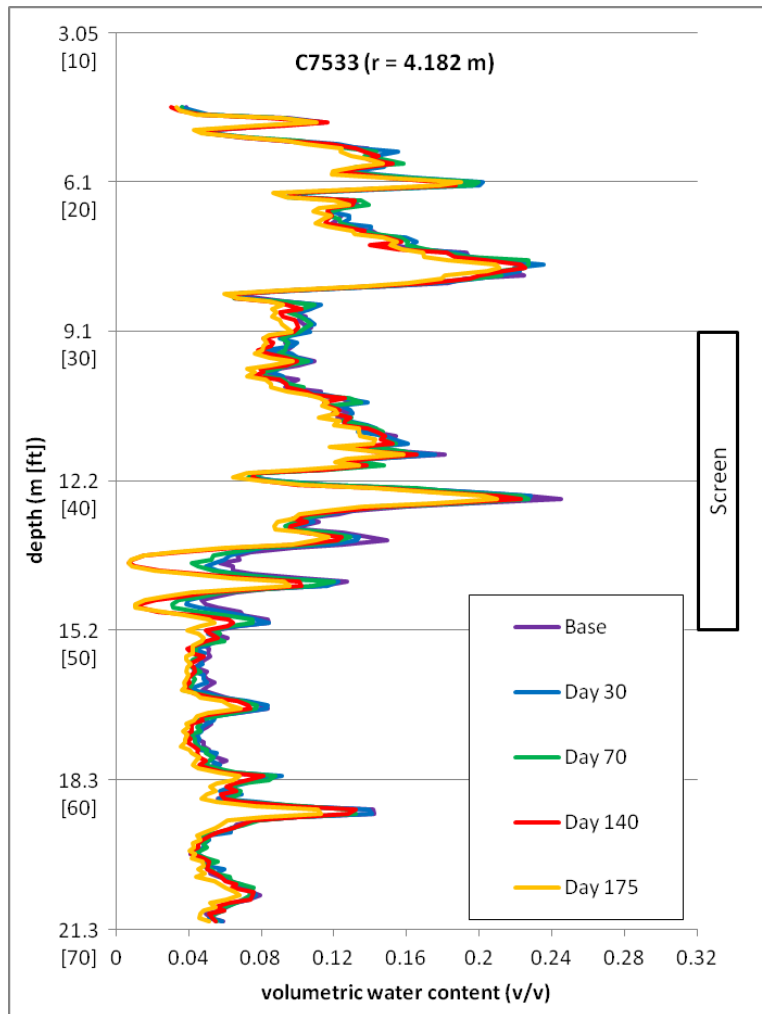
Figure 4.32. Neutron Moisture Probe Response over Time for Location C7533 (4.182 m [13.7 ft] from injection well). The base time is a logging event in December 2010, prior to the continuous active desiccation period. Other data are for logging events in nominal days from the start of active desiccation.
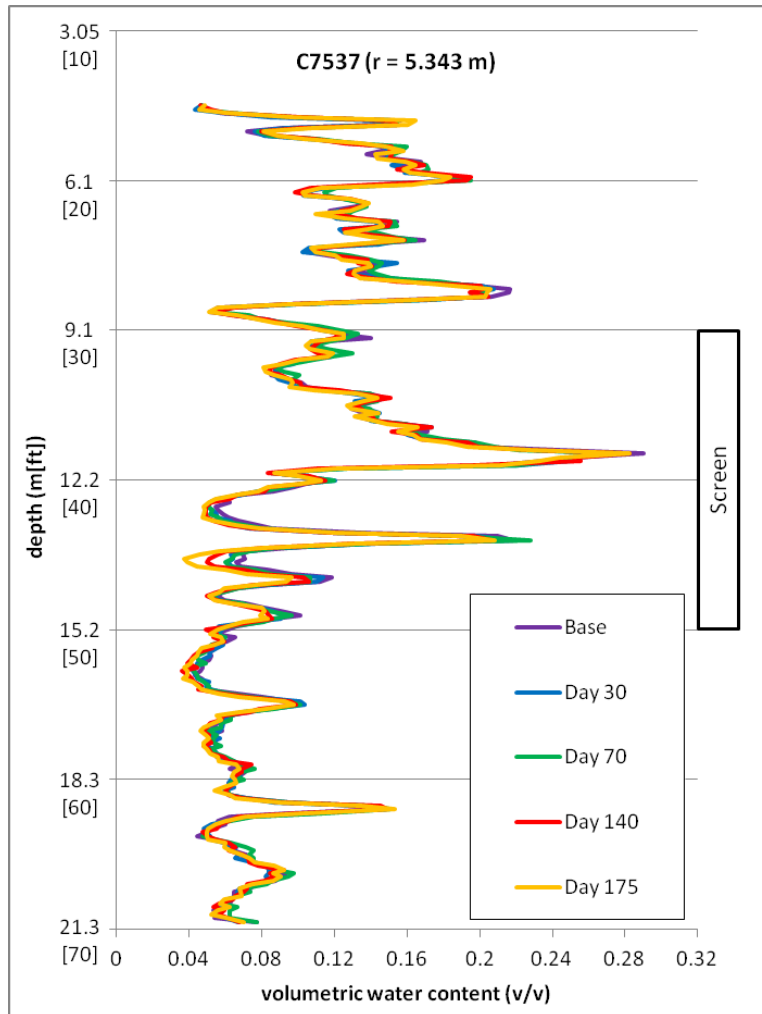
Figure 4.33. Neutron Moisture Probe Response over Time for Location C7537 (5.343 m [17.5 ft] from injection well). This location is along the axis between the injection and extraction wells. The base time is a logging event in December 2010, prior to the continuous active desiccation period. Other data are for logging events in nominal days from the start of active desiccation.
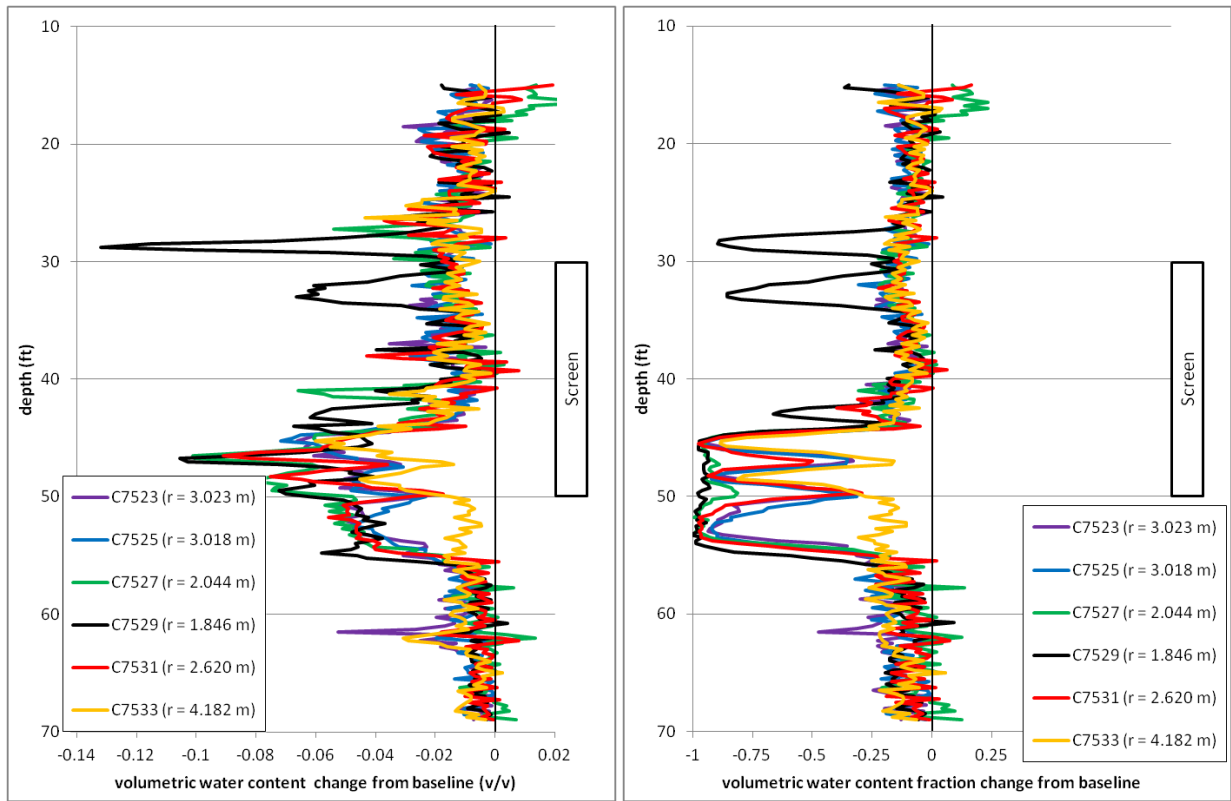
Figure 4.34. Change in Water Content at the End of Active Desiccation (day 175, July 2011) Compared to Pre-desiccation Baseline (December 2010) Based on Neutron Moisture Probe Data for Locations C7523, C7525, C7527, C7529, C7531, and C7533
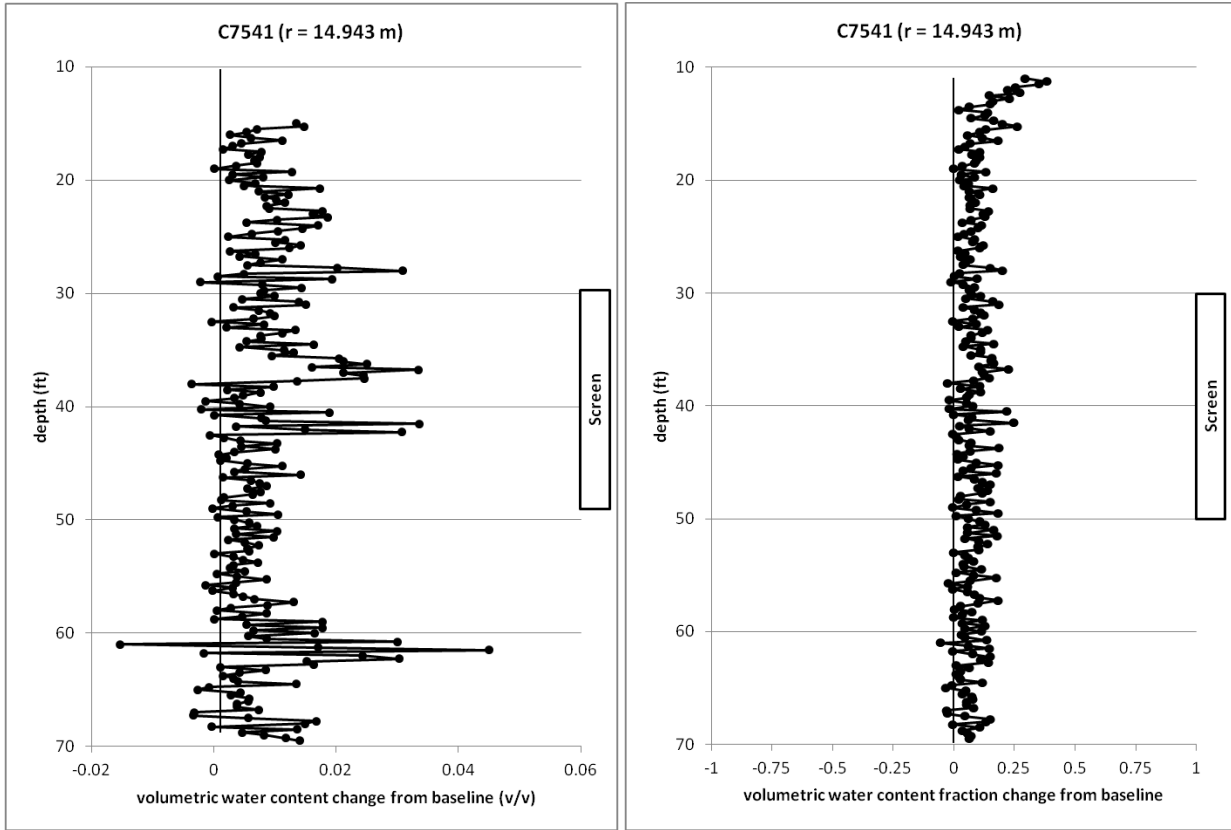
Figure 4.35. Change in Water Content at the End of Active Desiccation (day 175, July 2011) Compared to Pre-desiccation Baseline (December 2010) Based on Neutron Moisture Probe Data for Location C7541, Near the Extraction Well on the Side Opposite from the Injection Well
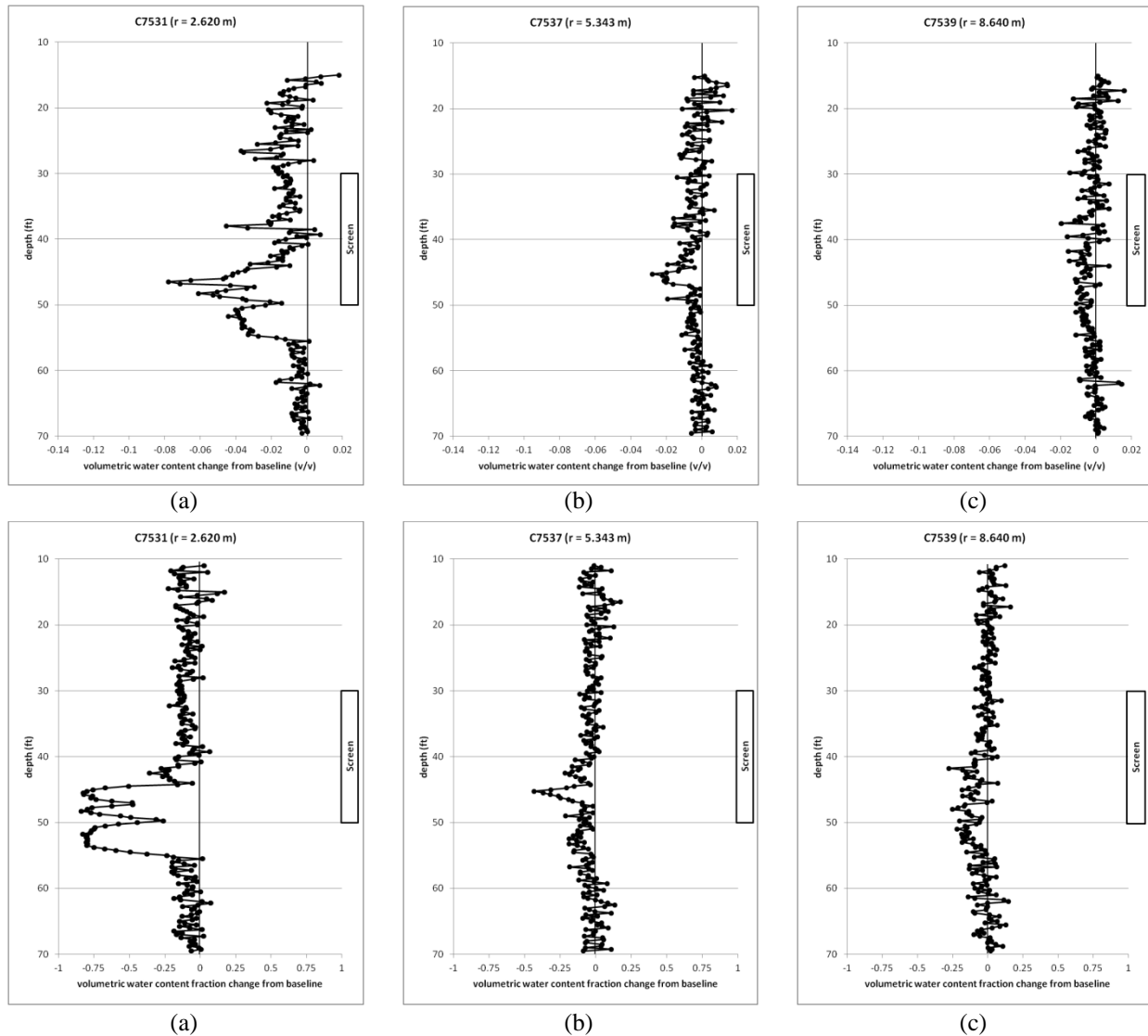
Figure 4.36. Change in Water Content at the End of Active Desiccation (day 175, July 2011) Compared to Pre-desiccation Baseline (December 2010) Based on Neutron Moisture Probe Data for Locations (a) C7531, (b) C7537, and (c) C7539, Along the Axis Between the Injection and Extraction Wells at Distances of 2.62 m, 5.343 m, and 8.64 m (8.5 ft, 17.5 ft, and 28 ft) from the Injection Well, Respectively
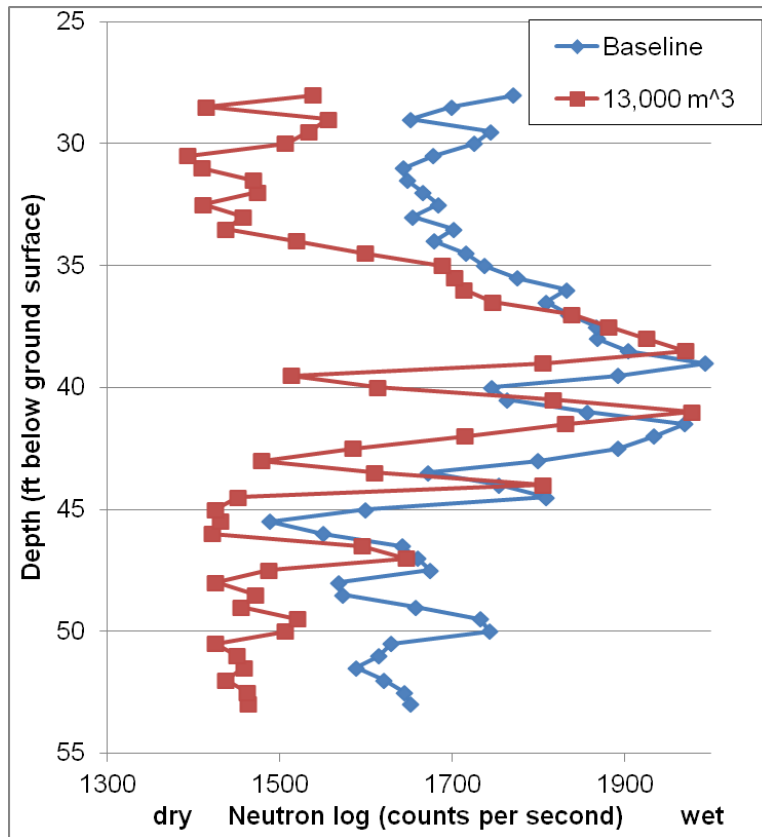
Figure 4.37. Neutron Moisture Log Response in the Injection Well Comparing Pre-injection (baseline) and after 13,000 m^3 of Dry Nitrogen Was Injected

Table 4.2. Post-Desiccation Sediment Core Analysis Results. Data from additional core samples for gravimetric and volumetric moisture content are shown in Appendix A.

Begin Depth Feet	End Depth Feet	Moisture Content % by Weight	Tc-99 µg/g dry	Tc-99 pCi/g dry	Nitrate µg/g dry
Core C8388					
20.15	22.65	9.94	<3.90E-05	<6.63E-01	1.48E+01
22	24.5	5.78	<3.92E-05	<6.66E-01	8.27E+00
24	26.5	6.19	<3.90E-05	<6.63E-01	8.57E+00
26.9	29.4	17.3	<3.90E-05	<6.63E-01	5.67E+01
29.7	32.2	5.87	3.87E-04	6.58E+00	9.68E+02
32.58	35.08	5.93	<3.90E-05	<6.63E-01	7.41E+01
35.5	38	6.57	2.74E-04	4.66E+00	4.25E+02
38.3	40.8	16.4	2.03E-03	3.45E+01	4.52E+03
40.5	43	10.5	5.59E-04	9.50E+00	1.45E+03
43.08	45.58	11.7	3.76E-03	6.39E+01	7.77E+03
45.2	47.7	0.319	9.71E-04	1.65E+01	2.04E+03
47.5	50	0.467	1.99E-03	3.38E+01	3.63E+03
50.1	52.6	0.408	4.12E-03	7.00E+01	5.23E+03
52.5	55	0.475	2.57E-03	4.37E+01	3.52E+03
55.6	58.1	3.03	1.60E-03	2.72E+01	3.00E+03
58	60.5	3.15	1.93E-03	3.28E+01	3.59E+03
Core C8387					
20	23.1	5.62	<3.90E-05	<6.63E-01	8.28E+00
22.3	24.8	5.07	<3.90E-05	<6.63E-01	5.44E+00
25	27.5	12.9	<3.90E-05	<6.63E-01	6.93E+01
27.5	30	4.58	<3.90E-05	<6.63E-01	2.36E+01
30	32.6	6.52	9.91E-05	1.68E+00	1.39E+02
32.8	35.3	6.86	<3.90E-05	<6.63E-01	3.90E+01
35.2	37.7	8.48	6.62E-04	1.13E+01	1.26E+03
37.5	40	9.02	4.10E-03	6.97E+01	7.45E+03
39.9	42.4	6.25	4.28E-03	7.28E+01	5.86E+03
42.7	45.2	4.15	2.06E-03	3.50E+01	3.54E+03
45.3	47.8	1.5	2.64E-03	4.49E+01	4.20E+03
47.6	50.1	2.78	9.54E-04	1.62E+01	3.03E+03
49.75	52.25	3.03	4.67E-03	7.94E+01	6.52E+03
52.8	55.3	2.24	4.18E-03	7.11E+01	5.61E+03
55.5	58	2.57	2.75E-03	4.68E+01	4.53E+03
58.3	60.8	3.12	2.84E-03	4.83E+01	4.27E+03

4.1.2.2   Spatial Analysis of Desiccation

Imaging of the desiccation process in two and three dimensions was also conducting using temperature, neutron, cross-hole ERT, and cross-hole GPR data. The numerous temperature sensors (0.6-m [2-ft] vertical interval) at the monitoring boreholes provided a spatially dense set of data for temperature. Thus,

temperature data were interpolated to produce two- and three-dimensional depictions of the temperature distribution at selected time points during the desiccation process. The neutron data were collected at frequent intervals (7.5 cm [3 in]) during vertical logging at the monitoring boreholes, providing a spatially dense set of data. Thus, the neutron moisture data were also interpolated to produce two- and three-dimensional depictions of the volumetric water content distribution at selected time points during the desiccation process. The ERT system enabled collection of cross-hole data twice daily. These data were interpreted to provide a temporal depiction of the two- and three-dimensional change in moisture conditions. Periodically, GPR data were collected from cross-borehole pairs and used to interpret moisture content changes for two-dimensional zones between logging locations. These two dimensional responses provided information about moisture content changes between monitoring locations.

Monitoring the progression of desiccation in the subsurface provides information to guide operational decisions such as modification of the injected gas temperature and flow rate. While nominal values for these injection parameters can be selected based on initial site characterization data, the impact of subsurface heterogeneities cannot be fully predicted and monitoring data to assess the impact of these heterogeneities on desiccation performance is needed. Monitoring data are also needed to determine when the size of the desiccated zone and the final moisture content are sufficient to meet the overall goals for the desiccation remedy. For desiccation, the performance in terms of slowing contaminant movement is a function of the final moisture content in relation to the residual moisture content value for the porous medium. When the moisture content is reduced below the residual moisture content value, porous medium water relative permeability is essentially zero and the remaining water cannot migrate as a result of pressure gradients. Additionally, the physical size of the desiccated zone and conditions at the desiccation zone boundaries impact the overall long-term performance of desiccation in reducing the moisture and contaminant flux to groundwater (Truex et al. 2011). The monitoring methods evaluated in the field test have the potential to provide the above type of data as part of implementing a desiccation remedy.

Temperature sensors can provide a means to monitor the progress and distribution of desiccation using an in situ network of sensors. Temperature decreases due to evaporative cooling until the desiccation front reaches the monitoring locations (i.e., the time when the sediment between the injection location and the monitoring location is desiccated). At that time, the temperature at the monitoring location begins to increase toward the temperature of the injected gas because evaporative cooling is no longer occurring in the sediment between the injection location and the monitoring location (Oostrom et al. 2009). There can be multiple inflection points if there are multiple layers that are being desiccated at different rates and these layers are within a region that can impact the temperature at the monitoring location. Figure 4.38 shows two-dimensional interpolations of temperature sensor data during active desiccation at days 20, 45, 90, and 164 (the end of dry gas injection) (see Appendix B for additional temperature plots). The progression of cooled zones shown at days 20 and 45 are indicators of desiccation activity and the related dominant injected dry gas flow pattern. By days 90 and 164, localized warming indicates that some zones have been desiccated, while desiccation, as indicated by cooler temperatures continues to occur at other locations.

Temperature variations impact the distribution of desiccation because temperature impacts the water-holding capacity of the gas. Evaporative cooling causes in situ temperature to decrease and the gas passing through the cooled zone evaporates water up to the water-holding capacity for the temperature of that zone. As the gas moves into warmer portions of the subsurface, the water-holding capacity increases and the gas evaporates more water. Thus, the impact of nonuniform temperature is to spatially spread out

the evaporation process. In laboratory flow cell tests, very sharp transitions between the zone of desiccation and nondesiccated zones were observed when temperature was relatively constant due to fast heat transfer from the flow cell walls that minimized evaporative cooling impact on temperature (Ward et al. 2008; Oostrom et al. 2009).

Figure 4.38. Interpolated Temperature Response Along the Axis Between the Injection and Extraction Wells, Indirectly Showing Desiccation Through the Evaporative Cooling Effect. Temperatures drop while a zone is being desiccated. Once a zone is fully desiccated, there is no more evaporative cooling and temperature rises toward the inlet temperature. Data from sensors at locations C7522–C7534 (Figure 3.4).

Temperature data do not directly enable quantification of moisture content decreases. However, temperature monitoring enables imaging of the nonuniform temperature distribution that affects the desiccation process and temperature inflections from cool to warm that indicate zones of significant desiccation. Temperature correction is also needed for the ERT analyses. Thermistors provide a robust sensor that can be monitored autonomously to provide high temporal and, potentially, high spatial resolution.

Neutron moisture logging of a borehole is a standard method for obtaining a high resolution vertical profile (~7.5 cm [3 in] vertical intervals) of volumetric moisture content. These data are a good representation of moisture content at the logging locations within the nominal measurement radius of about 30 cm. Figure 4.39 shows a two-dimensional interpolation of volumetric moisture content from neutron moisture logging data prior to active desiccation (December 2010) and at the end of active desiccation (see Appendix B for additional neutron moisture interpolation plots). This type of interpolation does not incorporate subsurface conditions that can impact the distribution of desiccation away from the measurement point. Thus, care is needed in interpreting the images with respect to the volumetric distribution of moisture content reduction.
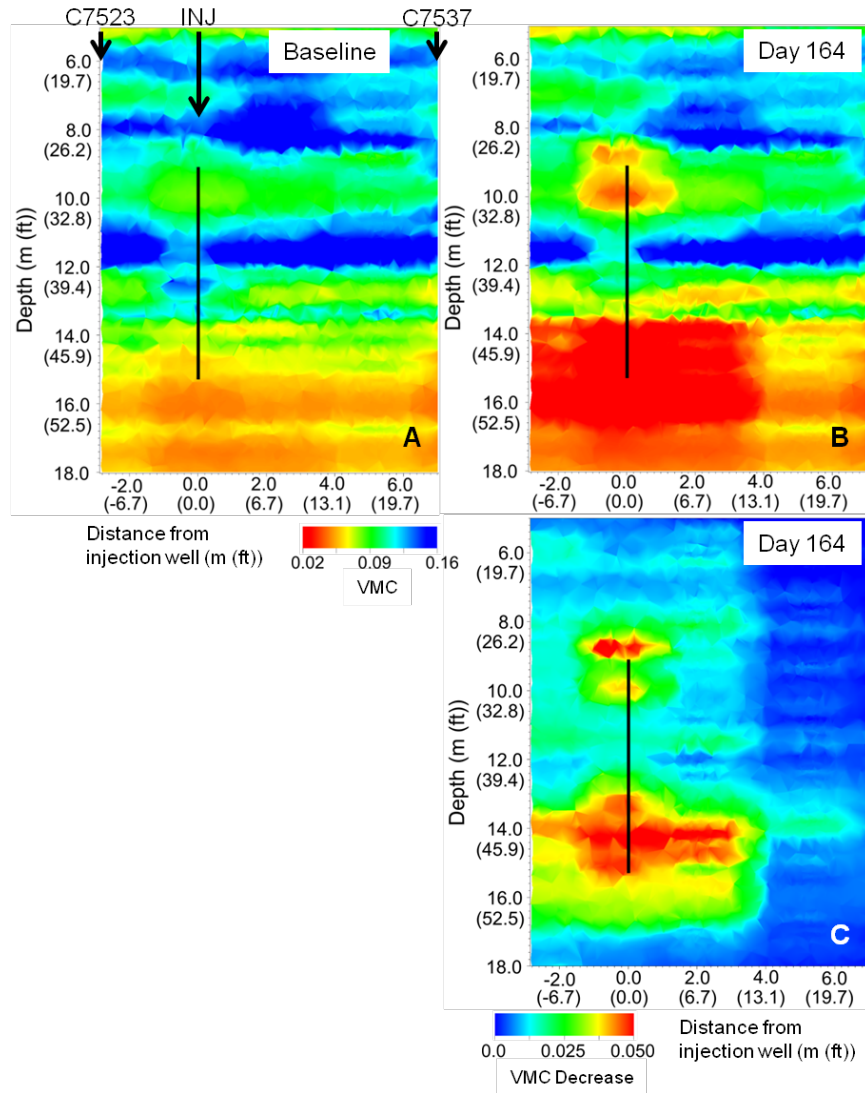
Figure 4.39. Interpolation of Volumetric Moisture Content (VMC) from Neutron Moisture Logging Data Along the Axis Between the Injection and Extraction Wells, Prior to (A) and at the End of Active Desiccation (B). Interpolation of the change in volumetric water content at the end of active desiccation (C) compared to the baseline volumetric moisture content distribution. Neutron moisture data are from logging at locations C7523–C7537 (Figure 3.4).

Cross-hole ERT reconstructs the electrical conductivity distribution between in situ electrode locations which can be related to the distribution of volumetric moisture content changes (Equation (3.5), Section 3.2.2.3). ERT monitoring can then be used to provide a temporal data set representing the three-dimensional distribution of desiccation via moisture content changes that represent conditions throughout the subsurface between electrode locations. The ERT data show changes in the volumetric moisture content expressed as the ratio of volumetric moisture content (VMC_t) at the time of the measurement to the baseline volumetric moisture content from an ERT data set collected prior to desiccation (VMC_0). Thus, a ratio of one designates areas that have not changed from the conditions prior to active desiccation. Ratios lower than one indicate desiccation, for instance, where a ratio of 0.75 means that the volumetric moisture content is 0.75 times what it was prior to desiccation. The progression and distribution of moisture content changes as imaged by ERT is shown in Figure 4.40. These two-dimensional sections were extracted from the three-dimensional ERT images along the transect between the injection and extraction wells. The resolution of the ERT data inversion is on the order of a cubic meter. Thus, the ERT images in Figure 4.40, cannot show sharp contrasts in wetting or drying zones over time, but show a "smoothed" image of how the subsurface is changing. Figure 4.40 shows the impact of non-uniform temperature (Figure 4.38) in the extended, but more moderate moisture content reduction along the path of dominant injection gas flow. There are four time points shown in Figure 4.40, but two ERT data sets were automatically collected each day such that a much higher temporal resolution could be imaged if needed (see Appendix B for additional ERT interpolation plots).

Cross-hole GPR provides means to monitor absolute volumetric moisture content and moisture content changes in two dimensions based on propagation of energy through the subsurface between two logging boreholes. Thus, it provides data for interpretation of volumetric moisture content distribution away from subsurface access points and does not require interpolation between access points like the neutron moisture logging data. However, high electrical conductivity at contaminated sites can severely impact the accuracy of the GPR estimate. When the ground has a high electrical conductivity the low-loss assumption is not valid and the electromagnetic velocity is affected by both conductivity and permittivity changes. As shown in Figure 4.41, pre-desiccation GPR moisture content estimates agree well with neutron moisture data above 12 m (39 ft) bgs where conductivity is low (Figure 4.42). However, below 12 m (39 ft) bgs, GPR estimates are significantly higher than the neutron moisture data where electrical conductivity is very high (Figure 4.42). In zones where neutron moisture data show significant desiccation by June, the GPR estimates much closer to the neutron moisture data. Figure 4.43 shows the two-dimensional GPR-imaged volumetric moisture content distribution prior to active desiccation (December 2010) and at the end of active desiccation for comparison to the neutron logging data interpolation (Figure 4.39) and ERT image (Figure 4.40). This figure shows volumetric moisture content changes similar to the other methods, although the absolute value of volumetric moisture content is higher by more than double compared to the neutron logging data for the pre-desiccation image and in parts of the post-desiccation image. As shown for the single logging location in Figure 4.41, the offset in Figure 4.43 is likely due to the changes in both electrical permittivity and conductivity that occurred during desiccation and because the low-loss assumption is not valid in some portions of the test site. However, in zones with significant desiccation, the electrical conductivity drops because moisture content decreases. In those zones, as shown in Figure 4.41, GPR moisture content determined through the Equation (3.6) correlation (Section 3.2.2.4) are much closer to those determined by neutron moisture logging. Neutron logging data is expected to be the more accurate localized indicator of volumetric moisture content because of its calibration to physical measurement of moisture content from sediment samples.
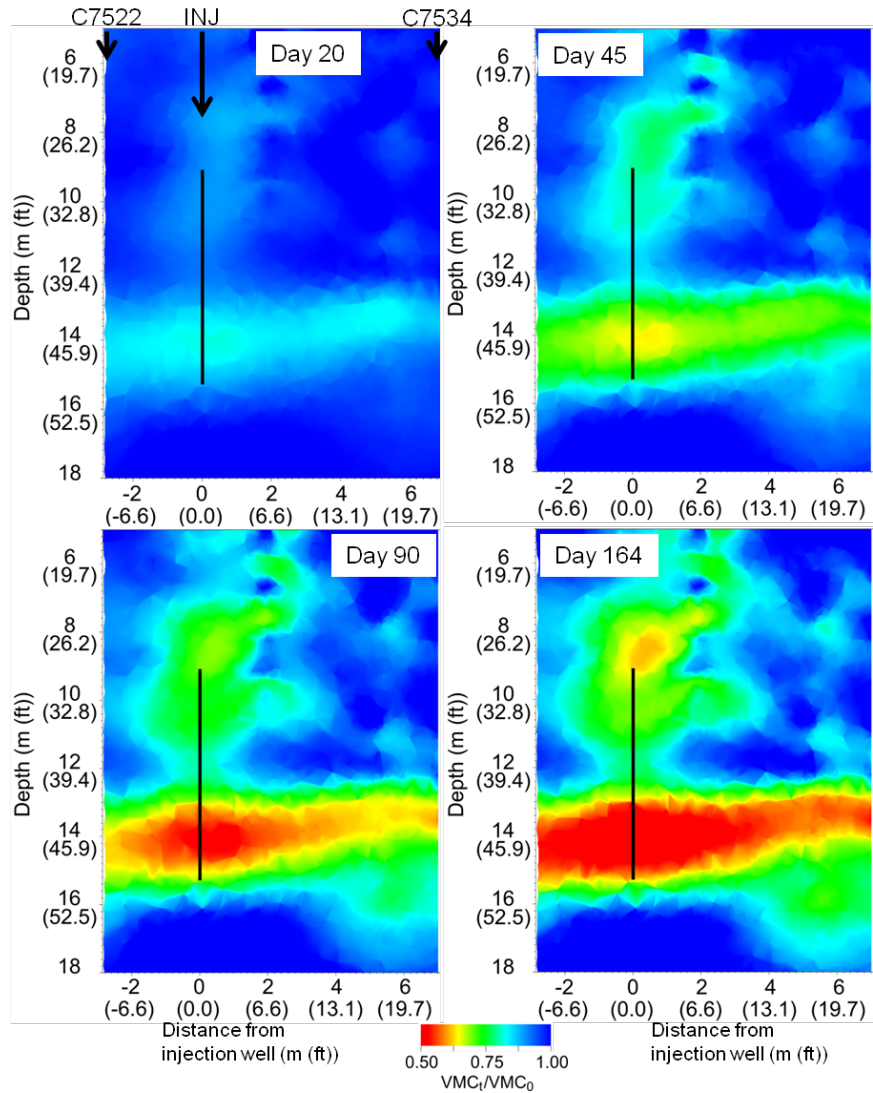
Figure 4.40. Ratio of Volumetric Moisture Content (VMC$_t$) to Pre-desiccation Volumetric Moisture Content (VMC$_0$) Over Time Along the Axis Between the Injection and Extraction Wells from Cross-Hole Electrical Resistivity Tomography. ERT data are from sensors at locations C7522–C7534 (Figure 4.34).
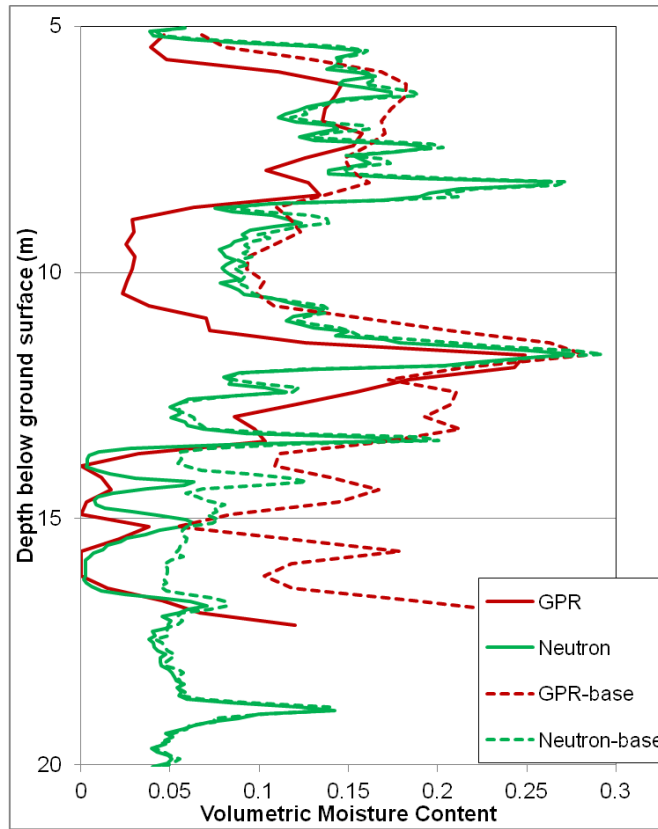
Figure 4.41. Volumetric Moisture Content Data Estimated for Location C7531 Using Neutron Moisture Logging and GPR. Base values are pre-desiccation data collected in December 2010. Neutron data were collected on June 6, 2011 (Day 140 after the start of desiccation). GPR data were collected on June 3, 2011.
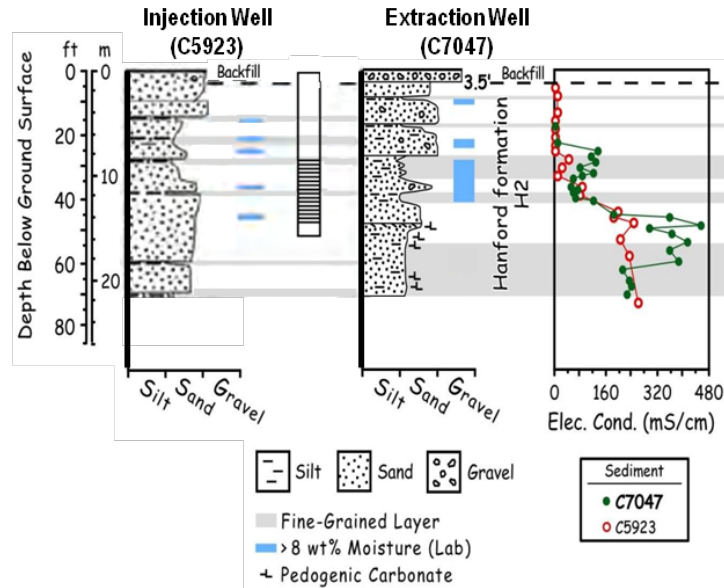
Figure 4.42. Injection and Extraction Well Borehole Data and Well Screened Interval (after DOE 2010a; Serne et al. 2009). Electrical conductivity was measured on pore water extracted from sediment samples.
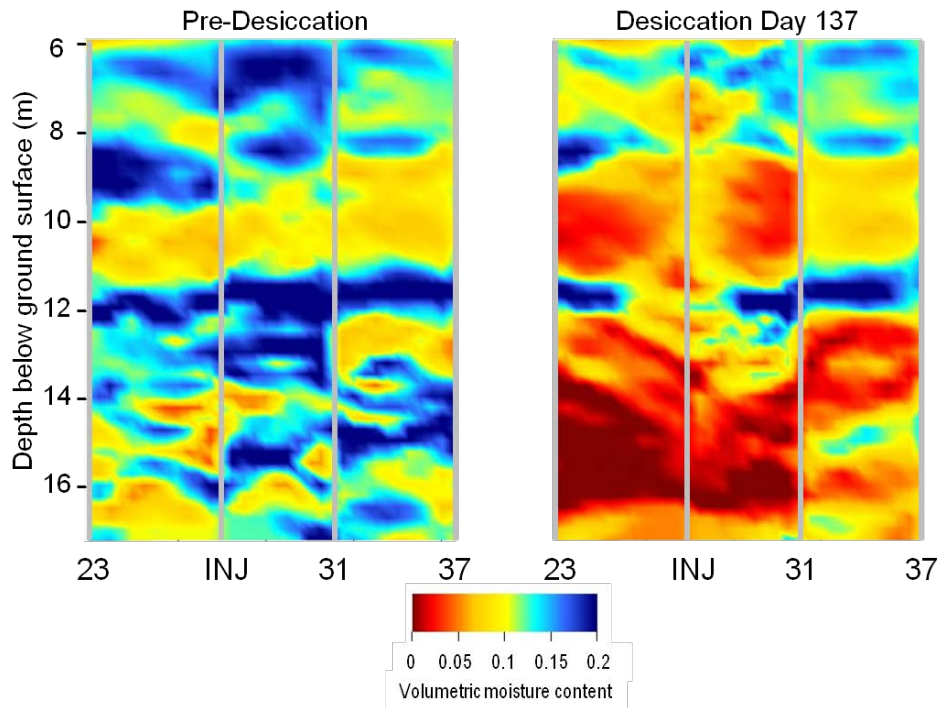
Figure 4.43. 2-D Interpretation of Volumetric Moisture Content from Cross-Hole Ground-Penetrating Radar Data Prior to Desiccation (left) and at Day 137 (June 3, 2011) After the Start of Active Desiccation (right)

4.1.2.3 Analysis of Condensate Collected During Active Desiccation

Condensate from the extracted soil gas was collected and analyzed periodically for Tc-99 and nitrate. These analyses were conducted because initial soil gas extraction testing had shown the potential for contamination to be present in the extraction stream (DOE 2010a). Contamination in condensate was observed for many of the samples collected over the duration of the active desiccation test (Table 4.3), either due to actual extraction of contaminants or due to residual in the extraction system from previous testing (see DOE 2010a). However, full-scale design for desiccation would not require an extraction well and issues associated with contaminant extraction can be avoided.

Table 4.3. Condensate Sampling Results

Sampling Date	Sample No.	Nitrate-N (µg/L)	Tc-99 (pCi/L)	Gross α (pCi/L)	Gross β(pCi/L)
12/02/2010	B29M54	0.155	69	U	U
12/02/2010	B29M59	0.162	87	U	22
2/03/2011	B29M55	U	U	U	6.4
6/13/2011	B29M56	U	58	U	U
6/13/2011	B29M56	-	99[a]	-	U[b]

(a) Sample reanalyzed; laboratory did not consider difference between this result and the original to be significant.
(b) Sample reanalyzed.

4.1.3 Post-Desiccation Data

The three primary types of monitoring—in situ sensor monitoring, neutron moisture logging, and GPR surveying—for the rewetting period (July 2011 through July 2017) are discussed, respectively, in the sections below on sensor, neutron, and geophysical data.

4.1.3.1 Sensor Data

In situ sensor monitoring was continued without interruption from the time of the last data reported in the prior year interim reports (Truex et al. 2013b, 2014, 2015). Figure 4.44 through Figure 4.51 show the temperature, matric potential, and humidity responses for the sensor locations where a response was observed during active desiccation. Data are shown from the end of active desiccation.
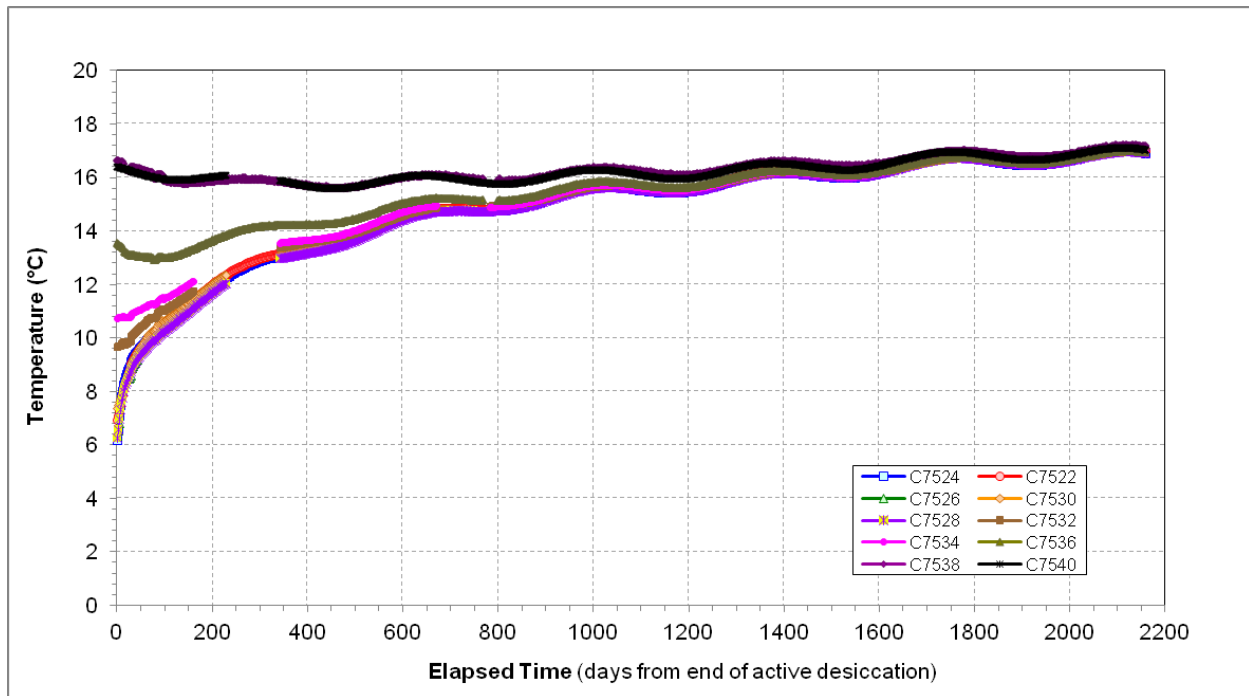
Figure 4.44. Post-desiccation Temperature Response over Time for the Sensors at a Depth of 32.5 ft (9.9 m) bgs
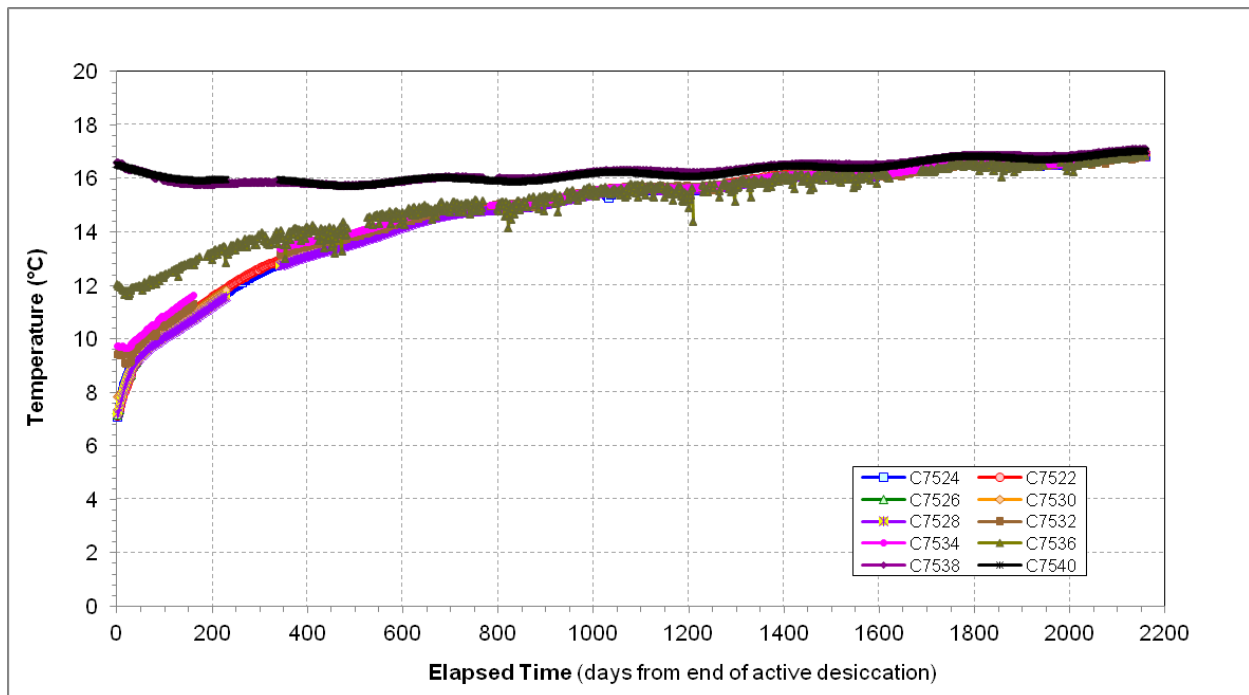
Figure 4.45. Post-desiccation Temperature Response over Time for the Sensors at a Depth of 36.5 ft (11.1 m) bgs
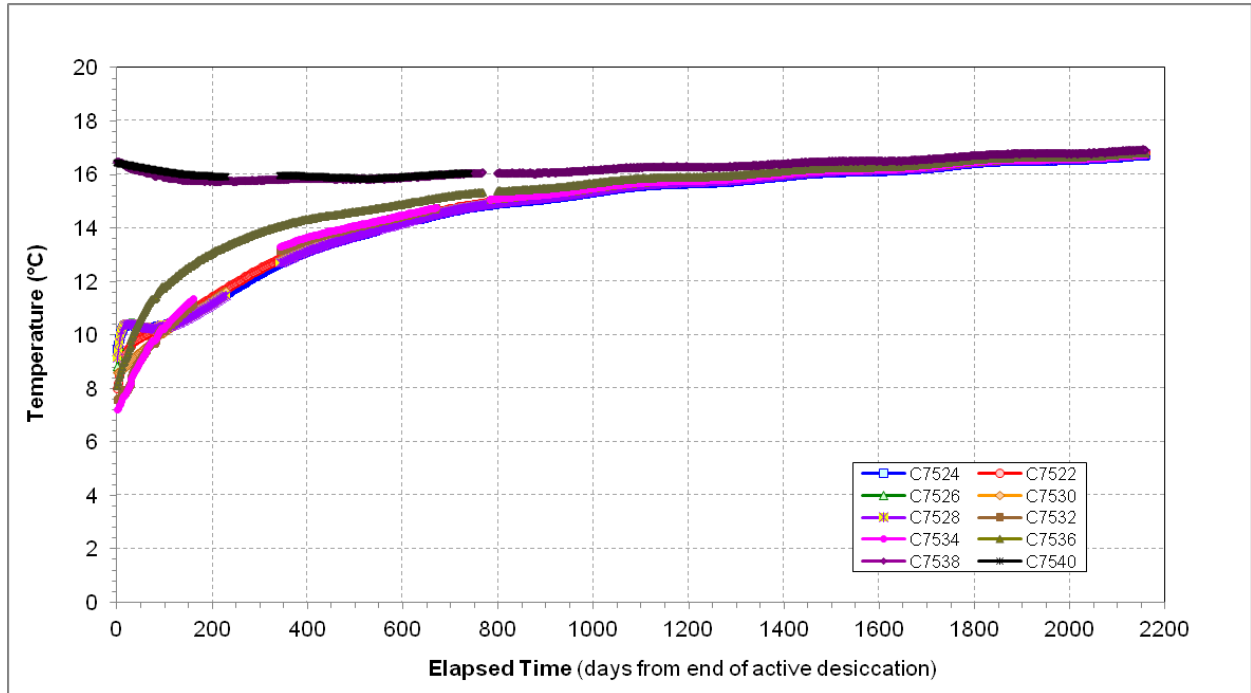
Figure 4.46. Post-desiccation Temperature Response over Time for the Sensors at a Depth of 42.5 ft (13 m) bgs
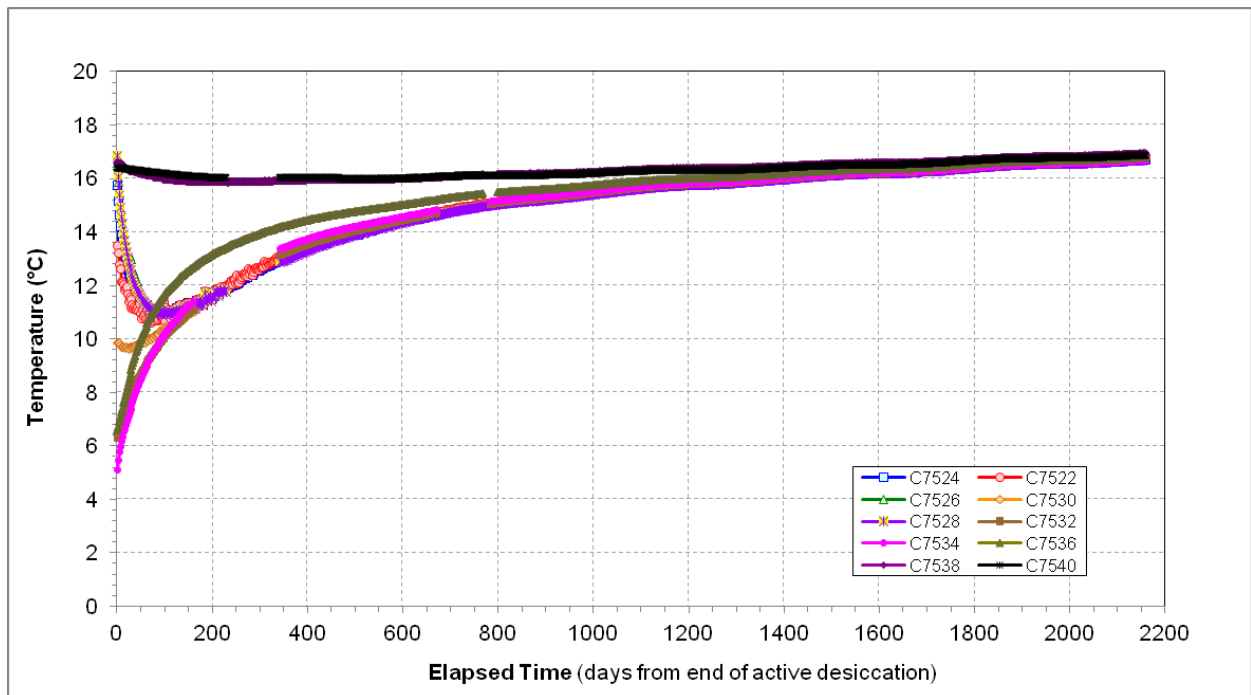
Figure 4.47. Post-desiccation Temperature Response over Time for the Sensors at a Depth of 46.5 ft (14.2 m) bgs

4.39
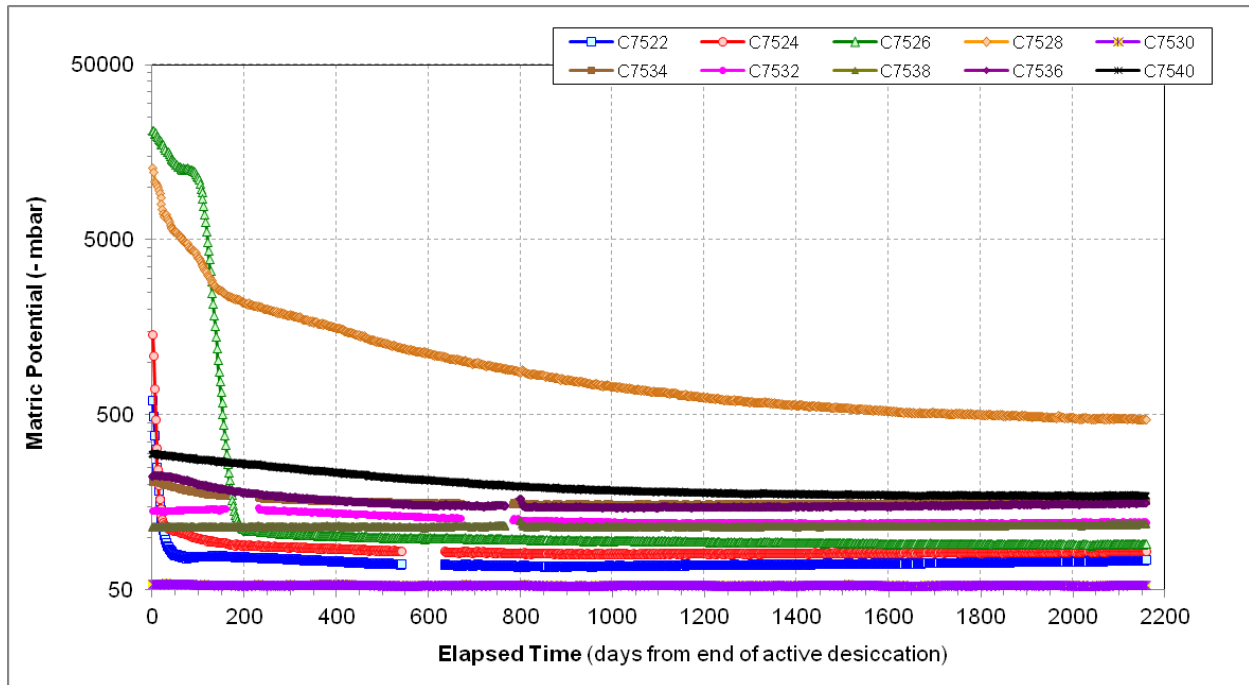
Figure 4.48. Post-desiccation Heat Dissipation Unit Response over Time for the Sensors at a Depth of 42.5 ft (13 m) bgs. Note that the y-axis uses a logarithmic scale.
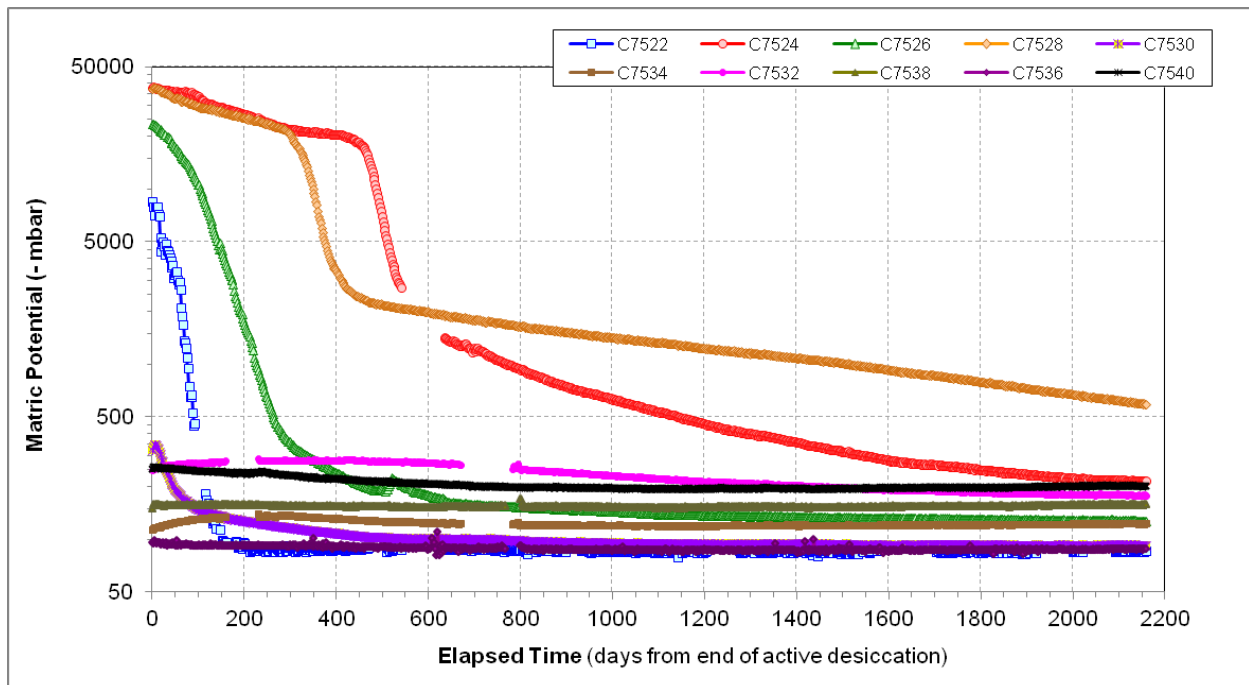
Figure 4.49. Post-desiccation Heat Dissipation Unit Response over Time for the Sensors at a Depth of 47.5 ft (14.5 m) bgs. Note that the y-axis uses a logarithmic scale.
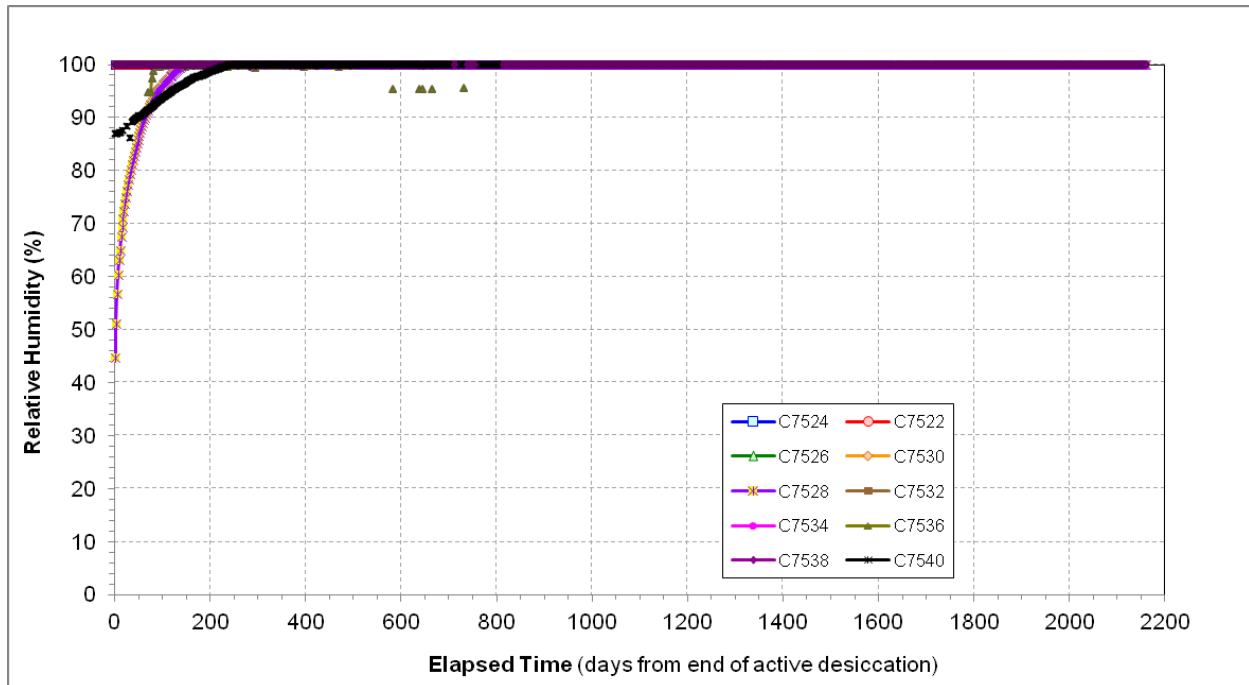
Figure 4.50. Post-desiccation Relative Humidity Probe Response Over Time for the Sensors at a Depth of 42.5 ft (13 m) bgs
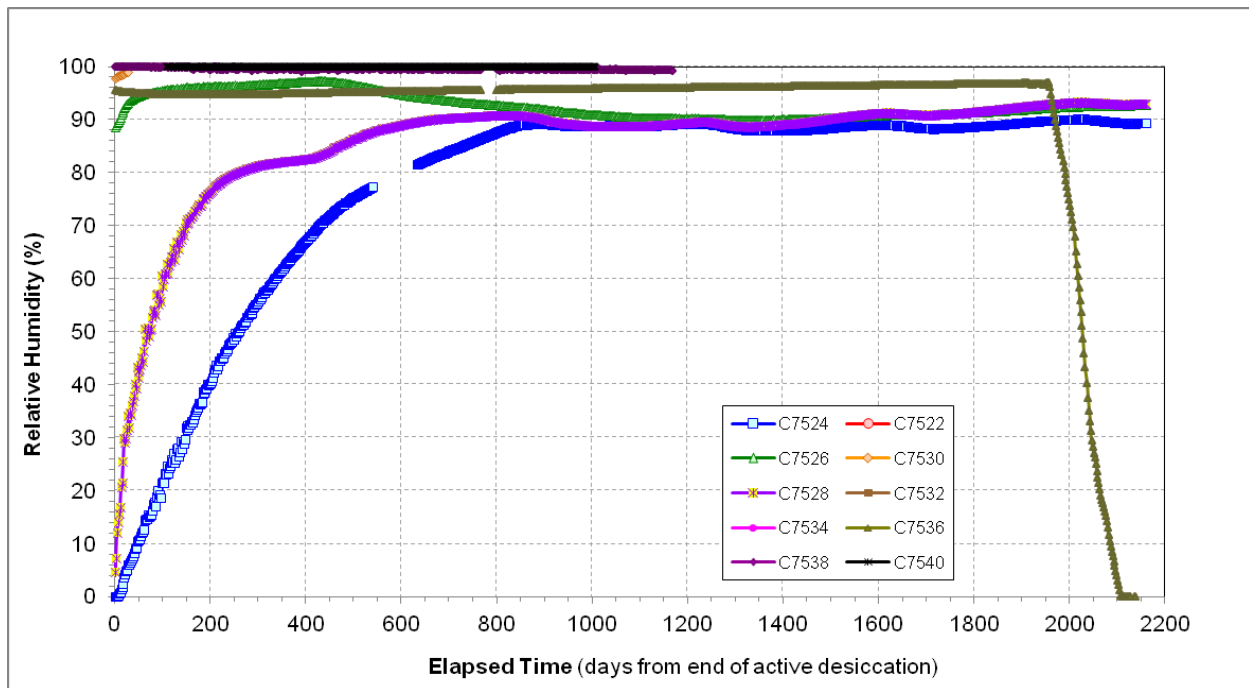
Figure 4.51. Post-desiccation Relative Humidity Probe Response Over Time for the Sensors at a Depth of 47.5 ft (14.5 m) bgs (note that the C7536 probe appears to have failed near the end of the test)

Temperatures at the key depths of 32.5, 36.5, 42.5, and 46.5 ft bgs exhibited some variation within about the first 100 days after the end of active desiccation. For the depth of 46.5 ft (14.2 m) bgs, several locations (C7524, C7522, C7526, C7528, and, to some extent, C7530) had reached a state of higher temperatures during active desiccation as a result of drying to the point where evaporative cooling was no longer occurring. In contrast, evaporative cooling was still occurring at locations C7532, C7534, and C7536 for the 46.5 ft bgs depth, so those locations had low temperatures at the end of active desiccation operations. By about 100 days after active desiccation, temperatures at all locations for the 46.5 ft bgs depth were converging. Beyond these initial post-active desiccation variations, the temperatures at all four key depths have continued a gradual increase over time at locations near the injection well and are now less than 1°C different from temperatures at distant/background locations. All temperatures at these four depths are converging to approximately 16-17°C.

Several locations at depths of 42.5 and 47.5 ft (13 and 14.5 m) bgs had exhibited a significant change in matric potential (as measured with the HDU sensors) to values between -5000 and -50000 mbar during active desiccation, indicating that significant drying occurred. After the end of active desiccation, the matric potential returned to nominally the pre-desiccation levels for most locations that had indicated drying. At a depth of 42.5 ft (13 m) bgs, the matric potential at locations C7522 and C7524 returned to around -75 to -100 mbar in a fairly short time frame (< 100 days) after the end of active desiccation. Matric potential at location C7526 for the 42.5 ft (13 m) bgs depth shows a 100-day lag before a relatively rapid change from -13000 mbar to values near -100 mbar by 200 days after end of active desiccation. At location C7528 for the 42.5 ft (13 m) depth, the matric potential indicated a more gradual rewetting, with conditions slowly getting wetter with current conditions at about -500 mbar, drier than pre-desiccation conditions (about -180 mbar). At the deeper 47.5 ft (14.5 m) locations, matric potential indicated a somewhat slower rewetting. Location C7530, which was just beginning to show changes in matric potential indicative of drying at the end of active desiccation, quickly returned to pre-desiccation levels within about 100 days. Matric potential at C7522 for the 47.5 ft (14.5 m) depth also had a relatively quick (within about 200 days) return to pre-desiccation matric potential. The return to pre-desiccation matric potential at the C7526 location for the 47.5 ft (14.5 m) depth was delayed and more gradual than observed by the corresponding sensor at the 42.5 ft (13 m) depth for that location. Matric potential at the 47.5 ft (14.5 m) depth at the C7528 location exhibited a similar gradual rewetting and has continued a slow rewetting rate with current readings at about -500 mbar. At the C7524 location for the 47.5 ft (14.5 m) depth, unlike the 42.5 ft (13 m) depth, the matric potential showed rewetting after a much longer delay (about 450 days after the end of active desiccation) and a more gradual rewetting that is currently approaching pre-desiccation conditions.

Several humidity sensors exhibited a transition to low relative humidity during active desiccation operation, indicating that drying was occurring. After the end of active desiccation, the lower relative humidity at a depth of 42.5 ft (13 m) for the C7528 location showed a relatively prompt (within about 150 days after the end of active desiccation) return to 100% relative humidity. While the humidity at a depth of 42.5 ft (13 m) for the C7540 location (background sensor) appeared to show a recovery to 100% relative humidity, this probe had previously shown essentially constant readings of about 85−90% since installation, so its readings are not considered accurate indications of humidity at that location. Humidity sensors at the 47.5 ft (14.5 m) depth for locations C7524 and C7528 have shown a much more gradual return to high humidity values. Since about 800 days after the end of active desiccation, these two sensors appear to have stabilized at around 90% relative humidity. At the C7526 location for the 47.5 ft (14.5 m) depth, moderate decreases in humidity were observed near the end of the active desiccation

period. The humidity quickly rebounded at this location, although the humidity values have drifted over time, showing a decrease to about 90% relative humidity in the most recent readings. Several of the humidity probes both during and after active desiccation have shown readings below 100% relative humidity when it was expected that the relative humidity should be 100%. Thus, it is unclear whether these readings are accurate.

4.1.3.2   Neutron Data

Vertical profiles from neutron moisture logging events conducted pre-desiccation, just after active desiccation, and for six years of annual surveys after desiccation are plotted in Figure 4.52 through Figure 4.58 to depict the relative rewetting that has occurred during this time frame. These data show a clear progression of rewetting. At the C7527 and C7529 monitoring locations, the thicker desiccated zones showed the slowest rewetting. These thicker desiccated zones were areas of high injected air flow due to the presence of coarser, lower-moisture content sediments. Plots containing all of the neutron surveys that have been conducted (pre-desiccation, July 2011, August 2011, September 2011, December 2011, February 2012, May 2013, August 2013, March 2014, August 2014, March 2015, August 2015 and June 2017) are included in Appendix C. For the June 2017 data, several boreholes show very shallow moisture changes (3 to 6 m [9.8 to 19.7 ft] bgs zone). These changes are interpreted as local annular flow of water at the borehole locations after a wet winter based on qualitative assessment of standing water at the top of these boreholes in the spring and the limited extent of the anomalous moisture increases.
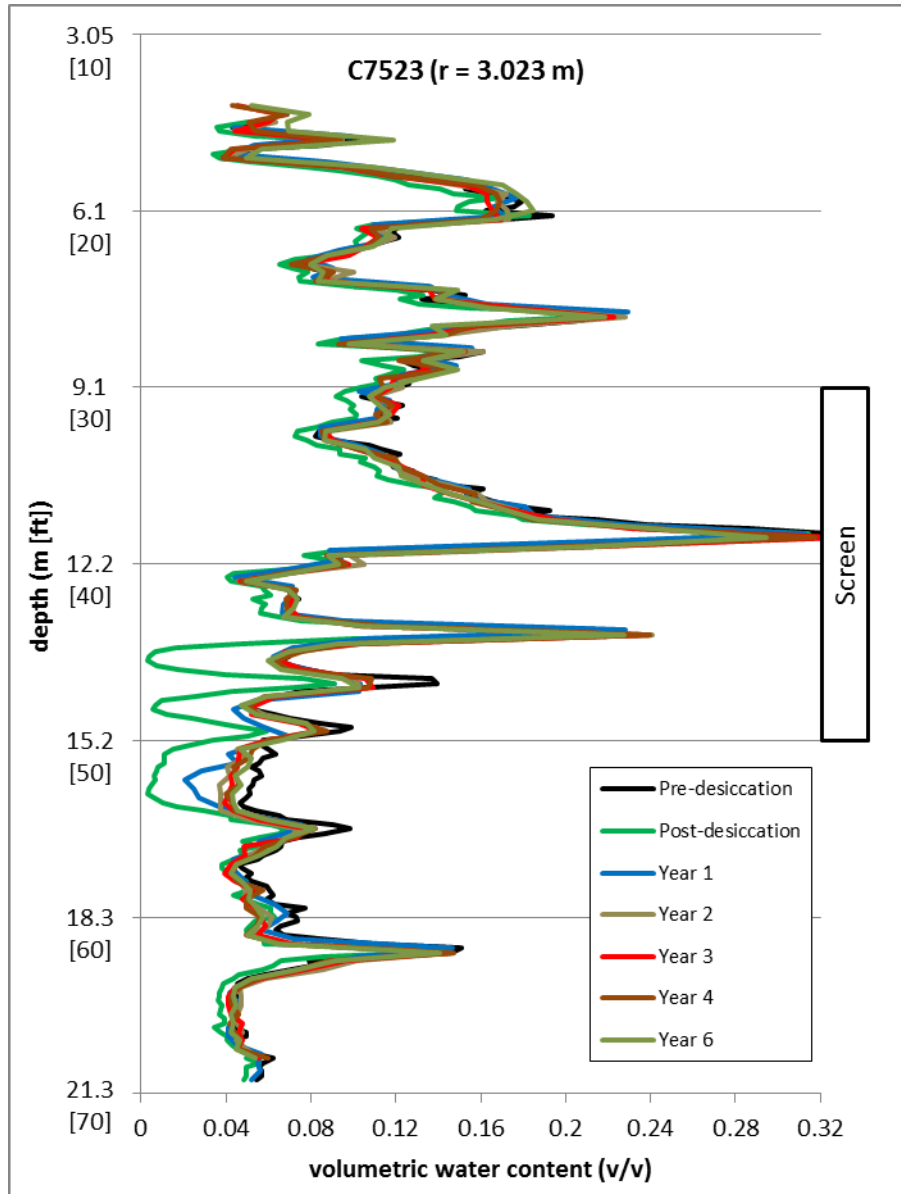
Figure 4.52. Neutron Moisture Probe Response over Time for Location C7523 (3.023 m [9.8 ft] from injection well). The pre-desiccation data are from a logging event in December 2010, prior to the continuous active desiccation period. Other data are for logging events after active desiccation ended.
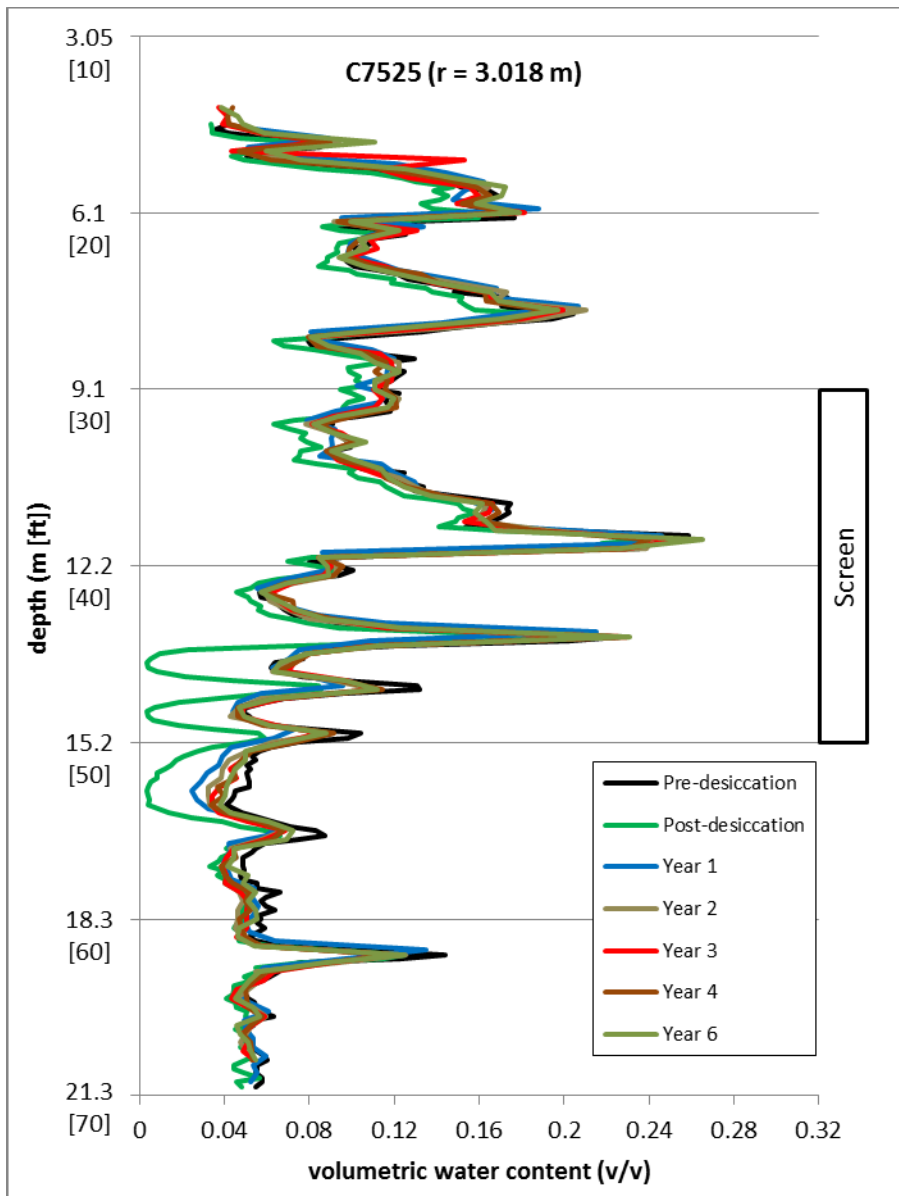
Figure 4.53. Neutron Moisture Probe Response over Time for Location C7525 (3.018 m [9.8 ft] from injection well). The pre-desiccation data are from a logging event in December 2010, prior to the continuous active desiccation period. Other data are for logging events after active desiccation ended.
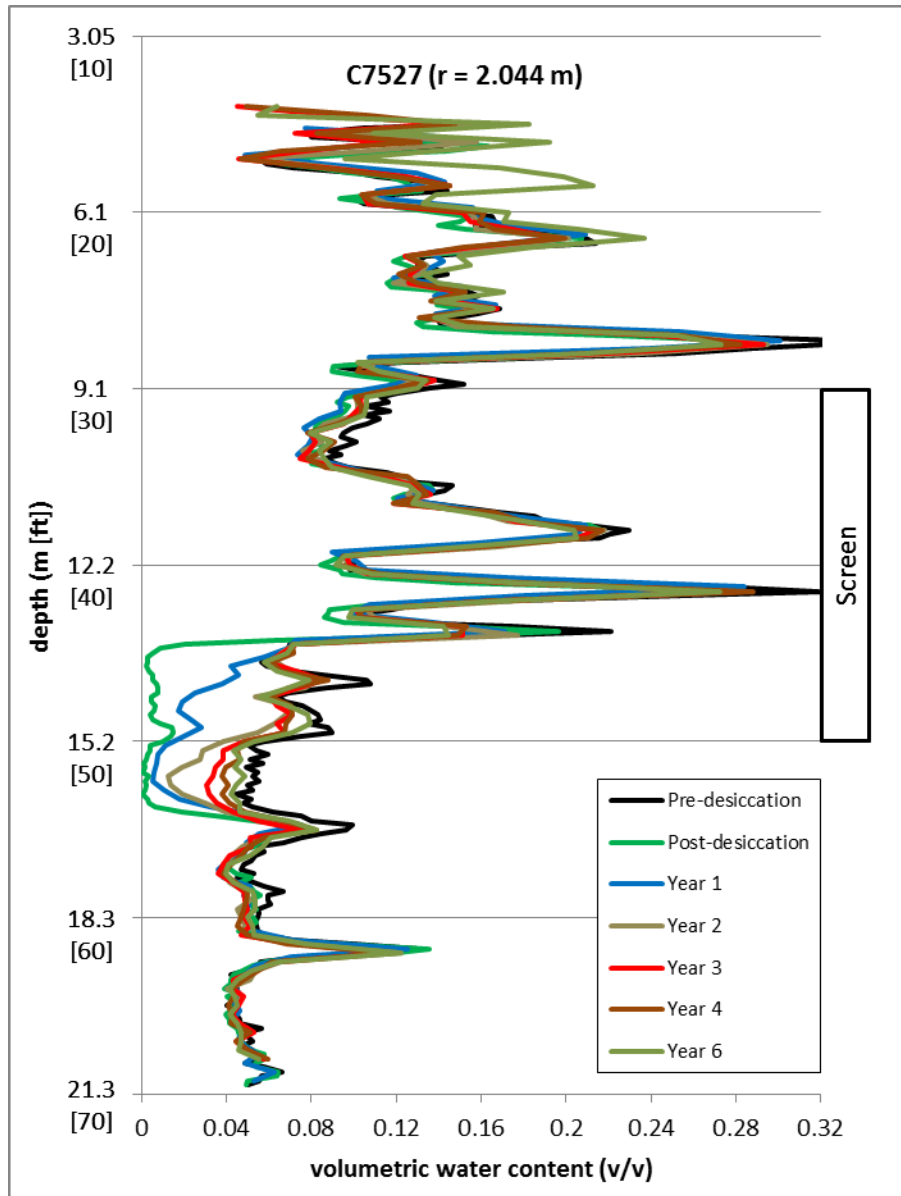
Figure 4.54. Neutron Moisture Probe Response over Time for Location C7527 (2.044 m [6.6 ft] from injection well). The pre-desiccation data are from a logging event in December 2010, prior to the continuous active desiccation period. Other data are for logging events after active desiccation ended.
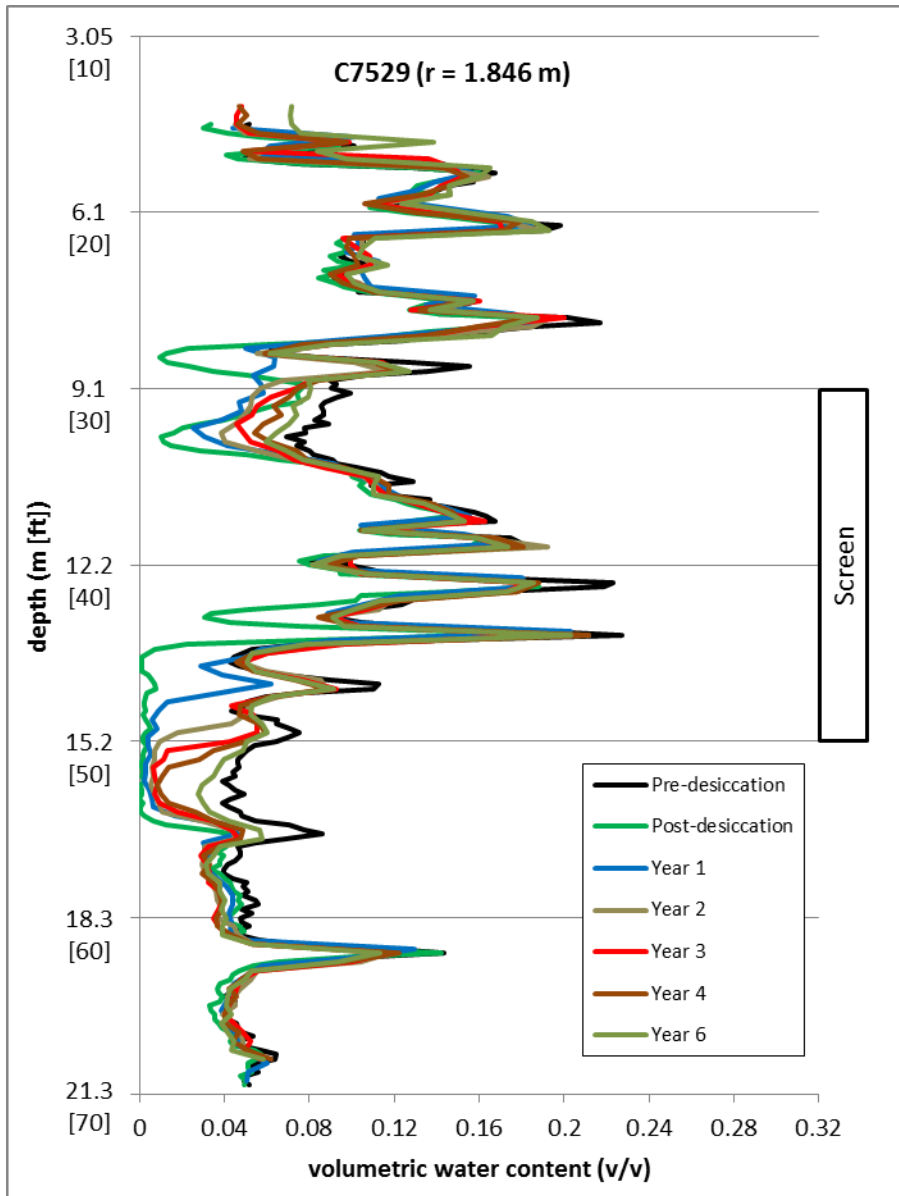
Figure 4.55. Neutron Moisture Probe Response over Time for Location C7529 (1.846 m [6 ft] from injection well). The pre-desiccation data are from a logging event in December 2010, prior to the continuous active desiccation period. Other data are for logging events after active desiccation ended.
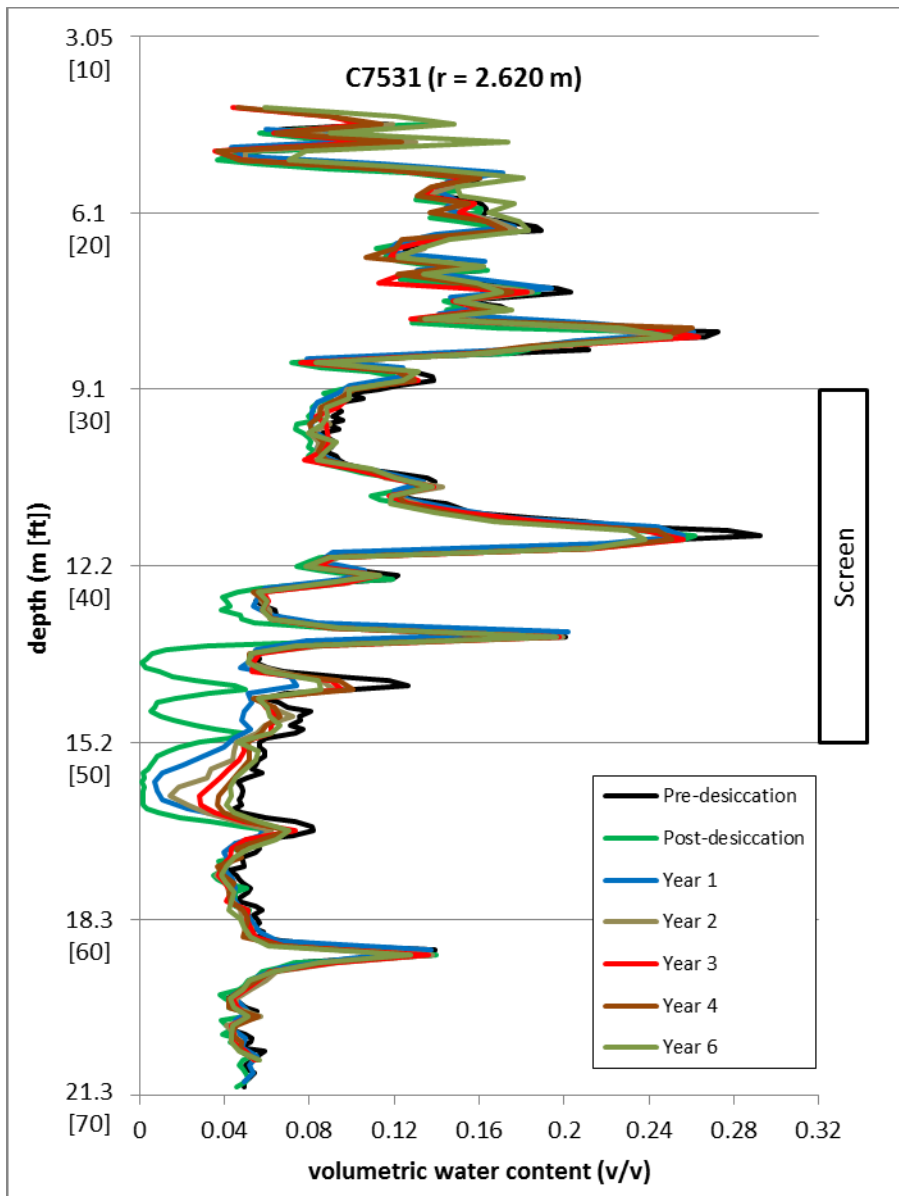
Figure 4.56. Neutron Moisture Probe Response over Time for Location C7531 (2.620 m [8.5 ft] from injection well). The pre-desiccation data are from a logging event in December 2010, prior to the continuous active desiccation period. Other data are for logging events after active desiccation ended.
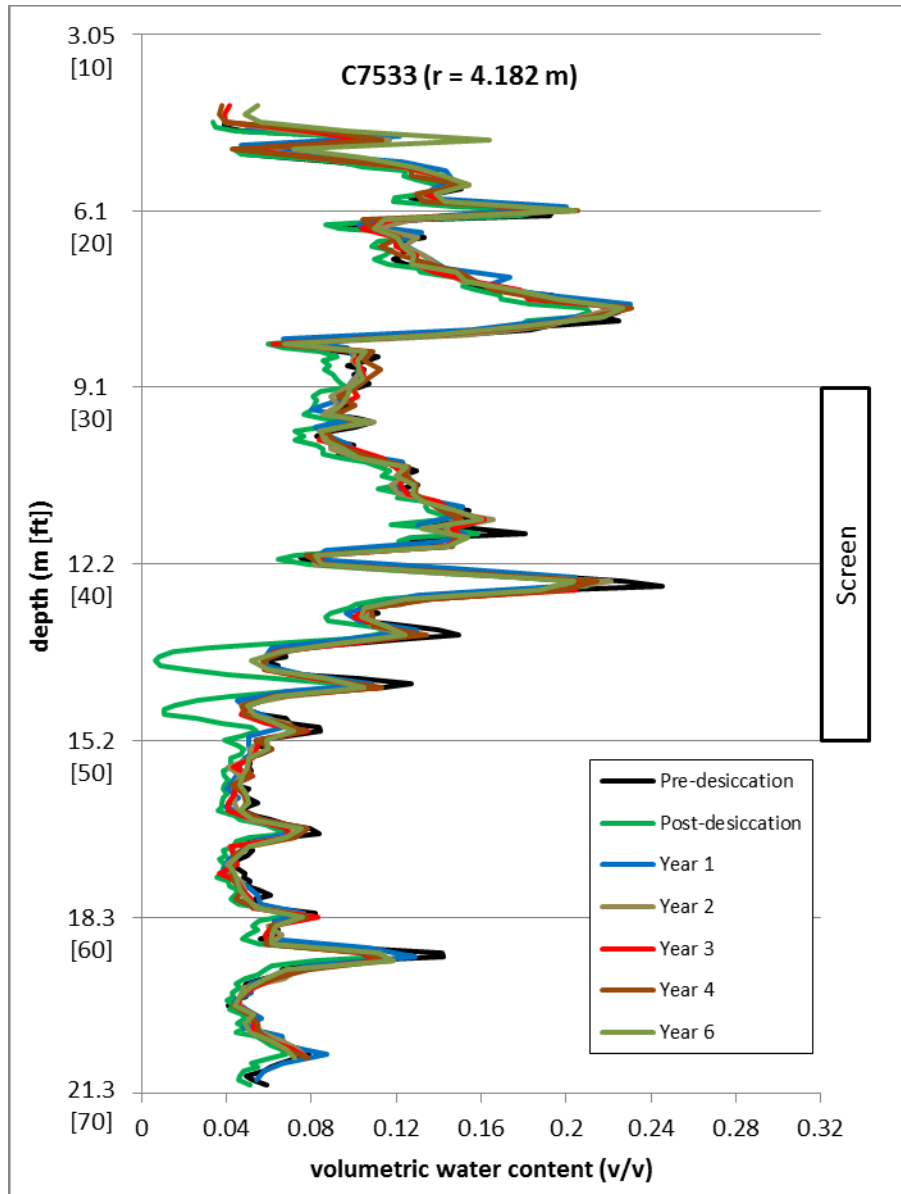
Figure 4.57. Neutron Moisture Probe Response over Time for Location C7533 (4.182 m [13.7 ft] from injection well). The pre-desiccation data are from a logging event in December 2010, prior to the continuous active desiccation period. Other data are for logging events after active desiccation ended.
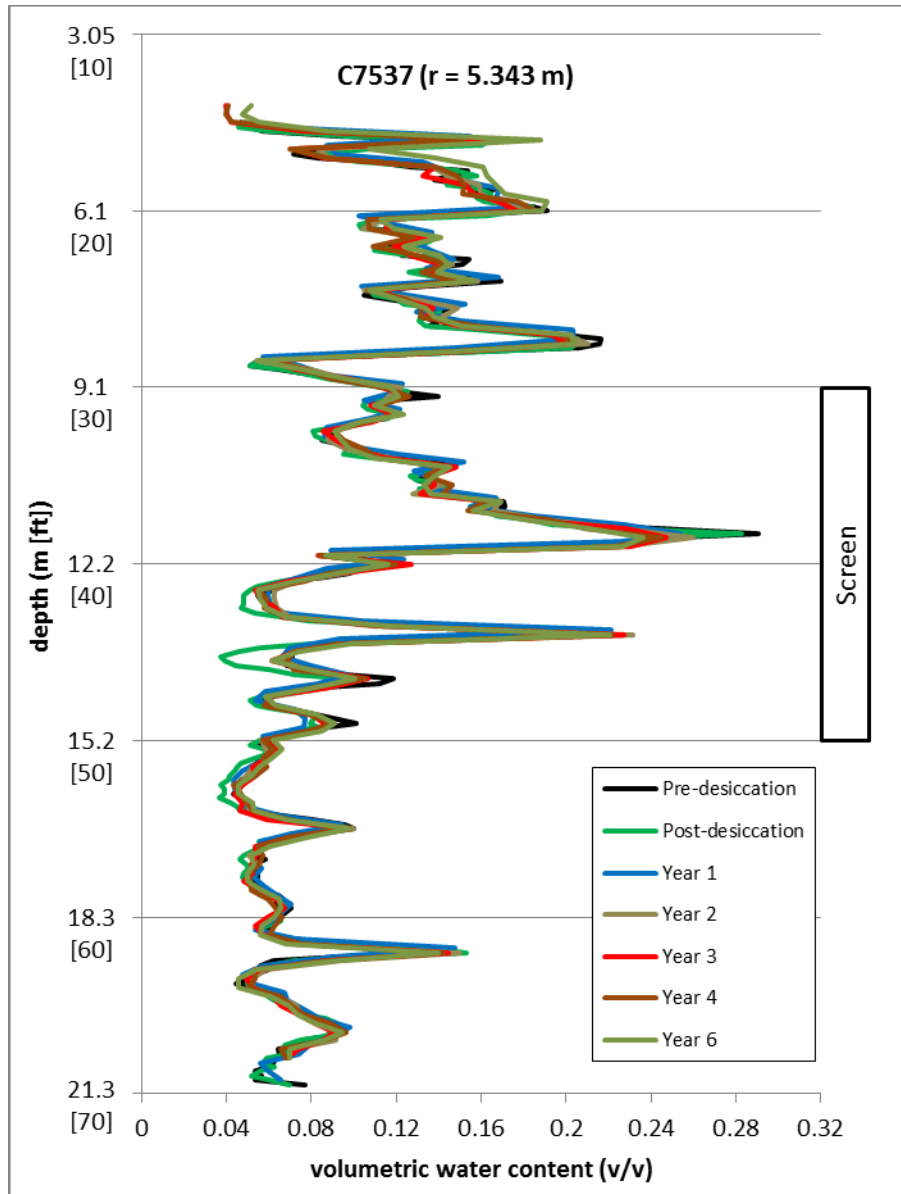
Figure 4.58. Neutron Moisture Probe Response over Time for Location C7537 (5.343 m [17.5 ft] from injection well). The pre-desiccation data are from a logging event in December 2010, prior to the continuous active desiccation period. Other data are for logging events after active desiccation ended.

4.1.3.3   Geophysical Data

Periodic GPR survey data were collected during post-desiccation monitoring. The GPR-interpreted volumetric moisture content distribution at day 137 during active desiccation and days 193, 265, 650, 770, 980, 1500 after the end of active desiccation are shown in Figure 4.59. Note that the GPR data at day 137, during desiccation, are prior to the end of active desiccation (e.g., day 164) such that conditions were likely dryer at the onset of the post-desiccation monitoring period. The post-desiccation GPR data show a general increase in volumetric moisture content over time within the 2-D survey cross section, approaching pre-desiccation conditions (Figure 4.60) by day 1500 after the end of active desiccation. The GPR survey at day 2100 after the end of active desiccation did not show any significant changes at the resolution of the imaging. These GPR data are consistent with the neutron moisture data, though the resolution of the GPR data is coarser.
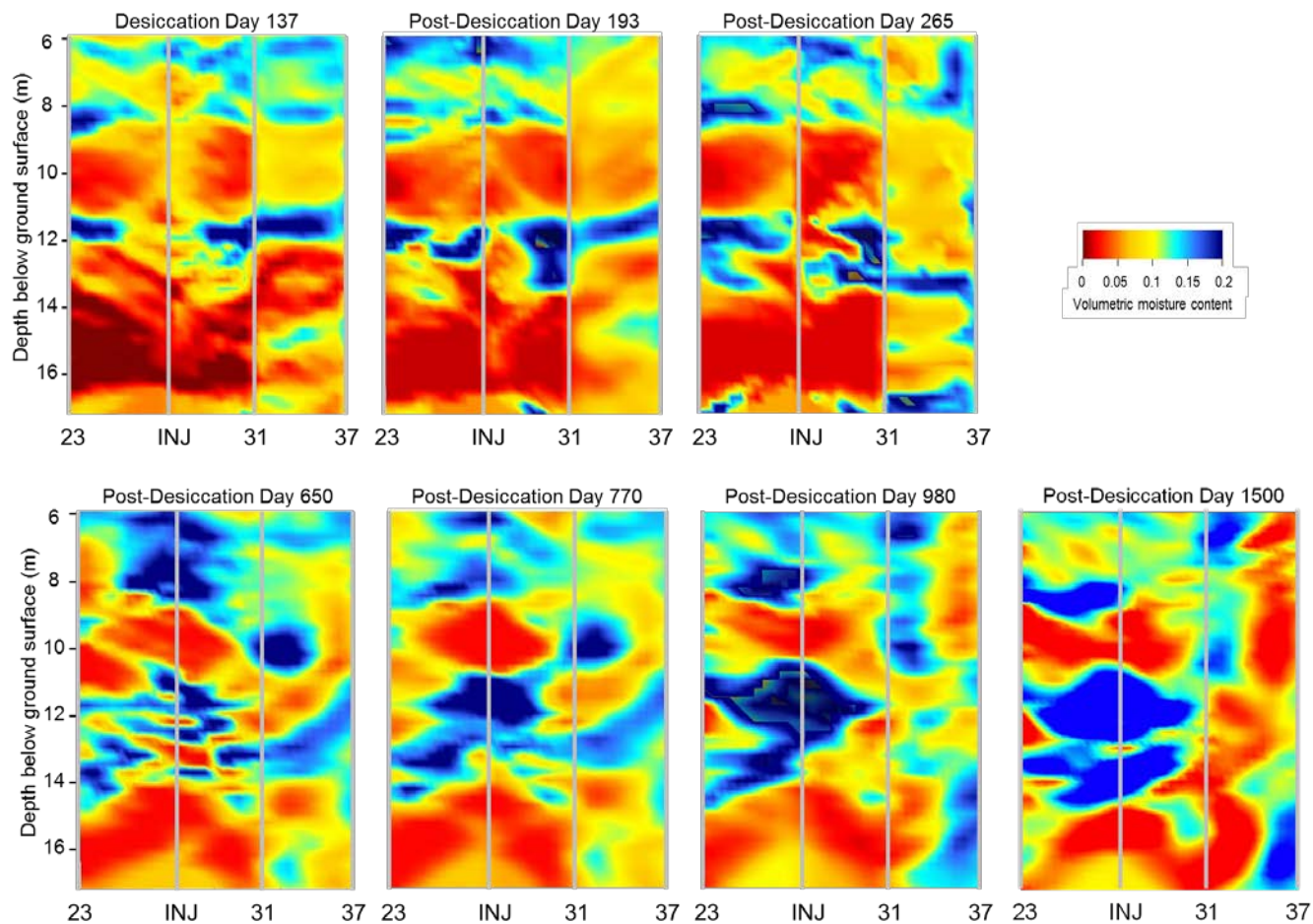
Figure 4.59. 2-D Interpretation of Volumetric Moisture Content from Cross-Hole Ground-Penetrating Radar Data during Desiccation (left) at Day 137 (June 3, 2011) and after the End of Active Desiccation. Locations are shown as INJ (injection well) and logging well locations are indicated by the last two numbers in the location identifier (e.g., 23 = C7523). Changes in GPR response between day 1500 and day 2100 were minimal in the context of the GPR resolution.
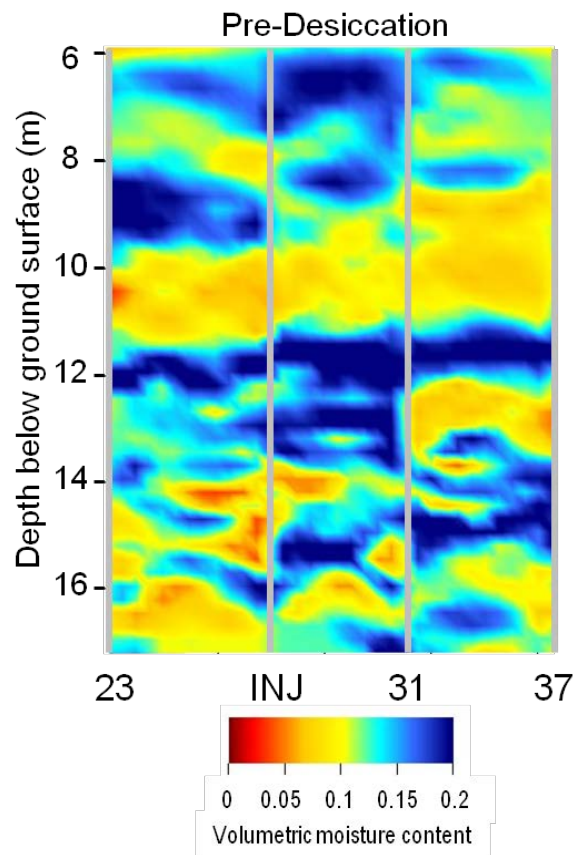
Figure 4.60. 2-D Interpretation of Initial Volumetric Moisture Content from Cross-Hole Ground-Penetrating Radar Data prior to Desiccation. Locations are shown as INJ (injection well) and logging well locations are indicated by the last two numbers in the location identifier (e.g., 23 = C7523).

Interpretation of the 2-D moisture content representation should consider that conversion of GPR-derived permittivity to VMC is affected by EC. Desiccation reduces the EC, which renders GPR data acquisition more favorable within desiccated zones, and improves the accuracy of the GPR-derived moisture content estimate. For example, Figure 4.61 shows the ERT-derived EC distribution along the GPR survey transect at the end of desiccation and at days 650, 770, 980, and 1500 post-desiccation. The black regions illustrate where low EC, or low-loss, assumptions may not be valid (EC >0.05 S/m). Prior to desiccation, the low-loss assumption was generally valid above a depth of 10 m (33 ft) and invalid below 10 m (33 ft). At the end of desiccation, low-conductivity conditions have been established within a zone from depths of approximately 13 m to 15 m (42.6 ft to 49.2 ft) (Figure 4.61). Within this depth interval, GPR-derived moisture content estimates correlated well with estimates from neutron moisture logging (Truex et al. 2012a). Within zones where desiccation has decreased the EC, GPR can be used with confidence to estimate the moisture content distribution between wells. At 650 days post-desiccation, low-loss conditions mostly remain within the 13-m to 15-m zone. However, by post-desiccation days 770 and 980, this zone appears to be recovering sufficiently such that low-loss conditions may no longer be applicable. By day 1500 (and confirmed by day 2100 data), data shows some apparent recovery of the low conductivity conditions, potentially related to moisture redistribution.
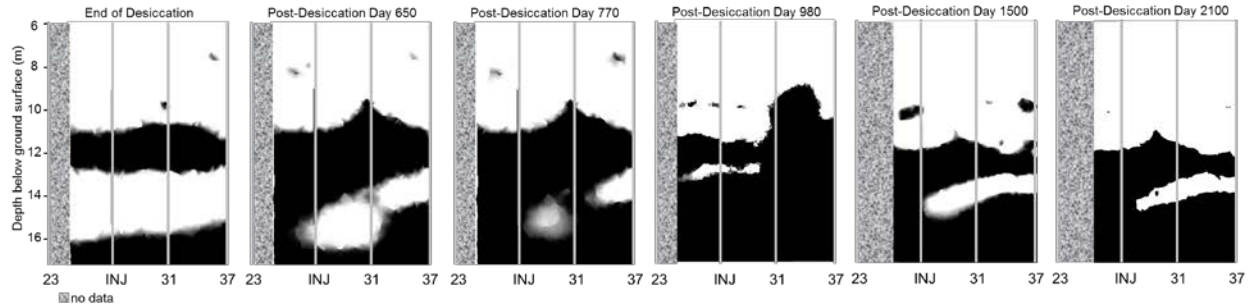
Figure 4.61. 2-D Image Showing Regions where GPR Low-Loss Conditions (white) Are Valid, Resulting in Higher Confidence in GPR-derived Moisture Content Estimates. Locations are shown as INJ (injection well) and logging well locations are indicated by the last two numbers in the location identifier (e.g., 23 = C7523).

ERT monitoring was continued without interruption after active desiccation was terminated. Figure 4.62 shows the ERT interpretation of changes in the VMC expressed as the ratio of VMC at the time of the measurement to the VMC at the end of active desiccation (VMC_0). A ratio of 1 designates areas that have not changed from the conditions at the end of active desiccation. Ratios higher than 1 indicate rewetting; for instance, a ratio of 3 means that the volumetric moisture content is 3 times higher than it was at the end of active desiccation. Ratios lower than 1 indicate drying; for instance, a ratio of 0.75 means that the VMC is 0.75 times what it was at the end of active desiccation. The resolution of the ERT data inversion is on the order of a cubic meter. Thus, the ERT images cannot show sharp contrasts in wetting or drying zones over time, but show a "smoothed" image of how the subsurface is changing. As time progresses, some regions in the test area get wetter (proceeding from green to yellow to orange in color). The moisture for rewetting is being drawn from adjacent regions, as shown by areas that have become dryer (darker blue color).
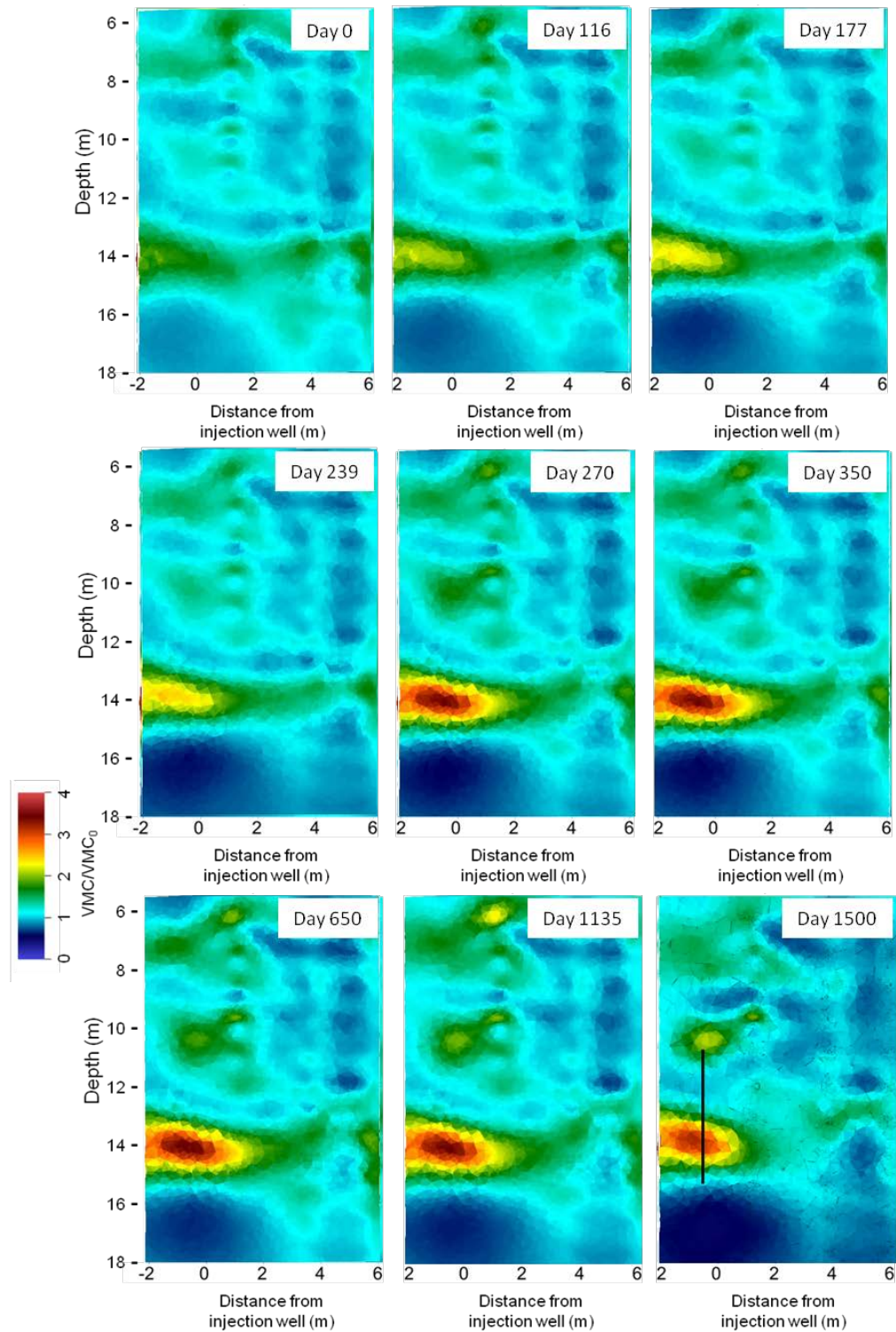
Figure 4.62. Ratio of Volumetric Moisture Content (VMC) to the Volumetric Moisture Content at the End of Active Desiccation (VMC_0) over Time along the Axis between the Injection and Extraction Wells from Cross-hole Electrical Resistivity Tomography. ERT data are from sensors at locations C7522–C7534 through day 1500 of the post-desiccation period (Figure

3.6). Changes in ERT response between day 1500 and day 2100 were not observable at the resolution of the ERT imaging.

4.2 Data Assessment with Respect to Field Test Objectives

Field test data and associated laboratory and numerical modeling results are interpreted with respect to each of the field test objectives.

4.2.1 Design Parameters

The first section (4.2.1.1) summarizes information collected and applied to support the field design. Specific design features are then discussed in the next section (4.2.1.2).

4.2.1.1 Design Information for the Field Test

Information supporting the design the desiccation field test was obtained through laboratory studies (4.2.1.1.1), field site characterization (4.2.1.1.2), and numerical modeling (4.2.1.1.3).

4.2.1.1.1 Laboratory Information Input to Desiccation Design

A vadose zone technical panel was convened in 2005 to evaluate potential vadose zone technologies, including desiccation (FHI 2006). In their evaluation, panel members provided guidance on the type of uncertainties that need to be resolved before applying desiccation as part of a remedy. This guidance, additional external technical review comments, and subsequent development of data quality objectives for the desiccation field test were used to guide design efforts in support of the desiccation treatability test. The primary conclusions of the laboratory and modeling efforts relevant to desiccation design are described below. These efforts are described in detail in Truex et al. (2011) and the additional reports and manuscripts cited below.

Impact of evaporative cooling on desiccation rate. Evaporative cooling occurs during desiccation at and adjacent to desiccation fronts to an extent that can be accurately quantified based on known processes (Oostrom et al. 2009; Ward et al. 2008; Truex et al. 2011). Temperature decreases due to evaporative cooling until the desiccation front reaches the monitoring locations (i.e., the time when the sediment between the injection location and the monitoring location is desiccated). At that time, the temperature at the monitoring location begins to increase toward the temperature of the injected gas because evaporative cooling is no longer occurring in the sediment between the injection location and the monitoring location (Oostrom et al. 2009). There can be multiple inflection points if there are multiple layers that are being desiccated at different rates and these layers are within a region that can impact the temperature at the monitoring location (Oostrom et al. 2009). The temperature response is less dramatic at larger distances from the injection well as the cooling front extends ahead of the desiccation front.

Temperature variations impact the distribution of desiccation because temperature impacts the water-holding capacity of the gas. Evaporative cooling causes in situ temperature to decrease and the gas passing through the cooled zone evaporates water up to the water-holding capacity for the temperature of that zone. As the gas moves into warmer portions of the subsurface, the water-holding capacity increases and the gas evaporates more water. Thus, the impact of nonuniform temperature is to spatially spread out

the evaporation process. In laboratory flow cell tests, very sharp transitions between the zone of desiccation and nondesiccated zones were observed when temperature was relatively constant due to fast heat transfer from the flow cell walls that minimized evaporative cooling impact on temp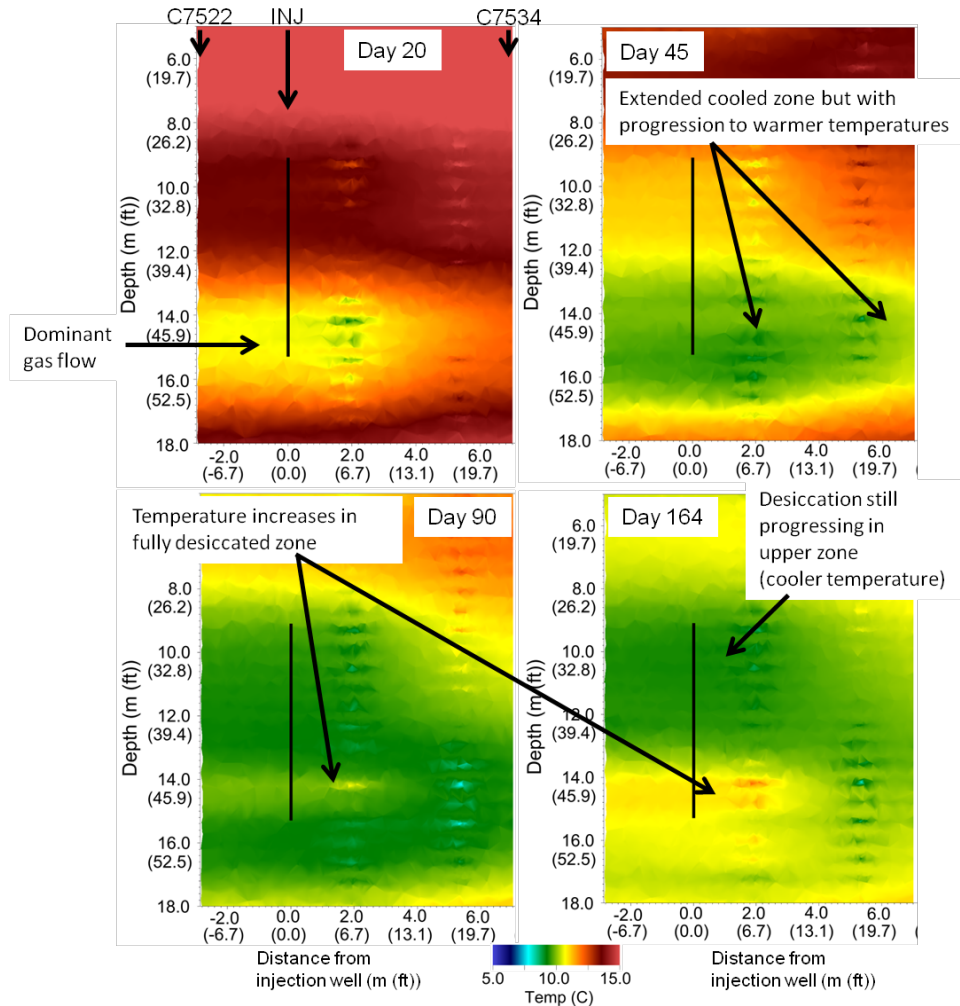erature (Ward et al. 2008; Oostrom et al. 2009). For field applications, however, evaporative cooling may decrease temperatures over a large area and more significantly impact the desiccation front characteristics.

Impact of solutes on desiccation and the fate of solutes during desiccation: Experiments demonstrated the desiccation rate is not a function of salt concentration. As such, inclusion of salt concentrations in estimates of desiccation rate is not necessary. The experimental results also suggest that for slowly moving desiccation fronts and high solute concentrations (>100 g/L), some redistribution of solute may occur in the soil moisture and in the direction of the solute concentration gradient. Because the sediment is relatively dry behind the desiccation front, solute migration will occur in the direction of the desiccation front movement or laterally at the edges of the desiccated area. Maximum concentration factors of about 120% of the initial concentration were observed in the one-dimensional column experiments. This moderate concentration increase does not affect the desiccation process because the desiccation rate is independent of the salt concentration.

Impact of porous media heterogeneity on desiccation. Desiccation rate is a function of soil gas flow rate. Thus, where layers of contrasting permeability are present, desiccation occurs to the greatest extent in higher permeability layers (Oostrom et al. 2009, 2012b; Ward et al. 2008). Nonuniform initial moisture conditions impact the desiccation volume because wetter zones require more dry gas contact to become desiccated. For instance, using a water-holding capacity of 14.6 g-water/m^3-gas (17°C), a porosity of 0.3, and a bulk density of 1900 kg/m^3, desiccating a porous medium to initially containing 5 wt % of water requires about 22,000 pore volumes of dry gas, whereas desiccating a porous medium initially containing 7 wt% of water requires about 30,000 pore volumes of dry gas. Thus, initially wetter zones require more dry gas contact than initially dryer zones and will lead to nonuniform drying even if the gas flow rate through each zone is the same. Nonuniform initial moisture content conditions also lead to relative gas-phase permeability contrasts between wetter and dryer zones that impede gas flow through the wetter zones and further accentuate the nonuniformity of the desiccation process.

Evaluation of rewetting phenomena after desiccation: The rate of rewetting is a function of the porous media properties of both the desiccated zone and the subsurface surrounding this zone and the moisture content distribution at the end of desiccation. After desiccation, the target zone will tend back toward the equilibrium moisture conditions for the porous media properties. Vapor-phase rewetting will occur, but has negligible impact on the overall rewetting process. Advective rewetting strongly depends on the porous media permeability within and surrounding the desiccated zone and the total thickness of the desiccated zone. Thus, targeting thick desiccated zones surrounded by lower permeability porous media will result in slower rewetting and an overall more significant effect on moisture flux toward the groundwater. More detailed discussion of rewetting is provided in Section 4.2.2.2.

Evaluation of gas tracers for use in monitoring desiccation: The application of gas-phase partitioning tracer tests was proposed to estimate initial water volumes and monitor progress of the desiccation process at pilot-test and field sites. Laboratory tracer tests were conducted in porous medium columns with various water saturations with sulfur hexafluoride as the conservative tracer and tricholoro-fluoromethane and difluoromethane as the water-partitioning tracers. Based on laboratory results, gas-phase partitioning tracer tests may be used to determine initial water volumes in sediments, provided the

initial water saturations are sufficiently large. However, these tracer tests cannot be used to detect and quantify water in relatively dry or desiccated sediments (Oostrom et al. 2011).

4.2.1.1.2 Field Input to Desiccation Design

In addition to the technical data obtained through laboratory experiments, field site characterization information is also used as input to the design for a specific application. At the pilot test site, pre-desiccation characterization efforts at the test site included the following activities.

- Sediment air permeability of the targeted desiccation depth interval (Serne et al. 2009)

- Sediment air permeability contrast, cone penetrometer tip pressure, and resistivity logging as a function of depth at five locations using the air permeameter technique (DOE 2010a)

- Extracted soil gas humidity, temperature, and pressure at selected volumetric flow rates (DOE 2010a)

- Quantification of contaminants in the extracted soil gas and extracted water (DOE 2010a)

- Logging and laboratory sediment data that characterizes the heterogeneity, especially in terms of the distribution of sandy and silty layers within the targeted desiccation depth interval (Serne et al. 2009)

- Intrinsic properties of key sediment types from borehole samples (Serne et al. 2009; DOE 2010a)

- Moisture content distribution at borehole locations (Serne et al. 2009; DOE 2010a)

- Permeability-moisture content relationships from borehole samples (Serne et al. 2009)

- Contaminant distribution from borehole samples and inferred from an electrical resistivity survey (Serne et al. 2009; Um et al. 2009, *Characterization of Sediments from the Soil Desiccation Pilot Test) (SDPT Site in the BC Cribs and Trenches Area*)

- Baseline neutron moisture logging and a GPR survey were conducted to evaluate the initial distribution of moisture content. A baseline ERT survey was also used to evaluate the lithology and contaminant distributions based on the distribution of conductivity.

- Once test infrastructure was installed, a gas tracer test was conducted to evaluate injected gas flow patterns.

- The equilibration of installed sensors to the in situ conditions was also monitored prior to start of active desiccation.

4.2.1.1.3 Modeling Input to Desiccation Design

Several types of modeling studies were conducted to provide input to the desiccation field test design. Simulations to estimate the overall performance of an idealized zone of desiccation in the subsurface in terms of slowing moisture and contaminant flux to groundwater were conducted to evaluate the relevant size of a desiccation zone for full-scale application and as a first investigation of the performance in terms of the target extent of moisture reduction during desiccation. Numerical modeling of the field scale desiccation process was also used to evaluate how operational and design factors impact the rate of desiccation and the magnitude of change in monitored parameters. Numerical modeling of the desiccation field test site conditions was also conducted to provide a comparative basis for evaluating field test results. These modeling studies are described in the sections below.

Identification of an appropriate performance target for desiccation. Simulations were used to evaluate the impact of desiccation on contaminant transport to the groundwater (Truex et al. 2011 and herein). In conjunction with a surface barrier, desiccation significantly delayed the concentration and arrival time of contaminants to the groundwater. The amount of delay is most impacted by the location and extent of the desiccated zone with respect to the zones of high contaminant and moisture content. Overall, desiccation in conjunction with a surface barrier reduces contaminant migration through the vadose zone more than a barrier alone. Desiccation can also be applied multiple times in the near term to enhance its overall effectiveness in the long term.

Numerical modeling of operational and design factors for the desiccation processes at field scale. Subsurface soil gas flow patterns and related desiccation rates in a homogeneous domain were used initially to evaluate field-test operational conditions. These simulations were targeted at defining appropriate well spacing, airflow, and parameters related to the test layout and equipment for the desiccation demonstration. A series of three-dimensional simulations were conducted using the STOMP simulator (White and Oostrom 2006) to examine different injection and extraction flow rates. Injection and extraction flow rates were varied in the range of 170 to 680 m^3/h (100 to 400 cfm) for both balanced (e.g., 510/510 m^3/h [300/300 cfm] injection/extraction) and unbalanced (e.g., 510/170 m^3/h [300/100 cfm] injection/extraction) conditions.

Unlike a single injection well or a single injection with multiple extraction well configurations, which owing to symmetry, can be simulated two-dimensionally with cylindrical coordinates, a dipole system requires a three-dimensional simulation. Figure 4.63 shows a cross sectional view of the conceptual model for simulating the dipole test. Two vertical wells of diameter d_W, with a screen from a depth d to a depth l, are installed in an effective homogeneous soil above a water table at depth b. For these simulations, d_W = 0.1524 m (0.5 ft), d = 9.7 m (30 ft), l = 15.8 m (50 ft), and b =103 m (338 ft). The injection and extraction wells are spaced 12 m (39 ft) apart.
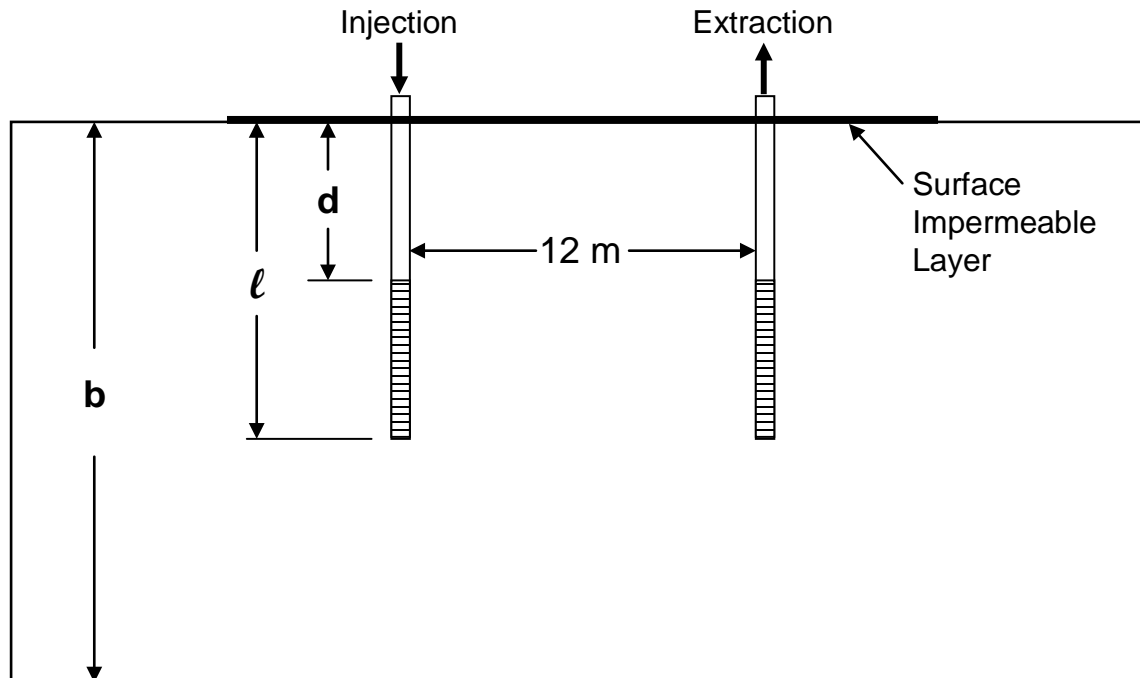
Figure 4.63. Conceptual Model of Well Configuration Used To Simulate Airflow between Two Wells

Boundary conditions are needed for the aqueous mass, gaseous mass, and energy conservation equations. At the surface (100 by 100 m), a no-flow (zero flux) boundary was specified for the aqueous phase across the entire surface. For the gas phase, a no-flow (zero flux) boundary was specified across the areal extent of the surface impermeable layer (46.95 m by 46.95 m [145 ft by 154 ft]) whereas the remainder of the surface was held constant at atmospheric pressure, P_{atm}. For the energy conservation equation, the upper surface is kept at a constant temperature of 23°C whereas the initial temperature in the domain is assumed to be 17°C. Owing to the presence of the water table at the bottom boundary, both the aqueous and gas pressures were held constant at P_{atm}, corrected for the difference in elevation. Temperature was held constant at groundwater temperature, T_{gw}, of 17°C. The four vertical boundaries of the three-dimensional domain were specified as hydraulic gradient boundaries for the aqueous and gaseous phases ($\delta P/\delta z = H$) and as outflow boundaries for energy.

Simulations used an air inlet temperature of 20°C with a 10% relative humidity, a subsurface initial temperature of 17°C, and an initial moisture content of 0.11 m^3/m^3. Thermal properties are also important in modeling the evaporation/condensation processes. Thermal properties of the porous media were estimated from Cass et al. (1981). The porous media pneumatic properties were homogeneous with no anisotropy ratio in the saturated hydraulic conductivity, and set to match the results from the constant rate permeability test. These simulations tend to be somewhat conservative (slow desiccation front move-ment) with respect to the most permeable portions of the test site because flow is more uniform than is expected in the field. In the field, lower permeability lenses are expected to focus flow in the higher permeability layers such that these would dry more quickly. However, the simulations likely over predict the reduction in moisture content within the dry zone because it does not account for drying of the less permeable lenses.

Under the simplified conditions of the simulations, desiccation volumes with time are similar to scoping calculations. For instance, the volume of desiccation over 100 days was approximately 50 m³-soil observed in simulations with a 510 m³/h [300-cfm] injection flow rate. A desiccation volume can also be hand-calculated assuming a 13-g/m³ water capacity of air (at ~15°C), a 510 m³/h [300-cfm] injection flow rate of air with 10% relative humidity, and a change in moisture content of 0.11 m³/m³. This hand-calculated value is ~48 m³-soil. Maintaining relatively higher injection rates (e.g., 510 m³/h [300 cfm]) provides for a larger desiccation volume within the targeted 6-month operational period. The larger desiccated volume is more favorable for monitoring because the desiccation front will intersect multiple monitoring locations. Lower injection flow rates (e.g., 170 m³/h [100 cfm]) require a well spacing likely infeasible for installation in the field (wells too closely spaced for drilling operations), or a longer operational time. For example, the time course of desiccation was simulated for three different injection/extraction conditions: 510/170 m³/h [300/100 cfm] (Figure 4.64), 100/100 (Figure 4.65), and 300/300 (Figure 4.66). These figures demonstrate that higher volumes of soil are desiccated at higher injection rates. Extracting at higher rates (e.g., 510/510 m³/h [300/300 cfm]) provides less of a benefit, and shows that moisture content is reduced by only a small measure (relative to the 510/170 m³/h [300/100 cfm] case). Note also that simulations predict some localized condensation near the extraction well due to the lowered subsurface temperature.
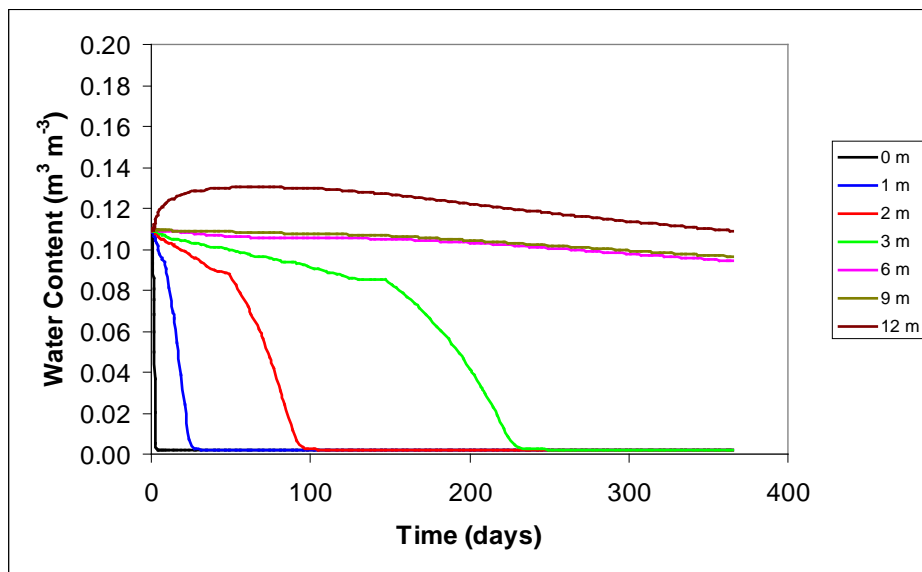
Figure 4.64. Simulated Desiccation (change in water content) Along the Centerline from the Injection to the Extraction Wells (mid-screen depth) for 510/170 m³/h [300/100 cfm] Injection/Extraction Flow Rates
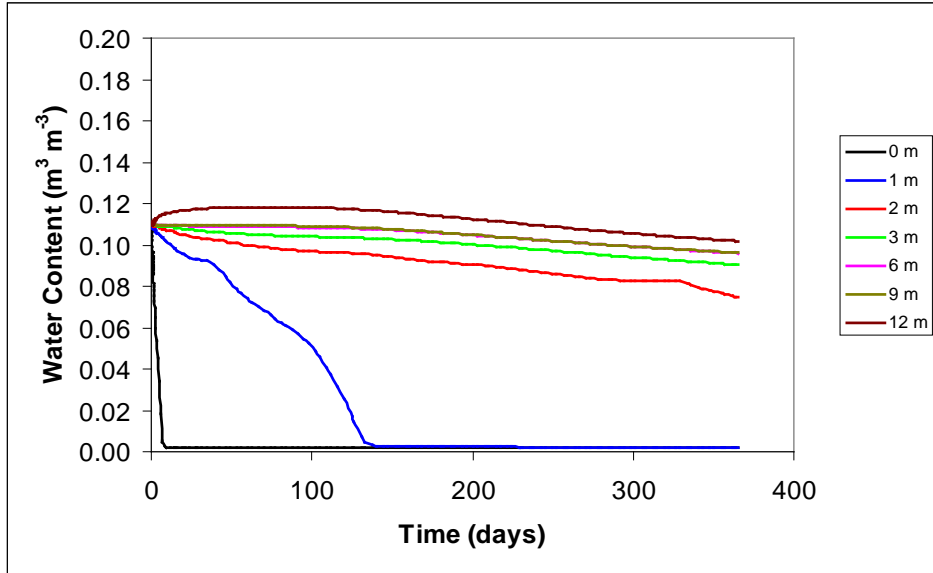
Figure 4.65. Simulated Desiccation (change in water content) Along the Centerline from the Injection to the Extraction Wells (mid-screen depth) for 170/170 m³/h [100/100 cfm] Injection/Extraction Flow Rates
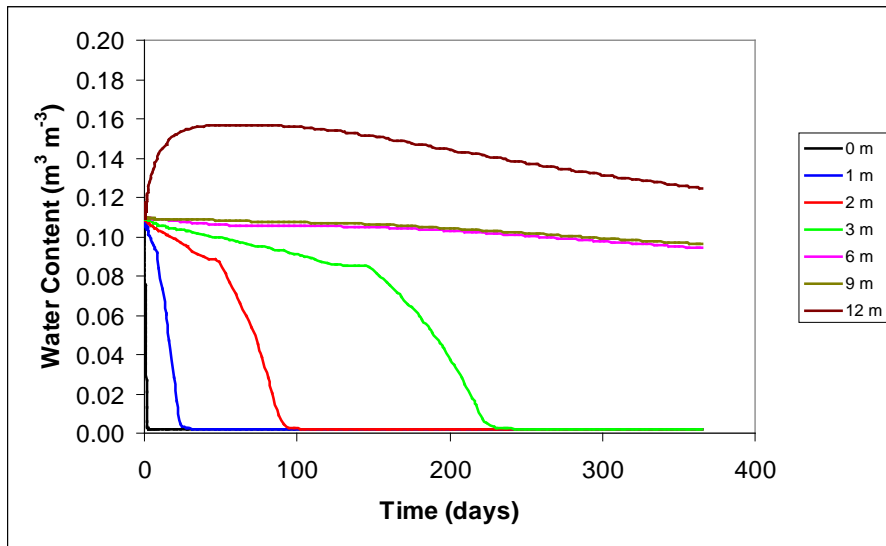
Figure 4.66. Simulated Desiccation (change in water content) Along the Centerline from the Injection to the Extraction Wells (mid-screen depth) for 510/510 m³/h [300/300 cfm] Injection/Extraction Flow Rates

Desiccation near the injection well (i.e., within 3 m [9.8 ft]) is primarily controlled by the injection flow rate. As shown in Figure 4.67 for a range of different injection/extraction rates, gas flow is directly proportional to the injection flow rate through a Y-Z plane located between the injection and extraction wells at a distance of 3 m (9.8 ft) from the injection well. The extraction rate has only a small impact on the gas flow rate at this distance from the extraction well. Table 4.4 shows the total gas flow rate at this plane for a cross sectional area of 57 m² (8.5 m [27.9 ft] in the y direction by 6.7 m [22 ft] in the z

direction) on the centerline between the injection and extraction wells. When the injection rate is 510 m³/h (300 cfm), the range of flow rates varies from 131 to 136 m³/h (77 to 80 cfm), whereas at 170 m³/h (100 cfm) the volumetric flow rate 3 m (9.8 ft) from the injection well is only 21 cfm. Due to the dipole arrangement of the wells, only 20%–30% of the injected airflow is captured at this distance from the injection well.
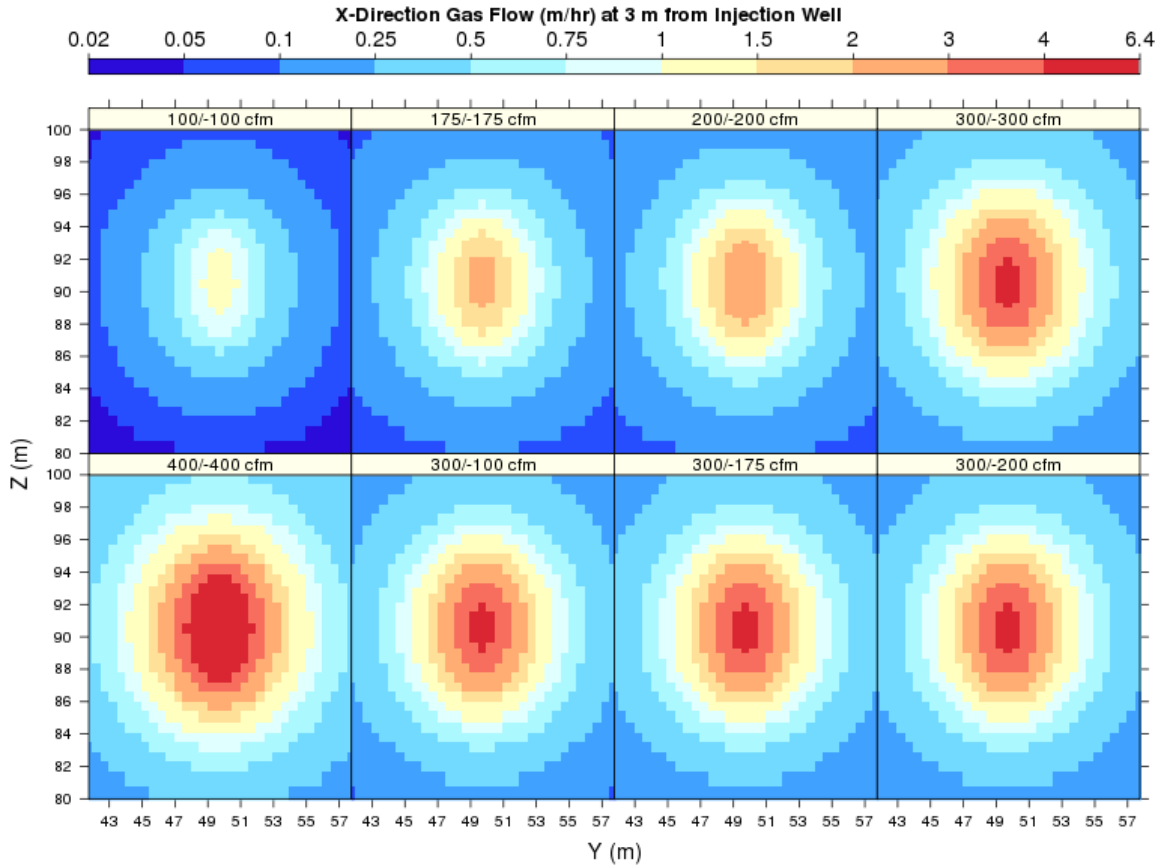
Figure 4.67. Depiction of Gas Flow Rate in a Y-Z Plane Located Between the Injection and Extraction Wells at a Distance of 3 m (9.8 ft) from the Injection Well. The extraction well is 12 m (39 ft) from the injection well. The flow rates are shown as injection/extraction. Note the flow rate through the plane increases with increasing injection flow rate. However, for a fixed injection flow rate of 510 m³/h (300 cfm), the extraction flow rate has little impact on the flow rate through the plane.

Table 4.4. Simulated Gas Flow Rate Through a Y-Z Plane Located between the Injection and Extraction Wells at a Distance of 3 m (9.8 ft) from the Injection Well in a Cross Sectional Area of 57 m² (8.5 m [27.9 ft] in the y direction by 6.7 m [22 ft] in the z direction) on the Centerline between the Injection and Extraction Wells

	Injection/Extraction Flow Rates (cfm)							
	100/100	175/175	200/200	300/300	400/400	300/100	300/175	300/200
Total gas flow rate through cross section (cfm)	21.19	40.46	47.57	79.79	116.77	77.94	78.66	78.88

At 9 m (29.5 ft) from the injection well, the impact of lower extraction rates on the gas flow rate can be observed (Figure 4.68). When the injection rate is fixed at 510 m³/h (300 cfm) and the extraction rate is lowered, the primary effect is a reduction in the gas flow rate along the centerline between the injection and extraction wells. Note the rate of desiccation is essentially the same for both a 510/170 m³/h (300/100 cfm) injection/extraction condition (Figure 4.64) compared to a 510/510 m³/h (300/300 cfm) injection/extraction condition (Figure 4.66) within the first 3 m of the injection well. Use of a dipole arrangement helps focus the soil gas flow to within a targeted monitoring zone and depth interval defined generally by the screened intervals of the wells. The extraction rate can be lower than the injection rate and still direct flow to the monitored test zone. This situation may be preferred for the test because 1) it maintains extraction flow rates lower than the critical velocity that may entrain droplets in the extracted soil gas; and 2) it helps minimize short circuiting between the injection and extraction wells due to the lower induced pressure gradients relative to higher extraction rates.
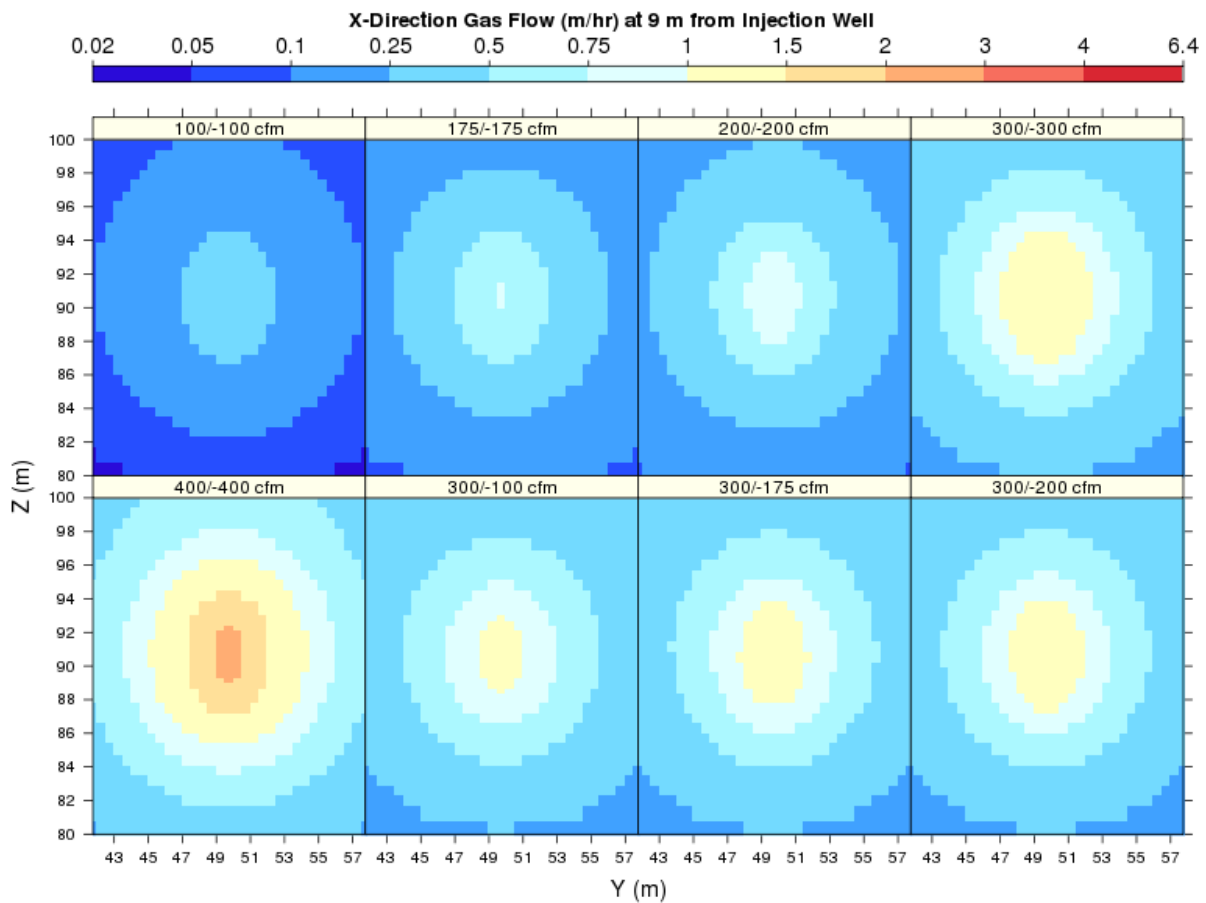
Figure 4.68. Depiction of Gas Flow Rate in a Y-Z Plane Located Between the Injection and Extraction Wells at a Distance of 9 m (29.5 ft) from the Injection Well. The extraction well is 12 m (39 ft) from the injection well. The flow rates are shown as injection/extraction. Note the flow rate through the plane increases with increasing injection flow rate. However, for a fixed injection flow rate of 510 m³/h (300 cfm), lower extraction flow rates diminish the flow rate through the plane, especially along the centerline between the injection and extraction wells.

Simulations also show a moderate increase in moisture content near the extraction well (see Figure 4.64 through Figure 4.66). While lower pressure tends to decrease relative humidity, the lower temperature induced at the extraction well in the simulations (see Figure 4.69 through Figure 4.71) causes condensation to occur. This condensation is focused around the extraction well because of the higher airflow rate through this region and because the extraction well draws soil gas from regions outside the desiccation zone where temperatures are higher compared to near the well.
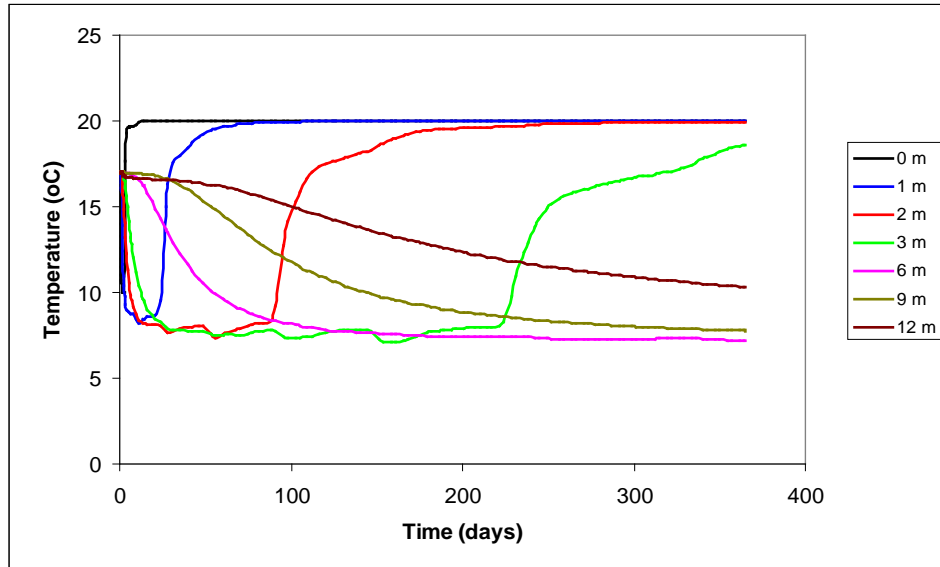
Figure 4.69. Simulated Temperature Profile During Desiccation Along the Centerline from the Injection to the Extraction Wells (mid-screen depth) for 510/170 m^3/h (300/100 cfm) Injection/Extraction Flow Rates. The injected air temperature is 20°C.
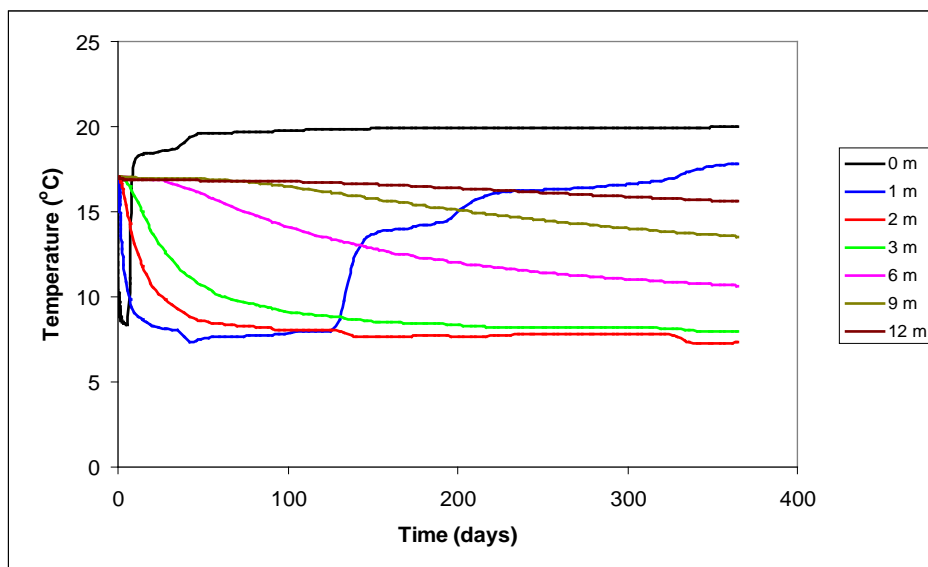
Figure 4.70. Simulated Temperature Profile During Desiccation Along the Centerline from the Injection to the Extraction Wells (mid-screen depth) for 170/170 m^3/h (100/100 cfm) Injection/Extraction Flow Rates. The injected air temperature is 20°C.
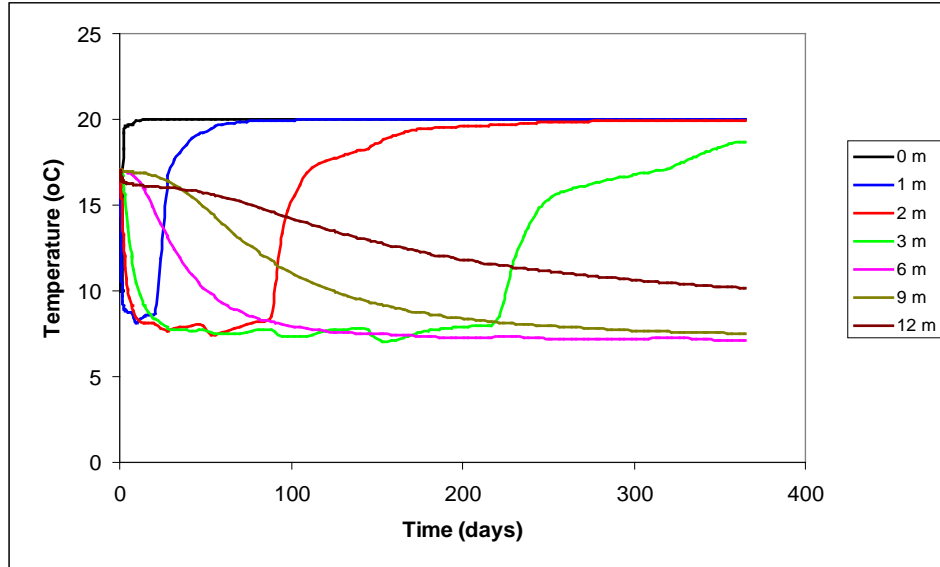
Figure 4.71. Simulated Temperature Profile During Desiccation Along the Centerline from the Injection to the Extraction Wells (mid-screen depth) for 510/510 m^3/h (300/300 cfm) Injection/Extraction Flow Rates. The injected air temperature is 20°C.

The simulation results suggest that field operations could be effectively initiated by selecting a desired influent airflow rate (e.g., 510 m^3/h [300 cfm]) based on a targeted desiccation volume and test timeframe. The extraction flow rate could then be increased until a desired flow pattern (e.g., as measured by pressure and tracer response) is obtained. Pressure gradients, and therefore the flow field, vary with the selected injection and extraction flow rates. For example, Figure 4.72, Figure 4.73, and Figure 4.74 show the pressure gradients for the 510/170 m^3/h (300/100 cfm) injection/extraction, the 170/170 m^3/h (100/100 cfm) injection/extraction, and the 510/510 m^3/h (300/300 cfm) injection/extraction conditions, respectively. Based on previous scoping simulations (Ward et al. 2008), increased injection air temperature could be used to increase the desiccation rate if necessary to reach targeted desiccation volumes within the test timeframe. Because monitoring instrumentation would be impacted by the injected air temperature, only moderate increases in injection air temperature should be considered.
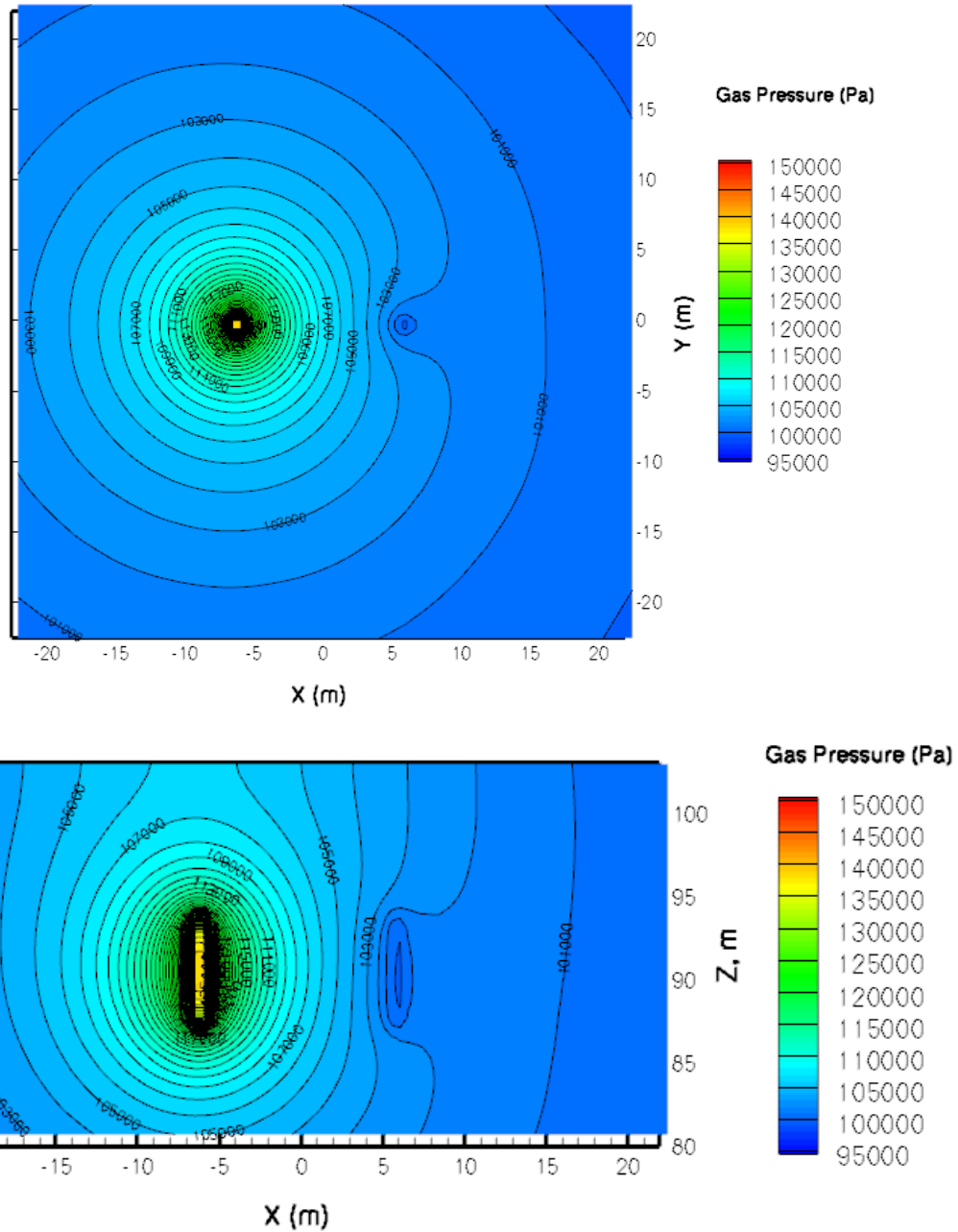
Figure 4.72. Simulated Plan (mid-screen depth) and Cross Sectional Views of the Pressure Gradients for 510/170 m^3/h (300/100 cfm) Injection/Extraction Flow Rates. Injection well is at - 6 m (-19.7 ft) and the extraction well is at 6 m (19.7 ft).
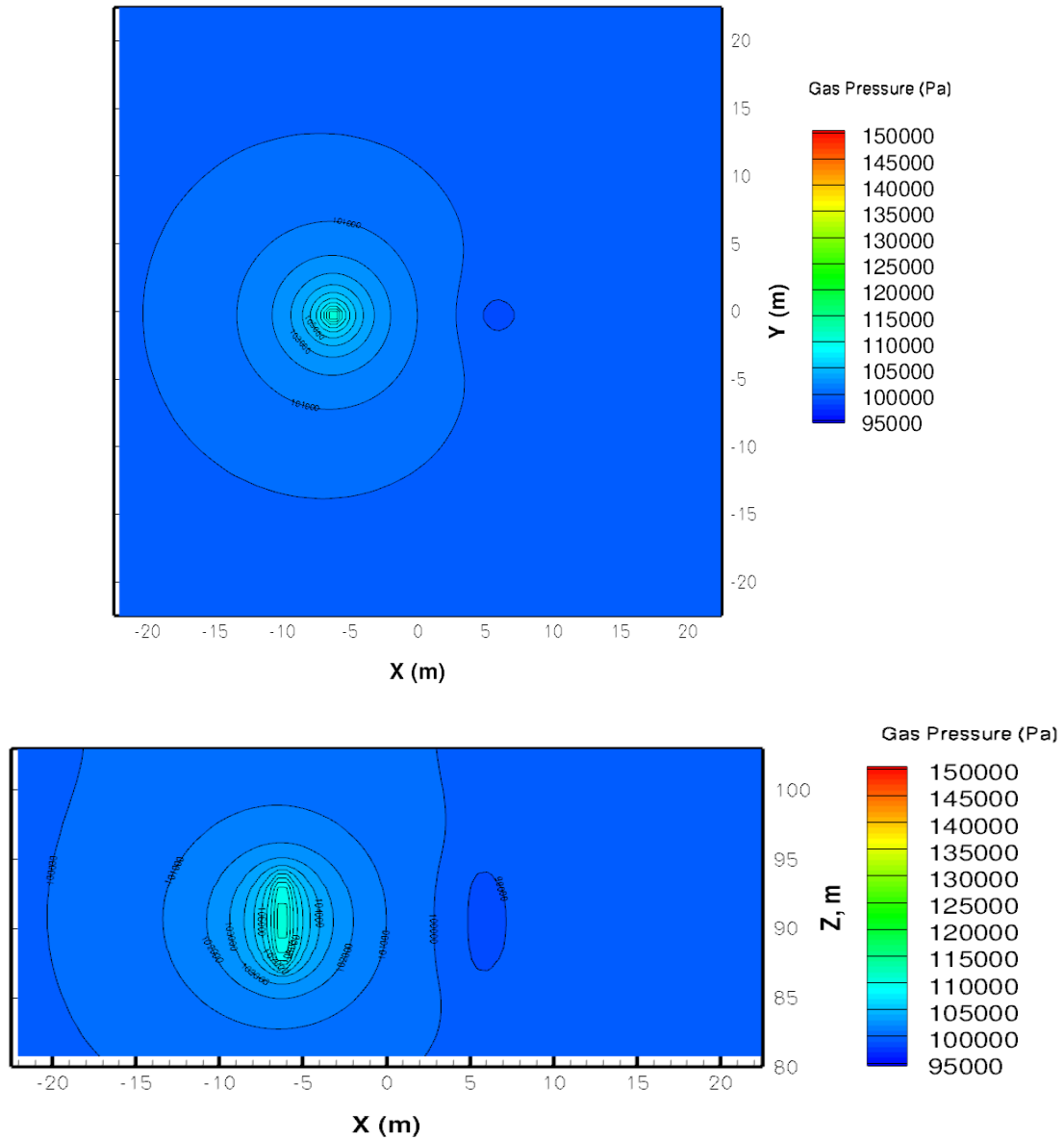
Figure 4.73. Simulated Plan (mid-screen depth) and Cross Sectional Views of the Pressure Gradients for 170/170 m³/h (100/100 cfm) Injection/Extraction Flow Rates. Injection well is at - 6 m (-19.7 ft) and the extraction well is at 6 m (19.7 ft).
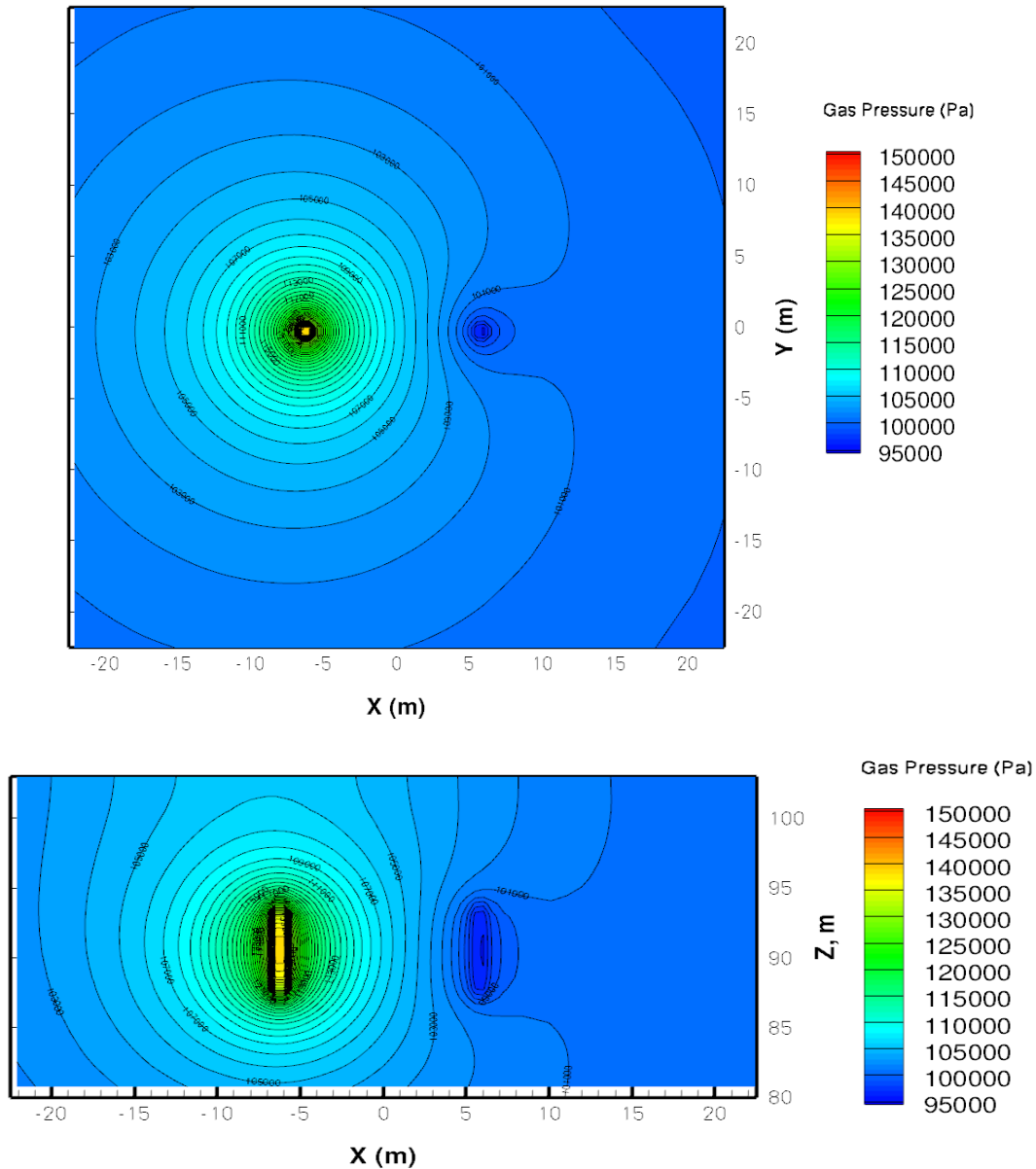
Figure 4.74. Simulated Plan (mid-screen depth) and Cross Sectional Views of the Pressure Gradients for 510/510 m³/h (300/300 cfm) Injection/Extraction Flow Rates. Injection Well is at –6 m (-19.7 ft)and the Extraction Well is at 6 m (19.7 ft).

Numerical modeling of the desiccation field test site. Pre-test simulations (above) were conducted using a homogeneous model domain based on the bulk subsurface property information available prior to having test infrastructure in place. Refined field simulations were conducted using the results of gas tracer testing at the test site (Section 4.1) to modify the model domain and account for the large-scale heterogeneity observed from these tracer data. Injected gas flow was significantly higher in the deeper monitored zone at the site compared to the upper zones. Thus, the model domain was modified to include a low permeability zone in the 98 to 131 m (30 to 40 ft) depth interval. Desiccation simulations were conducted using this model domain to provide an estimate for the temporal desiccation response at the site monitoring locations for use in comparing to the observed responses. Note that the simulated results

4.69

do not account for small-scale heterogeneity or lateral heterogeneity, so are expected to represent general, not specific, trends in desiccation progress.

Figure 4.75 through Figure 4.81 show the simulated moisture content, matric potential, humidity, and temperature responses at the monitoring locations. The responses are shown for each of the sensor depth intervals at these locations. Simulated results show desiccation responses occurring at C7522, C7524, C7526, C7528 at the 47.5 ft (14.5 m) sensor depth interval within 30 days, similar to the field results (Section 4.1). Within 60 days, the simulations show a desiccation response at C7530 at the 47.5 ft (14.5 m) sensor depth interval, also reflected in the field data. The simulations over-predict desiccation progress at C7532 and C7534 and for the 32, 37.5, and 42 ft (9.8, 11.4, 12.8 m) intervals. However, the extent of over-prediction is not known because the test was stopped after about 150 days of dry gas injection.
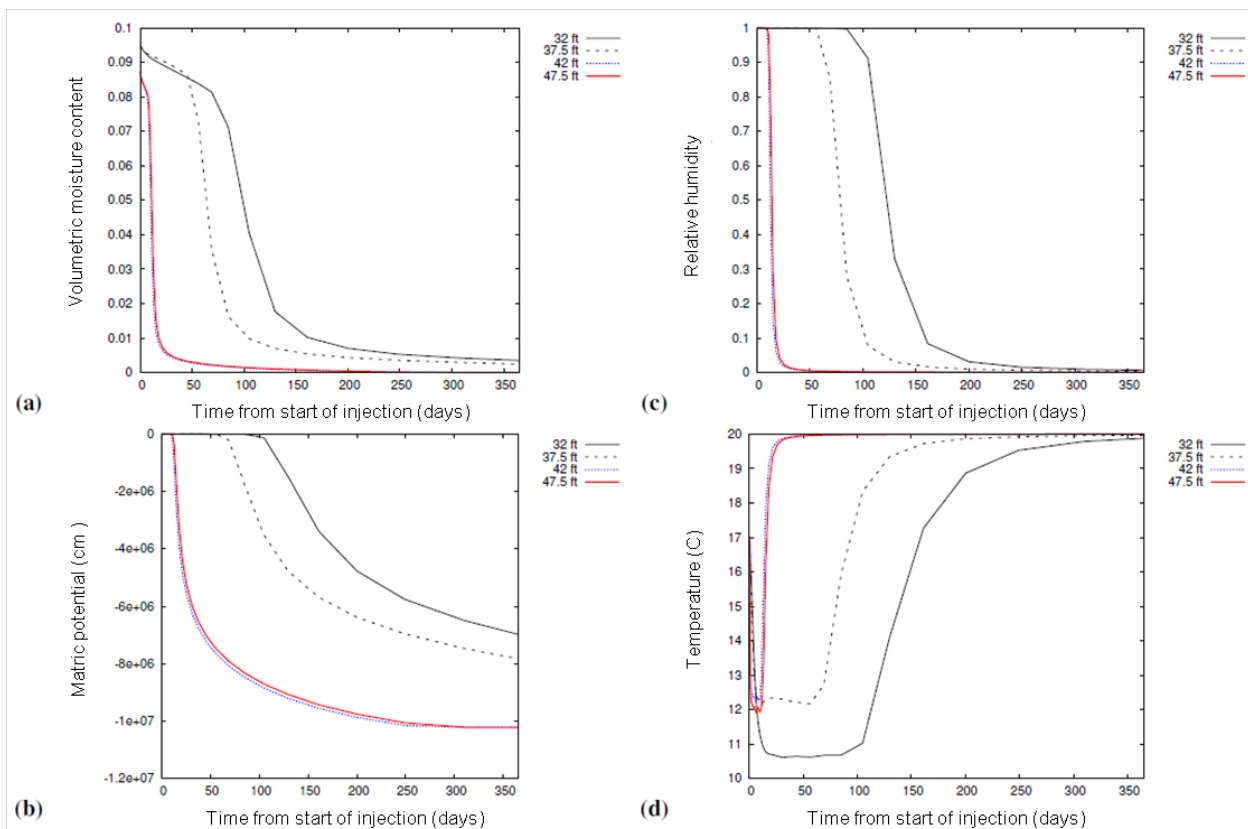
Figure 4.75. Simulated Desiccation Response at Location C7522 for a Layered Model Domain in Terms of (a) Volumetric Moisture Content, (b) Matric Potential, (c) Relative Humidity, and (d) Temperature Changes at the Nominal Mid-Depth of the Sensor Intervals for the Field Test (32, 37.5, 42, and 47.5 ft [9.8, 11.4, 12.8, and 14.5 m] bgs)

4.70
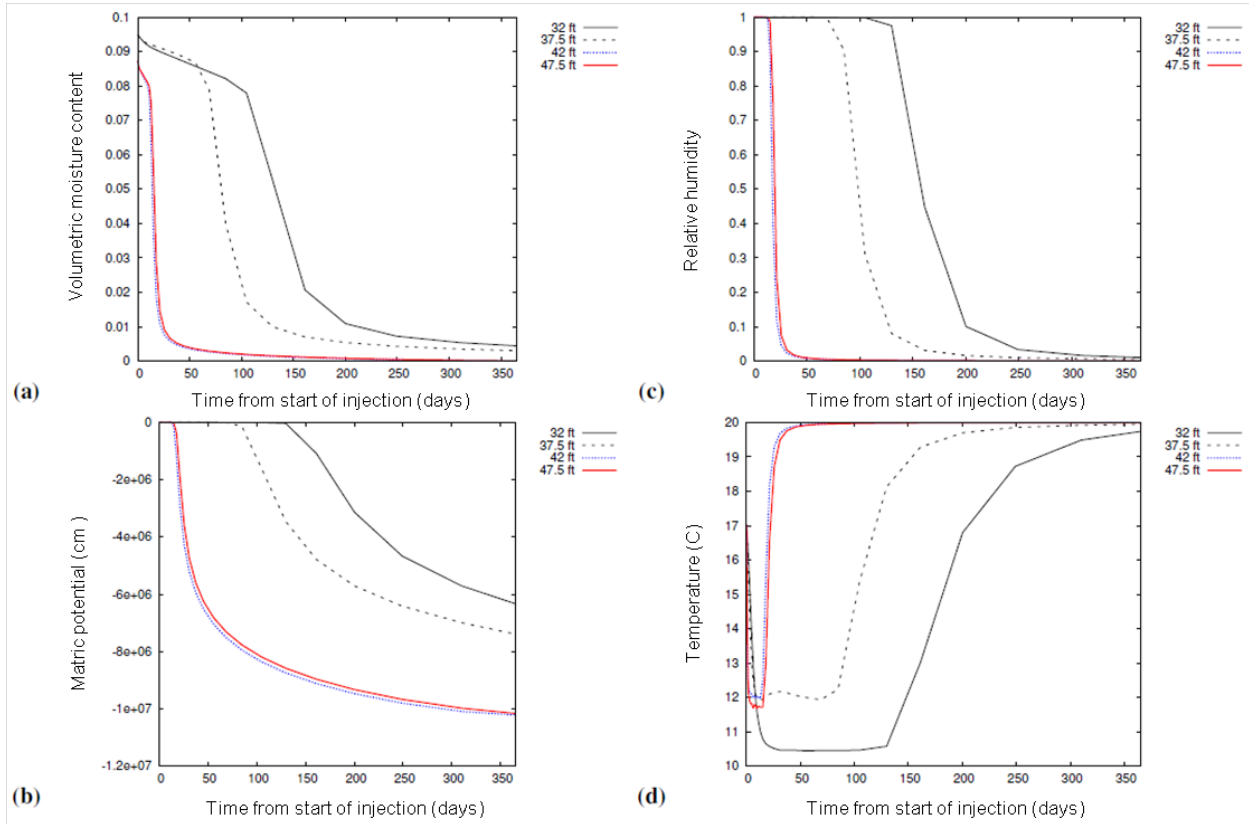
Figure 4.76. Simulated Desiccation Response at Location C7524 for a Layered Model Domain in Terms of (a) Volumetric Moisture Content, (b) Matric Potential, (c) Relative Humidity, and (d) Temperature Changes at the Nominal Mid-Depth of the Sensor Intervals for the Field Test (32, 37.5, 42, and 47.5 ft [9.8, 11.4, 12.8, and 14.5 m] bgs)
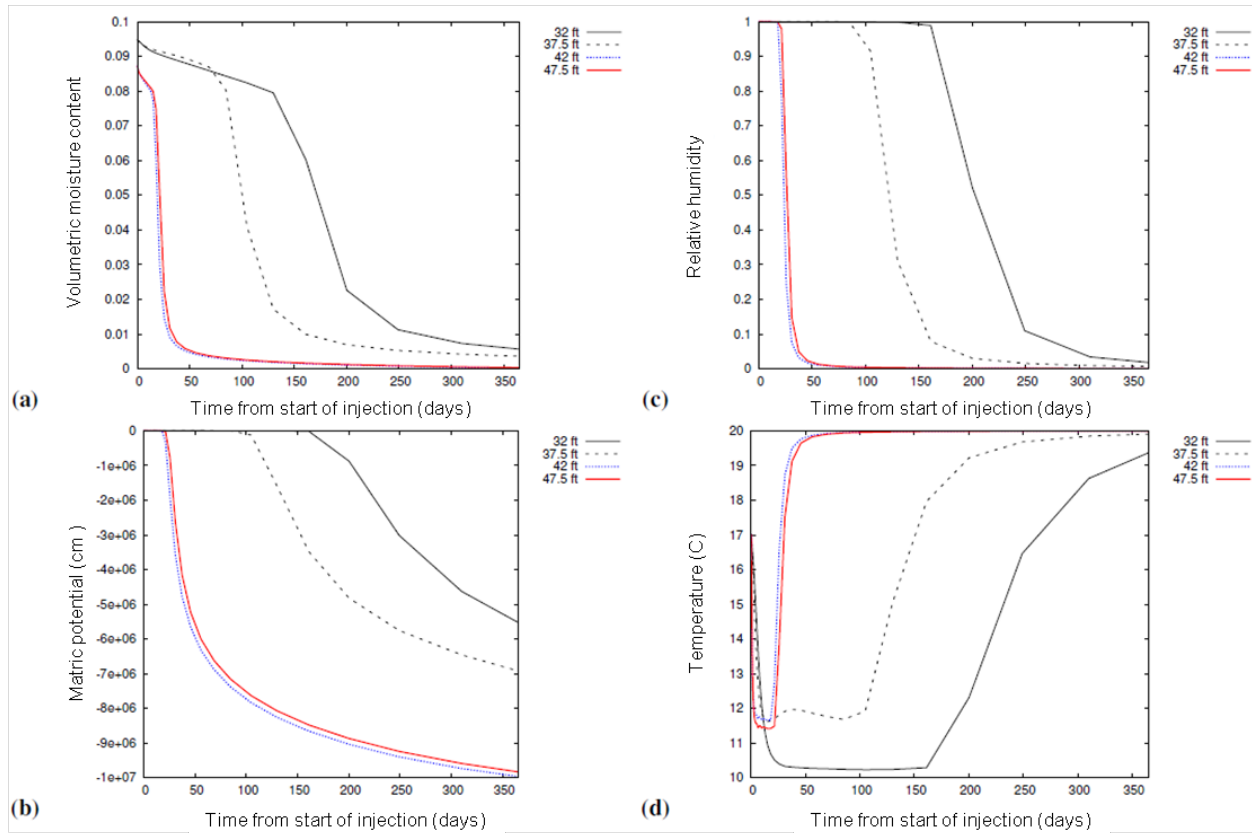
Figure 4.77. Simulated Desiccation Response at Location C7526 for a Layered Model Domain in Terms of (a) Volumetric Moisture Content, (b) Matric Potential, (c) Relative Humidity, and (d) Temperature Changes at the Nominal Mid-Depth of the Sensor Intervals for the Field Test (32, 37.5, 42, and 47.5 ft [9.8, 11.4, 12.8, and 14.5 m] bgs)
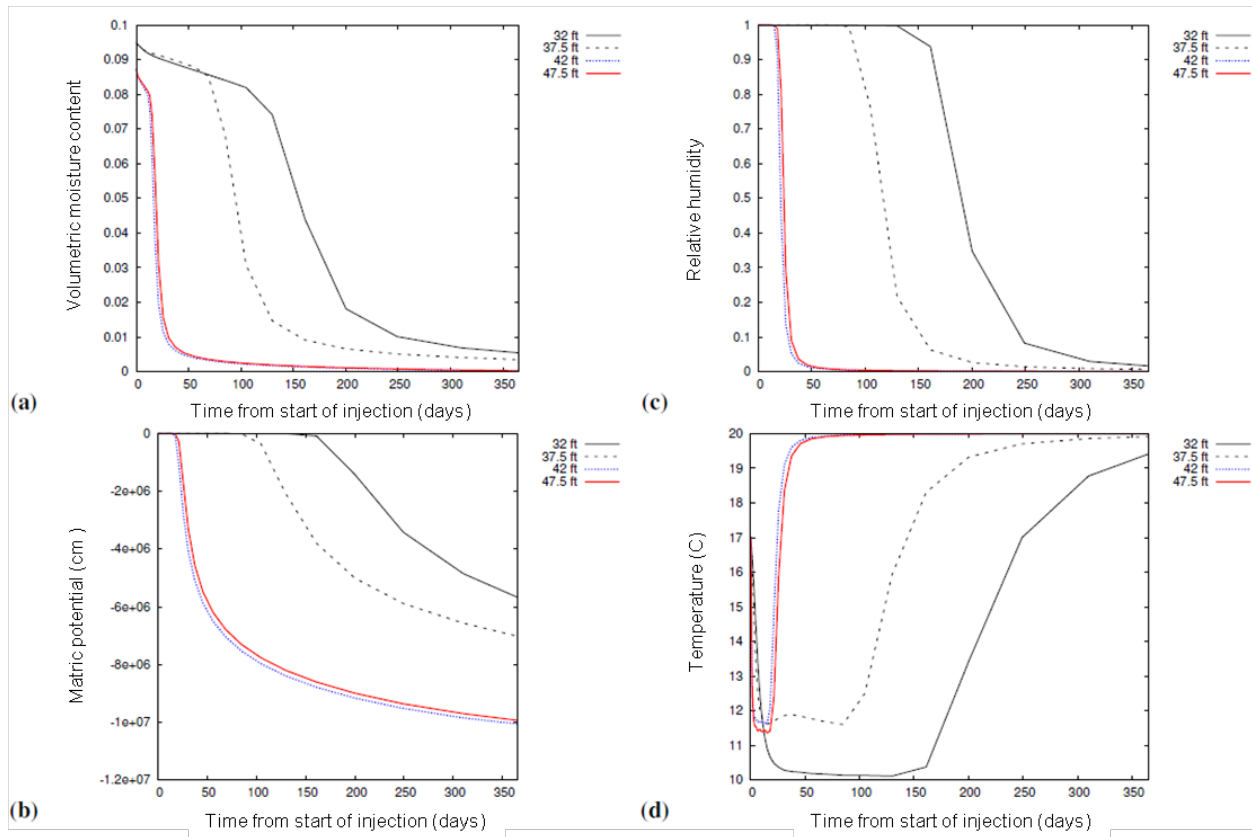
Figure 4.78. Simulated Desiccation Response at Location C7528 for a Layered Model Domain in Terms of (a) Volumetric Moisture Content, (b) Matric Potential, (c) Relative Humidity, and (d) Temperature Changes at the Nominal Mid-Depth of the Sensor Intervals for the Field Test (32, 37.5, 42, and 47.5 ft [9.8, 11.4, 12.8, and 14.5 m] bgs)
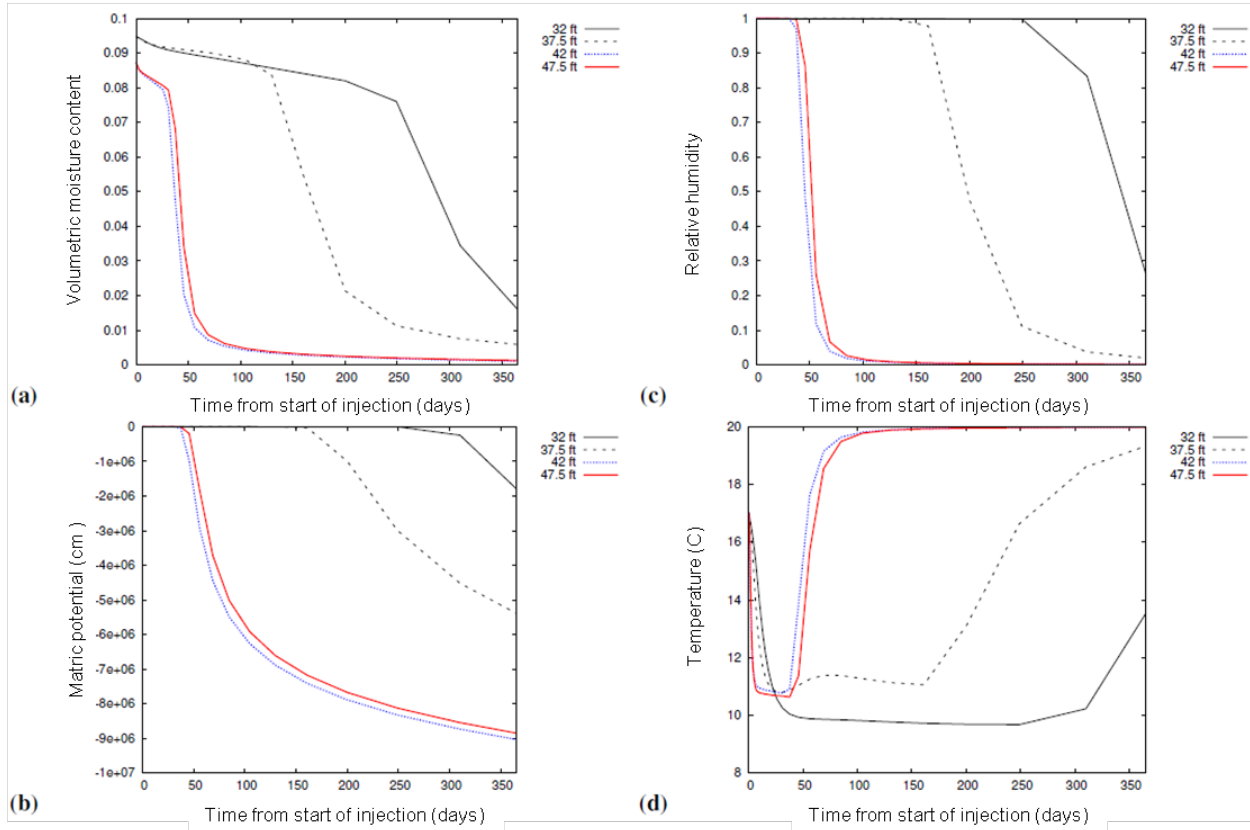
Figure 4.79. Simulated Desiccation Response at Location C7530 for a Layered Model Domain in Terms of (a) Volumetric Moisture Content, (b) Matric Potential, (c) Relative Humidity, and (d) Temperature Changes at the Nominal Mid-Depth of the Sensor Intervals for the Field Test (32, 37.5, 42, and 47.5 ft [9.8, 11.4, 12.8, and 14.5 m] bgs)
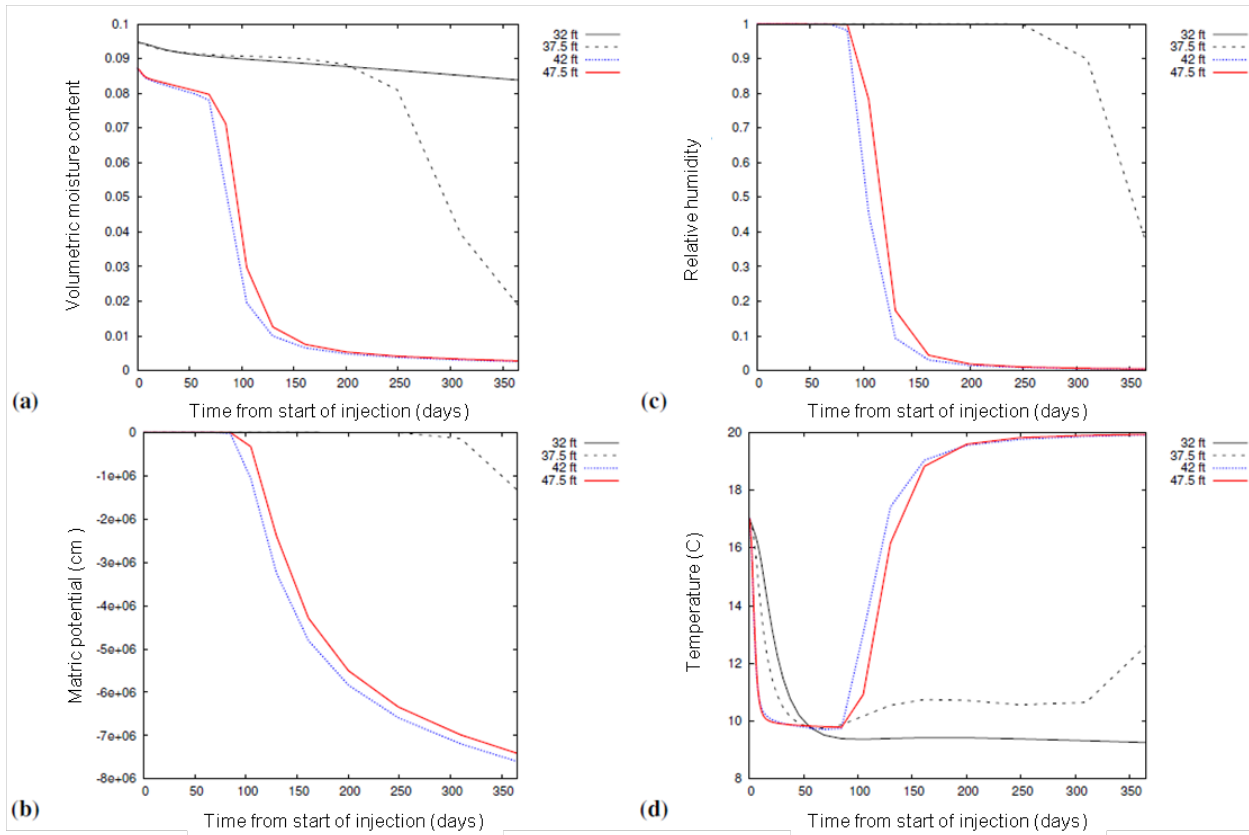
Figure 4.80. Simulated Desiccation Response at Location C7532 for a Layered Model Domain in Terms of (a) Volumetric Moisture Content, (b) Matric Potential, (c) Relative Humidity, and (d) Temperature Changes at the Nominal Mid-Depth of the Sensor Intervals for the Field Test (32, 37.5, 42, and 47.5 ft [9.8, 11.4, 12.8, and 14.5 m] bgs)
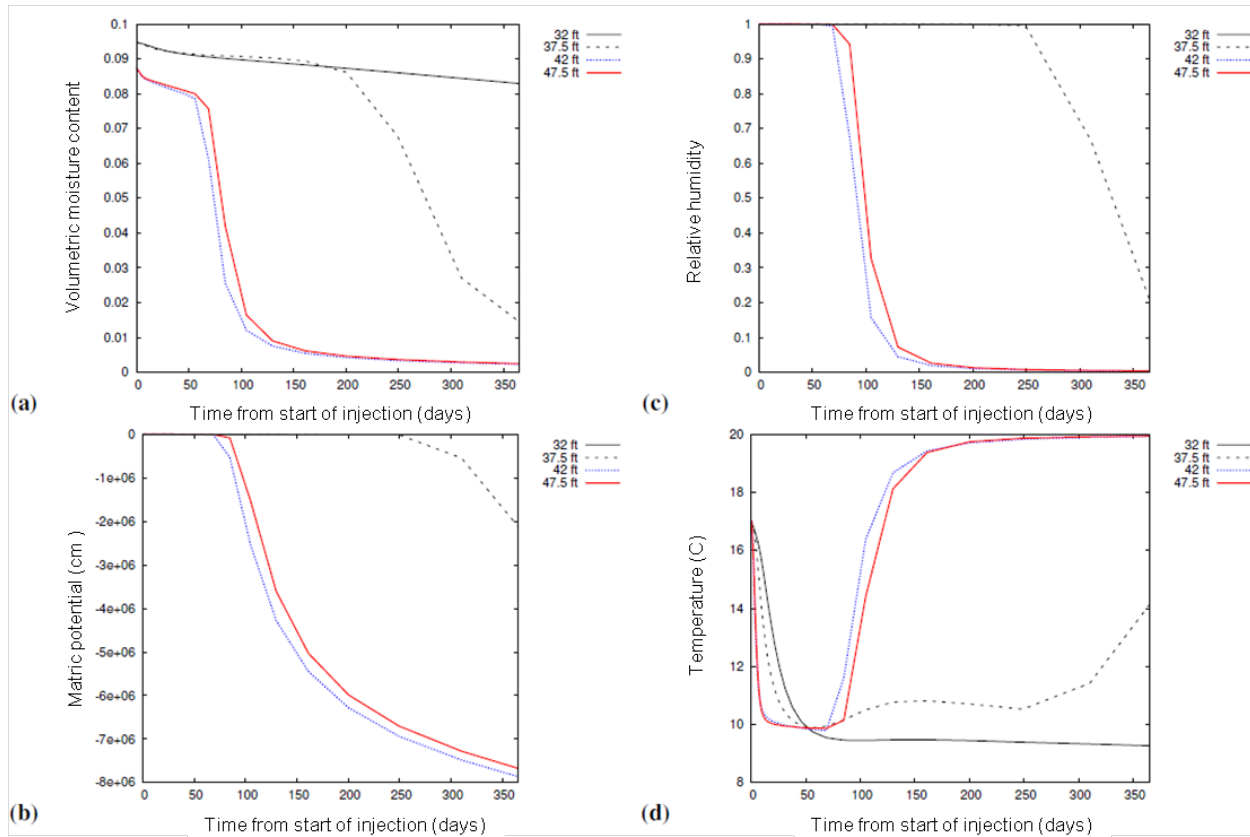
Figure 4.81. Simulated Desiccation Response at Location C7534 for a Layered Model Domain in Terms
of (a) Volumetric Moisture Content, (b) Matric Potential, (c) Relative Humidity, and
(d) Temperature Changes at the Nominal Mid-Depth of the Sensor Intervals for the Field
Test (32, 37.5, 42, and 47.5 ft [9.8, 11.4, 12.8, and 14.5 m] bgs)

4.2.1.2   Assessment of Desiccation Design Features

Several elements of the field test design are important to consider in a full-scale design for desiccation.
The material below summarizes important features related to 1) equipment and monitoring design, and 2)
field characterization information.

Equipment and Monitoring Design. The following elements should be considered in the design of the
monitoring system for a full-scale application.

- While in situ sensors provided information that was used to interpret desiccation performance during
  the field test, the only in situ sensors recommended for full-scale are thermistors (temperature
  sensing) and electrical resistivity electrodes (see Section 4.2.3). Emplacement of these sensors
  requires an access borehole into which a thermistor cable containing thermistors at a specific interval
  (e.g., every 0.6 m) and an electrical resistivity electrode cable with electrodes at specific intervals
  (e.g., every 2 m). With these cables in the borehole, the borehole should be backfilled with an
  alternating fill of sand and hydrated bentonite grout such that each individual electrical resistivity
  electrode is within grout material and there is sand separating each grouted zone from the grout zone
  above and below. The grout is needed to maintain good electrical contact between the electrode and

the formation. It should not be continuous, however, so that each electrode acts separately (e.g., is separated by an insulating material [sand]). Thermistors can be within either material.

- Cased wells installed for neutron logging should use the same design as used in the field test.

- The injection well can be designed to enable short term neutron moisture logging characterization of moisture content changes that correlate to injected gas flow. To enable neutron moisture logging, a stilling well can be installed in the injection well that allows access for a small diameter logging probe (see Figure 3.7). The rate of change in moisture at each depth interval during initial injection operations is related to the amount of gas flow within that depth interval.

For full-scale application, key field parameters important to desiccation design and performance evaluation and the associated characterization methodology are listed below. This recommendation assumes an injection-only design.

- Bulk permeability – rough estimate needed with additional quantification through measurements only if permeability may be low enough to cause air injection issues or significantly impact the air injection design.

- Distribution of permeability – estimate based on borehole lithology and vertical neutron probe data may be sufficient with additional information gathered if needed based on the uncertainties in the lateral heterogeneity or nature of permeability contrasts.

- Sediment properties from borehole samples – lithology description, moisture, contaminant, conductivity, and particle size information as a function of depth are needed at minimum to link to field measurements and estimate residual moisture content (used for setting target).

- Initial distribution of moisture and contaminants – sufficient information is needed to target desiccation and select appropriate performance goals (size of desiccated zone and extent of moisture reduction needed).

4.2.2   Desiccation Field Test Performance

The field test data can be interpreted with respect to the desiccation performance using the following categories of performance during active desiccation and after active desiccation (rewetting phase).

4.2.2.1   Active Desiccation Performance Assessment

Lateral Extent of Desiccation from Injection Well. Significant desiccation response was observed within the 13.7-16.8 m bgs (45–55 ft) depth interval out to a lateral extent of about 3 m (9.8 ft) from the injection well with a limited desiccation response (desiccation in less than 1-m-thick depth intervals) at 4 to 5.5 m (18 ft) distance by the end of active desiccation based on sensor and neutron logging data. Specifically, the neutron moisture log data show that the extent of drying depends on the initial moisture content and the distance from the injection well (see also Truex et al. 2012b). Examining the neutron moisture content data over time in the depth interval between 13.7 and 15.2 m (45 and 50 ft) bgs shows that, at locations C7529 and C7527 within 2 m (6.7 ft) of the injection well, the initially dryer zones, correlated to coarser higher permeability zones, dry first. However, with time, the initially wetter zones, correlated to finer-grained, lower permeability zones, are also desiccated. At larger radial distances from the injection well (e.g., locations C7531, C7523, C7525, C7533, and C7537) in this same depth interval,

moisture content is reduced over time primarily in the initially dryer zones, but by a much smaller extent in the initially wetter zones, especially as radial distance increases. Thus, while the leading edge of desiccation is following preferential flow pathways, the desiccated zone broadens over time and includes initially wetter regions closer to the injection well. This type of pattern of desiccation for adjacent coarse- and fine-grained layers has also been observed in laboratory flow cell tests (Oostrom et al. 2009, 2012b).

A rough comparison can be made to the expected radial influence calculated based on the amount of dry gas injected. About 1,800,000 m^3 of dry nitrogen was injected. This amount of dry gas, at the average temperature during the field test, is sufficient to fully desiccate a cylindrical region with a height of 6.1 m (20 ft) (screen length) and an initial moisture content of 0.0894 m^3-water/m^3-gas (initial average at the test site) to a radius of about 3.4 m (1 ft).

Volumetric Desiccation Estimate. Quantitative estimates of desiccation volume related to a specific threshold moisture content can be calculated using the neutron moisture logging data and the GPR data (ERT does not provide the necessary moisture content information). Neutron moisture logging data provides the vertical distribution of volumetric moisture content at the logging locations. The volumetric distribution of desiccation can be evaluated based on the volume reduced to below a specified threshold moisture content. Volumes were calculated by first identifying the neutron data locations (corresponding to a depth interval of 7.6 cm) along a neutron moisture log vertical profile where the final volumetric moisture content was below the specified threshold. Table 4.5 shows the number of neutron data intervals meeting each specified threshold value. The volume for each threshold location was then computed by multiplying the interval depth by the annular volumes between the monitoring point and the radial extent of the next inner monitoring location (or to the injection well for the innermost monitoring location). Finally, the volumes for each data interval meeting the specified threshold were added to provide the total volume below the specified threshold (Table 4.6). This estimate assumed a radial symmetry for the desiccation zone. Using the same type of calculation procedure for the neutron moisture logging data but with no specified threshold (e.g., all neutron data intervals where final moisture content values were lower than initial moisture content values), moisture content was reduced compared to initial conditions in a volume of 1300 m^3. Integrating the neutron data for the portion of the test site out to the radial distance to well C7537, the computed total amount of water removed during desiccation is 18,400 kg. Using a psychometric chart and the average test site temperature during desiccation of 12°C, the injected gas has a capacity to hold about 10.9 g-water/m^3-gas once it evaporates water and reaches a relative humidity of 100% at 12°C. With this water-holding capacity, the amount of water removed during desiccation computed based on the amount of dry gas injected during the test (1.8E+6 m^3) was 19,600 kg.

Table 4.5. Neutron Moisture Logging Data Showing the Number of 7.6-cm-thick Intervals at or below the Specified Threshold Volumetric Moisture Content at the End of Active Desiccation

Volumetric Moisture Content Threshold (m^3/m^3)	C7529 r = 1.85 m	C7527 r = 2.04 m	C7531 r = 2.62 m	C7525 r = 3.02 m	C7523 r = 3.02 m	C7533 r = 4.18 m	C7537 r = 5.34 m
0.01	41	33	22	18	15	3	0
0.02	48	38	30	24	24	7	0
0.03	56	44	35	33	30	16	0
0.04	89	54	62	56	62	40	11

Table 4.6. Computed Volume of Soil Desiccated to at or below the Specified Threshold Volumetric Moisture Content at the End of Active Desiccation Using the Data from Table 4.5, an Assumption of Radial Symmetry, and the Specified Radial Distances to Each Monitoring Location. Note that because locations C7523 and C7525 were at essentially the same radial distance, only the data from location C7523 was used in the calculation.

Volumetric Moisture Content Threshold (m^3/m^3)	Volume of soil (m^3) C7529 r = 1.85 m	Volume of soil (m^3) C7527 r = 2.04 m	Volume of soil (m^3) C7531 r = 2.62 m	Volume of soil (m^3) C7523 r = 3.02 m	Volume of soil (m^3) C7533 r = 4.18 m	Volume of soil (m^3) C7537 r = 5.34 m
0.01	33.5	6.1	14.2	8.2	6.0	0
0.02	39.2	7.0	19.3	13.1	14.0	0
0.03	45.7	8.1	22.5	16.3	32.0	0
0.04	72.6	10.0	39.9	33.8	80.0	29.1

Cross-hole GPR data were collected between the injection well and surrounding logging wells C7523, C7525, C7527, C7529, and C7531 and processed to produce a 2-D image of the estimated volumetric moisture content within the plane between the well pairs. For each well pair and at every depth the maximum distance from the injection well with volumetric water content less than a threshold of 0.01 m^3/m^3 cutoff was identified. A cylindrically symmetric volume was then calculated from the average distance at each depth from the well pair data. The GPR-based estimate of desiccation volume for desiccation to a volumetric moisture content equal to or less than 0.01 m^3/m^3 was 52 m^3. For comparison, the data from neutron moisture logging for the portion of the test site out to the radial distance to well C7531 was used to compute a desiccation volume of 62 m^3 at the same threshold.

Vertical Distribution of Desiccation. Significant variation in desiccation was observed across the vertical profile of the test site. This variation correlated to the initial moisture content, sediment texture, and amount of dry gas flow through a given vertical zone. The variation is evident in the neutron moisture logging profiles where initially wetter zones (finer materials) dried more slowly. Some of the thinner initially wet zones in the 13.7–16.8 m bgs (45–55 ft) depth interval dried over time, however, because of the high flow of dry gas adjacent to these zones (see neutron log for C7529, located about 1.8 m [6 ft] from the injection well). ERT, neutron, and GPR data depict some desiccation vertically above and below the injection well screen interval, likely the result of gas flow spreading in the relatively permeable zones above and below the screened interval.

Desiccation Moisture Endpoint. In zones that were fully desiccated, neutron moisture logging and post-desiccation core analysis show that the volumetric moisture content was reduced to less than 0.01 m^3/m^3. Sensors in highly desiccated zones showed matric potential values less than -10 bar. These field measurements are consistent with the extremely dry post-desiccation conditions observed in laboratory tests (Truex et al. 2011; Oostrom et al. 2009, 2012b).

Desiccation Rate. The desiccation rate is directly proportional to the rate at which dry gas is injected and the carrying capacity of that gas for water. For the field test, the injection flow rate was maintained at nominally 300 scfm with a relative humidity of zero. Using a psychometric chart and the approximate initial subsurface temperature of 17°C, the injected gas has a capacity to hold about 14.6 g-water/m^3-gas once it evaporates water and reaches a relative humidity of 100% at 17°C. Based on this information, the

nominal desiccation rate at the field test site would be about 180 L/d (water was transferred from the water phase to the gas phase). However, due to evaporative cooling, the average temperature within the field test site desiccation zone was about 12°C. At the lower temperature, injected gas has a capacity to hold about 10.9 g-water/m^3-gas and a corresponding desiccation rate would be about 130 L/d. The remainder of the overall capacity (50 L/d) would evaporate water from portions of the subsurface further away from the primary desiccation zone as the overall subsurface temperatures warmed toward 17°C. Maintaining higher and more uniform temperature would make the desiccation front more abrupt (e.g., keep more of the capacity within a target zone). When temperature drops at the desiccation zone, the holding capacity of the air decreases. As the gas moves outward to other areas, temperature increases and the gas picks up additional water. Thus, the transfer of water to gas phase occurs over distance. Keeping the temperature more constant minimizes the "spreading" of the desiccation process over distance.

In controlled laboratory experiments, injection of dry gas into moist homogeneous porous media causes drying to occur with a very sharp transition between the dried porous media (toward the injection location) and the moist porous media. In these conditions, the volume of dried sediment can be calculated using the approach presented above. Factors that make the transition between dried and moist zones occur over a larger distance include evaporative cooling effects (causing a lower water-holding capacity of the gas), and heterogeneity in gas flow (caused by heterogeneity in permeability and moisture content distribution). In the field, both of these conditions were present, and a simple volume calculation to estimate the fully desiccated zone is not directly applicable.

Impact of Evaporative Cooling. Significant evaporative cooling occurs during desiccation as observed both in laboratory tests and the field test. As discussed above, the evaporative cooling can impact the overall desiccation rate within the portion of the vadose zone where temperatures are lowered and tends to spread the desiccation process over distance. For scale-up, evaporative cooling must be considered in terms of the potential to condense water in the subsurface depending on the injected gas temperature and relative humidity and the subsurface temperature. This effect is discussed in Section 4.2.4. While evaporative cooling will always occur with desiccation, its impact can be evaluated and included in the desiccation design.

Operational Performance. System operations were very stable over time with the field test system. For a full-scale system, extraction of soil gas is not recommended, thus simplifying the system further. Injection of ambient air rather than dry nitrogen is recommended for full scale. Thus, operational reliability will be related to the reliability of the blower and air heater components. These are standardized equipment where reliability is expected to be high.

4.2.2.2   Post-Desiccation (Rewetting) Performance Assessment

Desiccation is intended to help meet remediation goals by slowing the movement of contaminated moisture through the vadose zone and thereby reducing the flux of contaminants into the groundwater. The rate at which moisture returns to the desiccated zone, here termed the rewetting rate, is important in the overall long-term performance of desiccation as part of a remedy. Rewetting phenomena and rates have been studied through laboratory and modeling efforts. Data were also being collected at the field test site after active desiccation was terminated.

4.2.2.2.1 Laboratory Evaluation of Rewetting

Laboratory data quantifying the rewetting process was collected and reported in Truex et al. (2011). Key conclusions were that vapor-phase rewetting can occur but rewets the desiccated zone only to a small extent, essentially to a level below the residual moisture content. Rewetting by aqueous transport occurs consistent with standard hydraulic phenomena such that desiccating to very low moisture content and creating very low aqueous phase hydraulic conductivity conditions leads to very low rates of aqueous transport rewetting.

4.2.2.2.2 Modeling Analysis of Rewetting

In earlier assessments of the rewetting process, Truex et al. (2013, 2014) showed that rewetting of the desiccated zones occurs relatively fast, consistent with expectations based on related laboratory analyses. Since the end of the desiccation period in 2011, a significant portion of the desiccated zone has been rewetted over a period of three years (Section 4.1; Truex et al. 2014). The numerical analysis reported in Truex et al. (2013) showed that although some lateral rewetting through water advection could occur, the observed desiccation in the field could not fully be explained by lateral migration alone. The initial modeling results indicated that a 3-D analysis is needed to fully assess subsurface rewetting. To this end, a 3-D model was developed, with numerical model implementation using the STOMP code (White and Oostrom 2006), to conduct a number of scoping simulations.

4.2.2.2.3 Desiccation Rewetting Modeling Methods

The conceptual model represents the subsurface at the Hanford Site 200-BC-2 Operable Unit between the 30 by 45 m (98 by 148 ft) geomembrane, emplaced in June 2009, and the water table at 105 bgs. Using a laser particle size distribution measurement method for sediment samples collected from well C8388, a layered system was developed using Loamy Sand, Sandy Loam, and Silt Loam layers in an otherwise Sand-dominated matrix. The hydraulic properties of these layers, according to Carsel and Parrish (1988), are shown in Table 4.7, with their depth intervals in the model listed in Table 4.8. In the simulations, the van Genuchten (1980) water content – capillary pressure relations are used and the Mualem (1976) model is used for the water relative permeability – water content relations.

Table 4.7. Hydraulic Properties of the Sediments Used in the STOMP Simulations (Carsel and Parrish 1988)

Sediment	van Genuchten α (1/cm)	van Genuchten n	Residual Volumetric Water Content (m^3_{liquid} / $m^3_{pore\ space}$)	Hydraulic Conductivity, K_{sat} (cm/hr)	Porosity (–)
Sand	1.45×10^{-1}	2.68	0.045	29.70	0.43
Sandy Loam	7.50×10^{-2}	1.89	0.035	4.42	0.41
Loamy Sand	1.24×10^{-1}	2.28	0.037	14.59	0.41
Silt Loam	2.00×10^{-2}	1.41	0.067	0.45	0.45

Table 4.8. Vertical Location of Lower-Permeability Layers. The layers in the desiccated zone (12.25 – 16 m bgs) are in bold.

Sediment	Layer Depths (m bgs)
Sandy Loam	5.5-6; 7.25 – 7.5; 11.25 - 11.875; **12.5 - 13**; **13.5 - 14**; 18.5 - 19
Loamy Sand	6 – 6.4; 7.5 – 7.75; 8.5 – 8.75; **12.25 – 12.5**; **14.75 – 15.25**
Silt Loam	8 - 8.5

A steady-state simulation was first conducted to establish the pre-operational conditions at the site. Assuming that all BC cribs were built at approximately the same time in 1955, it was assumed that prior to construction and operation, the area was most likely covered by Rupert Sand with a shrub steppe plant community. Based on recommendations by Last et al. (2006) a best estimate recharge rate of 4 mm/yr was assumed for this period. A steady-state pressure distribution for this recharge rate was used as the initial condition for the period from 1955 to the end of the desiccation period on June 30, 2011. In the simulation, a recharge rate of 30 mm/year was imposed for the operation period and post-operation period from 1955 through 1981 when the groundcover consisted of disturbed Rupert Sand with no vegetation (Last et al. 2006). In 1981 the BC-crib area was surface stabilized as a single area. All surface structures (risers and vents) were removed and the area was covered with 2.5 ft of soil and re-vegetated with wintergraze, thickspike, and crested Siberian wheatgrasses). The surface cover after stabilization and revegetation is estimated to be a disturbed Rupert Sand with a young shrub-steppe plant community. For this cover, Last et al. (2006) suggest a best estimate recharge rate of 8 mm/yr. This rate was used from 1981 through the middle of 2009 when the geomembrane was installed. For this cover, a recharge of 0 mm/yr was used. The pressure distribution on June 30 2011 was then used as the initial conditions of the rewetting simulations. For these simulations, it was assumed that either a 7 × 7 m or a 5 × 5 m zone was instantly desiccated between 12.25 and 16.0 m bgs by imposing a post-desiccation matrix potential of 5 bars. The position of the two areas related to the logging wells are shown in Figure 4.82. The vertical extent of the simulated desiccation zone was chosen based on observations reported in Truex et al. (2013). The rewetting simulation time was 100 years.
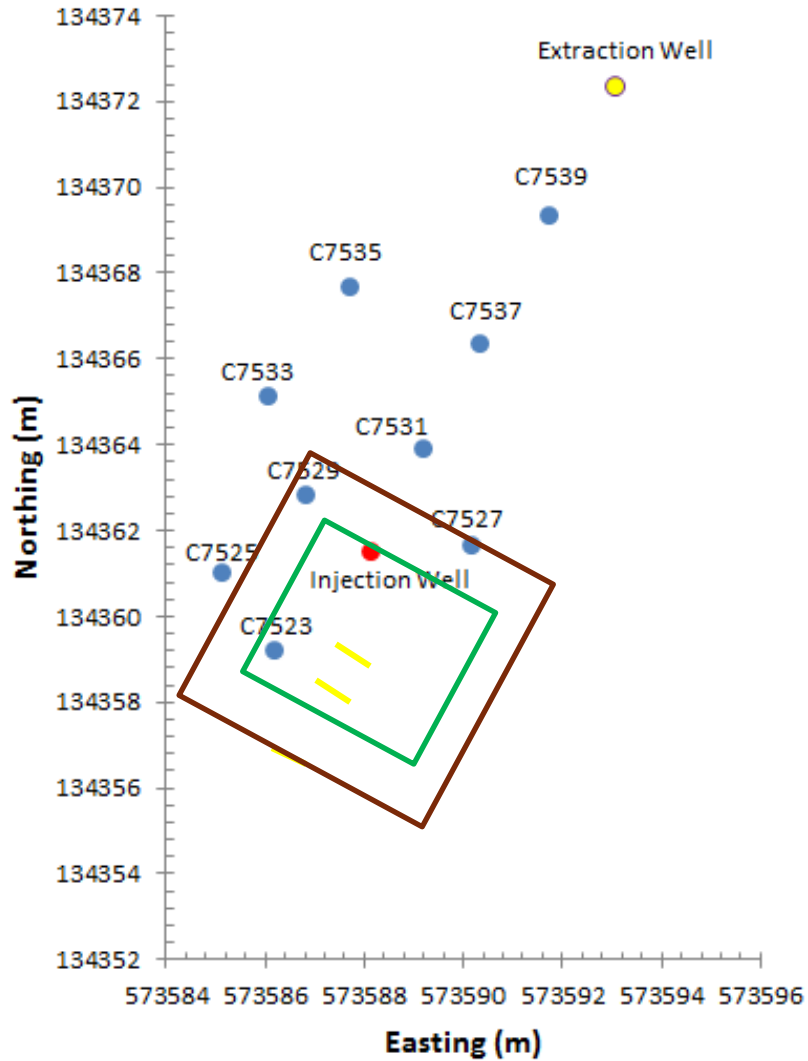
Figure 4.82. Location of Test Site Logging Wells, Injecting and Extraction Wells, and Plan Views of Desiccated Zones. The blue and green squares denote desiccated areas of 49 m^2 (7 × 7 m) and 25 m^2 (5 × 5 m), respectively, that are located between 12.25 m and 16 m bgs. The yellow lines indicate 1-m wide areas for which mass fluxes are shown in Figure 4.89.

4.2.2.2.4 Desiccation Rewetting Modeling Results

Simulation results for the 7 × 7 m desiccated zones are presented in Figure 4.83 through Figure 4.90. Volumetric water contents over time after desiccation for monitoring location C7523 are shown in Figure 4.83. At this location, near the edge of the desiccated zone, the water contents bounce back relatively quickly after desiccation. Rewetting in the upper sandy loam layer at 12.5 – 13 m bgs is more rapid than for the lower sandy loam layer at 13.5 – 14 m (Figure 4.83b). In the lower half of the zone, containing a loamy sand layer, the predicted rewetting is considerably slower than for the upper half with the two sandy loam layers. Above the desiccated zone, small reductions in water contents are observed, indicating a potential source for the rewetting observed in the desiccated zone. The results shown in

4.83

Figure 4.83 indicate that vertical downward migration from the region above the desiccated zone is an important component to the rewetting process.

In Figure 4.84, the rewetting at monitoring location C7527 is shown. This location is closer to the injection well and therefore further away from the imposed desiccated zone boundary than C7523 (see Figure 4.82 for well locations). The results for C7527 also show rapid rewetting but considerably slower than for C7523, especially in the lower half of the desiccated zone. The differences between results at these two locations are consistent with field observations where slower rewetting is reported for locations closer to the injection well (Section 4.1; Truex et al. 2014). The different rewetting rates at these locations suggest a diminishing impact of lateral rewetting with distance from the initial desiccation zone edge. The results also indicate that two major processes are involved in the rewetting process: migration as a result of capillary pressure difference between the desiccated and non-desiccated sediment, and drainage from above the desiccated zone. Outside the desiccation zone (monitoring location C7533), the water contents show only small decreases over time, consistent with slow moisture drainage and potential water migration towards the desiccated zone (Figure 4.85).

The behavior observed in the water content plots in Figure 4.83 through Figure 4.85through can be explained using water mass fluxes across the desiccated zone surfaces and the associated cumulative mass changes. The mass fluxes in Figure 4.86 show that migration through the vertical sides of the zone is a process that only occurs during the first 10 years after desiccation. Migration from the top is initially smaller but is sustained over much larger times. This behavior occurs because, over time, drainage from the sediment above the desiccated zone becomes the dominant rewetting process. After an initial spike in the mass flux through the top surface due to the localized response to rewetting at the interface between desiccated and not-desiccated zones, the mass flux quickly reduces to a value of approximately 400 kg/yr for the first few years (Figure 4.86a). That value is consistent with a recharge rate of 8 mm/yr over the 49 m^2 surface, a rate which was imposed on the domain top surface before the geomembrane was emplaced in 2009. Over time (Figure 4.86b), the rate from the top is reduced as the mobile water mass above the desiccated zone decreases. The water migration through the lower surface is of interest because initially water from below the desiccated zone is pulled upward into the desiccated zone due to the imposed capillary pressure. Over time, water drains from the bottom as water starts to migrate through the zone as part of the overall drainage process. The cumulative water masses shown in Figure 4.87 reinforce the observation that migration from the vertical sides occurs primarily over the first 10 years. The mass increase into the zone peaks at around 12 years and then slowly decreases as water drainage becomes the dominant flow process in the initially desiccated zone.

Figure 4.88 shows the diminishing effect of lateral water mass migration with distance from the desiccation zone outer edges. At the zone boundary (3.5 m from the injection well), a large initial rewetting response to desiccation is observed, driven by both lateral and vertical water migration. When moving closer to the inside of the zone, this effect rapidly diminishes. This figure shows that rewetting at the internal areas of the desiccated zone occurs primarily through water drainage from above the desiccated zone. The plots in Figure 4.89 show that the lateral migration through the vertical sides and vertical movement through the top are sustained by flow over considerable distance because the fluxes at the zone boundaries and at surfaces one meter away into the non-desiccated sediment are nearly similar. These results are important because it shows that the water rewetting the desiccated zone does not originate only from sediment directly adjacent to the desiccated zone, but is migrating from larger distances.

In Figure 4.90, the simulated fluxes for the desiccated zone are compared with fluxes at the same surfaces for the case when the same zone was not desiccated. For the non-desiccated case, there is no migration through the vertical sides, and the flow through the top and bottom are the result of drainage only as the system is responding to the emplacement of the geomembrane in 2009, reducing the recharge from 8 mm/yr to 0 mm/yr. The figure shows that the flux through the top is similar for both simulations after just a few years, indicating that the rewetting from the top quickly becomes dominated by drainage instead of movement due to the imposed capillary pressure in the desiccated zone. At the bottom of the zone it takes about 15 years for the fluxes from both simulations to merge. At this point in time, most of the effects of the initial desiccation have vanished.

In Figure 4.91 through Figure 4.93, the results of desiccating a smaller zone (5×5 m) are shown. The rewetting predicted at monitoring location C7527 is faster than for the larger desiccated zone (Figure 4.86) because the location is closer to the zone boundary. For this desiccated zone, monitoring location C7523 is outside that zone and no desiccation (and rewetting) occurs (Figure 4.92). Because the desiccated zone volume for the 5×5 m case is about half of that of the 7×7 m case, the predicted fluxes and cumulative amounts are also smaller, as shown in Figure 4.93 and Figure 4.94. As a result of the smaller size of the desiccated zone, the importance of migration through the top for the 5×5 m case is less than for the 7×7 m case.
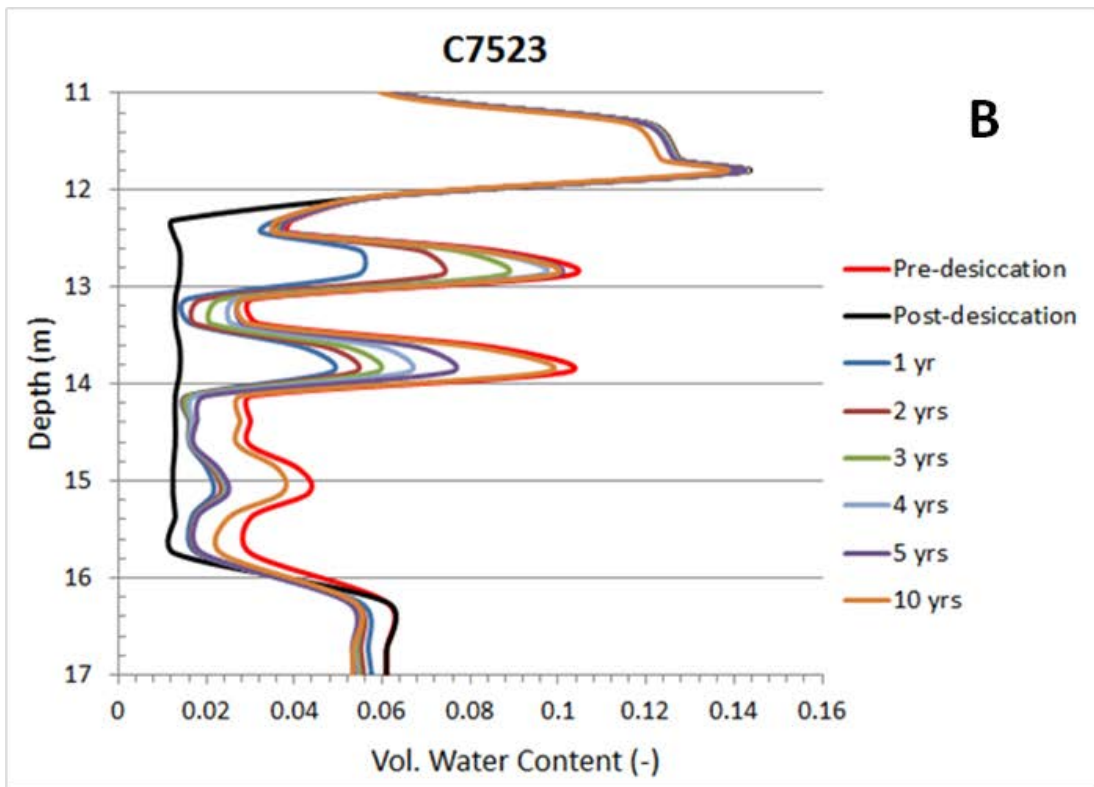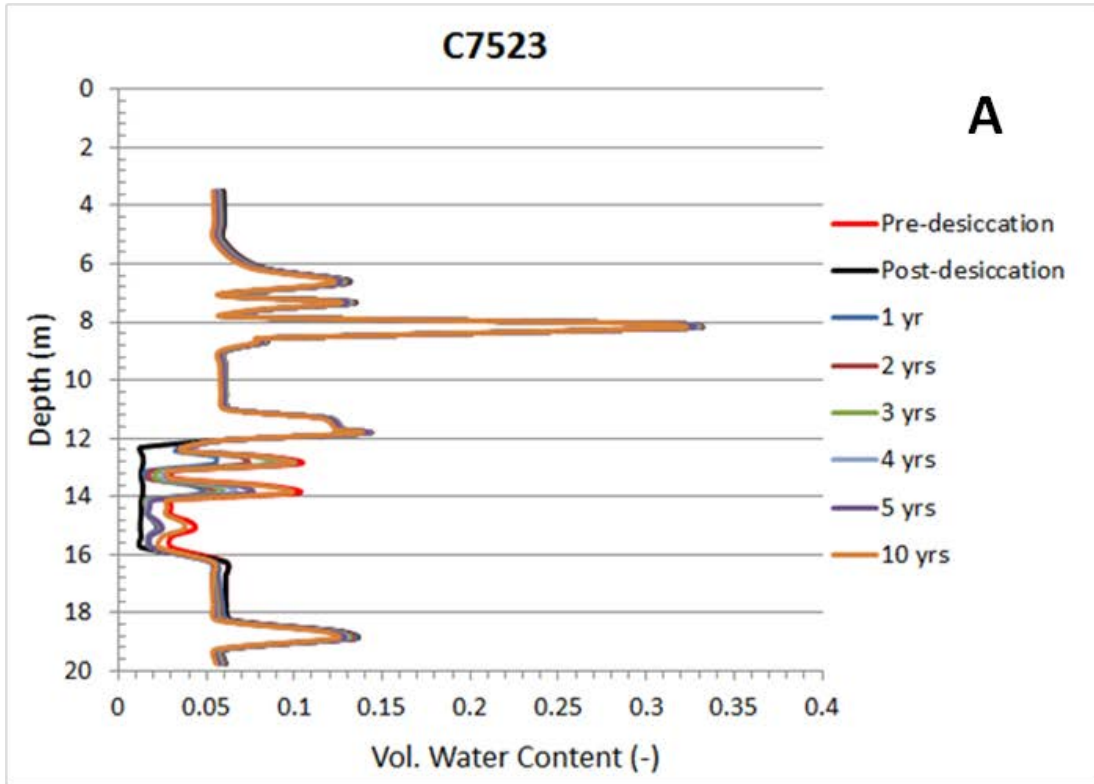
Figure 4.83. Simulated Volumetric Water Content Responses over Time at Location C7523 for the 7 × 7 m Desiccated Zone, Showing (A) the Full Depth Profile and (B) Details of the Rewetting Responses for the Desiccated Zone at 12.25–16 m bgs
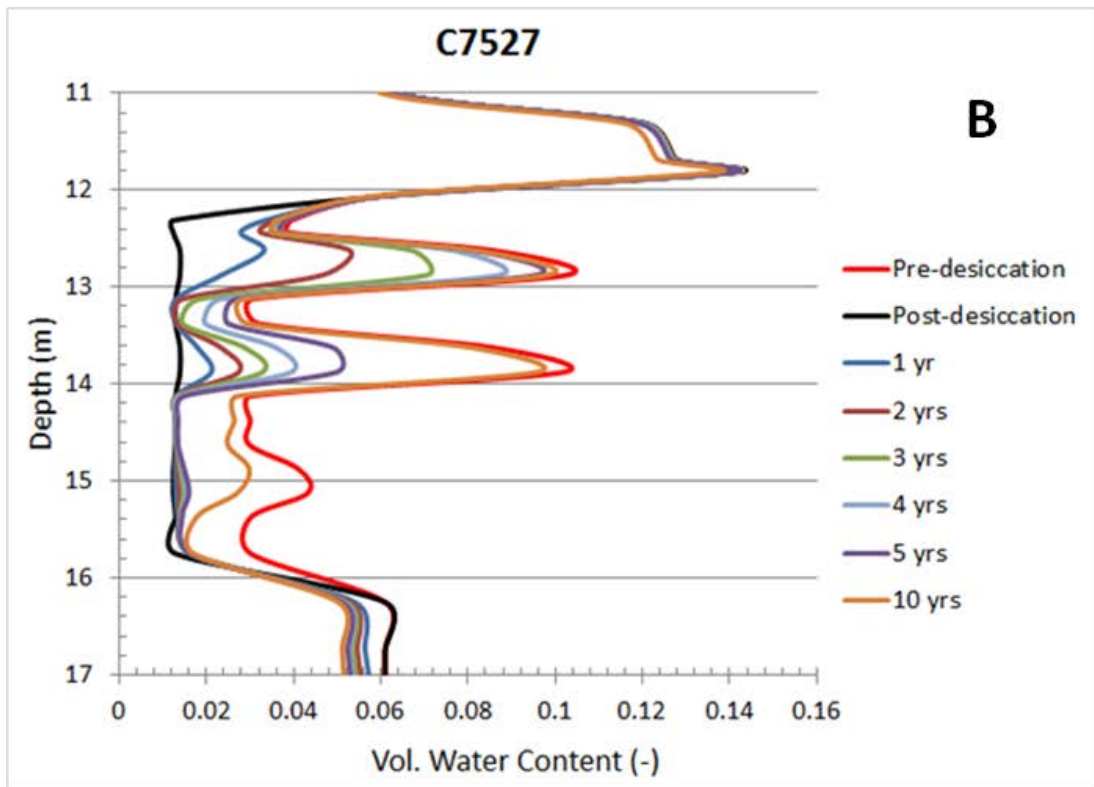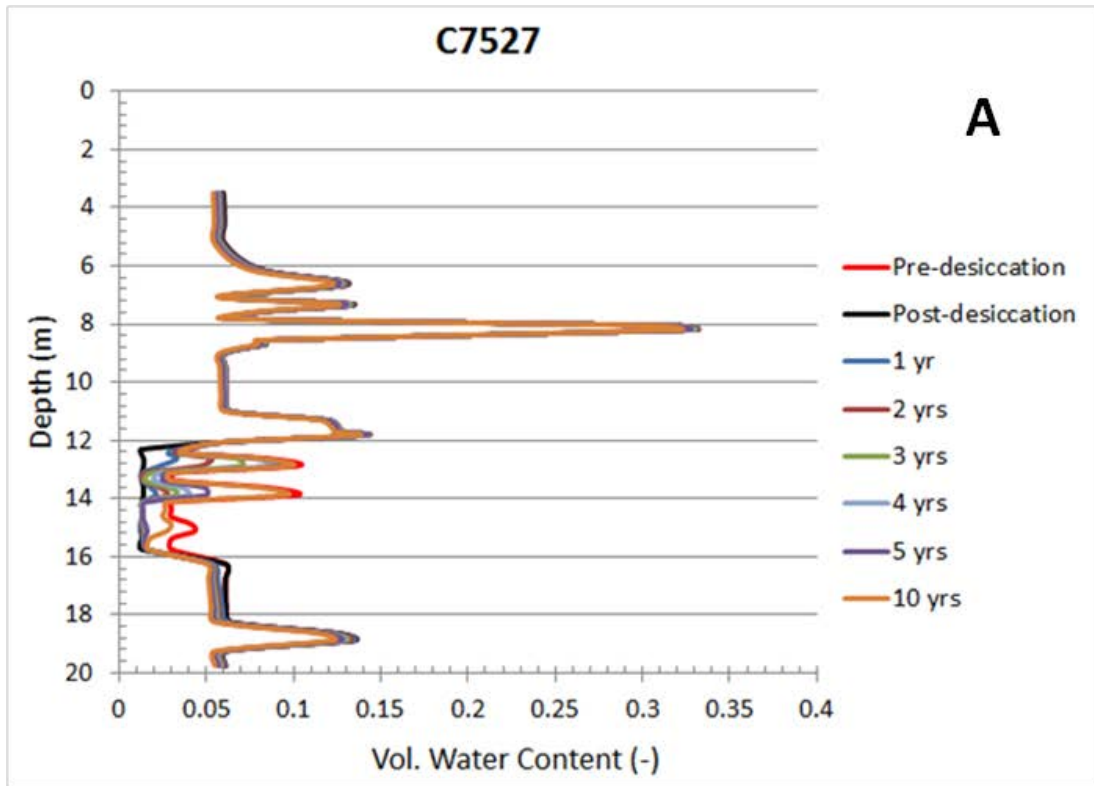
Figure 4.84. Simulated Volumetric Water Content Responses over Time at Location C7527 for the 7 × 7 m Desiccated Zone, Showing (A) the Full Depth Profile and (B) Details of the Rewetting Responses for the Desiccated Zone at 12.25–16 m bgs
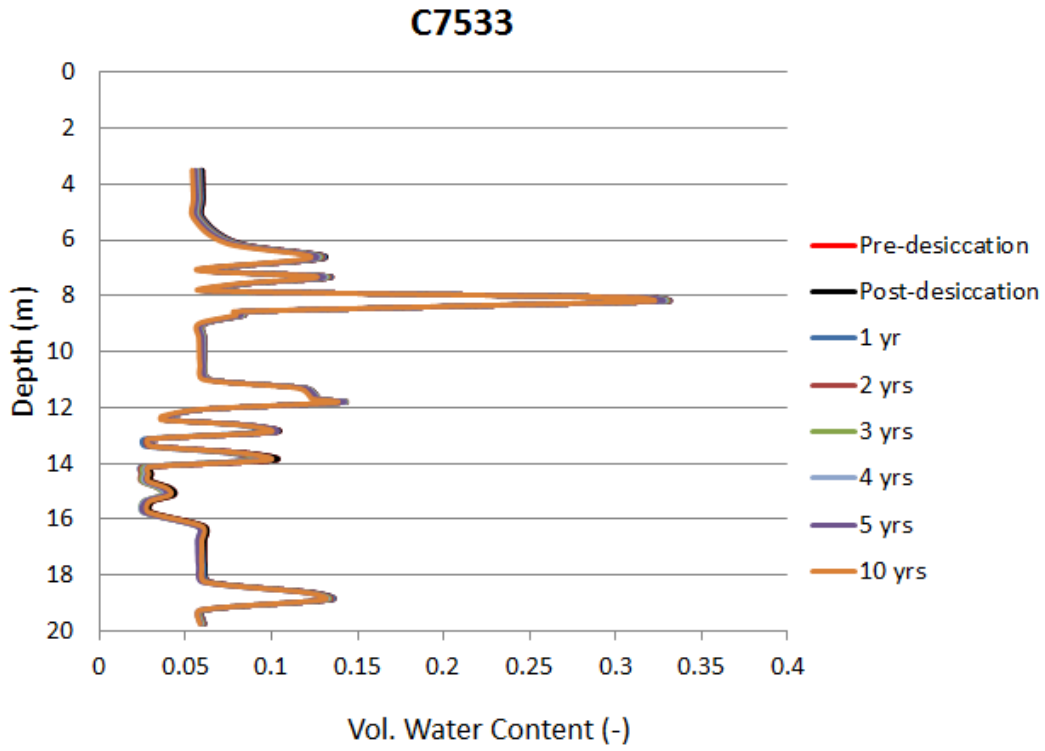
Figure 4.85. Simulated Volumetric Water Content Responses over Time at Location C7533 for the 7 × 7 m Desiccated Zone
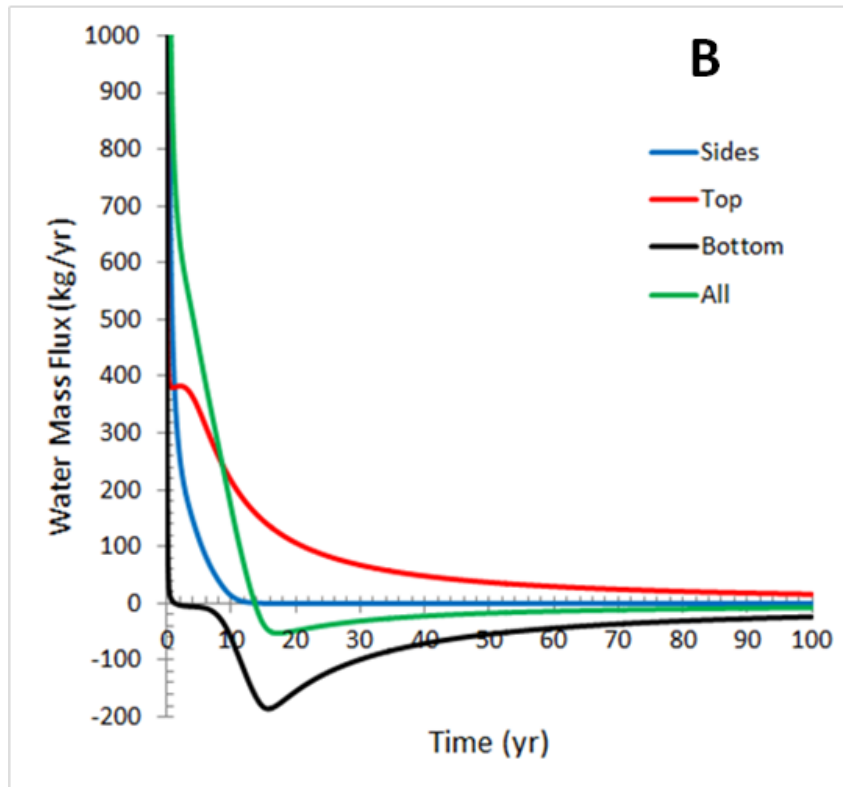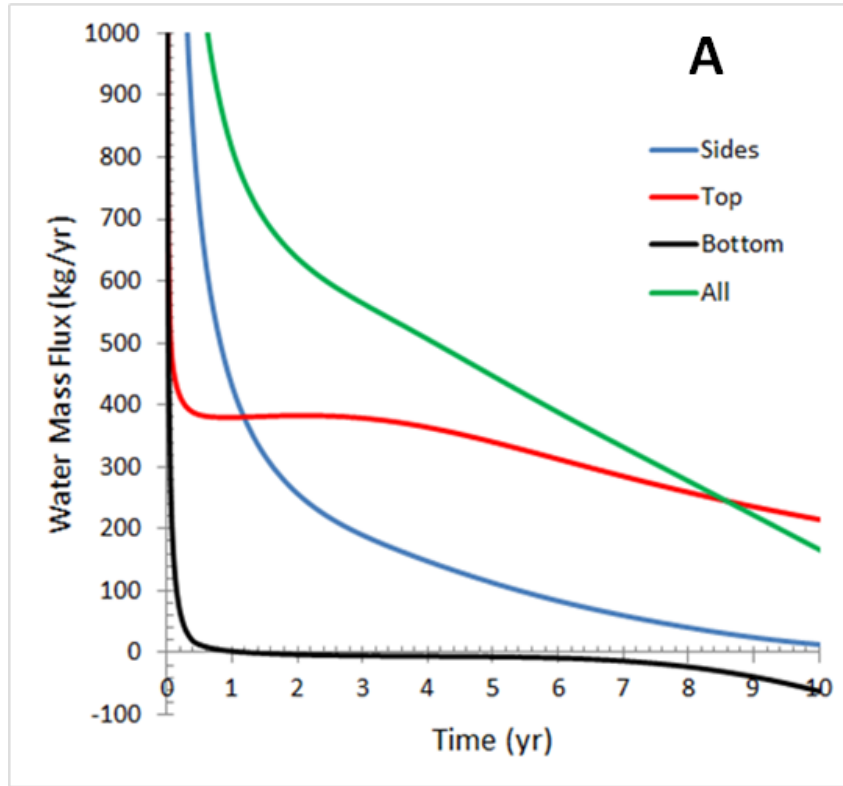
Figure 4.86. Water Mass Fluxes over Time across the Boundaries of the 7×7 m Desiccated Zone (12.25–16 m bgs) up to (A) 10 Years and (B) 100 Years after Desiccation. Positive values indicate migration into the initially desiccated zone
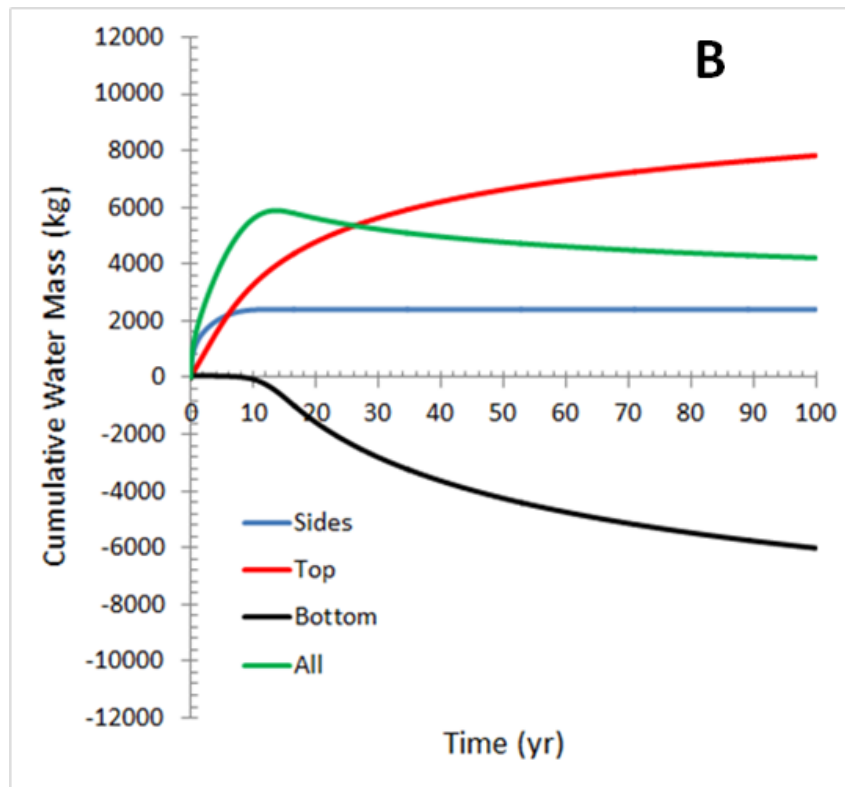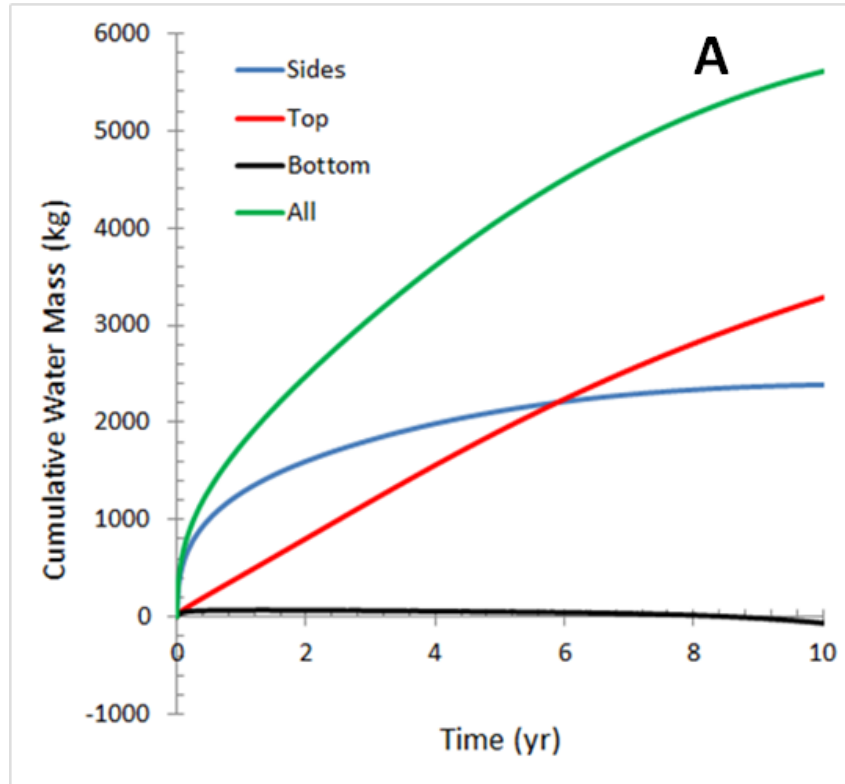
Figure 4.87. Cumulative Water Mass in the 7 × 7 m Desiccated Zone (12.25–16 m bgs) up to (A) 10 Years and (B) 100 Years after Desiccation. Positive values indicate an increase in water storage.
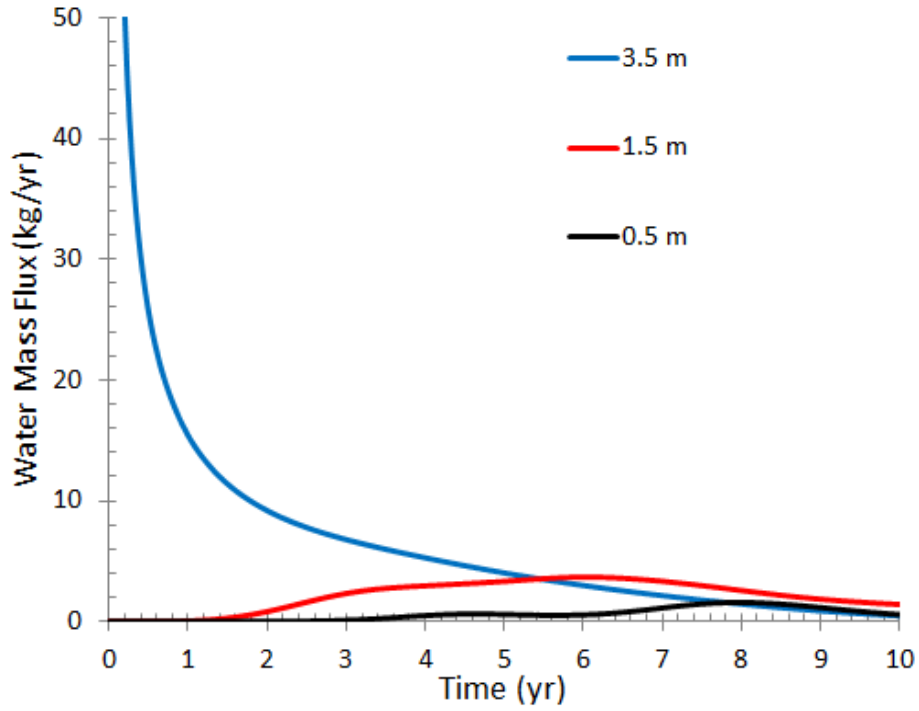
Figure 4.88. Comparison of Water Mass as a Function of Distance to the Injection Well. The fluxes are for1-m wide surfaces indicated in yellow in Figure 4.82.
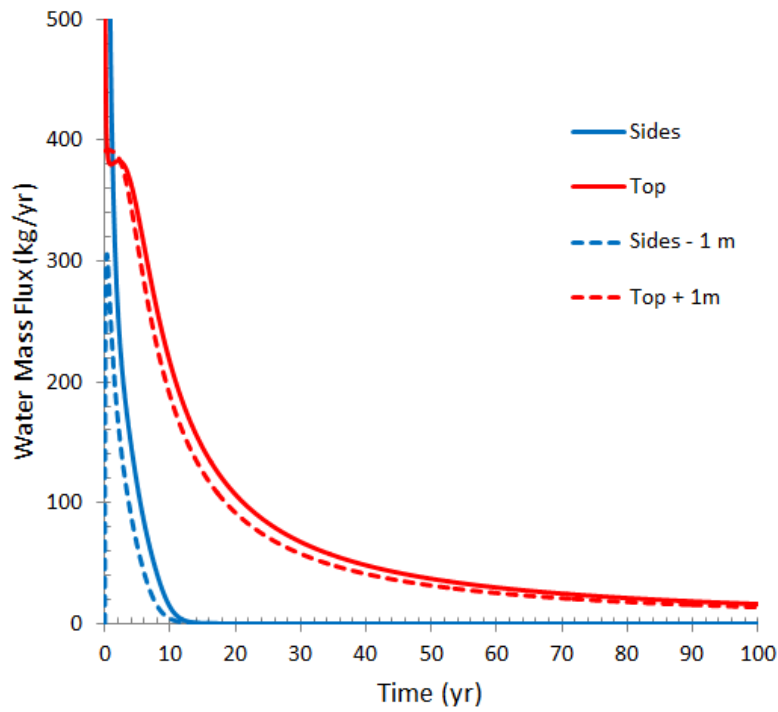
Figure 4.89. Comparison of Water Mass Fluxes at the Boundaries of the Initially 7×7 m Desiccated Zone between 12.25 and 16 m bgs and at Equal-Size Surfaces at a 1-meter Distance in the Undesiccated Sediment
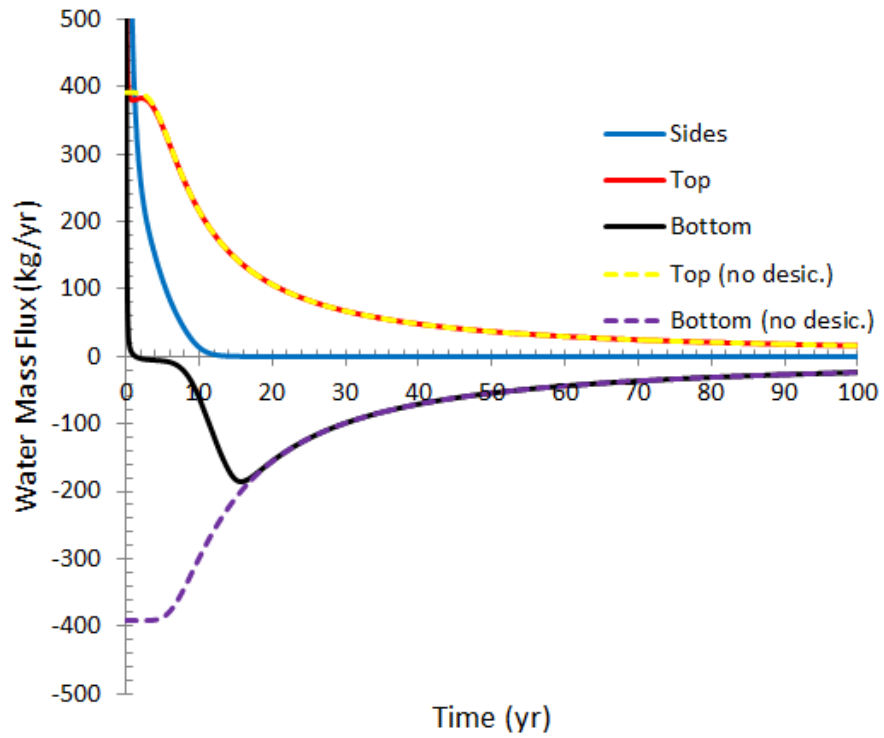
Figure 4.90. Comparison of Water Mass Fluxes For Simulations with and without the Initially 7×7 m Desiccated Zone between 12.25 and 16 m bgs
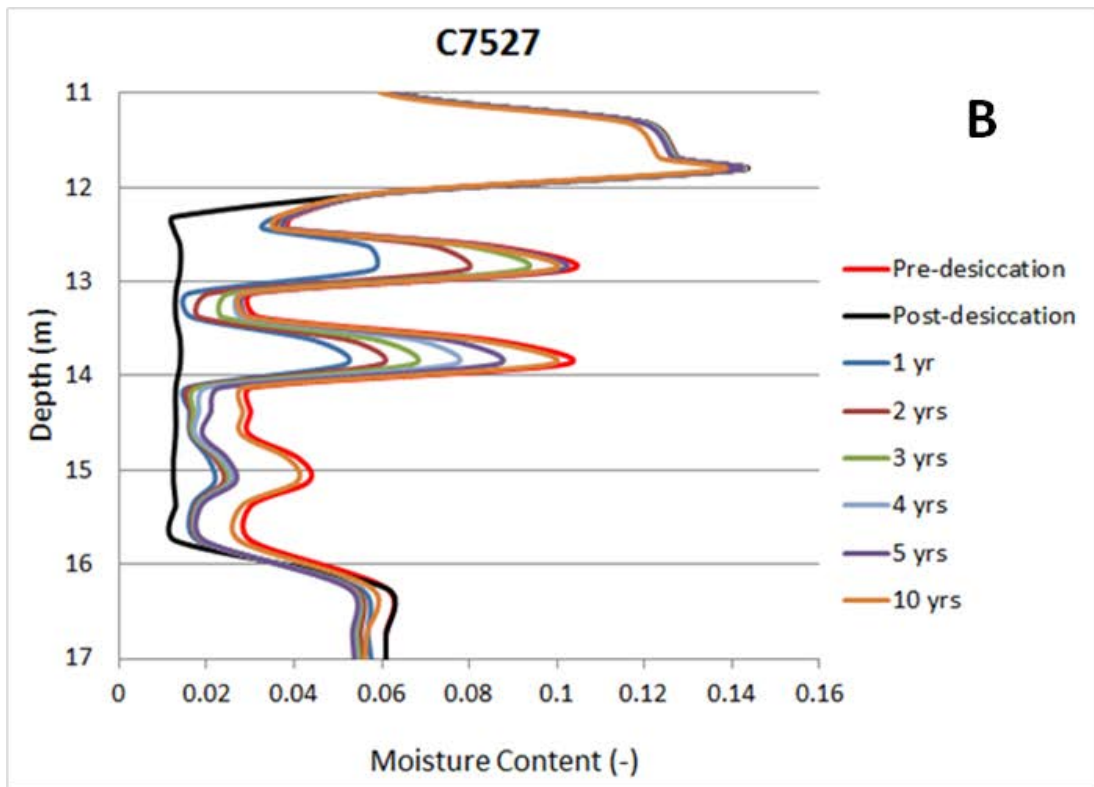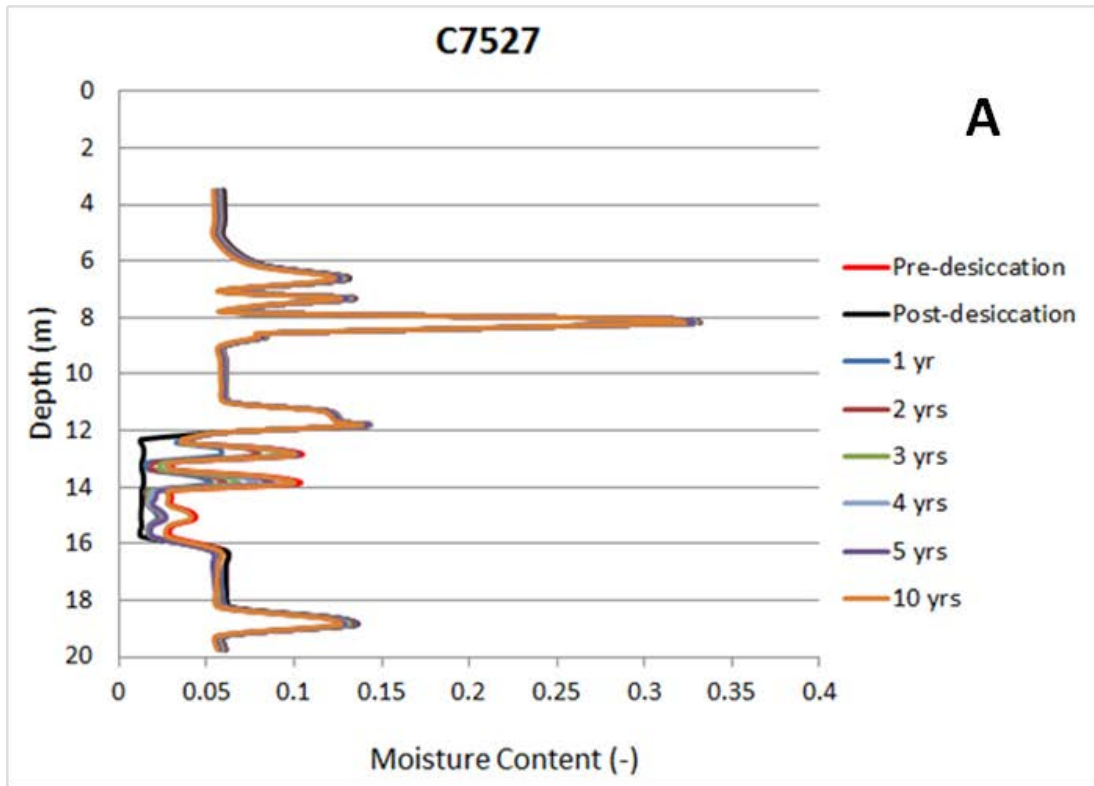
Figure 4.91. Simulated Volumetric Water Content Responses over Time at Location C7527 for the 5 × 5 m Desiccated Zone, Showing (A) the Full Depth Profile and (B) Details of the Rewetting Responses for the Desiccated Zone at 12.25–16 m bgs
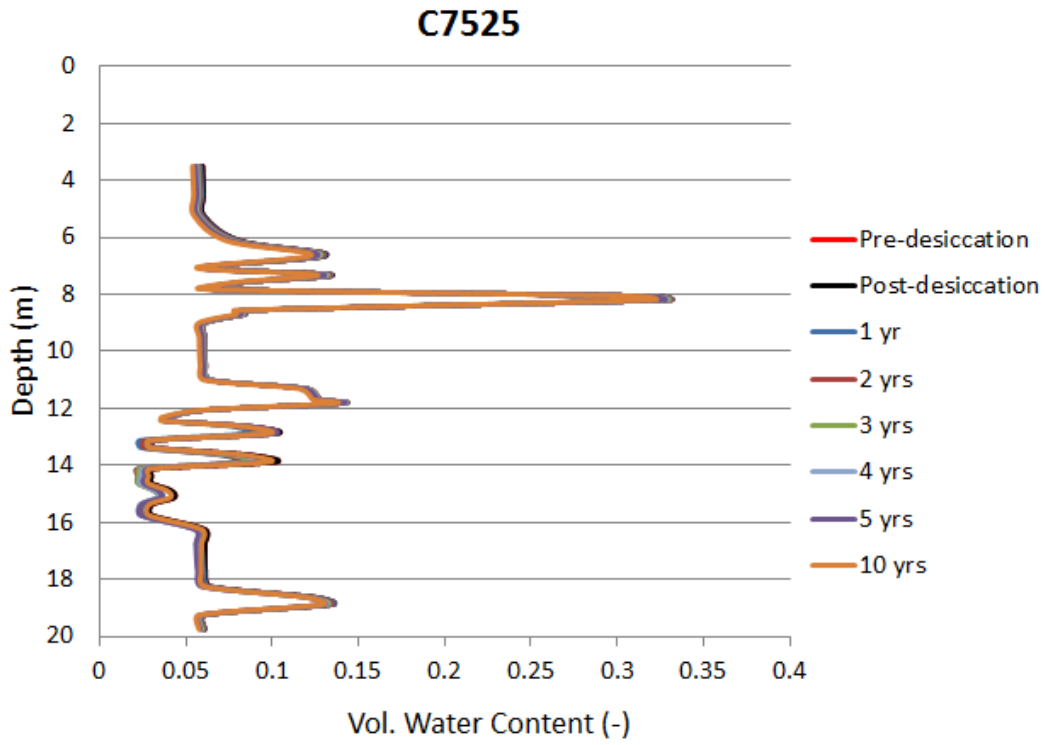
Figure 4.92. Simulated Volumetric Water Content Responses over Time at Location C7525 for the 5 × 5 m Desiccated Zone (12.25–16 m bgs)
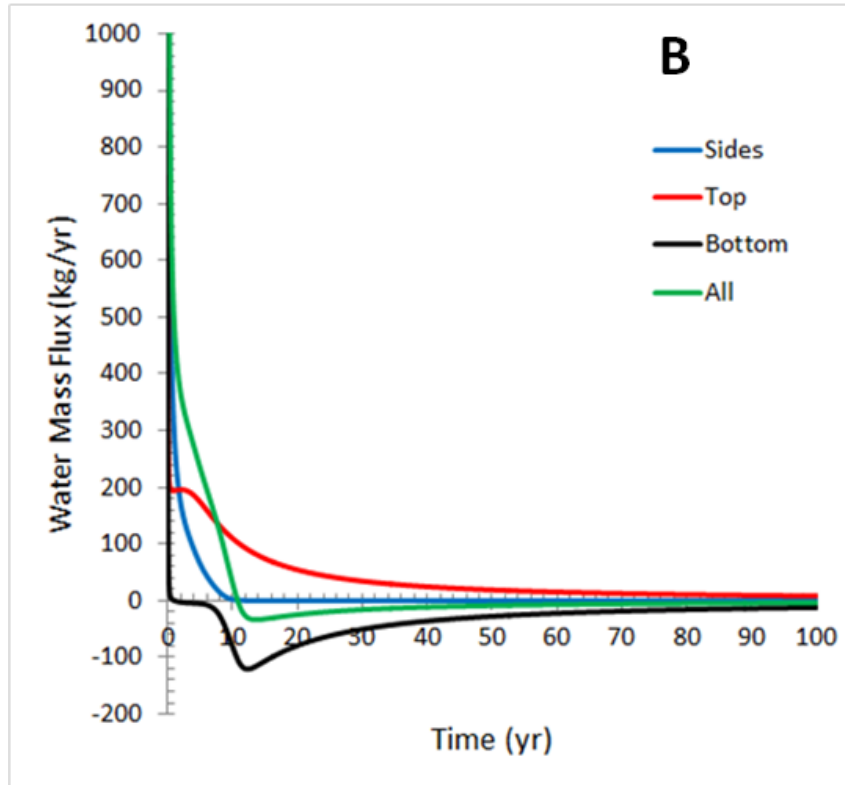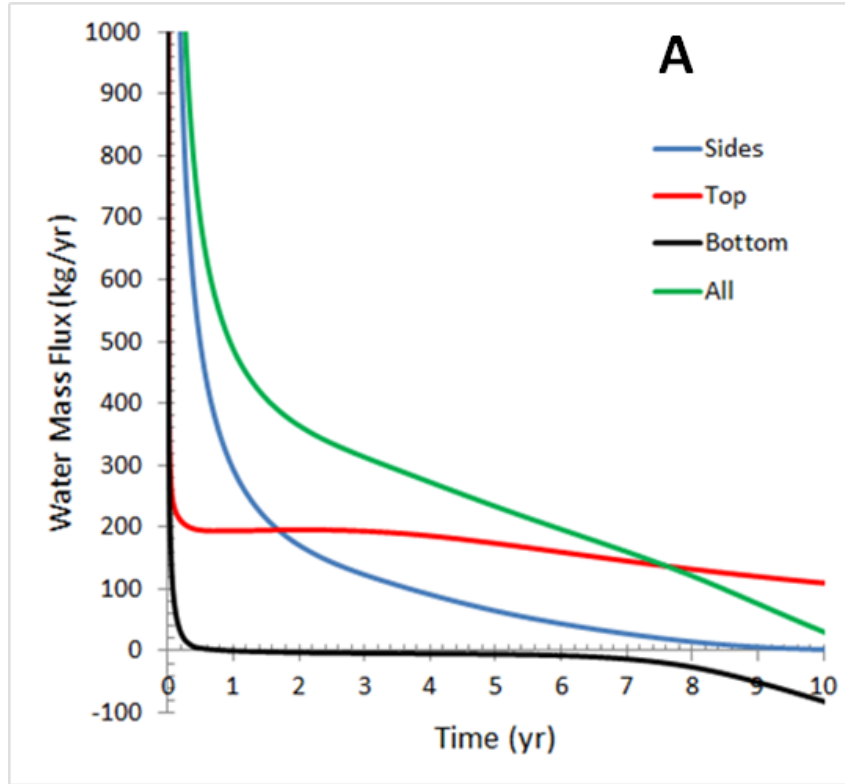
Figure 4.93. Water Mass Fluxes over Time across the Surfaces of the 5 × 5 m Desiccated Zone (12.25–16 m bgs) up to (A) 10 Years and (B) 100 Years after Desiccation. Positive values indicate migration into the initially desiccated zone.
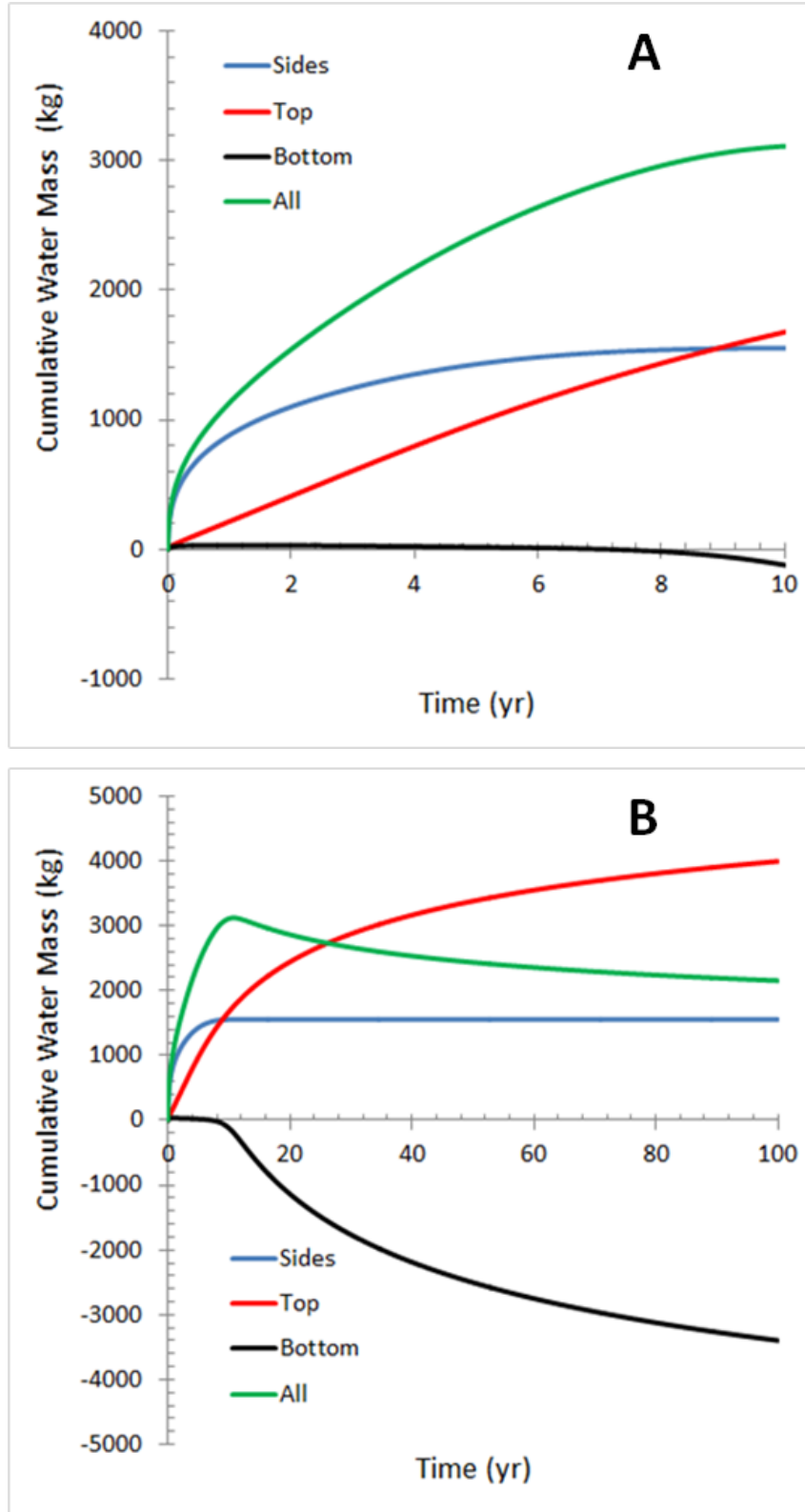
Figure 4.94. Water Mass Fluxes over Time across the Surfaces of the 5 × 5 m Desiccated Zone (12.25–16 m bgs) up to (A) 10 Years and (B) 100 Years after desiccation. Positive values indicate migration into the initially desiccated zone.

4.2.2.2.5 Conclusions from Modeling Assessment

The 3-D simulation results with imposed initial desiccated zones are consistent with field observations: (1) the simulations indicate a relative fast rewetting time (on the order of years); (2) the rewetting rate is faster at the top of the zones than near the bottom, and (3) rewetting is a function of the distance to the side boundaries of the desiccated zone, with faster rewetting near the edges. The results suggest that rewetting occurs due to the imposed capillary pressure gradients and due to drainage from the vadose zone above the desiccated zone. The magnitude of the latter process is mostly independent of the desiccated zone and occurs because of the changes in recharge rates at the site. Before emplacement of the geomembrane in 2009, the estimated site recharge was 8 mm/yr. Because of the reduction in recharge rate after 2009, water has to drain from the upper vadose zone and will migrate through the desiccated zone. This observation shows the importance of evaluating past recharge behavior and estimating water volumes (and rates) that are expected to drain through a desiccated zone. Rewetting of desiccated zones will be smaller if less drainage has to occur through these zones.

The simulation results show that the developed STOMP model can be used for field design and analysis of rewetting data. It is recommended that additional simulations be conducted that test the sensitivity of hydraulic properties, desiccated zone geometries, and operation scenarios. These simulations should be combined with contaminant transport to evaluate remedy effects on future flux to groundwater.

4.2.2.2.6 Post-Desiccation Monitoring Data Assessment

Desiccation is intended to help meet remediation goals by slowing the movement of contaminated moisture through the vadose zone and thereby reducing the flux of contaminants into the groundwater. The rate at which moisture returns to the desiccated zone, here termed the rewetting rate, is important in the overall long-term performance of desiccation as part of a remedy.

Rewetting phenomena and rates have previously been studied through laboratory and modeling efforts. Laboratory data quantifying the rewetting process were collected and reported by Truex et al. (2011). Key conclusions were that vapor-phase rewetting can occur but the process only rewets the desiccated zone to a small extent, essentially to a level below the residual moisture content. Rewetting by aqueous transport occurs, consistent with standard hydraulic phenomena, such that desiccating to very low moisture content and creating very low aqueous phase hydraulic conductivity conditions leads to low rates of aqueous transport rewetting.

Previous modeling efforts (Truex et al. 2012a, 2013b) concluded that the rate of rewetting is a function of the porous media properties of both the desiccated zone and the subsurface surrounding this zone, as well as the moisture content distribution at the end of active desiccation. After active desiccation, the moisture content distribution in the target zone will trend back toward the equilibrium moisture conditions for the porous media properties. Vapor-phase rewetting will occur, but has a negligible impact on the overall rewetting process. Advective rewetting in the aqueous phase strongly depends on the porous media permeability within and surrounding the desiccated zone, the moisture content surrounding the desiccated zone, and the total thickness of the desiccated zone. For example, at the C7527 and C7529 monitoring locations closest to injection well, the thicker desiccated zones have shown the least rewetting. These thicker desiccated zones were associated with areas of high injected air flow due to the presence of coarser, lower-moisture content sediments. While relatively wet sediments are present above these zones, the sediments below are also relatively coarse and dry. Rewetting of these zones has primarily occurred

from above. Analysis of rewetting in this zone after two years of rewetting was presented in Truex et al. (2013b). Additional rewetting analysis was presented in Section 4.2 herein and demonstrated the importance of 3-D moisture migration, and a dominant effect of vertical moisture migration due to drainage of water from the vadose zone above the desiccated zone.

Current data, 6-years after active desiccation was ended, show moisture redistribution in the subsurface at the test site associated with rewetting of desiccated areas. Areas that were moderately desiccated have largely returned to near pre-test conditions. Analysis demonstrates that the rewetting is partly from a local redistribution of water from wetter to dryer zones, but is primarily related to vertical moisture migration from above the desiccation zone. Rewetting is continuing for highly desiccated areas. Qualitatively, trends of moisture redistribution over a broad zone in the vicinity of the test site were observed in the GPR and ERT data.

4.2.3   Instrumentation and Monitoring Assessment

In situ remediation of the deep vadose zone for nonvolatile contaminants is largely in the developmental and demonstration stage. Thus, techniques for monitoring of remediation performance have not been fully evaluated. Desiccation, similarly to some other in situ remedies, imposes significant changes to subsurface conditions over a relatively short timeframe. Several types of instruments are available that monitor the type of properties affected by the desiccation process, but have not been previously used for monitoring desiccation. Candidate sensors were tested in the laboratory using a two-dimensional flow cell with imposed desiccation and rewetting conditions. These same sensors were also installed at the field test site. The sections below summarize the information and data available to date and interpret the sensor performance with respect to monitoring the desiccation process and subsequent rewetting of the desiccated zone.

4.2.3.1   Laboratory Evaluation of Instrumentation

Laboratory testing of in situ sensors was conducted and reported in Truex et al. (2011) and Oostrom et al. (2012a). In summary, the sensors installed at the desiccation field-test site were tested with respect to monitoring desiccation and rewetting in a laboratory flow cell. The thermistors, HDUs, and humidity probes provided useful information for both desiccation and rewetting. TCPs and DPHP instruments detected passage of the desiccation front, but were not useful thereafter. All instruments detect only very localized conditions, and changes in parameters must occur at the instrument location for the instrument to detect or quantify a change in conditions.

4.2.3.2   Field Test Information for Instrumentation

Sensor performance was also evaluated based on the data obtained during desiccation field testing. The results were generally consistent with the laboratory testing of the sensors. Using the neutron data as an indicator of where significant desiccation occurred, strong sensor responses would be expected at the 47 ft (14.5 m) bgs sensor intervals within 3 m of the injection well and moderate responses at the 42 ft (12.8 m) bgs sensor interval for the same wells. The HDUs and thermistors showed responses at the expected locations. Note that the thermistors were placed every 0.6 m (2 ft) between 3.1 and 21.3 m (10 and 70 ft) bgs. As such, the thermistors provided a good vertical indication of desiccation activity based on the

evaporative cooling response. Some responses were observed for humidity and moisture content sensors, but not for every location where a change in these parameters would be expected.

Reliability of sensors was also evaluated based on the number of sensors that stopped functioning or did not respond when a response was expected. Based on this assessment, the HDUs and thermistors were reliable with 100% of the thermistors and 39 of 40 HDU remaining functional throughout the test. Almost half of the humidity probes failed during the test (19/40) and 29 of 40 DPHP sensors failed. None of the TCPs provided meaningful data and 20 of 40 sensors completely failed (no signal).

Neutron moisture logging of a borehole is a standard method for obtaining a high resolution vertical profile (~7.5 cm vertical intervals) of volumetric moisture content. These data are a good representation of moisture content at the logging locations within the nominal measurement radius of about 30 cm. Measurement is manual, which may lead to lower temporal resolution than for methods that can operate autonomously. Interpolation of volumetric moisture content from neutron moisture logging data can be used to generate a three-dimensional image of moisture conditions. This type of interpolation does not incorporate subsurface conditions away from the measurement point that can impact the distribution of desiccation. The neutron moisture logging data provide robust information but over a small volumetric extent. Interpolation is impacted by the location of the drying front. For instance if drying has occurred at one location, but not yet at another location, interpolation cannot effectively project the extent of drying past the first location. A neutron logging image can show sharp moisture content contrasts that may not be physically accurate away from the logging locations. Thus, care is needed in interpreting the images with respect to the volumetric distribution of moisture content reduction.

Cross-hole ERT senses the electrical conductivity distribution between in situ electrode locations. As described in Equation (3.5) (Section 3.2.2.3), changes in the electrical conductivity distribution are related to changes in the volumetric moisture content distribution. While ERT measures only the change, not the absolute volumetric moisture content, the ERT data can be used to provide a temporal data set representing the distribution of desiccation via moisture content changes. These data are in response to conditions between electrodes, not just at the electrodes.

Overall, several factors impact the ERT estimate. Decreases in temperature and moisture content occur during desiccation, both of which cause a decrease in electrical conductivity. Thus, in order to quantitatively estimate the moisture content change using ERT, a temperature correction is necessary. This correction is moisture content dependent, but in practice, a constant temperature correction factor is applied in the data inversion. In addition, increasing fluid conductivity with decreasing moisture content is expected to dampen the ERT response and impact moisture content change estimates. With ERT, the resolution of the data inversion averages moisture content changes over a volume and the distribution of spatial moisture content change is depicted with lower contrast than actually exist, appearing as a smoothed or blurred representation of actual changes. Imaging resolution is related to electrode distribution which can also change over time if electrodes have to be dropped from the network because of electrical coupling issues as the porous medium is desiccated. In the field test, maintaining electrical coupling was difficult in heavily desiccated zones, likely due to bentonite contraction and subsequent separation from electrodes. Full-scale applications would need to consider improved wetting capability or nonshrinkable grout around electrodes to maintain adequate coupling (e.g., neat Portland cement).

Cross-hole ERT is implemented using robust in situ electrodes that can be monitored autonomously to provide high temporal resolution. Spatial resolution is related to the electrode distribution and proximity

to the desiccation zone, and can be selected to be appropriate for the scale of the desiccation target and the resolution needed based on the monitoring goals. For instance, the ERT applied at the test site imaged a zone about 12-m long by 6-m wide by 55-m thick with about 100 electrodes at 9 lateral locations. A volume twice as large could have been imaged using the same number of electrodes with a correspondingly scaled electrode spacing in the same number of lateral locations. In that case, image rendering would essentially look the same as shown in Figure 4.40, but the scale would be twice as large. For larger volumetric applications, neutron moisture logging could also be applied, although larger interpolation distances may misrepresent moisture content changes between logging locations, especially if there is significant heterogeneity, and there would be longer durations for desiccation to propagate from one logging location to the next. Thus, it may be advantageous at larger sites to use ERT imaging even through image resolution would need to be considered in interpreting the distribution and extent of moisture content reduction.

Cross-hole GPR provides means to monitor absolute volumetric moisture content and moisture content changes in two dimensions based on propagation of energy through the subsurface between two logging boreholes. Thus, it provides data for interpretation of volumetric moisture content distribution away from subsurface access points and does not require interpolation between access points like the neutron moisture logging data. However, high electrical conductivity at contaminated sites can severely impact the accuracy of the GPR estimate. When the ground has a high electrical conductivity the low-loss assumption is not valid and the EM velocity is affected by both electrical conductivity and permittivity changes. However, in zones with significant desiccation, the electrical conductivity drops because moisture content decreases. In those zones, GPR moisture content determined through the Equation (3.3) correlation are much closer to those determined by neutron moisture logging.

GPR provides a 2-D image of the subsurface moisture content using manual measurements, which may lead to lower temporal resolution than for methods that can operate autonomously. GPR logging borehole spacing is constrained by energy propagation and generally needs to be less than 10 m for the vadose zone and even much smaller for areas with high electrical conductivity (about 3 m at the desiccation test site). However, while the absolute value of moisture content is not accurate in areas of high electrical conductivity, GPR does image the location of moisture content changes and can provide accurate estimates of moisture content in highly desiccated zones, even when initial electrical conductivity is high. Thus, the GPR data may be suitable for identifying the distribution of highly desiccated zones and estimating the moisture content in these zones. Additionally, GPR can also be deployed to include measurement between the injection well (through the use of stilling well) and surrounding wells. ERT and neutron logging cannot effectively include data collection at the injection well because 1) the injection well configuration is not conducive to neutron logging or placement of ERT electrodes and 2) the subsurface adjacent to the injection well dries rapidly and creates conditions that are not suitable for ERT electrode operation (i.e., electrical coupling between the electrodes and the porous media is poor at low moisture content).

In summary, traditional moisture content monitoring through neutron moisture logging is well established and provides detailed vertical profile information at discrete logging locations. Interpolation of multiple logging locations is possible, but must be applied with caution because interpolation does not account for subsurface heterogeneities away from the logging locations and becomes less representative as the distance between logging locations increases. ERT implementation is readily scalable to larger sites. ERT data can be collected autonomously for good temporal resolution and can provide estimates of moisture content changes in three dimensions. GPR scaling is limited by the need for relatively closely

spaced subsurface access for logging. While moisture content estimates are impacted by high electrical conductivity, estimates in low conductivity and significantly desiccated zones appear to be similar to neutron moisture data. GPR also provides the ability to monitor directly surrounding the dry-gas injection well and may be useful for assessing near-well patterns of desiccation that relate to gas flow and are important for operational decisions. Interestingly, interpolation of temperature data, due to the evaporative cooling effect of desiccation, also provided useful three-dimensional information about the progress of desiccation and is a robust method for vadose zone implementation.

4.2.4   Scale-Up Assessment

The following sections address scale-up of desiccation with respect to design requirements, setting performance requirements, design calculations, and assessment of desiccation with respect to CERCLA feasibility study requirements.

4.2.4.1   Ambient Air Injection Assessment

The Water-Air-Energy mode of the STOMP simulator (White and Oostrom 2000; 2006) was used to simulate the desiccation process induced by injection of ambient air under a range of temperature (0°C to 30°C) and relative humidity (0% to 90%) conditions. Simulation results were evaluated in terms of desiccation efficiency and the potential for condensation of water within the subsurface as a function of the ambient air conditions.

4.2.4.1.1 Approach

A two-dimensional cylindrical coordinate system was used for the simulations (Figure 4.95). The 6-m-long injection well was located at the center of the 100-m thick domain, starting at 30 m bgs. Using symmetry, the simulations were conducted in two-dimensions with the injection well at the left edge of a domain consisting of a 45-degree wedge within the cylinder. Unlike the field test, no extraction well was used in the simulations, only injection of ambient air which was allowed to exit the right side of the domain. The water table was located at 100 m below the surface, as represented by the bottom boundary of the domain.
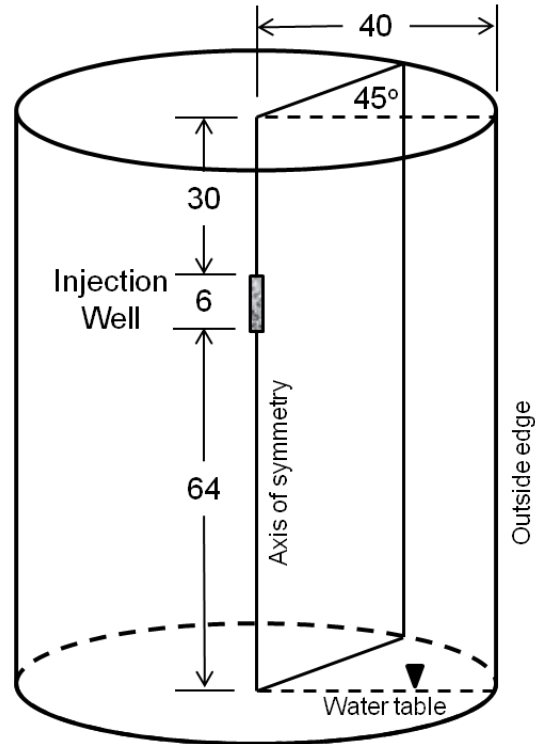
Figure 4.95. Schematic of Cylindrical Domain Used to Simulate Injection of Ambient Air. Dimensions
are in meters.

Grid convergence tests were performed to obtain the discretization used in the scoping simulations. The
40-m by 100-m domain was discretized into 60 nodes in the horizontal, and 400 nodes in the vertical,
yielding a total of 24,000 nodes in the domain. The domain was discretized with variable horizontal
spacing (0.25 to 1.0 m), which was refined near the injection well, but increased with distance from the
injection well.

Boundary conditions were set for the top, bottom, and outside edge of the domain. For the gas phase,
zero-flux boundaries were established at the top and bottom, representing use of a gas-impermeable
barrier at ground surface and the water table, respectively. The outside edge boundary condition
accounted for the weight of air along the vertical boundary using a gas pressure of 102494.5363 Pa at the
lowest cell. For the aqueous phase, a zero-flux boundary was set at the top of the domain. At the bottom,
a fixed (Dirichlet) pressure (102496.0000 Pa) was set to represent the water table (relative to an
atmospheric pressure of 101325 Pa at the top of the domain). At the outside edge boundary, similar to the
gas phase boundary condition, a hydrostatic condition was set that accounted for the weight of the water
column, with the aqueous pressure at the lowest cell set at 101269.7945 Pa. For energy transport, a fixed
temperature of 17°C was assumed for the top, bottom, and outside edge boundaries. At the injection well
axis boundary, no flow conditions outside of the injection well were assumed because this boundary
represented the axis of symmetry.

The domain was assumed to be homogeneous with hydraulic properties associated with a well-drained
sand (Table 4.9). A homogeneous domain was used so that impacts of desiccation and condensation
could be readily identified without confounding factors that could be attributed to subsurface
heterogeneities. The Webb extension (Webb 2000) was used in conjunction with the van Genuchten

equation (1980) to describe the pressure-saturation relationship for dry regions. Water retention relations such as the van Genuchten (1980) equation have a limitation at low aqueous saturations because they use residual or irreducible water saturation parameters (Webb 2000). When the irreducible water saturation (residual moisture content) is approached, the aqueous phase relative permeability approaches zero and the capillary pressure approaches infinity. This behavior of the capillary pressure-saturation curve can cause numerical problems at saturations near the irreducible water saturation (residual moisture content). The approach of using a finite irreducible saturation typically fails when the saturation drops below this value. The method by Webb (2000) extends the capillary pressure curves to zero liquid saturations, but does not necessitate refitting or experimental data for the van Genuchten portion of the curves. The details of the extension are discussed in Webb (2000).

Table 4.9. Hydraulic Properties of the Porous Medium

Saturated Hydraulic Conductivity (cm s^{-1})	2.270×10^{-3}
van Genuchten *alpha* (cm $^{-1}$)	0.061
van Genuchten *n*	2.031
Residual Saturation	0.080

Using the Webb extension with the van Genuchten equation for capillary pressure, three different sets of simulations were performed with continuous injection of ambient air for a period one year. Prior to injection of gas, an approximate steady-state condition was obtained by allowing the soil to drain for 1 year without desiccation and infiltration, yielding an initial water saturation of ~7%. The use of the Webb extension to the van Genuchten equation permits the saturation to drop slightly below the residual moisture content for the porous medium. In the first set of simulations (Case 1), ambient air was injected into the subsurface at a rate of 300 cubic feet per minute (cfm), the rate used in the desiccation field test. In the second set of simulations (Case 2), the same injection rate was used, but the initial saturation of the porous medium was set to 16% so that the effectiveness of desiccation and the potential for condensation could be observed at higher starting water saturation. In the third set of simulations (Case 3), the initial saturation of the domain was the same as for Case 1, but the injection rate was doubled to 600 cfm.

For all three cases, ambient air was injected at five different temperatures: 0°C, 10°C, 17°C, 20°C, and 30°C. At each temperature, the air was injected at 10 different relative humidity values: 0%, 10%, 20%, 30%, 40%, 50%, 60%, 70%, 80%, and 90%. Simulation results were analyzed primarily by examining trends in water saturation, temperature, relative humidity, and matric potential at an observation point located 5 m laterally from the injection well at a depth aligned with the midpoint of the injection screen.

4.2.4.1.2 Assessment Results

The same basic variation in responses for water saturation, temperature, relative humidity, and matric potential as a function of influent gas temperature and relative humidity were observed for each of the three cases simulated. Figure 4.96 through Figure 4.99 show the series of responses for different temperature and relative humidity combinations under Case 1 conditions. Each set of plots represent the response for a given temperature of the injected ambient air. Lines plotted in each set of plots represent the relative humidity of the injected air. In the plots below, several abbreviated axis legends are used. The legend "Aq Saturation" is the soil moisture saturation (volume water/volume pore space). The

legend "Aq matric potential, bar" is the matric potential in the soil in units of pressure (bar) where higher negative values equate to higher capillary pressures.
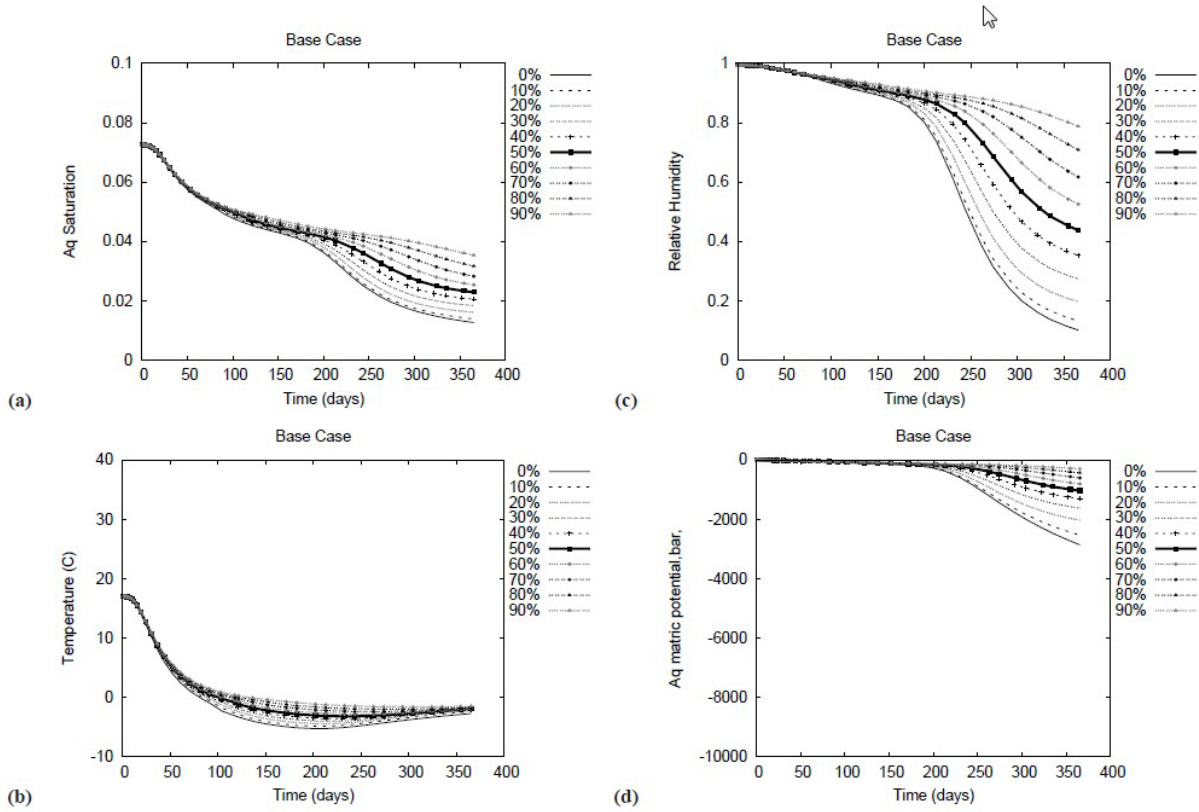
Figure 4.96. Ambient Air Desiccation as a Function of Injected Gas Relative Humidity for an Injected Gas Temperature of 0°C
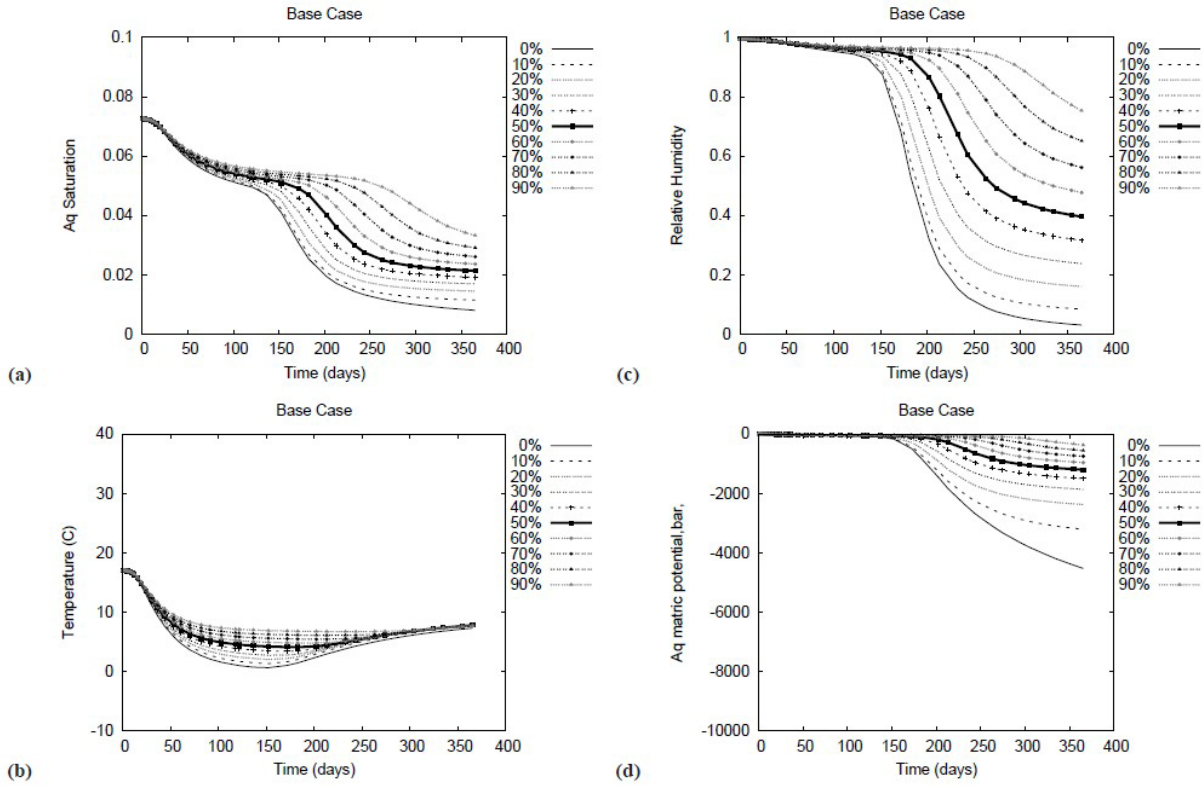
Figure 4.97. Ambient Air Desiccation as a Function of Injected Gas Relative Humidity for an Injected
Gas Temperature of 10°C
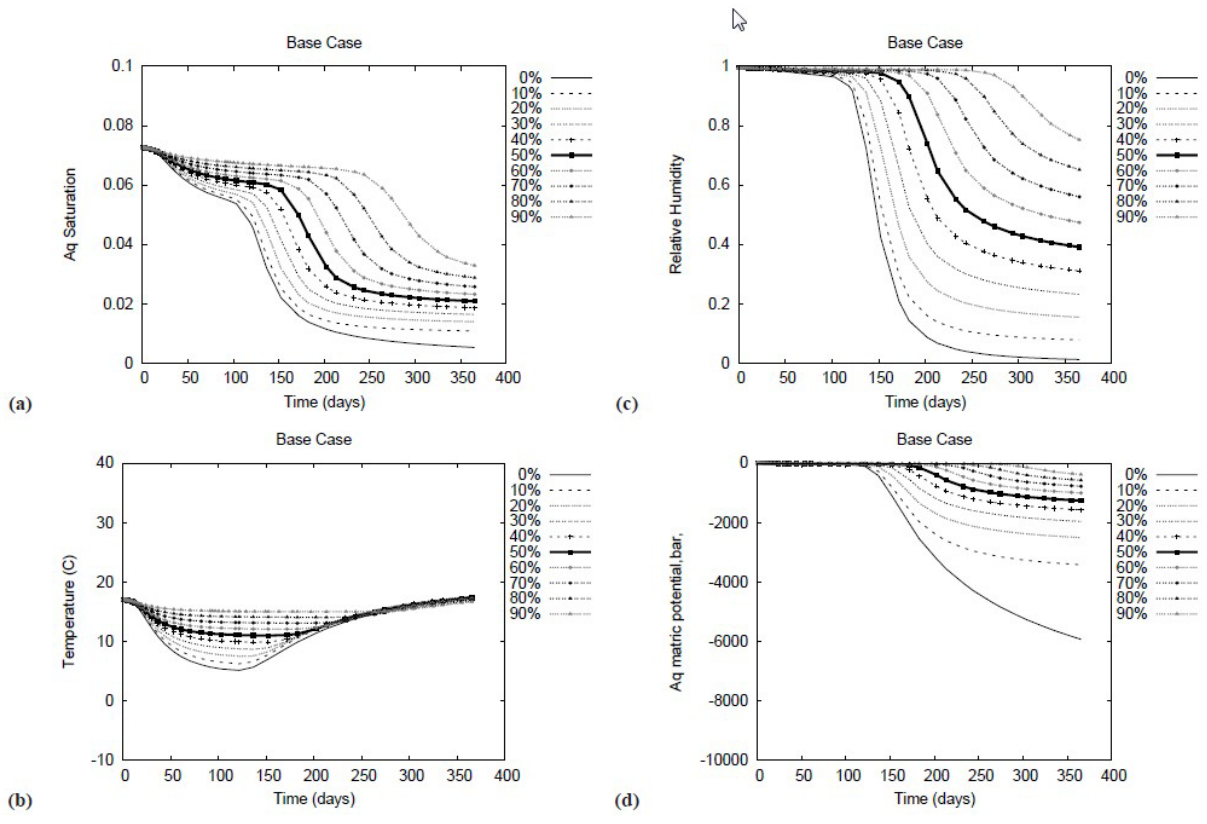
Figure 4.98. Ambient Air Desiccation as a Function of Injected Gas Relative Humidity for an Injected Gas Temperature of 20°C
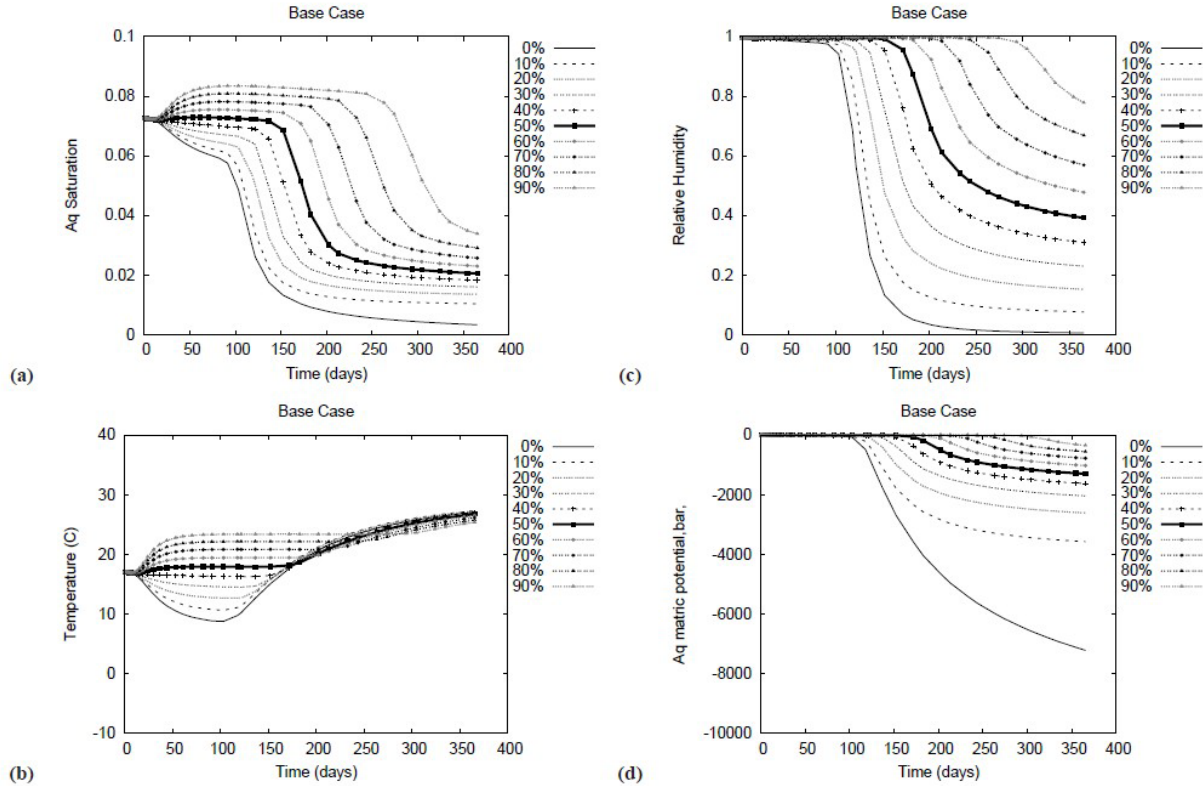
Figure 4.99. Ambient Air Desiccation as a Function of Injected Gas Relative Humidity for an Injected Gas Temperature of 30°C

Lower temperatures produce slower desiccation rates but did not generate conditions causing condensation of water in the subsurface. Higher temperatures result in quicker desiccation, but lead to the potential for condensation in the subsurface (as evidenced by temporary increased water saturations) at higher relative humidity values (e.g., above about 50%). The condensation is a temporary phenomenon that occurs until the temperature at the monitored point increases to where condensation does not occur. The temperature increase is from the heat in the influent gas and therefore, occurs slowly. The simulations showed moderate increases in water saturation until that time. However, potential issues caused by condensation and the amount of saturation increase for a specific site would need to be evaluated in the site-specific design to define an upper limit for relative humidity at higher influent gas temperatures.

The extent of desiccation is a function of the influent gas relative humidity. Note that in Figure 4.100 through Figure 4.104, the simulated water saturation is progressively higher as the relative humidity increases from 0% to 90%. The variation between water saturation is greater at higher temperatures. For a given site, the targeted water saturation endpoint should be considered in selecting appropriate ambient air conditions for desiccation operations. Lines plotted in each set of plots represent the temperature of the injected air.
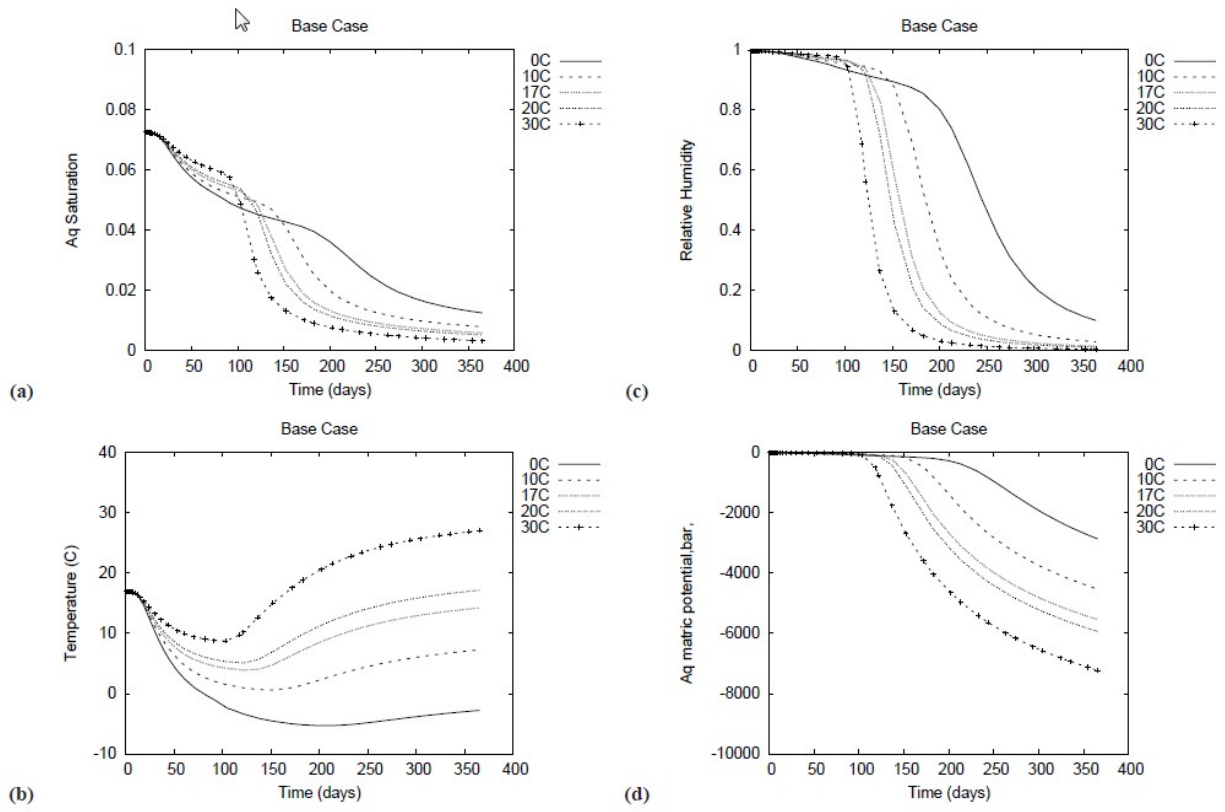
Figure 4.100. Ambient Air Desiccation as a Function of Injected Gas Temperature for an Injected Gas Relative Humidity of 0%
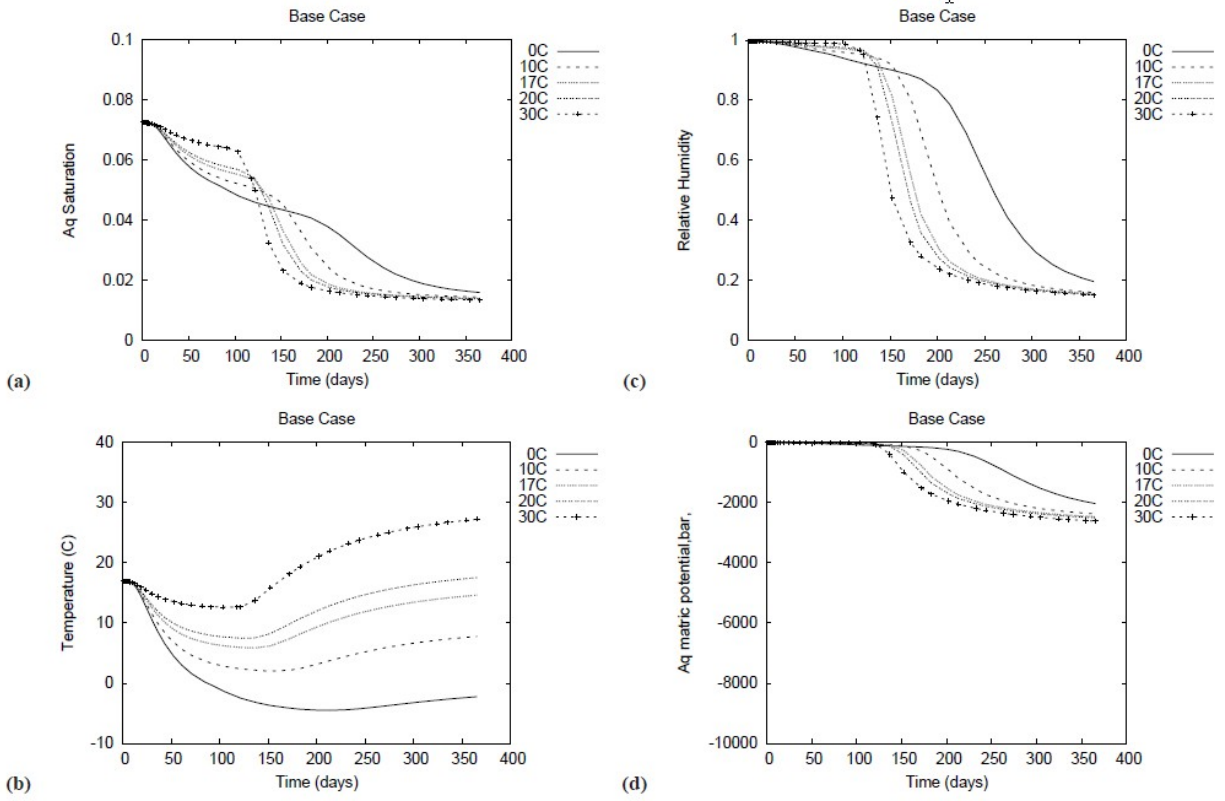
Figure 4.101. Ambient Air Desiccation as a Function of Injected Gas Temperature for an Injected Gas Relative Humidity of 20%
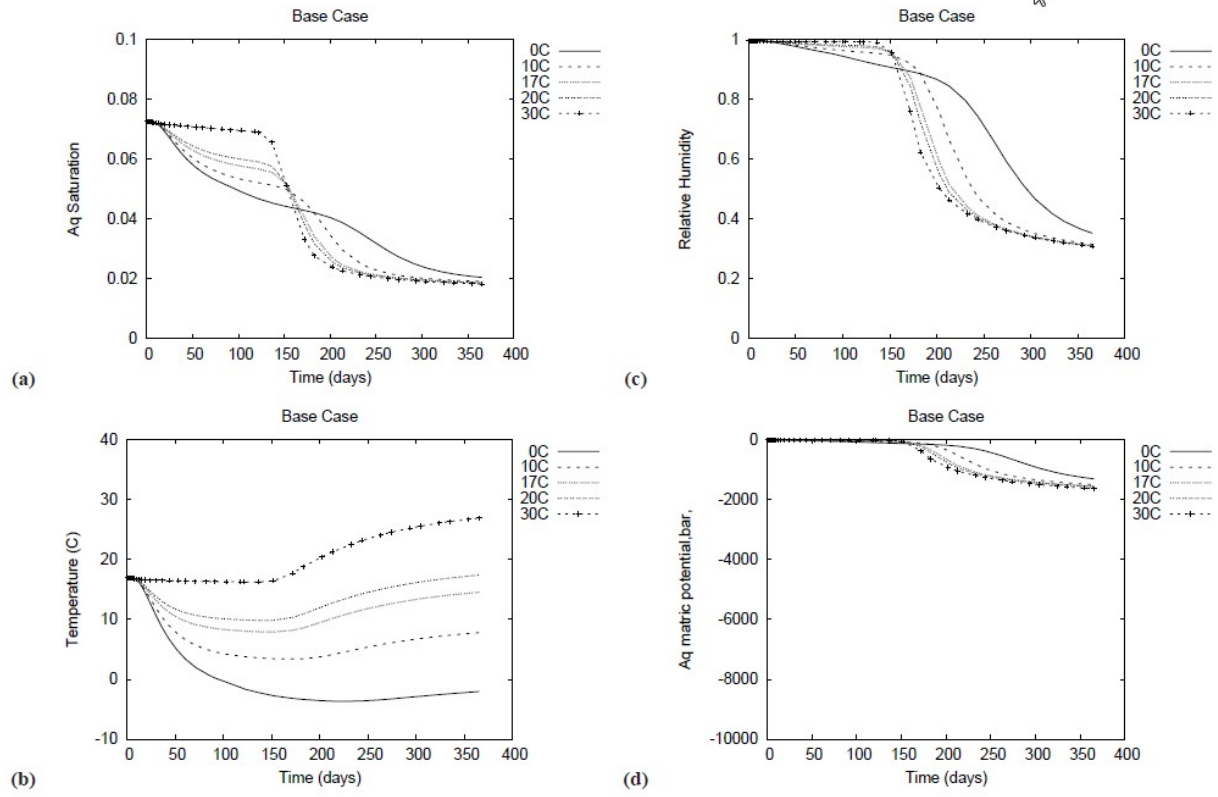
Figure 4.102. Ambient Air Desiccation as a Function of Injected Gas Temperature for an Injected Gas Relative Humidity of 40%
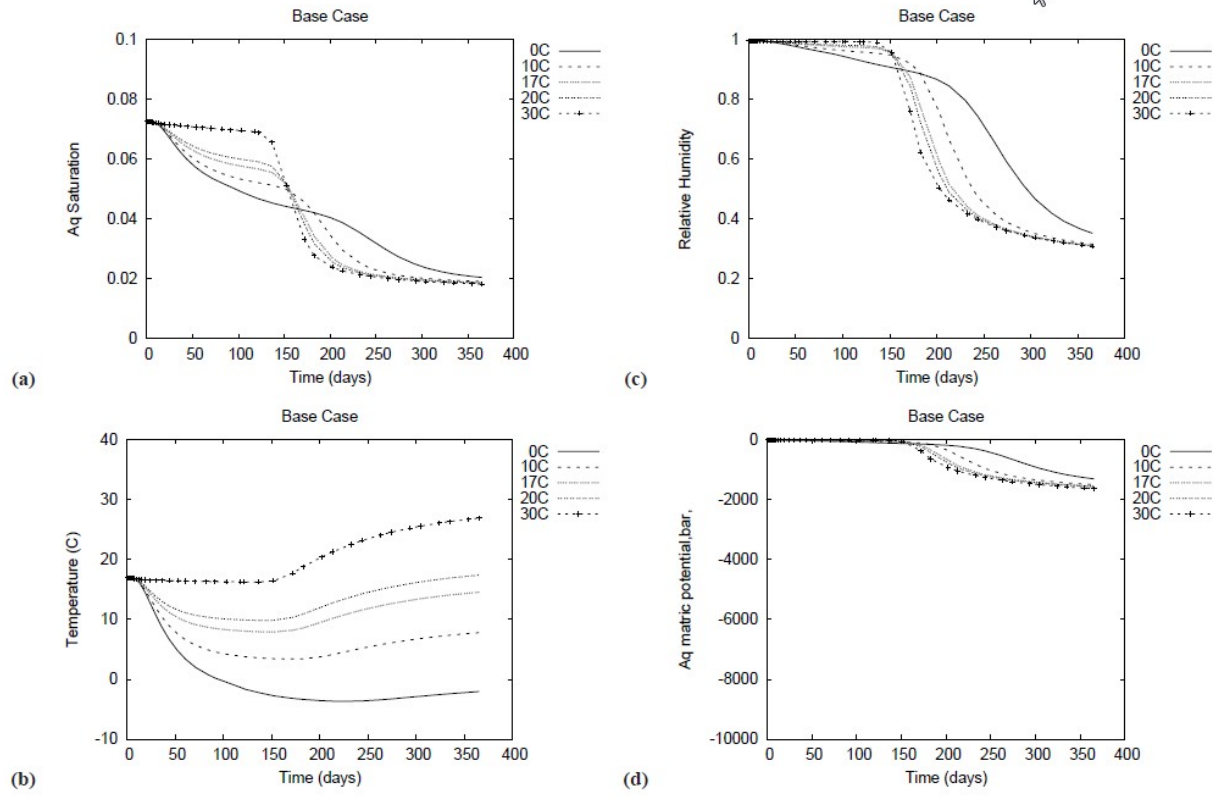
Figure 4.103. Ambient Air Desiccation as a Function of Injected Gas Temperature for an Injected Gas Relative Humidity of 60%
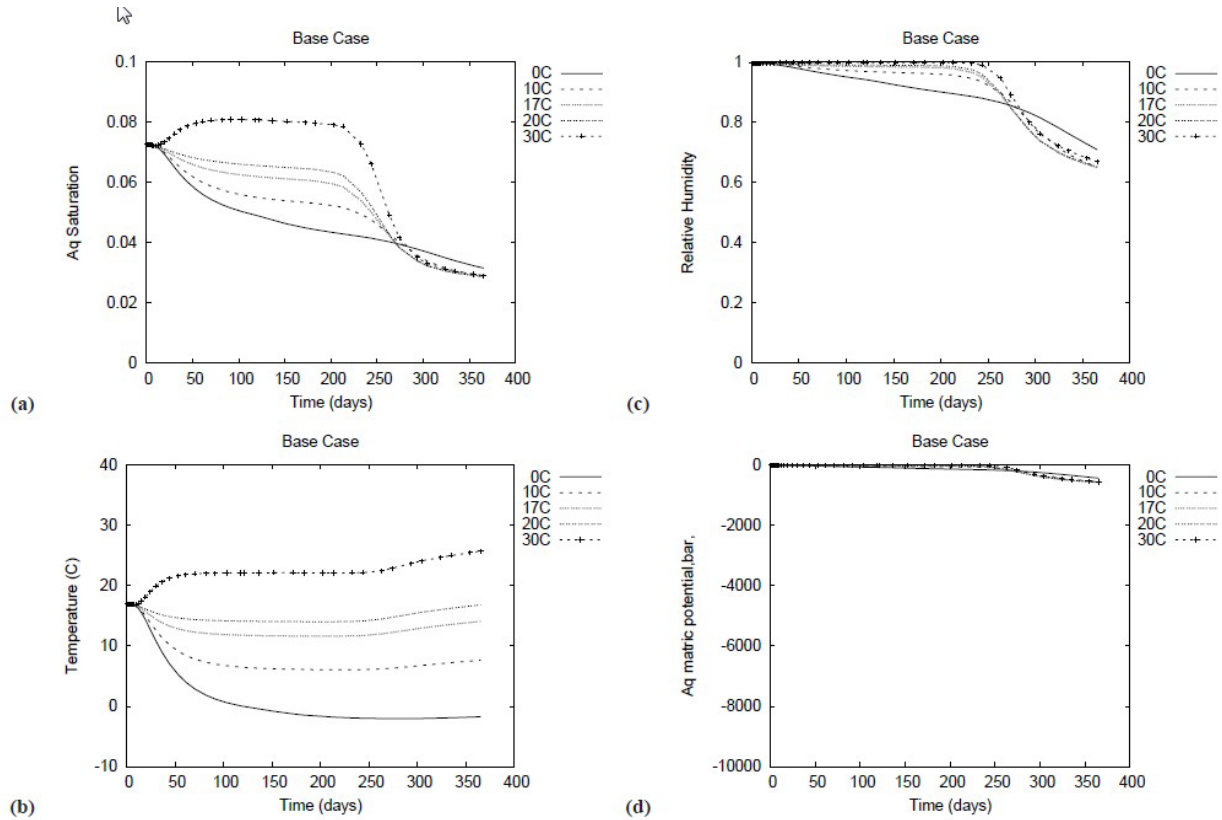
Figure 4.104. Ambient Air Desiccation as a Function of Injected Gas Temperature for an Injected Gas Relative Humidity of 80%

The same pattern of response to higher temperature and relative humidity were observed for Cases 2 and 3 (Figure 4.105 through Figure 4.112, respectively), but the duration and extent of relative water saturation change are different, as expected.
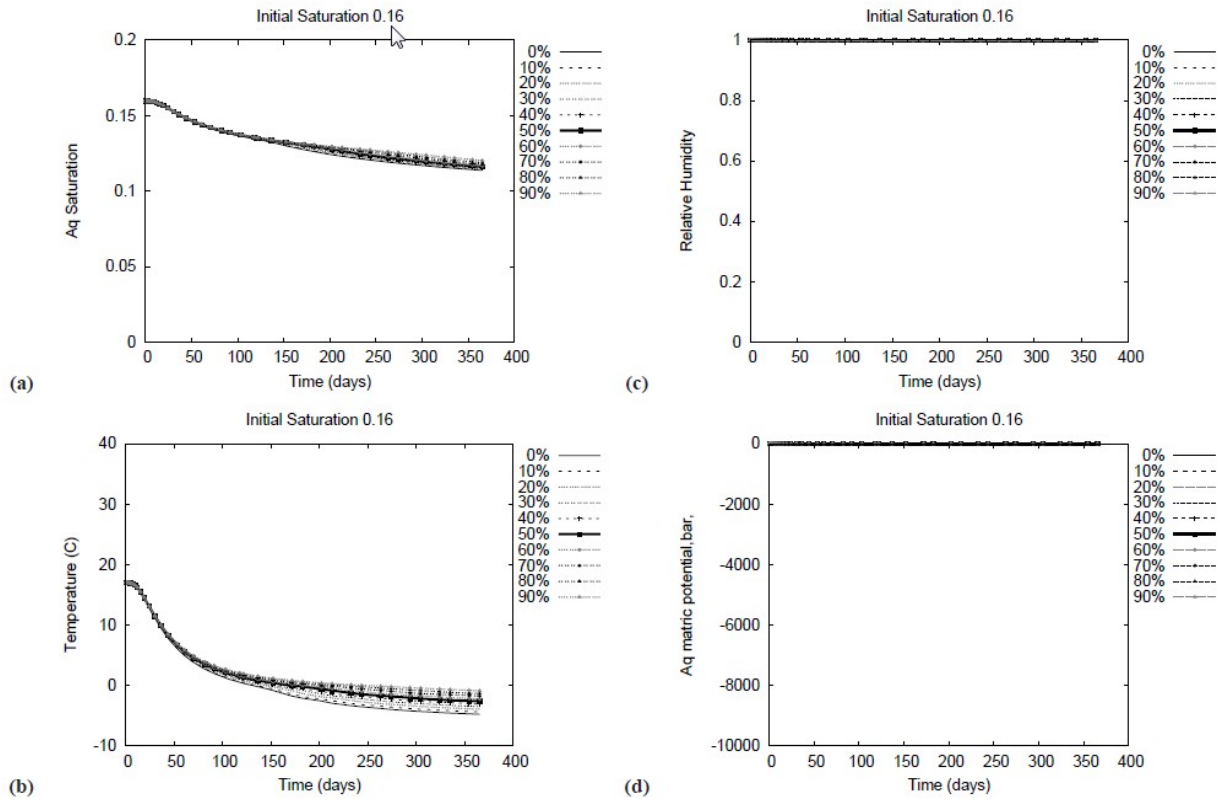
Figure 4.105. Ambient Air Desiccation as a Function of Injected Gas Relative Humidity for an Injected Gas Temperature of 0°C, High Initial Saturation Condition

4.114
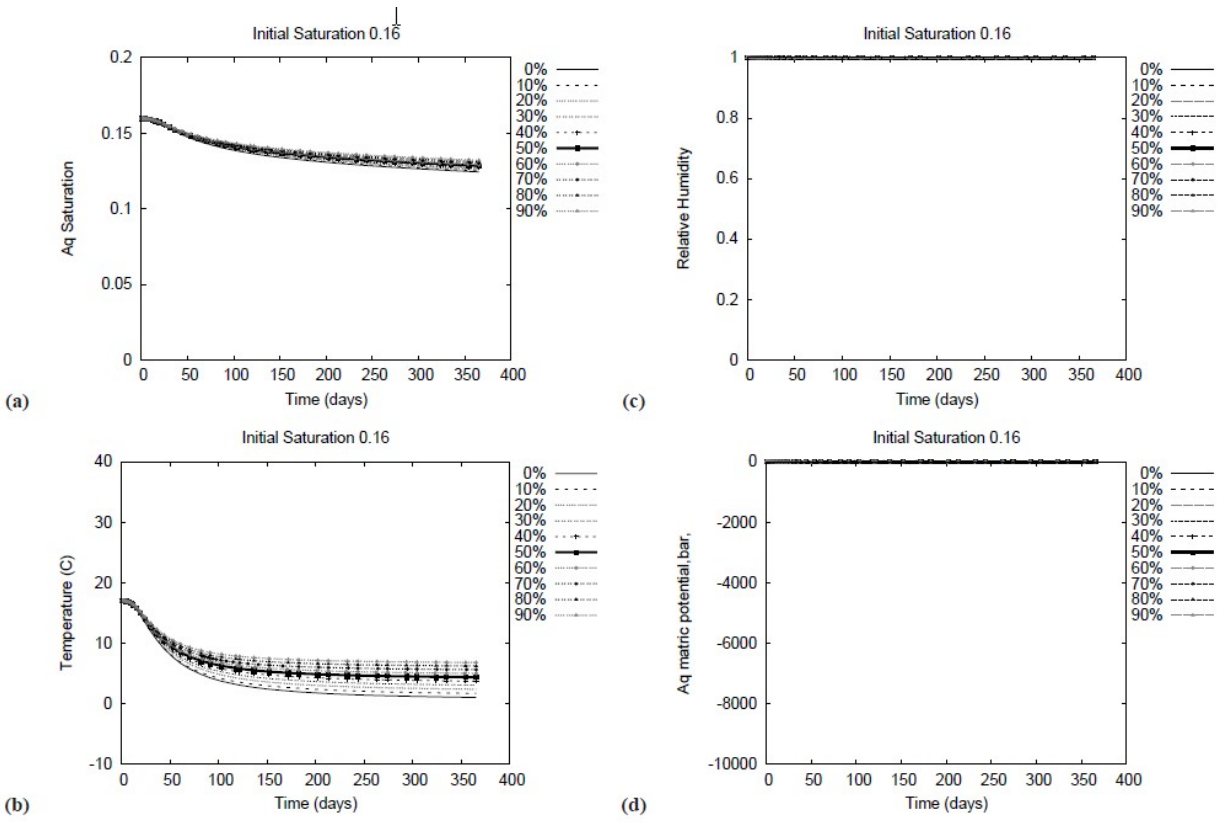
Figure 4.106. Ambient Air Desiccation as a Function of Injected Gas Relative Humidity for an Injected Gas Temperature of 10°C, High Initial Saturation Condition
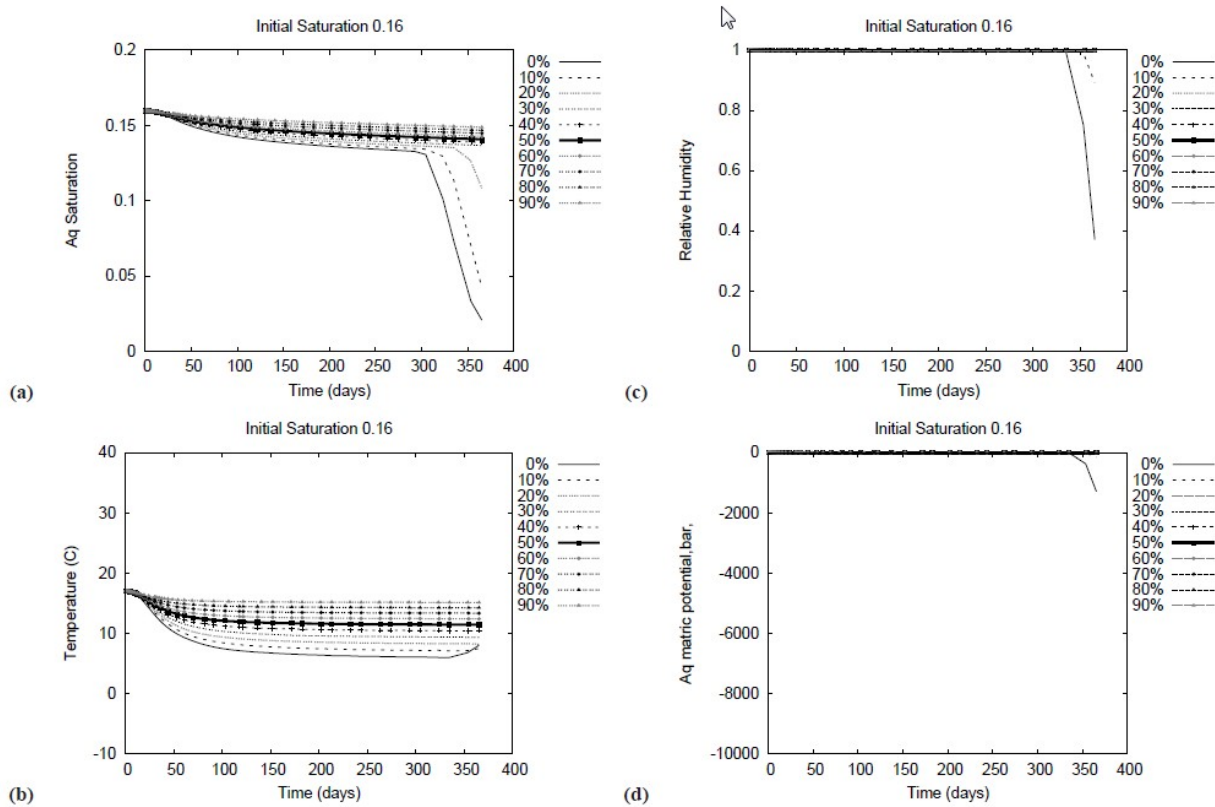
Figure 4.107. Ambient Air Desiccation as a Function of Injected Gas Relative Humidity for an Injected Gas Temperature of 20°C, High Initial Saturation Condition
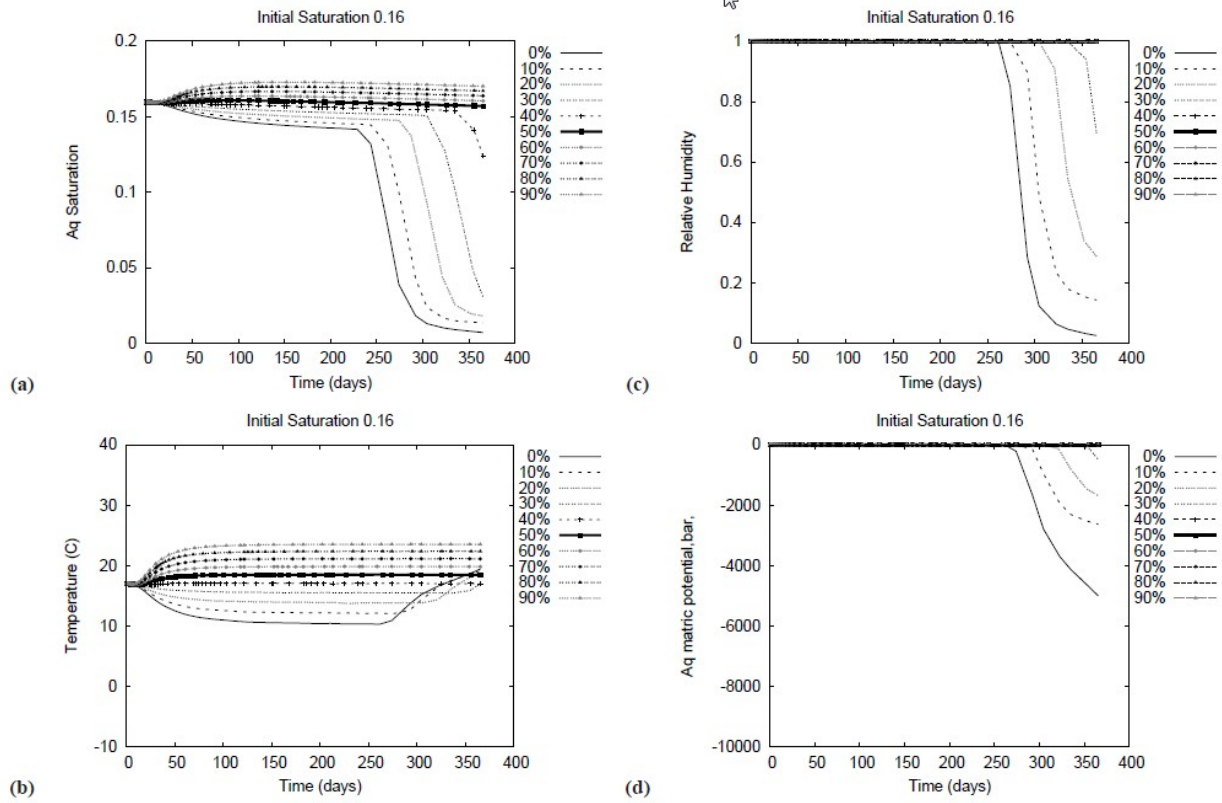
Figure 4.108. Ambient Air Desiccation as a Function of Injected Gas Relative Humidity for an Injected Gas Temperature of 30°C, High Initial Saturation Condition
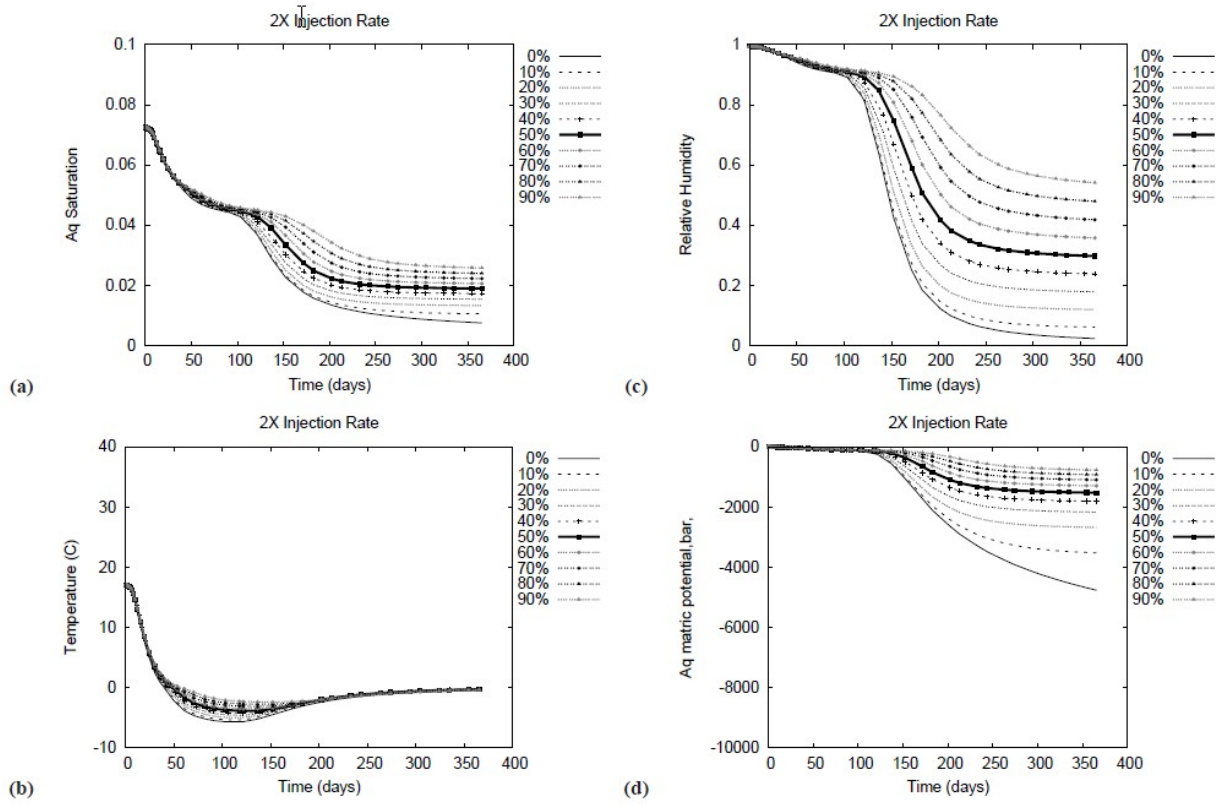
Figure 4.109. Ambient Air Desiccation as a Function of Injected Gas Relative Humidity for an Injected Gas Temperature of 0°C, High Injection Rate Condition
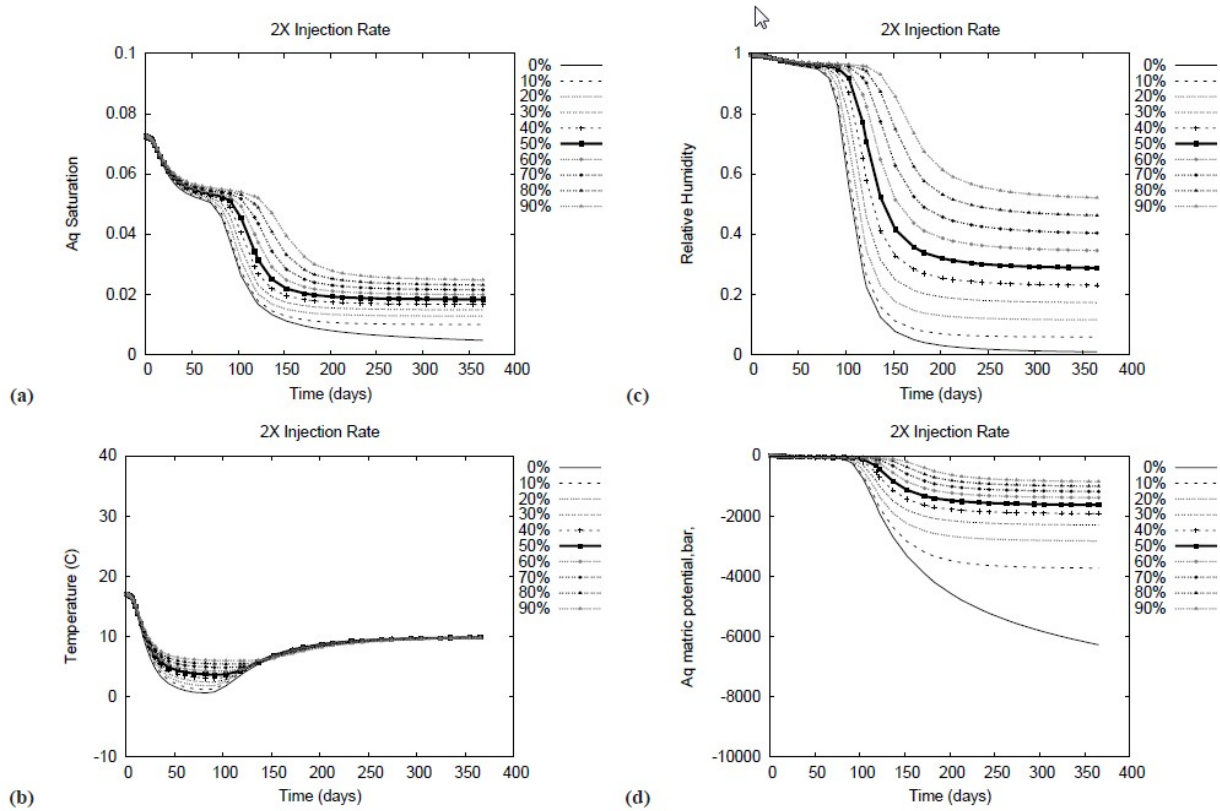
Figure 4.110. Ambient Air Desiccation as a Function of Injected Gas Relative Humidity for an Injected Gas Temperature of 10°C, High Injection Rate Condition
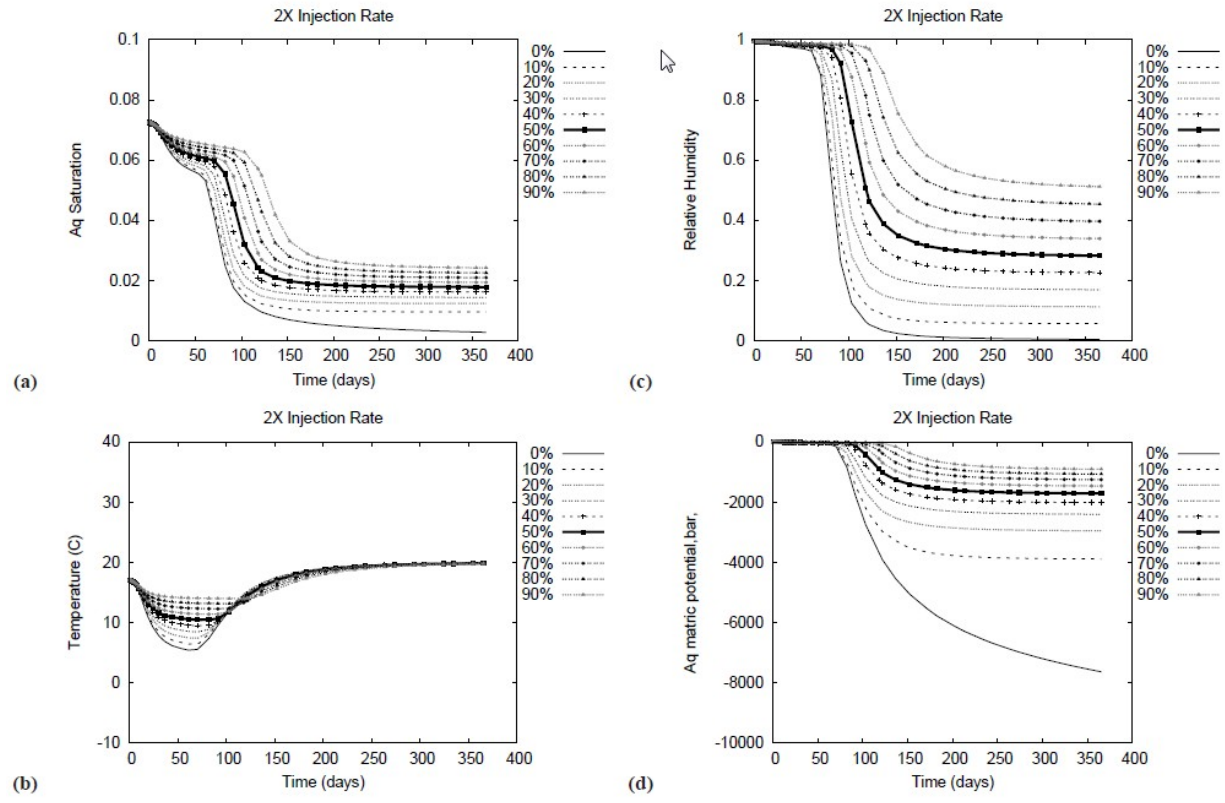
Figure 4.111. Ambient Air Desiccation as a Function of Injected Gas Relative Humidity for an Injected Gas Temperature of 20°C, High Injection Rate Condition
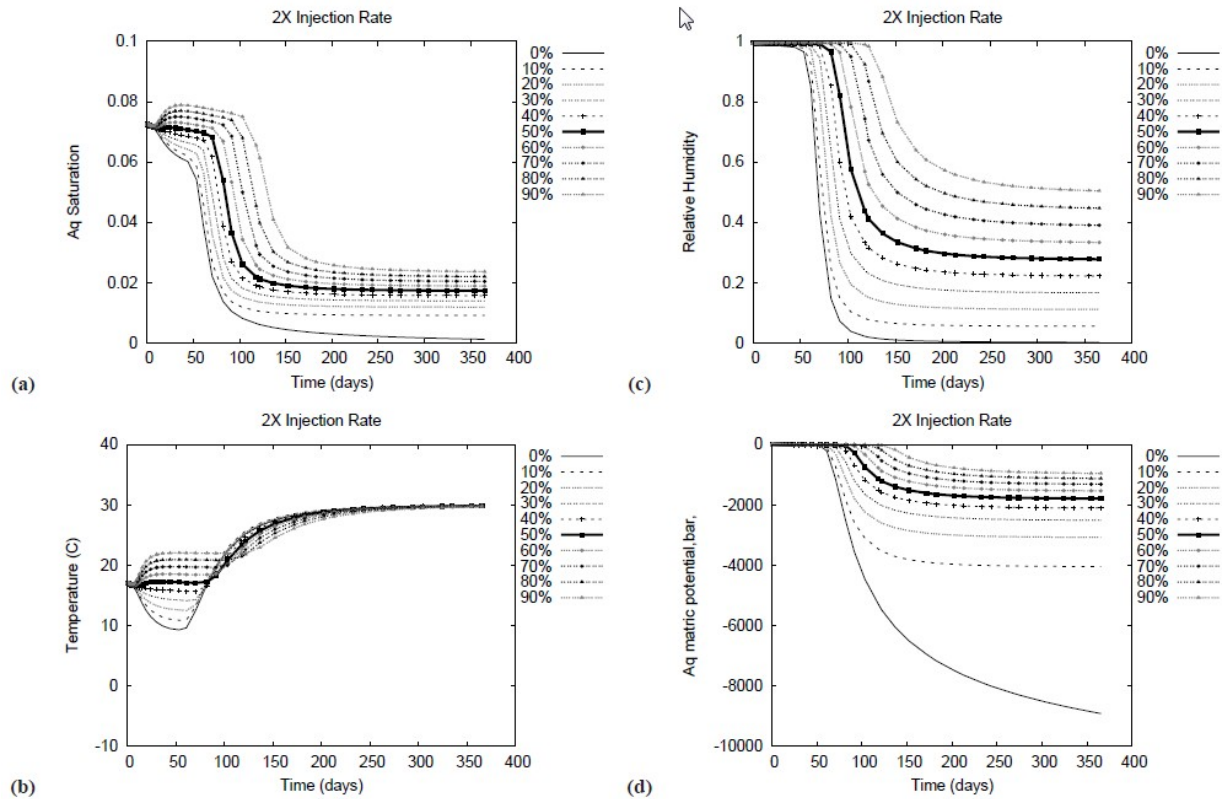
Figure 4.112. Ambient Air Desiccation as a Function of Injected Gas Relative Humidity for an Injected Gas Temperature of 30°C, High Injection Rate Condition

4.2.4.1.3 Ambient Air Assessment Conclusions

The simulation results suggest that ambient air under a wide range of temperature and relative humidity conditions could be used for desiccation. It appears that for Hanford, an injection process that enables heating of the influent air would enhance desiccation rate with ambient air. In that case, fall, spring, and winter air could be heated to reach an effective combination of temperature and relative humidity that increases the desiccation rate without risking condensation. Under a limited set of higher humidity, cooler temperature conditions, injection of air may need to be ceased until conditions change back to a favorable range. In the summer, heating would likely not be needed. However, a control to cease injection during higher humidity periods would be needed.

While the ambient air assessment results are for a generic homogeneous domain, the results along with meteorological data may be useful for designing desiccation based on use of ambient air at a level of detail appropriate for a feasibility study.

4.2.4.2   Assessment of Injection-Only Desiccation Operations

Simulations were conducted to evaluate the injected gas flow and resultant subsurface desiccation distribution as a function of depth for implementation of desiccation using an injection-only design. Desiccation occurs as a result of injection of dry gas that has the capacity to evaporate water from the subsurface. An extraction well can be used to help direct gas flow within the subsurface, but extraction of

soil gas does not directly cause any desiccation. Thus, if injection of dry gas can be effectively delivered to desiccate the targeted region, no extraction is needed.

Injected dry gas evaporates water until it reaches 100% relative humidity. This humid gas is then pushed outward from the injection point and would only release water back to the subsurface if temperature decreased and the related water-holding capacity of the gas thereby decreased. Because evaporative cooling occurs during desiccation, the injected gas flow is generally from cooler to warmer temperature after it has evaporated water from the subsurface. As such, the desiccation process tends to prevent condensation adjacent to the desiccation zone. Temperature changes may occur near the ground surface, however, due to seasonal weather conditions. Thus, it is of interest to understand the gas flux induced at the surface from an injection-only design because if the near-surface is cooler than deeper in the vadose zone, condensation may occur as gas is pushed upward.

The distribution of the desiccation zone and soil gas flux at the ground surface were simulated under several scenarios as part of evaluating an injection-only design. Figure 4.113 shows the model domain, although radial geometry and symmetry were used to simplify the simulations. Table 4.10 shows the simulation matrix.
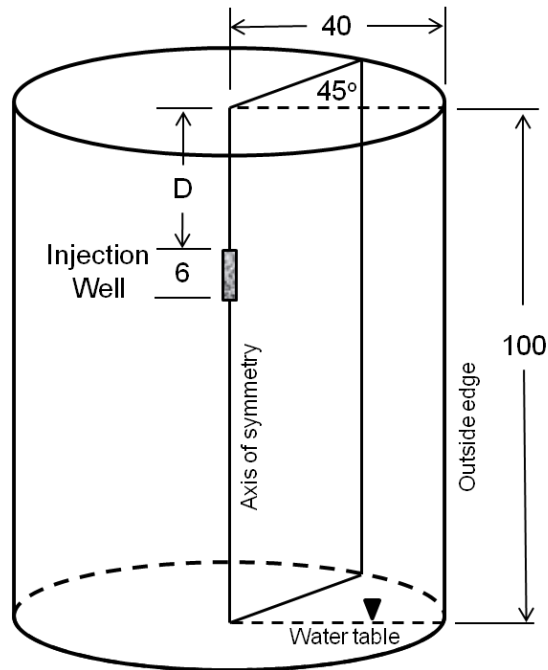
Figure 4.113. Model Domain

Table 4.10. Simulation Matrix

Simulation	Depth (D) (m)	Injection Flow Rate (cfm)	Anisotropy	No-flux surface (cover)
1	10	300	10:1	no
2	20	300	10:1	no
3	30	300	10:1	no
4	10	600	10:1	no
5	20	600	10:1	no
6	30	600	10:1	no
7	10	300	1:1	no
8	20	300	1:1	no
9	30	300	1:1	no
10	10	300	10:1	yes
11	20	300	10:1	yes
12	30	300	10:1	Yes

Figure 4.114 shows the simulation results in terms of the distribution of the desiccated zone after 1 year of desiccation. Note that the distribution of the desiccated zone is essentially the same at all simulated injection well screen depths. Thus, the proximity of the surface for the simulated scenarios, even without use of a barrier to gas flow, does not impact injected gas flow and skew the desiccated zone at shallower depths. Anisotropy (ratio of horizontal to vertical permeability) and injection flow rate have predictable impact on the desiccation distribution. Table 4.11 shows the gas flux at ground surface for each of the cases. Shallower injection wells have greater gas flux out of the ground surface and cold-weather-induced condensation would need to be considered in the desiccation design. The gas flux decreases with the depth of injection well screen, especially in the presence of moderate anisotropy.

While these simulations use a very generalized domain, the results suggest that an injection only-design is viable. For a specific site, consideration of the injection well screen depth and anisotropy can be used to evaluate the need for a barrier to gas flow at the surface.
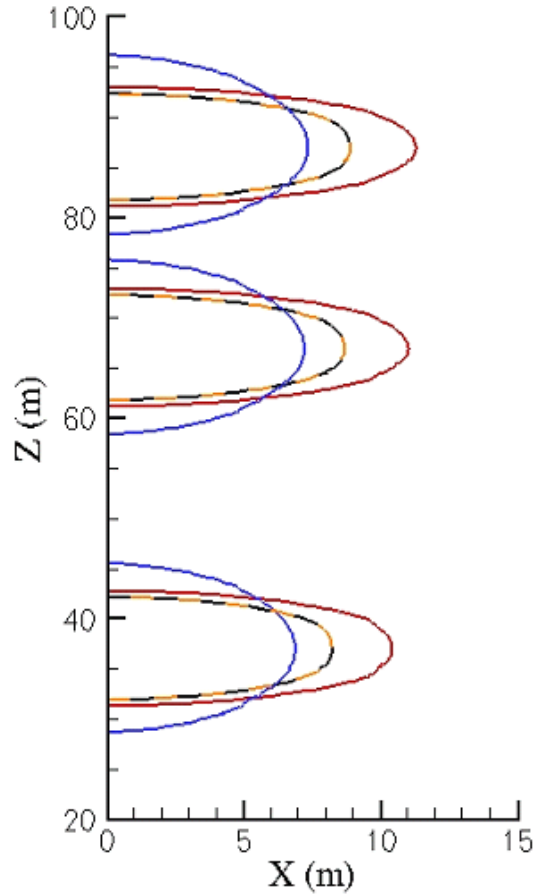
Figure 4.114. 3% Saturation Contour After 1 Year of Desiccation. The initial saturation was ~7%.
Black lines: Base Case (300 cfm; 10:1 anisotropy; no surface cover); Red lines: 600 cfm;
Blue lines: Isotropic; Orange dashed lines: Surface cover. Note that the orange dashed
and black lines are coincident.

Table 4.11. Gas Flow Rate Out of the Top Domain Surface

D(m)	Variable	Flux Out of Top Surface (L/min)
10	base case	140.9
10	600 cfm	276.3
10	isotropic	616.9
10	cover	0
30	base case	4.4
30	600 cfm	9.0
30	isotropic	227.0
30	cover	0
60	base case	0
60	600 cfm	0
60	isotropic	35.9
60	cover	0

4.2.4.3   Performance Requirements Based on Permeability Reduction and Rewetting

In zones that achieved considerable desiccation, the volumetric moisture content was reduced from values of up to 0.10 m^3/m^3 down to values near 0.01 m^3/m^3. The impact of reducing moisture content to this low level on the vertical movement of water and contaminants to groundwater is related to the change in water relative permeability caused by the moisture reduction. While sediment properties throughout the test site are not known, based on sediment characterization data, some of these sediments are similar in grain size to the 100-mesh sand installed in the sensor zones and to a well-characterized Hanford lysimeter sand used in desiccation flow cell experiments (Oostrom et al. 2012a,b). The Hanford lysimeter sand is a mixture of sands obtained from several Hanford locations and is considered to be representative of typical Hanford sand. Using the van Genuchten (1980) *n* and the residual moisture content values for the lysimeter sand, water relative permeability values as a function of moisture content can be computed using a relationship combining the Mualem (1976) relative permeability model with the van Genuchten (1980) pressure-saturation relation. The relative permeability relation for moisture contents ranging from the residual moisture content value up to 0.1 m^3/m^3 is plotted in Figure 4.115 as the gray line. The curve indicates that, theoretically, the water permeability approaches zero when the moisture content is reduced to the residual value of 0.042 m^3/m^3. If the moisture content is reduced below the residual moisture content value as a result of desiccation, the actual water relative permeability is essentially zero and the remaining water cannot migrate as a result of pressure gradients. Given that the residual moisture content is a fitting parameter and is not typically directly measured, the water relative permeability behavior for three additional residual moisture contents has also been included in Figure 4.115. The additional curves indicate that an endpoint moisture content of 0.01 m^3/m^3, as obtained for this field test, will have a non-zero water relative permeability only if the actual residual moisture content of the porous media is smaller than 0.01 m^3/m^3. Even for the most extreme case, with an imposed residual moisture content of zero, the relative permeability at a moisture content of 0.01 m^3/m^3 has been reduced to ~1.0E-5, representing a reduction of more than three orders of magnitude compared to the relative permeability for a moisture content of 0.1 m^3/m^3 (Figure 4.115).

In zones with less significant moisture reduction, rewetting from adjacent moist zones is expected to occur relatively quickly because the water relative permeability of the drier zone has not been significantly reduced. A range of moisture content reduction was observed at the desiccation field test site and moisture content is being monitored over the next few years to evaluate rewetting rates. In addition to rewetting from aqueous-phase movement, rewetting can also occur through movement of vapor-phase moisture (humid soil gas). Truex et al. (2011) demonstrated that vapor-phase rewetting can increase the moisture content to near the residual moisture content of tested porous media. However, the vapor-phase rewetting process is also very slow without soil gas advection because of the relatively low moisture content of soil gas and slow diffusion-driven movement of the humid gas.

The above phenomena are discussed in the context of rewetting processes in Section 4.2.2.2.2. While it is important to target moisture content reductions that result in low post-desiccation moisture content in relation to the residual moisture content for the porous media, it is also important to consider the overall porous media properties within and surrounding the desiccation zone. As shown in the rewetting analysis, the porous media permeability distribution and the overall thickness of the desiccated zone significantly impact the rewetting rate. Thus, site-specific performance targets must be developed considering the properties and the site heterogeneity.
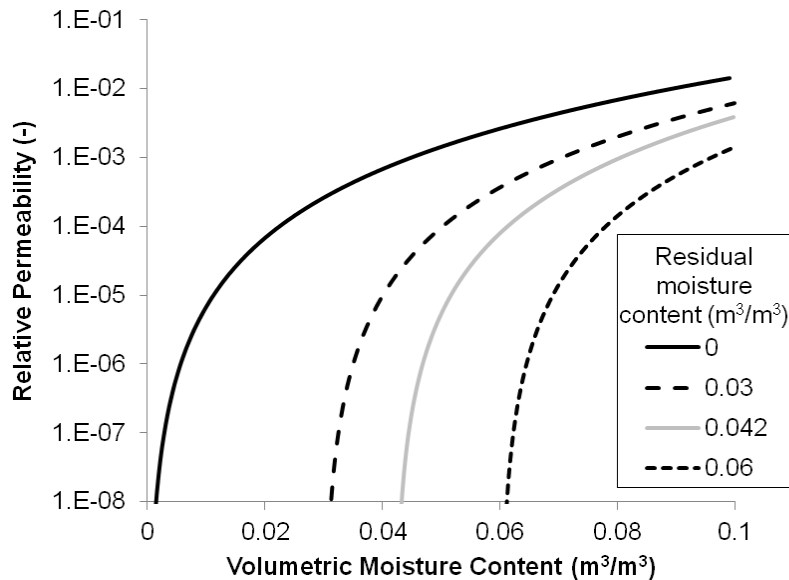
Figure 4.115. Relative Permeability (Mualem 1976) as a Function of Moisture Content, Using a van Genuchten (1980) *n* value of 3.64 and Residual Moisture Contents of 0, 0.03, 0.42, and 0.06. The van Genuchten *n* Value of 3.64 and residual moisture content of 0.42 (gray line) were derived from laboratory retention properties for the Hanford lysimeter sand (Oostrom et al. 2012b).

4.2.4.4   Design Calculations

Like many in situ technologies, numerical simulations provide a primary means to evaluate and select designs based on 1) flow and physical/chemical processes during implementation (e.g., injection of dry gas) and 2) predicted performance as a function of design. As shown in this report and previous studies (Truex et al. 2011; Ward et al. 2008), models are available for use in this design process. However there are also scoping-level calculations that can be used to support design of a desiccation system. Scoping calculations for desiccation are based on calculation of the water-holding capacity of injected gas and relating this factor to moisture removal in the subsurface. Results of laboratory tests and modeling have shown that desiccation processes can be reasonably represented by this type of calculation (Truex et al. 2011; Oostrom et al. 2009, 2012a,b).

The water-holding capacity of the injected gas is a function of its temperature and starting relative humidity. The temperature of the subsurface has been shown to vary significantly during desiccation due to evaporative cooling. For scoping purposes, the temperature used in the analysis could be selected as the starting subsurface temperature (e.g., ~17°C for Hanford) to define a maximum amount of moisture that will be removed. While temperature variation occurs in the vicinity of the zone that is being desiccated, injected gas will move into portions of the vadose zone that are at the starting temperature. Thus, in a more diffuse zone, the total water removed is related to the starting vadose zone temperature. A more conservative approach would be to use a lower temperature such as 12°C (observed average temperature in the field test site during desiccation). This lower temperature would represent the water-holding capacity within a more focused desiccation zone where it is more likely that significant reduction in moisture content will occur. Using the lower temperature is conservative in that the water-holding

capacity will be lower and the scoping calculations will estimate that a longer period of injection is needed to reach a specified moisture removal goal. For use of ambient air injection, the temperature and relative humidity of the injected gas will vary over time. In scoping calculations, meteorological data can be used to select a representative temperature and relative humidity for the design that is suitable for estimating the average water-holding capacity over a 1-year timeframe.

With the selected subsurface temperature and representative injected gas temperature and relative humidity, the water-holding capacity of the injected gas can be determined using a psychometric chart as the humidity ratio (kg_{water}/kg_{air}) at 100% relative humidity and the subsurface temperature minus the humidity ratio (kg_{water}/kg_{air}) at the injected gas relative humidity and temperature (dry bulb). This computation provides the water-holding capacity of the injected gas in mass of water per mass of air units. The ideal gas law can be used to compute the density of the influent air to convert the water-holding capacity to units of mass of water per volume of air (e.g., kg-water/m^3-gas). Desiccation volume in the subsurface is related to the water-holding capacity of the injected gas, the amount of gas injected (flow rate and duration of injection), and the amount of water per volume of soil (soil moisture content). A useful parameter for scoping level design at a site is the desiccation capacity of the injected gas in units of volume of soil desiccated per volume of gas injected. As shown in field and laboratory testing, desiccation will reduce soil moisture content to very low levels. Thus, the amount of water that will be removed from a target volume can be estimated as the average starting moisture content in the volume (e.g., kg-water/m^3-soil). By dividing the water-holding capacity of the injected gas by the gravimetric water content, a desiccation capacity can be computed in units of volume of soil desiccated per volume of gas injected (e.g., m^3-soil/m^3-gas). The desiccation capacity can then be used to estimate the total volume of gas that needs to be injected (product of the flow rate and duration) to reach a target desiccation volume. For an actual application, heterogeneity in the subsurface will cause variations in the starting moisture content and overall distribution of the desiccated zone. However, the scoping calculation reflects the physical linkage between the capacity of the injected gas to evaporate and carry away water and the amount of water that needs to be removed, and is therefore useful to assess the approximate duration of treatment for a given injection gas flow rate.

An example computation is shown below.

- Water-holding capacity of air at a relative humidity of 100% for 17°C subsurface temperature = 0.012 kg-water/kg-air (psychometric chart)

- Water-holding capacity of air at an assumed average relative humidity of 20% for an assumed average ambient air temperature of 15°C = 0.002 kg-water/kg-air (psychometric chart)

- Water-holding capacity of injected gas = 0.012 – 0.002 = 0.01 kg-water/kg-air

- Density of air at 17°C using the ideal gas law = 1.22 kg-air/m^3-air

- Water-holding capacity of injected gas = 0.01 × 1.22 = 0.0122 kg-water/m^3-air

- Average moisture content in target zone = 90 kg-water/m^3-soil (volumetric moisture content of 0.09)

- Desiccation capacity of injected gas = 0.0122/90 = 1.36E-4 m^3-soil/m^3-air

- The desiccation capacity can be used to estimate a desiccation volume for a selected flow rate and duration. For instance, injecting ambient air at 30 m^3/min (~1000 cfm) for 1 year is 1.58E+7 m^3-air. Using the desiccation capacity above, the desiccated volume = 1.36E-4 × 1.58E+7 = ~2000 m^3.

4.2.4.5 Assessment with Respect to CERCLA Feasibility Study Criteria

It will be necessary for the feasibility study author to evaluate soil desiccation using the seven CERCLA criteria, i.e., protectiveness of human health and the environment, compliance with applicable or relevant and appropriate requirements (ARARs); long-term effectiveness and permanence; reduction of toxicity, mobility, or volume; short-term effectiveness; implementability; and cost. The following section summarizes the information collected during the treatability test and how they relate to the CERLCA criteria.

4.2.4.5.1 Threshold Criteria: Protectiveness and ARARs

Numerical modeling will be a key tool in evaluating whether desiccation can meet remediation goals associated with the *Comprehensive Environmental Response, Compensation, and Liability Act* (CERCLA) feasibility study threshold criteria of 1) protection of human health and environment and 2) ARARs. Satisfying the CERCLA protectiveness criterion requires that groundwater not be contaminated above the defined groundwater remediation goals by future contaminant migration. The criteria determining remediation goals are the ARARs that define groundwater standards. It is expected that assessment of performance for evaluation purposes in the feasibility study will rely on fate and transport modeling. The treatability test collected data to improve the technical basis for this modeling and thereby increase site, regulator, and stakeholder confidence in the model results. Table 4.12 lists modeling and supporting laboratory information that were collected in the treatability test that relate to the threshold criteria.

Table 4.12. Information to Support Threshold Criteria

Element	Supporting Information
Model developed for application to desiccation	• Desiccation design modeling code enhancements to address very dry conditions obtained by desiccation have been developed and applied as part of the field test (Truex et al. 2011, 2015; Oostrom et al. 2009, 2012a; this report) • Numerical modeling of overall desiccation performance with respect to impact on groundwater has been conducted and provides a template for how this type of modeling can be applied in the future (Truex et al. 2011; this report) • Laboratory tests have been conducted to support the model development and evaluate modeling performance (Truex et al. 2011; Oostrom et al. 2009, 2012a)
Description and quantification of rewetting process	• Laboratory tests have been conducted to quantify and describe vapor-phase and aqueous-phase rewetting (Oostrom et al. 2012a; Truex et al. 2011) • An assessment of rewetting rate as a function of desiccation end point and surrounding conditions has been conducted (this report) • Rewetting data (6 years of rewetting) have been collected at the field site (this report)

4.2.4.5.2 Long-Term Effectiveness and Permanence

With respect to information from the treatability test, long-term effectiveness and permanence considers the magnitude of residual risk to human and ecological receptors (Table 4.13). Soil desiccation is not expected to remove contamination, but leave it relatively immobilized in the vadose zone. Over time, "rewetting" of the desiccation zone following treatment will occur. The rate of rewetting is important

with respect to the contaminant flux to the groundwater and resultant groundwater contaminant concentrations.

Table 4.13. Information to Support Long-Term Effectiveness and Permanence Criterion

Element	Supporting Information
What desiccation conditions mitigate vertical transport of water/solutes?	• The relationship between porous media properties, desiccation extent, and rewetting rate have been quantified (this report)
Description and quantification of rewetting process and how it relates to the longevity of the desiccation effect on contaminant migration to groundwater	• Laboratory tests have been conducted to quantify and describe vapor-phase and aqueous-phase rewetting (Oostrom et al. 2012a; Truex et al. 2011) • An assessment of rewetting rate as a function of desiccation end point and surrounding conditions has been conducted (this report) • Rewetting data (6 years of rewetting) have been collected at the field site (this report)
In a heterogeneous environment, how dry do the low permeability zones need to be and how does this correlate to future water migration?	• An assessment of rewetting rate as a function of desiccation end point and surrounding conditions has been conducted based on field data in heterogeneous portions of the test site (this report)

4.2.4.5.3 Reduction of Volume, Mobility, or Toxicity

By intent, soil desiccation will reduce the mobility of otherwise quite mobile contaminants (e.g., Tc-99 and nitrate). Desiccation does not address the volume or toxicity of the contamination. Ultimately, mobility is controlled by the rate of rewetting after desiccation (Table 4.14).

Table 4.14. Information to Support Reduction of Toxicity, Mobility, or Volume Criterion

Element	Supporting Information
What desiccation conditions mitigate vertical transport of water/solutes?	• The relationship between porous media properties, desiccation extent, and rewetting rate have been quantified (this report)
Description and quantification of rewetting process and related impact on mobility	• Laboratory tests have been conducted to quantify and describe vapor-phase and aqueous-phase rewetting (Oostrom et al. 2012a; Truex et al. 2011) • An assessment of rewetting rate as a function of desiccation end point and surrounding conditions has been conducted (this report) • Rewetting data (6 years of rewetting) have been collected at the field site (this report)

4.2.4.5.4 Short-Term Effectiveness

Short-term effectiveness considers potential effects on human health and the environment during the implementation phase of the remedy, and the time required to achieve the remedial action objectives (Table 4.15). Extraction of soil gas, as applied for the field test, could expose workers and/or the public (if it is contaminated, for instance, by volatile contaminants or if pore water extraction is induced into the extraction stream); however, extraction of soil gas is not recommended for the full-scale design and is therefore not considered as part of short-term effectiveness. However, a feasibility study may need to

consider issues for movement of soil gas to the ground surface due to desiccation if volatile contaminants are present. Another attribute of this criterion is the rate of desiccation in terms of the remediation timeframe.

Table 4.15. Information to Support Short-Term Effectiveness Criterion

Element	Supporting Information
Quantification of desiccation rate	• Laboratory tests have quantified the desiccation rate (Truex et al. 2011; Oostrom et al. 2009, 2012a,b) • Field test data were evaluated with respect to the desiccation rate (this report) • Desiccation design information includes information related to estimating the desiccation rate (this report)

4.2.4.5.5 Implementability

Implementability includes technical and administrative feasibility, and availability of services and materials. The only pertinent element of this criterion for the treatability test is technical feasibility (Table 4.16).

Table 4.16. Information to Support Implementability Criterion

Element	Supporting Information
Design information	• Desiccation design modeling code enhancements to address very dry conditions obtained by desiccation have been developed and applied as part of the field test (Truex et al. 2011, 2015; Oostrom et al. 2009, 2012a; this report) • Numerical modeling of overall desiccation performance with respect to impact on groundwater has been conducted and provides a template for how this type of modeling can be applied in the future (Truex et al. 2011, this report) • Laboratory tests have been conducted to support the model development and evaluate modeling performance (Truex et al. 2011; Oostrom et al. 2009, 2012a,b) • The relationship between porous media properties, desiccation extent, and rewetting rate have been quantified (this report) • Desiccation design information was generated from the treatability test, including use of ambient air and injection-only designs (this report)
Nature of equipment	• Field test equipment has been described, although some aspects of the field test design are not recommended as part of full-scale implementation (this report) • Desiccation design information was generated from the treatability test, including use of ambient air and injection-only designs (this report)
Subsurface property ranges and heterogeneity for implementing desiccation	• Desiccation design modeling code enhancements to address very dry conditions obtained by desiccation have been developed and applied as part of the field test (Truex et al. 2011, 2015; Oostrom et al. 2009, 2012a,b) • Numerical modeling of overall desiccation performance with respect to impact on groundwater has been conducted and provides a template for how this type of modeling can be applied in the future (Truex et al. 2011; this report) • Laboratory tests have been conducted to support the model development and evaluate modeling performance (Truex et al. 2011; Oostrom et al. 2009, 2012a,b)

4.2.4.5.6 Cost

Cost elements are needed to develop relative cost estimates for use in feasibility studies (Table 4.17). Historical data relating to Hanford well drilling/completion exists to estimate the cost of specific wells to be used for gas injection. Cost of air handling equipment to inject ambient air and providing monitoring capability can be obtained from engineering handbooks/vendors. No specialized equipment is necessary to implement desiccation.

Table 4.17. Information Supporting Estimating Cost for Desiccation

Element	Supporting Information
Design	• Field test equipment has been described, although some aspects of the field test design are not recommended as part of full-scale implementation (this report) • Desiccation design information was generated from the treatability test, including use of ambient air and injection-only designs (this report)
Operating timeframe	• Desiccation design information includes information related to estimating the desiccation rate (this report) • Desiccation design modeling include code enhancements to address very dry conditions obtained by desiccation has been developed and applied as part of the field test (Truex et al. 2011, 2015; Oostrom et al. 2009, 2012a,b; this report) • Laboratory tests have quantified the desiccation rate (Truex et al. 2011; Oostrom et al. 2009, 2012a,b) • Field test data were evaluated with respect to the desiccation rate (this report)
Monitoring	• Monitoring is needed during desiccation operations. The example design and monitoring equipment information in this report provide guidance for the type of monitoring that would be applied. • Long-term performance monitoring related to groundwater protection would also be part of a remedy using desiccation. This monitoring is expected to be the same as would be applied for other technologies being considered for reducing contaminant flux to the groundwater. Specific information about this type of monitoring was not compiled as part of the desiccation treatability test effort.
Surface barrier needs in conjunction with desiccation	• Numerical modeling of overall desiccation performance with respect to impact on groundwater have been conducted and provide a template for how this type of modeling can be applied in the future, including consideration of surface barriers (Truex et al. 2011; this report)

5.0 Quality Assurance Results

The *Data Quality Objectives Summary Report for the Soil Desiccation Pilot Test* (CHPRC 2009) defines principal study questions (PSQs) for the treatability test. Below are those questions and brief discussions of how each has been met.

PSQ #1: Will soil desiccation result in significant reduction of the sediment moisture content?

> Data were collected showing that desiccation reduced sediment moisture content to nearly zero in a significant portion of the zone targeted by the test. Data also showed that while desiccation proceeded initially in strata having higher permeability, adjacent strata with lower permeability began to dry as well.

PSQ #2: Will a significant rate of sediment desiccation be accomplished during the test?

> Data and associated data analysis from the test indicated that desiccation in the field proceeded as expected and consistent with previous laboratory quantification of desiccation rate which was correlated directly with the injection rate of the dry gas.

PSQ #3: Can soil desiccation be performed cost effectively?

> Test data were suitable to define desiccation cost factors and equipment, indicating that there are no specialized high-cost items or significant cost uncertainties. Extrapolation of test results to a proposed remediation indicates that cost elements include drilling injection wells and a comparable number of monitoring boreholes, blowers to inject ambient air, and heaters to condition the ambient air, as appropriate, for the duration required to desiccate the target region. All aspects of the remedy utilize readily available technology and robust equipment. Cost for the technology, which will be site specific depending on the vadose zone properties and contaminant distribution, can be adequately estimated using the information in the treatability test report at the level of accuracy required for a feasibility study.

PSQ #4: Can soil desiccation be accomplished such that it is effective in protecting groundwater in the long term?

> Test data provided information to support numerical simulations of example applications of desiccation for vadose-zone contamination. The simulation results showed that when desiccation is combined with a surface barrier, the contaminant flux to groundwater is reduced compared to desiccation only, surface-barrier only, and no-action scenarios.

Data collection and evaluation, and laboratory sample analysis were conducted in accordance with the methods and specifications described in the *Sampling and Analysis Plan for the Soil Desiccation Pilot Test* (DOE 2010c). A data quality assessment report was prepared described how the quality control limits were met for detection limits, accuracy, and precision (i.e., Table 1-2 and in accordance with Sections 2.3 and 2.4 of the *Sampling and Analysis Plan for the Soil Desiccation Pilot Test* [DOE 2010c]).

This report compiles data and text directly from previous publications that described the interim results of the desiccation test (Truex et al. 2012b, 2013b, 2014, 2015). New data collected in FY17 included 1) continuation of the temperature, humidity, and HDU sensor monitoring and 2) GPR, neutron moisture probe, and ERT surveys. These data were appended to the previous data for these monitoring elements.

In addition, new numerical modeling results were added in Section 2.2.1 as an example to illustrate design considerations for including desiccation in a remedial alternative.

6.0   Cost and Schedule

Overall cost of the desiccation pilot test, beginning October 2008 to conduct a data quality objectives (DQO) process for the characterization phase and continuing through design, construction, and implementation of the desiccation test was $6.4 million. Major cost elements and associated expenditures are shown in Table 6.1.

Table 6.1. Costs for Treatability Test Activities

Treatability Test Activity	$ (K)
Characterization phase DQO and sampling & analysis plan (permitting documentation)	208
Characterization equipment (design/procurement/installation)	270
Characterization phase borehole and extraction well drilling	414
Characterization phase data collection (sample collection & analysis, in situ sediment permeability)	638
Characterization testing reporting	55
Desiccation Field Test Plan and Sampling & Analysis Plan	102
Laboratory testing & numerical simulations (support test design)	1,372
Monitoring borehole drilling	340
Test site preparation (electric power, surface geomembrane installation)	198
Equipment/instrument design, procurement and installation	366
Conduct active portion of test	406
Nitrogen supply	595
Post-desiccation borehole drilling and sampling	161
Post-desiccation monitoring (rewetting, 1 year)	660
Data evaluation & reporting	615
Total	**6,400**

Costs shown above are not representative of what it would cost to implement a desiccation remedy. As discussed in Section 2.0 and Section 4.2.4 of this report, the design would be simplified due to the focus being remedy implementation rather than data collection related to evaluation of the desiccation process. For example, ambient air is recommended rather than dry nitrogen and desiccation progress monitoring would be accomplished with fewer instruments/sensors/geophysical methods and in a manner that maximizes autonomous data collection. Note also that a desiccation remedy would likely be combined with a permanent surface barrier, such as an evapotranspiration barrier, to limit recharge.

7.0   References

Archie GE. 1942. "The Electrical Resistivity Log as an Aid in Determining Some Reservoir Characteristics." *Petroleum Transactions of AIME* 146:54–62.

Basinger JM, GJ Kluitenberg, JM Ham, JM Frank, PL Barnes, and MB Kirkham. 2003. "Laboratory Evaluation of the Dual-Probe Heat-Pulse Method for Measuring Soil Water Content." *Vadose Zone Journal* 2:389–399.

Bilskie J, R Clawson, and J Ritter. 2007. "Calibration of Heat Pulse Sensors for Soil Water Matric Potential." *In* Annual Meetings Abstracts [CD] ASA, CSSA, and SSSA, Madison, Wisconsin.

Binley A, G Cassiani, R Middleton, and P Winship. 2002. "Vadose Zone Model Parameterisation Using Cross-Borehole Radar and Resistivity Imaging." *Journal of Hydrology* 267(3–4):147–159.

Brown RW and DL Bartos. 1982. *A Calibration Model for Screen-Caged Peltier Thermocouple Psychrometers*. Research Paper INT-293, U.S. Department of Agriculture Research, Forest Service, Intermountain Forest and Range Experimental Station, Ogden, Utah.

Carsel RF and RS Parrish. 1988. "Developing Joint Probability Distributions of Soil Water Retention Characteristics." *Water Resources Research* 24(5):755–769.

Campbell GS, C Calissendorif, and JH Williams. 1991. "Probe for Measuring Soil Specific Heat Using a Heat-Pulse Method." *Soil Science Society of America Journal* 55:(29):1–293.

Cass A, GS Campbell, and TL Jones. 1981. *Hydraulic and Thermal Properties of Soil Samples from the Buried Waste Test Facility*. PNL-4015, Pacific Northwest Laboratory, Richland, Washington.

CHPRC. 2009. *Data Quality Objectives Summary Report for the Soil Desiccation Pilot Test*. SGW-41327, Rev. 0, CH2M HILL Plateau Remediation Company, Richland, Washington.

Chronister GB, MJ Truex, and MW Benecke. 2012. "Soil Desiccation Techniques - Strategies for Immobilization of Deep Vadose Contaminants at the Hanford Central Plateau." In *Proceedings of Waste Management Symposia 2012*.

Corbin RA, BC Simpson, MJ Anderson, WF Danielson III, JG Field, TE Jones, and CT Kincaid. 2005. *Hanford Soil Inventory Model Rev. 1*. RPP-26744, Rev. 0, CH2M HILL Hanford Group, Inc., Richland Washington.

Daily W and E Owen. 1991. "Cross-Borehole Resistivity Tomography." *Geophysics* 56:1228–1235.

Day-Lewis FD, JM Harris, and SM Gorelick. 2002. "Time-lapse Inversion of Crosswell Radar Data." *Geophysics* 67:1740–1752.

DOE. 2008a. *Deep Vadose Zone Treatability Test Plan for the Hanford Central Plateau*. DOE/RL-2007-56, Rev. 0, U.S. Department of Energy Richland Office, Richland, Washington.

DOE. 2008b. *Sampling and Analysis Plan for Characterization of the Soil Desiccation Pilot Test Site*. DOE/RL-2008-67, Rev. 0, U.S. Department of Energy Richland Office, Richland, Washington.

DOE. 2009. *BC Cribs and Trenches Excavation-Based Treatability Test Report, Rev. 1 Reissue*. DOE/RL-2009-36, U.S. Department of Energy, Richland Operations Office, Richland, Washington.

DOE. 2010a. *Characterization of the Soil Desiccation Pilot Test Site*. DOE/RL-2009-119, Rev. 0, U.S. Department of Energy Richland Office, Richland, Washington.

DOE. 2010b. *Field Test Plan for the Soil Desiccation Pilot Test*. DOE/RL-2010-04, Rev. 0, U.S. Department of Energy Richland Office, Richland, Washington.

DOE. 2010c. *Sampling and Analysis Plan for the Soil Desiccation Pilot Test*. DOE/RL-2010-83, Rev. 0, U.S. Department of Energy Richland Office, Richland, Washington.

Dresel PE, DM Wellman, KJ Cantrell, and MJ Truex. 2011. "Review: Technical and Policy Challenges in Deep Vadose Zone Remediation of Metals and Radionuclides." *Environmental Science & Technology* 45(10):4207–4216.

Evett SR. 2005. *International Soil Moisture Sensor Comparison. In Irrigation Insights No. 1, Second Edition, Soil Water Monitoring*. P Charlesworth (ed.), Land & Water Australia, Braddon, Australia, pp. 68–71.

EPA. 1992. *Guidance for Conducting Treatability Studies under CERCLA*. EPA/540/R-92/071a, U.S. Environmental Protection Agency, Washington, D.C.

FHI. 2006. *Evaluation of Vadose Zone Treatment Technologies to Immobilize Technetium-99*. WMP-27397, Rev. 1, Fluor Hanford, Inc., Richland, Washington.

Flint AL, GS Campbell, KM Ellett, and C Calissendorff. 2002. "Calibration and Temperature Correction of Heat Dissipation Matric Potential Sensors." *Soil Science Society of America Journal* 66:1439–1445.

Friedman SP. 2005. "Soil Properties Influencing Apparent Electrical Conductivity: A Review." *Computers and Electronics in Agriculture* 46:47–50.

Greacen EL, RL Correll, RB Cunningham, OC Johns, and KD Nichols. 1981. "Calibration." In *Soil Water Assessment by the Neutron Method*, pp. 50–78, CSIRO, Melbourne, Australia.

Hamamoto S, P Moldup, K Kawamoto, T Komatsu. 2010. "Excluded-Volume Expansion of Archie's Law for Gas and Solute Diffusivities and Electrical and Thermal Conductivities in Variably Saturated Porous Media." *Water Resources Research*,46, doi:10.1029/2099WR00842r.

Han M, S Youssef, E Rosenberg, M Fleury, P Levitz. 2009. "Deviation from Archie's Law in Partially Saturated Porous Media: Wetting Film Versus Disconnectedness of the Conducting Phase." *Physical Review E*, 79,doi:10.1103/PhysRevE.79.031127.

Hignett C and SR Evett. 2002. "Neutron Thermalization." In *Methods of Soil Analysis. Part 4 – Physical Methods.* JH Dane and G Clarke Topp (eds.), pp. 501–521, Soil Science Society of America, Madison, Wisconsin.

Hubbard SS, JE Peterson, EL Majer, PT Zawislanski, J Roberts, KH Williams, and F Wobber. 1997. "Estimation of Permeable Pathways and Water Content Using Tomographic Radar Data." *The Leading Edge of Exploration* 16(11):1623–1628.

Huisman JA, C Sperl, W Bouten, and JM Verstraten. 2001. "Soil Water Content Measurements at Different Scales: Accuracy of Time Domain Reflectometry and Ground-Penetrating Radar." *Journal of Hydrology* 245:48–58.

Jackson MJ and DR Tweeton. 1994. *MIGRATOM - Geophysical Tomography Using Wavefront Migration and Fuzzy Constraints.* Bureau of Mines Report of Investigations 9497, 35 pp., Pittsburgh, Pennsylvania.

Johnson TC, RJ Versteeg, A Ward, FD Day-Lewis, and A Revil. 2010. "Improved Hydrogeophysical Characterization and Monitoring Through Parallel Modeling and Inversion of Time-Domain Resistivity and Induced Polarization Data." *Geophysics* 75(4):WA27–WA41.

Kincaid CT, PW Eslinger, RL Aaberg, TB Miley, IC Nelson, SL Strenge, and JC Evans, Jr. 2006. *Inventory Data Package for Hanford Assessments.* PNNL-15829, Rev. 0, Pacific Northwest National Laboratory, Richland, Washington.

Last GV, WE Nichols, and CT Kincaid. 2006. *Geographic and Operational Site Parameters List (GOSPL) for Hanford Assessments.* PNNL-14725, Rev. 1, Pacific Northwest National Laboratory, Richland, Washington.

Ledieu J, P De Ridder, P De Clerck, and S Dautrebande. 1986. "A Method of Measuring Soil Moisture by Time-Domain Reflectometry." *Journal of Hydrology* 88:319–328.

Li, J., DW Smith, SG Fityus, and DC Sheng. 2003. "The Numerical Analysis of Neutron Moisture Probe Measurements." *ASCE International Journal of Geomechanics* 3(1):11–20.

Maxfield HL. 1979. *Handbook 200 Area Waste Sites.* RHO-CD-673, Volumes 1, 2, and 3, Rockwell Hanford Operations, Richland, Washington.

Mualem Y. 1976. "A New Model for Predicting the Hydraulic Conductivity of Unsaturated Porous Media." *Water Resources Research* 12:513–522.

Oostrom M, TW Wietsma, JH Dane, MJ Truex, and AL Ward. 2009. "Desiccation of Unsaturated Porous Media: Intermediate-Scale Experiments and Numerical Simulation." *Vadose Zone Journal* 8:643–650.

Oostrom M, GD Tartakovsky, TW Wietsma, MJ Truex, and JH Dane. 2011. "Determination of Water Saturation in Relatively Dry and Desiccated Porous Media Using Gas-Phase Partitioning Tracer Tests." *Vadose Zone Journal* 10:1–8; doi:10.2136/vzj2010.0101.

Oostrom M, TW Wietsma, CE Strickland, VL Freedman, and MJ Truex. 2012a. "Instrument Testing During Desiccation and Rewetting at the Intermediate Laboratory Scale." *Vadose Zone Journal* doi:10.2136/vzj2011.0089.

Oostrom M, VL Freedman, TW Wietsma, and MJ Truex. 2012b. "Effects of porous medium heterogeneity on vadose zone desiccation: Intermediate-scale laboratory experiments and simulations." *Vadose Zone Journal* doi:10.2136/vzj2011.0168.

Ruijun M, A McBratney, B Whelan, B Minasny, and M Short. 2011. "Comparing Temperature Correction Models for Soil Electrical Conductivity Measurement." *Precision Agriculture* 12:55–66, doi:10.1007/s11119-009-9156-7.

Serne RJ, AL Ward, W Um, BN Bjornstad, DF Rucker, DC Lanigan, and MW Benecke. 2009. *Electrical Resistivity Correlation to Vadose Zone Sediment and Pore-Water Composition for the BC Cribs and Trenches Area*. PNNL-17821, Pacific Northwest National Laboratory, Richland, Washington.

Slater LD and DP Lesmes. 2002. "Electrical-Hydraulic Relationships Observed for Unconsolidated Sediments." *Water Resources Research* 38:1213–1225.

Topp GC and PA (Ty) Ferré. 2002. "Water Content." In *Methods of Soil Analysis Part 4, Physical Methods*, SSSA Book Series No. 5, JH Dane and GC Topp (eds.), Section 3.1, pp. 417–545, Soil Science Society of America, Inc., Madison, Wisconsin.

Truex MJ, M Oostrom, VL Freedman, C Strickland, and AL Ward. 2011. *Laboratory and Modeling Evaluations in Support of Field Testing for Desiccation at the Hanford Site*. PNNL-20146, Pacific Northwest National Laboratory, Richland, Washington.

Truex MJ, M Oostrom, CE Strickland, GB Chronister, MW Benecke, and CD Johnson. 2012a. "Field-Scale Assessment of Desiccation Implementation for Deep Vadose Zone Contaminants." *Vadose Zone Journal* doi:10.2136/vzj2011.0144

Truex MJ, M Oostrom, CE Strickland, TC Johnson, VL Freedman, CD Johnson, WJ Greenwood, AL Ward, RE Clayton, MJ Lindberg, JE Peterson, SS Hubbard, GB Chronister, and MW Benecke. 2012b. *Deep Vadose Zone Treatability Test for the Hanford Central Plateau: Soil Desiccation Pilot Test Results*. PNNL-21369, Pacific Northwest National Laboratory, Richland, Washington.

Truex MJ, TC Johnson, CE Strickland, JE Peterson, and SS Hubbard. 2013a. "Monitoring Vadose Zone Desiccation with Geophysical Methods." *Vadose Zone Journal* doi:10.2136/vzj2012.0147

Truex MJ, M Oostrom, CE Strickland, TC Johnson, CD Johnson, RE Clayton, and GB Chronister. 2013b. *Deep Vadose Zone Treatability Test for the Hanford Central Plateau: Interim Post-Desiccation Monitoring Results*. PNNL-22826, Pacific Northwest National Laboratory, Richland, Washington.

Truex MJ, M Oostrom, CE Strickland, TC Johnson, CD Johnson, RE Clayton, and GB Chronister. 2014. Deep Vadose Zone Treatability Test for the Hanford Central Plateau: Interim Post-Desiccation Monitoring Results, Fiscal Year 2014. PNNL-23731 Pacific Northwest National Laboratory, Richland, Washington.

Truex, MJ, CE Strickland, M Oostrom, CD Johnson, GD Tartakovsky TC Johnson, RE Clayton, and GB Chronister. 2015. Deep Vadose Zone Treatability Test for the Hanford Central Plateau: Interim Post-Desiccation Monitoring Results, Fiscal Year 2015. PNNL-24706, Pacific Northwest National Laboratory, Richland, WA.

Um W, RJ Serne, MJ Truex, AL Ward, MM Valenta, CF Brown, C Iovin, KN Geiszler, IV Kutnyakov, ET Clayton, H-S Chang, SR Baum, and DM Smith. 2009. *Characterization of Sediments from the Soil Desiccation Pilot Test (SDPT) Site in the BC Cribs and Trenches Area*. PNNL-18800, Pacific Northwest National Laboratory, Richland, Washington.

van Genuchten M Th. 1980. "A Closed-Form Equation for Predicting the Hydraulic Conductivity of Unsaturated Soils." *Soil Science Society of America Journal* 44:892–898.

van Overmeeren R, S Sariowan, and J Geherls. 1997. "Ground Penetrating Radar for Determining Volumetric Soil Water Content: Results of Comparative Measurements at Two Test Sites." *Journal of Hydrology* 197:316–338.

Ward AL, GW Gee, ZF Zhang, and JM Keller. 2004. *Vadose Zone Contaminant Fate and Transport Analysis for the 216-B-26 Trench*. PNNL-14907, Pacific Northwest National Laboratory, Richland, Washington.

Ward AL, M Oostrom, and DH Bacon. 2008. *Experimental and Numerical Investigations of Soil Desiccation for Vadose Zone Remediation: Report for Fiscal Year 2007*. PNNL-17274, Pacific Northwest National Laboratory, Richland, Washington.

Ward AL and RS Wittman. 2009. *Calibration of a Neutron Hydroprobe for Moisture Measurements in Small-Diameter Steel-Cased Boreholes*. PNNL-18539, Pacific Northwest National Laboratory, Richland, Washington.

Webb SW. 2000. "A Simple Extension of Two-Phase Characteristic Curves to Include the Dry Region." *Water Resources Research* 36:1425–1430.

White I and SJ Zegelin. 1995. "Electric and Dielectric Methods for Monitoring Soil-Water Content." In *Handbook of Vadose Zone Characterization and Monitoring*, LG Wilson, LG Everett, and S Cullen (eds.), Chapter 22, A. F. Lewis, New York.

White MD and M Oostrom. 2006. *STOMP Subsurface Transport Over Multiple Phases, Version 4.0, User's Guide*. PNNL-15782, Pacific Northwest National Laboratory, Richland, Washington.

White MD and M Oostrom. 2000. *STOMP Subsurface Transport Over Multiple Phase: Theory Guide*. PNNL-11216, Pacific Northwest National Laboratory, Richland, Washington.

Yao T, PJ Wierenga, AR Graham, and SP Neuman. 2004. "Neutron Probe Calibration in a Vertically Stratified Vadose Zone." *Vadose Zone Journal* 3:1400–1406.

Appendix A

Analytical Data Report for Sediment Samples Collected from Post-Desiccation Boreholes C8387 and C8388

Appendix A

Analytical Data Report for Sediment Samples Collected from Post-Desiccation Boreholes C8387 and C8388

Two boreholes were installed after the end of active desiccation. Samples were collected and analyzed for soil moisture and selected pore water chemistry as described in the detailed laboratory report shown below. Additional samples were analyzed to provide a more complete profile of the soil moisture distribution in the two boreholes than the more limited set of samples that were analyzed for soil moisture and selected pore water chemistry. These additional sample analyses used the same procedures as described in the laboratory report. Table A.1 and Table A.2 provide the results of these additional analyses.

A.2

Table A.1. BC Crib Borehole C8387

Shoe depth (ft bgs)	Interval #	Liner	Core Depth (ft)	Gravimetric Soil (gSoil/gTotal)	Gravimetric H$_2$0 (gH$_2$O/gSoil)	Gravimetric H$_2$0 (gH$_2$O/gTotal)	Core Soil Weight (g)	Bulk Density (g/cm^3)	Volumetric Moisture Content	Liner
23.1	242	D	21.1	0.9756	0.0250	0.0244	2021.853	1.739	0.0434	S.S
	242	C	21.6	0.9468	0.0562	0.0532	2011.353	1.686	0.0947	S.S
	242	B	22.1	0.9288	0.0767	0.0712	1927.571	1.649	0.1264	S.S
	242	A	22.6	0.9480	0.0549	0.0520	1639.336	1.737	0.0953	S.S
24.8	243	D	22.8	0.9318	0.0732	0.0682	2135.929	1.850	0.1354	S.S
	243	C	23.3	0.9517	0.0507	0.0483	2025.542	1.742	0.0884	S.S
	243	B	23.8	0.9397	0.0642	0.0603	2142.795	1.862	0.1195	S.S
	243	A	24.3	0.9283	0.0773	0.0717	1606.192	1.730	0.1337	S.S
27.5	244	D	25.5	0.8667	0.1538	0.1333	1816.046	1.586	0.2439	S.S
	244	C	26	0.8861	0.1285	0.1139	1778.685	1.530	0.1966	S.S
	244	B	26.5	0.9056	0.1042	0.0944	1801.553	1.552	0.1618	S.S
	244	A	27	0.9275	0.0782	0.0725	1454.546	1.577	0.1234	S.S
30	245	D	28	0.9501	0.0525	0.0499	2129.560	1.838	0.0964	S.S
	245	C	28.5	0.9562	0.0458	0.0438	2159.482	1.851	0.0847	S.S
	245	B	29	0.9379	0.0662	0.0621	1969.866	1.715	0.1136	S.S
	245	A	29.5	0.9489	0.0539	0.0511	1520.408	1.708	0.0920	S.S
32.6	246	D	30.6	0.9418	0.0618	0.0582	1976.165	1.735	0.1073	S.S
	246	C	31.1	0.9388	0.0652	0.0612	1884.380	1.621	0.1057	S.S
	246	B	31.6	0.9523	0.0500	0.0477	1900.233	1.648	0.0825	S.S
	246	A	32.1	0.9451	0.0581	0.0549	1563.495	1.642	0.0954	S.S
35.3	247	D	33.3	0.9457	0.0575	0.0543	1419.735	1.620	0.0931	S.S
	247	C	33.8	0.9358	0.0686	0.0642	1836.318	1.590	0.1091	S.S
	247	B	34.3	0.9393	0.0647	0.0607	1797.091	1.559	0.1008	S.S
	247	A	34.8	0.9218	0.0848	0.0782	1705.674	1.558	0.1321	S.S

Table A.1. (contd)

Shoe depth (ft bgs)	Interval #	Liner	Core Depth (ft)	Gravimetric Soil (gSoil/gTotal)	Gravimetric H20 (gH2O/gSoil)	Gravimetric H20 (gH2O/gTotal)	Core Soil Weight (g)	Bulk Density (g/cm3)	Volumetric Moisture Content	Liner
37.7	248	D	35.7	0.9183	0.0890	0.0817	1855.367	1.679	0.1495	lexan
	248	C	36.2	0.9219	0.0848	0.0781	1807.339	1.622	0.1374	lexan
	248	B	36.7	0.9216	0.0850	0.0784	1709.177	1.613	0.1371	lexan
	248	A	37.2	0.9190	0.0882	0.0810	1491.020	1.679	0.1481	lexan
40	249	D	38	0.8369	0.1949	0.1631	1769.562	1.615	0.3149	lexan
	249	C	38.5	0.9172	0.0902	0.0828	2065.194	1.869	0.1686	lexan
	249	B	39	0.8616	0.1607	0.1384	1811.489	1.694	0.2722	lexan
	249	A	39.5	0.9508	0.0518	0.0492	1845.906	1.872	0.0970	lexan
42.4	250	D	40.4	0.9631	0.0384	0.0369	2183.568	1.921	0.0737	S.S
	250	C	40.9	0.9412	0.0625	0.0588	2151.414	1.854	0.1159	S.S
	250	B	41.4	0.9582	0.0437	0.0418	2128.379	1.882	0.0822	S.S
	250	A	41.9	0.9620	0.0395	0.0380	1716.586	1.818	0.0717	S.S
45.2	251	D	43.2	0.9635	0.0379	0.0365	2200.939	1.946	0.0737	S.S
	251	C	43.7	0.9602	0.0415	0.0398	2212.550	1.846	0.0766	S.S
	251	B	44.2	0.9535	0.0487	0.0465	2079.005	1.797	0.0876	S.S
	251	A	44.7	0.9366	0.0677	0.0634	1657.068	1.828	0.1239	S.S
47.8	252	D	45.8	0.9884	0.0117	0.0116	1785.630	1.747	0.0204	lexan
	252	C	46.3	0.9852	0.0150	0.0148	1846.856	1.721	0.0258	lexan
	252	B	46.8	0.9748	0.0259	0.0252	1889.609	1.698	0.0440	lexan
	252	A	47.3	0.9590	0.0427	0.0410	1504.271	1.727	0.0737	lexan
50.1	253	D	48.1	0.9811	0.0193	0.0189	1926.402	1.913	0.0369	lexan
	253	C	48.6	0.9729	0.0278	0.0271	2105.944	1.942	0.0540	lexan
	253	B	49.1	0.9783	0.0222	0.0217	2216.295	1.985	0.0441	lexan
	253	A	49.6	0.9794	0.0211	0.0206	1802.544	2.017	0.0425	lexan
52.25	254	D	50.25	0.9759	0.0247	0.0241	2144.630	1.938	0.0478	lexan
	254	C	50.75	0.9705	0.0303	0.0295	1986.242	1.826	0.0554	lexan
	254	B	51.25	0.9823	0.0180	0.0177	2025.038	1.823	0.0328	lexan
	254	A	51.75	0.9803	0.0201	0.0197	1719.977	1.824	0.0366	lexan

Table A.1. (contd)

Shoe depth (ft bgs)	Interval #	Liner	Core Depth (ft)	Gravimetric Soil (gSoil/gTotal)	Gravimetric H20 (gH2O/gSoil)	Gravimetric H20 (gH2O/gTotal)	Core Soil Weight (g)	Bulk Density (g/cm3)	Volumetric Moisture Content	Liner
55.3	255	D	53.3	0.9791	0.0213	0.0209	1875.504	1.849	0.0394	lexan
	255	C	53.8	0.9781	0.0224	0.0219	1939.036	1.746	0.0391	lexan
	255	B	54.3	0.9815	0.0189	0.0185	1954.603	1.754	0.0331	lexan
	255	A	54.8	0.9751	0.0255	0.0249	1606.498	1.775	0.0453	lexan
58	256	D	56	0.9754	0.0252	0.0246	1858.719	1.773	0.0446	lexan
	256	C	56.5	0.9749	0.0257	0.0251	1905.450	1.721	0.0443	lexan
	256	B	57	0.9806	0.0198	0.0194	1884.272	1.747	0.0345	lexan
	256	A	57.5	0.9793	0.0211	0.0207	1682.015	1.784	0.0377	lexan
60.8	257	D	58.8	0.9712	0.0297	0.0288	1896.229	1.825	0.0542	lexan
	257	C	59.3	0.9697	0.0312	0.0303	1911.856	1.736	0.0542	lexan
	257	B	59.8	0.9775	0.0230	0.0225	1913.514	1.726	0.0397	lexan
	257	A	60.3	0.9744	0.0263	0.0256	1661.784	1.810	0.0476	Lexan

S.S. = Stainless steel.

Table A.2. BC Crib Borehole C8388

Shoe depth (ft bgs)	Interval #	Liner	Core Depth (ft)	Gravimetric Soil (gSoil/gTotal)	Gravimetric H20 (gH2O/gSoil)	Gravimetric H20 (gH2O/gTotal)	Core Soil Weight (g)	Bulk Density (g/cm3)	Volumetric Moisture Content	Liner
22.65	3K3	D	20.65	0.9385	0.0656	0.0615	2142.053	1.952	0.1280	lexan
	3K3	C	21.15	0.9096	0.0994	0.0904	2006.969	1.813	0.1803	lexan
	3K3	B	21.65	0.9408	0.0629	0.0592	1999.706	1.819	0.1144	lexan
	3K3	A	22.15	0.9002	0.1109	0.0998	1647.762	1.840	0.2041	lexan
24.5	3K4	D	22.5	0.9405	0.0632	0.0595	2079.084	1.945	0.1229	lexan
	3K4	C	23	0.9454	0.0578	0.0546	2126.613	1.883	0.1088	lexan
	3K4	B	23.5	0.9508	0.0518	0.0492	1956.198	1.849	0.0958	lexan
	3K4	A	24	0.9476	0.0553	0.0524	1973.296	1.792	0.0992	lexan
26.5	3K5	D	24.5	0.9326	0.0723	0.0674	2127.653	1.949	0.1409	lexan
	3K5	C	25	0.9417	0.0619	0.0583	2049.586	1.887	0.1169	lexan
	3K5	B	25.5	0.9229	0.0836	0.0771	1970.841	1.867	0.1560	lexan
	3K5	A	26	0.9253	0.0808	0.0747	1578.073	1.758	0.1420	lexan
29.4	3K6	D	27.4	0.8724	0.1463	0.1276	1873.455	1.734	0.2537	lexan
	3K6	C	27.9	0.8522	0.1734	0.1478	1808.040	1.653	0.2866	lexan
	3K6	B	28.4	0.8900	0.1237	0.1100	1649.540	1.562	0.1932	lexan
	3K6	A	28.9	0.9617	0.0398	0.0383	1696.923	1.786	0.0711	lexan
32.2	3K7	D	30.2	0.9454	0.0577	0.0546	1915.942	1.749	0.1009	lexan
	3K7	C	30.7	0.9446	0.0587	0.0554	1805.548	1.648	0.0967	lexan
	3K7	B	31.2	0.9387	0.0653	0.0613	1679.898	1.541	0.1006	lexan
	3K7	A	31.7	0.9429	0.0605	0.0571	1495.053	1.739	0.1052	lexan
35.08	3K8	D	33.08	0.9532	0.0491	0.0468	1730.562	1.593	0.0782	lexan
	3K8	C	33.58	0.9440	0.0593	0.0560	1717.657	1.549	0.0919	lexan
	3K8	B	34.08	0.9512	0.0513	0.0488	1758.257	1.597	0.0820	lexan
	3K8	A	34.58	0.9392	0.0648	0.0608	1407.363	1.605	0.1040	lexan

Shoe depth (ft bgs)	Interval #	Liner	Core Depth (ft)	Gravimetric Soil (gSoil/gTotal)	Gravimetric H$_2$0 (gH$_2$O/gSoil)	Gravimetric H$_2$0 (gH$_2$O/gTotal)	Core Soil Weight (g)	Bulk Density (g/cm^3)	Volumetric Moisture Content	Liner
38	3K9	D	36	0.9334	0.0714	0.0666	1722.603	1.614	0.1152	lexan
	3K9	C	36.5	0.9383	0.0657	0.0617	1781.458	1.599	0.1050	lexan
	3K9	B	37	0.9310	0.0741	0.0690	1759.204	1.597	0.1183	lexan
	3K9	A	37.5	0.9158	0.0920	0.0842	1435.497	1.662	0.1529	lexan
40.8	3L0	D	38.8	0.8791	0.1375	0.1209	1827.191	1.706	0.2347	lexan
	3L0	C	39.3	0.8591	0.1641	0.1409	1751.187	1.579	0.2591	lexan
	3L0	B	39.8	0.9640	0.0373	0.0360	1807.990	1.642	0.0613	lexan
	3L0	A	40.3	0.9532	0.0491	0.0468	2059.347	1.839	0.0903	lexan
43	3L1	D	41	0.9204	0.0865	0.0796	2123.792	1.906	0.1648	lexan
	3L1	C	41.5	0.9049	0.1051	0.0951	2017.399	1.907	0.2005	lexan
	3L1	B	42	0.8751	0.1428	0.1249	2026.234	1.818	0.2596	lexan
	3L1	A	42.5	0.9244	0.0818	0.0756	1718.685	1.582	0.1295	lexan
45.58	3L2	D	43.58	0.9582	0.0436	0.0418	2034.541	1.809	0.0789	S.S
	3L2	C	44.08	0.8951	0.1172	0.1049	1862.052	1.661	0.1947	S.S
	3L2	B	44.58	0.9720	0.0288	0.0280	2188.209	1.796	0.0518	S.S
	3L2	A	45.08	0.9785	0.0220	0.0215	1514.024	1.772	0.0390	S.S
47.7	3L3	D	45.7	0.9914	0.0087	0.0086	2054.515	1.866	0.0162	S.S.
	3L3	C	46.2	0.9968	0.0032	0.0032	1878.524	1.887	0.0060	lexan
	3L3	B	46.7	0.9957	0.0043	0.0043	1883.157	1.745	0.0076	S.S
	3L3	A	47.2	0.9942	0.0059	0.0058	1407.065	1.706	0.0100	S.S
50	3L4	D	48	0.9947	0.0053	0.0053	1861.472	2.014	0.0107	S.S.
	3L4	C	48.5	0.9954	0.0047	0.0046	2039.802	1.859	0.0087	S.S.
	3L4	B	49	0.9964	0.0036	0.0036	2085.788	1.803	0.0065	S.S.
	3L4	A	49.5	0.9833	0.0170	0.0167	1553.909	1.831	0.0311	S.S.
52.6	3L5	D	50.6	0.9934	0.0066	0.0066	1850.101	1.869	0.0123	S.S.
	3L5	C	51.1	0.9959	0.0041	0.0041	2137.602	1.897	0.0077	S.S.
	3L5	B	51.6	0.9996	0.0004	0.0004	1697.700	1.719	0.0006	S.S.

Table A.2. (contd)

Shoe depth (ft bgs)	Interval #	Liner	Core Depth (ft)	Gravimetric Soil (gSoil/gTotal)	Gravimetric H$_2$0 (gH$_2$O/gSoil)	Gravimetric H$_2$0 (gH$_2$O/gTotal)	Core Soil Weight (g)	Bulk Density (g/cm^3)	Volumetric Moisture Content	Liner
	3L5	A	52.1	0.9996	0.0004	0.0004	1441.798	1.703	0.0006	S.S.
55	3L6	D	53	0.9891	0.0110	0.0109	1556.227	1.702	0.0187	S.S.
	3L6	C	53.5	0.9953	0.0047	0.0047	1891.339	1.743	0.0083	S.S.
	3L6	B	54	0.9986	0.0014	0.0014	1796.795	1.739	0.0024	S.S.
	3L6	A	54.5	0.9989	0.0011	0.0011	1658.533	1.794	0.0019	S.S.
58.1	3L7	D	56.1	0.9778	0.0227	0.0222	2019.425	1.746	0.0397	S.S.
	3L7	C	56.6	0.9706	0.0303	0.0294	1962.817	1.682	0.0510	S.S.
	3L7	B	57.1	0.9774	0.0231	0.0226	1972.768	1.697	0.0392	S.S.
	3L7	A	57.6	0.9785	0.0219	0.0215	1624.707	1.789	0.0392	S.S.
60.5	3L8	D	58.5	0.9709	0.0300	0.0291	2119.794	1.801	0.0540	S.S.
	3L8	C	59	0.9695	0.0315	0.0305	2033.248	1.752	0.0552	S.S.
	3L8	B	59.5	0.9756	0.0251	0.0244	1962.153	1.682	0.0421	S.S.
	3L8	A	60	0.9717	0.0291	0.0283	1508.434	1.698	0.0494	S.S.

S.S. = Stainless steel.

A.1 Introduction

Between September 1, 2011, and September 14, 2011, sediment samples were received from post-desiccation boreholes and a subset of these samples were analyzed as described herein.

A.1.1   Analytical Results/Methodology

The analyses for this project were performed at the 331 Building in the 300 Area of the Hanford Site. Analyses were performed according to Pacific Northwest National Laboratory (PNNL) approved procedures and/or nationally recognized test procedures. The data sets include the sample identification numbers, analytical results, estimated quantification limits (EQL), and quality control data.

A.1.2   Quality Control

The preparatory and analytical quality control requirements, calibration requirements, acceptance criteria, and failure actions are defined in the online quality assurance plan, *Conducting Analytical Work in Support of Regulatory Programs* (PNNL 2010). This QA plan implements the *Hanford Analytical Services Quality Assurance Requirements Documents* (DOE/RL 2007 [HASQARD]) for PNNL.

A.1.3   Definitions

Dup   Duplicate

RPD   Relative Percent Difference

NR   No Recovery (percent recovery less than zero)

ND   Non-Detectable

%REC   Percent Recovery

A.1.4   Sample Receipt

Samples were received with a chain of custody (COC) and analyzed according to the sample identification numbers supplied by the client. All samples were refrigerated upon receipt until prepared for analysis. All samples were received with custody seals intact unless noted in the case narrative.

A.1.5   Holding Times

Holding time is defined as the time from sample preparation to the time of analyses. The prescribed holding times were met for all analytes unless noted in the case narrative.

A.1.6   Analytical Results

All reported analytical results meet the requirements of the CAW or client-specified statement of work unless noted in the case narrative.

A.2 Case Narrative Report

Hold Time

Due to a laboratory scheduling issue, the 48-hr hold times for nitrate analysis after extraction were not met.

Preparation Blank (PB)

No discrepancies noted.

Duplicate (DUP)

No discrepancies noted.

Laboratory Control Samples (LCS)

No discrepancies noted.

Post Spike (PS)

No discrepancies noted.

Matrix Spike (MS)

Not Applicable

Other QC Criteria

No discrepancies noted.

A.3 References

DOE/RL 2007. 2007. *Hanford Analytical Services Quality Assurance Requirements Document.* DOE/RL-96-68, Rev. 3, U.S. Department of Energy, Richland Operations Office, Richland, Washington.

PNNL. 2010. *Conducting Analytical Work in Support of Regulatory Programs.* PNNL-SA-63118, Pacific Northwest National Laboratory, Richland, Washington.

Samples Included in this Report

200-BC-1 Soil Desiccation Pilot Test

HEIS No.	Laboratory ID	Matrix	Date Collected		Date Received	
B2H3K3	1109002-01	Soil	8/30/11	09:40	9/1/11	13:05
B2H3K4	1109002-02	Soil	8/30/11	10:35	9/1/11	13:05
B2H3K5	1109002-03	Soil	8/30/11	13:40	9/1/11	13:05
B2H3K6	1109002-04	Soil	8/31/11	08:35	9/6/11	14:10
B2H3K7	1109002-05	Soil	8/31/11	09:45	9/6/11	14:10
B2H3K8	1109002-06	Soil	8/31/11	11:00	9/6/11	14:10
B2H3K9	1109002-07	Soil	8/31/11	13:30	9/6/11	14:10
B2H3L0	1109002-08	Soil	8/31/11	14:30	9/6/11	14:10
B2H3L1	1109002-09	Soil	9/1/11	09:05	9/7/11	11:06
B2H3L2	1109002-10	Soil	9/1/11	09:55	9/7/11	11:06
B2H3L3	1109002-11	Soil	9/1/11	11:25	9/7/11	11:06
B2H3L4	1109002-12	Soil	9/2/11	09:25	9/9/11	13:20
B2H3L5	1109002-13	Soil	9/2/11	10:15	9/9/11	13:20
B2H3L6	1109002-14	Soil	9/2/11	12:50	9/9/11	13:20
B2H3L7	1109002-15	Soil	9/2/11	13:55	9/9/11	13:20
B2H3L8	1109002-16	Soil	9/2/11	14:35	9/9/11	13:20
B2H242	1109002-17	Soil	9/8/11	09:18	9/14/11	13:30
B2H243	1109002-18	Soil	9/8/11	10:10	9/14/11	13:30
B2H244	1109002-19	Soil	9/8/11	11:10	9/14/11	13:30
B2H245	1109002-20	Soil	9/8/11	13:20	9/14/11	13:30
B2H246	1109002-21	Soil	9/8/11	14:20	9/14/11	13:30
B2H247	1109002-22	Soil	9/9/11	08:05	9/14/11	13:30
B2H248	1109002-23	Soil	9/9/11	09:20	9/14/11	13:30
B2H249	1109002-24	Soil	9/9/11	10:15	9/14/11	13:30
B2H250	1109002-25	Soil	9/9/11	11:17	9/14/11	13:30
B2H251	1109002-26	Soil	9/9/11	13:40	9/14/11	13:30
B2H252	1109002-27	Soil	9/9/11	14:45	9/14/11	13:30
B2H253	1109002-28	Soil	9/12/11	08:35	9/14/11	13:30
B2H254	1109002-29	Soil	9/12/11	09:45	9/14/11	13:30
B2H255	1109002-30	Soil	9/12/11	10:50	9/14/11	13:30
B2H256	1109002-31	Soil	9/12/11	13:15	9/14/11	13:30
B2H257	1109002-32	Soil	9/12/11	14:30	9/14/11	13:30
B2H258	1109002-33	Soil	9/9/11	13:40	9/14/11	13:30

Samples Analyzed in this Report

The following analyses were performed on the following samples included in this report:

Anions by Ion Chromatography
Moisture Content
Tc_U 1:1 DI Water Extract by ICPMS

HEIS No.	Laboratory ID	Matrix	Date Collected		Date Received	
B2H3K3	1109002-01	Soil	8/30/11	09:40	9/1/11	13:05
B2H3K4	1109002-02	Soil	8/30/11	10:35	9/1/11	13:05
B2H3K5	1109002-03	Soil	8/30/11	13:40	9/1/11	13:05
B2H3K6	1109002-04	Soil	8/31/11	08:35	9/6/11	14:10
B2H3K7	1109002-05	Soil	8/31/11	09:45	9/6/11	14:10
B2H3K8	1109002-06	Soil	8/31/11	11:00	9/6/11	14:10
B2H3K9	1109002-07	Soil	8/31/11	13:30	9/6/11	14:10
B2H3L0	1109002-08	Soil	8/31/11	14:30	9/6/11	14:10
B2H3L1	1109002-09	Soil	9/1/11	09:05	9/7/11	11:06
B2H3L2	1109002-10	Soil	9/1/11	09:55	9/7/11	11:06
B2H3L3	1109002-11	Soil	9/1/11	11:25	9/7/11	11:06
B2H3L4	1109002-12	Soil	9/2/11	09:25	9/9/11	13:20
B2H3L5	1109002-13	Soil	9/2/11	10:15	9/9/11	13:20
B2H3L6	1109002-14	Soil	9/2/11	12:50	9/9/11	13:20
B2H3L7	1109002-15	Soil	9/2/11	13:55	9/9/11	13:20
B2H3L8	1109002-16	Soil	9/2/11	14:35	9/9/11	13:20
B2H242	1109002-17	Soil	9/8/11	09:18	9/14/11	13:30
B2H243	1109002-18	Soil	9/8/11	10:10	9/14/11	13:30
B2H244	1109002-19	Soil	9/8/11	11:10	9/14/11	13:30
B2H245	1109002-20	Soil	9/8/11	13:20	9/14/11	13:30
B2H246	1109002-21	Soil	9/8/11	14:20	9/14/11	13:30
B2H247	1109002-22	Soil	9/9/11	08:05	9/14/11	13:30
B2H248	1109002-23	Soil	9/9/11	09:20	9/14/11	13:30
B2H249	1109002-24	Soil	9/9/11	10:15	9/14/11	13:30
B2H250	1109002-25	Soil	9/9/11	11:17	9/14/11	13:30
B2H251	1109002-26	Soil	9/9/11	13:40	9/14/11	13:30
B2H252	1109002-27	Soil	9/9/11	14:45	9/14/11	13:30
B2H253	1109002-28	Soil	9/12/11	08:35	9/14/11	13:30
B2H254	1109002-29	Soil	9/12/11	09:45	9/14/11	13:30
B2H255	1109002-30	Soil	9/12/11	10:50	9/14/11	13:30
B2H256	1109002-31	Soil	9/12/11	13:15	9/14/11	13:30
B2H257	1109002-32	Soil	9/12/11	14:30	9/14/11	13:30
B2H258	1109002-33	Soil	9/9/11	13:40	9/14/11	13:30

Wet Chemistry

Moisture Content (% by Weight) by AGG-WC-001

Lab ID	HEIS No.	Results	EQL	Analyzed	Batch
1109002-01	B2H3K3	9.94E0	N/A	9/15/11	1I12001
1109002-02	B2H3K4	5.78E0	N/A	9/15/11	1I12001
1109002-03	B2H3K5	6.19E0	N/A	9/15/11	1I12001
1109002-04	B2H3K6	1.73E1	N/A	9/15/11	1I12001
1109002-05	B2H3K7	5.87E0	N/A	9/15/11	1I12001
1109002-06	B2H3K8	5.93E0	N/A	9/15/11	1I12001
1109002-07	B2H3K9	6.57E0	N/A	9/15/11	1I12001
1109002-08	B2H3L0	1.64E1	N/A	9/15/11	1I12001
1109002-09	B2H3L1	1.05E1	N/A	9/15/11	1I12001
1109002-10	B2H3L2	1.71E1	N/A	9/15/11	1I12001
1109002-11	B2H3L3	3.19E-1	N/A	9/15/11	1I12001
1109002-12	B2H3L4	4.67E-1	N/A	9/15/11	1I12001
1109002-13	B2H3L5	4.08E-1	N/A	9/15/11	1I12001
1109002-14	B2H3L6	4.75E-1	N/A	9/15/11	1I12001
1109002-15	B2H3L7	3.03E0	N/A	9/15/11	1I12001
1109002-16	B2H3L8	3.15E0	N/A	9/15/11	1I12001
1109002-17	B2H242	5.62E0	N/A	9/19/11	1I15002
1109002-18	B2H243	5.07E0	N/A	9/19/11	1I15002
1109002-19	B2H244	1.29E1	N/A	9/19/11	1I15002
1109002-20	B2H245	4.58E0	N/A	9/19/11	1I15002
1109002-21	B2H246	6.52E0	N/A	9/19/11	1I15002
1109002-22	B2H247	6.86E0	N/A	9/19/11	1I15002
1109002-23	B2H248	8.48E0	N/A	9/19/11	1I15002
1109002-24	B2H249	9.02E0	N/A	9/19/11	1I15002
1109002-25	B2H250	6.25E0	N/A	9/19/11	1I15002
1109002-26	B2H251	4.15E0	N/A	9/19/11	1I15002
1109002-27	B2H252	1.50E0	N/A	9/19/11	1I15002
1109002-28	B2H253	2.78E0	N/A	9/19/11	1I15002
1109002-29	B2H254	3.03E0	N/A	9/19/11	1I15002
1109002-30	B2H255	2.24E0	N/A	9/19/11	1I15002
1109002-31	B2H256	2.57E0	N/A	9/19/11	1I15002
1109002-32	B2H257	3.12E0	N/A	9/19/11	1I15002
1109002-33	B2H258	3.92E0	N/A	9/19/11	1I15002

Anions by Ion Chromatography

CAS #	Analyte	Results	Units	EQL	Analyzed	Batch	Method
HEIS No.	**B2H3K3**	**Lab ID:**	**1109002-01**				
14797-55-8	Nitrate	1.48E1	µg/g dry	5.00E0	9/21/11	1I21001	AGG-IC-001
HEIS No.	**B2H3K4**	**Lab ID:**	**1109002-02**				
14797-55-8	Nitrate	8.27E0	µg/g dry	5.02E0	9/21/11	1I21001	AGG-IC-001
HEIS No.	**B2H3K5**	**Lab ID:**	**1109002-03**				
14797-55-8	Nitrate	8.57E0	µg/g dry	5.00E0	9/21/11	1I21001	AGG-IC-001
HEIS No.	**B2H3K6**	**Lab ID:**	**1109002-04**				
14797-55-8	Nitrate	5.67E1	µg/g dry	5.00E0	9/21/11	1I21001	AGG-IC-001
HEIS No.	**B2H3K7**	**Lab ID:**	**1109002-05**				
14797-55-8	Nitrate	9.68E2	µg/g dry	5.00E1	9/23/11	1I21001	AGG-IC-001
HEIS No.	**B2H3K8**	**Lab ID:**	**1109002-06**				
14797-55-8	Nitrate	7.41E1	µg/g dry	5.00E0	9/21/11	1I21001	AGG-IC-001
HEIS No.	**B2H3K9**	**Lab ID:**	**1109002-07**				
14797-55-8	Nitrate	4.25E2	µg/g dry	5.00E0	9/21/11	1I21001	AGG-IC-001
HEIS No.	**B2H3L0**	**Lab ID:**	**1109002-08**				
14797-55-8	Nitrate	4.52E3	µg/g dry	5.00E1	9/23/11	1I21001	AGG-IC-001
HEIS No.	**B2H3L1**	**Lab ID:**	**1109002-09**				
14797-55-8	Nitrate	1.45E3	µg/g dry	5.00E1	9/23/11	1I21001	AGG-IC-001
HEIS No.	**B2H3L2**	**Lab ID:**	**1109002-10**				
14797-55-8	Nitrate	7.77E3	µg/g dry	5.00E1	9/23/11	1I21001	AGG-IC-001
HEIS No.	**B2H3L3**	**Lab ID:**	**1109002-11**				
14797-55-8	Nitrate	2.04E3	µg/g dry	5.00E1	9/23/11	1I21001	AGG-IC-001
HEIS No.	**B2H3L4**	**Lab ID:**	**1109002-12**				
14797-55-8	Nitrate	3.63E3	µg/g dry	5.00E1	9/23/11	1I21001	AGG-IC-001
HEIS No.	**B2H3L5**	**Lab ID:**	**1109002-13**				
14797-55-8	Nitrate	5.23E3	µg/g dry	5.00E1	9/23/11	1I21001	AGG-IC-001
HEIS No.	**B2H3L6**	**Lab ID:**	**1109002-14**				
14797-55-8	Nitrate	3.52E3	µg/g dry	5.00E1	9/23/11	1I21001	AGG-IC-001
HEIS No.	**B2H3L7**	**Lab ID:**	**1109002-15**				
14797-55-8	Nitrate	3.00E3	µg/g dry	5.00E1	9/23/11	1I21001	AGG-IC-001
HEIS No.	**B2H3L8**	**Lab ID:**	**1109002-16**				
14797-55-8	Nitrate	3.59E3	µg/g dry	5.00E1	9/23/11	1I21001	AGG-IC-001
HEIS No.	**B2H242**	**Lab ID:**	**1109002-17**				
14797-55-8	Nitrate	8.28E0	µg/g dry	5.00E0	9/22/11	1I21002	AGG-IC-001
HEIS No.	**B2H243**	**Lab ID:**	**1109002-18**				
14797-55-8	Nitrate	5.44E0	µg/g dry	5.00E0	9/22/11	1I21002	AGG-IC-001
HEIS No.	**B2H244**	**Lab ID:**	**1109002-19**				
14797-55-8	Nitrate	6.93E1	µg/g dry	5.00E0	9/22/11	1I21002	AGG-IC-001
HEIS No.	**B2H245**	**Lab ID:**	**1109002-20**				
14797-55-8	Nitrate	2.36E1	µg/g dry	5.00E0	9/22/11	1I21002	AGG-IC-001
HEIS No.	**B2H246**	**Lab ID:**	**1109002-21**				
14797-55-8	Nitrate	1.39E2	µg/g dry	5.00E0	9/22/11	1I21002	AGG-IC-001

CAS #	Analyte	Results	Units	EQL	Analyzed	Batch	Method
HEIS No.	**B2H247**	**Lab ID:**	**1109002-22**				
14797-55-8	Nitrate	3.90E1	µg/g dry	5.00E0	9/22/11	1I21002	AGG-IC-001
HEIS No.	**B2H248**	**Lab ID:**	**1109002-23**				
14797-55-8	Nitrate	1.26E3	µg/g dry	5.00E1	9/23/11	1I21002	AGG-IC-001
HEIS No.	**B2H249**	**Lab ID:**	**1109002-24**				
14797-55-8	Nitrate	7.45E3	µg/g dry	5.00E1	9/23/11	1I21002	AGG-IC-001
HEIS No.	**B2H250**	**Lab ID:**	**1109002-25**				
14797-55-8	Nitrate	5.86E3	µg/g dry	5.00E1	9/23/11	1I21002	AGG-IC-001
HEIS No.	**B2H251**	**Lab ID:**	**1109002-26**				
14797-55-8	Nitrate	3.54E3	µg/g dry	5.00E1	9/23/11	1I21002	AGG-IC-001
HEIS No.	**B2H252**	**Lab ID:**	**1109002-27**				
14797-55-8	Nitrate	4.20E3	µg/g dry	5.00E1	9/23/11	1I21002	AGG-IC-001
HEIS No.	**B2H253**	**Lab ID:**	**1109002-28**				
14797-55-8	Nitrate	3.03E3	µg/g dry	5.03E1	9/24/11	1I21002	AGG-IC-001
HEIS No.	**B2H254**	**Lab ID:**	**1109002-29**				
14797-55-8	Nitrate	6.52E3	µg/g dry	5.00E1	9/24/11	1I21002	AGG-IC-001
HEIS No.	**B2H255**	**Lab ID:**	**1109002-30**				
14797-55-8	Nitrate	5.61E3	µg/g dry	5.00E1	9/24/11	1I21002	AGG-IC-001
HEIS No.	**B2H256**	**Lab ID:**	**1109002-31**				
14797-55-8	Nitrate	4.53E3	µg/g dry	5.00E1	9/24/11	1I21002	AGG-IC-001
HEIS No.	**B2H257**	**Lab ID:**	**1109002-32**				
14797-55-8	Nitrate	4.27E3	µg/g dry	5.00E1	9/24/11	1I21002	AGG-IC-001
HEIS No.	**B2H258**	**Lab ID:**	**1109002-33**				
14797-55-8	Nitrate	3.78E3	µg/g dry	5.47E1	9/24/11	1I21002	AGG-IC-001

Radionuclides by ICP-MS/1:1 Water Extract

CAS #	Analyte	Results	Units	EQL	Analyzed	Batch	Method
HEIS No.	**B2H3K3**	**Lab ID:**	**1109002-01**				
14133-76-7	Technetium-99	<3.90E-5	µg/g dry	3.90E-5	9/22/11	1I22001	PNNL-AGG-415
HEIS No.	**B2H3K4**	**Lab ID:**	**1109002-02**				
14133-76-7	Technetium-99	<3.92E-5	µg/g dry	3.92E-5	9/22/11	1I22001	PNNL-AGG-415
HEIS No.	**B2H3K5**	**Lab ID:**	**1109002-03**				
14133-76-7	Technetium-99	<3.90E-5	µg/g dry	3.90E-5	9/22/11	1I22001	PNNL-AGG-415
HEIS No.	**B2H3K6**	**Lab ID:**	**1109002-04**				
14133-76-7	Technetium-99	<3.90E-5	µg/g dry	3.90E-5	9/22/11	1I22001	PNNL-AGG-415
HEIS No.	**B2H3K7**	**Lab ID:**	**1109002-05**				
14133-76-7	Technetium-99	3.87E-4	µg/g dry	3.90E-5	9/22/11	1I22001	PNNL-AGG-415
HEIS No.	**B2H3K8**	**Lab ID:**	**1109002-06**				
14133-76-7	Technetium-99	<3.90E-5	µg/g dry	3.90E-5	9/22/11	1I22001	PNNL-AGG-415
HEIS No.	**B2H3K9**	**Lab ID:**	**1109002-07**				
14133-76-7	Technetium-99	2.74E-4	µg/g dry	3.91E-5	9/22/11	1I22001	PNNL-AGG-415
HEIS No.	**B2H3L0**	**Lab ID:**	**1109002-08**				
14133-76-7	Technetium-99	2.03E-3	µg/g dry	3.90E-5	9/22/11	1I22001	PNNL-AGG-415
HEIS No.	**B2H3L1**	**Lab ID:**	**1109002-09**				
14133-76-7	Technetium-99	5.59E-4	µg/g dry	3.90E-5	9/22/11	1I22001	PNNL-AGG-415
HEIS No.	**B2H3L2**	**Lab ID:**	**1109002-10**				
14133-76-7	Technetium-99	3.76E-3	µg/g dry	3.90E-5	9/22/11	1I22001	PNNL-AGG-415
HEIS No.	**B2H3L3**	**Lab ID:**	**1109002-11**				
14133-76-7	Technetium-99	9.71E-4	µg/g dry	3.90E-5	9/22/11	1I22001	PNNL-AGG-415
HEIS No.	**B2H3L4**	**Lab ID:**	**1109002-12**				
14133-76-7	Technetium-99	1.99E-3	µg/g dry	3.90E-5	9/22/11	1I22001	PNNL-AGG-415
HEIS No.	**B2H3L5**	**Lab ID:**	**1109002-13**				
14133-76-7	Technetium-99	4.12E-3	µg/g dry	3.90E-5	9/22/11	1I22001	PNNL-AGG-415
HEIS No.	**B2H3L6**	**Lab ID:**	**1109002-14**				
14133-76-7	Technetium-99	2.57E-3	µg/g dry	3.90E-5	9/22/11	1I22001	PNNL-AGG-415
HEIS No.	**B2H3L7**	**Lab ID:**	**1109002-15**				
14133-76-7	Technetium-99	1.60E-3	µg/g dry	3.90E-5	9/22/11	1I22001	PNNL-AGG-415
HEIS No.	**B2H3L8**	**Lab ID:**	**1109002-16**				
14133-76-7	Technetium-99	1.93E-3	µg/g dry	3.90E-5	9/22/11	1I22001	PNNL-AGG-415
HEIS No.	**B2H242**	**Lab ID:**	**1109002-17**				
14133-76-7	Technetium-99	<3.90E-5	µg/g dry	3.90E-5	9/22/11	1I22001	PNNL-AGG-415
HEIS No.	**B2H243**	**Lab ID:**	**1109002-18**				
14133-76-7	Technetium-99	<3.90E-5	µg/g dry	3.90E-5	9/22/11	1I22001	PNNL-AGG-415
HEIS No.	**B2H244**	**Lab ID:**	**1109002-19**				
14133-76-7	Technetium-99	<3.90E-5	µg/g dry	3.90E-5	9/22/11	1I22001	PNNL-AGG-415
HEIS No.	**B2H245**	**Lab ID:**	**1109002-20**				
14133-76-7	Technetium-99	<3.90E-5	µg/g dry	3.90E-5	9/22/11	1I22001	PNNL-AGG-415
HEIS No.	**B2H246**	**Lab ID:**	**1109002-21**				
14133-76-7	Technetium-99	9.91E-5	µg/g dry	3.90E-5	9/22/11	1I22002	PNNL-AGG-415

CAS #	Analyte	Results	Units	EQL	Analyzed	Batch	Method
HEIS No.	**B2H247**	**Lab ID:**	**1109002-22**				
14133-76-7	Technetium-99	<3.90E-5	µg/g dry	3.90E-5	9/22/11	1I22002	PNNL-AGG-415
HEIS No.	**B2H248**	**Lab ID:**	**1109002-23**				
14133-76-7	Technetium-99	6.62E-4	µg/g dry	3.90E-5	9/22/11	1I22002	PNNL-AGG-415
HEIS No.	**B2H249**	**Lab ID:**	**1109002-24**				
14133-76-7	Technetium-99	4.10E-3	µg/g dry	3.90E-5	9/22/11	1I22002	PNNL-AGG-415
HEIS No.	**B2H250**	**Lab ID:**	**1109002-25**				
14133-76-7	Technetium-99	4.28E-3	µg/g dry	3.90E-5	9/22/11	1I22002	PNNL-AGG-415
HEIS No.	**B2H251**	**Lab ID:**	**1109002-26**				
14133-76-7	Technetium-99	2.06E-3	µg/g dry	3.90E-5	9/22/11	1I22002	PNNL-AGG-415
HEIS No.	**B2H252**	**Lab ID:**	**1109002-27**				
14133-76-7	Technetium-99	2.64E-3	µg/g dry	3.90E-5	9/22/11	1I22002	PNNL-AGG-415
HEIS No.	**B2H253**	**Lab ID:**	**1109002-28**				
14133-76-7	Technetium-99	9.54E-4	µg/g dry	3.90E-5	9/22/11	1I22002	PNNL-AGG-415
HEIS No.	**B2H254**	**Lab ID:**	**1109002-29**				
14133-76-7	Technetium-99	4.67E-3	µg/g dry	3.90E-5	9/22/11	1I22002	PNNL-AGG-415
HEIS No.	**B2H255**	**Lab ID:**	**1109002-30**				
14133-76-7	Technetium-99	4.18E-3	µg/g dry	3.90E-5	9/22/11	1I22002	PNNL-AGG-415
HEIS No.	**B2H256**	**Lab ID:**	**1109002-31**				
14133-76-7	Technetium-99	2.75E-3	µg/g dry	3.90E-5	9/22/11	1I22002	PNNL-AGG-415
HEIS No.	**B2H257**	**Lab ID:**	**1109002-32**				
14133-76-7	Technetium-99	2.84E-3	µg/g dry	3.90E-5	9/22/11	1I22002	PNNL-AGG-415
HEIS No.	**B2H258**	**Lab ID:**	**1109002-33**				
14133-76-7	Technetium-99	2.19E-3	µg/g dry	4.27E-5	9/22/11	1I22002	PNNL-AGG-415

Wet Chemistry – Quality Control

Environmental Science Laboratory

Analyte	Result	Reporting Limit	Units	Spike Level	Source Result	%REC	%REC Limits	RPD	RPD Limit	Notes
Batch 1I12001 – Moisture Prep										
Duplicate (1I12001-DUP1)			**Source: 1109002-04**		Prepared and Analyzed: 09/15/11					
Moisture Content	1.79E1	N/A	% by weight		1.73E1			3.24	35	
Batch 1I15002 – Moisture Prep										
Duplicate (1I15002-DUP1)			**Source: 1109002-25**		Prepared: 09/15/11		Analyzed: 09/19/11			
Moisture Content	6.26E0	N/A	% by weight		6.25E0			0.112	35	

Anions by Ion Chromatography – Quality Control

Environmental Science Laboratory

Analyte	Result	Reporting Limit	Units	Spike Level	Source Result	%REC	%REC Limits	RPD	RPD Limit	Notes
Batch 1I12001 – 1:1 Water Extract (IC)										
Blank (1I12001-BLK1)					Prepared: 09/21/11		Analyzed: 09/21/11			
Nitrate	<5.00E-1	5.00E-1	µg/g wet							
LCS (1I21001-BS1					Prepared: 09/21/11		Analyzed: 09/21/11			
Nitrate	1.07E1	5.00E-1	µg/g wet	1.00E1		107	80–120			
Duplicate (1I21001-DUP1)			**Source: 1109002-04**		Prepared: 09/21/11		Analyzed: 09/21/11			
Nitrate	5.92E1	5.09E0	µg/g dry		5.67E1			4.27	20	
Post Spike (1I21001-PS1)			**Source: 1109002-01**		Prepared: 09/21/11		Analyzed: 09/21/11			
Nitrate	5.39E0	N/A	µg/mL	3.85E0	1.48E0	101	75–125			
Batch 1I21002 – 1:1 Water Extract (IC)										
Blank (1I21002-BLK1)					Prepared: 09/21/11		Analyzed: 09/22/11			
Nitrate	<5.00E-1	5.00E-1	µg/g wet							
LCS (1I21002-BS1)					Prepared: 09/21/11		Analyzed: 09/23/11			
Nitrate	1.04E1	500E-1	µg/g wet	1.00E1		104	80–120			
Duplicate (1I21002-DUP1)			**Source: 1109002-25**		Prepared: 09/21/11		Analyzed: 09/24/11			
Nitrate	5.86E3	5.00E1	µg/g dry		5.86E3			0.0326	20	
Post Spike (1I21002-PS1)			**Source: 1109002-17**		Prepared: 09/21/11		Analyzed: 09/23/11			
Nitrate	5.07E0	N/A	µg/mL	3.85E0	8.27E-1	110	75–125			

Radionuclides by ICP-MS/1:1 Water Extract – Quality Control

Environmental Science Laboratory

Analyte	Result	Reporting Limit	Units	Spike Level	Source Result	%REC	%REC Limits	RPD	RPD Limit	Notes
Batch 1I22001 – 1:1 Water Extract (ICP/ICPMS)										
Blank (1I22001-BLK1)						Prepared and Analyzed: 09/22/11				
Technetium-99	<3.90E-5	3.90E-5	µg/g wet							
Duplicate (1I22001-DUP1)			**Source: 1109002-04**			Prepared and Analyzed: 09/22/11				
Technetium-99	<3.97E-5	3.97E-5	µg/g dry		ND				35	
Post Spike (1I22001-PS1)			**Source: 1109002-01**			Prepared and Analyzed: 09/22/11				
Technetium-99	1.09E0	N/A	µg/L	1.09E0	1.40E-3	101	75–125			
Batch 1I22002 – 1:1 Water Extract (ICP/ICPMS)										
Blank (1I22002-BLK1)						Prepared and Analyzed: 09/22/11				
Technetium-99	<3.90E-5	3.90E-5	µg/g wet							
Duplicate (1I22002-DUP1)			**Source: 1109002-25**			Prepared and Analyzed: 09/22/11				
Technetium-99	3.35E-5	3.90E-5	µg/g dry		4.28E-3			24.3	35	

Pacific Northwest National Laboratory	**CORE LOG**	Boring/Well No C8387	Depth 20-35'	Date 9-16-11	Sheet
		Location BC Cribs	Project BC Soil Dessication		1 of 3

Logged by _____ Bruce Bjornstad _____ (Print) _____ (Sign)   Drilling Contractor _____

Reviewed by _____ (Print) _____ (Sign) _____ Date _____   Driller _____

Lithologic Class. Scheme _____ Procedure _____ Rev _____   Drill Method _____

DEPTH (ft)	SAMPLES TYPE	SAMPLES ID NUMBER	MOIS-TURE	GRAPHIC LOG C Z S G	LITHOLOGIC DESCRIPTION (particle size distribution, sorting, mineralogy, roundness, color, reaction to HCl, maximum grain size, consolidation, structure, etc.)	COMMENTS
21	s.s.	D B2H242 B A shoe	M		S, fn-crs sand, loose; mod. sorted; 2.5Y5/2 (grayish brn); max part. size = crs sand; wk rxn w/Hcl, 30-40% basalt zS, silty fn sand; compact; well sorted; 2.5Y5/4 (lt. olive brn); max part size = fn sand; mod rxn w/ HCl	4" dia stainless steel liners; 6" long
22						
23	s.s	shoe B2H243 B A shoe	M		S, fn-crs; loose; 2.5Y5/2 (grayish brn); 30-40% basalt; wk rxn w/Hcl zS, silty fn sand; compact; 2.5Y 5/4 (lt.olive brn); mod rxn w/ HCl, well sorted	
24						
25	s.s.	D B2H244 B A shoe	M		zS; silty fn sand with stringers of fn-md sand; laminated; cohesive/compact; 2.5Y 4/4 (olive brn); max part. size = md sand; well sorted	
26						
27						
28	s.s.	D B2H245 B A shoe	SM		zS; silty fn-crs sand; sl. compact; poorly sorted; max. part size = v. crs sand; 2.5Y6/2 (lt.brnish gray); HCl rxn moderate to strong	slough?
29						
30						
31	s.s.	D B2H246 B A shoe	SM		S, fn-md sand; sl. compact; well sorted; 2.5Y5/4 (lt. olive brn); laminated; strng rxn w/ HCl	
32						
33						
34	s.s.	D B2H247 B A	SM		zS; silty fn sand; laminated; compact; well sorted; 2.5Y5/4 (lt olive brn; max part. size = med. sand; strng rxn w/ HCl	

W = Wet, M = Moist, SM = Slightly Moist, D = Dry   s.s: split spoon

Page 15 of 35

2006/DCL/FORMS/CoreLog/001 (006/09)

Pacific Northwest National Laboratory	CORE LOG	Boring/Well No C8387	Depth 35-50'	Date 9-16-11	Sheet
		Location BC Cribs	Project BC Soil Dessication		2 of 3

Logged by Bruce Bjornstad _____ (Print) _____ (Sign) _____ Drilling Contractor _____

Reviewed by _____ (Print) _____ (Sign) _____ Date _____ Driller _____

Lithologic Class. Scheme _____ Procedure _____ Rev _____ Drill Method _____

DEPTH (ft)	SAMPLES TYPE	SAMPLES ID NUMBER	MOIS-TURE	GRAPHIC LOG C Z S G	LITHOLOGIC DESCRIPTION (particle size distribution, sorting, mineralogy, roundness, color, reaction to HCl, maximum grain size, consolidation, structure, etc.)	COMMENTS
36	s.s.	shoe D B2H248 B A	SM		zS; silty fn sand; compact; massive; well sorted; max. part. size = md sand; strng rxn w/ HCl	lexan liner "C"
37						
38 39	s.s.	shoe B2H249 B A	M		zS interbedded with md-crs sand; z fnS; compact; well sorted; 2.5Y5/4 (lt. olive brn); strng rxn w/HCl md-crs sand; 2.5Y5/2 (grayish brn); 30-40% basalt; mod. sorted; no rxn w/ HCl	steel liner
40 41 42	s.s.	shoe D B2H250 B A	SM		zS, silty fn sand at top and bottom separated by md-crs sand z fnS; well sorted; compact; md-crs sand; 2.5Y 5/4 (lt. olive brn); loose; 20-30% basalt; mod. sorted; wk rxn w/ HCl	steel liner
43 44 45	s.s.	shoe D B2H251 B A shoe	D		zS; silty fn-crs sand; compact; poorly sorted; lots of white crushed? grains ∴ redrilled slough?; 2.5Y 7/2 (lt. gray)	steel liner - handled as rad sample in fume hood; slough?
46 47	s.s.	D B2H252 B A	D		S, md-crs sand; loose; mod sorted; 20-30% basalt; max. part. size = v. crs. sand; 2.5Y7/2 (lt. gray)	lexan liner
48 49	s.s.	shoe B2H253 B A shoe	SM		S, fn-md sand, 2.5Y 6/2 (lt. brnishgray), mod. sorted, sl. compact, micaceous zS, silty fn sand; compact; well sorted, 2.5Y 7/4 (pale yellow)	lexan liner

W = Wet, M = Moist, SM = Slightly Moist, D = Dry

A.22

Pacific Northwest National Laboratory	CORE LOG	Boring/Well No _C8387_	Depth _50-61'_	Date _9-16-11_	Sheet
		Location _BC Cribs_	Project _BC Soil Dessication_		_3_ of _3_

Logged by ___Bruce Bjornstad___
Print   Sign

Reviewed by ___
Print   Sign   Date ___

Lithologic Class. Scheme ___   Procedure ___   Rev ___

Drilling Contractor ___
Driller ___
Drill Method ___

DEPTH (ft)	SAMPLES TYPE	SAMPLES ID NUMBER	MOIS-TURE	GRAPHIC LOG C Z S G	LITHOLOGIC DESCRIPTION (particle size distribution, sorting, mineralogy, roundness, color, reaction to HCl, maximum grain size, consolidation, structure, etc.)	COMMENTS
51	s.s.	D B2H254 B A shoe	SM	▨	S, md-crs sand; sl. compact; mod. sorted; 2.5Y6/2 (lt. brnish gray); 15-25% basalt; max. part. size = v. crs sand	lexan liner
52						
53	s.s.	D B2H255 B A shoe	SM	▨	S, md-crs sand; sl. compact; mod sorted; 2.5Y6/2 (lt. brnish gray; 15-25% basalt; max. part. size = v. crs. sand, massive	lexan
54						
55						
56	s.s.	D B2H256 B A shoe	SM	▨	S, md-crs sand; sl. compact; mod. sorted; 2.5Y6/2 (lt. brnish gray; 10-20% basalt; max. part. size = crs sand, mod. rxn w/ HCl, massive	lexan
57						
58						
59	s.s.	D B2H257 B A shoe	M	▨	same as above	lexan
60						
61						

Page 17 of 85

W = Wet, M = Moist, SM = Slightly Moist, D = Dry

2006/DCL/FORMS/CoreLog/001 (006/09)

Pacific Northwest National Laboratory	CORE LOG	Boring/Well No _C8388_		Depth _20-35'_ Date _9-14-11_	Sheet
		Location _BC Cribs_		Project _BC Cribs Soil Desic._	_1_ of _3_

Logged by _Bruce Bjornstad_   Print _____ Sign _____   Drilling Contractor _____

Reviewed by _____ Print _____ Sign _____ Date _____   Driller _____

Lithologic Class. Scheme _____ Procedure _____ Rev _____   Drill Method _____

DEPTH (ft)	SAMPLES		MOIS-TURE	GRAPHIC LOG				LITHOLOGIC DESCRIPTION (particle size distribution, sorting, mineralogy, roundness, color, reaction to HCl, maximum grain size, consolidation, structure, etc.)	COMMENTS
	TYPE	ID NUMBER		C	Z	S	G		*Hanford formation* *All "C" liners*
		D							4" dia. lexan-lined cores; 6" long;
21	S.S.	B2H3K3	SM					S, fn-md sand, massive, mod. sorted, micaceous, 10YR6/2 (lt. brnish gray), max. part. size = crs sand; faint stratification	split spoon
		B						under camera lights; sl. cohesive, mod. rxn w/HCl	C liner 20.1-22.65'
22		A							0.5' overlap
		shoe							
23		D						zfnS, silty fn sand, laminated; 10YR5/3 (brn); compact; well sorted, mod rxn. w/ HCl	
	S.S.	B2H3K4	SM					S, fn sand, well sorted; wk laminated; 10YR6/3 (pale brn); sl. compact,	sharp contact
24		B						mod rxn w/ HCl; max. part. size = fn sand	overlap
		A						zfnS, silty fn sand, 10YR5/2 (grayish brn); compact; wk laminated;	sharp contact
25	S.S.	B2H3K5	SM					mod. sorted, mod rxn to HCl	
		B						S, md-crs sand; sl. compact; grayish brn; mod. sorted, basaltic mod. rxn. to HCl	
26		A							
		shoe							
27									
		D						fnsZ - fnS, fine sandy silt to fn sand; well laminated and interlayered;	
28	S.S.	B2H3K6	SM					compact; 10YR5/2 (grayish brn); max part. size = fine sand;	
		B						strong rxn w/ HCl; mod-well sorted;	
29		A							
		shoe							
30		D						S, fn-md sand at bottom grades up into crs sand; 10YR5/3 (brn); mod.	
	S.S.	B2H3K7	SM					compact; wk laminated; 30-40% basalt in crs sand; mod	
31		B						rxn w/ HCl; max. part. size = crs sand; mod sorted	
		A							
32		shoe							
33		D						S, md sand; homogeneous; 10YR6/3 (pale brn); massive; max part. size =	
	S.S.	B2H3K8	SM					crs. sand; mod sorted; strng rxn w/ HCl; 30-40% basalt	
34		B							
		A							
		shoe							

W = Wet, M = Moist, SM = Slightly Moist, D = Dry   S.S = split spoon   2006/DCL/FORMS/CoreLog/001 (006/09)

Pacific Northwest National Laboratory		**CORE LOG**	Boring/Well No __C8388__	Depth __35-50__	Date __9-14-11__	**Sheet**	
			Location __BC Cribs__	Project __BC Soil Dessication__		__2__ of __3__	

Logged by ___Bruce Bjornstad___ Print ___ Sign ___   Drilling Contractor _____

Reviewed by ___ Print ___ Sign ___ Date ___   Driller _____

Lithologic Class. Scheme _____ Procedure _____ Rev ___   Drill Method _____

DEPTH (ft)	SAMPLES		MOIS-TURE	GRAPHIC LOG C Z S G	LITHOLOGIC DESCRIPTION (particle size distribution, sorting, mineralogy, roundness, color, reaction to HCl, maximum grain size, consolidation, structure, etc.)	COMMENTS
	TYPE	ID NUMBER				
36	s.s.	D B2H3K9 B A shoe	SM		S, fn-md sand; 10YR6/4 (lt. yel. brn); sl. compact; mod. sorted; wk laminated; max part. size = md sand; 20-30% basalt; strng rxn w/ HCl	Hanford formation "C" liner
37						
38						
39	s.s.	D B2H3L0 B A shoe	SM		zfnS, silty fn sand; compact; well sorted; 10YR6/3 (pale brn); wk. laminated; micaceous; strng rxn w/ HCl S, md-v.crs sand; mod. sorted; sl. compact; 10YR5/2 (grayish brn); mod. rxn w/ HCl; 40-50% basalt; salt and pepper sand	sharp contact
	s.s.	B2H3L1 B A shoe	SM		z fn-md S; silty fn-md sand; compact; wk. laminated; mod. sorted; strng rxn w/ HCl S, fn-v.crs. sand; mod. sorted; sl. compact; 30-40% basalt; 20-30% basalt	overlap 0.5 B liner? based on grading and drag folding
42						lexan
43						
44	s.s.	B2H3L2 B A shoe	SM		S, md-crs sand, loose, 2.5Y6/2 (lt. brnish gray); mod. sorted; 30-40% basalt; strng rxn w/ HCl zS, silty fn sand, compact; laminated; 10YR6/3 (pale brn); mod rxn. w/ HCl	beginning of stain-less steel liners	Steel
45						
46	s.s.	B2H3L3 B A shoe	D		zS, silty fn-v.crs sand; loose; v. dry; very poorly sorted; 2.5Y7/2 (lt. gray); 15-25% basalt; angular to subangular sand, mod. rxn to HCl	0.5' overlap Dessig-ated? V. loose - sediment pours out of liner - no layering preserved	lexan
47						
48	s.s.	D B2H3L4 B A shoe	D		Same as above (zS)		Steel
49						

W = Wet, M = Moist, SM = Slightly Moist, D = Dry

2006/DCL/FORMS/CoreLog/001 (006/09)

Pacific Northwest National Laboratory	CORE LOG	Boring/Well No _C8388_		Depth _50-6_	Date _9-14-11_	Sheet
		Location _BC Cribs_		Project _BC Soil Dessication_		_3_ of _3_

Logged by _Bruce Bjornstad_   Drilling Contractor ____

Reviewed by ____   Date ____   Driller ____

Lithologic Class. Scheme ____   Procedure ____ Rev ____   Drill Method ____

DEPTH (ft)	SAMPLES TYPE	SAMPLES ID NUMBER	MOIS-TURE	GRAPHIC LOG C Z S G	LITHOLOGIC DESCRIPTION (particle size distribution, sorting, mineralogy, roundness, color, reaction to HCl, maximum grain size, consolidation, structure, etc.)	COMMENTS
51 52	s.s.	D B2H3L5 B A shoe	D		zS, silty fn-v.crs. sand, v. poorly sorted, v. loose and dry; pours out of liner; 2.5Y8/1 (white); 10-15% basalt; mod rxn w/ HCl; ~20% silt, max part. size = granule	Hanford formation steel liner, dessicated
53 54 5	s.s.	D C B2H3L6 A shoe	D		zS, v. loose and dry – same as previous liner	C + B inverted? (core-catcher marks on D liner) steel
5 56 57 58	s.s.	B2H3L7 B A shoe	SM		S, fn-crs sand; mod sorted, sl. cohesive (due to moisture); 2.5Y6/2 (lt. brnish gray); 15-25% basalt; wk rxn w/ HCl, max. part. size = f.crs. sand, homogeneous	steel liner
59 60 61	s.s.	B2H3L8 B A shoe	SM		S, same as above except lgst particle = granule, mod rxn w/ HCl	steel liner

W = Wet, M = Moist, SM = Slightly Moist, D = Dry   2006/DCL/FORMS/CoreLog/001 (006/09)

C8387   B2H242   20.6-23.1 ft   Core

Borehole ID   Sample Number   Page 21 of 85   Depth   Sample

C8387   B2H243   22.3-24.8 ft   Core

Borehole ID   Sample Number   Depth   Sample

A.26

C8387	B2H244	25.0-27.5 ft	Core
Borehole ID	Sample Number	Depth	Sample

C8387	B2H245	27.5-30.0 ft	Core
Borehole ID	Sample Number	Depth	Sample

C8387   B2H246   30.1-32.6 ft   Core
Borehole ID   Sample Number   Depth   Sample

C8387   B2H247   32.8-35.3 ft   Core
Borehole ID   Sample Number   Depth   Sample

A.28

C8387	B2H248	35.2-37.7 ft	Core
Borehole ID	Sample Number	Depth	Sample

C8387	B2H249	37.5-40.0 ft	Core
Borehole ID	Sample Number	Depth	Sample

| C8387 | B2H250 | 40.0-42.5 ft | Core |
| Borehole ID | Sample Number | Depth | Sample |

| C8387 | B2H251 | 42.7-45.2 ft | Core |
| Borehole ID | Sample Number | Depth | Sample |

| C8387 | B2H252 | 45.3-47.8 ft | Core |
| Borehole ID | Sample Number | Depth | Sample |

| C8387 | B2H253 | 47.6-50.1 ft | Core |
| Borehole ID | Sample Number | Depth | Sample |

A.31

C8387 B2H254 49.75-52.25 ft Core
Borehole ID Sample Number Depth Sample

C8387 B2H255 52.8-55.3 ft Core
Borehole ID Sample Number Depth Sample

A.32

| C8387 | B2H256 | 55.5-58 ft | Core |
| Borehole ID | Sample Number ___ | Depth | Sample |

| C8387 | B2H257 | 58.3-60.8 ft | Core |
| Borehole ID | Sample Number ___ | Depth | Sample |

A.33

C8388   B2H3K3   20-23 ft   Core Sample

Borehole ID   Sample Number   Depth from Chain-of-Custody

C8388   B2H3K4   22-25 ft   Core Sample

Borehole ID   Sample Number   Depth from Chain-of-Custody

A.34

C8388   B2H3K5   24-2~~7~~5ft 26.5ft   Core

Borehole ID   Sample Number   Depth from Chain-of-Custody   Sample

C8388   B2H3K6   27-29.4ft   Core

Borehole ID   Sample Number   Depth from Chain-of-Custody   Sample

A.35

C8388   B2H3K7   30-32 ft
                        29.7   Core

Borehole ID   Sample Number   Depth from Chain-of-Custody   Sample

C8388   B2H3K8   33-35 ft
                        32.58 - 35.08   Core

Borehole ID   Sample Number   Depth from Chain-of-Custody   Sample

A.36

C8388 B2H3K9 36-38 ft Core

35.5 - 38

Borehole ID Sample Number Depth from Chain-of-Custody Sample

C8388 B2H3L0 38-41 ft Core

38.3 — 40.8

Borehole ID Sample Number Depth from Chain-of-Custody Sample

A.37

| C8388 | B2H3L1 | 40.5-43.0 ft | Core |
| Borehole ID | Sample Number | Depth from Chain-of-Custody | Sample |

| C8388 | B2H3L2 | 43.08-45.58 ft | Core |
| Borehole ID | Sample Number | Depth from Chain-of-Custody | Sample |

A.38

C8388   B2H3L3   45.2-47.7 ft   Core

Borehole ID   Sample Number   Depth from Chain-of-Custody   Sample

C8388   B2H3L4   47.5-50.0 ft   Core

Borehole ID   Sample Number   Depth from Chain-of-Custody   Sample

C8388	B2H3L5	50.1-52.6 ft	Core
Borehole ID	Sample Number	Depth from Chain-of-Custody	Sample

C8388	B2H3L6	52.5-55.0 ft	Core
Borehole ID	Sample Number	Depth from Chain-of-Custody	Sample

C8388   B2H3L7   55.6-58.1 ft   Core

Borehole ID   Sample Number   Depth from Chain-of-Custody   Sample

C8388   B2H3L8   58.0-60.5 ft   Core

Borehole ID   Sample Number   Depth from Chain-of-Custody   Sample

COLLECTOR	COMPANY CONTACT	TELEPHONE NO.	PROJECT COORDINATOR	PRICE CODE	8H	DATA TURNAROUND
Tvrner, Oaks, Anderson	LUKE, SN	372-1667	LUKE, SN			
SAMPLING LOCATION	**PROJECT DESIGNATION**		**SAF NO.**	**AIR QUALITY**	L	30 Days / 30 Days
Sample 1	200-BC-1 Soil Desiccation Pilot Test - Soil		F11-155			
ICE CHEST NO.	**FIELD LOGBOOK NO.**	**ACTUAL SAMPLE DEPTH**	**COA**	**METHOD OF SHIPMENT**		**ORIGINAL**
_N/A_	_HNF-N-585-1 pg 46_	_20.15-22.65 ft_	301405ES10	GOVERNMENT VEHICLE		
SHIPPED TO	**OFFSITE PROPERTY NO.**		**BILL OF LADING/AIR BILL NO.**			
Environmental Sciences Laboratory	N/A		N/A			

MATRIX*	POSSIBLE SAMPLE HAZARDS/ REMARKS	
A = Air DL = Drum Liquids DS = Drum Solids L = Liquid O = Oil S = Soil SE = Sediment T = Tissue V = Vegetation W = Water WI = Wipe X = Other	Contains Radioactive Material at concentrations that may or may not be regulated for transportation per 49 CFR / IATA Dangerous Goods Regulations but are not releasable per DOE Order 5400.5 (1990/1993)	
	PRESERVATION	Cool ~4C
	HOLDING TIME	28 Days/48 Hours
	TYPE OF CONTAINER	Liner
	NO. OF CONTAINER(S)	4
	VOLUME	1000g
SPECIAL HANDLING AND/OR STORAGE RADIOACTIVE TIE TO: B2H3H5	**SAMPLE ANALYSIS**	SEE ITEM (1) IN SPECIAL INSTRUCTIONS

SAMPLE NO.	MATRIX*	SAMPLE DATE	SAMPLE TIME	
B2H3K3	SOIL	_8-30-11_	_0940_	_X_

A.42

CHAIN OF POSSESSION		SIGN/ PRINT NAMES	
RELINQUISHED BY/REMOVED FROM	DATE/TIME	RECEIVED BY/STORED IN	DATE/TIME
A. Turner	_8-30-11_ _1435_	_MO 413 SSU_ _R)_	_8-30-11_ _1435_
MO-413 SSU-R1	_9/1/11_ _1220_	_J. Garcia_ _+CO_	_9/1/11_ _1220_
J. Garcia _+G_	_9/1/11_ _1305_	_Amanda Lawter_ _and_	_9/1/11_ _1305_
RELINQUISHED BY/REMOVED FROM	DATE/TIME	RECEIVED BY/STORED IN	DATE/TIME
RELINQUISHED BY/REMOVED FROM	DATE/TIME	RECEIVED BY/STORED IN	DATE/TIME
RELINQUISHED BY/REMOVED FROM	DATE/TIME	RECEIVED BY/STORED IN	DATE/TIME

LABORATORY SECTION	RECEIVED BY	
FINAL SAMPLE DISPOSITION	DISPOSAL METHOD	

SPECIAL INSTRUCTIONS

** The CACN for all analytical work at ESL laboratory is 301405ES20 (under Contract 00036402 Release 00045).

** ESL will perform all analyses as outlined on the Field Sampling Requirements from the material of the liner selected from the four liners of each sleeve that they will be receiving.

** The 200 Area S&GRP Characterization and Monitoring Sampling and Analysis GKI applies to this SAF.
(1) IC Anions - 9056 {Nitrate}; Moisture Content - D2216 {Percent moisture (wet sample)}; Tc-99 by ICPMS {Technetium-99};

SRM #13564

TITLE	DATE/TIME
DISPOSED BY	DATE/TIME

PRINTED ON 8/24/2011

SDG# _ESL 090025_

A-6003-618 (REV 2)

CH2MHill Plateau Remediation Company			CHAIN OF CUSTODY/SAMPLE ANALYSIS REQUEST			F11-155-064		PAGE 1 OF 1

COLLECTOR
Tuner, Bates, Anderson

COMPANY CONTACT
LUKE, SN

TELEPHONE NO.
372-1667

PROJECT COORDINATOR
LUKE, SN

PRICE CODE 8H

DATA TURNAROUND
30 Days / 30 Days

SAMPLING LOCATION
Sample 2

PROJECT DESIGNATION
200-BC-1 Soil Desiccation Pilot Test - Soil

SAF NO.
F11-155

AIR QUALITY 7

ICE CHEST NO.
N/A

FIELD LOGBOOK NO.
HNF-N-585-1 pg 46

ACTUAL SAMPLE DEPTH
22 - 24.5 ft

COA
301405ES10

METHOD OF SHIPMENT
GOVERNMENT VEHICLE

ORIGINAL

SHIPPED TO
Environmental Sciences Laboratory

OFFSITE PROPERTY NO.
N/A

BILL OF LADING/AIR BILL NO.
N/A

MATRIX*
A - Air
DI = Drum Liquids
DS = Drum Solids
L - Liquid
O = Oil
S - Soil
SE = Sediment
T = Tissue
V - Vegetation
W = Water
WI = Wipe
X - Other

POSSIBLE SAMPLE HAZARDS/ REMARKS
Contains Radioactive Material at concentrations that may or may not be regulated for transportation per 49 CFR / IATA Dangerous Goods Regulations but are not releasable per DOE Order 5400.5 (1990/1993)

PRESERVATION Cool~4C

HOLDING TIME 28 Days/48 Hours

TYPE OF CONTAINER Liner

NO. OF CONTAINER(S) 4

VOLUME 1000g

SAMPLE ANALYSIS SEE ITEM (1) IN SPECIAL INSTRUCTIONS

SPECIAL HANDLING AND/OR STORAGE
RADIOACTIVE TIE TO: B2H3H6

SAMPLE NO.	MATRIX*	SAMPLE DATE	SAMPLE TIME	
B2H3K4	SOIL	8-30-11	1035	A

CHAIN OF POSSESSION

RELINQUISHED BY/REMOVED FROM	DATE/TIME	RECEIVED BY/STORED IN	DATE/TIME
A. Tuner MZ 8-30-11	1435	M0413 SSU R) 8-30-11	1435
MO-413 SSU- R1 9/1/11	1220	J. Garcia +G 9/1/11	1220
J. Garcia +G 9/1/11	1305	Amanda Lawler am 9/1/11	1305
RELINQUISHED BY/REMOVED FROM	DATE/TIME	RECEIVED BY/STORED IN	DATE/TIME
RELINQUISHED BY/REMOVED FROM	DATE/TIME	RECEIVED BY/STORED IN	DATE/TIME
RELINQUISHED BY/REMOVED FROM	DATE/TIME	RECEIVED BY/STORED IN	DATE/TIME

SPECIAL INSTRUCTIONS

** The CACN for all analytical work at ESL laboratory is 301405ES20 (under Contract 00036402 Release 00045).

** ESL will perform all analyses as outlined on the Field Sampling Requirements from the material of the liner selected from the four liners of each sleeve that they will be receiving.

** The 200 Area S&GRP Characterization and Monitoring Sampling and Analysis GKI applies to this SAF.
(1) IC Anions - 9056 {Nitrate}; Moisture Content - D2216 {Percent moisture (wet sample)}; Tc-99 by ICPMS {Technetium-99};

BRM # 13564

LABORATORY SECTION	RECEIVED BY		TITLE	DATE/TIME
FINAL SAMPLE DISPOSITION	DISPOSAL METHOD		DISPOSED BY	DATE/TIME

PRINTED ON 8/24/2011

A-6003-618 (REV Z)

CH2MHill Plateau Remediation Company | CHAIN OF CUSTODY/SAMPLE ANALYSIS REQUEST | F11-155-065 | PAGE 1 OF 1

COLLECTOR				
Turner, Bates, Anderson				

COMPANY CONTACT	TELEPHONE NO.	PROJECT COORDINATOR	PRICE CODE 8H	DATA TURNAROUND
LUKE, SN	372-1667	LUKE, SN		30 Days / 30 Days

SAMPLING LOCATION
Sample 3

PROJECT DESIGNATION
200-BC-1 Soil Desiccation Pilot Test - Soil

SAF NO. F11-155 | **AIR QUALITY**

ICE CHEST NO.
N/A

FIELD LOGBOOK NO.
HNF-N-585-105 46 | **ACTUAL SAMPLE DEPTH** 24-26.5Pt

COA 301405ES10 | **METHOD OF SHIPMENT** GOVERNMENT VEHICLE | **ORIGINAL**

SHIPPED TO
Environmental Sciences Laboratory

OFFSITE PROPERTY NO.
N/A

BILL OF LADING/AIR BILL NO.
N/A

MATRIX*	POSSIBLE SAMPLE HAZARDS/ REMARKS	PRESERVATION	Cool~4C
A=Air	Contains Radioactive Material at concentrations		
DL=Drum	that may or may not be regulated for	HOLDING TIME	28 Days/48 Hours
Lquids	transportation per 49 CFR / IATA Dangerous		
DS=Drum	Goods Regulations but are not releasable per		
Solids	DOE Order 5400.5 (1990/1993)	TYPE OF CONTAINER	Liner
L=Liquid			
O=Oil			
S=Soil		NO. OF CONTAINER(S)	4
SE=Sediment			
T=Tissue			
V=Vegetation		VOLUME	1000g
W=Water			
WI=Wipe			
X=Other	SPECIAL HANDLING AND/OR STORAGE RADIOACTIVE TIE TO: B2H3H7	SAMPLE ANALYSIS	SEE ITEM (1) IN SPECIAL INSTRUCTIONS

SAMPLE NO.	MATRIX*	SAMPLE DATE	SAMPLE TIME	
B2H3K5	SOIL	8-30-11	1340	X

CHAIN OF POSSESSION

RELINQUISHED BY/REMOVED FROM	DATE/TIME	RECEIVED BY/STORED IN	DATE/TIME
A. Turner M	8-30-11 1435	MO 413 SS4 R1	8-3-11 1435
MO-413 SSU-R1	9/1/11 1220	J. Garcia +Co	9/1/11 1220
J. Garcia +Co	9/1/11 1305	Amanda Lawter	9/1/11 1305
RELINQUISHED BY/REMOVED FROM	DATE/TIME	RECEIVED BY/STORED IN	DATE/TIME
RELINQUISHED BY/REMOVED FROM	DATE/TIME	RECEIVED BY/STORED IN	DATE/TIME
RELINQUISHED BY/REMOVED FROM	DATE/TIME	RECEIVED BY/STORED IN	DATE/TIME

LABORATORY SECTION	RECEIVED BY		
FINAL SAMPLE DISPOSITION	DISPOSAL METHOD		

SPECIAL INSTRUCTIONS
** The CACN for all analytical work at ESL laboratory is 301405ES20 (under Contract 00036402 Release 00045).

** ESL will perform all analyses as outlined on the Field Sampling Requirements from the material of the liner selected from the four liners of each sleeve that they will be receiving.

** The 200 Area S&GRP Characterization and Monitoring Sampling and Analysis GK1 applies to this SAF.
(1) IC Anions - 9056 {Nitrate}; Moisture Content - D2216 {Percent moisture (wet sample)}; Tc-99 by ICPMS {Technetium-99};

BRM # 13564

TITLE	DATE/TIME
DISPOSED BY	DATE/TIME

PRINTED ON 8/24/2011

A-6003-618 (REV 2)

CH2MHill Plateau Remediation Company

CHAIN OF CUSTODY/SAMPLE ANALYSIS REQUEST

F11-155-066 | PAGE 1 OF 1

COLLECTOR	COMPANY CONTACT	TELEPHONE NO.	PROJECT COORDINATOR	PRICE CODE	8H	DATA TURNAROUND
Turner, chacon, Anderson	LUKE, SN	372-1667	LUKE, SN			
SAMPLING LOCATION	PROJECT DESIGNATION		SAF NO.	AIR QUALITY	_	30 Days / 30 Days
Sample 4	200-BC-1 Soil Desiccation Pilot Test - Soil		F11-155			
ICE CHEST NO.	FIELD LOGBOOK NO.	ACTUAL SAMPLE DEPTH	COA	METHOD OF SHIPMENT		ORIGINAL
N/A	HNF-N-585-1 Pg 47 26.9-29.9ft		301405ES10	GOVERNMENT VEHICLE		
SHIPPED TO	OFFSITE PROPERTY NO.		BILL OF LADING/AIR BILL NO.			
Environmental Sciences Laboratory	N/A		N/A			

MATRIX*
A =Air
Dl.=Drum Liquids
DS=Drum Solids
L=Liquid
O=Oil
S=Soil
SE=Sediment
T=Tissue
V=Vegetation
W=Water
WI=Wipe
X=Other

POSSIBLE SAMPLE HAZARDS/ REMARKS		
Contains Radioactive Material at concentrations that may or may not be regulated for transportation per 49 CFR / IATA Dangerous Goods Regulations but are not releasable per DOE Order 5400.5 (1990/1993)	PRESERVATION	Cool~4C
	HOLDING TIME	28 Days/48 Hours
	TYPE OF CONTAINER	Liner
	NO. OF CONTAINER(S)	4
SPECIAL HANDLING AND/OR STORAGE RADIOACTIVE TIE TO: B2H3H8	VOLUME	1000g
	SAMPLE ANALYSIS	SEE ITEM (1) IN SPECIAL INSTRUCTIONS

SAMPLE NO.	MATRIX*	SAMPLE DATE	SAMPLE TIME	
B2H3K6	SOIL	8-31-11	0835	X

CHAIN OF POSSESSION				
RELINQUISHED BY/REMOVED FROM	DATE/TIME	RECEIVED BY/STORED IN	DATE/TIME	
A. Turner	8-31-11 1520	MP4/35SG R1	8-31-11 1520	
RELINQUISHED BY/REMOVED FROM	DATE/TIME	RECEIVED BY/STORED IN	DATE/TIME	
7 0413 SSU-R1	SEP 06 2011 1300	M. A. White Ma White	SEP 06 2011 1300	
RELINQUISHED BY/REMOVED FROM	DATE/TIME	RECEIVED BY/STORED IN	DATE/TIME	
M. A. White Ma White	SEP 06 2011 1410	L. Kustnyako L. Kustnyako	SEP 06 2011 1410	
RELINQUISHED BY/REMOVED FROM	DATE/TIME	RECEIVED BY/STORED IN	DATE/TIME	
RELINQUISHED BY/REMOVED FROM	DATE/TIME	RECEIVED BY/STORED IN	DATE/TIME	
RELINQUISHED BY/REMOVED FROM	DATE/TIME	RECEIVED BY/STORED IN	DATE/TIME	

LABORATORY SECTION	RECEIVED BY
FINAL SAMPLE DISPOSITION	DISPOSAL METHOD

PRINTED ON 8/24/2011

SPECIAL INSTRUCTIONS

** The CACN for all analytical work at ESL laboratory is 301405ES20 (under Contract 00036402 Release 00045).

** ESL will perform all analyses as outlined on the Field Sampling Requirements from the material of the liner selected from the four liners of each sleeve that they will be receiving.

** The 200 Area S&GRP Characterization and Monitoring Sampling and Analysis GKI applies to this SAF.
(1) IC Anions - 9056 {Nitrate}; Moisture Content - D2216 {Percent moisture (wet sample)}; Tc-99 by ICPMS {Technetium-99};

BRM# 13569

TITLE	DATE/TIME
DISPOSED BY	DATE/TIME

Page 56 of 85

SDG# ESL090026

A-6003-618 (REV 2)

COLLECTOR	COMPANY CONTACT	TELEPHONE NO.	PROJECT COORDINATOR	PRICE CODE 8H	DATA TURNAROUND
Turner, Chacon, Anderson	LUKE, SN	372-1667	LUKE, SN		30 Days / 30 Days

SAMPLING LOCATION	PROJECT DESIGNATION		SAF NO.	AIR QUALITY ☐	
Sample 5	200-BC-1 Soil Desiccation Pilot Test - Soil		F11-155		

ICE CHEST NO.	FIELD LOGBOOK NO.	ACTUAL SAMPLE DEPTH	COA	METHOD OF SHIPMENT	ORIGINAL
N/C	HNF-N-535-1 Pg 47	29.7 - 32.2 Ft	301405ES10	GOVERNMENT VEHICLE	

SHIPPED TO	OFFSITE PROPERTY NO.	BILL OF LADING/AIR BILL NO.
Environmental Sciences Laboratory	N/A	N/A

MATRIX*
A=Air
DL=Drum Liquids
DS=Drum Solids
L=Liquid
O=Oil
S=Soil
SE=Sediment
T=Tissue
V=Vegetation
W=Water
WI=Wipe
X=Other

POSSIBLE SAMPLE HAZARDS/ REMARKS
Contains Radioactive Material at concentrations that may or may not be regulated for transportation per 49 CFR / IATA Dangerous Goods Regulations but are not releasable per DOE Order 5400.5 (1990/1993)

SPECIAL HANDLING AND/OR STORAGE
RADIOACTIVE TIE TO: B2H3H9

PRESERVATION	Cool~4C
HOLDING TIME	28 Days/48 Hours
TYPE OF CONTAINER	Liner
NO. OF CONTAINER(S)	4
VOLUME	1000g
SAMPLE ANALYSIS	SEE ITEM (1) IN SPECIAL INSTRUCTIONS

SAMPLE NO.	MATRIX*	SAMPLE DATE	SAMPLE TIME	
B2H3K7	SOIL	8-31-11	0945	X

CHAIN OF POSSESSION

RELINQUISHED BY/REMOVED FROM	DATE/TIME	RECEIVED BY/STORED IN	DATE/TIME
A. Turner 8-31-11	1520	M0413 SSU R1 8-31-11	1520
Mo 413 SSU-R1	SEP 06 2011 1300	M. A. White	SEP 06 2011 1300
M. A. White	SEP 06 2011 1410	L. Kudujka	SEP 06 2011 1410
RELINQUISHED BY/REMOVED FROM	DATE/TIME	RECEIVED BY/STORED IN	DATE/TIME
RELINQUISHED BY/REMOVED FROM	DATE/TIME	RECEIVED BY/STORED IN	DATE/TIME
RELINQUISHED BY/REMOVED FROM	DATE/TIME	RECEIVED BY/STORED IN	DATE/TIME

SPECIAL INSTRUCTIONS

** The CACN for all analytical work at ESL laboratory is 301405ES20 (under Contract 00036402 Release 00045).

** ESL will perform all analyses as outlined on the Field Sampling Requirements from the material of the liner selected from the four liners of each sleeve that they will be receiving.

** The 200 Area S&GRP Characterization and Monitoring Sampling and Analysis GKI applies to this SAF.
(1) IC Anions - 9056 {Nitrate}; Moisture Content - D2216 {Percent moisture (wet sample)}; Tc-99 by ICPMS {Technetium-99};

BRM # 13564

LABORATORY SECTION	RECEIVED BY	TITLE	DATE/TIME
FINAL SAMPLE DISPOSITION	DISPOSAL METHOD	DISPOSED BY	DATE/TIME

PRINTED ON 8/24/2011

A 6003-618 (REV 2)

CH2MHill Plateau Remediation Company | CHAIN OF CUSTODY/SAMPLE ANALYSIS REQUEST | F11-155-068 | PAGE 1 OF 1

COLLECTOR	COMPANY CONTACT	TELEPHONE NO.	PROJECT COORDINATOR	PRICE CODE	8H	DATA TURNAROUND
Turner, Charon, Anderson	LUKE, SN	372-1667	LUKE, SN			30 Days / 30 Days

SAMPLING LOCATION
Sample 6

	PROJECT DESIGNATION		SAF NO.	AIR QUALITY	⌐
	200-BC-1 Soil Desiccation Pilot Test - Soil		F11-155		

ICE CHEST NO.

N/a

	FIELD LOGBOOK NO.	ACTUAL SAMPLE DEPTH	COA	METHOD OF SHIPMENT	ORIGINAL
	HNF-N-585-1 pg 47	32.58-35.08 Ft	301405ES10	GOVERNMENT VEHICLE	

SHIPPED TO

Environmental Sciences Laboratory

	OFFSITE PROPERTY NO.		BILL OF LADING/AIR BILL NO.
	N/A		N/A

MATRIX*
A= Air
DL=Drum Liquids
DS=Drum Solids
L =Liquid
O=Oil
S=Soil
SE=Sediment
T =Tissue
V=Vegetation
W=Water
WI=Wipe
X -Other

POSSIBLE SAMPLE HAZARDS/ REMARKS
Contains Radioactive Material at concentrations that may or may not be regulated for transportation per 49 CFR / IATA Dangerous Goods Regulations but are not releasable per DOE Order 5400.5 (1990/1993)

SPECIAL HANDLING AND/OR STORAGE
RADIOACTIVE TIE TO: B2H3J0

PRESERVATION	Cool~4C
HOLDING TIME	28 Days/48 Hours
TYPE OF CONTAINER	Liner
NO. OF CONTAINER(S)	4
VOLUME	1000g
SAMPLE ANALYSIS	SEE ITEM (1) IN SPECIAL INSTRUCTIONS

SAMPLE NO.	MATRIX*	SAMPLE DATE	SAMPLE TIME	
B2H3K8	SOIL	8-31-11	1100	

CHAIN OF POSSESSION

RELINQUISHED BY/REMOVED FROM	DATE/TIME	RECEIVED BY/STORED IN	DATE/TIME
A. Turner AZ	8-31-11 1520	MO413 SS4 R1	8-31-11 1520
MO413 SSU-R1	SEP 06 2011 1300	M.A. White	SEP 06 2011 1300
M.A. White	SEP 06 2011 1410	I. Kudnyakov	SEP 06 2011 1410
RELINQUISHED BY/REMOVED FROM	DATE/TIME	RECEIVED BY/STORED IN	DATE/TIME
RELINQUISHED BY/REMOVED FROM	DATE/TIME	RECEIVED BY/STORED IN	DATE/TIME
RELINQUISHED BY/REMOVED FROM	DATE/TIME	RECEIVED BY/STORED IN	DATE/TIME

LABORATORY SECTION	RECEIVED BY
FINAL SAMPLE DISPOSITION	DISPOSAL METHOD

SPECIAL INSTRUCTIONS
** The CACN for all analytical work at ESL laboratory is 301405ES20 (under Contract 00036402 Release 00045).

** ESL will perform all analyses as outlined on the Field Sampling Requirements from the material of the liner selected from the four liners of each sleeve that they will be receiving.

** The 200 Area S&GRP Characterization and Monitoring Sampling and Analysis GKI applies to this SAF.
(1) IC Anions - 9056 {Nitrate}; Moisture Content - D2216 {Percent moisture (wet sample)}; Tc-99 by ICPMS {Technetium-99};

BRM # 13564

TITLE	DATE/TIME
DISPOSED BY	DATE/TIME

PRINTED ON 8/24/2011

A-6003-618 (REV 2)

CH2MHill Plateau Remediation Company

COLLECTOR

Turner, Crow, Anderson

SAMPLING LOCATION

Sample 7

ICE CHEST NO.

N/A

SHIPPED TO

Environmental Sciences Laboratory

MATRIX*
A=Air
DL=Drum
Liquids
DS=Drum
Solids
L=Liquid
O=Oil
S=Soil
SE=Sediment
T=Tissue
V=Vegetation
W=Water
WI=Wipe
X=Other

POSSIBLE SAMPLE HAZARDS/ REMARKS
Contains Radioactive Material at concentrations that may or may not be regulated for transportation per 49 CFR / IATA Dangerous Goods Regulations but are not releasable per DOE Order 5400.5 (1990/1993)

SPECIAL HANDLING AND/OR STORAGE
RADIOACTIVE TIE TO: B2H3J1

CHAIN OF CUSTODY/SAMPLE ANALYSIS REQUEST

COMPANY CONTACT	TELEPHONE NO.
LUKE, SN	372-1667

PROJECT DESIGNATION
200-BC-1 Soil Desiccation Pilot Test - Soil

FIELD LOGBOOK NO.	ACTUAL SAMPLE DEPTH
HNF-N-SBS-1 PG 47	*35.5-38 FT*

OFFSITE PROPERTY NO.
N/A

PRESERVATION	Cool~4C
HOLDING TIME	28 Days/48 Hours
TYPE OF CONTAINER	Liner
NO. OF CONTAINER(S)	4
VOLUME	1000g
SAMPLE ANALYSIS	SEE ITEM (1) IN SPECIAL INSTRUCTIONS

PROJECT COORDINATOR	
LUKE, SN	
SAF NO.	
F11-155	
COA	
301405ES10	
BILL OF LADING/AIR BILL NO.	
N/A	

F11-155-069	PAGE 1 OF 1
PRICE CODE	8H	DATA TURNAROUND
AIR QUALITY	....	30 Days / 30 Days
METHOD OF SHIPMENT	
GOVERNMENT VEHICLE	**ORIGINAL**

SAMPLE NO.	MATRIX*	SAMPLE DATE	SAMPLE TIME	
B2H3K9	SOIL	*8-31-11*	*1330*	*X*

CHAIN OF POSSESSION

RELINQUISHED BY/REMOVED FROM	DATE/TIME	RECEIVED BY/STORED IN	DATE/TIME
A. Turner	*8-31-11* *1520*	*M0413 SS4 K1*	*8-31-11* *1520*
SSU-R1	SEP 06 2011 *1318*	M. A. White	SEP 06 2011 *1300*
M.A. White	SEP 06 2011 *1410*	*L Kudray Kov*	SEP 06 2011 *1410*
RELINQUISHED BY/REMOVED FROM	DATE/TIME	RECEIVED BY/STORED IN	DATE/TIME
RELINQUISHED BY/REMOVED FROM	DATE/TIME	RECEIVED BY/STORED IN	DATE/TIME
RELINQUISHED BY/REMOVED FROM	DATE/TIME	RECEIVED BY/STORED IN	DATE/TIME

LABORATORY SECTION	RECEIVED BY
FINAL SAMPLE DISPOSITION	DISPOSAL METHOD

PRINTED ON 8/24/2011

SPECIAL INSTRUCTIONS

** The CACN for all analytical work at ESL laboratory is 301405ES20 (under Contract 00036402 Release 00045).

** ESL will perform all analyses as outlined on the Field Sampling Requirements from the material of the liner selected from the four liners of each sleeve that they will be receiving.

** The 200 Area S&GRP Characterization and Monitoring Sampling and Analysis GKI applies to this SAF.
(1) IC Anions - 9056 {Nitrate}; Moisture Content - D2216 {Percent moisture (wet sample)}; Tc-99 by ICPMS {Technetium-99};

BRM # 13564

TITLE	DATE/TIME
DISPOSED BY	DATE/TIME

A-6003-618 (REV 2)

CH2MHill Plateau Remediation Company | CHAIN OF CUSTODY/SAMPLE ANALYSIS REQUEST | F11-155-070 | PAGE 1 OF 1

COLLECTOR	COMPANY CONTACT	TELEPHONE NO.	PROJECT COORDINATOR	PRICE CODE	8H	DATA TURNAROUND
Turner,Crow, Anderson	LUKE, SN	372-1667	LUKE, SN			
SAMPLING LOCATION	PROJECT DESIGNATION		SAF NO.	AIR QUALITY	[ ]	30 Days / 30 Days
Sample 8	200-BC-1 Soil Desiccation Pilot Test - Soil		F11-155			
ICE CHEST NO.	FIELD LOGBOOK NO.	ACTUAL SAMPLE DEPTH	COA	METHOD OF SHIPMENT		ORIGINAL
N/A	HNF-N-585-1 *1647*	38.3-40.8 ft	301405ES10	GOVERNMENT VEHICLE		
SHIPPED TO	OFFSITE PROPERTY NO.		BILL OF LADING/AIR BILL NO.			
Environmental Sciences Laboratory	N/A		N/A			

MATRIX*	POSSIBLE SAMPLE HAZARDS/ REMARKS		
A=Air DL=Drum Liquids DS=Drum Solids L=Liquid O=Oil S=Soil SE=Sediment T=Tissue V=Vegetation W=Water WI=Wipe X=Other	Contains Radioactive Material at concentrations that may or may not be regulated for transportation per 49 CFR / IATA Dangerous Goods Regulations but are not releasable per DOE Order 5400.5 (1990/1993)	PRESERVATION	Cool~4C
		HOLDING TIME	28 Days/48 Hours
		TYPE OF CONTAINER	Liner
		NO. OF CONTAINER(S)	4
		VOLUME	1000g
	SPECIAL HANDLING AND/OR STORAGE RADIOACTIVE TIE TO: B2H3J2	SAMPLE ANALYSIS	SEE ITEM (1) IN SPECIAL INSTRUCTIONS

SAMPLE NO.	MATRIX*	SAMPLE DATE	SAMPLE TIME	
B2H3L0	SOIL	8-31-11	1430	▓

CHAIN OF POSSESSION		SIGN/ PRINT NAMES		SPECIAL INSTRUCTIONS
RELINQUISHED BY/REMOVED FROM	DATE/TIME	RECEIVED BY/STORED IN	DATE/TIME	** The CACN for all analytical work at ESL laboratory is 301405ES20 (under Contract 00036402 Release 00045).
A.Turner *A C* 8-31-11	1520	*M0413 SSM R1* 8-31-11	1520	
M0413 SSU-R1 SEP 0 6 2011	*0800*	M. A. White *Mawte* SEP 0 6 2011	*0800*	** ESL will perform all analyses as outlined on the Field Sampling Requirements from the material of the liner selected from the four liners of each sleeve that they will be receiving.
M. A. White *Mawte* SEP 0 6 2011	1410	*L. Kutnyakov* SEP 0 6 2011	1410	
RELINQUISHED BY/REMOVED FROM	DATE/TIME	RECEIVED BY/STORED IN	DATE/TIME	** The 200 Area S&GRP Characterization and Monitoring Sampling and Analysis GKI applies to this SAF.
RELINQUISHED BY/REMOVED FROM	DATE/TIME	RECEIVED BY/STORED IN	DATE/TIME	(1) IC Anions - 9056 {Nitrate}; Moisture Content - D2216 {Percent moisture (wet sample)}; Tc-99 by ICPMS {Technetium-99};
RELINQUISHED BY/REMOVED FROM	DATE/TIME	RECEIVED BY/STORED IN	DATE/TIME	*BRM #93564*

LABORATORY SECTION	RECEIVED BY		TITLE	DATE/TIME
FINAL SAMPLE DISPOSITION	DISPOSAL METHOD		DISPOSED BY	DATE/TIME

PRINTED ON 8/24/2011

A-6003-618 (REV 2)

COLLECTOR
Turner, Bates, Anderson

COMPANY CONTACT
LUKE, SN

TELEPHONE NO.
372-1667

PROJECT COORDINATOR
LUKE, SN

PRICE CODE 8H

DATA TURNAROUND
30 Days / 30 Days

SAMPLING LOCATION
Sample 9

PROJECT DESIGNATION
200-BC-1 Soil Desiccation Pilot Test - Soil

SAF NO.
F11-155

AIR QUALITY

ICE CHEST NO.
N/A

FIELD LOGBOOK NO.
HNF-N-585-1 pg 48

ACTUAL SAMPLE DEPTH
40.5-43 Ft

COA
301405ES10

METHOD OF SHIPMENT
GOVERNMENT VEHICLE

ORIGINAL

SHIPPED TO
Environmental Sciences Laboratory

OFFSITE PROPERTY NO.
N/A

BILL OF LADING/AIR BILL NO.
N/A

MATRIX*
A=Air
DL=Drum
Liquids
DS=Drum Solids
L=Liquid
O=Oil
S=Soil
SE=Sediment
T=Tissue
V=Vegetation
W=Water
WI=Wipe
X=Other

POSSIBLE SAMPLE HAZARDS/ REMARKS
Contains Radioactive Material at concentrations that may or may not be regulated for transportation per 49 CFR / IATA Dangerous Goods Regulations but are not releasable per DOE Order 5400.5 (1990/1993)

SPECIAL HANDLING AND/OR STORAGE
RADIOACTIVE TIE TO: B2H3J3

PRESERVATION Cool~4C

HOLDING TIME 28 Days/48 Hours

TYPE OF CONTAINER Liner

NO. OF CONTAINER(S) 4

VOLUME 1000g

SAMPLE ANALYSIS SEE ITEM (1) IN SPECIAL INSTRUCTIONS

SAMPLE NO.	MATRIX*	SAMPLE DATE	SAMPLE TIME	
B2H3L1	SOIL	9-1-11	0905	A

CHAIN OF POSSESSION

RELINQUISHED BY/REMOVED FROM	DATE/TIME	RECEIVED BY/STORED IN	DATE/TIME
A Turner MZ	9-1-11 1410	M0413 SS4 R)	9-1-11 1410
Mo-413 SSO-121	9-7-11 0800	Calvin Jarvis (Calvin Jan)	9-7-11 0800
Calvin Jarvis/Calvin Jan	9-7-11 11:06	Amanda Lawter Am Lt	9-7-11 11:06
RELINQUISHED BY/REMOVED FROM	DATE/TIME	RECEIVED BY/STORED IN	DATE/TIME
RELINQUISHED BY/REMOVED FROM	DATE/TIME	RECEIVED BY/STORED IN	DATE/TIME
RELINQUISHED BY/REMOVED FROM	DATE/TIME	RECEIVED BY/STORED IN	DATE/TIME

SPECIAL INSTRUCTIONS
** The CACN for all analytical work at ESL laboratory is 301405ES20 (under Contract 00036402 Release 00045).

** ESL will perform all analyses as outlined on the Field Sampling Requirements from the material of the liner selected from the four liners of each sleeve that they will be receiving.

** The 200 Area S&GRP Characterization and Monitoring Sampling and Analysis GKI applies to this SAF.
(1) IC Anions - 9056 {Nitrate}; Moisture Content - D2216 {Percent moisture (wet sample)}; Tc-99 by ICPMS {Technetium-99};

BRM# 13569

LABORATORY SECTION	RECEIVED BY		TITLE	DATE/TIME
FINAL SAMPLE DISPOSITION	DISPOSAL METHOD		DISPOSED BY	DATE/TIME

PRINTED ON 8/24/2011

A-6003-618 (REV 2)

A.50

CH2MHill Plateau Remediation Company	CHAIN OF CUSTODY/SAMPLE ANALYSIS REQUEST		F11-155-072	PAGE 1 OF 1

COLLECTOR
Turner, Bartos, Anderson

SAMPLING LOCATION
Sample 10

ICE CHEST NO.
N/A

SHIPPED TO
Environmental Sciences Laboratory

COMPANY CONTACT
LUKE, SN

TELEPHONE NO.
372-1667

PROJECT DESIGNATION
200-BC-1 Soil Desiccation Pilot Test - Soil

FIELD LOGBOOK NO.
HNF-N-585-1 PG 48

ACTUAL SAMPLE DEPTH
43.08 - 45.58 ft

OFFSITE PROPERTY NO.
N/A

PROJECT COORDINATOR
LUKE, SN

SAF NO.
F11-155

COA
301405ES10

BILL OF LADING/AIR BILL NO.
N/A

PRICE CODE 8H

AIR QUALITY

METHOD OF SHIPMENT
GOVERNMENT VEHICLE

DATA TURNAROUND
30 Days / 30 Days

ORIGINAL

MATRIX*
A =Air
DL=Drum Liquids
DS=Drum Solids
L=Liquid
O=Oil
S=Soil
SE=Sediment
T=Tissue
V=Vegetation
W=Water
WI=Wipe
X=Other

POSSIBLE SAMPLE HAZARDS/ REMARKS
Contains Radioactive Material at concentrations that may or may not be regulated for transportation per 49 CFR / IATA Dangerous Goods Regulations but are not releasable per DOE Order 5400.5 (1990/1993)

SPECIAL HANDLING AND/OR STORAGE
RADIOACTIVE TIE TO: B2H3J4

PRESERVATION	Cool~4C
HOLDING TIME	28 Days/48 Hours
TYPE OF CONTAINER	Liner
NO. OF CONTAINER(S)	4
VOLUME	1000g
SAMPLE ANALYSIS	SEE ITEM (1) IN SPECIAL INSTRUCTIONS

SAMPLE NO.	MATRIX*	SAMPLE DATE	SAMPLE TIME	
B2H3L2	SOIL	9-1-11	0955	X

CHAIN OF POSSESSION

RELINQUISHED BY/REMOVED FROM	DATE/TIME	RECEIVED BY/STORED IN	DATE/TIME
A - Turner M Z	9-1-11 1410	MP 413 SS4 R1	9-1-11 1410
MO-413 SS0-R)	9-7-11 0800	Calvin Farris / Calvin Farris	9-7-11 0800
Calvin Farris / Calvin Farris	9-7-11 1106	Amanda Lawter	9-7-11 1106
RELINQUISHED BY/REMOVED FROM	DATE/TIME	RECEIVED BY/STORED IN	DATE/TIME
RELINQUISHED BY/REMOVED FROM	DATE/TIME	RECEIVED BY/STORED IN	DATE/TIME
RELINQUISHED BY/REMOVED FROM	DATE/TIME	RECEIVED BY/STORED IN	DATE/TIME

LABORATORY SECTION	RECEIVED BY
FINAL SAMPLE DISPOSITION	DISPOSAL METHOD

SPECIAL INSTRUCTIONS
** The CACN for all analytical work at ESL laboratory is 301405ES20 (under Contract 00036402 Release 00045).

** ESL will perform all analyses as outlined on the Field Sampling Requirements from the material of the liner selected from the four liners of each sleeve that they will be receiving.

** The 200 Area S&GRP Characterization and Monitoring Sampling and Analysis GKI applies to this SAF.
(1) IC Anions - 9056 {Nitrate}; Moisture Content - D2216 {Percent moisture (wet sample)}; Tc-99 by ICPMS {Technetium-99};

BRM# 13564

TITLE **DATE/TIME**

DISPOSED BY **DATE/TIME**

Page 62 of 85

PRINTED ON 8/24/2011

A-6003-618 (REV 2)

CH2MHill Plateau Remediation Company | CHAIN OF CUSTODY/SAMPLE ANALYSIS REQUEST | F11-155-073 | PAGE 1 OF 1

COLLECTOR		
Turner, Bates, Anderson		

COMPANY CONTACT	TELEPHONE NO.	PROJECT COORDINATOR	PRICE CODE	8H	DATA TURNAROUND
LUKE, SN	372-1667	LUKE, SN			30 Days / 30 Days

SAMPLING LOCATION
Sample 11

PROJECT DESIGNATION
200-BC-1 Soil Desiccation Pilot Test - Soil

SAF NO. F11-155	AIR QUALITY

ICE CHEST NO.
N/A

FIELD LOGBOOK NO.	ACTUAL SAMPLE DEPTH	COA	METHOD OF SHIPMENT
HNF-N-585-1 pb 48	45.2-47.7 Ft	301405ES10	GOVERNMENT VEHICLE

ORIGINAL

SHIPPED TO
Environmental Sciences Laboratory

OFFSITE PROPERTY NO.
N/A

BILL OF LADING/AIR BILL NO.
N/A

MATRIX*	POSSIBLE SAMPLE HAZARDS/ REMARKS	PRESERVATION	Cool~4C
A=Air	Contains Radioactive Material at concentrations		
DL=Drum	that may or may not be regulated for	HOLDING TIME	28 Days/48 Hours
Liquids	transportation per 49 CFR / IATA Dangerous		
DS=Drum	Goods Regulations but are not releasable per	TYPE OF CONTAINER	Liner
Solids	DOE Order 5400.5 (1990/1993)		
L=Liquid		NO. OF CONTAINER(S)	4
O=Oil			
S=Soil		VOLUME	1000g
SE=Sediment			
I=Tissue		SAMPLE ANALYSIS	SEE ITEM (1) IN SPECIAL INSTRUCTIONS
V=Vegetation			
W=Water			
WI=Wipe	SPECIAL HANDLING AND/OR STORAGE		
X=Other	RADIOACTIVE TIE TO: B2H3J5		

SAMPLE NO.	MATRIX*	SAMPLE DATE	SAMPLE TIME	▉
B2H3L3	SOIL	9-1-11	1125	X

CHAIN OF POSSESSION		SIGN/ PRINT NAMES	
RELINQUISHED BY/REMOVED FROM	DATE/TIME	RECEIVED BY/STORED IN	DATE/TIME
A. Turner AZ 9-1-11	1410	MO 413 SS4 R1 9-1-11	1410
RELINQUISHED BY/REMOVED FROM	DATE/TIME	RECEIVED BY/STORED IN	DATE/TIME
MO-413 SSU-R1 9-7-11	0800	Calvofacis/Calo7an	9-7-11 0800
RELINQUISHED BY/REMOVED FROM	DATE/TIME	RECEIVED BY/STORED IN	DATE/TIME
Calvofacis/Calo7an 9-7-11	11:06	Amanda Canter	9-7-11 11:06
RELINQUISHED BY/REMOVED FROM	DATE/TIME	RECEIVED BY/STORED IN	DATE/TIME
RELINQUISHED BY/REMOVED FROM	DATE/TIME	RECEIVED BY/STORED IN	DATE/TIME
RELINQUISHED BY/REMOVED FROM	DATE/TIME	RECEIVED BY/STORED IN	DATE/TIME

SPECIAL INSTRUCTIONS
** The CACN for all analytical work at ESL laboratory is 301405ES20 (under Contract 00036402 Release 00045).

** ESL will perform all analyses as outlined on the Field Sampling Requirements from the material of the liner selected from the four liners of each sleeve that they will be receiving.

** The 200 Area S&GRP Characterization and Monitoring Sampling and Analysis GKI applies to this SAF.
(1) IC Anions - 9056 {Nitrate}; Moisture Content - D2216 {Percent moisture (wet sample)}; Tc-99 by ICPMS {Technetium-99};

BRM # 13564

LABORATORY SECTION	RECEIVED BY		TITLE		DATE/TIME
FINAL SAMPLE DISPOSITION	DISPOSAL METHOD		DISPOSED BY		DATE/TIME

PRINTED ON 8/24/2011

A-6003-618 (REV 2)

CH2MHill Plateau Remediation Company		CHAIN OF CUSTODY/SAMPLE ANALYSIS REQUEST		F11-155-074		PAGE 1 OF 1

COLLECTOR Emerson
Turner, Bates, Anderson

SAMPLING LOCATION AT9-2~11
Sample 12

ICE CHEST NO.
N|A

SHIPPED TO
Environmental Sciences Laboratory

COMPANY CONTACT LUKE, SN
TELEPHONE NO. 372-1667

PROJECT DESIGNATION
200-BC-1 Soil Desiccation Pilot Test - Soil

FIELD LOGBOOK NO. #NF-N-5851 pg 48
ACTUAL SAMPLE DEPTH 47.5-50 ft

OFFSITE PROPERTY NO.
N/A

PROJECT COORDINATOR LUKE, SN
PRICE CODE 8H

SAF NO. F11-155
AIR QUALITY —

COA 301405ES10
METHOD OF SHIPMENT GOVERNMENT VEHICLE

BILL OF LADING/AIR BILL NO.
N/A

DATA TURNAROUND 30 Days / 30 Days

ORIGINAL

MATRIX*
A=Air
DL=Drum Liquids
DS - Drum Solids
L=Liquid
O=Oil
S=Soil
St=Sediment
T=Tissue
V=Vegetation
W=Water
WI=Wipe
X=Other

POSSIBLE SAMPLE HAZARDS/ REMARKS
Contains Radioactive Material at concentrations that may or may not be regulated for transportation per 49 CFR / IATA Dangerous Goods Regulations but are not releasable per DOE Order 5400.5 (1990/1993)

SPECIAL HANDLING AND/OR STORAGE
RADIOACTIVE TIE TO: B2H3J6

PRESERVATION Cool~4C
HOLDING TIME 28 Days/48 Hours
TYPE OF CONTAINER Liner
NO. OF CONTAINER(S) 4
VOLUME 1000g
SAMPLE ANALYSIS SEE ITEM (1) IN SPECIAL INSTRUCTIONS

SAMPLE NO.	MATRIX*	SAMPLE DATE	SAMPLE TIME	
B2H3L4	SOIL	9-2-11	0925	X

CHAIN OF POSSESSION

RELINQUISHED BY/REMOVED FROM	DATE/TIME	RECEIVED BY/STORED IN	DATE/TIME
A. Turner 9-2-11	1500	SSU-R1 Mo-4/3 9-2-11	1500
SSU-R1 Mo-4/3 9-9-11	1000	Calimfaris/Calo7az 9-9-11	1000
Calimfaris/Calo7az 9-9-11	13 20	I. Kufnyakov 9-9-11	13 20
RELINQUISHED BY/REMOVED FROM	DATE/TIME	RECEIVED BY/STORED IN	DATE/TIME
RELINQUISHED BY/REMOVED FROM	DATE/TIME	RECEIVED BY/STORED IN	DATE/TIME
RELINQUISHED BY/REMOVED FROM	DATE/TIME	RECEIVED BY/STORED IN	DATE/TIME

LABORATORY SECTION	RECEIVED BY	
FINAL SAMPLE DISPOSITION	DISPOSAL METHOD	

PRINTED ON 8/24/2011

SPECIAL INSTRUCTIONS
** The CACN for all analytical work at ESL laboratory is 301405ES20 (under Contract 00036402 Release 00045).

** ESL will perform all analyses as outlined on the Field Sampling Requirements from the material of the liner selected from the four liners of each sleeve that they will be receiving.

** The 200 Area S&GRP Characterization and Monitoring Sampling and Analysis GKI applies to this SAF.
(1) IC Anions - 9056 {Nitrate}; Moisture Content - D2216 {Percent moisture (wet sample)}; Tc-99 by ICPMS {Technetium-99};

BRM# 13564

TITLE	DATE/TIME
DISPOSED BY	DATE/TIME

Page 64 of 85

SDG# ESL 09D026

A-6003-618 (REV 2)

CH2MHill Plateau Remediation Company

CHAIN OF CUSTODY/SAMPLE ANALYSIS REQUEST

F11-155-075   PAGE 1 OF 1

COLLECTOR	COMPANY CONTACT	TELEPHONE NO.	PROJECT COORDINATOR	PRICE CODE	8H	DATA TURNAROUND

Turner, Emerson, Anderson

SAMPLING LOCATION	LUKE, SN	372-1667	LUKE, SN	AIR QUALITY	30 Days / 30 Days
Sample 13	PROJECT DESIGNATION		SAF NO.		
ICE CHEST NO.	200-BC-1 Soil Desiccation Pilot Test - Soil		F11-155		
	FIELD LOGBOOK NO.	ACTUAL SAMPLE DEPTH	COA	METHOD OF SHIPMENT	ORIGINAL
N/A	HNF-N-585-1 pg 47	50.1-52.6 Ft	30140SES10	GOVERNMENT VEHICLE	
SHIPPED TO	OFFSITE PROPERTY NO.		BILL OF LADING/AIR BILL NO.		
Environmental Sciences Laboratory	N/A		N/A		

MATRIX*
A=Air
DL – Drum
Liquids
DS=Drum
Solids
L=Liquid
O=Oil
S=Soil
SE=Sediment
T=Tissue
V=Vegetation
W=Water
WI=Wipe
X=Other

POSSIBLE SAMPLE HAZARDS/ REMARKS
Contains Radioactive Material at concentrations that may or may not be regulated for transportation per 49 CFR / IATA Dangerous Goods Regulations but are not releasable per DOE Order 5400.5 (1990/1993)

SPECIAL HANDLING AND/OR STORAGE
RADIOACTIVE TIE TO: B2H3J7

PRESERVATION	Cool~4C
HOLDING TIME	28 Days/48 Hours
TYPE OF CONTAINER	Liner
NO. OF CONTAINER(S)	4
VOLUME	1000g
SAMPLE ANALYSIS	SEE ITEM (1) IN SPECIAL INSTRUCTIONS

SAMPLE NO.	MATRIX*	SAMPLE DATE	SAMPLE TIME	
B2H3L5	SOIL	9-2-11	1015	A

CHAIN OF POSSESSION

RELINQUISHED BY/REMOVED FROM	DATE/TIME	RECEIVED BY/STORED IN	DATE/TIME
A-Turner	9-2-11 1500	Mo-413 SSU-R1	9-2-11 1500
Mo-413 SSU R1	9-9-11 1000	Colven Faris/Calzton	9-9-11 1000
Colven Faris/Calzton	9-9-11 1320	I. Kufnyako	9-9-11 1320
RELINQUISHED BY/REMOVED FROM	DATE/TIME	RECEIVED BY/STORED IN	DATE/TIME
RELINQUISHED BY/REMOVED FROM	DATE/TIME	RECEIVED BY/STORED IN	DATE/TIME
RELINQUISHED BY/REMOVED FROM	DATE/TIME	RECEIVED BY/STORED IN	DATE/TIME

LABORATORY SECTION	RECEIVED BY
FINAL SAMPLE DISPOSITION	DISPOSAL METHOD

PRINTED ON 8/24/2011

SPECIAL INSTRUCTIONS

** The CACN for all analytical work at ESL laboratory is 301405ES20 (under Contract 00036402 Release 00045).

** ESL will perform all analyses as outlined on the Field Sampling Requirements from the material of the liner selected from the four liners of each sleeve that they will be receiving.

** The 200 Area S&GRP Characterization and Monitoring Sampling and Analysis GKI applies to this SAF.
(1) IC Anions - 9056 {Nitrate}; Moisture Content - D2216 {Percent moisture (wet sample)}; Tc-99 by ICPMS {Technetium-99};

BRM# 13564

TITLE	DATE/TIME
DISPOSED BY	DATE/TIME

A-6003-618 (REV 2)

CH2MHill Plateau Remediation Company   CHAIN OF CUSTODY/SAMPLE ANALYSIS REQUEST   F11-155-076   PAGE 1 OF 1

COLLECTOR	COMPANY CONTACT	TELEPHONE NO.	PROJECT COORDINATOR	PRICE CODE	8H	DATA TURNAROUND
Turner, Emerson, Anderson	LUKE, SN	372-1667	LUKE, SN			30 Days / 30 Days

SAMPLING LOCATION	PROJECT DESIGNATION		SAF NO.	AIR QUALITY	
Sample 14	200-BC-1 Soil Desiccation Pilot Test - Soil		F11-155		

ICE CHEST NO.	FIELD LOGBOOK NO.	ACTUAL SAMPLE DEPTH	COA	METHOD OF SHIPMENT	
N/A	HNF-N-585-1 pg 49	52.5 - 55A	301405ES10	GOVERNMENT VEHICLE	ORIGINAL

SHIPPED TO	OFFSITE PROPERTY NO.	BILL OF LADING/AIR BILL NO.
Environmental Sciences Laboratory	N/A	N/A

MATRIX* A=Air DL=Drum Liquids DS=Drum Solids L=Liquid O=Oil S=Soil SE=Sediment T=Tissue V=Vegetation W=Water WI=Wipe X=Other	POSSIBLE SAMPLE HAZARDS/ REMARKS	PRESERVATION	Cool~4C
	Contains Radioactive Material at concentrations that may or may not be regulated for transportation per 49 CFR / IATA Dangerous Goods Regulations but are not releasable per DOE Order 5400.5 (1990/1993)	HOLDING TIME	28 Days/48 Hours
		TYPE OF CONTAINER	Liner
		NO. OF CONTAINER(S)	4
		VOLUME	1000g
	SPECIAL HANDLING AND/OR STORAGE RADIOACTIVE TIE TO: B2H3J8	SAMPLE ANALYSIS	SEE ITEM (1) IN SPECIAL INSTRUCTIONS

SAMPLE NO.	MATRIX*	SAMPLE DATE	SAMPLE TIME	
B2H3L6	SOIL	9-2-11	1250	A

CHAIN OF POSSESSION				
RELINQUISHED BY/REMOVED FROM	DATE/TIME	RECEIVED BY/STORED IN	DATE/TIME	
A-Turner M	9-2-11 1800	Mo-413SSU-R1	9-2-11 1500	
Mo-413 SSU-R1	9-9-11 1000	Calvin Farris/Calp Tan	9-9-11 1000	
Calvin Farris/Calp Tan	9-9-11 1320	J. Kutnyak Kov	9-9-11 1320	
RELINQUISHED BY/REMOVED FROM	DATE/TIME	RECEIVED BY/STORED IN	DATE/TIME	
RELINQUISHED BY/REMOVED FROM	DATE/TIME	RECEIVED BY/STORED IN	DATE/TIME	
RELINQUISHED BY/REMOVED FROM	DATE/TIME	RECEIVED BY/STORED IN	DATE/TIME	

SPECIAL INSTRUCTIONS

** The CACN for all analytical work at ESL laboratory is 301405ES20 (under Contract 00036402 Release 00045).

** ESL will perform all analyses as outlined on the Field Sampling Requirements from the material of the liner selected from the four liners of each sleeve that they will be receiving.

** The 200 Area S&GRP Characterization and Monitoring Sampling and Analysis GKI applies to this SAF.
(1) IC Anions - 9056 {Nitrate}; Moisture Content - D2216 {Percent moisture (wet sample)}; Tc-99 by ICPMS {Technetium-99};

BRM # 13564

LABORATORY SECTION	RECEIVED BY		TITLE	DATE/TIME
FINAL SAMPLE DISPOSITION	DISPOSAL METHOD		DISPOSED BY	DATE/TIME

PRINTED ON 8/24/2011   A-6003-618 (REV 2)

CH2MHill Plateau Remediation Company | CHAIN OF CUSTODY/SAMPLE ANALYSIS REQUEST | F11-155-077 | PAGE 1 OF 1

COLLECTOR	COMPANY CONTACT	TELEPHONE NO.	PROJECT COORDINATOR	PRICE CODE	8H	DATA TURNAROUND
Turner, Anderson, Emerson	LUKE, SN	372-1667	LUKE, SN			30 Days / 30 Days

SAMPLING LOCATION
Sample 15

PROJECT DESIGNATION
200-BC-1 Soil Desiccation Pilot Test - Soil

SAF NO.
F11-155

AIR QUALITY ⌐1

ICE CHEST NO.
N/A

FIELD LOGBOOK NO.
HNF-N-595-1 Pb49

ACTUAL SAMPLE DEPTH
55.6-58.1 Ft

COA
301405ES10

METHOD OF SHIPMENT
GOVERNMENT VEHICLE

ORIGINAL

SHIPPED TO
Environmental Sciences Laboratory

OFFSITE PROPERTY NO.
N/A

BILL OF LADING/AIR BILL NO.
N/A

MATRIX*
A=Air
DL=Drum Liquids
DS=Drum Solids
L=Liquid
O=Oil
S=Soil
SE=Sediment
T=Tissue
V=Vegetation
W=Water
WI=Wipe
X=Other

POSSIBLE SAMPLE HAZARDS/ REMARKS
Contains Radioactive Material at concentrations that may or may not be regulated for transportation per 49 CFR / IATA Dangerous Goods Regulations but are not releasable per DOE Order 5400.5 (1990/1993)

SPECIAL HANDLING AND/OR STORAGE
RADIOACTIVE TIE TO: B2H3J9

PRESERVATION	Cool~4C
HOLDING TIME	28 Days/48 Hours
TYPE OF CONTAINER	Liner
NO. OF CONTAINER(S)	4
VOLUME	1000g
SAMPLE ANALYSIS	SEE ITEM (1) IN SPECIAL INSTRUCTIONS

SAMPLE NO.	MATRIX*	SAMPLE DATE	SAMPLE TIME	
B2H3L7	SOIL	9-2-11	1355	X

CHAIN OF POSSESSION

RELINQUISHED BY/REMOVED FROM	DATE/TIME	RECEIVED BY/STORED IN	DATE/TIME
A-Turner AMC	9-2-11 1500	SSU-R1	9-2-11 1500
Mo-413	9-9-11 1000	Calinfarris Colston	9-9-11 1000
Calinfarris Colston	9-9-11 1320	L. Intruyah	9-9-11 1320

SPECIAL INSTRUCTIONS

** The CACN for all analytical work at ESL laboratory is 301405ES20 (under Contract 00036402 Release 00045).

** ESL will perform all analyses as outlined on the Field Sampling Requirements from the material of the liner selected from the four liners of each sleeve that they will be receiving.

** The 200 Area S&GRP Characterization and Monitoring Sampling and Analysis GKI applies to this SAF.
(1) IC Anions - 9056 {Nitrate}; Moisture Content - D2216 {Percent moisture (wet sample)}; Tc-99 by ICPMS {Technetium-99};

BRM# 13564

LABORATORY SECTION	RECEIVED BY		TITLE	DATE/TIME
FINAL SAMPLE DISPOSITION	DISPOSAL METHOD		DISPOSED BY	DATE/TIME

Page 67 of 85

PRINTED ON 8/24/2011

A-6003-618 (REV 2)

| CH2MHill Plateau Remediation Company | | CHAIN OF CUSTODY/SAMPLE ANALYSIS REQUEST | | | F11-155-078 | | PAGE 1 OF 1 |

COLLECTOR
Turner, Emerson

SAMPLING LOCATION
Sample 16

ICE CHEST NO.
N/A

SHIPPED TO
Environmental Sciences Laboratory

COMPANY CONTACT
LUKE, SN

TELEPHONE NO.
372-1667

PROJECT DESIGNATION
200-BC-1 Soil Desiccation Pilot Test - Soil

FIELD LOGBOOK NO.
HNF-N-585-1 pg 49

ACTUAL SAMPLE DEPTH
58-60.5Ft

OFFSITE PROPERTY NO.
N/A

PROJECT COORDINATOR
LUKE, SN

SAF NO.
F11-155

COA
301405ES10

BILL OF LADING/AIR BILL NO.
N/A

PRICE CODE BH

AIR QUALITY L

METHOD OF SHIPMENT
GOVERNMENT VEHICLE

DATA TURNAROUND
30 Days / 30 Days

ORIGINAL

MATRIX*
A=Air
DL=Drum Liquids
DS=Drum Solids
L=Liquid
O=Oil
S=Soil
SE=Sediment
T=Tissue
V=Vegetation
W=Water
WI=Wipe
X=Other

POSSIBLE SAMPLE HAZARDS/ REMARKS
Contains Radioactive Material at concentrations that may or may not be regulated for transportation per 49 CFR / IATA Dangerous Goods Regulations but are not releasable per DOE Order 5400.5 (1990/1993)

SPECIAL HANDLING AND/OR STORAGE
RADIOACTIVE TIE TO: B2H3K0

PRESERVATION Cool~4C

HOLDING TIME 28 Days/48 Hours

TYPE OF CONTAINER Liner

NO. OF CONTAINER(S) 4

VOLUME 1000g

SAMPLE ANALYSIS SEE ITEM (1) IN SPECIAL INSTRUCTIONS

SAMPLE NO.	MATRIX*	SAMPLE DATE	SAMPLE TIME	
B2H3L8	SOIL	9-2-11	1435	X

CHAIN OF POSSESSION

RELINQUISHED BY/REMOVED FROM	DATE/TIME	RECEIVED BY/STORED IN	DATE/TIME
A. Turner	9-2-11 1500	SSU-R1	9-2-11 1500
Mo-413 SSU-R1	9-9-11 1000	Calvin Farris	9-9-11 1000
Calvin Farris	9-9-11 1320	L. Lusby	9-9-11 1320

LABORATORY SECTION | RECEIVED BY

FINAL SAMPLE DISPOSITION | DISPOSAL METHOD

SPECIAL INSTRUCTIONS
** The CACN for all analytical work at ESL laboratory is 301405ES20 (under Contract 00036402 Release 00045).

** ESL will perform all analyses as outlined on the Field Sampling Requirements from the material of the liner selected from the four liners of each sleeve that they will be receiving.

** The 200 Area S&GRP Characterization and Monitoring Sampling and Analysis GKI applies to this SAF.
(1) IC Anions - 9056 {Nitrate}; Moisture Content - D2216 {Percent moisture (wet sample)}; Tc-99 by ICPMS {Technetium-99};

BRM# 13569

TITLE | **DATE/TIME**

DISPOSED BY | **DATE/TIME**

Page 68 of 85

PRINTED ON 8/24/2011

A-6003-618 (REV 2)

CH2MHill Plateau Remediation Company

CHAIN OF CUSTODY/SAMPLE ANALYSIS REQUEST

F11-155-019   PAGE 1 OF 1

COLLECTOR	COMPANY CONTACT	TELEPHONE NO.	PROJECT COORDINATOR	PRICE CODE BH	DATA TURNAROUND
Bates, Anderson, Turner	LUKE, SN	372-1667	LUKE, SN		

SAMPLING LOCATION
Sample 1

PROJECT DESIGNATION
200-BC-1 Soil Desiccation Pilot Test - Soil

SAF NO.
F11-155

AIR QUALITY LI

30 Days / 30 Days

ICE CHEST NO.
N/A

FIELD LOGBOOK NO.
HNF-N-585-1 pg 51

ACTUAL SAMPLE DEPTH
20.6

COA
301405ES10

METHOD OF SHIPMENT
GOVERNMENT VEHICLE

ORIGINAL

SHIPPED TO
Environmental Sciences Laboratory

OFFSITE PROPERTY NO.
N/A

BILL OF LADING/AIR BILL NO.
N/A

MATRIX*
A=Air
DL=Drum Liquids
DS=Drum Solids
L=Liquid
O=Oil
S=Soil
SE=Sediment
T=Tissue
V=Vegetation
W=Water
WI=Wipe
X=Other

POSSIBLE SAMPLE HAZARDS/ REMARKS
Contains Radioactive Material at concentrations that may or may not be regulated for transportation per 49 CFR / IATA Dangerous Goods Regulations but are not releasable per DOE Order 5400.5 (1990/1993)

SPECIAL HANDLING AND/OR STORAGE
RADIOACTIVE TIE TO: B2H224

PRESERVATION	Cool~4C
HOLDING TIME	28 Days/48 Hours
TYPE OF CONTAINER	Liner
NO. OF CONTAINER(S)	4
VOLUME	1000g
SAMPLE ANALYSIS	SEE ITEM (1) IN SPECIAL INSTRUCTIONS

SAMPLE NO.	MATRIX*	SAMPLE DATE	SAMPLE TIME	
B2H242	SOIL	9-8-11	0918	

CHAIN OF POSSESSION

RELINQUISHED BY/REMOVED FROM	DATE/TIME	RECEIVED BY/STORED IN	DATE/TIME
Dale Bates	9-1-11 1515	M0413 SSU-R1	9-8-11 1515
SSU-R2	SEP 14 2011 1240	Columbarris/Calisto	SEP 14 2011 1240
Columbarris/Calisto	SEP 14 2011 1330	J. Kudzapu	9-14-11 1330

LABORATORY SECTION	RECEIVED BY
FINAL SAMPLE DISPOSITION	DISPOSAL METHOD

PRINTED ON 8/24/2011

SPECIAL INSTRUCTIONS
** The CACN for all analytical work at ESL laboratory is 301405ES20 (under Contract 00036402 Release 00045).

** ESL will perform all analyses as outlined on the Field Sampling Requirements from the material of the liner selected from the four liners of each sleeve that they will be receiving.

** The 200 Area S&GRP Characterization and Monitoring Sampling and Analysis GKI applies to this SAF.
(1) IC Anions - 9056 {Nitrate}; Moisture Content - D2216 {Percent moisture (wet sample)}; Tc-99 by ICPMS {Technetium-99};

BRM# 13564

TITLE	DATE/TIME
DISPOSED BY	DATE/TIME

SDG# ESL 090026

A-6003-618 (REV 2)

| CH2MHill Plateau Remediation Company | | CHAIN OF CUSTODY/SAMPLE ANALYSIS REQUEST | | F11-155-020 | | PAGE 1 OF 1 |

COLLECTOR
Bates, Anderson, Turner

COMPANY CONTACT
LUKE, SN

TELEPHONE NO.
372-1667

PROJECT COORDINATOR
LUKE, SN

PRICE CODE 8H

DATA TURNAROUND
30 Days / 30 Days

SAMPLING LOCATION
Sample 2

PROJECT DESIGNATION
200-BC-1 Soil Desiccation Pilot Test - Soil

SAF NO.
F11-155

AIR QUALITY

ICE CHEST NO.
N/A

FIELD LOGBOOK NO.
HNF-N-585-1 pg 51

ACTUAL SAMPLE DEPTH
22.3

COA
301405ES10

METHOD OF SHIPMENT
GOVERNMENT VEHICLE

ORIGINAL

SHIPPED TO
Environmental Sciences Laboratory

OFFSITE PROPERTY NO.
N/A

BILL OF LADING/AIR BILL NO.
N/A

MATRIX*
A=Air
DL=Drum
Liquids
DS=Drum
Solids
L=Liquid
O=Oil
S=Soil
SE=Sediment
T=Tissue
V=Vegetation
W=Water
WI=Wipe
X=Other

POSSIBLE SAMPLE HAZARDS/ REMARKS
Contains Radioactive Material at concentrations that may or may not be regulated for transportation per 49 CFR / IATA Dangerous Goods Regulations but are not releasable per DOE Order 5400.5 (1990/1993)

SPECIAL HANDLING AND/OR STORAGE
RADIOACTIVE TIE TO: B2H225

PRESERVATION Cool~4C

HOLDING TIME 28 Days/48 Hours

TYPE OF CONTAINER Liner

NO. OF CONTAINER(S) 4

VOLUME 1000g

SAMPLE ANALYSIS SEE ITEM (1) IN SPECIAL INSTRUCTIONS

SAMPLE NO.	MATRIX*	SAMPLE DATE	SAMPLE TIME	
B2H243	SOIL	9-8-4	1010	

CHAIN OF POSSESSION

RELINQUISHED BY/REMOVED FROM	DATE/TIME	RECEIVED BY/STORED IN	DATE/TIME
Bates	9-8-11 1515	MO 413 SSU-121	9-8-11 1515
MO413 SSU-R2	SEP 14 2011 1240	Colin Farris Colista	SEP 14 2011 1240
Colin Farris Colista	SEP 14 2011 1330	T. Kushnata L Lindmay	9-14-11 1330
RELINQUISHED BY/REMOVED FROM	DATE/TIME	RECEIVED BY/STORED IN	DATE/TIME
RELINQUISHED BY/REMOVED FROM	DATE/TIME	RECEIVED BY/STORED IN	DATE/TIME
RELINQUISHED BY/REMOVED FROM	DATE/TIME	RECEIVED BY/STORED IN	DATE/TIME

SPECIAL INSTRUCTIONS
** The CACN for all analytical work at ESL laboratory is 301405ES20 (under Contract 00036402 Release 00045).

** ESL will perform all analyses as outlined on the Field Sampling Requirements from the material of the liner selected from the four liners of each sleeve that they will be receiving.

** The 200 Area S&GRP Characterization and Monitoring Sampling and Analysis GKI applies to this SAF.
(1) IC Anions - 9056 {Nitrate}; Moisture Content - D2216 {Percent moisture (wet sample)}; Tc-99 by ICPMS {Technetium-99};

BRM# 13564

LABORATORY SECTION	RECEIVED BY		TITLE	DATE/TIME
FINAL SAMPLE DISPOSITION	DISPOSAL METHOD		DISPOSED BY	DATE/TIME

PRINTED ON 8/24/2011

A-6003-618 (REV 2)

CH2MHill Plateau Remediation Company

CHAIN OF CUSTODY/SAMPLE ANALYSIS REQUEST

F11-155-021   PAGE 1 OF 1

COLLECTOR						

Bates, Anderson, Turner

COMPANY CONTACT	TELEPHONE NO.	PROJECT COORDINATOR	PRICE CODE	8H	DATA TURNAROUND
LUKE, SN	372-1667	LUKE, SN			30 Days / 30 Days

SAMPLING LOCATION
Sample 3

PROJECT DESIGNATION		SAF NO.	AIR QUALITY	☐
200-BC-1 Soil Desiccation Pilot Test - Soil		F11-155		

ICE CHEST NO.   N/A

FIELD LOGBOOK NO.	ACTUAL SAMPLE DEPTH	COA	METHOD OF SHIPMENT	ORIGINAL
HNF-N-585-1 pg 51	25	301405ES10	GOVERNMENT VEHICLE	

SHIPPED TO
Environmental Sciences Laboratory

OFFSITE PROPERTY NO.	BILL OF LADING/AIR BILL NO.
N/A	N/A

MATRIX*
A=Air
DL=Drum Liquids
DS=Drum Solids
L=Liquid
O=Oil
S=Soil
SE=Sediment
T=Tissue
V=Vegetation
W=Water
WI=Wipe
X=Other

POSSIBLE SAMPLE HAZARDS/ REMARKS
Contains Radioactive Material at concentrations that may or may not be regulated for transportation per 49 CFR / IATA Dangerous Goods Regulations but are not releasable per DOE Order 5400.5 (1990/1993)

SPECIAL HANDLING AND/OR STORAGE
RADIOACTIVE TIE TO: B2H226

PRESERVATION	Cool~4C
HOLDING TIME	28 Days/48 Hours
TYPE OF CONTAINER	Liner
NO. OF CONTAINER(S)	4
VOLUME	1000g
SAMPLE ANALYSIS	SEE ITEM (1) IN SPECIAL INSTRUCTIONS

SAMPLE NO.	MATRIX*	SAMPLE DATE	SAMPLE TIME	
B2H244	SOIL	9-8-11	1110	

CHAIN OF POSSESSION

RELINQUISHED BY/REMOVED FROM	DATE/TIME	RECEIVED BY/STORED IN	DATE/TIME
Dale Bates 9-8-11	1515	*m0413 SSU-R2* 9-8-11	1515
m0413 SSU-R2	SEP 14 2011 1240	*Cal Farris/Cal*	SEP 14 2011 1240
Cal Farris/Cal SEP 14 2011	1530	*T. Kutnyak* 9-14-11	1530
RELINQUISHED BY/REMOVED FROM	DATE/TIME	RECEIVED BY/STORED IN	DATE/TIME
RELINQUISHED BY/REMOVED FROM	DATE/TIME	RECEIVED BY/STORED IN	DATE/TIME
RELINQUISHED BY/REMOVED FROM	DATE/TIME	RECEIVED BY/STORED IN	DATE/TIME

LABORATORY SECTION	RECEIVED BY	
FINAL SAMPLE DISPOSITION	DISPOSAL METHOD	

SPECIAL INSTRUCTIONS
** The CACN for all analytical work at ESL laboratory is 301405ES20 (under Contract 00036402 Release 00045).

** ESL will perform all analyses as outlined on the Field Sampling Requirements from the material of the liner selected from the four liners of each sleeve that they will be receiving.

** The 200 Area S&GRP Characterization and Monitoring Sampling and Analysis GKI applies to this SAF.
(1) IC Anions - 9056 {Nitrate}; Moisture Content - D2216 {Percent moisture (wet sample)}; Tc-99 by ICPMS {Technetium-99};

BRM# 13564

TITLE	DATE/TIME
DISPOSED BY	DATE/TIME

PRINTED ON 8/24/2011

A-6003-618 (REV 2)

CH2MHill Plateau Remediation Company   CHAIN OF CUSTODY/SAMPLE ANALYSIS REQUEST   F11-155-022   PAGE 1 OF 1

COLLECTOR	COMPANY CONTACT	TELEPHONE NO.	PROJECT COORDINATOR	PRICE CODE	BH	DATA TURNAROUND
Bates, Turner	LUKE, SN	372-1667	LUKE, SN			30 Days / 30 Days

SAMPLING LOCATION	PROJECT DESIGNATION		SAF NO.	AIR QUALITY	
Sample 4	200-BC-1 Soil Desiccation Pilot Test - Soil		F11-155		

ICE CHEST NO.	FIELD LOGBOOK NO.	ACTUAL SAMPLE DEPTH	COA	METHOD OF SHIPMENT	ORIGINAL
N/A	*HNF-N-545-1 pg 51*	*27.5*	301405ES10	GOVERNMENT VEHICLE	

SHIPPED TO	OFFSITE PROPERTY NO.	BILL OF LADING/AIR BILL NO.
Environmental Sciences Laboratory	N/A	N/A

MATRIX*	POSSIBLE SAMPLE HAZARDS/ REMARKS	PRESERVATION	Cool~4C
A=Air	Contains Radioactive Material at concentrations that may or may not be regulated for transportation per 49 CFR / IATA Dangerous Goods Regulations but are not releasable per DOE Order 5400.5 (1990/1993)	HOLDING TIME	28 Days/48 Hours
DL~Drum Liquids			
DS=Drum Solids		TYPE OF CONTAINER	Liner
L=Liquid			
O=Oil			
S=Soil		NO. OF CONTAINER(S)	4
SE=Sediment			
T=Tissue			
V=Vegetation		VOLUME	1000g
W=Water			
WI=Wipe			SEE ITEM (1)
X=Other	SPECIAL HANDLING AND/OR STORAGE	SAMPLE ANALYSIS	IN SPECIAL INSTRUCTIONS
	RADIOACTIVE TIE TO: B2H227		

SAMPLE NO.	MATRIX*	SAMPLE DATE	SAMPLE TIME	
B2H245	SOIL	*9-8-11*	*1320*	▮

CHAIN OF POSSESSION		SIGN/ PRINT NAMES		SPECIAL INSTRUCTIONS

RELINQUISHED BY/REMOVED FROM	DATE/TIME	RECEIVED BY/STORED IN	DATE/TIME
Dale Bates	*9-8-11 1515*	*M0413 SSU-R1 9-8-11*	*1515*
M0413 SSU-R2	*SEP 14 2011 1240*	*Cabanfaos 9-14-11 SEP 14 2011 1240*	
Cabanfaos SEP 14 2011 1330		*J. Kutanya 9-14-11*	*1330*
RELINQUISHED BY/REMOVED FROM	DATE/TIME	RECEIVED BY/STORED IN	DATE/TIME
RELINQUISHED BY/REMOVED FROM	DATE/TIME	RECEIVED BY/STORED IN	DATE/TIME
RELINQUISHED BY/REMOVED FROM	DATE/TIME	RECEIVED BY/STORED IN	DATE/TIME

SPECIAL INSTRUCTIONS

** The CACN for all analytical work at ESL laboratory is 301405ES20 (under Contract 00036402 Release 00045).

** ESL will perform all analyses as outlined on the Field Sampling Requirements from the material of the liner selected from the four liners of each sleeve that they will be receiving.

** The 200 Area S&GRP Characterization and Monitoring Sampling and Analysis GKI applies to this SAF.
(1) IC Anions - 9056 {Nitrate}; Moisture Content - D2216 {Percent moisture (wet sample)}; Tc-99 by ICPMS {Technetium-99};

BRM# 13564

LABORATORY SECTION	RECEIVED BY		TITLE	DATE/TIME
FINAL SAMPLE DISPOSITION	DISPOSAL METHOD		DISPOSED BY	DATE/TIME

Page 72 of 85

PRINTED ON 8/24/2011   A-6003-618 (REV 2)

CH2MHill Plateau Remediation Company

CHAIN OF CUSTODY/SAMPLE ANALYSIS REQUEST

F11-155-023 | PAGE 1 OF 1

COLLECTOR		
Bates, Turner, Billingsley		

COMPANY CONTACT	TELEPHONE NO.	PROJECT COORDINATOR
LUKE, SN	372-1667	LUKE, SN

PRICE CODE	8H

DATA TURNAROUND

SAMPLING LOCATION
Sample 5

PROJECT DESIGNATION		SAF NO.
200-BC-1 Soil Desiccation Pilot Test - Soil		F11-155

AIR QUALITY

30 Days / 30 Days

ICE CHEST NO.
N/A

FIELD LOGBOOK NO.	ACTUAL SAMPLE DEPTH	COA
HNF-N-585-1 pg 51	30.1	301405ES10

METHOD OF SHIPMENT
GOVERNMENT VEHICLE

ORIGINAL

SHIPPED TO
Environmental Sciences Laboratory

OFFSITE PROPERTY NO.	BILL OF LADING/AIR BILL NO.
N/A	N/A

MATRIX*
A=Air
DL=Drum Liquids
DS=Drum Solids
L=Liquid
O=Oil
S=Soil
SE=Sediment
T=Tissue
V=Vegetation
W=Water
WI=Wipe
X=Other

POSSIBLE SAMPLE HAZARDS/ REMARKS
Contains Radioactive Material at concentrations that may or may not be regulated for transportation per 49 CFR / IATA Dangerous Goods Regulations but are not releasable per DOE Order 5400.5 (1990/1993)

SPECIAL HANDLING AND/OR STORAGE
RADIOACTIVE TIE TO: B2H228

PRESERVATION	Cool~4C
HOLDING TIME	28 Days/48 Hours
TYPE OF CONTAINER	Liner
NO. OF CONTAINER(S)	4
VOLUME	1000g
SAMPLE ANALYSIS	SEE ITEM (1) IN SPECIAL INSTRUCTIONS

SAMPLE NO.	MATRIX*	SAMPLE DATE	SAMPLE TIME	
B2H246	SOIL	9-8-11	1420	

CHAIN OF POSSESSION

RELINQUISHED BY/REMOVED FROM	DATE/TIME	RECEIVED BY/STORED IN	DATE/TIME
Bates	9-8-11 / 1515	*mo413 SSU-R1* 9-8-11	1515
mo413 SSU-R2	SEP 14 2011 1240	*Calvin Ears*	SEP 14 2011 1240
Calvin Ears	SEP 14 2011 1330	*J. Kudzaka* 9-14-11	1330

SPECIAL INSTRUCTIONS

** The CACN for all analytical work at ESL laboratory is 301405ES20 (under Contract 00036402 Release 00045).

** ESL will perform all analyses as outlined on the Field Sampling Requirements from the material of the liner selected from the four liners of each sleeve that they will be receiving.

** The 200 Area S&GRP Characterization and Monitoring Sampling and Analysis GKI applies to this SAF.
(1) IC Anions - 9056 {Nitrate}; Moisture Content - D2216 {Percent moisture (wet sample)}; Tc-99 by ICPMS {Technetium-99};

BRM# 13564

LABORATORY SECTION	RECEIVED BY		TITLE	DATE/TIME
FINAL SAMPLE DISPOSITION	DISPOSAL METHOD		DISPOSED BY	DATE/TIME

PRINTED ON 8/24/2011

A-6003-618 (REV 2)

A.63

COLLECTOR	COMPANY CONTACT	TELEPHONE NO.	PROJECT COORDINATOR	PRICE CODE	8H	DATA TURNAROUND
Bates, Cross, Anderson	LUKE, SN	372-1667	LUKE, SN			

SAMPLING LOCATION
Sample 6

PROJECT DESIGNATION
200-BC-1 Soil Desiccation Pilot Test - Soil

SAF NO.
F11-155

AIR QUALITY ☐

30 Days / 30 Days

ICE CHEST NO.
n/A

FIELD LOGBOOK NO.
HNF-N-585-1 page 52   72.8

ACTUAL SAMPLE DEPTH

COA
301405ES10

METHOD OF SHIPMENT
GOVERNMENT VEHICLE

ORIGINAL

SHIPPED TO
Environmental Sciences Laboratory

OFFSITE PROPERTY NO.
N/A

BILL OF LADING/AIR BILL NO.
N/A

MATRIX*	POSSIBLE SAMPLE HAZARDS/ REMARKS	PRESERVATION	Cool~4C
A=Air	Contains Radioactive Material at concentrations that may or may not be regulated for transportation per 49 CFR / IATA Dangerous Goods Regulations but are not releasable per DOE Order 5400.5 (1990/1993)	HOLDING TIME	28 Days/48 Hours
DL=Drum Liquids			
DS=Drum Solids		TYPE OF CONTAINER	Liner
L=Liquid			
O=Oil		NO. OF CONTAINER(S)	4
S=Soil			
SE=Sediment		VOLUME	1000g
T=Tissue			
V=Vegetation			
W=Water			
WI=Wipe			
X=Other	SPECIAL HANDLING AND/OR STORAGE RADIOACTIVE TIE TO: B2H229	SAMPLE ANALYSIS	SEE ITEM (1) IN SPECIAL INSTRUCTIONS

SAMPLE NO.	MATRIX*	SAMPLE DATE	SAMPLE TIME	
B2H247	SOIL	9-9-11	0805	

CHAIN OF POSSESSION

RELINQUISHED BY/REMOVED FROM	DATE/TIME	RECEIVED BY/STORED IN	DATE/TIME
Dale Bates	9-9-11	1520	SSU-R1	9-9-11	1520
SSU-R2	SEP 14 2011 1240	Quintaris Kale	SEP 14 2011 1240
Quintaris/Cal SEP 14 2011 1330	J. Kutryak 9-14-11 1330
RELINQUISHED BY/REMOVED FROM	DATE/TIME	RECEIVED BY/STORED IN	DATE/TIME
RELINQUISHED BY/REMOVED FROM	DATE/TIME	RECEIVED BY/STORED IN	DATE/TIME
RELINQUISHED BY/REMOVED FROM	DATE/TIME	RECEIVED BY/STORED IN	DATE/TIME

SIGN/ PRINT NAMES

SPECIAL INSTRUCTIONS

** The CACN for all analytical work at ESL laboratory is 301405ES20 (under Contract 00036402 Release 00045).

** ESL will perform all analyses as outlined on the Field Sampling Requirements from the material of the liner selected from the four liners of each sleeve that they will be receiving.

** The 200 Area S&GRP Characterization and Monitoring Sampling and Analysis GKI applies to this SAF.
(1) IC Anions - 9056 {Nitrate}; Moisture Content - D2216 {Percent moisture (wet sample)}; Tc-99 by ICPMS {Technetium-99};

BRM# 13564

LABORATORY SECTION	RECEIVED BY	TITLE	DATE/TIME
FINAL SAMPLE DISPOSITION	DISPOSAL METHOD	DISPOSED BY	DATE/TIME

PRINTED ON 9/8/2011

A-6003-618 (REV 2)

CH2MHill Plateau Remediation Company | CHAIN OF CUSTODY/SAMPLE ANALYSIS REQUEST | F11-155-025 | PAGE 1 OF 1

COLLECTOR *Anderson, Bates, Cra~*

COMPANY CONTACT	TELEPHONE NO.	PROJECT COORDINATOR	PRICE CODE	BH	DATA TURNAROUND
LUKE, SN	372-1667	LUKE, SN			30 Days / 30 Days

SAMPLING LOCATION
Sample 7

PROJECT DESIGNATION		SAF NO.	AIR QUALITY ☐	
200-BC-1 Soil Desiccation Pilot Test - Soil		F11-155		

ICE CHEST NO. *N/A*

FIELD LOGBOOK NO.	ACTUAL SAMPLE DEPTH	COA	METHOD OF SHIPMENT
HaF-N-545-1 pg 52	35.2	301405ES10	GOVERNMENT VEHICLE

ORIGINAL

SHIPPED TO
Environmental Sciences Laboratory

OFFSITE PROPERTY NO.	BILL OF LADING/AIR BILL NO.
N/A	N/A

MATRIX*
A=Air
DL=Drum Liquids
DS=Drum Solids
1=Liquid
O=Oil
S=Soil
SE=Sediment
T=Tissue
V=Vegetation
W=Water
WI=Wipe
X=Other

POSSIBLE SAMPLE HAZARDS/ REMARKS
Contains Radioactive Material at concentrations that may or may not be regulated for transportation per 49 CFR / IATA Dangerous Goods Regulations but are not releasable per DOE Order 5400.5 (1990/1993)

PRESERVATION	Cool~4C
HOLDING TIME	28 Days/48 Hours
TYPE OF CONTAINER	Liner
NO. OF CONTAINER(S)	4
VOLUME	1000g
SAMPLE ANALYSIS	SEE ITEM (1) IN SPECIAL INSTRUCTIONS

SPECIAL HANDLING AND/OR STORAGE
RADIOACTIVE TIE TO: B2H230

SAMPLE NO.	MATRIX*	SAMPLE DATE	SAMPLE TIME	
B2H248	SOIL	9-9-4	0920	

CHAIN OF POSSESSION

RELINQUISHED BY/REMOVED FROM	DATE/TIME	RECEIVED BY/STORED IN	DATE/TIME
Dale Bates	9-9-4 1520	*mou13* SSU-R1 9-9-11	1520
mou13 SSU-R2	SEP 14 2011 1240	*Calutaris/Clotz*	SEP 14 2011 1240
Calutaris/Clotz	SEP 14 2011 1530	*J. Kutryak* 9-14-11	1330

SPECIAL INSTRUCTIONS

** The CACN for all analytical work at ESL laboratory is 301405ES20 (under Contract 00036402 Release 00045).

** ESL will perform all analyses as outlined on the Field Sampling Requirements from the material of the liner selected from the four liners of each sleeve that they will be receiving.

** The 200 Area S&GRP Characterization and Monitoring Sampling and Analysis GKI applies to this SAF.
(1) IC Anions - 9056 {Nitrate}; Moisture Content - D2216 {Percent moisture (wet sample)}; Tc-99 by ICPMS {Technetium-99};

BRM# 13564

LABORATORY SECTION	RECEIVED BY		TITLE	DATE/TIME
FINAL SAMPLE DISPOSITION	DISPOSAL METHOD		DISPOSED BY	DATE/TIME

PRINTED ON 8/24/2011

A 6003-618 (REV 2)

CH2MHill Plateau Remediation Company

F11-155-026 | PAGE 1 OF 1

COLLECTOR	COMPANY CONTACT	TELEPHONE NO.	PROJECT COORDINATOR	PRICE CODE	8H	DATA TURNAROUND
Anderson	LUKE, SN	372-1667	LUKE, SN			30 Days / 30 Days

SAMPLING LOCATION	PROJECT DESIGNATION	SAF NO.	AIR QUALITY	
Sample 8	200-BC-1 Soil Desiccation Pilot Test - Soil	F11-155		

ICE CHEST NO.	FIELD LOGBOOK NO.	ACTUAL SAMPLE DEPTH	COA	METHOD OF SHIPMENT	
N/A	HNF-N-585-1 pg 52	37.5	301405ES10	GOVERNMENT VEHICLE	**ORIGINAL**

SHIPPED TO	OFFSITE PROPERTY NO.	BILL OF LADING/AIR BILL NO.
Environmental Sciences Laboratory	N/A	N/A

MATRIX*
A=Air
DL=Drum Liquids
DS=Drum Solids
L=Liquid
O=Oil
S=Soil
SE=Sediment
T=Tissue
V=Vegetation
W=Water
WI=Wipe
X=Other

POSSIBLE SAMPLE HAZARDS / REMARKS
Contains Radioactive Material at concentrations that may or may not be regulated for transportation per 49 CFR / IATA Dangerous Goods Regulations but are not releasable per DOE Order 5400.5 (1990/1993)

SPECIAL HANDLING AND/OR STORAGE
RADIOACTIVE TIE TO: B2H231

PRESERVATION	Cool ~4C
HOLDING TIME	28 Days/48 Hours
TYPE OF CONTAINER	Liner
NO. OF CONTAINER(S)	4
VOLUME	1000g
SAMPLE ANALYSIS	SEE ITEM (1) IN SPECIAL INSTRUCTIONS

SAMPLE NO.	MATRIX*	SAMPLE DATE	SAMPLE TIME	
B2H249	SOIL	9-9-11	1015	

CHAIN OF POSSESSION

RELINQUISHED BY/REMOVED FROM	DATE/TIME	RECEIVED BY/STORED IN	DATE/TIME
(signature) 9-9-11	1520	N0417 SSU-R1 9-9-11	1520
N0413 SSU-R2	SEP 14 2011 1240	Colinfarns/Col-7	SEP 14 2011 1240
Colinfarns/Col-7	SEP 14 2011 1330	L. Kubriak	9-14-11 1330

SPECIAL INSTRUCTIONS
** The CACN for all analytical work at ESL laboratory is 301405ES20 (under Contract 00036402 Release 00045).

** ESL will perform all analyses as outlined on the Field Sampling Requirements from the material of the liner selected from the four liners of each sleeve that they will be receiving.

** The 200 Area S&GRP Characterization and Monitoring Sampling and Analysis GKI applies to this SAF.
(1) IC Anions - 9056 {Nitrate}; Moisture Content - D2216 {Percent moisture (wet sample)}; Tc-99 by ICPMS {Technetium-99};

BRM# 13564

LABORATORY SECTION	RECEIVED BY		TITLE	DATE/TIME
FINAL SAMPLE DISPOSITION	DISPOSAL METHOD		DISPOSED BY	DATE/TIME

PRINTED ON 8/24/2011

A-6003-618 (REV 2)

CH2MHill Plateau Remediation Company

CHAIN OF CUSTODY/SAMPLE ANALYSIS REQUEST

F11-155-027

PAGE 1 OF 1

COLLECTOR	COMPANY CONTACT	TELEPHONE NO.	PROJECT COORDINATOR	PRICE CODE	8H	DATA TURNAROUND
	LUKE, SN	372-1667	LUKE, SN			30 Days / 30 Days

SAMPLING LOCATION	PROJECT DESIGNATION	SAF NO.	AIR QUALITY	
Sample 9	200-BC-1 Soil Desiccation Pilot Test - Soil	F11-155		

ICE CHEST NO.	FIELD LOGBOOK NO.	ACTUAL SAMPLE DEPTH	COA	METHOD OF SHIPMENT	
N/A	HNF-N-585-1 pg 52	39.9	301405ES10	GOVERNMENT VEHICLE	**ORIGINAL**

SHIPPED TO	OFFSITE PROPERTY NO.	BILL OF LADING/AIR BILL NO.
Environmental Sciences Laboratory	N/A	N/A

MATRIX*
A=Air
DL=Drum Liquids
DS=Drum Solids
L=Liquid
O=Oil
S=Soil
SE=Sediment
T=Tissue
V=Vegetation
W=Water
WI=Wipe
X=Other

POSSIBLE SAMPLE HAZARDS/ REMARKS
Contains Radioactive Material at concentrations that may or may not be regulated for transportation per 49 CFR / IATA Dangerous Goods Regulations but are not releasable per DOE Order 5400.5 (1990/1993)

SPECIAL HANDLING AND/OR STORAGE
RADIOACTIVE TIE TO: B2H232

PRESERVATION	Cool~4C
HOLDING TIME	28 Days/48 Hours
TYPE OF CONTAINER	Liner
NO. OF CONTAINER(S)	4
VOLUME	1000g
SAMPLE ANALYSIS	SEE ITEM (1) IN SPECIAL INSTRUCTIONS

SAMPLE NO.	MATRIX*	SAMPLE DATE	SAMPLE TIME	
B2H250	SOIL	9-9-11	1117	

CHAIN OF POSSESSION

RELINQUISHED BY/REMOVED FROM	DATE/TIME	RECEIVED BY/STORED IN	DATE/TIME
Dale Bakesbestos	9-9-11 1520	MO413 SSU-R1	9-9-11 1520
mm3 SSU-R2	SEP 14 2011 1240	CalvinFocris	SEP 14 2011 1240
CalvinFocris	SEP 14 2011 1330	L. Kutyak	9-14-11 1330
RELINQUISHED BY/REMOVED FROM	DATE/TIME	RECEIVED BY/STORED IN	DATE/TIME
RELINQUISHED BY/REMOVED FROM	DATE/TIME	RECEIVED BY/STORED IN	DATE/TIME
RELINQUISHED BY/REMOVED FROM	DATE/TIME	RECEIVED BY/STORED IN	DATE/TIME

LABORATORY SECTION	RECEIVED BY
FINAL SAMPLE DISPOSITION	DISPOSAL METHOD

SPECIAL INSTRUCTIONS

** The CACN for all analytical work at ESL laboratory is 301405ES20 (under Contract 00036402 Release 00045).

** ESL will perform all analyses as outlined on the Field Sampling Requirements from the material of the liner selected from the four liners of each sleeve that they will be receiving.

** The 200 Area S&GRP Characterization and Monitoring Sampling and Analysis GKI applies to this SAF.
(1) IC Anions - 9056 {Nitrate}; Moisture Content - D2216 {Percent moisture (wet sample)}; Tc-99 by ICPMS {Technetium-99};

BRM# 13564

TITLE	DATE/TIME
DISPOSED BY	DATE/TIME

PRINTED ON 8/24/2011

A-6003-618 (REV 2)

CH2MHill Plateau Remediation Company | CHAIN OF CUSTODY/SAMPLE ANALYSIS REQUEST | F11-155-02B | PAGE 1 OF 1

COLLECTOR

SAMPLING LOCATION
Sample 10

ICE CHEST NO. N/A

SHIPPED TO
Environmental Sciences Laboratory

COMPANY CONTACT LUKE, SN	**TELEPHONE NO.** 372-1667
PROJECT DESIGNATION 200-BC-1 Soil Desiccation Pilot Test - Soil	
FIELD LOGBOOK NO. HNF-N-585-1pg 52	**ACTUAL SAMPLE DEPTH** 42.7
OFFSITE PROPERTY NO. N/A	

PROJECT COORDINATOR LUKE, SN	**PRICE CODE** 8H
SAF NO. F11-155	**AIR QUALITY**
COA 301405ES10	**METHOD OF SHIPMENT** GOVERNMENT VEHICLE
BILL OF LADING/AIR BILL NO. N/A	

DATA TURNAROUND 30 Days / 30 Days

ORIGINAL

MATRIX*
A=Air
DL=Drum Liquids
DS=Drum Solids
L=Liquid
O=Oil
S=Soil
SE=Sediment
T=Tissue
V=Vegetation
W=Water
WI=Wipe
X=Other

POSSIBLE SAMPLE HAZARDS/ REMARKS
Contains Radioactive Material at concentrations that may or may not be regulated for transportation per 49 CFR / IATA Dangerous Goods Regulations but are not releasable per DOE Order 5400.5 (1990/1993)

SPECIAL HANDLING AND/OR STORAGE
RADIOACTIVE TIE TO: B2H233

PRESERVATION	Cool~4C
HOLDING TIME	28 Days/48 Hours
TYPE OF CONTAINER	Liner
NO. OF CONTAINER(S)	4
VOLUME	1000g
SAMPLE ANALYSIS	SEE ITEM (1) IN SPECIAL INSTRUCTIONS

SAMPLE NO.	MATRIX*	SAMPLE DATE	SAMPLE TIME	
B2H251	SOIL	9-9-11	1340	

CHAIN OF POSSESSION

RELINQUISHED BY/REMOVED FROM	DATE/TIME	RECEIVED BY/STORED IN	DATE/TIME
	9-9-11	no413 SSU-R1	9-9-11 1520
SSU-R2 mo413	SEP 14 2011 1240	Colvin, Farris	SEP 14 2011 1240
Colvin, Farris	SEP 14 2011 1330		9-14-11 1330

LABORATORY SECTION	RECEIVED BY			TITLE	DATE/TIME
FINAL SAMPLE DISPOSITION	DISPOSAL METHOD			DISPOSED BY	DATE/TIME

SPECIAL INSTRUCTIONS
** The CACN for all analytical work at ESL laboratory is 301405ES20 (under Contract 00036402 Release 00045).

** ESL will perform all analyses as outlined on the Field Sampling Requirements from the material of the liner selected from the four liners of each sleeve that they will be receiving.

** The 200 Area S&GRP Characterization and Monitoring Sampling and Analysis GKI applies to this SAF.
(1) IC Anions - 9056 {Nitrate}; Moisture Content - D2216 {Percent moisture (wet sample)}; Tc-99 by ICPMS {Technetium-99};
BRM # 13564

PRINTED ON 8/24/2011

A-6003-618 (REV 2)

CH2MHill Plateau Remediation Company

CHAIN OF CUSTODY/SAMPLE ANALYSIS REQUEST

F11-155-029 | PAGE 1 OF 1

COLLECTOR		
Anderson Bates Crew		

COMPANY CONTACT	TELEPHONE NO.
LUKE, SN	372-1667

PROJECT COORDINATOR	PRICE CODE	8H	DATA TURNAROUND
LUKE, SN			30 Days / 30 Days

SAMPLING LOCATION
Sample 11

PROJECT DESIGNATION
200-BC-1 Soil Desiccation Pilot Test - Soil

SAF NO.	AIR QUALITY	L
F11-155		

ICE CHEST NO.
N/A

FIELD LOGBOOK NO.	ACTUAL SAMPLE DEPTH
HNF-N-585-1 pg 52 45.3	

COA	METHOD OF SHIPMENT
301405ES10	GOVERNMENT VEHICLE

ORIGINAL

SHIPPED TO
Environmental Sciences Laboratory

OFFSITE PROPERTY NO.
N/A

BILL OF LADING/AIR BILL NO.
N/A

MATRIX*
A=Air
DL=Drum
Liquids
DS=Drum
Solids
L=Liquid
O=Oil
S=Soil
SE=Sediment
T=Tissue
V=Vegetation
W=Water
WI=Wipe
X=Other

POSSIBLE SAMPLE HAZARDS/ REMARKS
Contains Radioactive Material at concentrations that may or may not be regulated for transportation per 49 CFR / IATA Dangerous Goods Regulations but are not releasable per DOE Order 5400.5 (1990/1993)

SPECIAL HANDLING AND/OR STORAGE
RADIOACTIVE TIE TO: B2H234

PRESERVATION	Cool~4C
HOLDING TIME	28 Days/48 Hours
TYPE OF CONTAINER	Liner
NO. OF CONTAINER(S)	4
VOLUME	1000g
SAMPLE ANALYSIS	SEE ITEM (1) IN SPECIAL INSTRUCTIONS

SAMPLE NO.	MATRIX*	SAMPLE DATE	SAMPLE TIME	
B2H252	SOIL	9-9-11	1445	

CHAIN OF POSSESSION

RELINQUISHED BY/REMOVED FROM	DATE/TIME	RECEIVED BY/STORED IN	DATE/TIME
Dale Bates 9-9-11	1520	*no413 SSU-R1* 9-9-11	1920
no413 SSU-R2	SEP 14 2011 1240	*Olvifaris*	SEP 14 2011 1240
Olivaris SEP 14 2011 1330		*L. Lutyah* 9-14-11	1330

LABORATORY SECTION	RECEIVED BY		
FINAL SAMPLE DISPOSITION	DISPOSAL METHOD		

SPECIAL INSTRUCTIONS

** The CACN for all analytical work at ESL laboratory is 301405ES20 (under Contract 00036402 Release 00045).

** ESL will perform all analyses as outlined on the Field Sampling Requirements from the material of the liner selected from the four liners of each sleeve that they will be receiving.

** The 200 Area S&GRP Characterization and Monitoring Sampling and Analysis GKI applies to this SAF.
(1) IC Anions - 9056 {Nitrate}; Moisture Content - D2216 {Percent moisture (wet sample)}; Tc-99 by ICPMS {Technetium-99};

BRM# 13564

TITLE	DATE/TIME
DISPOSED BY	DATE/TIME

PRINTED ON 8/24/2011

A-6003-618 (REV 2)

CH2MHill Plateau Remediation Company | **CHAIN OF CUSTODY/SAMPLE ANALYSIS REQUEST** | **F11-155-030** | **PAGE 1 OF 1**

COLLECTOR	COMPANY CONTACT	TELEPHONE NO.	PROJECT COORDINATOR	PRICE CODE	8H	DATA TURNAROUND
Turner, Anderson, wallace	LUKE, SN	372-1667	LUKE, SN			30 Days / 30 Days

SAMPLING LOCATION	PROJECT DESIGNATION		SAF NO.	AIR QUALITY	
Sample 12	200-BC-1 Soil Desiccation Pilot Test - Soil		F11-155		

ICE CHEST NO.	FIELD LOGBOOK NO.	ACTUAL SAMPLE DEPTH	COA	METHOD OF SHIPMENT	
N/A	HNF-N-585-1 pg 53	47.6-50.1 FT	301405ES10	GOVERNMENT VEHICLE	**ORIGINAL**

SHIPPED TO	OFFSITE PROPERTY NO.	BILL OF LADING/AIR BILL NO.
Environmental Sciences Laboratory	N/A	N/A

MATRIX*
A=Air
DL=Drum Liquids
DS=Drum Solids
L=Liquid
O=Oil
S=Soil
SE=Sediment
T=Tissue
V=Vegetation
W=Water
WI=Wipe
X=Other

POSSIBLE SAMPLE HAZARDS/ REMARKS
Contains Radioactive Material at concentrations that may or may not be regulated for transportation per 49 CFR / IATA Dangerous Goods Regulations but are not releasable per DOE Order 5400.5 (1990/1993)

SPECIAL HANDLING AND/OR STORAGE
RADIOACTIVE TIE TO: B2H235

PRESERVATION	Cool~4C
HOLDING TIME	28 Days/48 Hours
TYPE OF CONTAINER	Liner
NO. OF CONTAINER(S)	4
VOLUME	1000g
SAMPLE ANALYSIS	SEE ITEM (1) IN SPECIAL INSTRUCTIONS

SAMPLE NO.	MATRIX*	SAMPLE DATE	SAMPLE TIME	
B2H253	SOIL	9-12-11	0835	X

CHAIN OF POSSESSION

RELINQUISHED BY/REMOVED FROM	DATE/TIME	RECEIVED BY/STORED IN	DATE/TIME
A. Turner	9-12-11 / 1530	SSU-R2	SEP 12 2011 /1530
SSU-R2	SEP 14 2011 1240	Columfaris/Cal	SEP 14 2011 1240
Columfaris/Cal	SEP 14 2011 1330	KULTAYA	9-14-11 1330

LABORATORY SECTION	RECEIVED BY	TITLE	DATE/TIME
FINAL SAMPLE DISPOSITION	DISPOSAL METHOD	DISPOSED BY	DATE/TIME

SPECIAL INSTRUCTIONS
** The CACN for all analytical work at ESL laboratory is 301405ES20 (under Contract 00036402 Release 00045).

** ESL will perform all analyses as outlined on the Field Sampling Requirements from the material of the liner selected from the four liners of each sleeve that they will be receiving.

** The 200 Area S&GRP Characterization and Monitoring Sampling and Analysis GKI applies to this SAF.
(1) IC Anions - 9056 {Nitrate}; Moisture Content - D2216 {Percent moisture (wet sample)}; Tc-99 by ICPMS {Technetium-99};

BRM# 13564

Page 80 of 85

PRINTED ON 8/24/2011

A-6003-618 (REV 2)

CH2MHill Plateau Remediation Company | CHAIN OF CUSTODY/SAMPLE ANALYSIS REQUEST | F11-155-031 | PAGE 1 OF 1

COLLECTOR	COMPANY CONTACT	TELEPHONE NO.	PROJECT COORDINATOR	PRICE CODE 8H	DATA TURNAROUND
Tim	LUKE, SN	372-1667	LUKE, SN		
SAMPLING LOCATION	PROJECT DESIGNATION		SAF NO.	AIR QUALITY	30 Days / 30 Days
Sample 13	200-BC-1 Soil Desiccation Pilot Test - Soil		F11-155		
ICE CHEST NO.	FIELD LOGBOOK NO.	ACTUAL SAMPLE DEPTH	COA	METHOD OF SHIPMENT	
N/A	*HNF-N-585-1 pg 52*	*49.75-52.25 ft*	301405ES10	GOVERNMENT VEHICLE	**ORIGINAL**
SHIPPED TO	OFFSITE PROPERTY NO.		BILL OF LADING/AIR BILL NO.		
Environmental Sciences Laboratory	N/A		N/A		

MATRIX*				
A=Air	POSSIBLE SAMPLE HAZARDS/ REMARKS	PRESERVATION	Cool~4C	
DL=Drum Liquids	Contains Radioactive Material at concentrations that may or may not be regulated for transportation per 49 CFR / IATA Dangerous Goods Regulations but are not releasable per DOE Order 5400.5 (1990/1993)	HOLDING TIME	28 Days/48 Hours	
DS=Drum Solids				
L=Liquid		TYPE OF CONTAINER	Liner	
O=Oil				
S=Soil		NO. OF CONTAINER(S)	4	
St=Sediment				
T=Tissue				
V=Vegetation		VOLUME	1000g	
W=Water				
WI=Wipe				
X=Other	SPECIAL HANDLING AND/OR STORAGE RADIOACTIVE TIE TO: B2H236	SAMPLE ANALYSIS	SEE ITEM (1) IN SPECIAL INSTRUCTIONS	

SAMPLE NO.	MATRIX*	SAMPLE DATE	SAMPLE TIME	
B2H254	SOIL	*9-12-11*	*0945*	*X*

CHAIN OF POSSESSION			
RELINQUISHED BY/REMOVED FROM	DATE/TIME	RECEIVED BY/STORED IN	DATE/TIME
A. Tim	*9-12-11 1530*	*SSU-R2* SEP 1 2 2011	*1530*
SSU-R2	SEP 1 4 2011	*Colin Faris/Col.* SEP 1 4 2011	*1240*
Col.Faris/Col.	SEP 1 4 2011 *1330*	*L. Kutooski 9-14-11*	*1330*
RELINQUISHED BY/REMOVED FROM	DATE/TIME	RECEIVED BY/STORED IN	DATE/TIME
RELINQUISHED BY/REMOVED FROM	DATE/TIME	RECEIVED BY/STORED IN	DATE/TIME
RELINQUISHED BY/REMOVED FROM	DATE/TIME	RECEIVED BY/STORED IN	DATE/TIME

LABORATORY SECTION	RECEIVED BY		TITLE	DATE/TIME
FINAL SAMPLE DISPOSITION	DISPOSAL METHOD		DISPOSED BY	DATE/TIME

SPECIAL INSTRUCTIONS

** The CACN for all analytical work at ESL laboratory is 301405ES20 (under Contract 00036402 Release 00045).

** ESL will perform all analyses as outlined on the Field Sampling Requirements from the material of the liner selected from the four liners of each sleeve that they will be receiving.

** The 200 Area S&GRP Characterization and Monitoring Sampling and Analysis GKI applies to this SAF.
(1) IC Anions - 9056 {Nitrate}; Moisture Content - D2216 {Percent moisture (wet sample)}; Tc-99 by ICPMS {Technetium-99};

BRM# 13564

Page 81 of 85

PRINTED ON 8/24/2011

A 6003-618 (REV 2)

CH2MHill Plateau Remediation Company | CHAIN OF CUSTODY/SAMPLE ANALYSIS REQUEST | F11-155-032 | PAGE 1 OF 1

COLLECTOR	COMPANY CONTACT	TELEPHONE NO.	PROJECT COORDINATOR	PRICE CODE	8H	DATA TURNAROUND
Thmer	LUKE, SN	372-1667	LUKE, SN			30 Days / 30 Days

SAMPLING LOCATION	PROJECT DESIGNATION		SAF NO.	AIR QUALITY ☐
Sample 14	200-BC-1 Soil Desiccation Pilot Test - Soil		F11-155	

ICE CHEST NO.	FIELD LOGBOOK NO.	ACTUAL SAMPLE DEPTH	COA	METHOD OF SHIPMENT
UIA	HNF-N-585-1 PG 52	52.6 - 55.3 ft	301405ES10	GOVERNMENT VEHICLE

ORIGINAL

SHIPPED TO	OFFSITE PROPERTY NO.	BILL OF LADING/AIR BILL NO.
Environmental Sciences Laboratory	N/A	N/A

MATRIX*	POSSIBLE SAMPLE HAZARDS/ REMARKS	PRESERVATION	Cool~4C
A=Air	Contains Radioactive Material at concentrations		
DL=Drum Liquids	that may or may not be regulated for	HOLDING TIME	28 Days/48 Hours
DS=Drum Solids	transportation per 49 CFR / IATA Dangerous		
L=Liquid	Goods Regulations but are not releasable per	TYPE OF CONTAINER	Liner
O=Oil	DOE Order 5400.5 (1990/1993)		
S=Soil		NO. OF CONTAINER(S)	4
SE=Sediment			
T=Tissue		VOLUME	1000g
V=Vegetation			
W=Water			
WI=Wipe		SAMPLE ANALYSIS	SEE ITEM (1) IN SPECIAL INSTRUCTIONS
X=Other	SPECIAL HANDLING AND/OR STORAGE RADIOACTIVE TIE TO: 82H237		

SAMPLE NO.	MATRIX*	SAMPLE DATE	SAMPLE TIME	
B2H255	SOIL	9-12-11	1050	X

CHAIN OF POSSESSION		SPECIAL INSTRUCTIONS

RELINQUISHED BY/REMOVED FROM	DATE/TIME	RECEIVED BY/STORED IN	DATE/TIME
A. Thmer	9-12-11 1530	mo 413 SSU-R2	SEP 1 2 2011 1530
mo 413 SSU-R2	SEP 1 4 2011 1240	Calixfarris/Cal2z	SEP 1 4 2011 1240
Calixfarris/Cal2z	SEP 1 4 2011 1330	L Kahya	9-14-11 1330

SPECIAL INSTRUCTIONS

** The CACN for all analytical work at ESL laboratory is 301405ES20 (under Contract 00036402 Release 00045).

** ESL will perform all analyses as outlined on the Field Sampling Requirements from the material of the liner selected from the four liners of each sleeve that they will be receiving.

** The 200 Area S&GRP Characterization and Monitoring Sampling and Analysis GKI applies to this SAF.
(1) IC Anions - 9056 {Nitrate}; Moisture Content - D2216 {Percent moisture (wet sample)}; Tc-99 by ICPMS {Technetium-99};

BRM# 13564

LABORATORY SECTION	RECEIVED BY		TITLE	DATE/TIME
FINAL SAMPLE DISPOSITION	DISPOSAL METHOD		DISPOSED BY	DATE/TIME

PRINTED ON 8/24/2011

A 6003-618 (REV 2)

| CH2MHill Plateau Remediation Company | | CHAIN OF CUSTODY/SAMPLE ANALYSIS REQUEST | | F11-155-033 | PAGE 1 OF 1 |

CH2MHill Plateau Remediation Company

CHAIN OF CUSTODY/SAMPLE ANALYSIS REQUEST

F11-155-033 PAGE 1 OF 1

COLLECTOR	COMPANY CONTACT	TELEPHONE NO.	PROJECT COORDINATOR	PRICE CODE 8H	DATA TURNAROUND
Tw^v	LUKE, SN	372-1667	LUKE, SN		
SAMPLING LOCATION	**PROJECT DESIGNATION**		**SAF NO.**	**AIR QUALITY** [ ]	30 Days / 30 Days
Sample 15	200-BC-1 Soil Desiccation Pilot Test - Soil		F11-155		
ICE CHEST NO.	**FIELD LOGBOOK NO.**	**ACTUAL SAMPLE DEPTH**	**COA**	**METHOD OF SHIPMENT**	
OIA	HNF-N-585-1 pg 62	SS.5 - SB Ft	301405ES10	GOVERNMENT VEHICLE	**ORIGINAL**
SHIPPED TO	**OFFSITE PROPERTY NO.**		**BILL OF LADING/AIR BILL NO.**		
Environmental Sciences Laboratory	N/A		N/A		

MATRIX*
A=Air
DL=Drum Liquids
DS=Drum Solids
L=Liquid
O=Oil
S=Soil
SE=Sediment
T=Tissue
V=Vegetation
W=Water
WI=Wipe
X=Other

POSSIBLE SAMPLE HAZARDS/ REMARKS
Contains Radioactive Material at concentrations that may or may not be regulated for transportation per 49 CFR / IATA Dangerous Goods Regulations but are not releasable per DOE Order 5400.5 (1990/1993)

SPECIAL HANDLING AND/OR STORAGE
RADIOACTIVE TIE TO: B2H238

PRESERVATION	Cool~4C
HOLDING TIME	28 Days/48 Hours
TYPE OF CONTAINER	Liner
NO. OF CONTAINER(S)	4
VOLUME	1000g
SAMPLE ANALYSIS	SEE ITEM (1) IN SPECIAL INSTRUCTIONS

SAMPLE NO.	MATRIX*	SAMPLE DATE	SAMPLE TIME	
B2H256	SOIL	9-12-11	1315	X

CHAIN OF POSSESSION

RELINQUISHED BY/REMOVED FROM	DATE/TIME	RECEIVED BY/STORED IN	DATE/TIME
A. Tw~ M~ 9-13-11	1530	mov SSU-R2	SEP 1 2 2011 1530
Mo-413 SSU-R2	SEP 1 4 2011	Calivanis/Calo	SEP 1 4 2011 1240
Calivanis/Calo	SEP 1 4 2011 1330	I. Kuthyakov 9-14-11	1330

SIGN/ PRINT NAMES

SPECIAL INSTRUCTIONS
** The CACN for all analytical work at ESL laboratory is 301405ES20 (under Contract 00036402 Release 00045).

** ESL will perform all analyses as outlined on the Field Sampling Requirements from the material of the liner selected from the four liners of each sleeve that they will be receiving.

** The 200 Area S&GRP Characterization and Monitoring Sampling and Analysis GKI applies to this SAF.
(1) IC Anions - 9056 {Nitrate}; Moisture Content - D2216 {Percent moisture (wet sample)}; Tc-99 by ICPMS {Technetium-99};

BRM# 13569

LABORATORY SECTION	RECEIVED BY	TITLE	DATE/TIME
FINAL SAMPLE DISPOSITION	DISPOSAL METHOD	DISPOSED BY	DATE/TIME

PRINTED ON 8/24/2011

A-6003-618 (REV 2)

CH2MHill Plateau Remediation Company | CHAIN OF CUSTODY/SAMPLE ANALYSIS REQUEST | F11-155-034 | PAGE 1 OF 1

COLLECTOR	COMPANY CONTACT	TELEPHONE NO.	PROJECT COORDINATOR	PRICE CODE	8H	DATA TURNAROUND
Turner	LUKE, SN	372-1667	LUKE, SN			30 Days / 30 Days

SAMPLING LOCATION	PROJECT DESIGNATION		SAF NO.	AIR QUALITY	☐	
Sample 16	200-BC-1 Soil Desiccation Pilot Test - Soil		F11-155			

ICE CHEST NO.	FIELD LOGBOOK NO.	ACTUAL SAMPLE DEPTH	COA	METHOD OF SHIPMENT	ORIGINAL
_N/A_	_HNF-N-585-1 PG 52_	_58.3 - 60.8 ft_	301405ES10	GOVERNMENT VEHICLE	

SHIPPED TO	OFFSITE PROPERTY NO.	BILL OF LADING/AIR BILL NO.
Environmental Sciences Laboratory	N/A	N/A

MATRIX*	POSSIBLE SAMPLE HAZARDS/ REMARKS		
A=Air	Contains Radioactive Material at concentrations that may or may not be regulated for transportation per 49 CFR / IATA Dangerous Goods Regulations but are not releasable per DOE Order 5400.5 (1990/1993)	PRESERVATION	Cool~4C
DL=Drum		HOLDING TIME	28 Days/48 Hours
Liquids			
DS=Drum			
Solids		TYPE OF CONTAINER	Liner
L=Liquid			
O=Oil		NO. OF CONTAINER(S)	4
S=Soil			
SE=Sediment			
T=Tissue		VOLUME	1000g
V=Vegetation			
W=Water			
WI=Wipe		SAMPLE ANALYSIS	SEE ITEM (1) IN SPECIAL INSTRUCTIONS
X=Other	SPECIAL HANDLING AND/OR STORAGE RADIOACTIVE TIE TO: B2H239		

SAMPLE NO.	MATRIX*	SAMPLE DATE	SAMPLE TIME	████
B2H257	SOIL	9-12-11	1430	X

CHAIN OF POSSESSION		SIGN/ PRINT NAMES	
RELINQUISHED BY/REMOVED FROM	DATE/TIME	RECEIVED BY/STORED IN	DATE/TIME
A. Turner	_9-12-11 1530_	_mo43 SSU-R2_ SEP 1 2 2011	_1530_
mo43 SSU-R2	SEP 1 4 2011 _1240_	_Colin Sarris/Colo 2_ SEP 1 4 2011	_1240_
Colin Sarris/Colo 2 SEP 1 4 2011	_1330_	_L. Kathyakov_ 9-14-11	_1330_
RELINQUISHED BY/REMOVED FROM	DATE/TIME	RECEIVED BY/STORED IN	DATE/TIME
RELINQUISHED BY/REMOVED FROM	DATE/TIME	RECEIVED BY/STORED IN	DATE/TIME
RELINQUISHED BY/REMOVED FROM	DATE/TIME	RECEIVED BY/STORED IN	DATE/TIME

LABORATORY SECTION	RECEIVED BY		TITLE		DATE/TIME
FINAL SAMPLE DISPOSITION	DISPOSAL METHOD		DISPOSED BY		DATE/TIME

SPECIAL INSTRUCTIONS

** The CACN for all analytical work at ESL laboratory is 301405ES20 (under Contract 00036402 Release 00045).

** ESL will perform all analyses as outlined on the Field Sampling Requirements from the material of the liner selected from the four liners of each sleeve that they will be receiving.

** The 200 Area S&GRP Characterization and Monitoring Sampling and Analysis GKI applies to this SAF.
(1) IC Anions - 9056 {Nitrate}; Moisture Content - D2216 {Percent moisture (wet sample)}; Tc-99 by ICPMS {Technetium-99};

BRM # 13564

PRINTED ON 8/24/2011

A-6003-618 (REV 2)

CH2MHill Plateau Remediation Company		CHAIN OF CUSTODY/SAMPLE ANALYSIS REQUEST			F11-155-035	PAGE 1 OF 1

COLLECTOR	COMPANY CONTACT	TELEPHONE NO.	PROJECT COORDINATOR	PRICE CODE	8H	DATA TURNAROUND
Crow	LUKE, SN	372-1667	LUKE, SN			
SAMPLING LOCATION	**PROJECT DESIGNATION**		**SAF NO.**	**AIR QUALITY**		30 Days / 30 Days
Sample 17	200-BC-1 Soil Desiccation Pilot Test - Soil		F11-155			
ICE CHEST NO.	**FIELD LOGBOOK NO.**	**ACTUAL SAMPLE DEPTH**	**COA**	**METHOD OF SHIPMENT**		**ORIGINAL**
N/A	HNF-N-585-1	42.7'	301405ES10	GOVERNMENT VEHICLE		
SHIPPED TO	**OFFSITE PROPERTY NO.**		**BILL OF LADING/AIR BILL NO.**			
Environmental Sciences Laboratory	N/A		N/A			

MATRIX*	POSSIBLE SAMPLE HAZARDS/ REMARKS	PRESERVATION	Cool~4C
A=Air DL=Drum Liquids DS=Drum Solids L=Liquid O=Oil S=Soil SE=Sediment T=Tissue V=Vegetation W=Water WI=Wipe X=Other	Contains Radioactive Material at concentrations that may or may not be regulated for transportation per 49 CFR / IATA Dangerous Goods Regulations but are not releasable per DOE Order 5400.5 (1990/1993)	HOLDING TIME	28 Days/48 Hours
		TYPE OF CONTAINER	Liner
		NO. OF CONTAINER(S)	C KS 8/24/11
		VOLUME	1000g
	SPECIAL HANDLING AND/OR STORAGE RADIOACTIVE TIE TO: B2H233	SAMPLE ANALYSIS	SEE ITEM (1) IN SPECIAL INSTRUCTIONS

SAMPLE NO.	MATRIX*	SAMPLE DATE	SAMPLE TIME	
B2H258	SOIL	9-9-11	1445 1340	

IVK 9/9/11

CHAIN OF POSSESSION

RELINQUISHED BY/REMOVED FROM	DATE/TIME	RECEIVED BY/STORED IN	DATE/TIME
R Crow /R Crow	9-9-11 1520	MO-413 SSU-R1	9-9-11 1520
MO-413 SSU-R2	SEP 14 2011 1240	Calimbas's/Cab7	SEP 14 2011 1240
Calimbas's/Cab7	SEP 14 2011 1330	L. Lutyakw	9-14-11 1330

SPECIAL INSTRUCTIONS

** The CACN for all analytical work at ESL laboratory is 301405ES20 (under Contract 00036402 Release 00045).

** ESL is to prepare this sample as a duplicate of Sample 10 and use HEIS # B2H258.

** The 200 Area S&GRP Characterization and Monitoring Sampling and Analysis GKI applies to this SAF.
(1) IC Anions - 9056 {Nitrate}; Moisture Content - D2216 {Percent moisture (wet sample)}; Tc-99 by ICPMS {Technetium-99};

SRM# 13564

LABORATORY SECTION	RECEIVED BY		TITLE	DATE/TIME
FINAL SAMPLE DISPOSITION	DISPOSAL METHOD		DISPOSED BY	DATE/TIME

PRINTED ON 8/24/2011

A-6003-618 (REV 2)

Appendix B

Supplemental Temperature, Neutron Moisture Log, Electrical Resistivity Tomography, and Ground Penetrating Radar Data Plots

Appendix B

Supplemental Temperature, Neutron Moisture Log, Electrical Resistivity Tomography, and Ground Penetrating Radar Data Plots

This appendix contains supplemental data plots for temperature, neutron moisture log, electrical resistivity tomography, and ground penetrating radar data collected during active desiccation. These plots expand on those presented in the main text of the report by providing additional time points or three-dimensional images.

Temperature Data Interpolation Plots
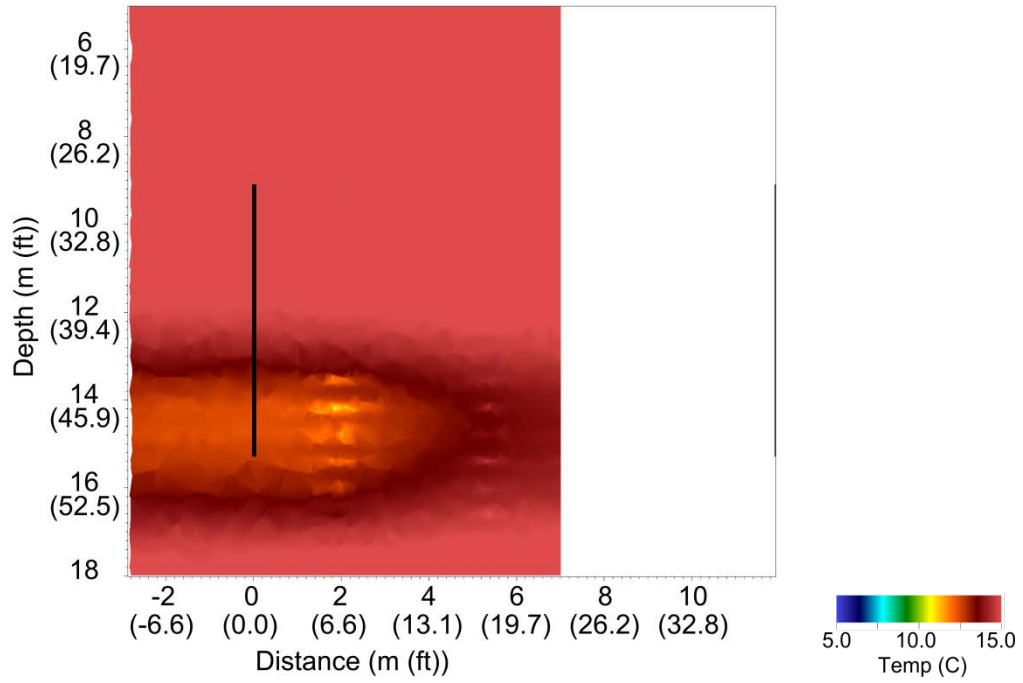
January 31, 2011 (Desiccation Day 14)
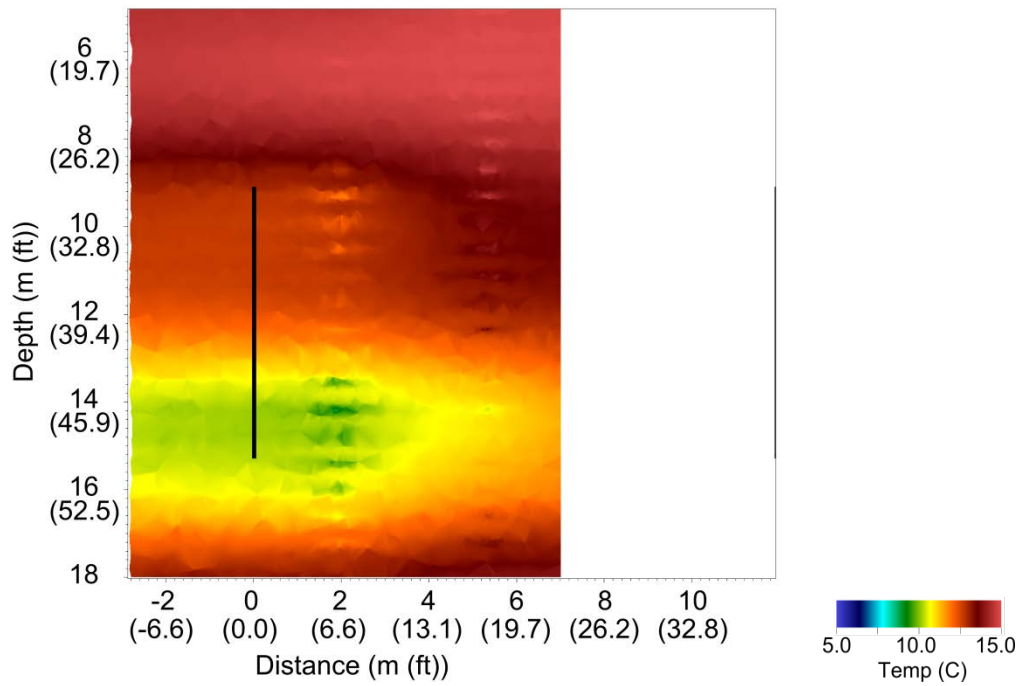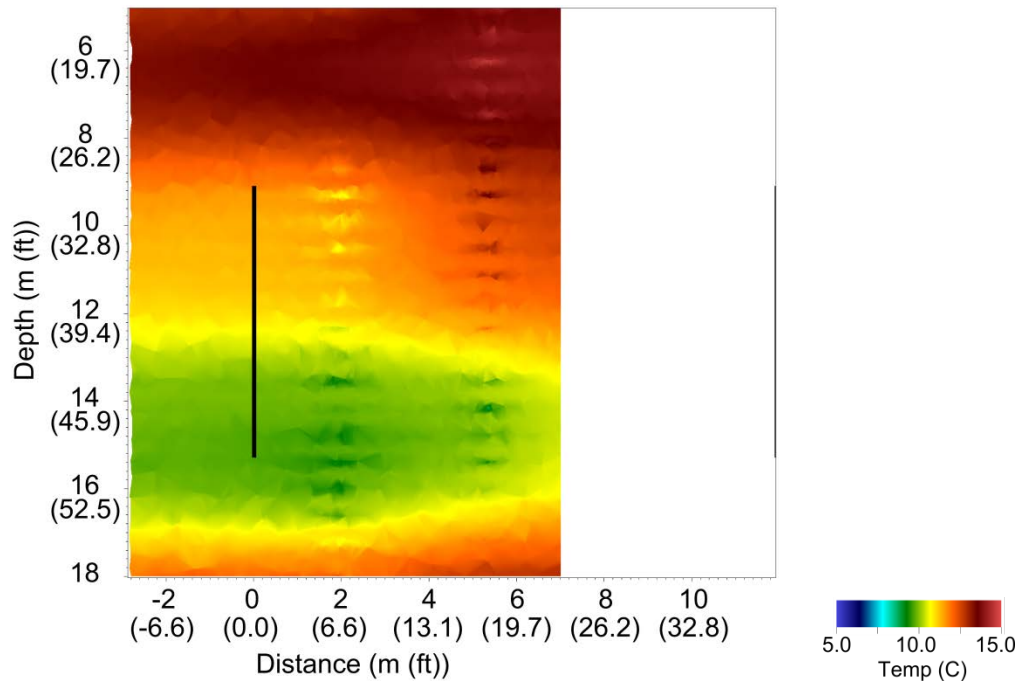
February 14, 2011 (Desiccation Day 28)

B.2

February 28, 2011 (Desiccation Day 42)

March 14, 2011 (Desiccation Day 56)

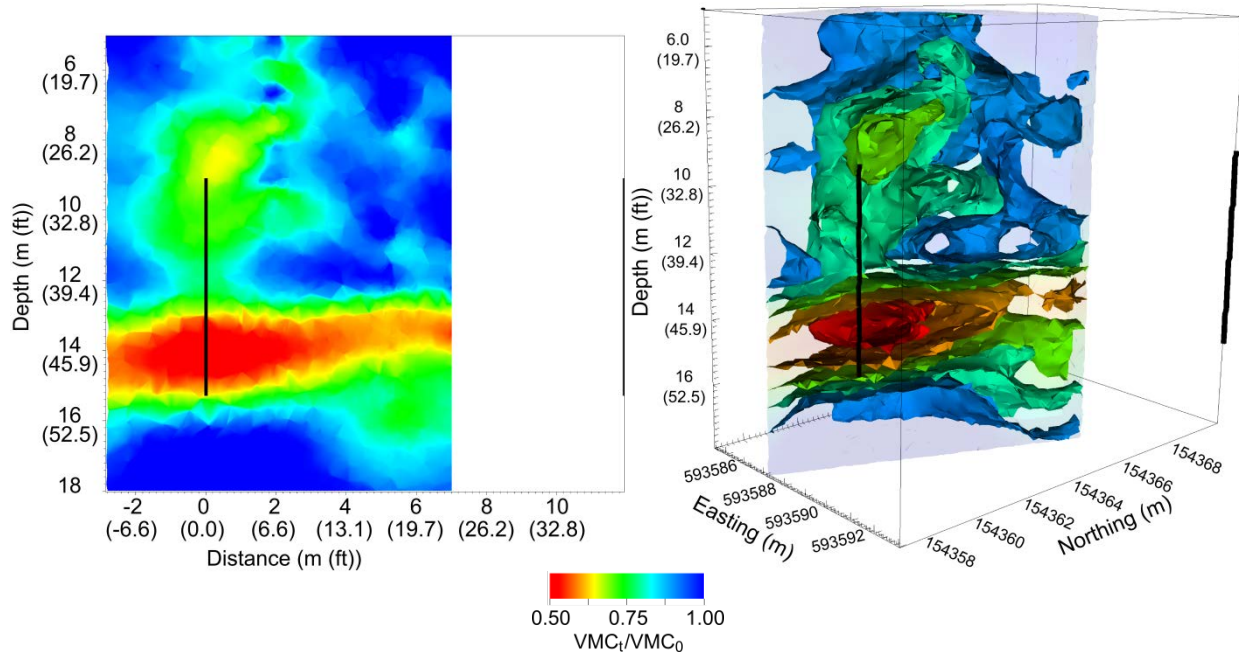March 28, 2011 (Desiccation Day 70)
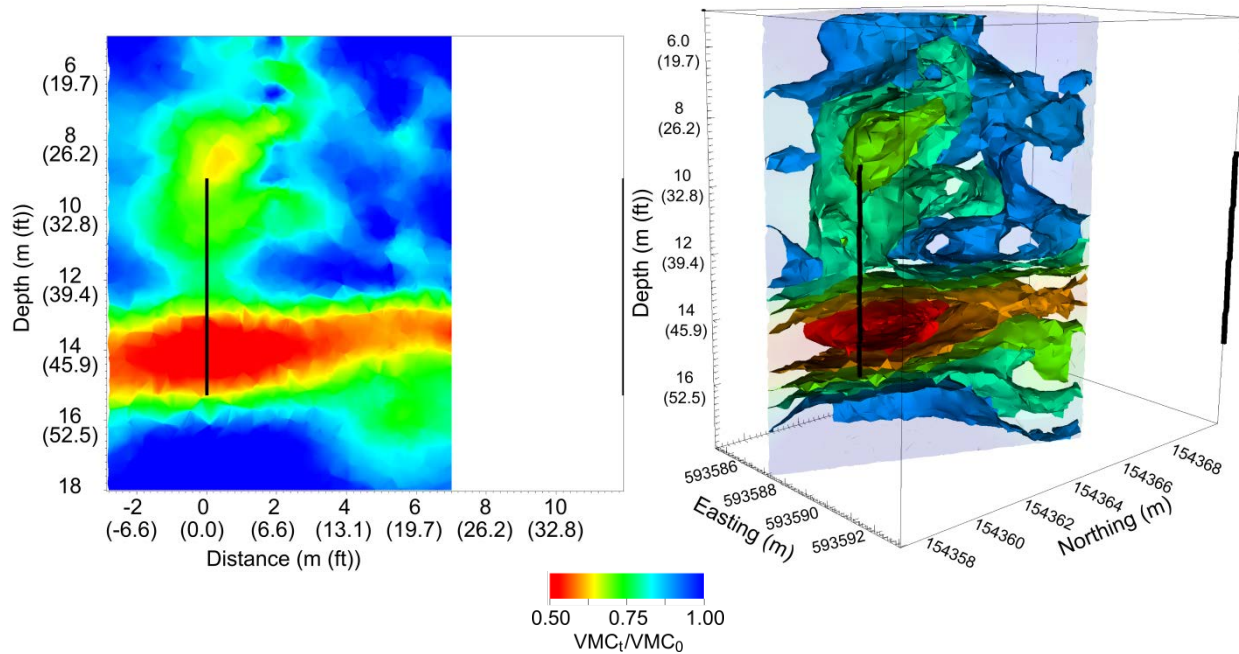

April 11, 2011 (Desiccation Day 84)

April 25, 2011 (Desiccation Day 98)

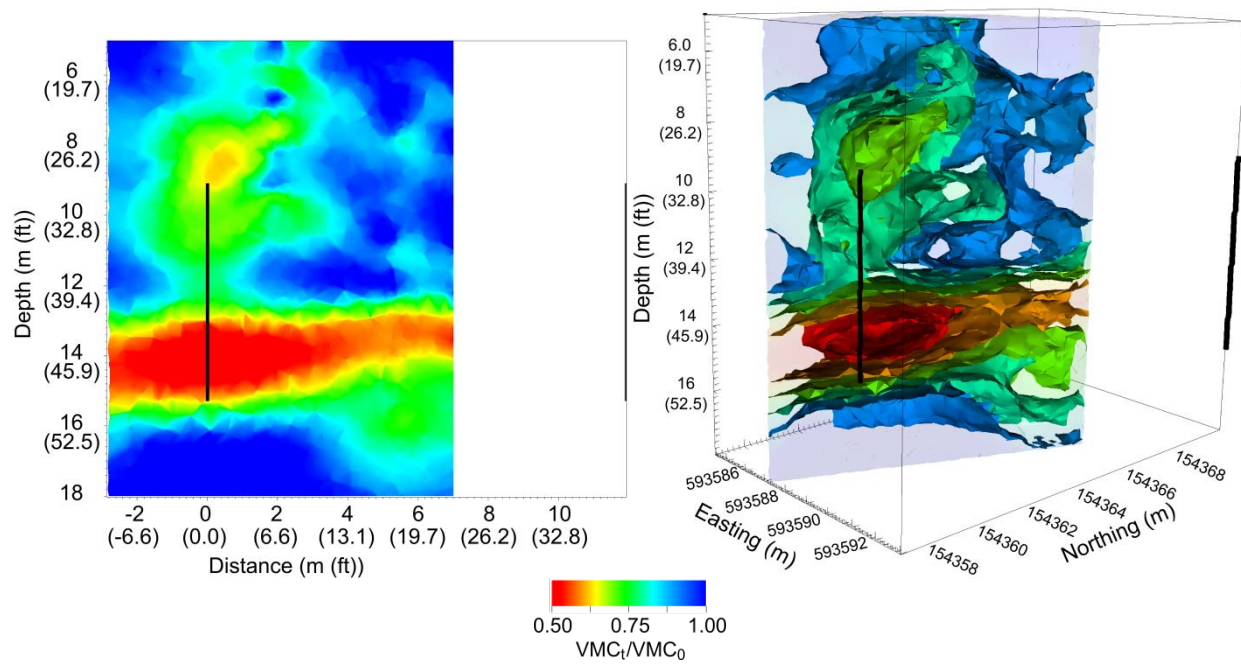

May 9, 2011 (Desiccation Day 112)

B.5
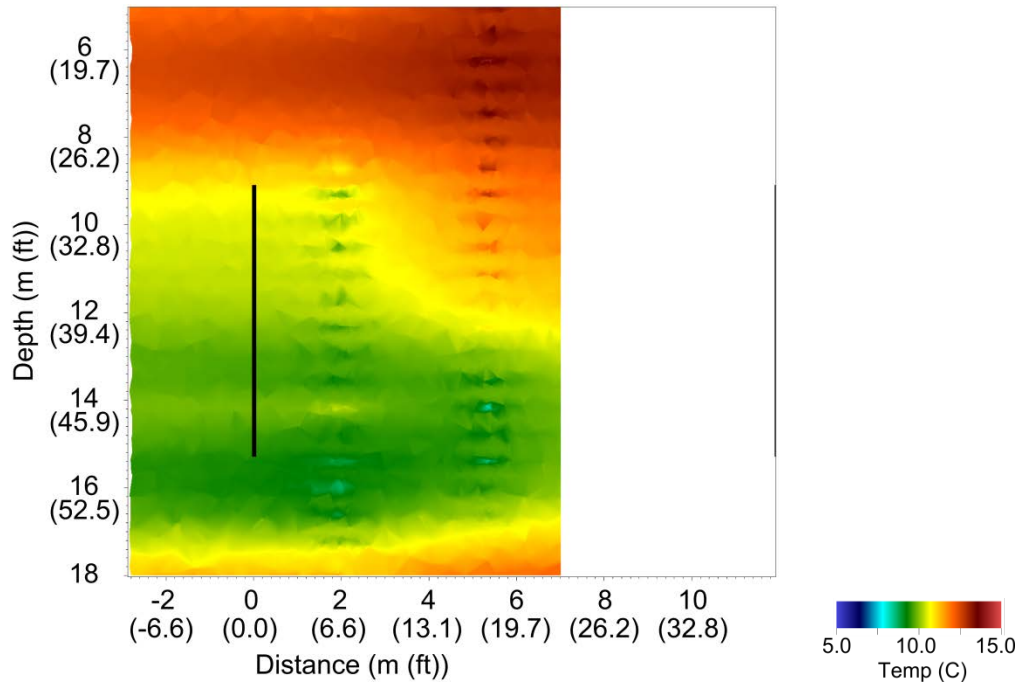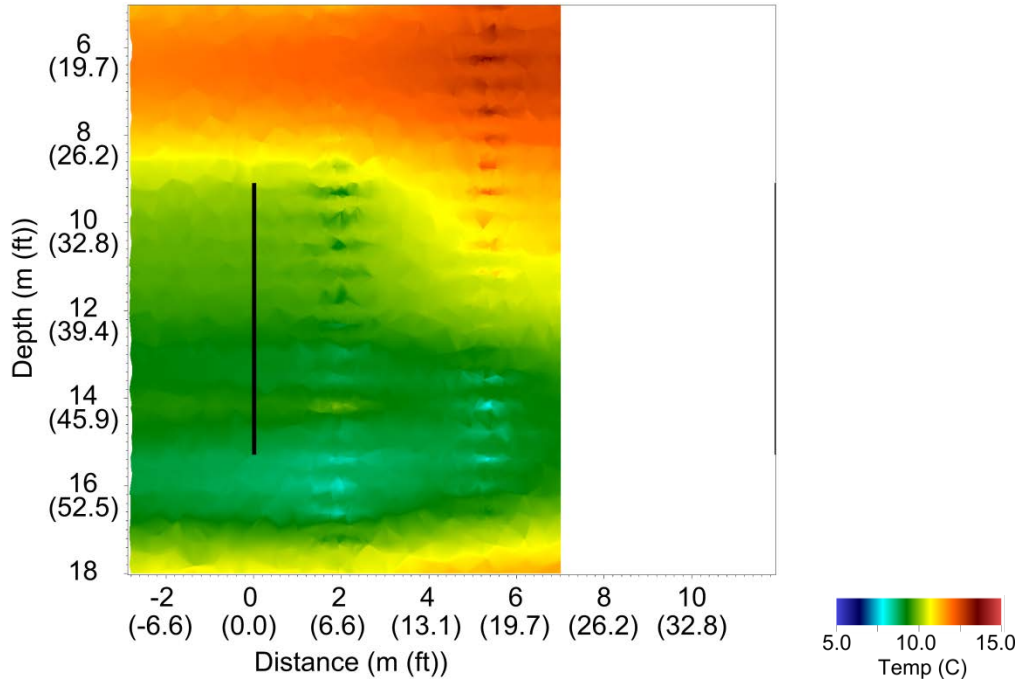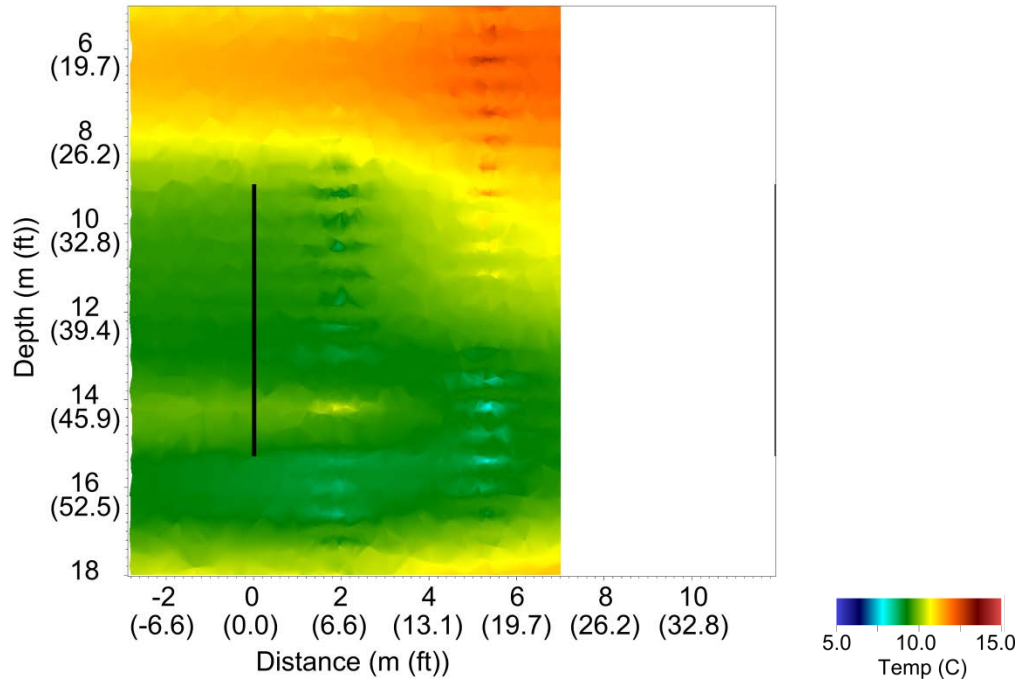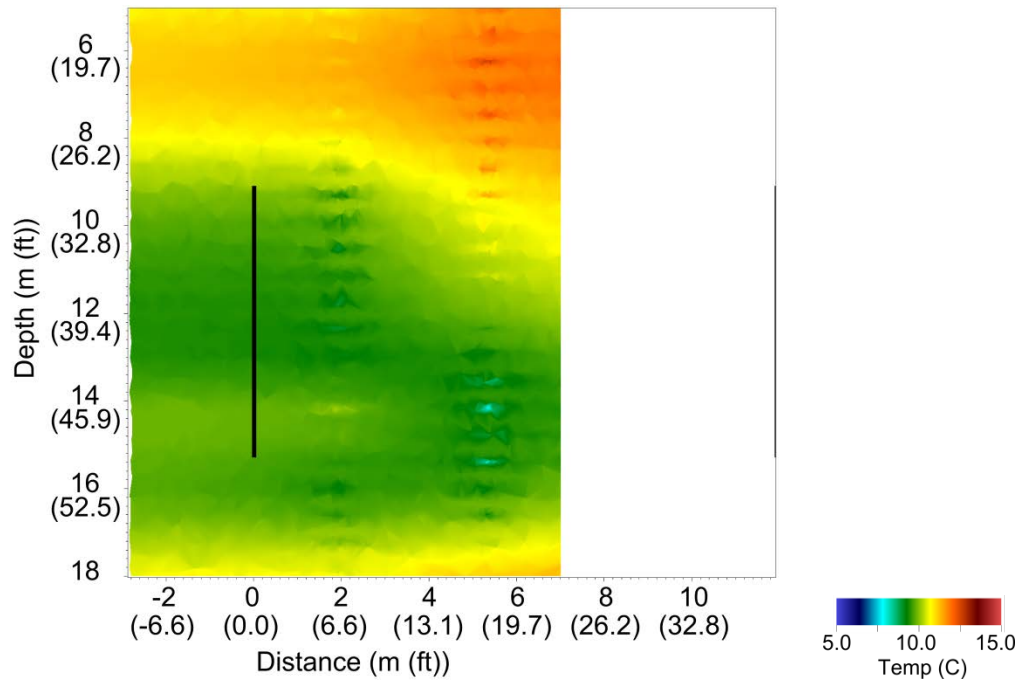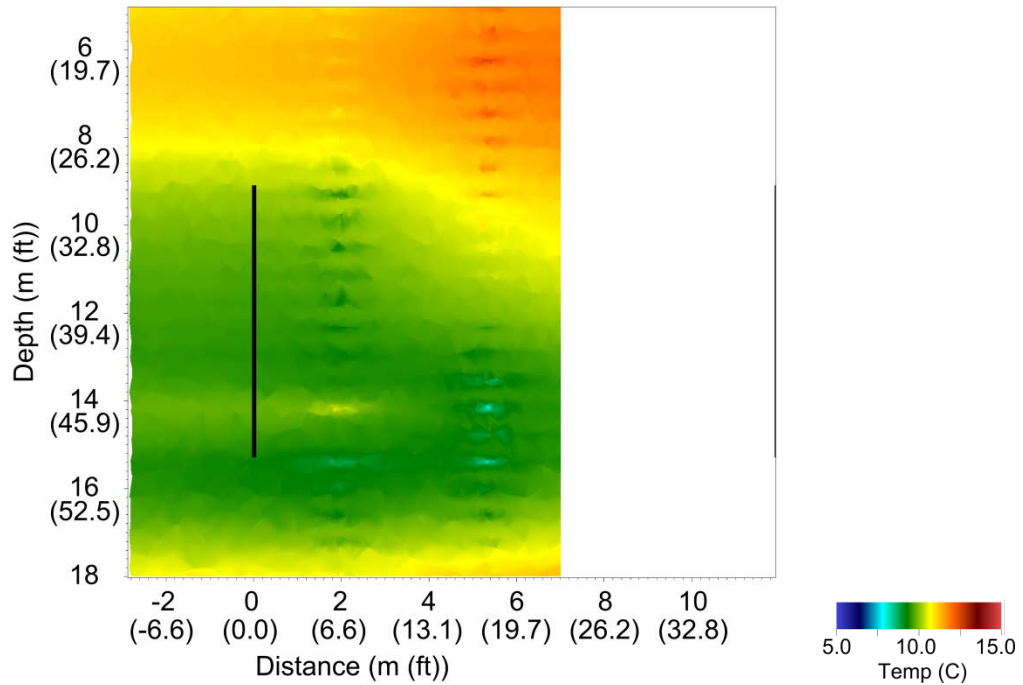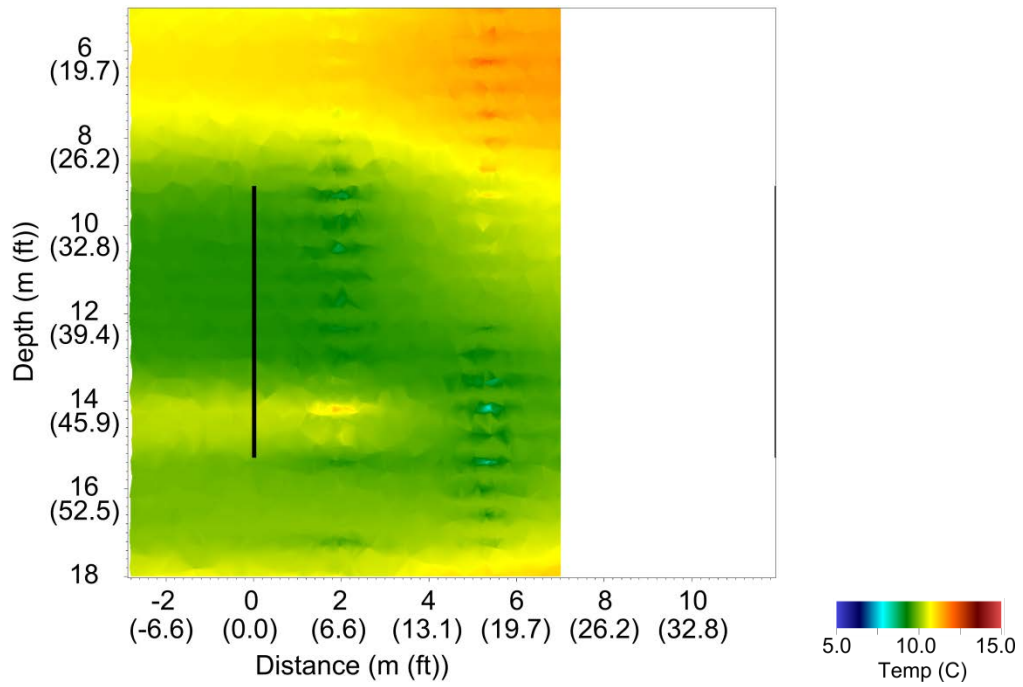
May 23, 2011 (Desiccation Day 126)
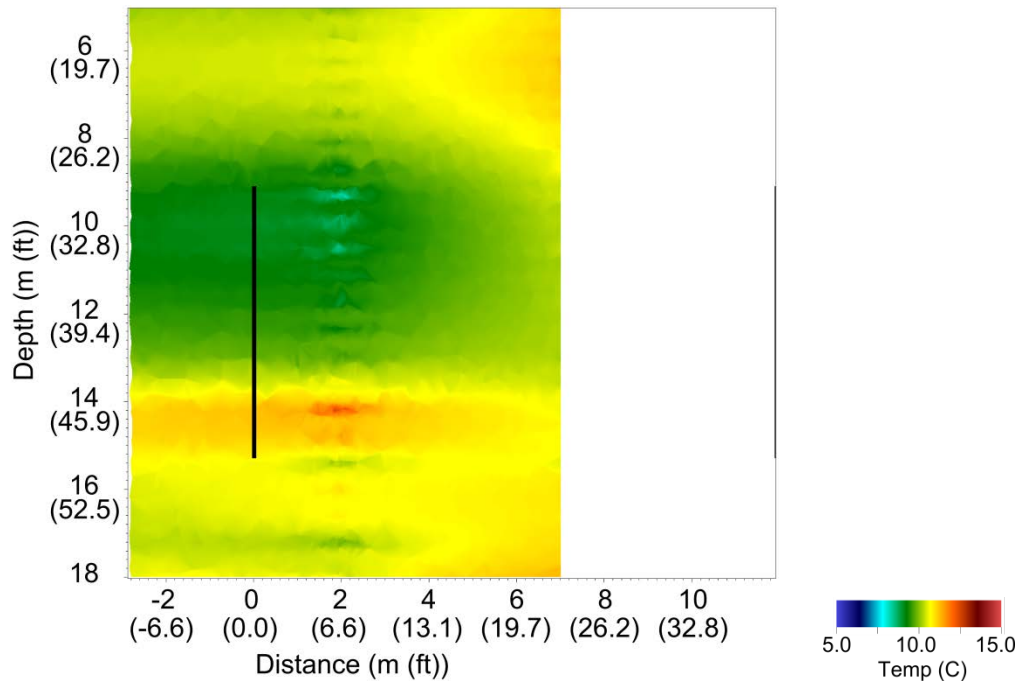
June 6, 2011 (Desiccation Day 140)
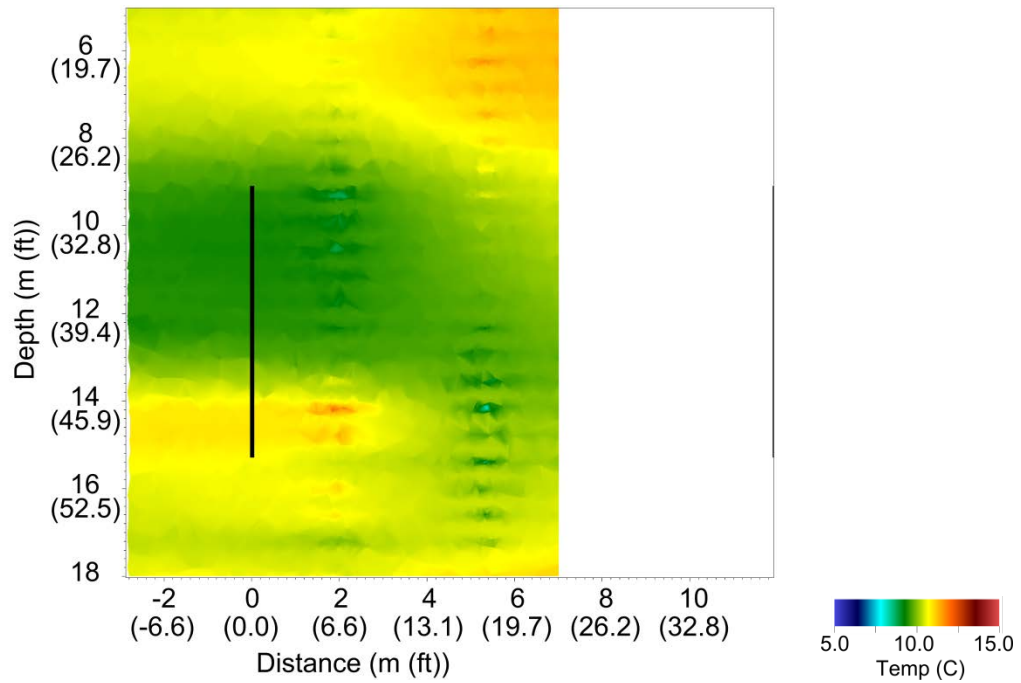
June 20, 2011 (Desiccation Day 154)
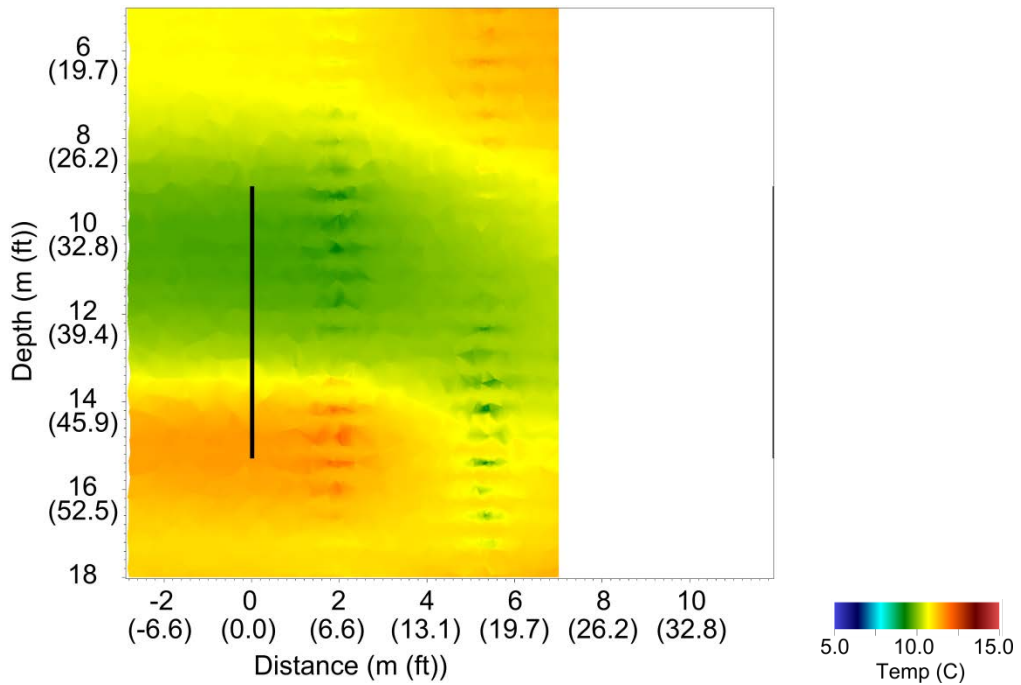
July 4, 2011 (Day 4 post-desiccation)

Neutron Moisture Logging Data Interpolation
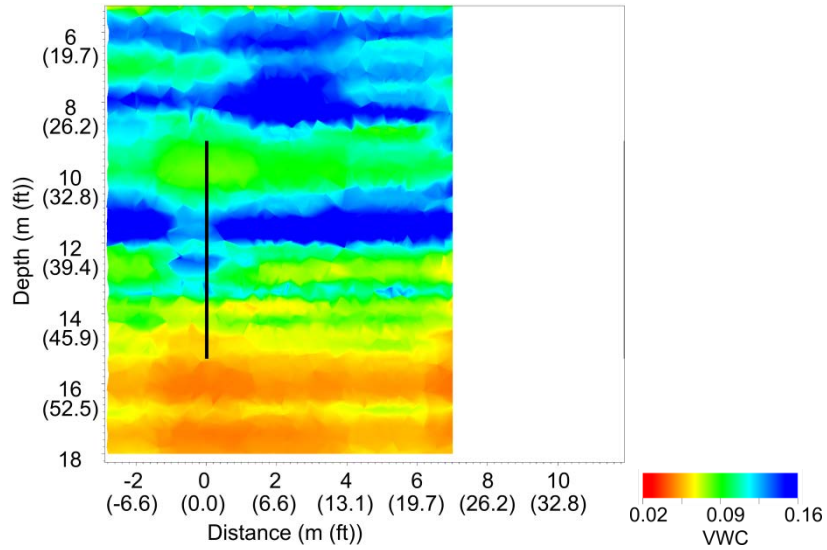
December 2010 (Baseline Pre-desiccation)
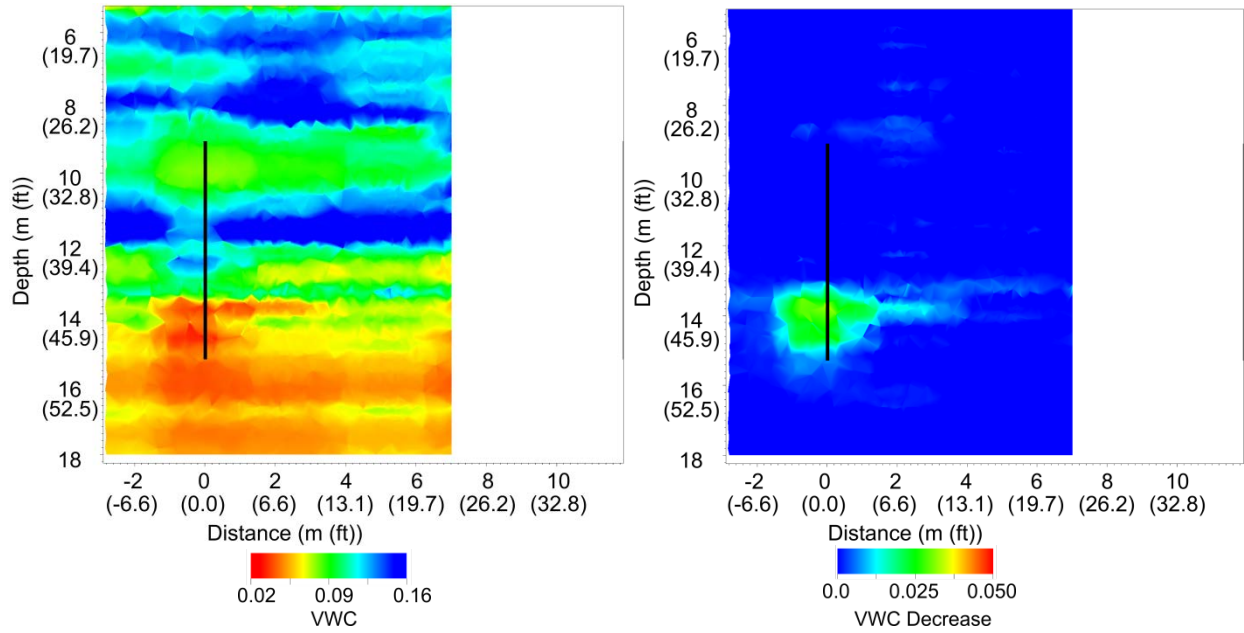
February 16, 2011 (Desiccation Day 30)
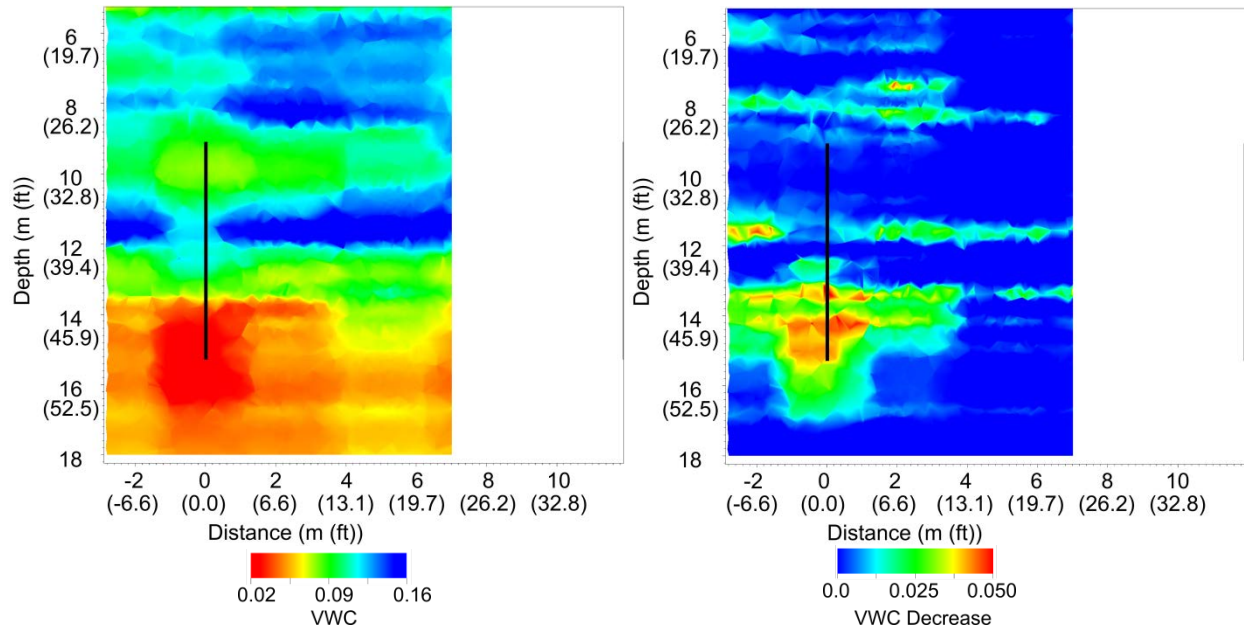
March 28, 2011 (Desiccation Day 70)
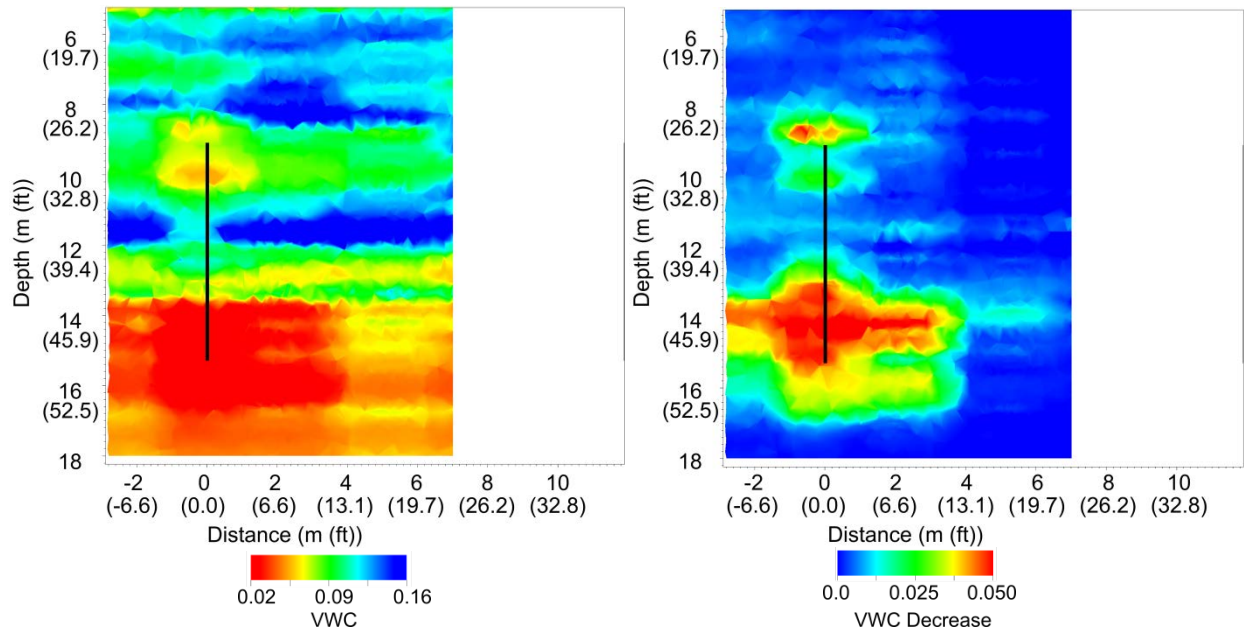
June 6, 2011 (Desiccation Day 140)
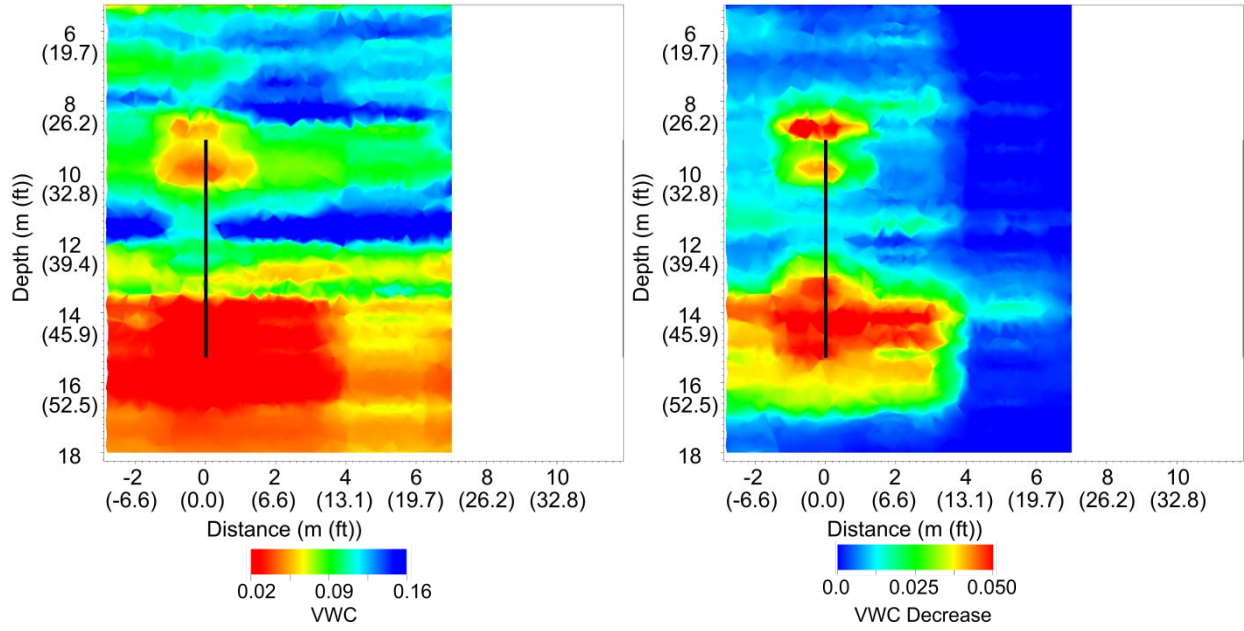
July 11, 2011 (Desiccation Day 175, considered representative of final desiccation moisture content where desiccation ended on day 164)

Electrical Resistivity Tomography Data Interpretation

January 31, 2011 (Desiccation Day 14)

February 14, 2011 (Desiccation Day 28)

B.11

February 28, 2011 (Desiccation Day 42)

March 14, 2011 (Desiccation Day 56)

March 28, 2011 (Desiccation Day 70)

April 11, 2011 (Desiccation Day 84)

April 25, 2011 (Desiccation Day 98)

May 9, 2011 (Desiccation Day 112)

B.14

May 23, 2011 (Desiccation Day 126)

June 6, 2011 (Desiccation Day 140)

B.15

June 20, 2011 (Desiccation Day 154)

Ground Penetrating Radar Data Interpretation
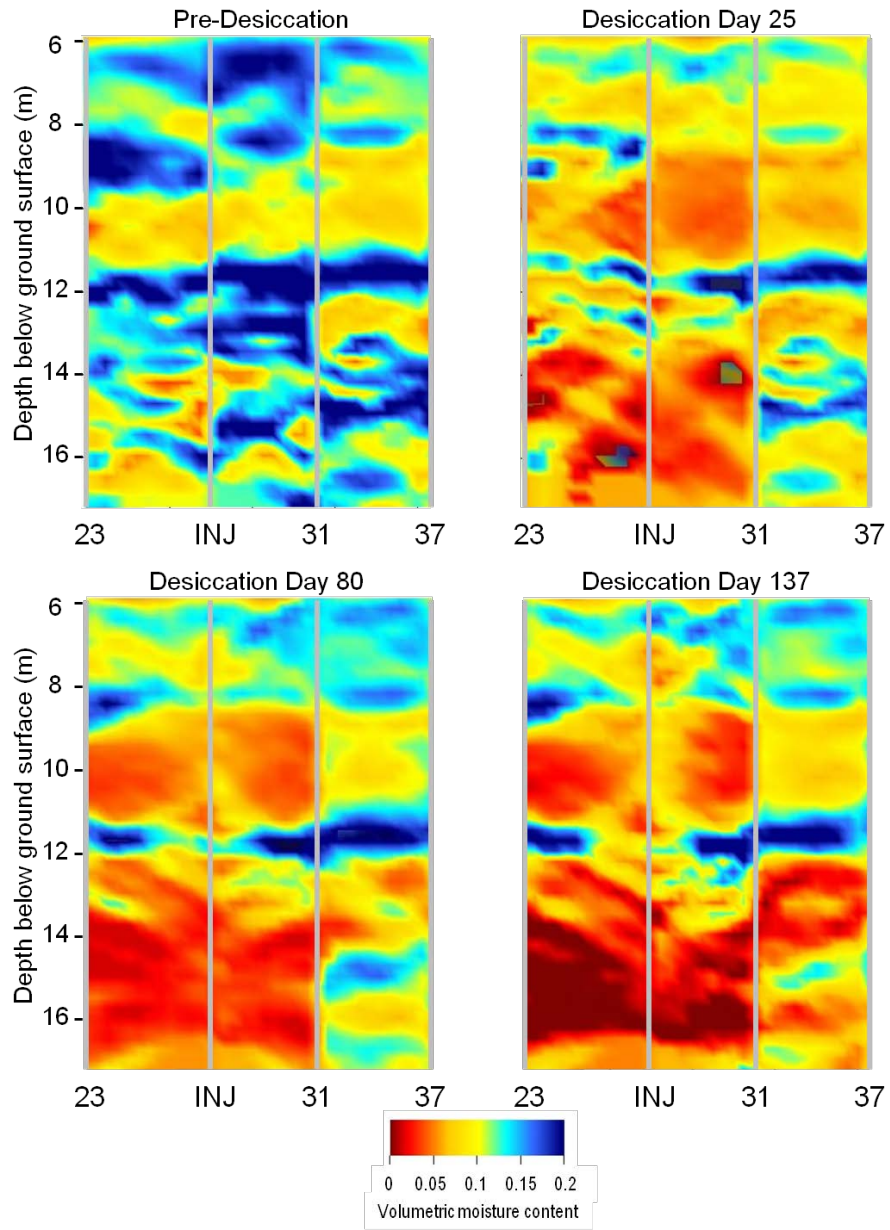
Active Desiccation (X-axis shows logging access locations where INJ = the injection well and other locations represent the last two digits of the location name [i.e., 23 = C7523])

Appendix C

Post-Desiccation Neutron Moisture Probe Data

Appendix C

Neutron Moisture Probe Data
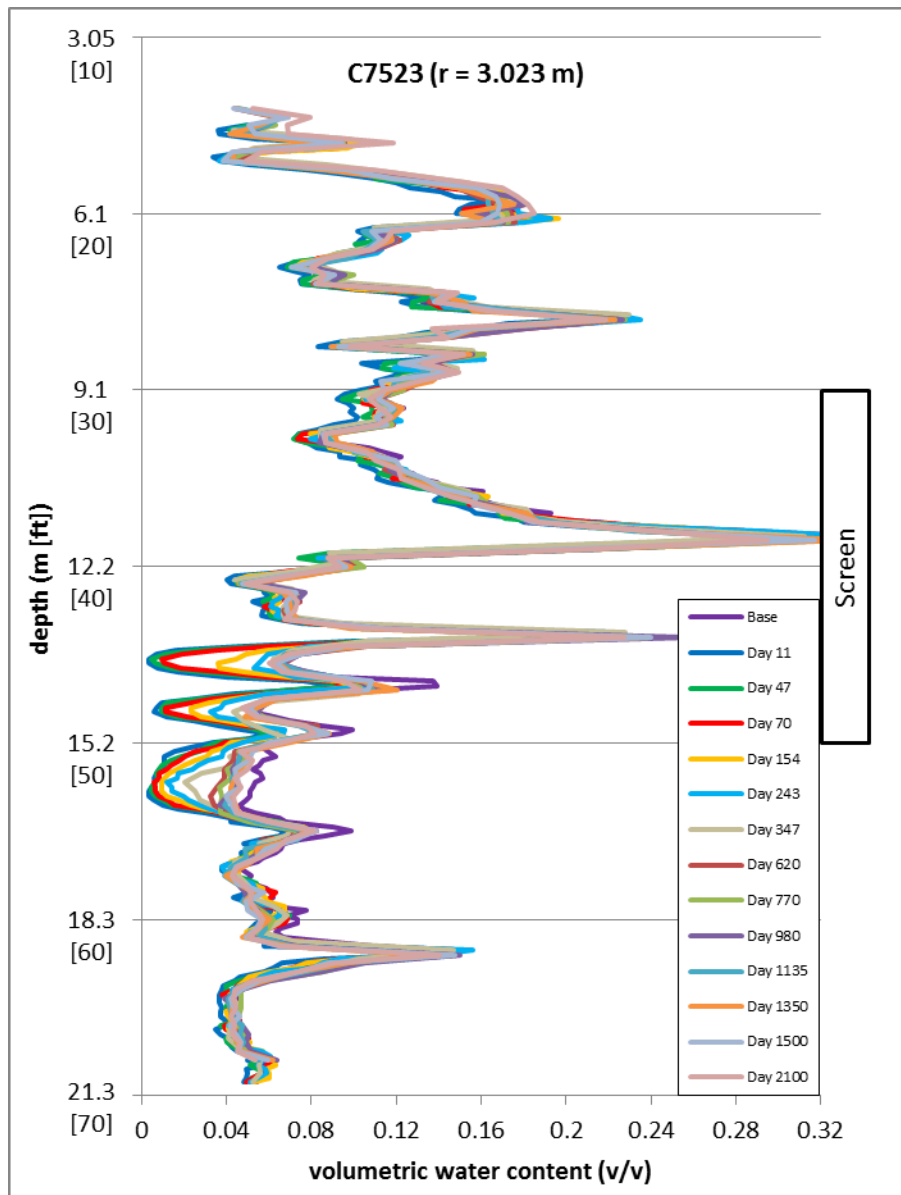
Figure C.1. Neutron Moisture Probe Response over Time for Location C7523 (3.023 m from injection well). The pre-desiccation data (Base) are for a logging event in December 2010, prior to the continuous active desiccation period. Other data are for logging events after active desiccation ended.
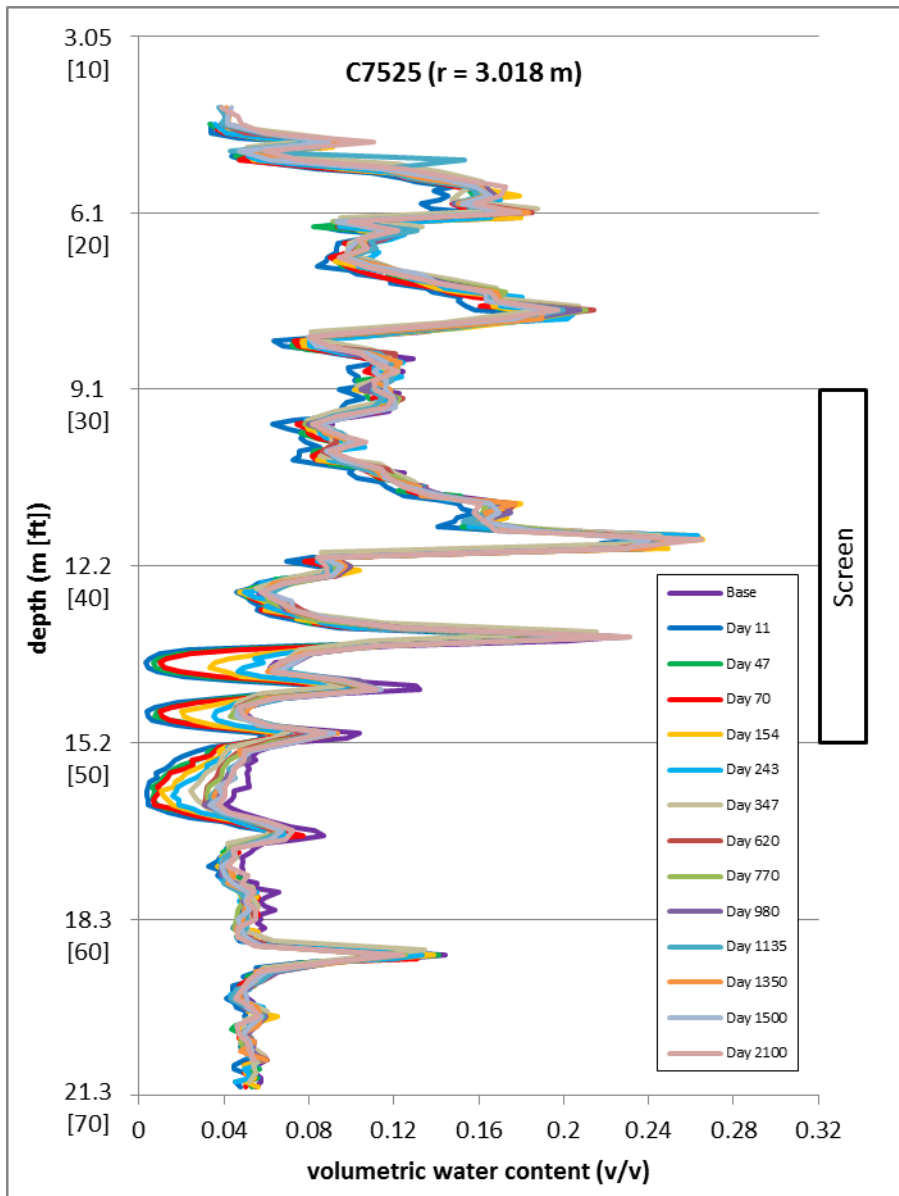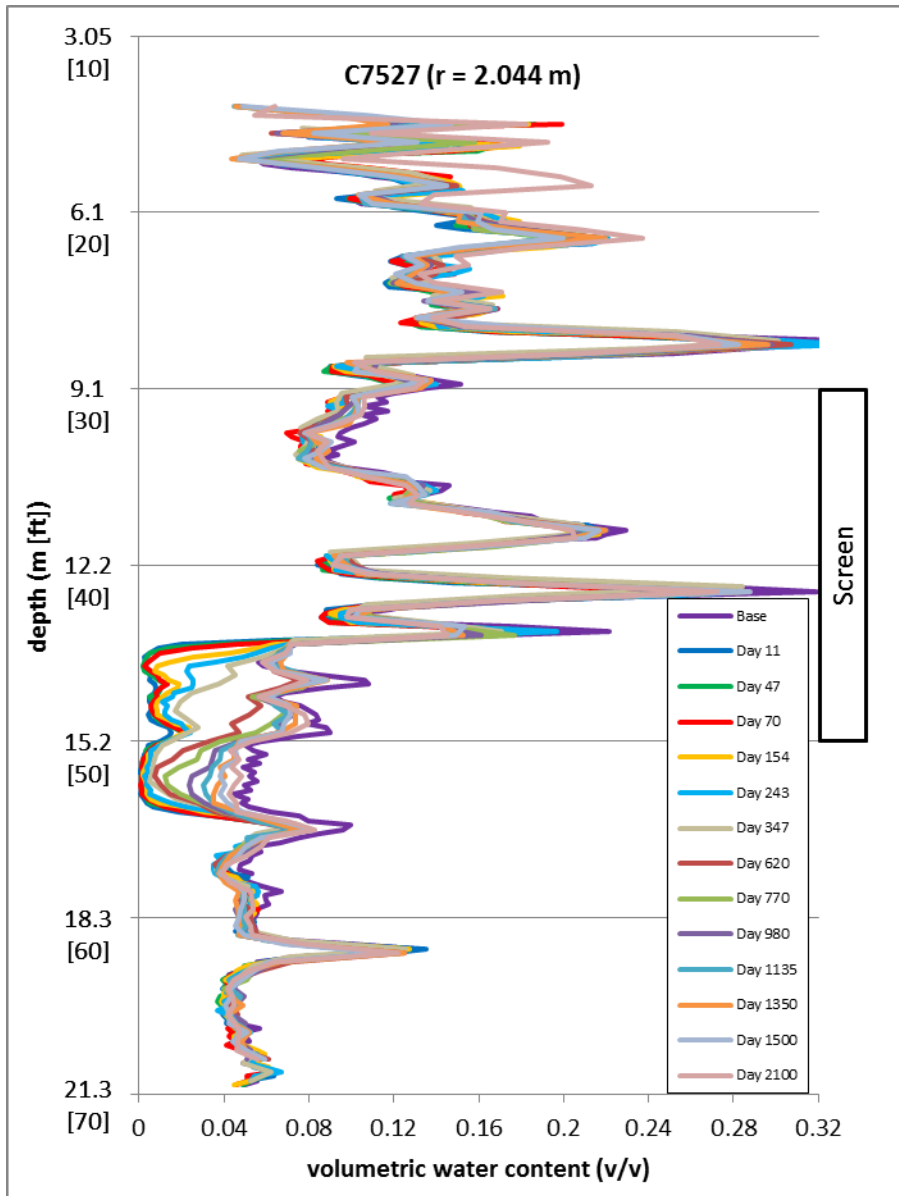
Figure C.2. Neutron Moisture Probe Response over Time for Location C7525 (3.018 m from injection well). The pre-desiccation data (Base) are for a logging event in December 2010, prior to the continuous active desiccation period. Other data are for logging events after active desiccation ended.
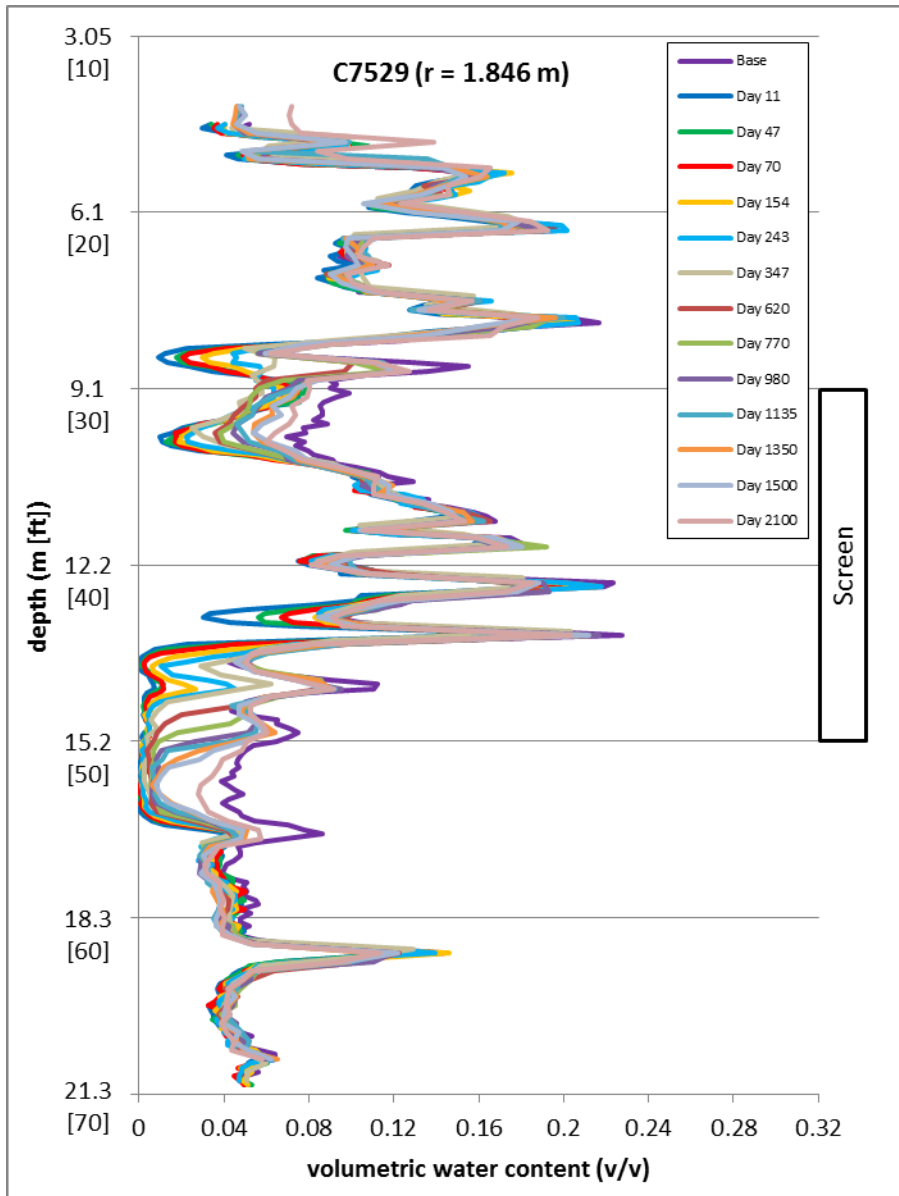
C.2

Figure C.3. Neutron Moisture Probe Response over Time for Location C7527 (2.044 m from injection well). The pre-desiccation data (Base) are for a logging event in December 2010, prior to the continuous active desiccation period. Other data are for logging events after active desiccation ended.
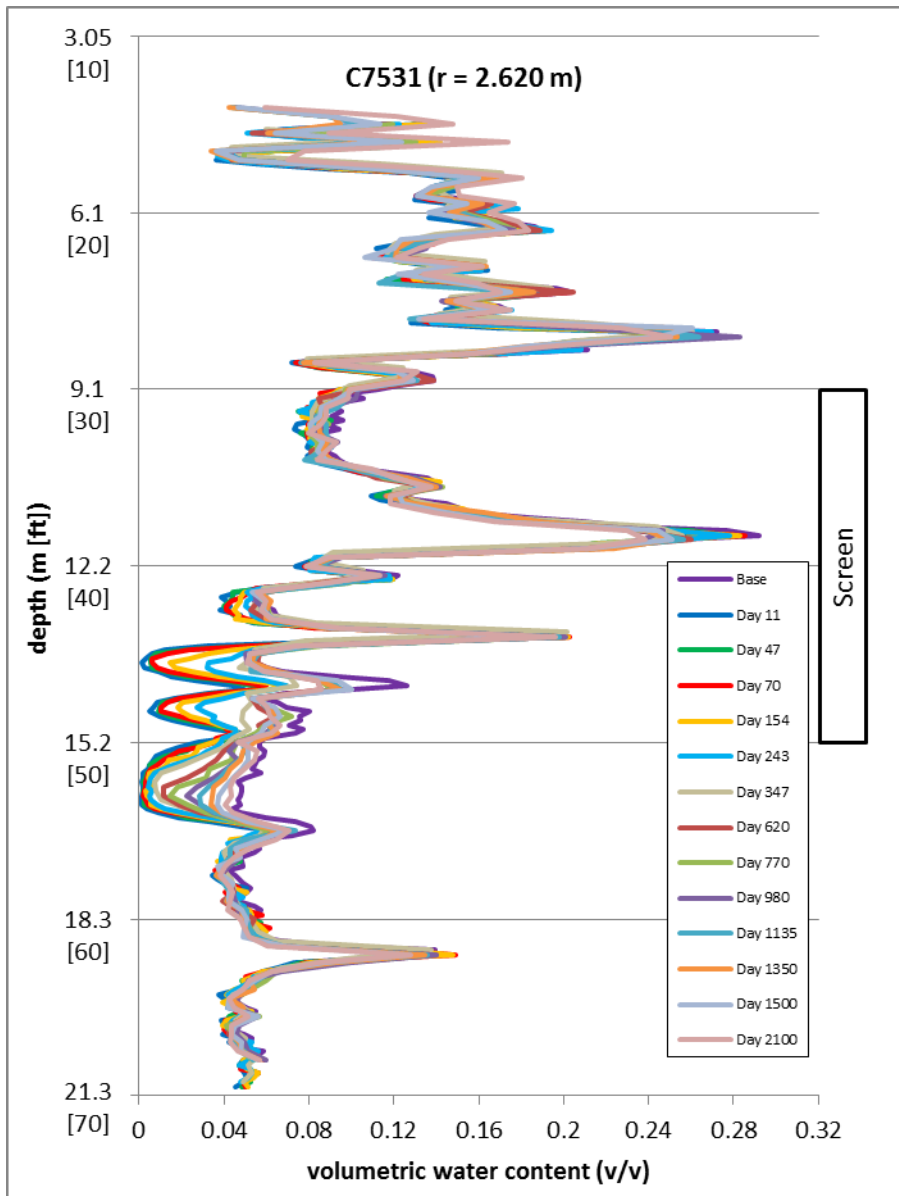
Figure C.4. Neutron Moisture Probe Response over Time for Location C7529 (1.846 m from injection well). The pre-desiccation data (Base) are for a logging event in December 2010, prior to the continuous active desiccation period. Other data are for logging events after active desiccation ended.

Figure C.5. Neutron Moisture Probe Response over Time for Location C7531 (2.620 m from injection well). The pre-desiccation data (Base) are for a logging event in December 2010, prior to the continuous active desiccation period. Other data are for logging events after active desiccation ended.
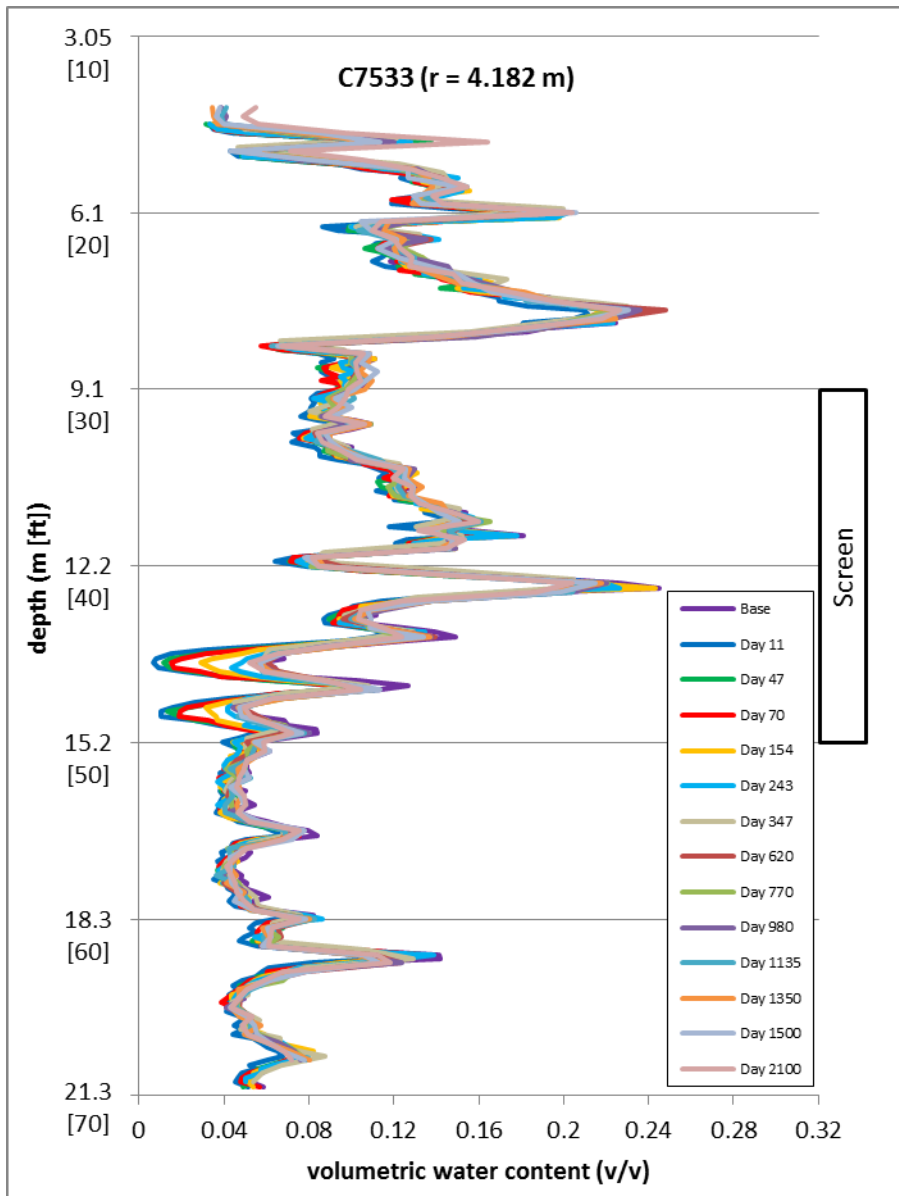
Figure C.6. Neutron Moisture Probe Response over Time for Location C7533 (4.182 m from injection well). The pre-desiccation data (Base) are for a logging event in December 2010, prior to the continuous active desiccation period. Other data are for logging events after active desiccation ended.
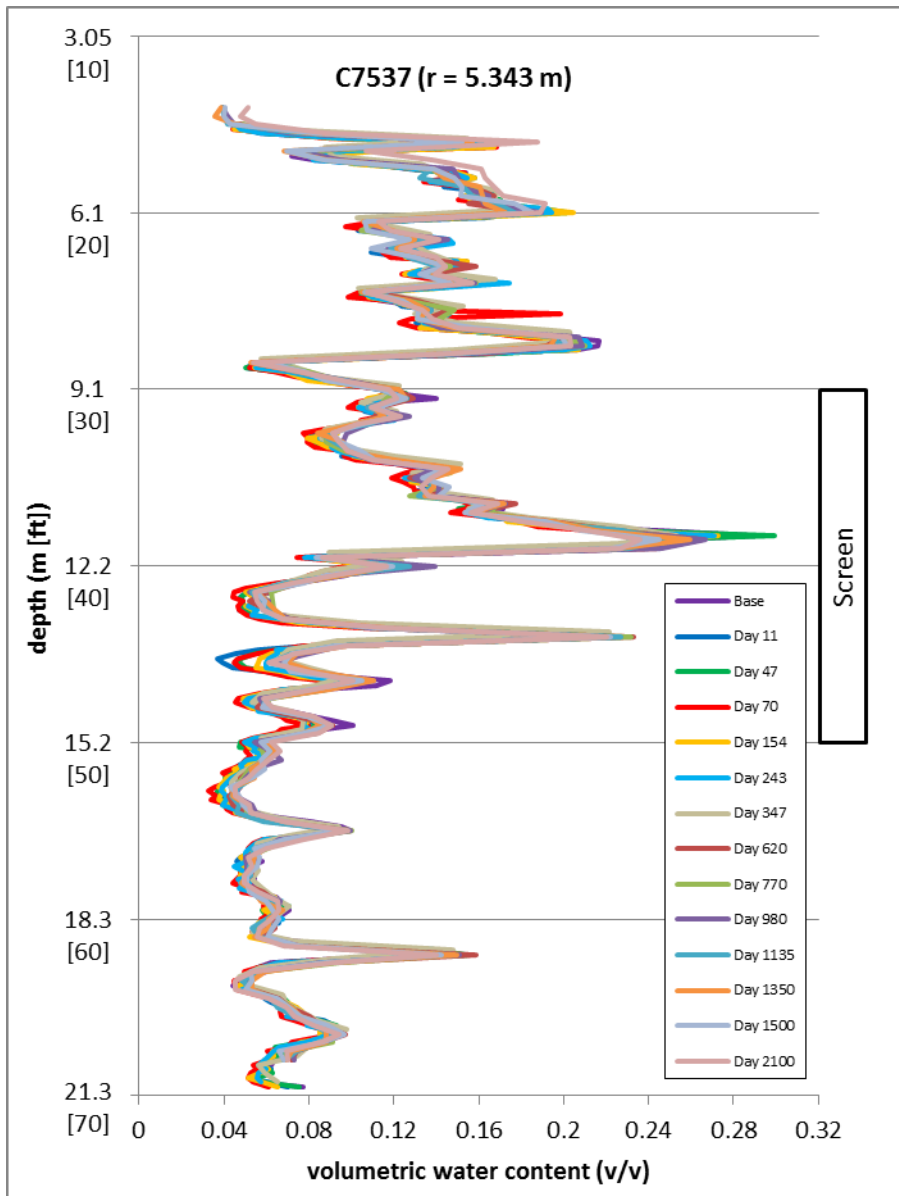
Figure C.7. Neutron Moisture Probe Response over Time for Location C7537 (5.343 m from injection well). The pre-desiccation data (Base) are for a logging event in December 2010, prior to the continuous active desiccation period. Other data are for logging events after active desiccation ended.

Distribution

No. of
Copies

No. of
Copies

\# **Hanford Distribution**
CHPRC
  Dave St. John (PDF)

\# **Local Distribution**
Pacific Northwest National Laboratory
  MJ Truex (PDF)

Pacific Northwest
NATIONAL LABORATORY

Proudly Operated by **Battelle** *Since 1965*

902 Battelle Boulevard
P.O. Box 999
Richland, WA 99352
1-888-375-PNNL (7665)

U.S. DEPARTMENT OF
ENERGY

www.pnnl.gov